PhD program in Chemical and Pharmaceutical Sciences, and Related Industrial Innovation XXXIV cycle

Oxo-rhenium-catalyzed Biomimetic Cyclizations and Late-stage Electrochemical C–H Oxidation of Unactivated C(sp^3)–H Bonds

Academic year: 2020–2021

PhD student: Debora Chiodi

Supervisor: Prof. Alessio Porta

Supervisor signature:

Internship of 19 months at Scripps Research (LA JOLLA, CA, USA) under the supervision of Prof. Phil S. Baran

Table of Contents

Abstract

Part A: Oxo-rhenium-promoted Biomimetic Cyclization

From a synthetic point of view, biomimetic cyclizations are remarkable tools because a significant increase in molecular complexity can be obtained in a single step. In fact, using an acyclic, properly tailored substrate, it is possible to build a complex polycyclic structural motif. It is well known that transition metals can promote the biomimetic cyclization of polyunsaturated chains to form carbocyclic systems. There are a variety of ways to activate an "unactivated", electron-neutral olefin that usually behaves like a weak nucleophile: the most common way is to exploit the Lewis acidity of a metallic species to induce a cyclization reaction. Usually, transition-metal-catalyzed biomimetic cyclizations are intramolecular processes. In fact, both the nucleophile and the electrophile that participate in the reaction are present in the same backbone to make the cyclization reaction fast enough in order to minimize the formation of byproducts and to avoid possible side polymerization reactions. Except for some organocatalytic intermolecular examples in which the electrophiles and nucleophiles that undergo the biomimetic cyclization are not part of the same molecule, examples that involve a metallic species remain limited. In the first part of this PhD thesis, a new method to promote biomimetic cyclizations of terpenoid-like starting materials using an oxo-rhenium complex as a catalyst is described. This proof of concept, if further explored, will give access to useful building blocks that can be employed for the total synthesis of natural products.

Part B: Electrochemical C–H Oxidation

The site-specific oxidation of "strong", non-acidic C(sp^3)–H bonds is a rewarding, yet difficult topic in organic synthesis. In an academic setting, this could lead to a drastic simplification of synthetic plans; in an industrial/pharmaceutical setting, late-stage oxidative access to metabolites and late-stage diversification of lead compounds could save much time and effort in drug discovery and development. Therefore, there is a growing need for new reagents and methods to achieve such transformations. One drawback of current chemical reagents is the lack of diversity with regard to structure and reactivity that prevent rapid screening to be employed. In the biochemical realm, directed evolution still holds the greatest promise for achieving complex C–H oxidations in a variety of settings. In the second part of this PhD thesis, *N*-ammonium ylides are described as tunable, electrochemically driven oxidants for site-specific, chemoselective C(sp^3)–H oxidation. Using a computationally guided approach, these new mediators were synthesized with simple building blocks, and rapidly expanded into a library. This ylide-based approach to C–H oxidation exhibits a unique selectivity relative to other classes of chemical oxidants, and can be applied to real-world problems in the agricultural and pharmaceutical sectors.

Chapter 1: Rhenium Chemistry

1.1 Chapter Abstract

In this chapter, an overview of reactions in organic synthesis catalyzed by rhenium complexes will be discussed. In particular, attention will be placed on high-valence oxo-rhenium complexes, which have proved to be efficient catalysts for C–C and C–X bond formation, given the dual nature of these complexes to behave both as Lewis acids and as oxidants promoting oxygen atom transfer reactions (OAT). Furthermore, rhenium carbonyl complexes, which can promote a variety of annulation reactions, will be discussed. The beauty of rhenium chemistry lies in its simplicity: The reaction conditions often involve only the starting material(s), a rhenium catalyst, and solvent. It is the aim of this thesis to demonstrate how this underutilized transition metal can simplify aspects of modern organic synthesis.

1.2 Introduction

Rhenium (Re) is a transition metal located in Group 7 of the Periodic Table of Elements. Rhenium is in the same group as manganese and is located in the middle of all the transition metal groups in the Periodic Table. Given its "special" position in the Periodic Table, rhenium complexes have some features and properties belonging to both the early and late transition metals. For example, rhenium exhibits lower electronegativity in comparison with some late transition metals like rhodium, ruthenium and palladium, which explains why Re–X (X = C, N, O) bonds are more polarized than the corresponding M–X bonds of late transition metals under the same experimental conditions. Hence, the Re–X bond in a rhenium complex possesses relatively stronger nucleophilicity, providing benefits for nucleophilic addition to unsaturated substrates with an electron-withdrawing group. Moreover, some rhenium complexes can also behave like late transition metal complexes undergoing, for example, oxidative addition, reductive elimination, and β-hydride elimination. One of the most important features of rhenium is the wide range of oxidation states that it can access, ranging from –1 to +7, offering a great opportunity for the development of new chemical transformations using rhenium as catalyst.

The chemistry of oxo-rhenium complexes has been the subject of extensive research due to their applications in various industrial and biological settings. The generally favorable features of oxo-rhenium(V) complexes, such as convenient synthesis, large scope of possible ligands, and easy handling (moisture and oxygen stability), resulted in the diverse application of oxo-rhenium complexes in organic synthesis as homogeneous catalysts [1–3].
The synthesis of oxo-rhenium complexes has also attracted significant interest in medicinal chemistry due to their biological properties including anticancer, antibacterial, and antifungal activity [4–7], and also in diagnostic nuclear medicine and radioimmunotherapy as a result of the attractive nuclear properties of ^{186}Re and ^{188}Re isotopes [8,9].

Over many years, high-valent rhenium complexes were employed as excellent catalysts for oxidation reactions, such as the oxidation of alkenes, sulfides, and pyridines [10]. In the last two decades, several new developments in rhenium catalysis were reported. In particular, important progress has been made in high valence oxo-rhenium catalysis [11] and in rhenium carbonyl catalysis. For the latter, particular emphasis will be given to annulation reactions based on C–H and C–C bond cleavage. [12,13]

1.3 Oxo-rhenium Catalysis

The class of rhenium-based organometallic oxides appeared for the first time about 50 years ago thanks to the pioneering research of the Fisher and Wilkinson groups (late 1960s), and subsequently by the Herrman group, which optimized the synthesis of methyltrioxorhenium (MTO) and its application in catalysis. MTO was extensively studied, and the importance of this rhenium oxide species as a catalyst is well known in many oxidation reactions like the epoxidation of olefins [14a–14c], C–H oxidation of sp^2 C–H bonds [14d,14e], and less frequently, of sp^3 C–H bonds [14f] (Figure 1.1). MTO is also employed in the reduction of epoxides [14g] and 1,2-diols in a Corey–Winter-type reaction [14h,14i]. Occasionally, MTO is employed in olefin metathesis and aldehyde olefination [15,16].

Despite the importance of MTO in catalysis, it is not the aim of this thesis to further describe the reactivity of this type of rhenium species. The discovery of MTO paved the way for the exploration of a new oxo-rhenium species, which led to unprecedented reactivity both in oxidation reactions and in Lewis acid catalysis.

High-valent oxo-rhenium complexes proved to be efficient catalysts for the synthesis of C–X bonds. The Toste group's research was particularly relevant for this field. They explored the powerful catalytic activity of some oxo-rhenium complexes [$ReOCl_3$(dppm)] and [$ReOCl_3(SMe_2)(OPPh_3)$] in C–C, C–O, C–N and C–S bond-forming reactions under mild conditions (Figure 1.2).[17]

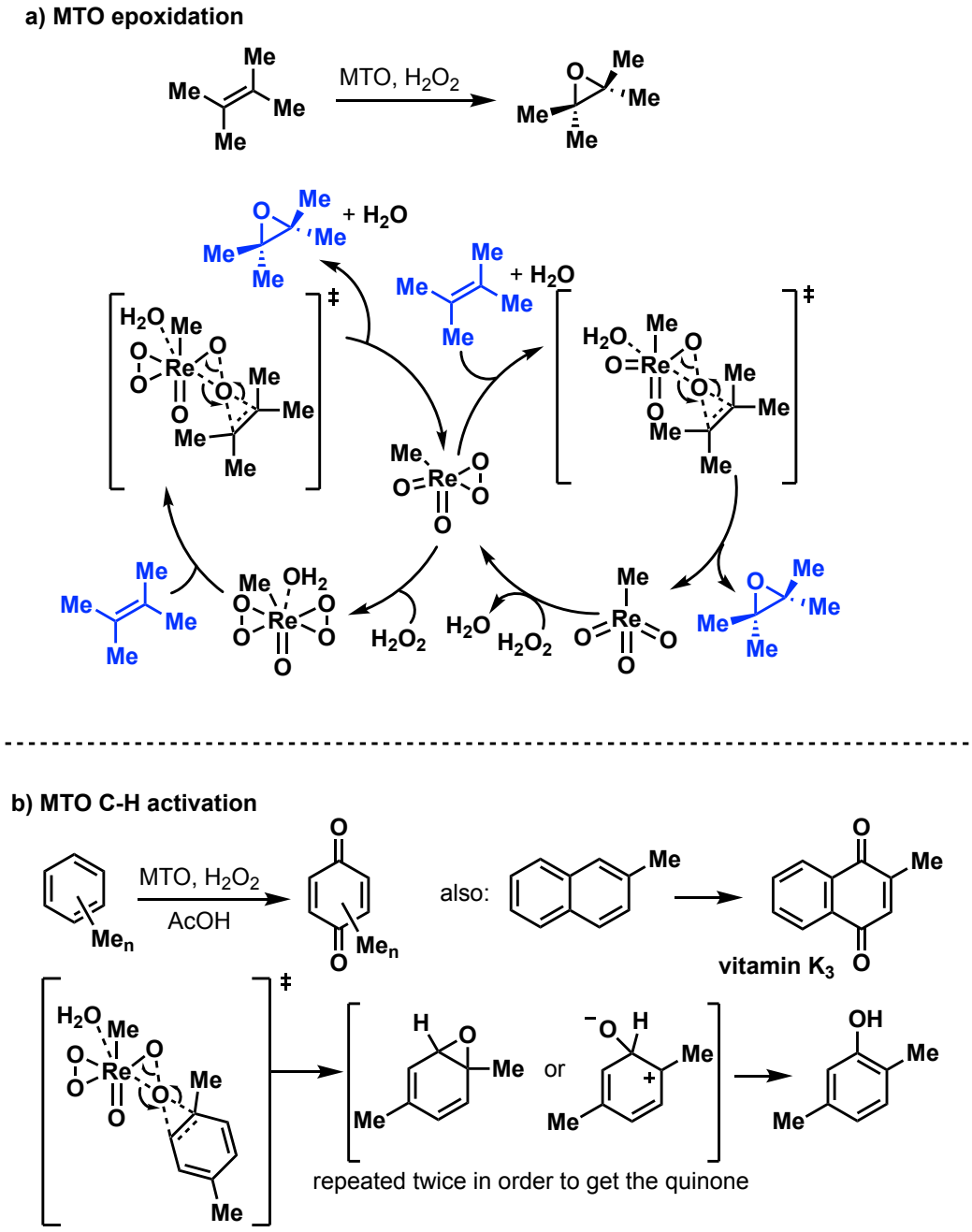

Figure 1.1 a) MTO-catalyzed oxidation of olefins and its catalytic cycle. b) MTO-catalyzed C–H oxidation of sp^2 and sp^3 C–H bonds.

C–X bond formation

Oxocarbenium / anomeric carbon functionalization:

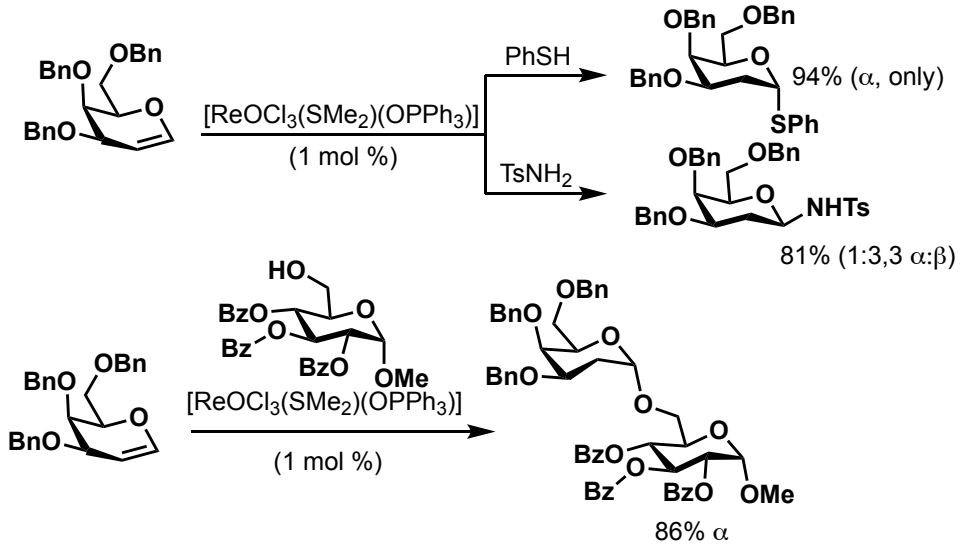

C–C bond formation: Coupling

Sakurai-type reaction:

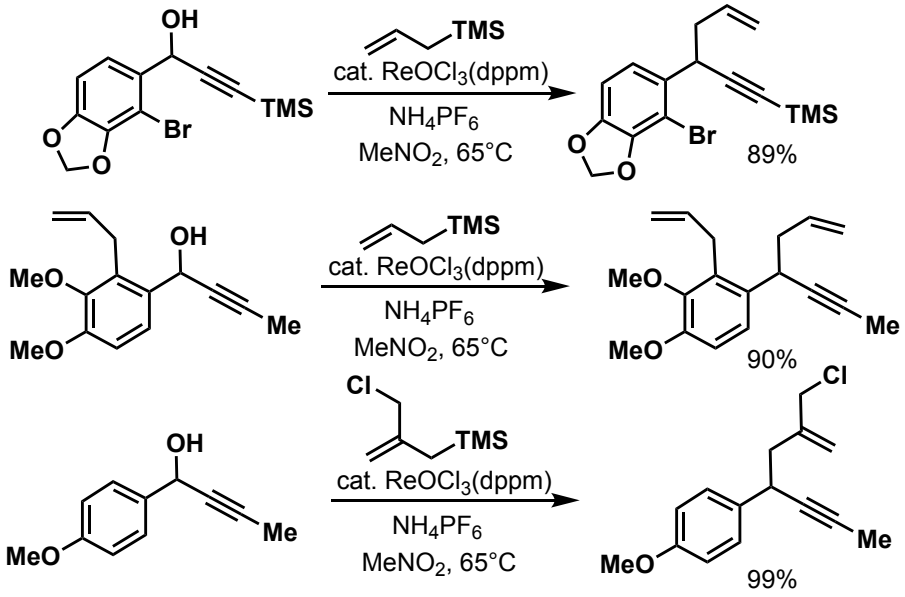

Figure 1.2 Examples of oxo-rhenium(V)-catalyzed C–X and C–C bond formation by Toste and co-workers.

Toste's group's purpose was to use the Lewis acidity of the rhenium complexes in order to promote the generation of stabilized cations, mainly propargyl cations and oxocarbenium ions, as exemplified by a large variety of compounds. A similar type of chemistry was recently applied to furanosides employing a variety of nucleophiles like azides and silyl enol ethers, expanding the applicability of this oxo-rhenium catalyst for the functionalization of sugar-based compounds.[17c] Toste's group also reported a mild method for the regioselective synthesis of propargyl ethers by coupling propargyl alcohols with a range of other alcohols

using [$ReOCl_3$(dppm)] as catalyst (Figure 1.3).[18] This reaction is compatible with a variety of functional groups on the propargyl alcohol motif, including heteroaromatic, electron-rich aromatics and sterically hindered *ortho*-disubstituted aryl groups. Both primary and secondary alcohols can be used as nucleophiles in this reaction without a significant difference in reactivity, however, tertiary alcohols afforded only moderate yields.

C–X bond formation

Propargylic alcohol S_N1-type reaction:

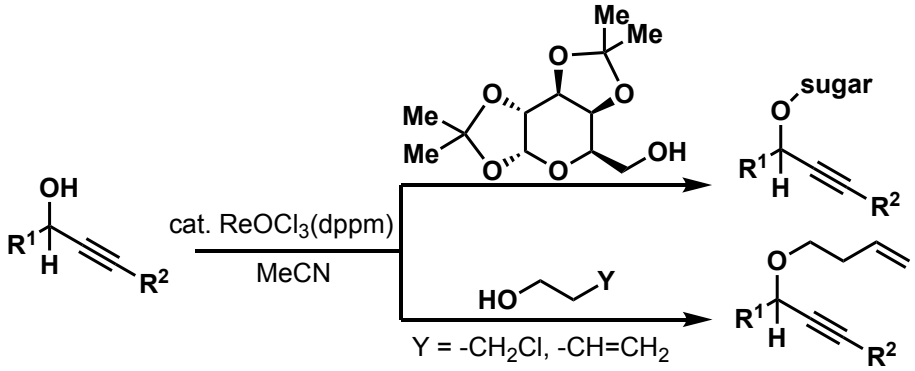

Figure 1.3 Propargyl ether synthesis promoted by an oxo-Re(V) complex.

Toste and co-workers also evaluated the efficiency of the oxo complex [$ReOCl_3$(dppm)] in the formation of C–C bonds in a Sakurai-type reaction between allylsilanes and propargyl alcohols to afford 1,5-enynes as shown in Figure 1.2.[17b] This reaction was also applied to electron-rich and electron-poor aromatic alcohols containing several alkynyl substituents in good yields, without competitive rearrangement to the enone, using 5 mol% of potassium hexafluorophosphate in nitromethane at 65 °C (Figure 1.4).[19]

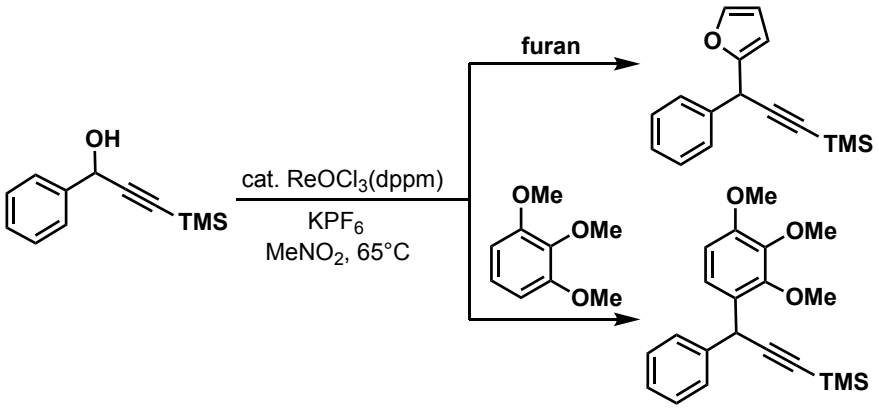

Figure 1.4 Examples of an S_N1-type trapping of propargyl cations with an electron-rich aromatic ring catalyzed by an oxo-Re(V) complex.

This method was also successfully employed in the synthesis of intermediates en route to biologically relevant natural products like *O*-Me-detrol and podophyllotoxin (Figure 1.5). [19]

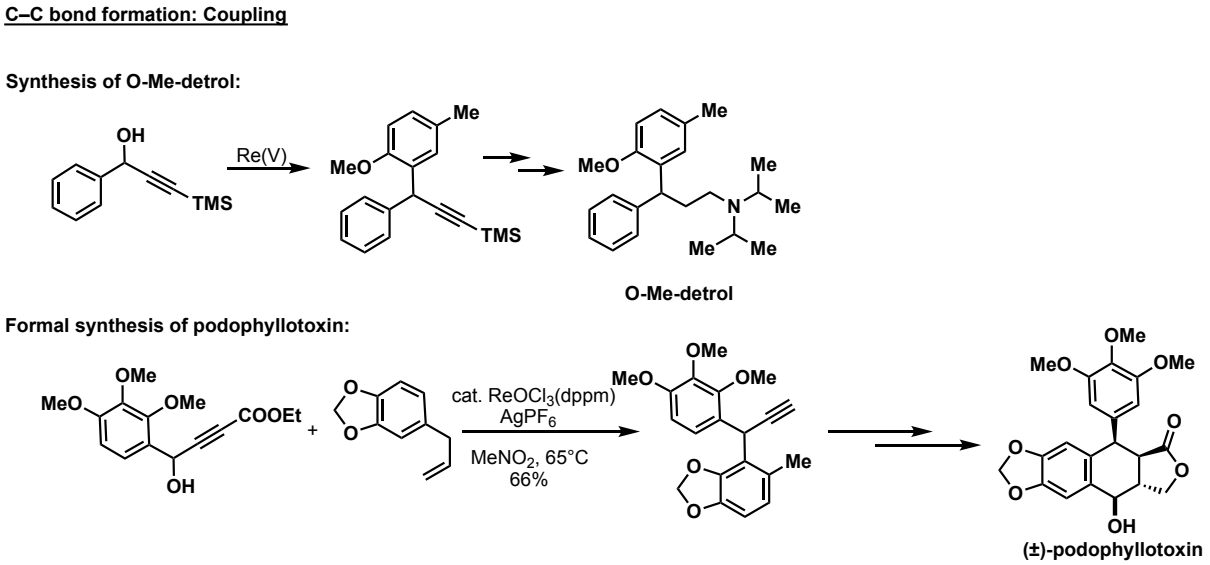

Figure 1.5 Synthetic application of an S_N1-type trapping of propargyl cations with electron-rich aromatic ring catalyzed by an oxo-Re(V) complex.

The oxo-rhenium complex [$ReOCl_3$(dppm)] also proved to be efficient for the regioselective synthesis of propargylamines, generating a propargyl cation from propargyl alcohols and trapping it with tosylamines and carbamates. This reaction was valuable for the construction of C–N bonds given its compatibility with many functional groups. The applicability of this reaction was demonstrated in the preparation of a useful intermediate in the synthesis of pentabromopseudilin, which is known as a potent lipoxygenase inhibitor (Figure 1.6). [20]

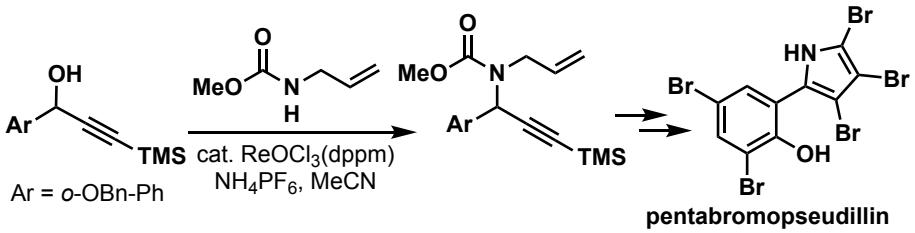

Figure 1.6 Synthetic application of an S_N1-type trapping of propargyl cations with carbamates catalyzed by an oxo-Re(V) complex.

The synthesis of *O*-, *N*-, and *S*-*α*-glycosides was investigated by Toste and co-workers using oxocarbenium ions of glycals as electrophiles and trapping them with a wide range of nucleophiles including alcohols, sulfonamides, and thiols. The oxo-rhenium complex [$ReOCl_3(SMe)_2(OPPh_3)$] was employed as a Lewis acid in order to promote the generation of oxocarbenium ions on the sugar motif. Some examples of sugar glycosylation were previously shown in Figure 1.2. [17] A variety of 2-deoxysugars were prepared with this method in excellent yields, tolerating a variety of protecting groups such as isopropylidene acetals, alkyl and silyl ethers, acetates, and benzoates. Interestingly, the catalytic addition of thiols to glycals resulted in good yields of 2-thioglycosides with no observable catalyst poisoning.

Another interesting application of oxo-Re complexes is the ability of promoting oxygen atom transfer reactions that catalyze oxidations and redox-neutral isomerizations. Most of the oxidation reactions previously described for MTO catalysis exploit this mechanism in which the oxidation process catalyzed by oxo-rhenium species happens mostly in an asynchronous concerted manner, as exemplified by the MTO oxidation of olefins (see Figure 1.1). Similarly, this mechanism was also observed in some redox-neutral rearrangements catalyzed by some oxo-rhenium species, like the isomerization of allylic alcohols [21] and in the Meyer–Schuster rearrangement of propargylic alcohols for the synthesis of enones (Figure 1.7). [22] In particular, the oxo-Re(V)-promoted Meyer–Schuster rearrangement was efficiently employed in the total synthesis of alpha-ionone, a molecule widely employed in the fragrance industry.

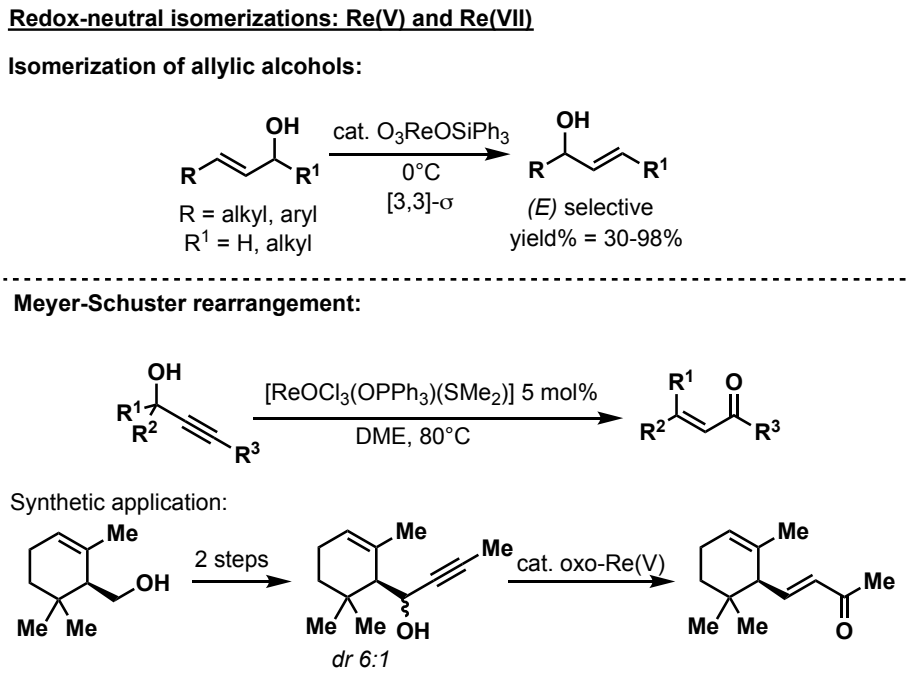

Figure 1.7 Redox-neutral isomerizations catalyzed by Re(V) and Re (VII) species.

Calculations regarding the mechanism indicate a [3,3]-sigmatropic rearrangement,[23] which proceeds through a chair-like transition state containing an anionic perrhenate moiety and a cationic allyl moiety, suggesting that the high catalytic activity of $[ReOCl_3(OPPh_3)(SMe_2)]$ arises from the stabilizing effect of its spectator oxo ligands. Depending on the nature of the substituents R^1, R^2, and R^3 on the propargylic alcohol, the [3,3]-sigmatropic rearrangement can be synchronous or asynchronous (e.g., through cationic intermediates), and as such, the reaction can be *E*/*Z*-specific or result in an *E*/*Z* mixture.[22a, 24] It is possible to use these non-selective processes with reversible trapping by electrophiles, which results in cyclization reactions where regio- and stereocontrol are dictated by thermodynamics. In certain cases, the cationic intermediates that are generated in the reaction can also be employed as electrophiles in promoting intra- or intermolecular dehydrative reactions with a variety of nucleophiles. [24] This type of reactivity can be applied to the synthesis of a variety of heterocyclic and carbocyclic motifs.

A remarkable example of this type of reactivity is shown in Figure 1.8, in which the formation of these spirocyclic products results from the transposition and cyclization of ketones or ketals that are flanked by two allylic alcohols.

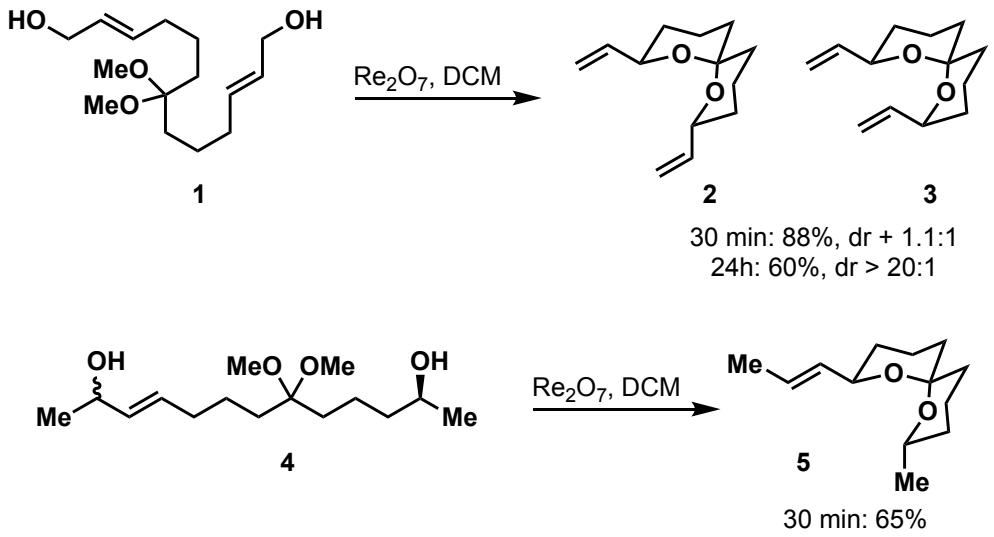

Figure 1.8 Remote stereoinduction in spiroketal formation promoted by Re_2O_7.

In the spiroketal formation reaction of diol **1**, the reaction initially gives a ~1:1 mixture of diastereomers **2** and **3**, but a prolonged reaction time led to exclusive generation of the thermodynamic product **2** as a single diastereomer. Enantiomerically enriched products can be prepared instead by employing substrates such as **4**, in which the absolute stereochemical configuration of the nonallylic alcohol is defined. Treatment of this substrate with Re_2O_7 provided spiroketal **5** with no loss of enantiomeric excess.

Exploiting the same concept described above for the spiroketalization, it is possible to use the oxygen atom of an epoxide as a nucleophile and, through an epoxonium ion intermediate that subsequently collapses, the desired cyclization products can form. If the epoxide is enantiomerically pure, the stereochemical configuration will be retained during the cyclization reaction (Figure 1.9).

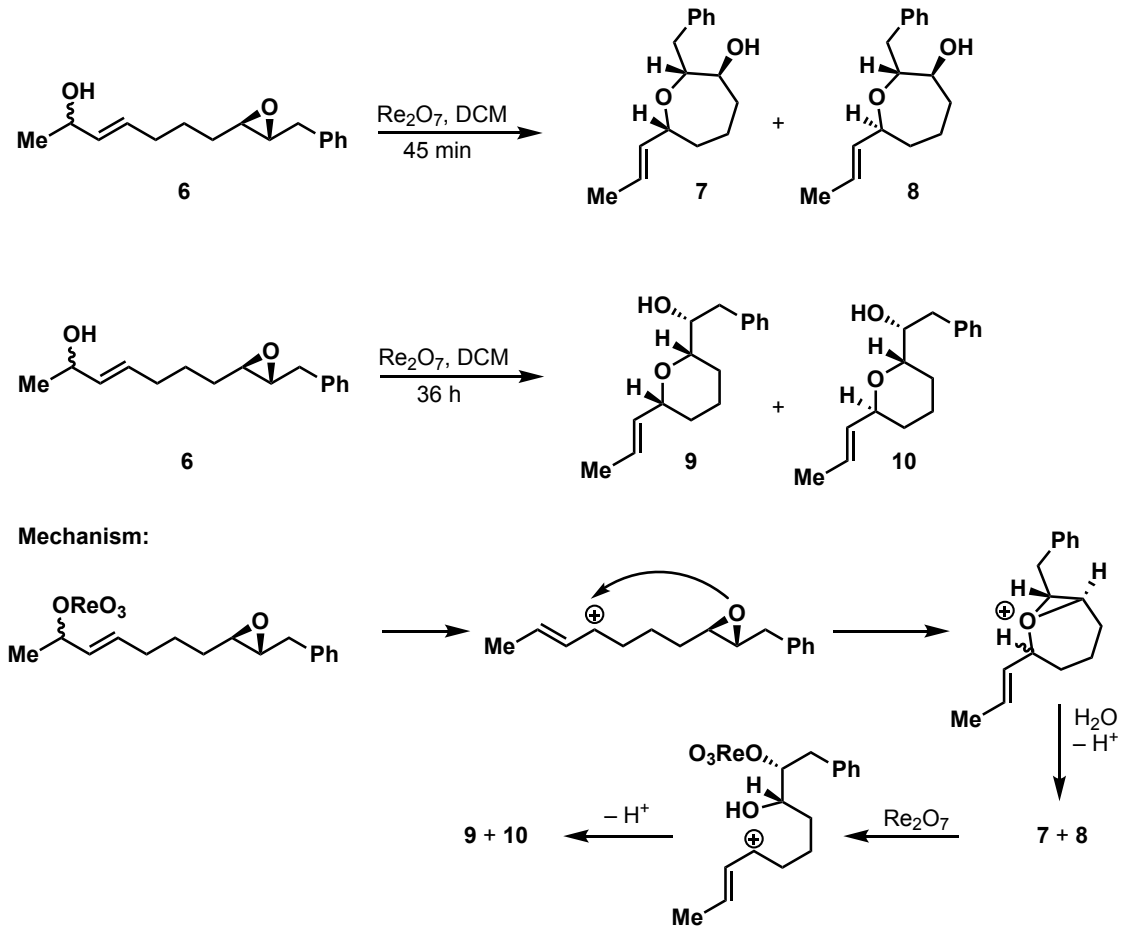

Figure 1.9 Rhenium-catalyzed epoxide cyclization.

The regiochemistry of the nucleophilic addition is consistent with calculations performed by the Houk group, in which it was shown that the *endo*-C–O bond in bicyclo[5.1.0]epoxonium ions is weaker than the *exo*-C–O bond.[25] Then, conversion of the oxepanes **7** + **8** into tetrahydropyrans **9** + **10** results from the ionization of the allylic ether to form an allyl cation, followed by nucleophilic addition by the hydroxy group to form the tetrahydropyran.

Another interesting example is shown in Figure 1.10 where C–C bond formation is achieved in the final step in a Sakurai–Hosomi-type reaction. Stereocontrol in nucleophilic additions to five-membered cyclic oxocarbenium ions follows Woerpel's model [26] whereby the nucleophile approaches opposite to the methyl group in the conformation depicted by intermediate **13**. Carbon–carbon bond-forming reactions to form tetrahydropyrans proved to be unsuccessful under the standard conditions. This is attributed to the greater energetic barrier for the formation of six-membered oxocarbenium ions relative to that of their lower homologues [27] and to the lower nucleophilicity of allylic silanes relative to hydrosilanes. In order to enhance the reactivity of Re_2O_7 and/or by improving the nucleofugacity of perrhenate, a hydrogen-bonding catalyst to enhance Brønsted acidity was employed. Thanks to this dual catalysis, an efficient and stereoselective conversion of **14** into **16** was achieved in the presence of sulfamide catalyst **15**.

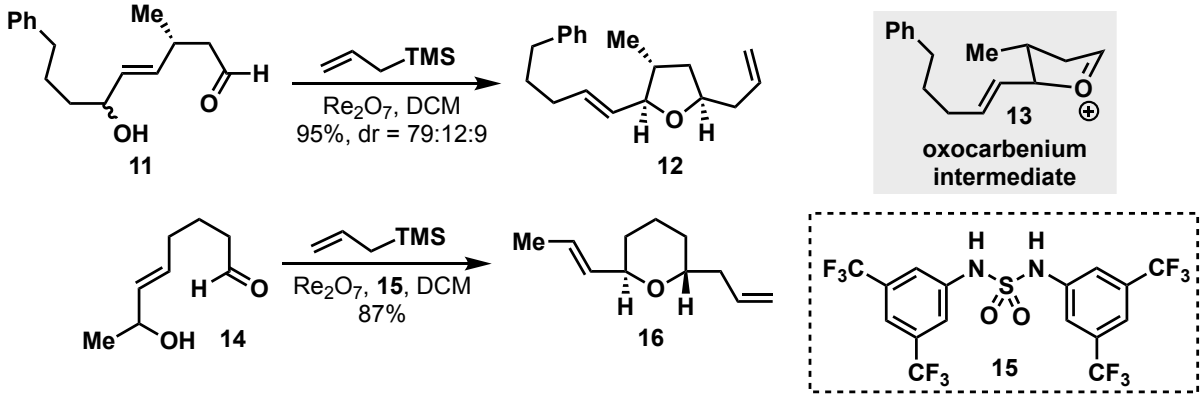

Figure 1.10 Intercepted cationic rhenium-catalyzed cyclization.

Another interesting application for the generation of cations by an oxo-rhenium species was described by Floreancig and co-workers in 2020 for the synthesis of nitrogen-containing heterocycles. They exploited the ability of Re_2O_7 to catalyze a dehydrative cyclization using allylic alcohols as allyl cation precursors (Figure 1.11). [27, 28]

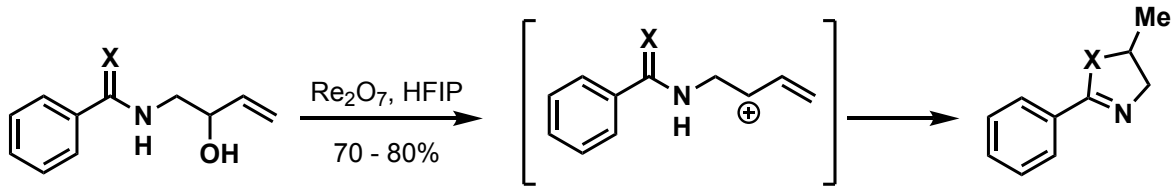

Figure 1.11 Synthesis of nitrogen-containing heterocycles using Re_2O_7 as a catalyst.

1.4 Rhenium-Catalyzed Annulation Reactions

The synthesis of complex organic molecules, especially cyclic compounds, starting from simple substrates is one of the main pursuits of organic chemistry. Transition-metal-catalyzed annulation reactions are widely employed as efficient and convenient methods for the synthesis of carbocycles and heterocycles. In recent years, breakthroughs have been made in this field through the use of late transition metal catalysis.[29] However, there are still many challenges that need to be overcome: (1) prefunctionalization of substrates is often needed to promote cyclization reactions, (2) stoichiometric oxidants are often required to oxidize the active metal centers to complete the catalytic cycles, and (3) stoichiometric byproducts usually accompany the process of annulation reactions. Rhenium catalysts, thanks to its Lewis acidity, π bond affinity, and ability to function without stoichiometric additives, have the potential to address many of these concerns.

In 2005, Takai and Kuninobu's group showed for the first time examples of a rhenium-catalyzed addition of active methylene compounds to terminal alkynes using $[ReBr(CO)_3(thf)]_2$

as a catalyst.[30] Thanks to this new chemistry, they achieved intermolecular reactions between 1,3-dicarbonyl compounds and terminal alkynes to give the corresponding alkenyl 1,3-dicarbonyl products. This strategy could also be rendered intramolecular, resulting in cyclized products in excellent yield (Figure 1.12). This resulted in a redox-neutral cyclization without pre-functionalization or stoichiometric waste. The authors suggested two possible reaction pathways. In *path a*, the rhenium catalyst first coordinates to the alkyne moiety and to the enol form of the 1,3-dicarbonyl system. Then, the complex undergoes an intramolecular oxidative addition forming the 5-membered metallocycle, and subsequent detachment of the rhenium atom gives the desired product. The alternative *path b* is an oxidative cyclization which gives a rhenacyclopentene species, followed by β-hydride elimination and reductive elimination to generate the desired product.

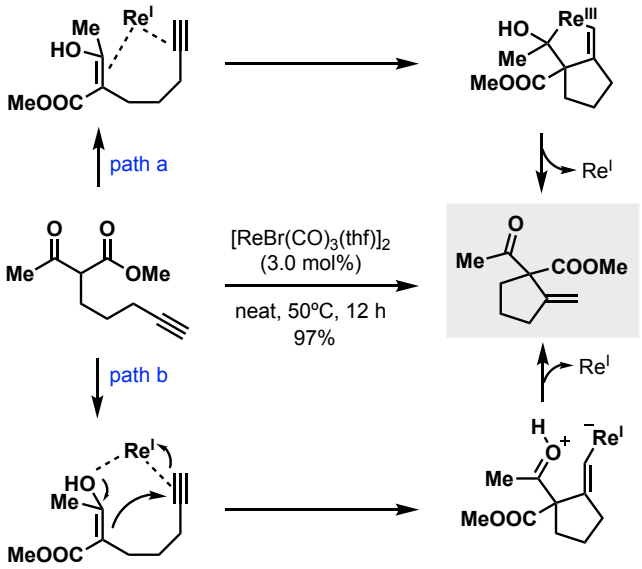

Figure 1.12 Rhenium-catalyzed intramolecular nucleophilic addition of an active methylene system onto a terminal alkyne moiety.

The same research group demonstrated a rhenium-catalyzed [2+2] cycloaddition between olefins and alkynes.[31, 32] In particular, when a simple olefin like norbornene reacted with alkynes in the presence of a catalytic amount of $[ReBr(CO)_3(thf)]_2$ and isocyanide, cyclobutene derivatives were formed in moderate to good yields (Figure 1.13).

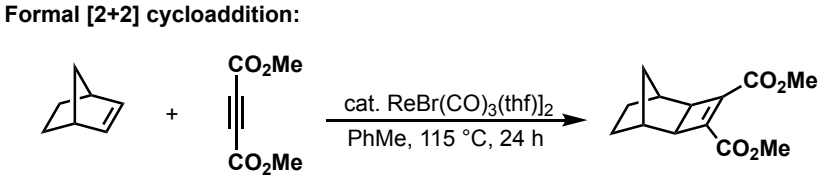

Figure 1.13 Rhenium-catalyzed [2+2] cycloaddition between olefins and alkynes.

In this methodology, electron-deficient internal and terminal alkynes reacted very well, whereas phenylacetylene gave only a very low yield of the desired product. The mechanism that the author suggested starts with coordination of the rhenium complex to the substrate. Then, the two substrates (the norbornene and the alkyne unit) undergo an oxidative cyclization

generating a metallocycle with rhenium, followed by a reductive elimination to give the product.

The Takai–Kuninobu group, thanks to the extensive data available in the literature regarding rhenium-catalyzed reactions between 1,3-dicarbonyl systems and acetylene groups,[30] decided to investigate in depth the Re-catalyzed reactions of 1,3-dicarbonyl compounds with allenes. This led to the discovery of a new formal [3+2] reaction for the synthesis of polysubstituted cyclopentenes from β-ketoesters and aliphatic allenes using catalytic $Re_2(CO)_{10}$ (Figure 1.14).[32]

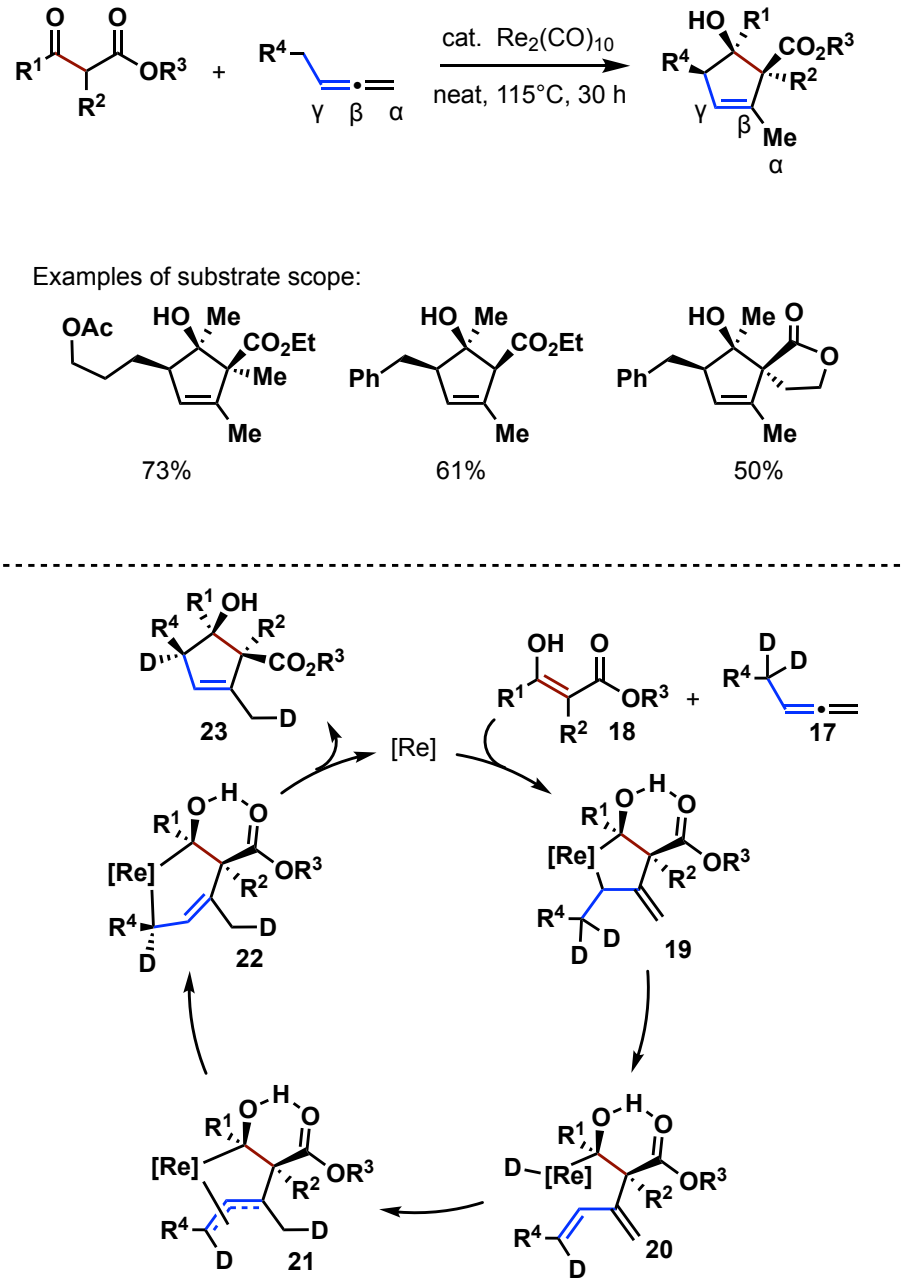

Figure 1.14 Rhenium-catalyzed [3+2] synthesis of stereodefined cyclopentenes, along with its proposed mechanism.

It is important to note that the allene substrate in the above example reacts at the β- and γ-positions and at the allylic methylene position, but instead, similar reactions known in the literature occur at the three carbon atoms of the α-, β-, and γ-positions.[33] It is worth noting that this reaction occurs with high stereoselectivity, as this outcome is probably driven by the hydrogen bonding between the hydroxy and ester groups. This method has a broad substrate scope, and bicyclic/spirocyclic products can also be synthesized when employing cyclic 1,3-dicarbonyl substrates. From a mechanistic standpoint, the authors suggested the mechanism shown in Figure 1.14 and they supported it with controlled experiments to rule out the possibility of rhenium-catalyzed isomerization of aliphatic allenes to 1,3-dienes or aliphatic methyl alkynes. In the catalytic cycle, compound **19** was obtained from a formal insertion of the allene **17** starting material into the C–H bond between the two carbonyl groups. After a series of deuterium-labeling experiments, the authors suggested the following reaction mechanism: The first step is an oxidative cyclization of the rhenium catalyst and the two starting materials, giving rhenacyclopentane **19**; the second step is a β-hydride/deuterium elimination of **19** giving compound **20**, followed by insertion of the exocyclic double bond of **20** into the Re–H/D bond to give (π-allyl)rhenium intermediate **21**; in the last step, compound **21** rearranges to give the σ-allyl intermediate **22**, which finally undergoes reductive elimination to give the product **23** while regenerating the rhenium catalyst (Figure 1.14).

Another interesting application of rhenium-catalyzed cyclizations is a formal [2+2+2] that led to the synthesis of multi-substituted aromatic rings (Figure 1.15).[34] Rhenium is necessary for the incorporation of the first alkyne group, forming a pyrone; a second alkyne group is incorporated in a thermal [4+2] cycloaddition, giving rise to a hexa-substituted benzene product.

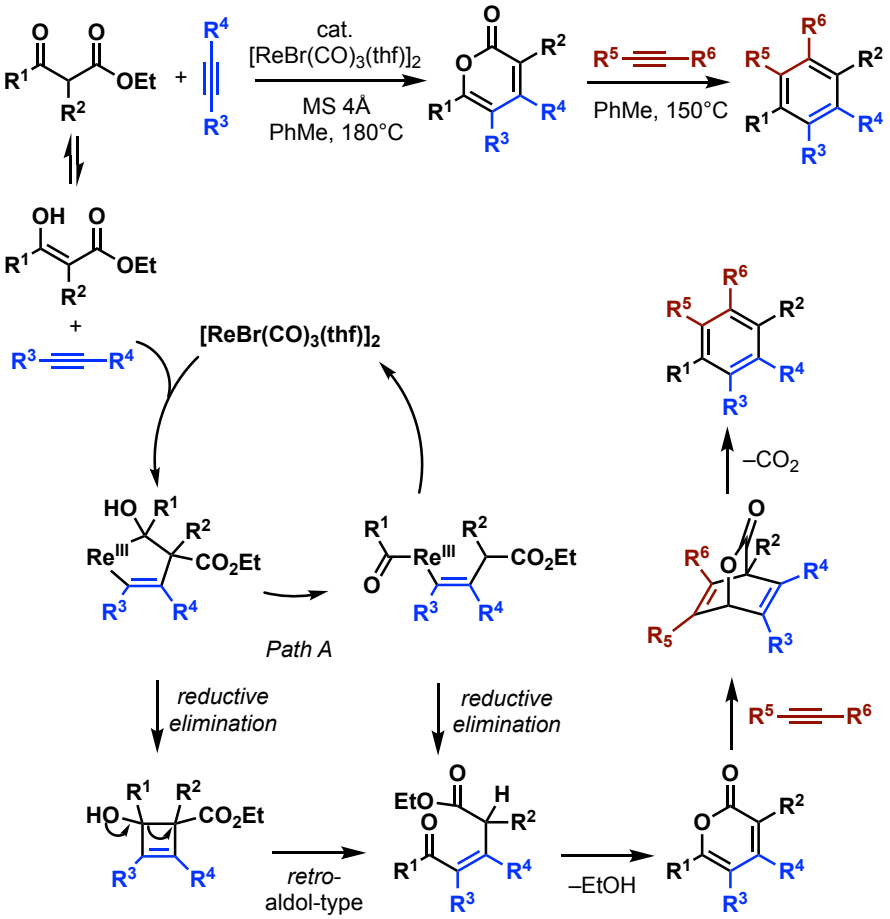

Figure 1.15 Rhenium-catalyzed synthesis of multi-substituted arenes from β-keto esters and two alkynes.

In 2006, the Takai–Kuninobu group described a ring expansion protocol based on 1,3-dicarbonyl compounds and arylacetylenes using catalytic $[ReBr(CO)_3(thf)]_2$ and benzyl isocyanide (Figure 1.16).[35] In this methodology, different arylacetylenes were tested, giving the desired ring expansion products in good yields, with the exception of alkylacetylenes that failed under these reaction conditions. Even simple enyne substrates reacted, giving the desired products in good yield. While this method can give rise to eight-, nine-, and 10-membered-rings, seven-membered rings cannot be made using this protocol. Furthermore, β-keto esters and β-diketones were successfully employed, giving the corresponding products in good yields. A control experiment demonstrated that ring expansion did not occur via a C–H alkenylation intermediate. In the proposed reaction mechanism, the rhenium catalyst reacts with a β-keto ester and an acetylene to generate a rhenacyclopentene. Then, ring opening by C–C bond cleavage/ isomerization/reductive elimination gives the final product (*path a*). Alternatively, a different sequence of reductive elimination/ring opening/isomerization is also possible for this reaction (*path b*).

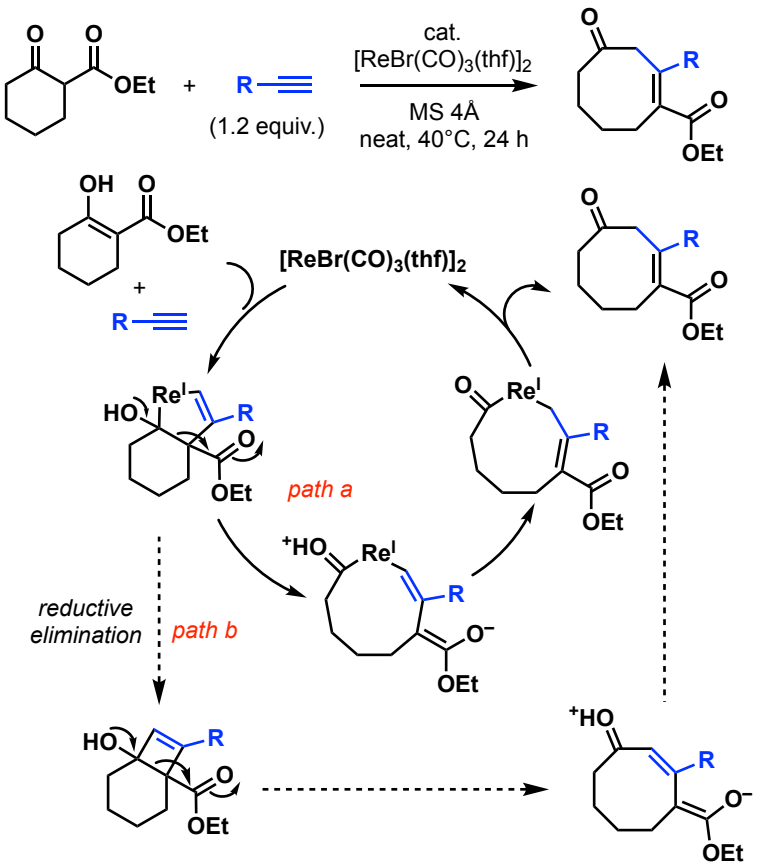

Figure 1.16 Rhenium-catalyzed insertion of an alkyne two-carbon motif into a cyclohexane framework.

As demonstrated above, rhenium chemistry is versatile and intriguing, and can result in complex products in one step when planned correctly. Its affinity to π bonds (π acidity), its Lewis acidity (σ acidity), its low electronegativity leading to polarized Re–C and Re–X bonds, among other unique properties, can allow for tandem reactions while maintaining simple reaction conditions. Typically, only the Re catalyst is used in the reaction, without many additives: No co-oxidant or co-reductant is necessary, and stoichiometric by-products do not form. It is with these advantages that rhenium chemistry was pursued in this thesis, and this research interest was coupled to a widely known tandem reaction—the concept of biomimetic cyclization—as described in Chapter 2.

1.5 References

1. Romão, C. C.; Herrmann, W. A. *Chem. Rev*. **1997**, *97*, 3197.
2. Espenson, J. H. *Coord. Chem. Rev*. **2005**, *249*, 329.
3. Machura, B.; Wolff, M.; Gryca, I. *Coord. Chem. Rev.* **2014**, *275*, 154.
4. Suntharalingam, K.; Awuah, S. G.; Bruno, P. M.; Johnstone, T. C.; Wang, F.; Lin, W.; Zheng, Y.-R.; Page, J. E.; Hemann, M. T.; Lippard, S. J. *J. Am. Chem. Soc*. **2015**, *137*, 2967.

5. Segal, I.; Zablotskaya, A.; Kniess, T.; Shestakova, I. *Chem. Heterocycl. Compd.* **2012**, *48*, 296.

6. Nguyen, H. H.; Jegathesh, J. J.; Maia, P. I. S.; Deflon, V. M.; Gust, R.; Bergemann, S.; Abram, U. *Inorg. Chem.* **2009**, *48*, 9356.

7. Mosi, R.; Baird, I. R.; Cox, J.; Anastassov, V.; Cameron, B.; Skerlj, R. T.; Fricker, S. P. *J. Med. Chem.* **2006**, *49*, 5262.

8. Hahna, E. M.; Casinib, A.; Kühn, F. E. *Coord. Chem. Rev*. **2014**, *276*, 97.

9. Santos, I.; Paulo, A.; Correia, J. D. G. *Top. Curr. Chem.* **2005**, *252*, 45.

10. Owens, G. S.; Arias, J.; Abu-Omar, M. M. *Catal. Today,* **2000***, 55,* 317.

11. James E*.“Rhenium: Properties, Uses and Occurrence”*, Nova Science Publishers Inc, **2017**.

12. Mao, G.; Huang, Q.; Wang, C. *Eur. J. Org. Chem.* **2017**, *25*, 3549.

13. Kuninobu, Y.; Takai, K. Chem. Rev. **2011**, *111*, 1938.

14. (a) Herrmann, W.A.; Fischer, R.W.; Marz, D.W. *Angew. Chem. Int. Ed.* **1991**, *30*, 1638; (b) Tan, H.; Espenson, J. H. *Inorg. Chem.* **1998**, *37*, 467; (c) Jacob, J.; Espenson, J. H. *Inorg. Chim. Acta* **1998***, 270*, 55; (d) Adam, W.; Herrmann, W. A.; Lin, J.; Saha-Moeller, C. R. *J. Org. Chem.* **1994**, *59*, 8281; (e) Adam, W.; Lin, J.; Saha-Möller, C. R.; Herrmann, W. A.; Fischer, R. W.; Correia, J. D. *Angew. Chem. Int. Ed.* **1995***, 33*, 2475; (f) Schuchardt, U.; Mandelli, D.; Shul'pin, G. B. *Tetrahedron Lett.* **1996**, 37, 6487; (g) Nakagiri, T.; Murai, M.; Takai, K. *Org. Lett*. **2015**, *17*, 3346; (h) Liu, S.; Senocak, A.; Smeltz, J. L.; Yang, L.; Wegenhart, B.; Yi, J.; Kenttämaa, H. I.; Ison, E. A.; Abu-Omar, M. M. *Organometallics* **2013**, *32*, 3210; (i) Gable, K. P.; Zhuravlev, F. A. *J. Am. Chem. Soc.* **2002**, *124*, 3970.

15. Herrmann, W.A.; Wagner, W.; Flessner, U.N.; Volkhardt, U.; Komber, H. *Angew. Chem. Int. Ed*. **1991**, *30*, 1636.

16. Herrmann, W. A.; Wang, M. *Angew. Chem. Int. Ed.* **1991**, *30*, 1641.

17. a) Sherry, B. D.; Loy, R. N.; Toste, F. D.; *J. Am. Chem. Soc.* **2004**, *126*, 4510; b) Luzung, M. R.; Toste, F. D. *J. Am. Chem. Soc.* **2003**, *125*, 15760; c) Casali, E.; Sirwan, O. T.; Dezaye, A. A.; Chiodi, D.; Porta, A.; Zanoni, G. *J. Org. Chem.* **2021**, *86*, 7672.

18. Sherry, B. D.; Radosevich, A. T.; Toste, F. D. *J. Am. Chem. Soc*. **2003**, *125*, 6076.

19. Kennedy-Smith, J. J.; Young, L. A.; Toste, F. D. *Org. Lett.* **2004***, 6*, 1325.

20. Ohri, R. V.; Radosevich, A. T.; Hrovat, K. J.; Musich, C.; Huang, D.; Holman, T. R.; Toste, F. D. *Org. Lett.* **2005**, *7*, 2501.

21. Morrill, C.; Grubbs, R. H. *J. Am. Chem. Soc.* **2005**, *127*, 2842.

22. a) Stefanoni, M.; Luparia, M.; Porta, A.; Zanoni, G.; Vidari, G. *Chem. Eur. J.* **2009**, *15*, 3940; b) Bugoni, S.; Porta, A.; Valiullina, Z.; Zanoni, G.; Vidari, G. *Eur. J. Org. Chem.* **2016**, 4900; c) Mattia, E.; Porta, A.; Merlini, V.; Zanoni, G.; Vidari, G. *Chemistry* **2012**, *18*, 11894.

23. Bellemin–Laponnaz, S.; Le Ny, J.-P.; Dedieu, A. *Chem. Eur. J.* **1999***, 5,* 57.

24. Floreancig, P. *Synlett* **2021**; 32, 1406.

25. Wan, S.; Gunaydin, H.; Houk, K. N.; Floreancig, P. E. *J. Am. Chem. Soc.* **2007**, *129*, 7915.

26. Smith, D. M.; Tran, M. B.; Woerpel, K. A. *J. Am. Chem. Soc.* **2003***, 125,* 14149.

27. a) Kruse, C. G.; Poels, E. K.; Jonkers, F. L.; Van der Gen, A. *J. Org. Chem.* **1978***, 43,* 3548; b) Green, M. E.; Rech, J. C.; Floreancig, P. E. *Angew. Chem., Int. Ed.* **2008***, 47,* 7317.

28. Rodriguez del Rey, F. O.; Floreancig, P. E. *Org. Lett.* **2021***, 23,* 150.

29. a) Larock, R. C. *Top. Organomet. Chem.* **2005***, 14,* 147; b) Majum- dar, K. C.; Samanta, S.; Sinha, B. *Synthesis* **2012***, 44,* 817; c) Palmes, J. A.; Aponick, A. *Synthesis* **2012**, *44,* 3699*;* d) Abbiati, G.; Marinelli, F.; Rossi, E.; Arcadi, A. *Isr. J. Chem*. **2013**, *53,* 856; e) Mannathan, S.; Cheng, C. H. *J. Chin. Chem. Soc.* **2014**, *61,* 59; *f)* Abbiati, G.; Arcadi, A.; Marinelli, F.; Rossi, E. *Synthesis* **2014**, *46*, 687; *g)* Chen, J. R.; Hu, X. Q.; Lu, L. Q.; Xiao, W. J. *Chem. Rev.* **2015***, 115,* 5301.

30. Kuninobu, Y.; Kawata, A.; Takai, K. *Org. Lett.* **2005**, *7,* 4823.

31. Kuninobu, Y.; Yu, P.; Takai, K. *Chem. Lett.* **2007**, *36,* 1162.

32. Kuninobu, Y.; Takai, K. *Angew. Chem. Int. Ed*. **2008**, 47, 9318.

33. a) Zimmer, R.; Dinesh, C. U.; Nandanan, E.; Khan, F. A. *Chem. Rev.* **2000**, *100,* 3067; b) Ma, S. *Chem. Rev.* **2005***, 105,* 2829; c) Brummond, K. M.; DeForrest, J. E. *Synthesis* **2007**, 795; d) Ma, S. *Aldrichim. Acta* **2007**, *40,* 91; e) Hassan, H. H. A. M. *Curr. Org. Synth.* **2007**, *4*, 413.

34. a) Kuninobu, Y.; Takata, H.; Kawata, A.; Takai, K. *Org. Lett.* **2008**, *10,* 3133; b) Kuninobu, Y.; Kawata, A.; Nishi, M.; Takata, H.; Takai, K. *Chem. Commun.* **2008***, 47,* 6360.

35. Kuninobu, Y.; Kawata, A.; Nishi, M.; Yudha S, S.; Chen, J.; Takai, K. *Chem. Asian J.* **2009**, *4*, 1424.

Chapter 2: Metal-promoted Biomimetic Cyclizations

2.1 Chapter Abstract

In this chapter, an overview of biomimetic cyclizations catalyzed by metal reagents will be discussed. In particular, attention will be placed on electrophilic and/or oxophilic metal reagents that behave as Lewis acids to initiate polyolefin cyclizations. This results in the simultaneous formation of multiple C–C bonds, thereby rapidly generating complexity. Perhaps because of its biomimetic nature, the reaction conditions are usually simple, only involving the starting material, a metal catalyst, and solvent. It is the aim of this thesis to demonstrate how biomimetic cyclizations have impacted both organic chemistry as well as our understanding of natural product biosynthesis. Of note, radical-initiated biomimetic cyclizations exist as well, but these are beyond the scope of this PhD thesis.

2.2 Introduction

Biomimetic electrophilic cyclizations of terpenoid-like polyolefins have been investigated over many years by prominent chemists such as Stork [1], Eschenmoser and Ruzicka [2], Johnson [3], and Van Tamelen [4]. From a synthetic point of view, this type of reaction simulates the mechanism of oxido-squalene cyclases and squalene-hopene cyclases, which generate different terpenoid-based polycycles like lanosterol, cycloartenol and hopenes starting from a variety of linear unsaturated chains [5]. The connection between biomimicry and natural product total synthesis has been discussed in several reviews [6-12], and it has been stated by Yoder and Johnston that organic synthesis and biosynthetic studies have been synergistic, as each has evolved in parallel with the other. [13]

From a synthetic point of view, biomimetic cyclization is a remarkable synthetic tool because a significant increase in molecular complexity can be obtained in a single step. In fact, using an acyclic, well-designed substrate as the starting material, it is possible to build up a complex polycyclic structural motif. The stereochemical configuration of these cyclic products in some cases can be predicted on the assumption that acyclic polyene precursors react with a defined conformation. For example, it can assume a chair- or boat-like conformation in a six-membered transition state, undergoing an antiperiplanar addition to the double bonds present in the molecule. This conformational insight is explained in seminal works by Stork and Eschenmoser, [14] resulting in what is now called the "*Stork–Eschenmoser hypothesis*". This is one of the guiding principles used when discussing cation-olefin cyclization, and proposes a direct stereoelectronic rationalization for the course of the cyclization. In particular, each double bond undergoes a stereoselective *anti* addition with the transition state being distinguished by chair-like conformations of the nascent rings. The conclusion of this hypothesis is that *trans* double bonds should generate *trans* ring junctions and *cis* double bonds should lead to *cis* fused systems (Figure 2.1).

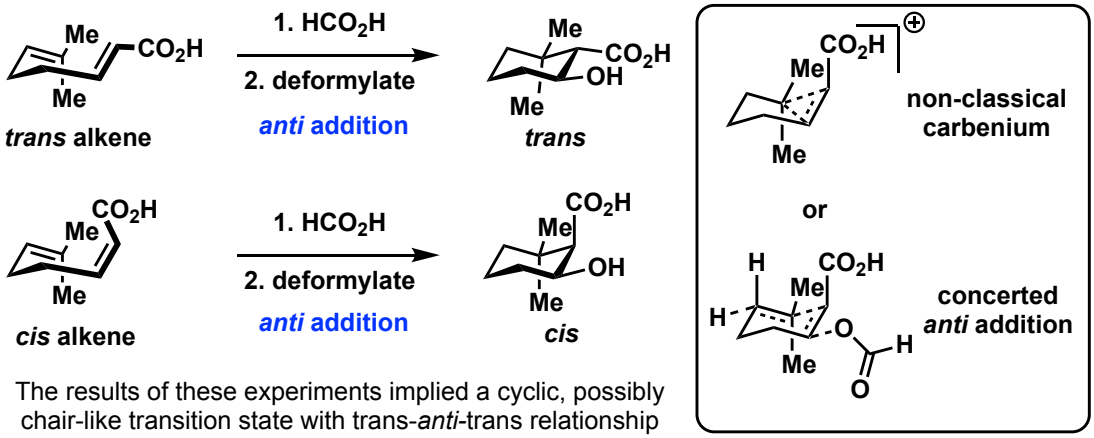

Figure 2.1. A simplified explanation of the Stork–Eschenmoser hypothesis. Eschenmoser presented cyclization evidence that suggests an *anti-carbenium addition to an olefin (or possibly a carbenium intermediate).*

This biomimetic process is important and is worth further discussion, particularly regarding key factors that determine the ring size, stereochemistry (that is governed largely by the Stork–Eschenmoser hypothesis), and functional patterning of products based on the initiation and chain termination. The main goal of this chapter is to focus specifically on recent advances made in the polyene cyclization field in the last two decades. As shown in many sections of this chapter, a broad range of novel variants for the biomimetic cyclization process was developed using metals and their properties (e.g., their ability to behave as Lewis acids or radical initiators) in an innovative fashion. These methods have led to the discovery of many new chiral reagents and catalysts that are able to reach (and in some cases exceed) the levels of selectivity that nature can accomplish with the use of enzymes. New activating groups and reagents have been developed, allowing for highly enantioselective metal-mediated cyclizations that were not previously achievable even in their racemic version. Furthermore, completely different mechanisms of activation that go beyond the traditional electrophilic activation of polyunsaturated linear chains, such as radical initiation, have been explored in order to access analogous structural motifs. In certain cases, these approaches offer products with different or even opposite stereocontrol, ring size, and order of ring formation, which make these methods essential as new tools for the total synthesis of terpene-like molecules. However, many frontiers still remain unexplored, and there is still a need to further expand the synthetic power of this cation-π chemistry in terpenoid-like systems.

2.3 Lewis-acid-assisted Brønsted-acid (LBA)-mediated Cyclizations

It is well known in the literature that nature uses enzymes called cyclases in order to selectively deliver a proton to the terminal olefin of polyunsaturated terpenoid systems, forming complex, polycyclized products as single enantiomers. An example of such a transformation is reported in bacterial metabolism for the synthesis of hopene employing squalene as the starting material. [15] Inspired by nature, synthetic chemists in the past have utilized proton-initiated cyclizations of unfunctionalized polyenes in order to get poly-carbocyclic products, but the majority of

these reactions just delivered mixtures of isomers in racemic form. Only recently, the available synthetic tools are allowing the synthetic organic chemist to compete, at least partially, with the power of these cyclase enzymes. Thanks to these improvements, various research groups have been able to produce examples of enantioselective, proton-induced polyene cyclizations. The small size of a proton, even when associated to bulky counterions, often makes asymmetric protonation very challenging due to the high conformational flexibility of many substrates. In this section, recent examples of chiral proton-induced polyene cyclizations will be discussed, highlighting advantages and limitations therein.

One of the most famous pioneers in the area of enantioselective proton-induced cyclizations is Yamamoto. In many of his seminal publications, it was shown that the adduct between a chiral Brønsted acid and a properly chosen Lewis acid, called Lewis-acid-assisted Brønsted acids (LBAs), is able to behave like an artificial cyclase enzyme, promoting the enantioselective protonation of carefully designed polyenes. Some examples of LBA complexes are shown in Figure 2.2.

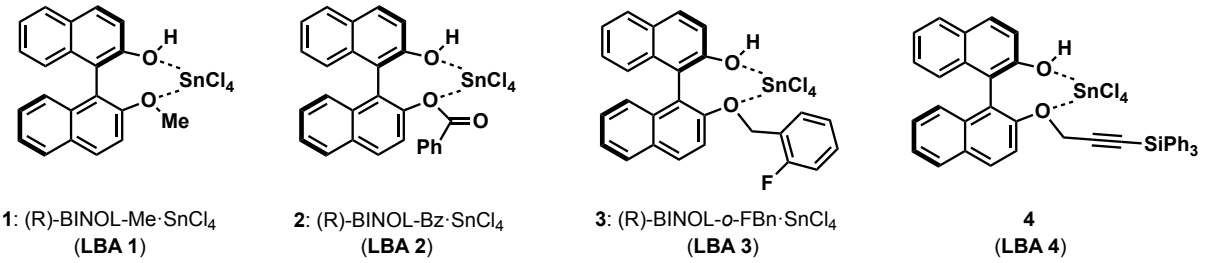

1: (R)-BINOL-Me·$SnCl_4$ (**LBA 1**) | **2**: (R)-BINOL-Bz·$SnCl_4$ (**LBA 2**) | **3**: (R)-BINOL-*o*-FBn·$SnCl_4$ (**LBA 3**) | **4** (**LBA 4**)

Figure 2.2 Selected examples of LBA complexes used by Yamamoto and co-workers in enantioselective proton-induced cyclizations.

In these examples, a functionalized BINOL is coordinated in a bidentate fashion to tin(IV) chloride. This coordination decreases the conformational flexibility of the O–H bond and increases the acidity of that proton. In some of the earliest examples of LBA-promoted biomimetic cyclizations, geranyl alcohols and *o*-geranyl phenols were employed as substrates and efficiently cyclized using stoichiometric amounts of LBA, promoting the formation of *trans*-fused products with modest enantioselectivity.[16] These LBAs were also employed in the total synthesis of enantioenriched (–)-ambrox (compound **6**, Figure 2.3). This compound is a commonly used substrate in the fragrance industry. **6** was the major product obtained from the cyclization of **5** (42% *ee*) even though a few other diastereoisomers (compounds **7**–**9**) were isolated using **LBA 1** as the catalyst. Subsequently, it was observed that using a catalytic amount of a second-generation complex, **LBA 2**, still furnished the cyclization product. Employing geranyl phenolic ethers like compound **10** gave the same products as *o*-geranyl phenols but with much higher enantioselectivity and diastereoselectivity at the trans-fused junction of **12**. Even though the product obtained using these different complexes is the same, from a mechanistic point of view, the cyclization promoted by **LBA 2** is different, and most likely proceeds through an abnormal Claisen rearrangement followed by the key polyene cyclization step.

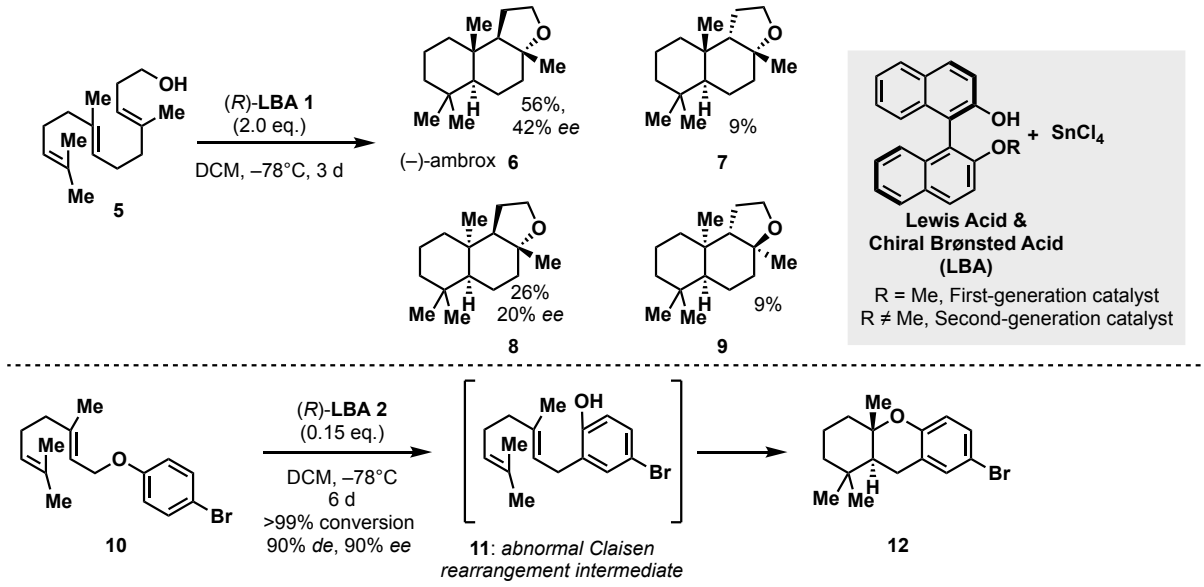

Figure 2.3 First enantioselective cyclization using BINOL-based ligands and $SnCl_4$ as the catalyst (i.e., the LBA system) by Yamamoto and co-workers.

The enantioselective synthesis of bi- and tricyclic polyenes starting from polyolefins with aromatic rings as the terminator group can also be done using LBA complexes. However, usually this type of terminating group alone is not capable of pushing the cyclization forward (it is difficult to form more than one ring when using this terminating group). This is exemplified in Figure 2.4 in which compound **13** is converted into a mixture of **14** and **15**, favoring the partially cyclized product **15**, especially when catalyst **4** is employed. [17] In order to fully convert the partially cyclized product **15** into **16**, it is oftentimes necessary to add an extra step that involves a diasteroselective cyclization promoted by either Brønsted or Lewis acids (e.g., BF_3•Et_2O). In this case, a Lewis acid was employed to push the reaction to completion, and after treatment of the mixture of **14** and **15** with BF_3•Et_2O, compound **16** was obtained in 89% overall yield and 75% *ee*. It is important to note that the acetate protection of the phenol moiety was crucial for enantioselectivity. A similar strategy was employed in the total synthesis of a natural product isolated from a Tasmanian tasmanite sediment with high efficiency (65% yield) and enantioselectivity (77% *ee).*[18] Previously, Corey and co-workers tried to synthesize this natural product using a chiral epoxide at the distal double bond in order to initiate the biomimetic cyclization of the polyene chain, affording the corresponding secondary alcohol, which had to be removed after the cyclization [19]. Thus, the ability to effect a direct, enantioselective proton-based cyclization, as it is most likely achieved in nature, can afford a more efficient solution to this particular challenge.

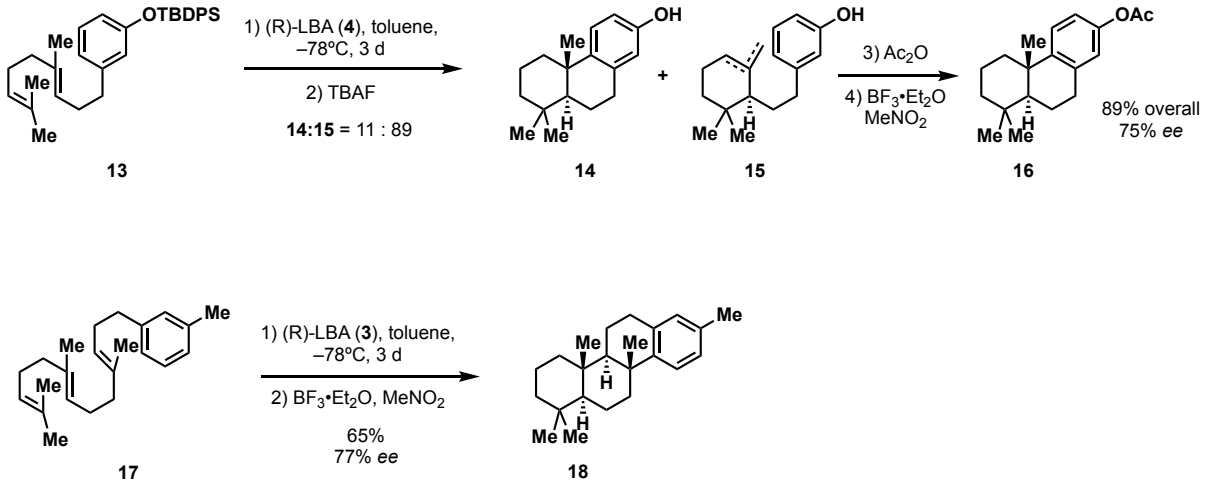

Figure 2.4 The use of LBA catalysts to effect enantioselective cation-π cyclizations.

A very important role in determining the success of a biomimetic cyclization in terms of enantioselectivity and regioselectivity is the type of terminating group that is employed. In fact, many research groups tried to use BINOL-derived LBA complexes in order to affect the stereochemistry of polyene cyclizations terminated by alcohols or phenols, but the outcome was not very satisfying, only giving modest stereoselectivities. The reason behind these results is most likely the OH group coordinating Lewis acids in a non-productive fashion. After screening Lewis acids, it was found that catechol-derived LBA complex **19**, which has a smaller five-membered coordination sphere, could efficiently cyclize polyenes terminated by a nucleophilic alcohol group, as well as by arenes, to form tri-, tetra-, and pentacyclic structures with improved enantioselectivity (Figure 2.5A).[17] A great example of the use of this complex is the cyclization of compound **20** to give **21** in a two-step sequence, achieving moderate diastereoselectivity and 88% *ee*. In order to get a better enantiomeric excess, recrystallization was successfully performed, enhancing the optical purity. After deprotection of the methyl ether in the aromatic moiety, (–)-chromazonarol (**22**) was obtained in excellent yield. Another interesting aspect of the catalyst LBA **19** is its ability to promote catalyst-controlled diastereoselectivity when starting materials containing chiral centers were used. [18] An example of this property is apparent when starting from the enantioenriched compound **23**, and treating it with the two different enantiomers of LBA **19** (Figure 2.5B). The two newly formed stereocenters were governed by catalyst control, irrespective of the configuration of the pre-existing stereocenter. This important property shows that is possible to effectively override any substrate bias and substrate-dependent induction. To this end, LBA **19** was brilliantly used in the enantiodivergent synthesis of (–)-caparrapi oxide **26** and (+)-8-epicaparrapi oxide **27** starting from a common intermediate.

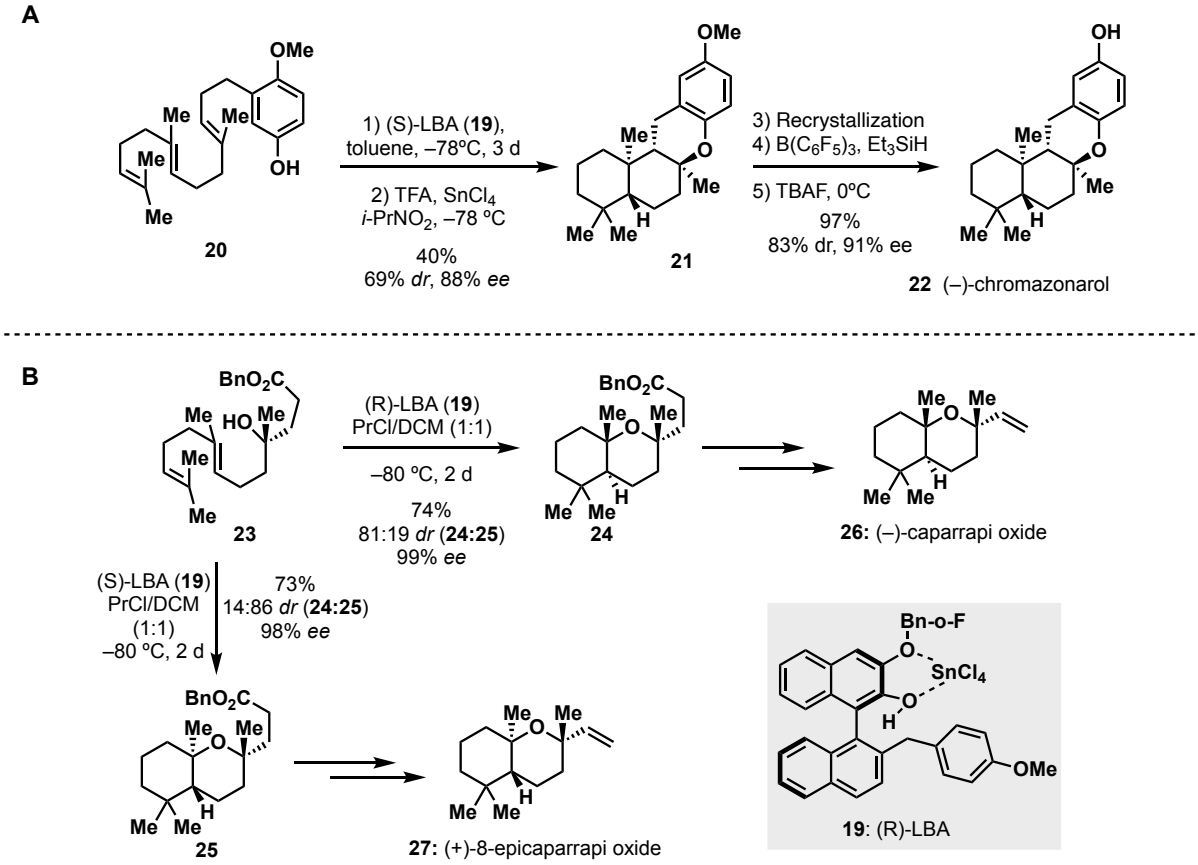

Figure 2.5 Total synthesis of natural products using LBA complex **19**.

Another interesting example of Lewis-acid-promoted biomimetic cyclization is the one reported by Corey and coworkers, who discovered that a chiral BINOL complex ligated to $SbCl_5$ is able to promote a polyene cyclization, furnishing the desired product with high yields and enantioselectivity (Figure 2.6).[20] A practical feature of this cyclization is that this reagent leads to reaction times that are on the order of hours (at –78 ºC) and it does not require subsequent treatment with Lewis acid to close the final ring system. In fact, (*R*)-*o,o*-dichloro-BINOL• $SbCl_5$ **29** was capable of fully cyclizing several substrates containing both electron-rich as well as unactivated aryl rings with great yield, diastereoselectivity, and enantioselectivity. Other Lewis acids screened with this ligand showed much slower reaction times and diminished enantioselectivity. The efficiency shown by these antimony-based complexes (like **29**) can be explained by the fact that $SbCl_5$ is both a bulkier and stronger Lewis acid than $SnCl_4$.

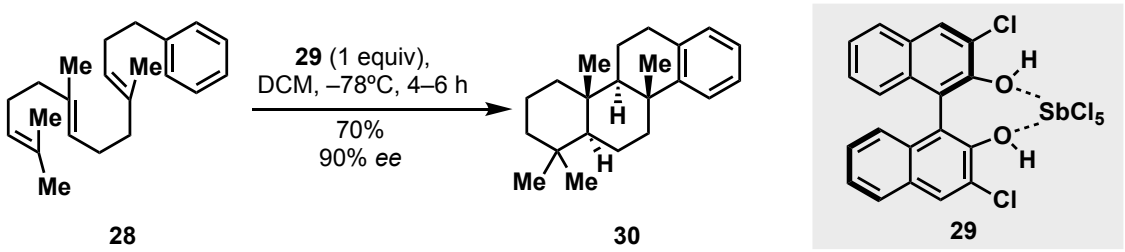

Figure 2.6 Corey's BINOL-$SbCl_5$ complex created a fully cyclized framework without additional Lewis acids.

Lewis-base-assisted Brønsted-acid (LBBA)-mediated cyclizations, usually promoted by chiral phosphorus(III) Lewis basic complexes, is a curious discovery that will not be discussed in this chapter since it is mainly focused on metal-promoted biomimetic cyclizations.

2.4 Cation-π Cascades Initiated by Epoxide Opening

Another approach that nature uses for the synthesis of polycyclic terpenes is to convert the triterpene squalene into squalene oxide, and using that intermediate for subsequent cyclizations. This transformation is catalyzed by squalene monooxygenase, which delivers 2,3-oxidosqualene selectively (Figure 2.7). This is then used as a starting material that is cyclized to give lanosterol and other steroid derivatives, depending on the enzyme involved. [15] With these inspirations derived from terpene biosynthesis, synthetic chemists have strived to utilize the same key transformation in their efforts at biomimicry, and excellent results have been achieved.

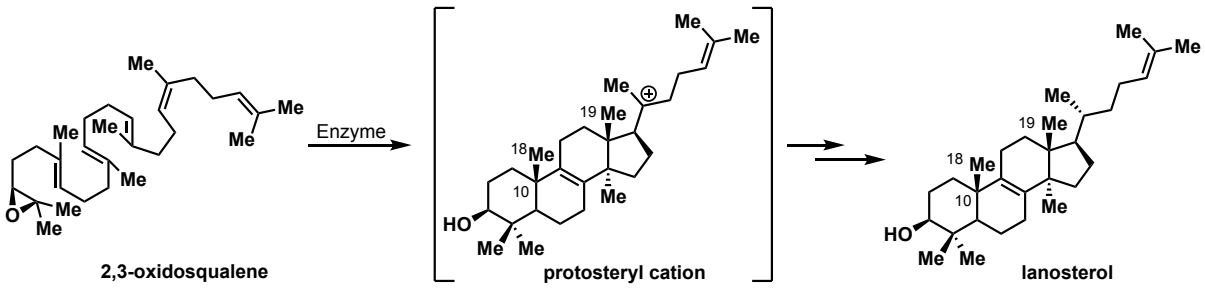

Figure 2.7 Nature uses an epoxide-initiated cascade reaction to generate lanosterol and other steroid frameworks.

2.5 Use of Enol Silane Terminating Groups in Synthesis

One of the most critical steps in a biomimetic cyclization, from a chemical point of view, is the initiation process because it often requires a challenging pre-functionalization of the polyene starting material. In many cases, nature exploits the oxidation ability of various enzymes to promote site-selective asymmetric epoxidations. Over the years, many research groups worked in order to develop our own synthetic toolkit to promote similar asymmetric epoxidations of olefins in a highly enantio- and diastereoselective manner (whether through direct means, or through multistep processes such as asymmetric dihydroxylation, leaving group formation, and cyclization). Even though this key problem has mostly been addressed, there is still one longstanding challenge in the polyene cyclization that needs to be solved: the termination process. Especially for biomimetic multiple cyclizations of a polyene starting material (e.g., the tetracyclization of squalene derivatives without the aid of enzymes), there is a tendency for the last ring in the sequence (e.g., the D ring in cholesterol) to be generated as a five-membered ring rather than the desired six-membered ring. E. J. Corey was the first to find a solution in the mid-1990s, whereby in order to solve this selectivity issue, a nucleophilic enol silane was employed to terminate the cyclization cascade, obtaining the desired six-membered ring. [21,22] An example of this type of termination reaction is shown in Figure 2.8. Compound **32** at this point is prone to undergo the polycyclization reaction using Me_2AlCl as a Lewis acid, which after silyl deprotection and subsequent hydrolysis of the dithiane protecting group, gives the desired tricyclic **35** in 42% overall yield with high stereoselectivity. Given the high selectivity achieved, compound **35** was employed as a key intermediate for the total synthesis of dammarenediol II (**36**), the primary product of the cyclization of 2,3-epoxidosqualene in plants.

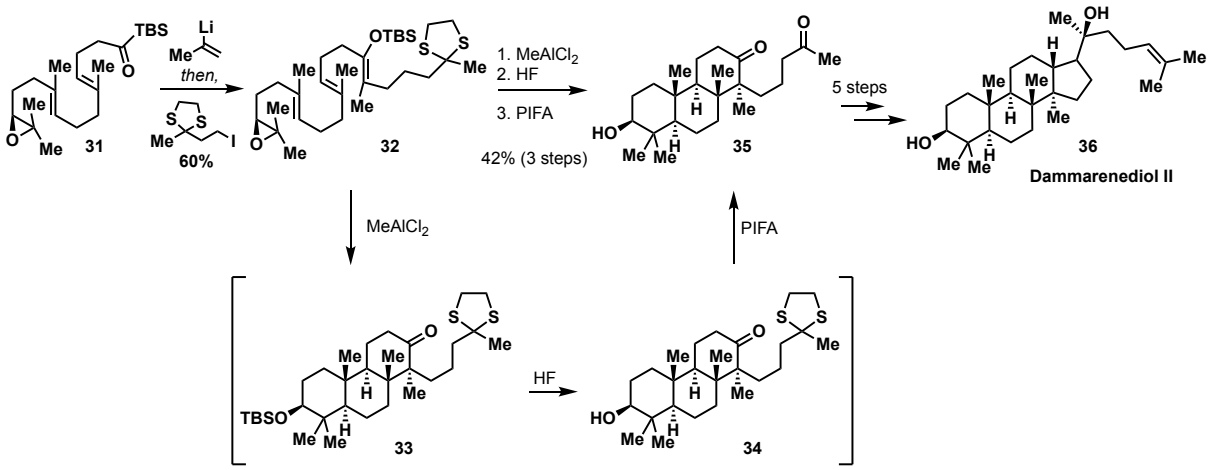

Figure 2.8 Corey's total synthesis of dammarenediol II, using a key six-membered ring-forming cyclization cascade with an enol silane terminating group.

The enol silane terminating group was also employed for the generation of polycyclic systems containing more than three carbocyclic rings. A relevant example is shown in Figure 2.9 where compound **37** undergoes tetracyclization after treatment with $MeAlCl_2$. [23] After selective silyl deprotection and equilibration of the stereocenter adjacent to the carbonyl, the desired product **38** was obtained in 30% overall yield. Then, **38** was used as a key intermediate for the synthesis of the natural product sclarenedial (**39**). It is important to note that the chiral epoxide was strategically used to control both the enantio- and diastereoselectivity of this cationic cyclization, but the resultant alcohol was later removed from the product using a radical deoxygenation.

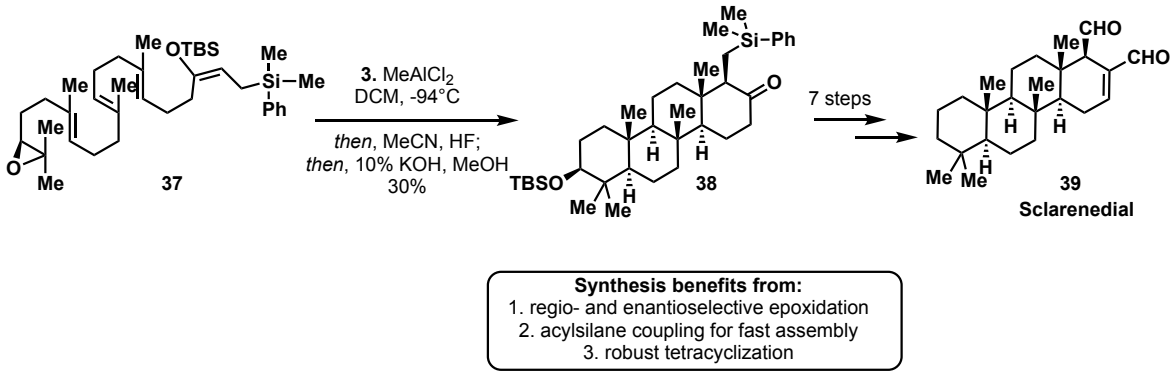

Figure 2.9 A tetracyclization cascade culminating in a six-membered ring formation by using an enol silane terminating group.

Another interesting application is the use of a TMS group (instead of silyl enol ethers) as a terminating agent (Figure 2.10). Vidari and co-workers discovered that an unusual reagent, TiF_4, efficiently promotes the addition-cyclization of compound **41** to aliphatic aldehydes **40**, affording 1,3-disubstituted methylenecyclohexane derivatives **43**, **44** and 4**5** in good yields (ranging from 40 to 85% of **43** + **44** + 4**5**) and high *cis* diastereoselectivity (Figure 2.10). The selectivity of the elimination process for quenching the carbocation was fully controlled thanks to the introduction of a TMS group in the starting material. It is important to note that this reaction was very sensitive to the temperature and to the order of addition of every reagent, therefore it was crucial to use the optimal 1:2:4 molar ratio of **40**, **41**, and TiF_4, as well as the right temperature (the initial exposure of the aldehyde to TiF_4 must be at –40 °C for 10 min prior to the addition of **41** that happens at 0 °C). [24]

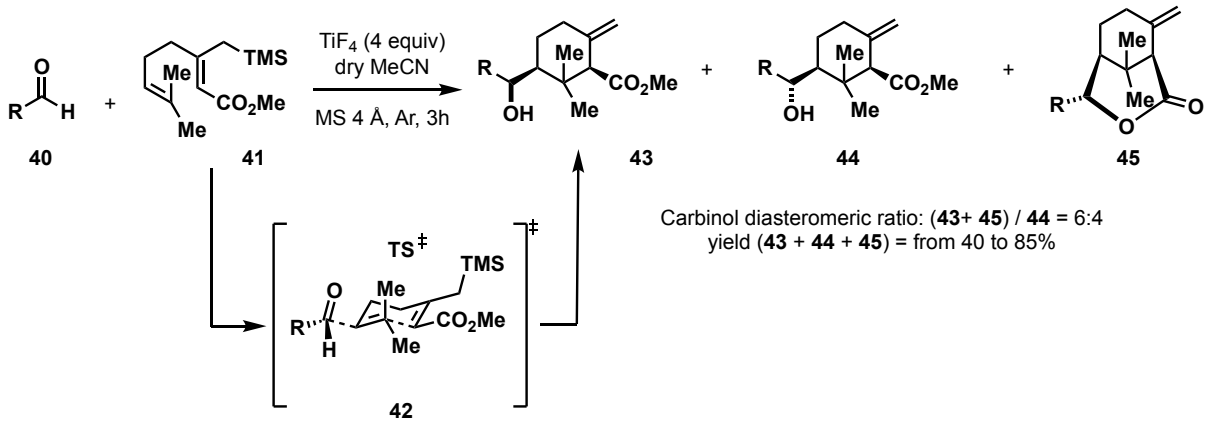

Figure 2.10 Vidari's use of an allylsilane to control the selectivity of six-membered ring formation.

2.6 Use of Other Terminating Groups in Epoxide-based Polyene Cyclizations

In epoxide-opening-initiated polyene cyclizations, the terminating groups can also be aryl rings and styrenyl alkenes. A great example by Overman and co-workers showed the termination of an epoxide-initiated tetracyclization using an aryl ring (Figure 2.11). The obtained scaffold was subsequently employed for the enantioselective synthesis of adociasulfate 1 (**48**), a kinesin motor protein inhibitor extracted from the *Haliclona* family of sea sponges.[25] In Overman's work, the chiral epoxide of **46** was installed using Sharpless asymmetric epoxidation reaction with 95% *ee.* Compound **46** was then treated with $Sc(OTf)_3$, affording the polycyclic structure **47** in 15% yield. In this cyclization, the presence of an electron-donating phenyl allyl ether was essential for the completion of the final cyclization, because without this motif, only partially cyclized products were obtained. It is worth noting that using Me_2AlCl, a stronger and more commonly used Lewis acid for epoxide-opening cascades, on the same system gave trace amounts of the desired product **47** (>5%). However, this is a substrate-dependent result: Corey and co-workers reported examples in which Me_2AlCl (as a mixture with $MeAlCl_2$) is capable of initiating epoxide opening of tri- and tetracyclizations terminated by arenes or styrenyl olefins.[26] In this type of tricyclization, both activated and unactivated arenes delivered the desired products in good yield. The intermediate **50** generated using this method was employed for the enantioselective synthesis of lupeol (**51**).[27]

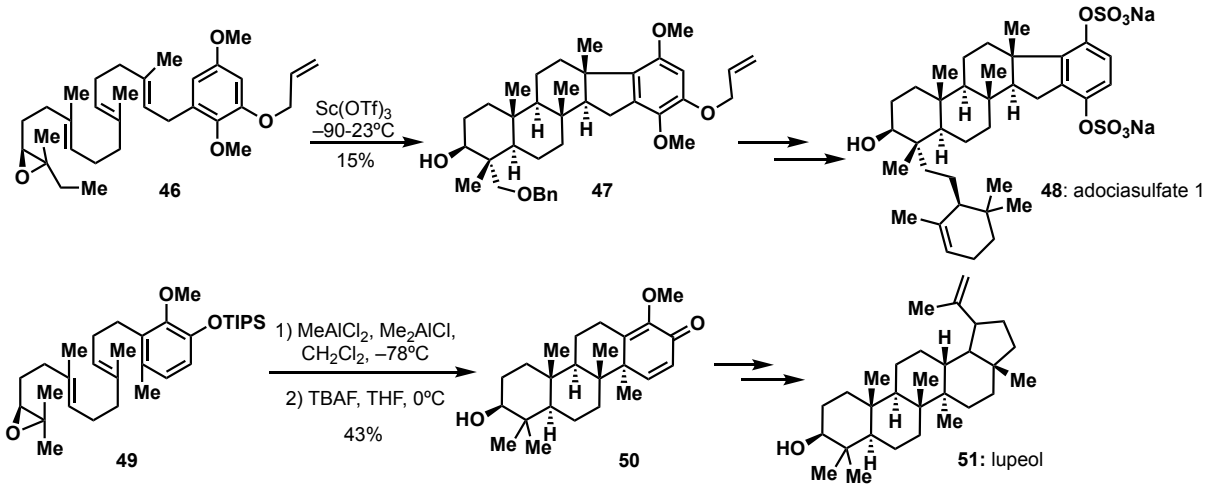

Figure 2.11 The use of aryl terminating groups in epoxide-initiated cyclization cascades.

2.7 Other Functional Groups for Cation-π Cascade Initiation

Among the different methods for initiating a cation-π cyclization cascade, electrophilic activators are worth mentioning. The most important method is the one that requires the use of oxocarbenium and *N*-acyliminium ions to activate the terminus of a polyene chain for cyclization. This way to initiate the cyclization was explored by several research groups, in particular by Johnson and co-workers that almost 50 years ago demonstrated the possibility to initiate an asymmetric polyene cyclization using a Lewis acid opening of optically active acetals (Figure 2.14) [28]. This methodology was employed by Johnson and co-workers for the preparation of a key intermediate for the synthesis of vitamin D metabolites (**54**). In this reaction, acetal **52** was treated with Ti(IV) chloride, which promoted the cyclization reaction giving optically pure **53** with high yield and diastereoselectivity.[29] In order to obtain a five-membered ring selectively in the last ring closure, a propargylic silane was used as the terminating group. Another interesting example from the same research group is the Sn(IV)-promoted pentacyclization of compound **55** to give **56** with 5.5:1 dr in favor of the α-disposed product.[30] It is interesting that a fluorine atom was used in order to help the stabilization of the positive charge in the transition state, allowing the pentacyclization to go to completion. The presence of the fluorine atom also helped in controlling the regioselectivity in the formation of the C ring, giving a six-membered ring rather than its five-membered alternative.

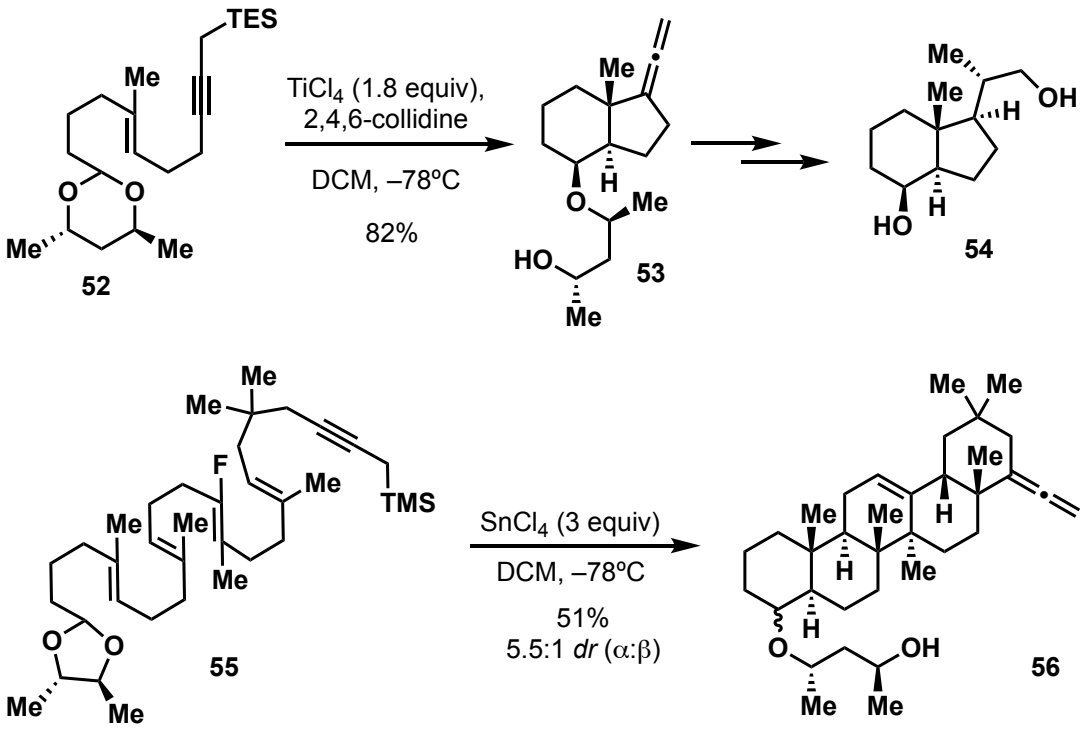

Figure 2.14 Examples of cyclization cascades initiated by chiral ketals and terminated by propargyl silanes.

While in the approach reported by Johnson and co-workers, the enantioselectivity is governed by the chiral auxiliary on the polyolefin starting material, in the approach described by Loh and co-workers, the chirality is dictated by a chiral acetal reagent that reacts in an intermolecular biomimetic cyclization with a non-chiral polyolefin starting material (Figure 2.15).[31] In this example, the Lewis acid $SnCl_4$ promoted the formation of a chiral oxocarbenium ion *in situ*, which in turn gave the desired chiral products in high yield and with good enantioselectivity. The authors exemplified the utility of this biomimetic cyclization protocol in the total synthesis of antiochic acid (**72**).[32] In a similar fashion, this procedure was successfully applied to chiral amino alcohol derivatives, wherein cyclization precursor **73** reacted with a chiral amino alcohol to give compound **74** in 54% yield, with 93:7 dr and 71% ee.[33]

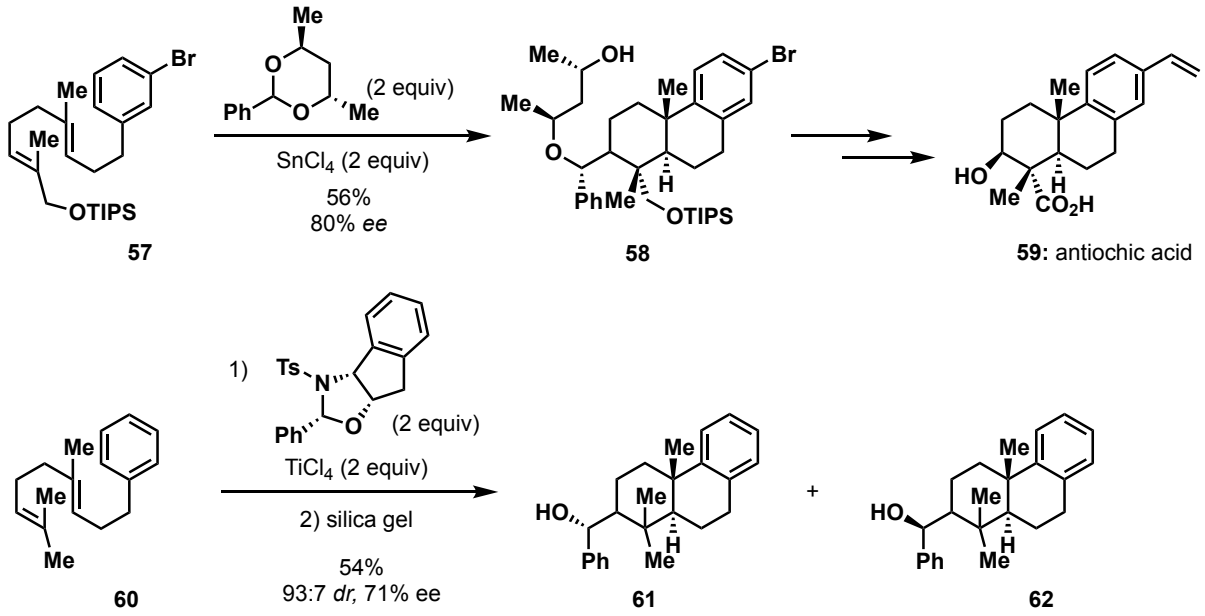

Figure 2.15 The use of a chiral acetal or an aminoalcohol-based reagent to induce stereochemistry onto achiral polyolefin starting materials.

2.8 Miscellaneous Polyene Cyclizations Initiated by Metal Activation of Simple Olefins

Other than the traditional electrophilic activation, there is another interesting method of activation that is possible to employ: the transition-metal-based activation. This type of activation process has been explored in several different contexts: stoichiometric incorporation of metals within cyclized products, catalytic activation of polyenes, and carbometallation-induced cyclizations.

One of the first examples of this mode of activation was reported by Nishizawa and co-workers, where a stoichiometric amount of Hg(II) catalyzed the biomimetic cyclization of polyolefins (Figure 2.16).[34] When substrate **63** was treated with $Hg(OTf)_2$, it underwent cyclization to give **64** in 60% yield, which was subsequently used for the synthesis of 8a-hydroxypolypoda-13,17,21-triene (**65**).[35] The cyclized organomercurial intermediate **64** was easily isolated as a stable crystalline solid that can also be easily demetallated using a simple reducing agent like $NaBH_4$ or other nucleophiles like selenium and halogens. Even though this strategy has clear limitations like the high toxicity of the reagents and low atom economy (the metal is used in a stoichiometric amount), there are still some important advantages. Firstly, this method cyclizes polyenes that terminate with electron-deficient alkenes, like **63** bearing an ester group; and secondly, this method allows for the replacement of the organomercurial group with other nucleophiles with retention of configuration.

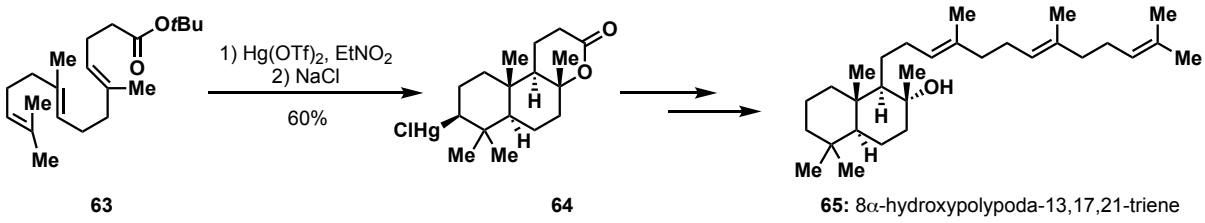

Figure 2.16 Hg-mediated polyolefin cyclization without electron-rich olefins as terminating groups.

Other metals that were efficiently used for this activation mode were described by Gagné and coworkers, wherein Pt(II) and Pd(II) pincer ligand complexes were used in polyolefin cyclizations terminated by alcohols, phenols, amines, and simple olefin nucleophiles.[36,37] One of the main features of Pd(II) and Pt(II) is that, unlike other transition metals, these cationic complexes usually coordinate to the less substituted side of the alkenes, giving access to a variety of polycyclic compounds that otherwise would not be possible to get through standard polyene cyclization.[38] In fact, in the example shown in Figure 2.17, the cationic Pd complex **67** promoted the biomimetic cyclization of polyene **66** with good diastereoselectivity, giving compound **69** in 90% yield upon demetallation with $NaBH_4$.

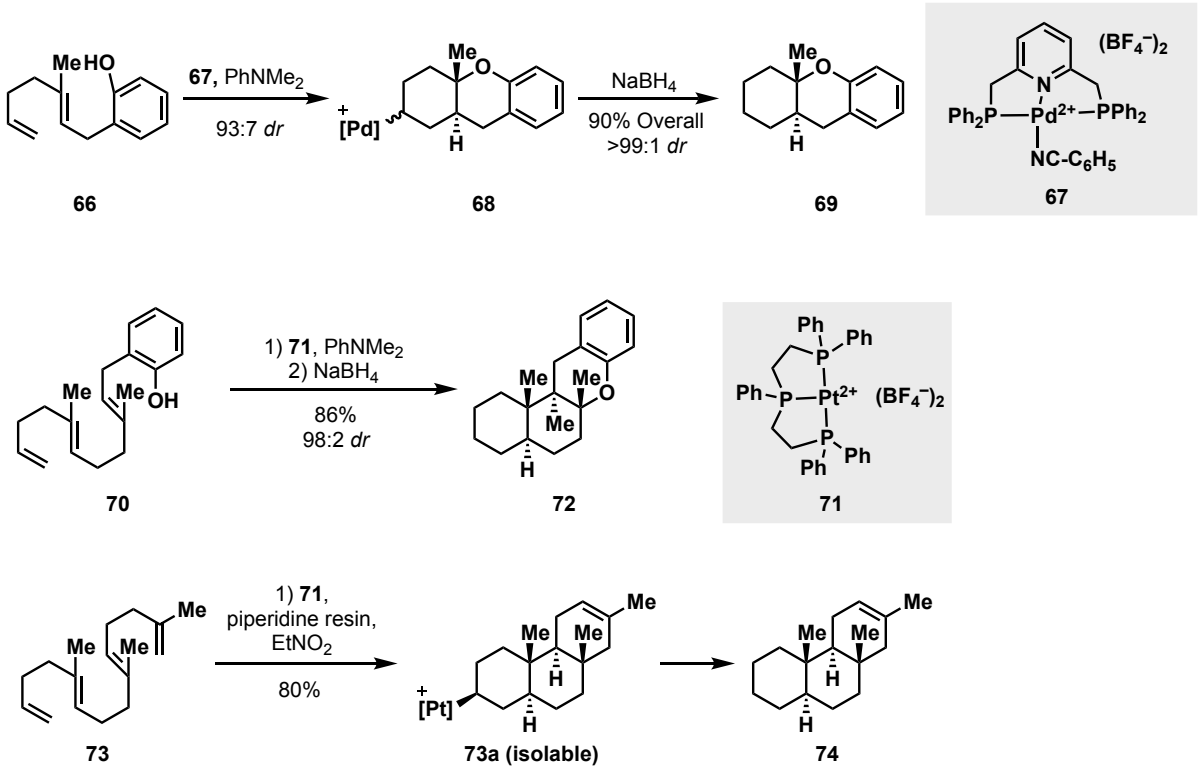

Figure 2.17 Cationic palladium and platinum complexes capable of initiating cation-π cyclization cascades without the traditional trisubstituted olefin terminus.

Another metal that works well in promoting biomimetic cyclizations with a similar activation mode is bismuth. In fact, a recent paper published by Dunach and co-workers reported a highly efficient $Bi(OTf)_3$-catalyzed cyclization of simple polyenes, in which either aryl rings or simple olefins were used as terminating groups (Figure 2.18).[39] In this example, compound **75** was treated with a catalytic amount of $Bi(OTf)_3$, giving bicyclic compound **76** in 90% yield. The resulting product is likely obtained by a 1,2-hydride shift of the less stable carbocationic intermediate **77** giving the intermediate **78**, which then undergoes a 1,2-methyl shift and elimination to give the desired product **76**. The role of the metal in this reaction mechanism is unclear, and it is possible that this cyclization cascade is a result of the TfOH generated by the side reaction of $Bi(OTf)_3$ with moisture.

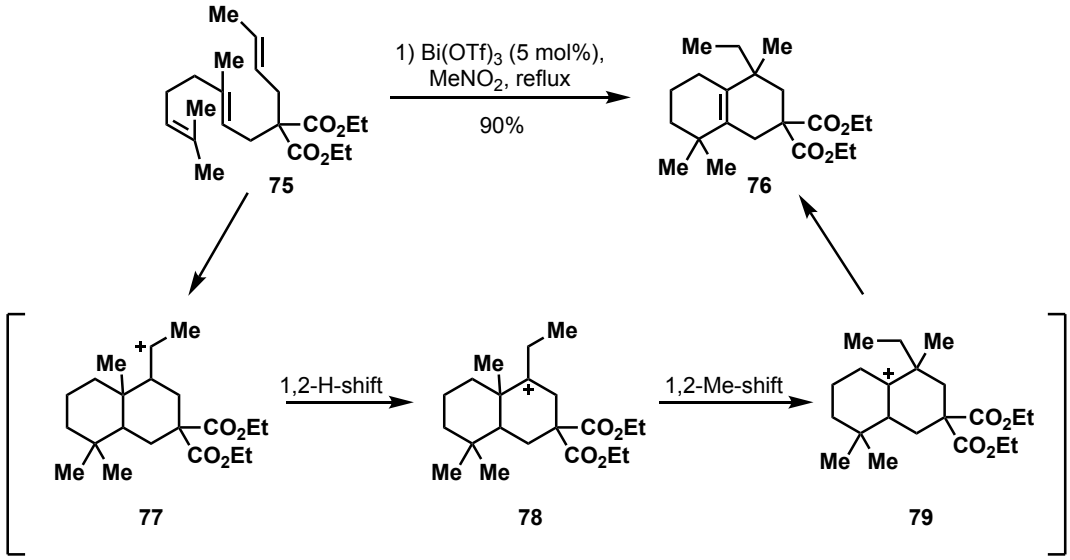

Figure 2.18 Bi-catalyzed cation-π cyclization terminated by an olefin.

2.9 References

1. Stork, G.; Burgstahler, A. W. *J. Am. Chem. Soc.* **1955***, 77,* 5068.
2. Eschenmoser, A.; Ruzicka, L.; Jeger, O.; Arigoni, D. *Helv. Chim. Acta* **1955**, *38*, 1890.
3. Johnson, W. S. *Acc. Chem. Res.,* **1968**, *1,* 1.
4. Van Tamelen, E. E. *Acc. Chem. Res.,* **1968**, *1,* 111.
5. Dewick, P. M. *Medicinal Natural Products,* John Wiley & Sons, Ltd: Chichester, England, **2001**.
6. Johnson, W. S. *Angew. Chem. Int. Ed.* **1976**, *15,* 9.
7. Bartlett, P. A. *In Asymmetric Synthesis,* Morrison, J. D., Ed.; Academic Press: New York Vol. 3, pp. 341–409, **1984**.
8. a) Yoder, R. A.; Johnston, J. N. *Chem. Rev.* **2005**, *105*, 4730; b) Yamamoto, H.; Futatsugi, K. *Angew. Chem. Int. Ed.* **2005**, *44*, 1924.
9. Sutherland, J. K. *Chem. Soc. Rev., **1980**, 9,* 265.
10. Sutherland, J. K. *In Comprehensive Organic Synthesis.* Trost, B. M., Fleming, I., Eds; Pergamon: Oxford, Vol. 3, pp. 341-377, **1991**.
11. Fürstner, A.; Davies, P. W. *Angew. Chem. Int. Ed.* **2007**, 3410.
12. Taylor, S. K. *Organic Preparations and Procedures Int.* **1992***, 24,* 245.
13. Yoder, R. A.; Johnston, J. N. *Chem. Rev.* **2005***, 105,* 4730.
14. a) Eschenmoser, A.; Arigoni, D. *Helv. Chim. Acta, **2005**, 88,* 3011; b) Stork, G.; Conroy, H. *J. Am. Chem. Soc***. 1951***, 73*, 4748; c) Yoder, R. A.; Johnston, J. N. *Chem. Rev.* **2005**, *105*, 4730.
15. Wendt, K. U.; Schulz, G. E.; Corey, E. J.; Liu, D. R. *Angew. Chem. Int. Ed.* **2000**, *39,* 2812.
16. a) Ishihara, K.; Nakamura, S.; Yamamoto, H. *J. Am. Chem. Soc.* **1999**, *121*, 4906; b) Nakamura, S.; Ishihara, K.; Yamamoto, H. *J. Am. Chem. Soc.* **2000**, *122*, 8131.
17. Ishibashi, H.; Ishihara, K.; Yamamoto, H. *J. Am. Chem. Soc.* **2004**, *126*, 11122.
18. Uyanik, M.; Ishibashi, H.; Ishihara, K.; Yamamoto, H. *Org. Lett.* **2005**, *7,* 1601.
19. Corey, E. J.; Luo, G.; Lin, L. S. *Angew. Chem. Int. Ed.* **1998**, *37,* 1126.
20. Surendra, K.; Corey, E. J. *J. Am. Chem. Soc.* **2012**, *134*, 11992.

21. a) Corey, E. J.; Lin, S. *J. Am. Chem. Soc.* **1996**, *118*, 8765; b) Van Tamelen, E. E.; Willet, J.; Schwartz, M.; Nadeau, R. *J. Am. Chem. Soc.* **1966**, *88*, 5937.

22. Corey, E. J.; Lin, S.; Luo, G. *Tetrahedron Lett.* **1997**, *38*, 5771.

23. Corey, E. J.; Luo, G.; Lin, L. S. *J. Am. Chem. Soc.* **1997**, *119*, 9927.

24. Anastasia, L.; Giannini, E.; Zanoni, G.; Vidari, G. *Tetrahedron* **2005**, *46*, 5803.

25. a) Bogenstatter, M.; Limberg, A.; Overman, L. E.; Tomasi, A. L. *J. Am. Chem. Soc.* **1999**, *121*, 12206 b) Lindel, T.; Hopmann, C. *Polyene Cyclization to Adociasulfate 1. In Organic Synthesis Highlights V*; Schmalz, H.-G., Wirth, T., Eds.; Wiley-VCH: Weinheim, pp 342–349, **2003**.

26. Surendra, K.; Corey, E. J. *J. Am. Chem. Soc.* **2008**, *130*, 8865.

27. Surendra, K.; Corey, E. J. *J. Am. Chem. Soc.* **2009**, *131*, 13928.

28. a) Johnson, W. S.; Harbert, C. A.; Stipanovic, R. D. *J. Am. Chem. Soc.* **1968**, *90*, 5279; b) Johnson, W. S.; Harbert, C. A.; Ratcliffe, B. E.; Stipanovic, R. D. *J. Am. Chem. Soc.* **1976**, *98*, 6188; c) Bartlett, P. A.; Johnson, W. S.; Elliot, J. D. *J. Am. Chem. Soc.* **1983**, *105*, 2088.

29. Johnson, W. S.; Elliot, J. D.; Hanson, G. J. J. *Am. Chem. Soc.* **1984**, *106*, 1138.

30. a) Fish, P. V.; Johnson, W. S. *J. Org. Chem.* **1994**, *59*, 2324; b) Fish, P. V.; Johnson, W. S.; Jones, G. S.; Tham, F. S.; Kullnig, R. K. *J. Org. Chem.* **1994**, *59*, 6150.

31. Zhao, Y.-J.; Chng, S. S.; Loh, T.-P. *J. Am. Chem. Soc.* **2007**, *129*, 492.

32. Zhao, Y.-J.; Loh, T.-P. *Org. Lett.* **2008**, *10*, 2143.

33. Zhao, Y.-J.; Loh, T.-P. *J. Am. Chem. Soc.* **2008**, *130*, 10024.

34. Nishizawa, M.; Takenaka, H.; Hirotsu, K.; Higuchi, T.; Hayashi, Y. *J. Am. Chem. Soc.* **1984**, *106*, 4290.

35. Takao, H.; Wakabayashi, A.;Takahashi, K.; Imagawa, H.; Sugihara, T.; Nishizawa, M. *Tetrahedron Lett.* **2004**, *45*, 1079.

36. Nishizawa, M.; Takao, H.; Kanoh, N.; Asoh, K.; Hatakeyama, S.; Yamada, H. *Tetrahedron Lett.* **1994**, *35*, 5693.

37. Koh, J. H.; Gagné, M. R. *Angew. Chem. Int. Ed.* **2004**, *43*, 3459.

38. Sokol, J. G.; Korapala, C. S.; White, P. S.; Becker, J. J.; Gagné, M. R. *Angew. Chem. Int. Ed*. **2011**, *123*, 5658.

39. Godeau, J.; Olivero, S.; Antoniotti, S.; Dunach, E. *Org. Lett.* **2011**, *13*, 3320.

Chapter 3: Oxo-rhenium(V)-catalyzed Biomimetic Cyclization

3.1 Chapter Abstract

The two previous chapters described an overview of rhenium chemistry and metal-promoted biomimetic cyclizations. There is an overlap between these two research interests because: a) both involve Lewis acid chemistry; b) both can result in ring formation; and c) both are typically carried out under simple reaction conditions where additives are rarely necessary, and stoichiometric waste is not produced. In this chapter, the result of an amalgamation of these concepts is described: oxo-rhenium(V)-catalyzed biomimetic cyclization.

3.2 Introduction

As previously described, it is well known in the literature how transition metals can promote the biomimetic cyclization of polyunsaturated chains to form carbocyclic systems. There are a variety of ways to engage an unactivated olefin (which usually behaves like a weak nucleophile): the most common way is to exploit the Lewis acid property of a metallic species to induce a cyclization reaction. Usually, transition-metal-catalyzed biomimetic cyclizations are intramolecular cascade processes where all the nucleophiles and electrophiles react simultaneously to make the cyclization reaction fast enough and minimize the formation of byproducts. Except for some literature examples related to organocatalytic systems in which the electrophiles and nucleophiles that undergo the biomimetic cyclization are completely disjoint and promote an intermolecular biomimetic cyclization, examples that involve a metallic species remain limited.

The most relevant example of metal-catalyzed intermolecular biomimetic cyclization was described in 2005 by Vidari and co-workers, in which they treated a carefully designed dienyl allyl silane (**2**) with an over-stoichiometric amount of TiF_4 (Figure 3.1). This reaction also worked with $TiCl_4$, albeit in poor yield, in which the major byproducts were halogenated derivatives obtained by trapping the carbocation in the polyene structure with Cl anions. Other Lewis acids such as BF_3•Et_2O and $SnCl_4$ were completely ineffective in cyclizing compound **2**. [2] More details about the TiF_4-promoted biomimetic cyclization have already been described in Chapter 2.

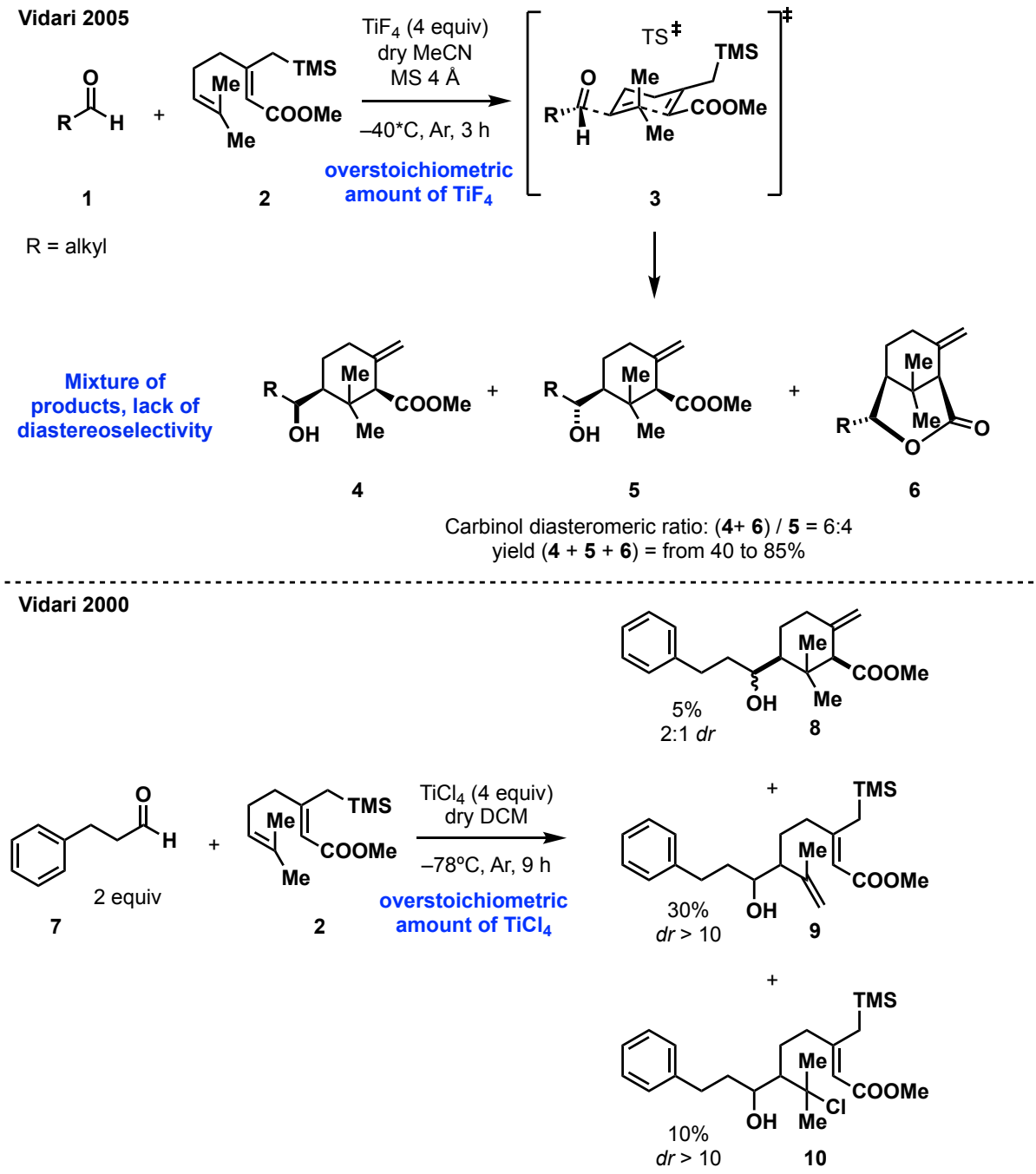

Figure 3.1 Titanium-promoted intermolecular biomimetic cyclization reported by Vidari and co-workers.

The Vidari group attempted to improve this biomimetic cyclization, employing a variety of known Lewis acids and reaction conditions, but to no avail over the past decade. Meanwhile, I had gained experience with oxo-rhenium chemistry and its application in the total synthesis of small polyketides during my master's degree. It was then conjectured that the interesting reactivity of oxo-rhenium(V) complexes could be exploited as a simple solution for this unsolved problem. In particular, taking inspiration from a rhenium-catalyzed Sakurai–Hosomi-type reaction on furanoside derivatives, it was hypothesized that aldehydes could be activated

under mild conditions through a bimetallic system composed by an oxo-Re(V) complex (**12**) and $Cu(OTf)_2$ (Figure 3.2). The role of the thiophilic $Cu(OTf)_2$ is to remove the labile ligand SMe_2 from the coordination sphere of the oxo-Re(V) complex **12** giving the highly reactive species **16** through unstable bimetallic adduct **15**. $CoCl_2$ can also serve as a co-catalyst in this reaction. In the presence of only $Cu(OTf)_2$ (or $CoCl_2$), without the rhenium precatalyst **12**, the reaction does not work at all. Moreover, when only the Re(V) complex is present, a much lower yield resulted (between 30 and 45% depending on the substituent on the furanoside moiety), demonstrating the efficiency of this mild co-catalytic system.

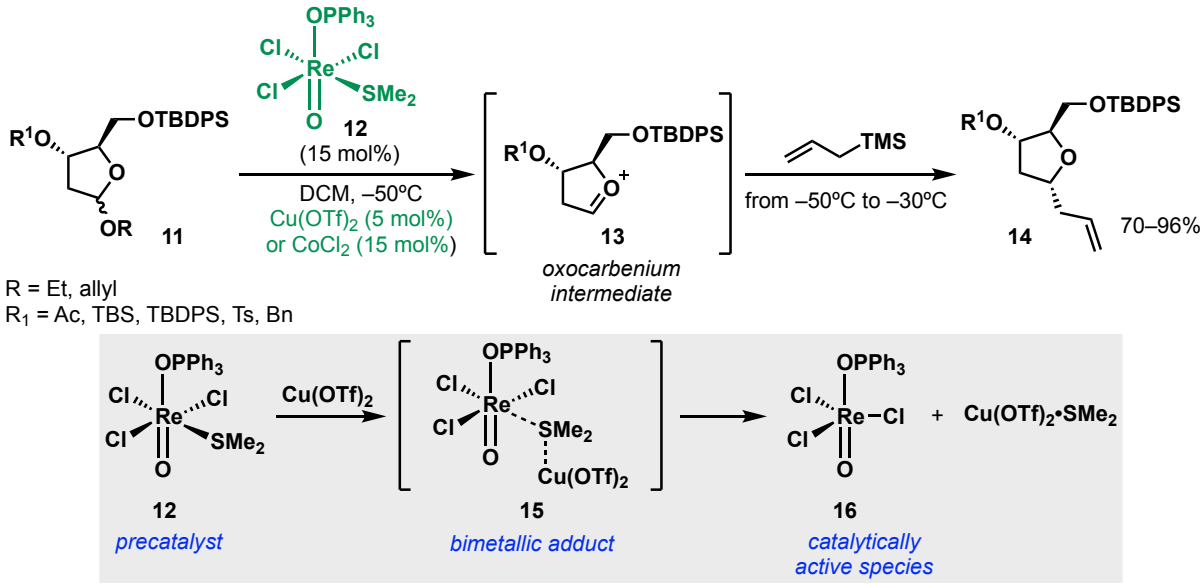

Figure 3.2 Merging rhenium chemistry with cation-olefin reaction methodology in a furanoside system.

3.3 Experimental Results and Discussion

In order to validate the hypothesis regarding the ability of the oxo-rhenium complex **12** to activate aldehydes, the reactivity of this unprecedented catalytic system was tested on a simple acyclic system (Figure 3.3). In this model system, the benzaldehyde reacted first with the rhenium complex to form adduct **18**, and subsequently it underwent the Sakurai reaction with the TMS allyl silane, giving allylic alcohol **19** in good yield (73%). The conditions shown below were identified as the best conditions after a brief screening.

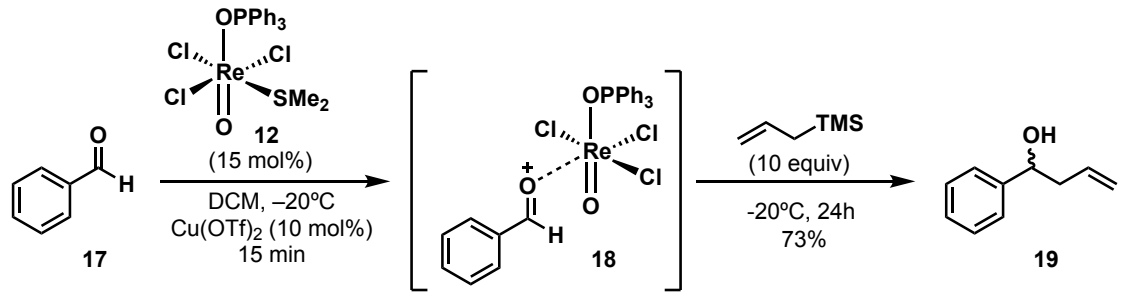

Figure 3.3 Testing the ability of oxo-rhenium complex **12** to activate aldehydes.

After this promising result, the same conditions were applied to a more complex substrate **2**, which approximates terpene-like systems by virtue of an embedded isoprene unit (Figure 3.5). Substrate **2** for this biomimetic cyclization was not commercially available and was therefore synthesized in one pot from readily available starting materials (Figure 3.4). In this catalytic cyclization reaction, commercially available phenylpropionaldehyde (**7**), after coordination with the rhenium complex **12**, reacted with dienyl allyl silane **2** in a biomimetic cyclization to give olefinic lactone **17**.

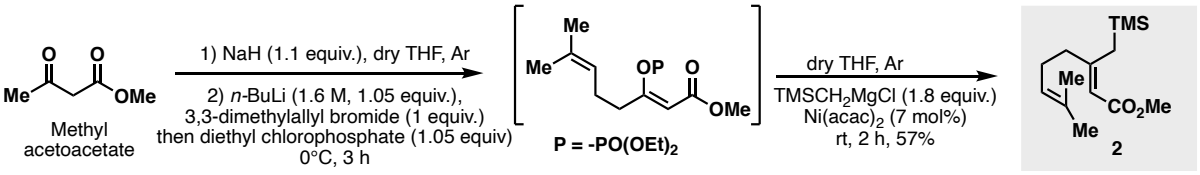

Figure 3.4 A one-pot synthesis of polyisoprene-like diene **49**.

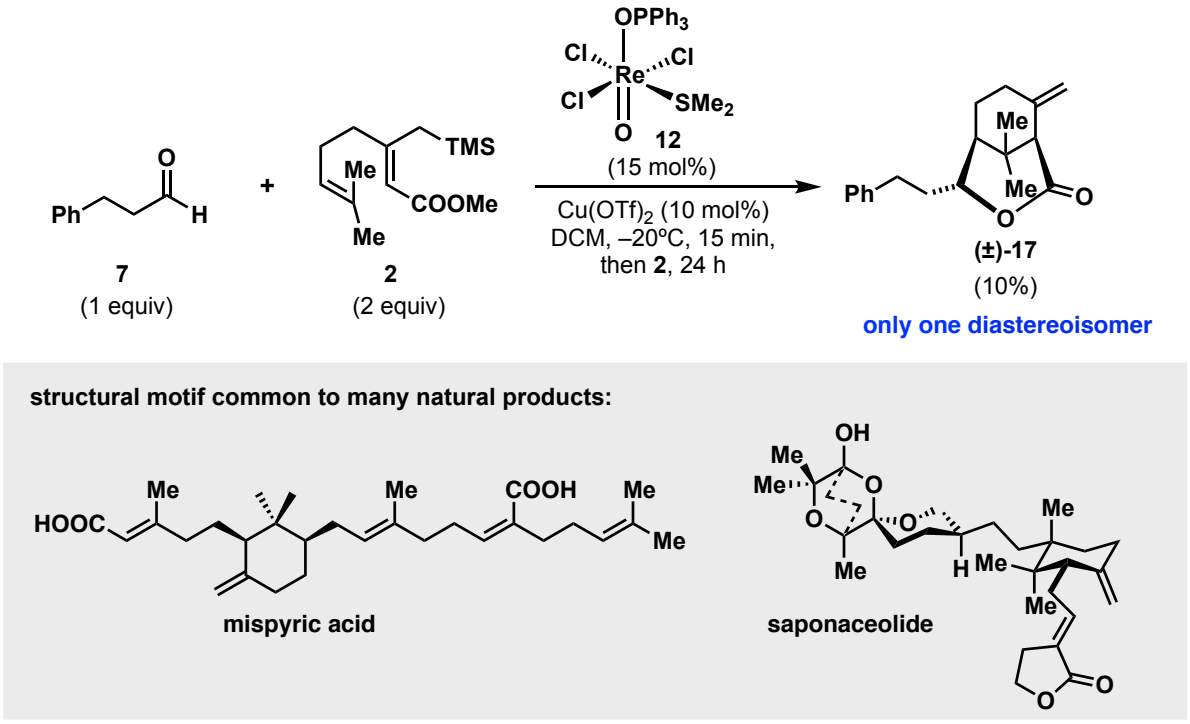

Figure 3.5 A rhenium-catalyzed merger of an aldehyde and a dienyl system, resulting in the first "hit" in obtaining a cyclization product.

Surprisingly, even though the isolated yield was low (10% yield), only one diastereoisomer of **17** was observed. The only identified by-product was the self-condensation product of aldehyde **7**. The reaction went to full conversion and the diene in excess (2 equivalents) was recovered. This result was very promising, given that it was just the first attempt, and it was possible to obtain, in a catalytic fashion, what was previously possible only when using a large amount of TiF_4. Thus, an optimization process was undertaken to see if a better result could be achieved when compared to the old method with TiF_4, both in terms of yield and diastereoselectivity. It is important to underline that this structural motif is common to many natural products of the terpene family, two of which are mispyric acid and saponaceolide (see Figure 3.5). For this reason, this method could pave the way to a simplified access of key intermediates for the synthesis of terpenoid natural products.

After an extensive screening of conditions, optimal conditions for the model reaction between phenylpropionaldehyde **7** and dienyl allyl silane **2** were found (Table 3.1). There are many parameters that affect the outcome of this reaction, one of them being the temperature at which the aldehyde gets coordinated by the oxo-rhenium complex **12**. In fact, decreasing the temperature from –10 °C (entries 3 and 4) to –40 °C (entries 2 and 7–14) made a significant difference in isolated yield (from 5% to 51%). Another important parameter to consider is the amount of co-catalyst: increasing the amount of $Cu(OTf)_2$ led to a lower yield (entries 3–8), and it even led to decomposition when 40 mol% of Cu(II) was employed (entry 6). This behavior can be explained by the strong Lewis acid properties of $Cu(OTf)_2$, since the major product observed was the self-condensation of the aldehyde. Thus, a lower amount of Cu(II) was employed, and it was found that 5 mol% (entry 10) is the optimal amount, since 2.5 mol% of copper led to trace product (entry 9). Other co-catalysts were tested, the most relevant being $CoCl_2$ given its moderate thiophilicity and its moderate Lewis acidity (but much weaker than $Cu(OTf)_2$); however, it resulted in trace product (entry 12). Also, the combination of $Cu(OTf)_2/CoCl_2$ was tested, but only a poor yield was obtained (entry 11). Even though the temperature of precomplexation and the amount of copper are the main parameters that affect this reaction, the reaction temperature *after* the addition of dienyl allyl silane **12** has an effect. The lower the temperature, the better the yield, but when the reaction was cooled too much (e.g., lower than –30 °C), the reaction stopped and the yield decreased. The right balance between all these parameters gave the best result, which is highlighted in blue in Table 3.1.

Table 3.1 Optimization of the reaction temperature (both for pre-complexation as well as for the reaction) and the amounts of catalyst/co-catalyst.

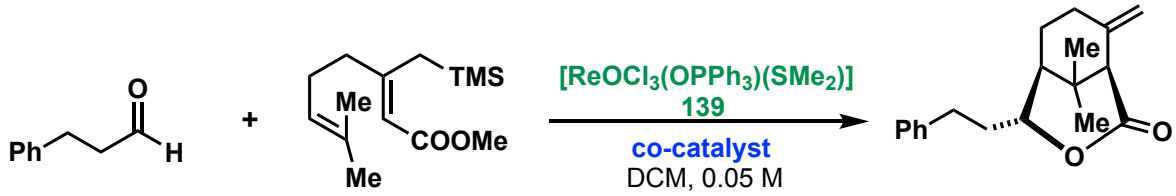

7 2 (±)-17

Entry	Equiv. Compound 7	Equiv. Compound 2	mmol compound 7	mol % oxo-Re(V)	mol % co-catalyst	Pre-complexation T(°C), t(min)	Reaction T(°C), t(min)	Isolated yield %
1	1	2	0.40	15 mol %	$Cu(OTf)_2$, 5 mol%	-23°C, 15 min	5°C, 15 h	Decomposition
2	1	2	0.40	15 mol %	$Cu(OTf)_2$, 5 mol%	-40°C, 15 min	-30°C, 15 h	27%
3	1	2	0.40	15 mol %	$Cu(OTf)_2$,10mol%	-10°C, 30 min	25°C, 15 h	Decomposition
4	1	2	0.40	15 mol %	$Cu(OTf)_2$,10mol%	-10°C, 30 min	-10°C, 15 h	5%
5	1	2	0.40	15 mol %	$Cu(OTf)_2$,10mol%	-20°C, 30 min	0°C, 15 h	10%
6	1	2	0.40	40 mol %	$Cu(OTf)_2$,40mol%	-20°C, 30 min	0°C, 15 h	Decomposition
7	1	2	0.40	15 mol %	$Cu(OTf)_2$,10mol%	-40°C, 30 min	-30°C, 15 h	36%
8	1	2	0.40	18 mol %	$Cu(OTf)_2$,12mol%	-40°C, 30 min	-23°C, 15 h	30%
9	1	2	0.40	15 mol %	$Cu(OTf)_2$, 2.5mol%	-40°C, 30 min	-23°C, 15 h	6%
10	1	2	0.40	15 mol %	$Cu(OTf)_2$, 5 mol%	-40°C, 30 min	-30°C, 15 h	51%
11	1	2	0.40	15 mol %	$Cu(OTf)_2$, 5mol%, $CoCl_2$, 10 mol%	-40°C, 30 min	-23°C, 15 h	15%
12	1	2	0.40	15 mol %	$CoCl_2$, 10 mol%	-40°C, 30 min	-23°C, 15 h	7%
13	1	1.5	0.40	15 mol %	$Cu(OTf)_2$, 5 mol%	-40°C, 30 min	-30°C, 15 h	42%
14	1	1.5	0.40	10 mol %	$Cu(OTf)_2$, 5 mol%	-40°C, 30 min	-23°C, 15 h	39%

With the optimized conditions in hand, a substrate scope was generated, wherein the dienyl allyl silane was kept constant and the aldehyde structure was varied (Table 3.2).

Table 3.2 A substrate scope that varies the aldehyde component. Compound **2** (2 equiv., 0.7 mmol), aldehydes (1 equiv., 0.35 mmol), [$Re^{v}O(SMe_2)(OPPh_3)Cl_3$] = 15 mol %, $Cu(OTf)_2$ = 5 mol %, dry DCM (0.05 M), pre-complexation at –40 °C for 30 min, then reaction at –30 °C for 16 h. Each reaction was tested 3 times (except for entry **5** that was run just one time) and the reported isolated yields are averaged over 3 reactions.

Entry	Aldehyde Structure	Product structure	Isolated yield%	Observations
1	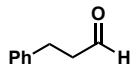 7	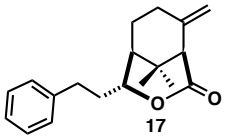 17	51%	None
2	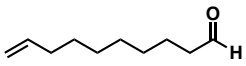 18	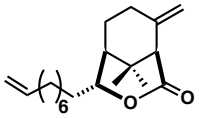 19	43%	Aldehyde not completely dry
3	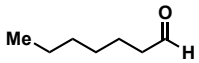 20	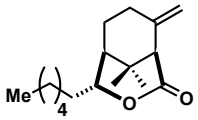 21	47%	None
4	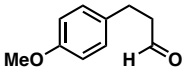 22	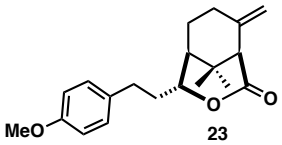 23	5%	The major product : 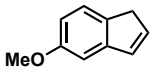 24
5	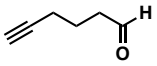 25	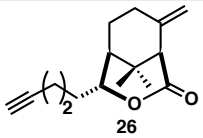 26	No reaction	Self-condensation of aldehyde and one unknown product
6	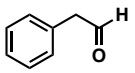 27	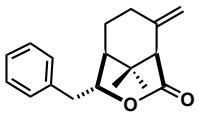 28	No reaction	Self-condensation of aldehyde only
7	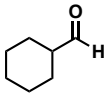 29	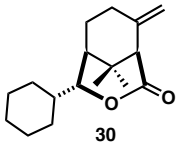 30	No reaction	Self-condensation of aldehyde only
8	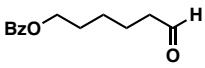 31	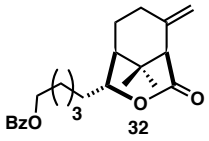 32	No reaction	Maybe a bicoordination of Re(V) inhibits cyclization
9	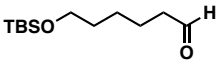 33	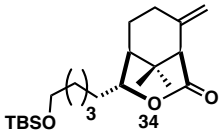 34	No reaction	Self-condensation of aldehyde only
10	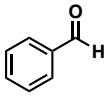 35	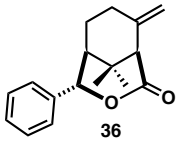 36	No reaction	Self-condensation of aldehyde only
11	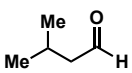 37	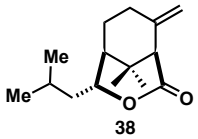 38	No reaction	Self-condensation of aldehyde only

The only entries that delivered a good yield were entries 1 to 3. Entry 4 only gave 5% isolated yield, and the main product was 5-methoxy-1*H*-indene (**24**) due to the high electron-rich character of aldehyde **22** that spontaneously cyclizes in the presence of a Lewis acid. For other entries (entries 6, 7, 10, and 11), they did not deliver the desired product, as the only observed product was the self-condensation of the corresponding aldehyde. Entry 5 gave a slightly different outcome, as the aldehyde self-condensation was observed, as well as a significant amount of an unknown byproduct. With the aldehyde of entry 8, no product formation was observed, and we suspect some kind of coordination effect that inhibits the reactivity of the catalyst. Lastly, entry 9 delivered just the deprotected aldehyde with a free hydroxy group.

The standard conditions were tested with other oxygen-containing electrophiles like ketones, enoate esters, acetals, and epoxides, but no product formation was observed (Figure 3.6).

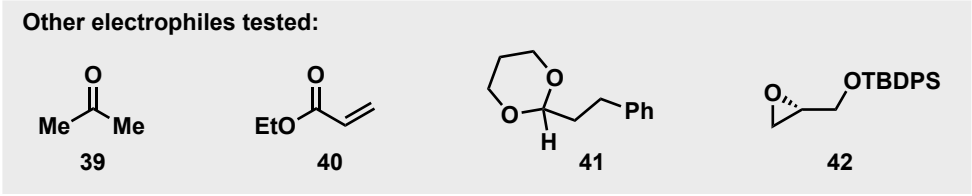

Figure 3.6 Other oxygen-containing electrophiles that were tested instead of aldehydes.

Furthermore, a different set of diene nucleophiles were tested, but none of them delivered the desired product (Table 3.3). Only self-condensation of the starting aldehyde **7** was observed.

Table 3.3 A substrate scope that varies the diene component. Aldehyde **7** (1 equiv., 0.35 mmol), nucleophile (2 equiv., 0.70 mmol), $[Re^{V}O(SMe_2)(OPPh_3)Cl_3]$ = 15 mol %, $Cu(OTf)_2$ = 5 mol %, dry DCM (0.05 M), pre-complexation at –40 °C for 30 min, then reaction at –30 °C for 16 h. Each reaction was tested 3 times.

Entry	Aldehyde Structure	Product structure	Isolated yield%	Observations
1	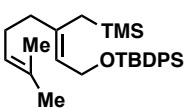 39	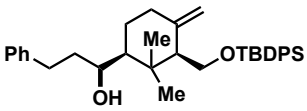 40	No reaction	Self-condensation of aldehyde only
2	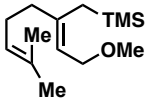 41	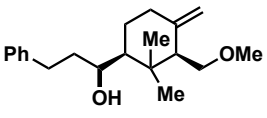 42	No reaction	Self-condensation of aldehyde only
3	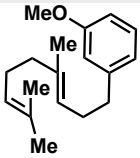 43	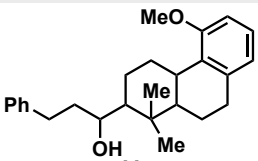 44	No reaction	Self-condensation of aldehyde only

This preliminary data helped rationalize the structure of the reagents required for this methodology. The structural requirements of both the nucleophile and electrophile are summarized below:

- The nucleophile requires a carbonyl moiety that is directly conjugated to the double bond of the allylsilane moiety (perhaps because it gets coordinated by the catalyst, or it helps polarize that olefin).
- The nucleophile requires a silane as the terminator group.
- Aldehydes are the only active electrophiles in this transformation.
- The aldehydes require both the α and β positions as methylene groups, since further substituents are not tolerated at these positions with the current reaction conditions.
- Terminal alkynes and other coordinating groups (like hydroxy groups or ethers) in the aldehyde side chain could inhibit the catalytic activity of the oxo-Re(V) catalyst (a color change in the reaction medium was observed, which was different from the working reaction).

The features required for both the nucleophile and the electrophile are highlighted in Figure 3.7 (grey box). Since the aldehydes require methylene groups at the α and β positions, a general synthesis of such aldehydes was necessary. To this end, a very simple and efficient method was used to synthesize a broad range of aldehydes who fit this requirement. This sequence was used for the synthesis of compound **22**, as well as for other aldehydes that contain halogenated aromatic rings. (These aldehydes have not yet been tested with the optimized conditions for the biomimetic cyclization and, for this reason, they are not reported in this thesis.)

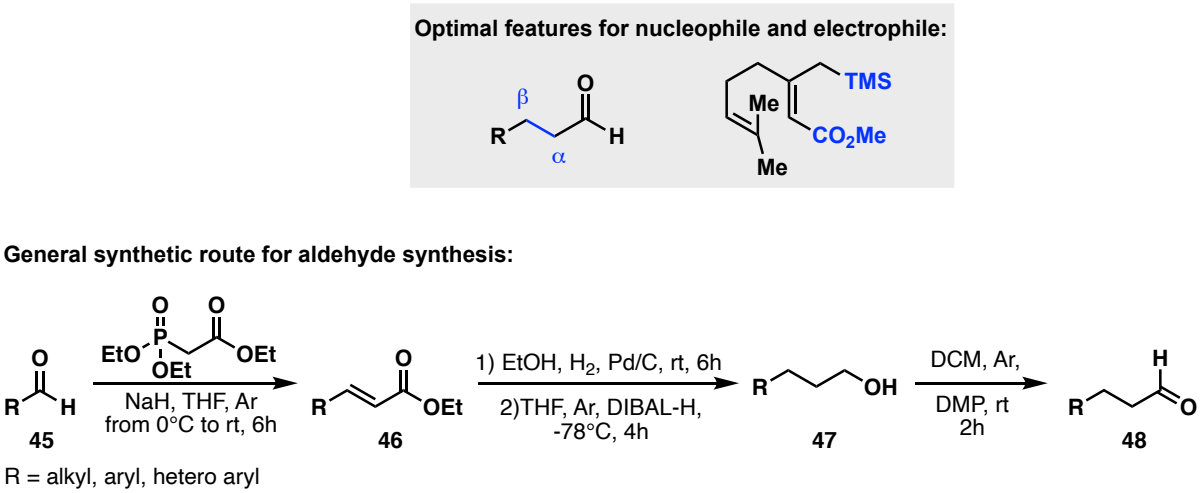

Figure 3.7 Optimal features regarding the nucleophile and the electrophile for the reaction, as well as a general route for the synthesis of aldehydes used in this project.

3.4 Theoretical Results and Discussion

To investigate the diastereoselectivity and the mechanistic manifold of this reaction, a DFT study was undertaken, and the proposed catalytic cycle is shown below (Figure 3.8).]

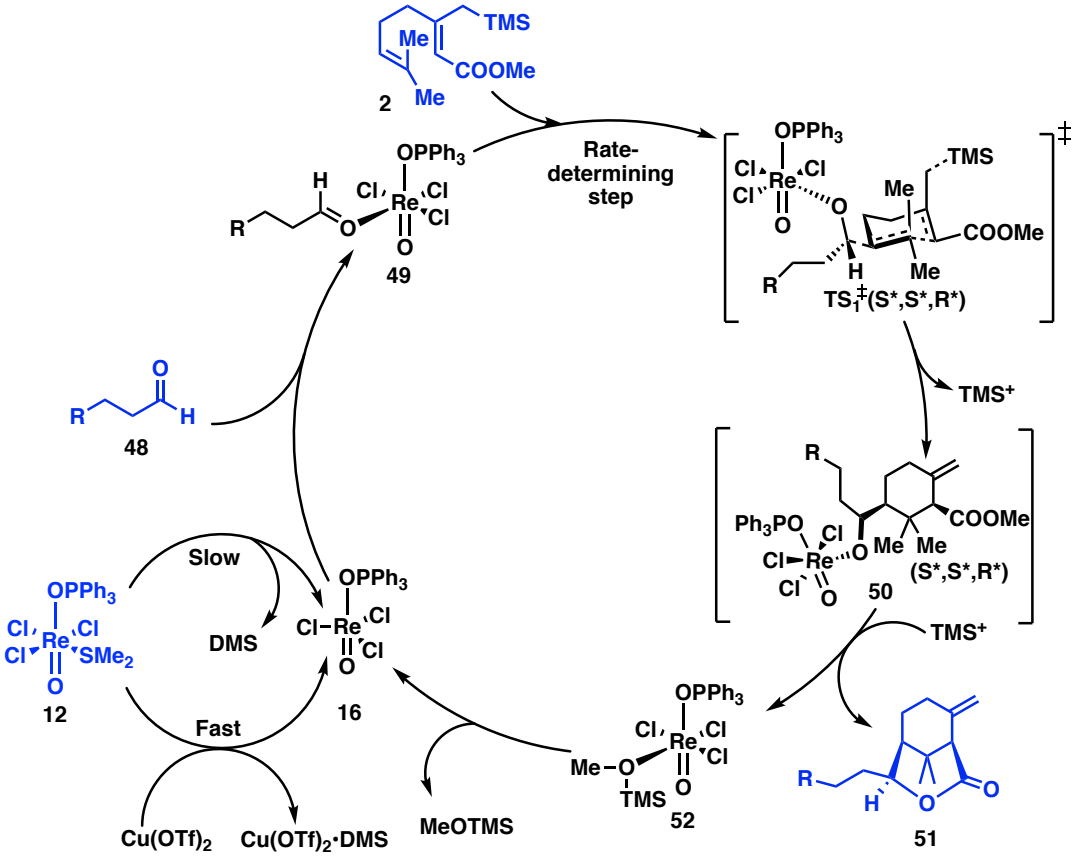

Figure 3.8 The catalytic cycle evaluated using differentiate level of theory: H, C, O, S, Cl, Si, P 6-31+g (d,p) and Cu, Re LANL2DZ (ECP method)

In this proposed catalytic cycle, complex **12** first undergoes spontaneous loss of the labile ligand dimethylsulfide (DMS) giving **16**, which, thanks to its high Lewis acidity, reacts with substrate **48** to give complex **49**. Preliminary studies have suggested that the ligand exchange is likely to be dissociative rather than associative. To confirm that the ligand exchange occurs in a dissociative manner, the associative process was also studied. In fact, comparing the energies involved for both processes, the dissociative mechanism is much more advantageous from an energetic point of view, in which **48** displaces DMS from the rhenium coordination sphere. The rate-determining step of the entire catalytic system is the reaction and cyclization between **49** and **2** that gives **50** through **TS 1**. The desired product **51** was subsequently obtained by intramolecular lactonization and ligand exchange in the rhenium coordination sphere, releasing complex **52** and the cascade product **51**. The efficiency of this catalytic system was also confirmed by the fact that other oxo-rhenium complexes such as [(dppm)ReOCl$_3$], [(dppe)ReOCl$_3$] and [(dppp)ReOCl$_3$] did not provide any product, even when

these complexes were used in stoichiometric amounts. This can be explained by the lack of a displaceable ligand in these rhenium complexes.

Unfortunately, the transition state for the lactonization process is not yet found and, in this preliminary computational study, the effect of the ester moiety in affecting the rhenium catalysis (that is clearly important from an experimental point of view) has not yet been rationalized.

Moreover, to promote the generation of the catalytically active species **16**, as previously mentioned, a thiophilic metal like $Cu(OTf)_2$ was employed. This co-catalyst proved to be fundamental in accelerating the formation of the complex **16** (and consequently that of the entire process) as highlighted in the energy profile below (grey box, Figure 3.9). In fact, without the presence of this Cu salt, the catalytic activity dramatically decreased, and no product was observed.

The energy profile of the entire catalytic cycle (DFT / B3LYP with differentiated basis set) is shown in Figure 3.9. Acetaldehyde was used as the model aldehyde in order to simplify the system. After the dissociative ligand exchange (from complex **12** to **16**), complex **49a** reacts with compound **2**. The two species could undergo four possible transition states (TS_1, TS_2, TS_3, TS_4), all with different conformations and relative stereochemistry. Based on the calculated ΔE, the transition state that is the most favored is TS_1 with the relative stereochemistry (S*, S*, R*), which possesses the lowest energy with 24.2 kcal/mol (compared with the other transition states that respectively have 26.1, 28.3, and 37.0 kcal/mol), and is thus the most thermodynamically stable. The product obtained after this cyclization process is compound **50a** with a relative energy of –13.3 kcal/mol. Very pleasingly, this result matched the experimental data, in which the relative stereochemistry of the product is (S*, S*, R*) based on NMR analysis through comparison with a literature substrate. After the rate-determining step, **50a** changes its conformation, assuming a di-axial conformation to allow the intramolecular lactonization reaction. Unfortunately, the transition state for the intramolecular lactonization is not yet available, but additional studies are currently ongoing.

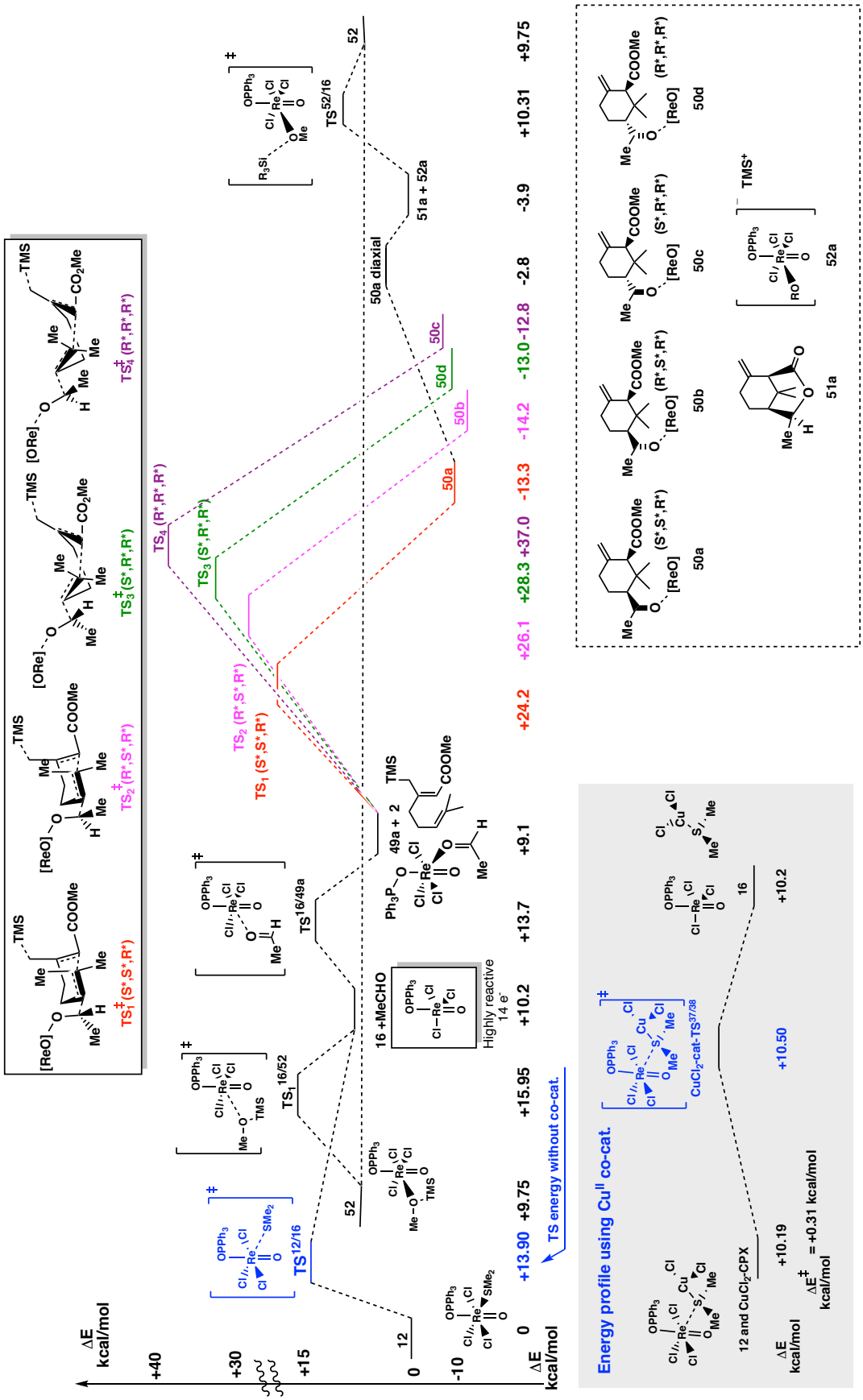

Figure 3.9 An energy diagram showcasing the relative energies of the reaction intermediates and transition states for the aldehyde-diene cyclization reaction.

3.5 Further Studies for Enantioselectivity

A further attempt to evaluate the potential of this reaction was made by performing the same transformation in an enantioselective fashion. To explore this possibility, the synthesis of chiral rhenium complexes was undertaken. When designing these rhenium complexes, it was important to keep intact the reactivity and geometry of the complex (Figure 3.10). The chiral information was installed by substituting one or two of the chlorine ligands with one or two anionic ligands (e.g., a BINOL-type ligand), while keeping the labile dimethylsulfide ligand that is a key requirement for the biomimetic cyclization.

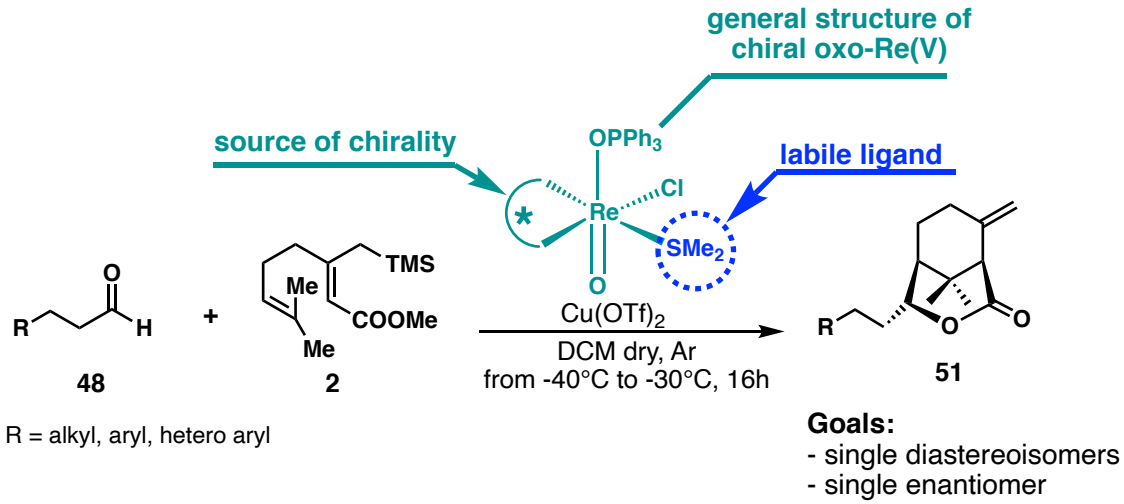

Figure 3.10 Elements of design for a chiral Re catalyst to promote an enantioselective cyclization cascade.

Two new chiral oxo-rhenium complexes were synthesized, and their syntheses are shown in Figure 3.11. In both syntheses, Ag_2CO_3 was used for promoting the displacement of chlorine with BINOL derivatives by exploiting the favorable K_{sp} value for the precipitation of Ag_2CO_3. Upon completion of chiral complexes **56** and **58**, they were employed in the biomimetic cyclization (Table 3.4). Although the reaction with both catalysts gave modest yields of product, there was some induction of enantiomeric excess of 11% and 9%, respectively. This demonstrated that the chirality of the rhenium complex can indeed be transferred to the chirality of the product.

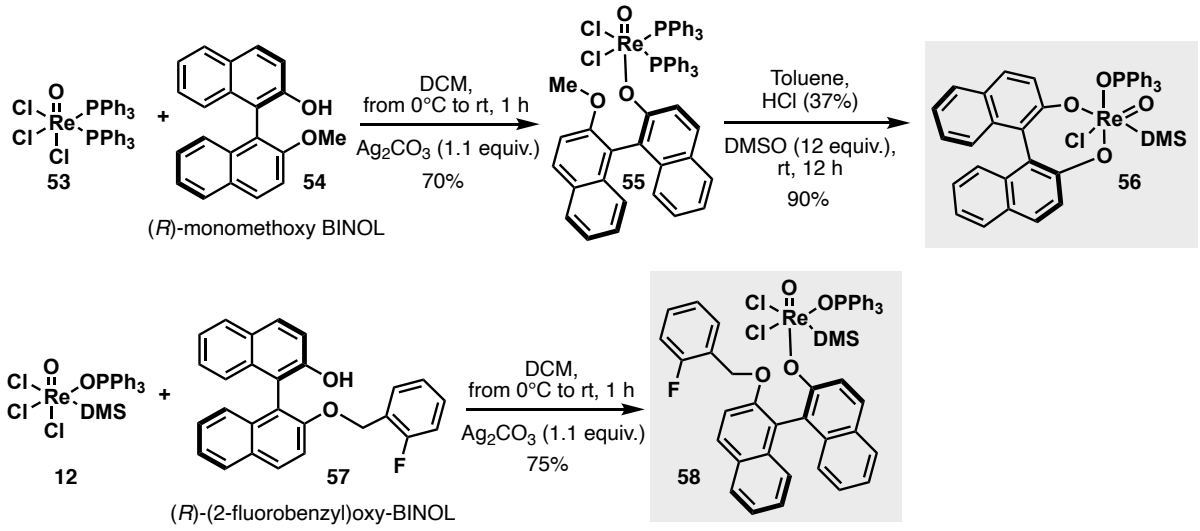

Figure 3.11 Synthesis of chiral Re complexes **56** and **58**. Note: The exact position of the ligands in complexes **56** and **58** is not known: only NMR spectra and ESI-MS are available, and obtaining suitable crystals for X-ray diffraction was difficult.

Table 3.4 Attempts at enantioselective biomimetic cyclization using chiral oxo-Re(V) complexes **56** and **58**.

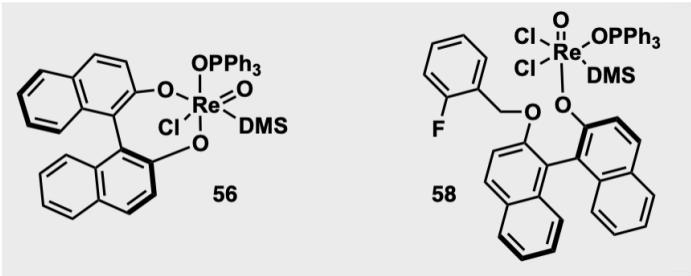

Entry	mol% chiral oxo-Re(V) complex used	Equiv. compound 7	Equiv. compound 2	Isolated yield% of compound 17	%ee
1	Compound **56**, 15 mol%	1 equiv. (0.35 mmol)	2 equiv. (0.70 mmol)	37%	11%
2	Compound **58**, 15 mol%	1 equiv. (0.35 mmol)	2 equiv. (0.70 mmol)	35%	9%

Reaction conditions: 5 mol% $Cu(OTf)_2$, dry DCM (0.05 M), pre-complexation at –40 °C for 30 min, then reaction at –30 °C for 16 h. Each reaction was tested 3 times and the reported isolated yields are averaged over 3 reactions. *%ee* was determined using chiral HPLC column IA-3, with flow of 1 mL/min using 95:5 *n*-heptane/iPrOH, with UV detection at 220 nm.

3.6 Conclusions and Future Work

In conclusion, this project demonstrated the feasibility of using oxo-rhenium complexes to catalyze biomimetic cyclizations of polyisoprene-like starting materials to give terpene-like products. The data showed in this chapter are a proof of concept that will be expanded in the future. Possible areas of development are listed here: 1) complete the substrate scope by using many different aldehydes (or other different electrophiles) that fits the requirements of this

reaction; 2) expand the utility of the method by trying the reaction with extended polyenes; 3) experimentally demonstrate each step of the proposed catalytic cycle; 4) fully characterize the new, chiral Re complexes; 5) optimize the enantioselectivity of this transformation by using different chiral rhenium complexes; and 6) use the scaffolds obtained with this methodology in the total synthesis of bioactive molecules and natural products.

3.7 References

1. Anastasia, L.; Giannini, E.; Zanoni, G.; Vidari, G. *Tetrahedron* **2005**, *46*, 5803.
2. Vidari, G.; Bonicelli, M. P.; Anastasia, L.; Zanoni, G. *Tetrahedron Lett*., **2000**, *41*, 3471–3474. Anastasia, L.; Giannini, E.; Zanoni, G.; Vidari, G. *Tetrahedron Lett.*, **2005**, *46*, 5803–5806.

Chapter 4: Electrochemical C–H oxidation

4.1 Chapter Abstract

In this chapter, an overview of organic electrochemical methods is described, with particular attention on electrochemical C–H oxidation. The motivation is two-fold: 1) organic electrochemistry has recently witnessed a resurgence as a simplifying method that is complementary to organometallic chemistry and photochemistry; and 2) C–H oxidation is the pinnacle of complexity-generating methodology, which can greatly streamline multistep organic synthesis. Combined together, electrochemical C–H oxidation would be a powerful alternative to traditional C–H oxidation methods because it would avoid the use of stoichiometric oxidants (that are typically expensive, toxic, and/or explosive on large scale) and it would utilize the renewable resource of electricity. General concepts of electrochemical oxidation will be described, which will then set the stage for electrochemical C–H oxidation.

4.2 Copyright/disclaimers

To construct this chapter, two main sources were used, both of which are published papers from Prof. Phil Baran's laboratory: "*Synthetic Organic Electrochemical Methods Since 2000: On the Verge of a Renaissance"* [1] and *"A Survival Guide for the Electro-curious"*.[2] These two reviews were chosen as main sources for this chapter because, during my research experience in the Baran Laboratory, I found that they were the most comprehensive, especially for the electrochemical C–H oxidation that I was investigating. Many portions of this section are reprinted/adapted with permission from: *Chem. Rev.* **2017**, *117*, 13230–13319, Copyright 2017 American Chemical Society; *Acc. Chem. Res.* **2020**, *53*, 72–83, Copyright 2020 American Chemical Society. A copyright permission document is shown at the end of this thesis (p. 272).

4.3 Introduction

The term organic electrochemistry can be simply described as the reduction and oxidation of organic molecules at electrodes: therefore, it is simply redox chemistry. These types of reactions that happen at the electrode surface are conceptually not that different from reactions of inner sphere, ion pairing or complexation reactions. Thus, in many respects, electrochemical reactions are similar to their homogeneous counterparts except for the topology: an electrode is a 2D structure (as in electrode surface area) placed in a 3D volume (as in reaction solution), while molecular redox species are generally dispersed throughout the solution. From a historical point of view, electrochemistry is one of the oldest forms of reaction setups explored in a laboratory. In fact, the first example of an electrochemical reaction dates back to 1800, when the invention of the Volta Pile, the first electric battery, allowed the continual movement of electrons through a circuit.[2] The most important events in the development of electrochemistry and, more specifically, organic electrochemistry, are highlighted in the timeline shown in Figure 4.1.

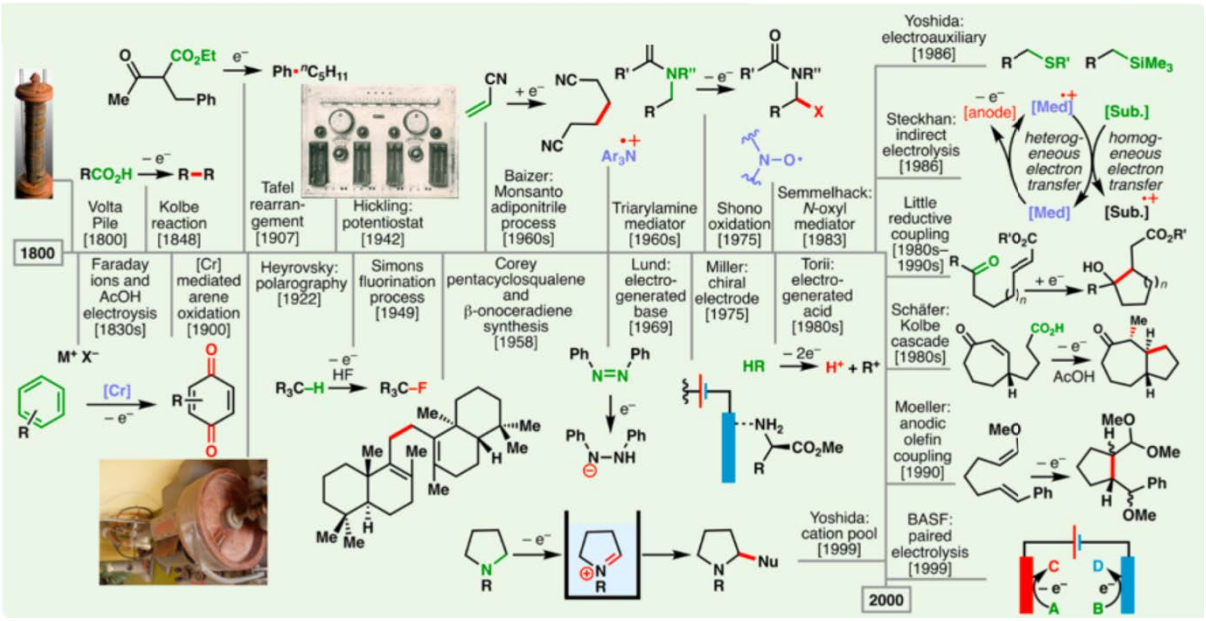

Figure 4.1 A timeline of 200 years of electroorganic chemistry with selected examples. [Reprinted/adapted with permission from: *Chem. Rev.* **2017**, *117*, 13230–13319, Copyright 2017 American Chemical Society].

4.4 Electrochemistry: Basic Concepts

Before describing the most relevant electrochemical transformations, some basic concepts in electrochemistry will be summarized. Comparing an electrochemical reaction with a canonical one, we can identify four basic differences (Figure 4.2A).

1) An electrochemical cell needs a power source (e.g., battery, potentiostat) and it is connected to three different electrodes: anode, cathode, and reference electrode. The term "(+)X/(−)Y" is often used to denote the anodic (X) and cathodic (Y) materials.

2) The driving force of an electrochemical reaction, which is a redox process, is the reaction potential (often described as voltage). In order to achieve this driving force, the power source in the circuit generates an electric potential. This causes an electric imbalance that pushes electrons into the cathode from the anode, creating a reductive environment at the cathode and an oxidative environment at the anode. From a practical point of view, the power source connected to the electrochemical cell controls the potential between the "working electrode" and the reference electrode. It is important to specify that: a) the working electrode is the one where the desired reaction occurs; b) the counter electrode is the other electrode which closes the circuit (either the anode or cathode could be denoted as the "working electrode"); c) the reference electrode is not directly involved in the electrochemical reaction, and is used for the voltage difference between the anode and the cathode that will be controlled by a power source.

3) A parameter that needs to be considered in an electrochemical reaction is the current. The current is defined as the rate of electron movement per unit of time, resulting in redox processes. The current and potential (from #2 above) are linked together.

4) In an electrochemical reaction, the reactants or electrocatalysts in solution undergo a heterogeneous interaction with either the anode (by donating electrons and getting oxidized) or the cathode (by accepting electrons and getting reduced). In order to close the circuit, both oxidative and reductive processes have to occur concurrently.

In order to understand how an electrochemical reaction works, it is important to know how an electrochemical cell is built up (Figure 4.2B). The three main components of an electrochemical cell are:

1) The **power source**. It exists in a variety of forms, and the most common ones are the constant current (galvanostatic conditions) and constant potential (potentiostatic conditions), so depending on the external power source employed, we could perform experiments either with galvanostats or potentiostats. In the modern era, commercial power sources for electrochemistry can perform both modes of electrolysis and are colloquially (and somewhat incorrectly) referred to as potentiostats.

2) The **electrodes.** They can vary in terms of their constitution (material), surface area, and reusability (some anodes may be partially consumed during a reaction, and some anodes are resistant). As electron transfer takes place on the surface of the electrodes, the choice of electrode can impact the outcome of a reaction.

3) The **reference electrode**. When a fixed potential is required, a third electrode, called the "reference" electrode, is employed. This electrode is not essential to perform preparative constant potential experiments, but it is necessary in cases when an accurate and specific potential is required (including cyclic voltammetry). Like any electrical circuit, increasing conductivity/reducing resistance is essential.

Depending on the situation, we use one of the two modes of electrolysis: constant current or constant potential. Every mode of electrolysis has advantages and disadvantages that are summarized below.

1) **Constant Current** *(Recommended).*

- Features: the potential drifts until the substrates for oxidation and reduction are found to maintain current.

- Advantages: easier setup; full conversion.

- Disadvantages: selectivity can be an issue due to over-oxidation or over-reduction.

2) **Constant Potential**

- Features: current adjusts over time to maintain the cell potential.

- Advantages: selectivity can be higher in this mode.

- Disadvantages: requires a reference electrode and full conversion is often not achieved.

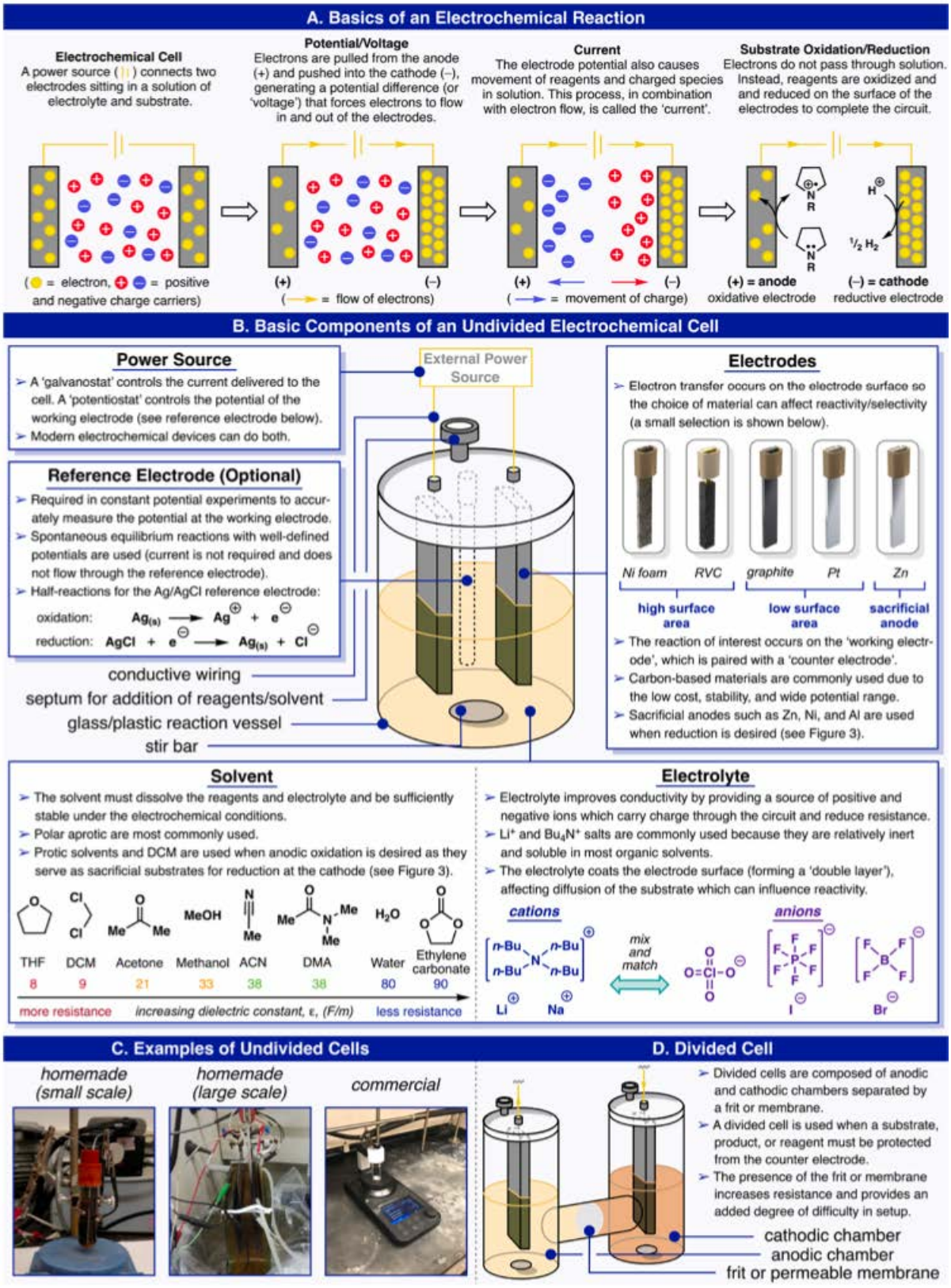

Figure 4.2 (A) Basic features of an electrochemical reaction. (B) Overview of an undivided electrochemical cell. (C) Various types of undivided cells. (D) The divided cell. [Reprinted/adapted with permission from: *Acc. Chem. Res.* **2020**, *53*, 72–83, Copyright 2020 American Chemical Society].

In an electrochemical reaction, the solvent and the electrolyte (a charged species) largely influence the conductivity and the electric resistance in the solution of an electrochemical cell. Ammonium and alkali-metal-based salts are the most commonly employed electrolytes.[3]

One of the key challenges for the field of organic electrochemistry was the non-standardized nature of available equipment options, as most literature examples had relied on homemade electrochemical setups with variable reproducibility (Figure 2C). This issue has been addressed by a number of researchers,[4] and in particular, Professor Phil Baran's laboratory had a significant contribution in this regard, especially in the collaboration with IKA and the launch of ElectraSyn 2.0, a device for organic electrochemistry.[5-6] The IKA ElectraSyn 2.0 is a standardized device that reduces reproducibility problems, and in turn encourages the adoption of electrochemistry in both academic and industrial laboratories.

In certain scenarios, it might be desirable for a species formed at one electrode to not react at another, in which an alternative setup referred to as a "divided cell" can be employed (Figure 4.2D). In this setup, the electrodes are located in two chambers separated by a permeable membrane or a frit. Such setups are often more complicated for the user (e.g., due to the separative membranes, as well as inherently higher resistance), and therefore the use of an undivided cell is generally preferred. In any organic chemistry methodology, the most practical reactions rely on their ability to be scaled up, and thus several groups have developed electrochemical flow setups that overcome challenges of mass transfer, rate, and stability of electrode materials to enable large scale transformations. All these advances in experimental setups and conditions have recently made electrochemistry a powerful and user-friendly synthetic tool.[7,8]

4.5 Electrochemical Oxidation

In this section, examples of electrochemical oxidation will be discussed. Most examples in the literature regard the decarboxylative Kolbe reaction, C–H oxidations α to a nitrogen atom (Shono oxidation), alcohol oxidation, and benzylic C–H oxidation, since these are systems that are more susceptible to oxidation. However, advances in electrochemistry needed to achieve these transformations have recently culminated in the electrochemical oxidation of "unactivated" C–H bonds. The purpose of this section is to highlight the great potential this chemistry is capable of, and how the field has grown over the past decade.

4.5.1 Kolbe reaction

One of the most famous electrochemical oxidations is the classical Kolbe Reaction. Although not formally an oxidation of a C–H bond, this reaction is included for historical purposes, as well as setting the stage for other oxidation mechanisms. This transformation starts with the anodic oxidation of alkyl carboxylates, and subsequently, the resulting radical undergoes facile decarboxylation. The alkyl radical that is generated in this oxidation process then dimerizes, forming a C−C bond. The Kolbe electrochemical oxidation was investigated by several

research groups, especially before the year 2000, and all the discoveries before that year had already been summarized in several reviews. [9–11] In recent years, this transformation has been utilized for the synthesis of benzathine, [12] the construction of bis-phosphine oxide ligands, [13] and dimerization of silylacetic acids [14–16] and fatty acids. [17] Unlike the classical Kolbe reaction, in which the dimerization reaction happens between two molecules of the same carboxylic acid species, the mixed Kolbe reaction is a heterodimerization between two different alkyl carboxylic acids. This is less commonly known, and since a statistical mixture of homodimerized and heterodimerized products typically forms, an excess of one acid component is often necessary to favor the latter. [18] Renaud and co-workers used a mixed-Kolbe electrolysis for the synthesis of dihydropertusaric acid (Figure 4.3A). [19] In this case, the ketal-containing carboxylic acid was used in large excess (8 equiv.).

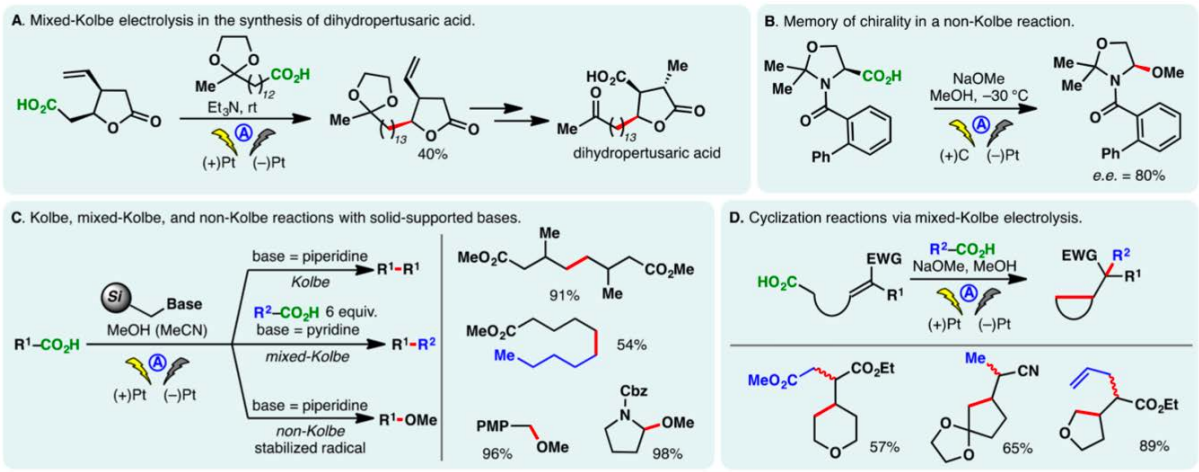

Figure 4.3 Oxidation of carboxylates: the Kolbe reaction and related processes. [Reprinted/adapted with permission from: *Chem. Rev.* **2017**, *117*, 13230–13319, Copyright 2017 American Chemical Society].

Since this reaction follows trends in radical stability, carboxylic acids with an α substituent are able to stabilize the radical obtained from the electrochemical decarboxylation process (e.g., an α-amino group in an amino acid). Interestingly, when Kolbe electrolysis is performed on such substrates, further electrochemical oxidation can occur, and the resulting cation (e.g., an acyl iminium cation) can be trapped with an external nucleophile, undergoing a non-Kolbe reaction. An interesting example of a non-Kolbe reaction is shown in Figure 4.3B.[20] In this example reported by Matsumura and co-workers, the electrochemical oxidation of an *N*-acylated serine derivative exhibited some "memory of chirality" and the methoxylated product was afforded in 80% ee. [21, 22]

In terms of reaction conditions, in the Kolbe electrolysis, usually a base is added into a solution of carboxylic acids, forming the corresponding carboxylate salts. In this way, the substrate not only serves as the molecule that undergoes the decarboxylation reaction, but also acts as an electrolyte for the electrochemical transformation. Interestingly, as shown in Figure 4.3C, the Tajima and Fuchigami groups developed protocols to conduct Kolbe,[23] mixed-Kolbe,[24] and non-Kolbe [25,26] reactions using solid-supported bases like piperidine or pyridine. In

these protocols, after completion of the electrolysis, the base could be removed simply through filtration, making the process much simpler from an operational standpoint. Other important improvements in this regard were achieved by the Chiba group, who reported an efficient protocol for the Kolbe reaction using cycloalkane-based thermomorphic systems. [27] In addition, Compton and co-workers developed an aqueous protocol for running the Kolbe reaction of water-immiscible aliphatic acids through ultrasonication and emulsion formation. [28]

An extension of the Kolbe reaction is a cyclization cascade developed by Schäfer.[9, 29] In this process, a carboxylic acid generates an alkyl radical electrochemically, after which it cyclizes onto a tethered olefin intramolecularly. The resulting radical can then combine intermolecularly with an alkyl radical derived from the anodic decarboxylation of another carboxylic acid. More recently, Marko and co-workers reported a method to prepare five- and six-membered rings using this cascade reaction (Figure 4.3D). [30] The use of an electron-deficient olefin is necessary in this reaction because of the nucleophilic character of alkyl radicals. Addition onto Michael acceptors [31,32] and the use of bis-carboxylic acids (i.e., malonic acids) [33] have also been described.

4.5.2 α-Oxidation of amines and amides: Shono-type oxidation

Shono oxidation is a classic organic electrochemistry reaction in which an *N*-acylamine is oxidized to form an iminium ion, which can then be trapped by various nucleophiles. There are two parts to this reaction: oxidation at the anode, and reduction at the cathode. For example, in the Shono oxidation of *N*-Boc-pyrrolidine in methanol, the pyrrolidine substrate loses two electrons at the anode (i.e., gets oxidized), resulting in an acyliminium ion and a proton (Figure 4.4). This oxidation is likely achieved in two steps: a one-electron oxidation to an *N*-centered radical cation, followed by another one-electron oxidation to release a proton and generate an iminium ion. The two electrons thus freed can then travel from the anode to the cathode. At the cathode, two molecules of methanol gain two electrons (i.e., gets reduced) to form a molecule of hydrogen and two methoxide ions. The iminium ion is then trapped by methoxide to form the final α-oxidation product. It is indeed a combination reaction between an oxidized species and a reduced species, both of which are charged. A key additive in this reaction is the electrolyte, which is typically an organic salt such as Et_4NBF_4. This electrolyte facilitates the movement of the formed ionic species and helps maintain an ionic medium such that the electrons can move freely from the anode to the cathode. The amount of electrons extracted from the anodic oxidation must equal that of the electrons consumed in the cathodic reduction. The two half-reactions at the anode and the cathode must both be efficient, since problems with either one of the two will affect the flow of electrons and prevent the electrochemical redox reaction from taking place (Figure 4.4).

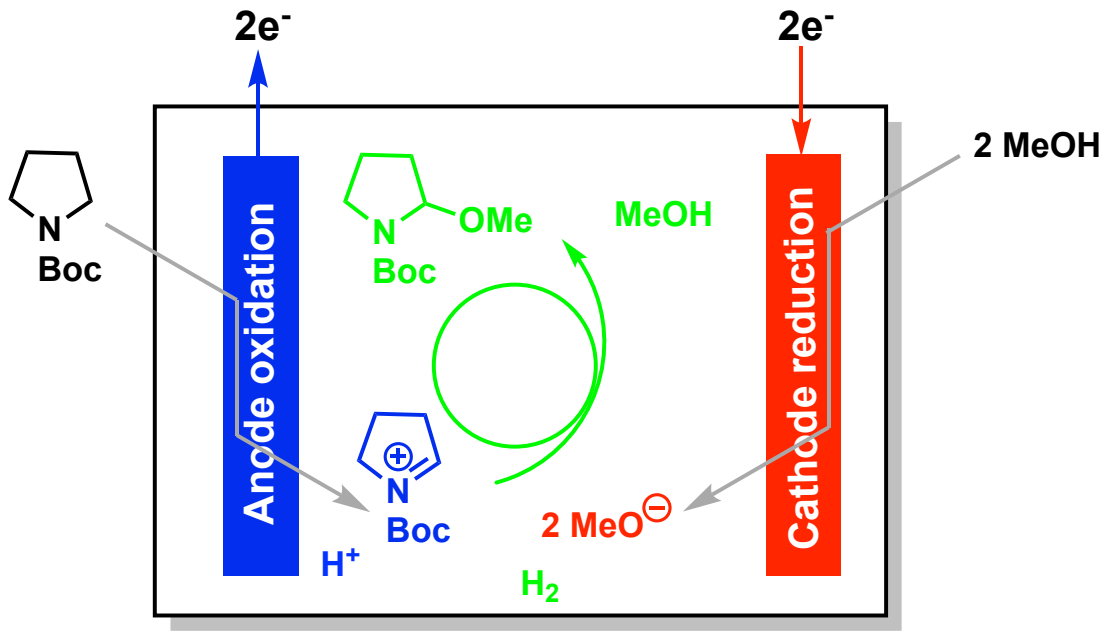

Figure 4.4 Schematic representation of the two half-reactions (anodic oxidation and cathodic reduction) of a Shono oxidation.

The Shono-type oxidation reaction described above is useful for generating *N*-acyl or *N*-carbamoyl iminium ions,[34,35] which is then trapped as an isolable *N*,*O*-acetal when the reaction is conducted in alcoholic solvent. This species can then be reverted to an acyliminium ion upon treatment with acid to allow for further functionalizations. Recent efforts have been made to render this sequence asymmetric with chiral auxiliaries (Figure 4.5A). For example, Shono methoxylation of chiral carbamates, [36–39] phosphoramides, [40, 41] and sulfinamides [42] has been developed (Figure 4.5A, (1)−(3)). Typically, the methoxylation step results in poor diastereoselectivity, but this is inconsequential; it is the nucleophilic addition (e.g., of an allyl silane) onto the iminium species that imparts stereoselectivity. Good stereoselectivity (d.r. >20:1) of the initial electrochemical oxidation was observed when the alkoxy nucleophile was tethered with chiral cyclic amides, however, analogous acyclic amides led to virtually no selectivity (d.r. 1.4:1; Figure 4.5A, (4)). [43] Evans oxazolidinone chemistry has also been fitted into a Shono oxidation paradigm to give enantiomerically enriched Mannich adducts.[44]

When an unsymmetrical cyclic system is used, the Shono oxidation typically occurs at the less substituted position (Figure 4.5B). However, the regiochemical outcome of the methoxylation step may be reversed by using *N*-cyanoamines.[45] Interestingly, the cyano group substantially stabilized the more substituted iminium ion, thereby favoring methoxylation at the more substituted position, but this effect was not observed with carbamates (*N*-alkoxycarbonyl amines). The Shono oxidation of bicyclic carbamates mainly occurs at the ring junction, but with little stereocontrol (Figure 4.5C).[46] The use of a trifluoromethyl group in place of the carbamate carbonyl group enhanced the regio- and stereoselectivity of the process.

Despite the low, and seemingly accessible, redox potentials of amines, anodic oxidation of alkyl amines is performed to a lesser extent compared to amides. This might be due to the

instability of the aminyl radical cations and imines. Despite this, Gallardo and co-workers have achieved the anodic oxidation of alkyl amines to synthesize substituted imidazoliniums, tetrahydropyrimidiniums,[47] and hindered alkyl diamines.[48] When a nucleophile is tethered to the amine component, the reactive intermediates can be trapped intramolecularly, giving cyclized products (Figure 4.5D).[49, 50] Furthermore, the Shono-type oxidation is more useful with anilines or benzyl amines, which form more stabilized radical cation intermediates.[51]

A mediator is a species that "mediates" the electrochemical oxidation by getting oxidized first, and then transfers this oxidation to the substrate thereafter. This allows the reaction to proceed in a selective manner. As such, a sensitive substrate does not suffer the full extent of the electrochemical potential that is applied, and it can undergo oxidation with minimal degradation. For example, electrochemical oxidation of dialkyl anilines was achieved when using a specific mediator, a stabilized nitroxyl mediator (4-OBz-TEMPO) (Figure 4.5E).[52] The reaction takes place at the less substituted position, wherein the *N*-methyl group is preferentially oxidized, furnishing a formamide. Other additives can sometimes be beneficial to an electrochemical reaction. For example, in the Shono-type oxidation of imidates and imines (Figure 4.5F),[53], the addition of ammonium sulfate was found to improve the reaction yield. Although its role is unclear, ammonium sulfate presumably maintains a neutral pH in the electrochemical cell, thus suppressing the oxidation of cathodically generated methoxide. A similar α-methoxylation/acetoxylation of imines can be achieved, this time with the aid of tetraethylammonium bromide as a mediator (Figure 4.5F, right).

In an interesting application of Shono-type chemistry, instead of oxidizing the C–H bonds at the α-carbon of amides and carbamates, allyl and benzyl groups at that position were cleaved (Figure 4.5G).[54] In this C–C cleavage reaction, preliminary mechanistic studies revealed that the process involves allyl cationic species rather than the analogous radicals.

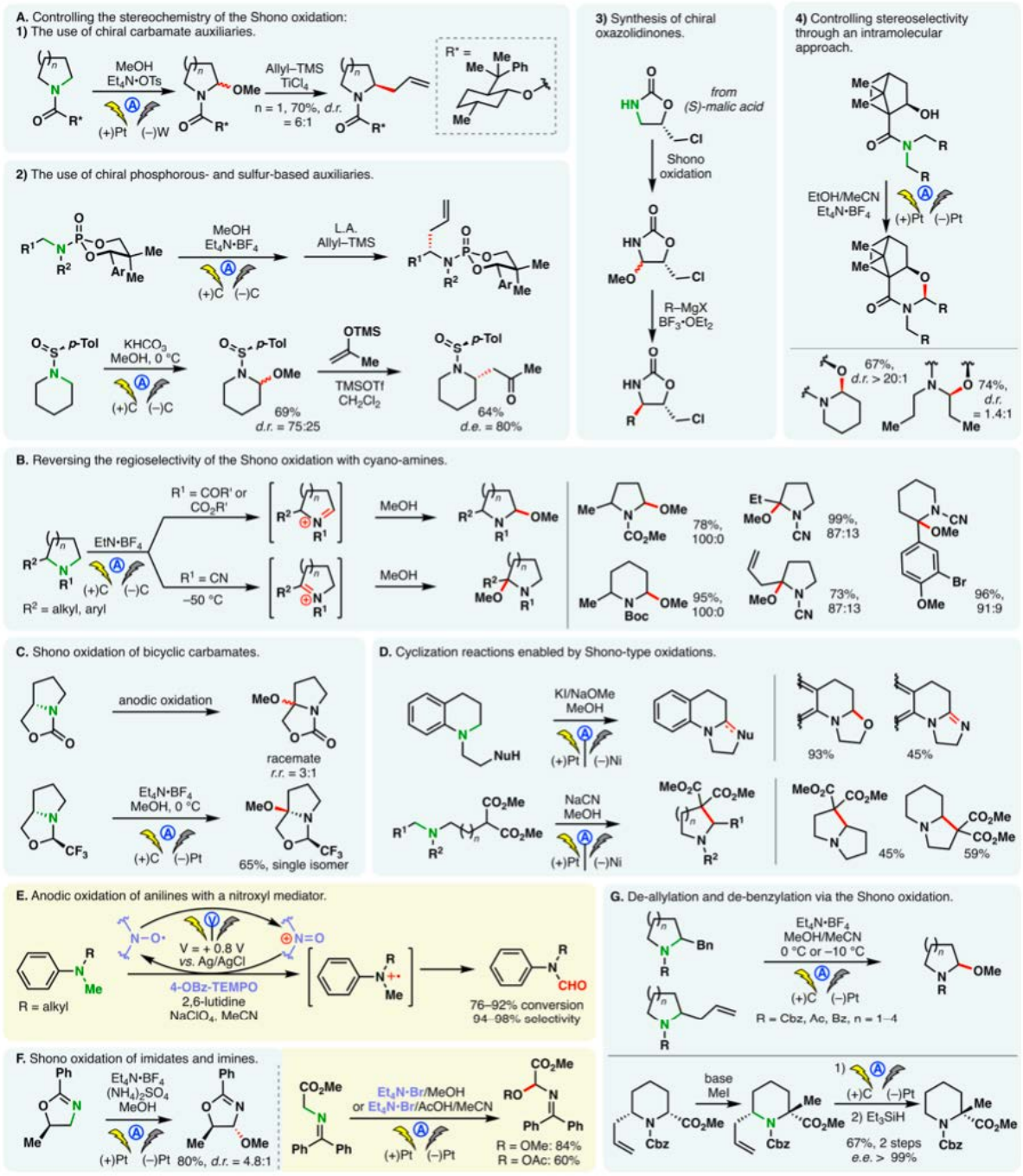

Figure 4.5 Shono oxidation: variation of nitrogen substituents. [Reprinted/adapted with permission from: *Chem. Rev.* **2017**, *117*, 13230–13319, Copyright 2017 American Chemical Society].

Shono-type oxidations are most commonly observed with alcohols as nucleophiles due to their relatively high oxidation potential compared to amides/carbamates. Although conceptually feasible, trapping the intermediary iminium with carbon-centered nucleophiles such as cyanides or enol ethers can be complicated by competing anodic oxidations of these nucleophiles. Instead, a two-step process might be beneficial, wherein an *N*,*O*- acetal is first

formed electrochemically and isolated, then subjected to further chemical manipulations. Triphenylphosphine,[55] sulfone,[56] and benzotriazole [57] are examples of nucleophiles that are enabled in this manner.

To shorten this two-step process, Tajima and co-workers devised a one-step anodic α-cyanation reaction based on the principle of "site isolation" (Figure 4.6A).[58] $Bu_4N \cdot BF_4$ and the cyanide salt of a solid-supported quaternary ammonium cation (PS-$NMe_3 \cdot CN$) were introduced into the reaction: the former served as the supporting electrolyte, while the latter reduced the effective concentration of cyanide in the solution phase, keeping CN^- in vicinity to the polymer support. Cyanide oxidation was thus suppressed, as evidenced by cyclic voltammetry (see Figure 4.6A inset). Similarly, using a "phase separation" approach, Atobe reported an example of direct Shono allylation (Figure 4.6B).[59] In this case, an ionic liquid ($EMM \cdot BF_4$) [60] was chosen as the reaction medium, wherein the nucleophile (allyl−TMS) has minimal solubility. Although sufficient interaction between the nucleophile and the anodically generated iminium can be achieved by sonication, oxidation of the nucleophile is minimized by virtue of its poor solubility and conductivity.

Tajima also reported a one-pot allylation of lactams (Figure 4.6C).[61] This strategy involved a Shono oxidation with hexafluoroisopropanol (HFIP) as the trapping electrophile, after which the hexafluoroisopropoxy group can be readily displaced by carbon-based nucleophiles such as allyl-TMS. A key aspect of this reaction is the use of a solid-supported base: the base allows for the *in situ* generation of electrolytes, and it may be removed through a simple filtration. Furthermore, the use of solid-supported bases in MeOH has enabled a series of electrochemical methoxylation reactions wherein methoxide anions are generated *in situ*.[62–64] Continuing the theme of amide α-allylation using allyl-TMS, undesired oxidation of the allyl nucleophile can be minimized with a flow chemistry approach (Figure 4.6D). [65, 66]

Onomura showed that a one-step anodic cyanation of amides/carbamates is also possible using TMSCN as the nucleophile (Figure 4.6E). [67]. The addition of methanesulfonic acid ($MeSO_3H$) was found to be crucial for this reaction. Furthermore, Huang and co-workers demonstrated that anilines could be introduced to the α-position of lactams through direct anodic oxidation when the lactam was used in excess (Figure 4.6F).[68] Maintaining a high current density at the anode was found to be critical: even though the oxidation potential of anilines is lower than that of lactams, the more concentrated lactam could undergo preferential oxidation at high current densities.

For the α-oxidation of amine substrates, clever solutions were employed. Luo and co-workers developed an anodic coupling between tetrahydroisoquinoline derivatives and alkyl ketones through the combination of Shono-type oxidation and enamine catalysis, giving enantioenriched products (Figure 4.6G).[69] For the imidation of aliphatic amines, Wang and co-workers used tosyl azide, giving *N*-tosylamidines (Figure 4.6H).[70] The anodically generated imine/iminium likely tautomerizes into the corresponding enamine, which can engage tosyl azides in a cycloaddition, upon which fragmentation of the cycloadduct affords the amidine products.

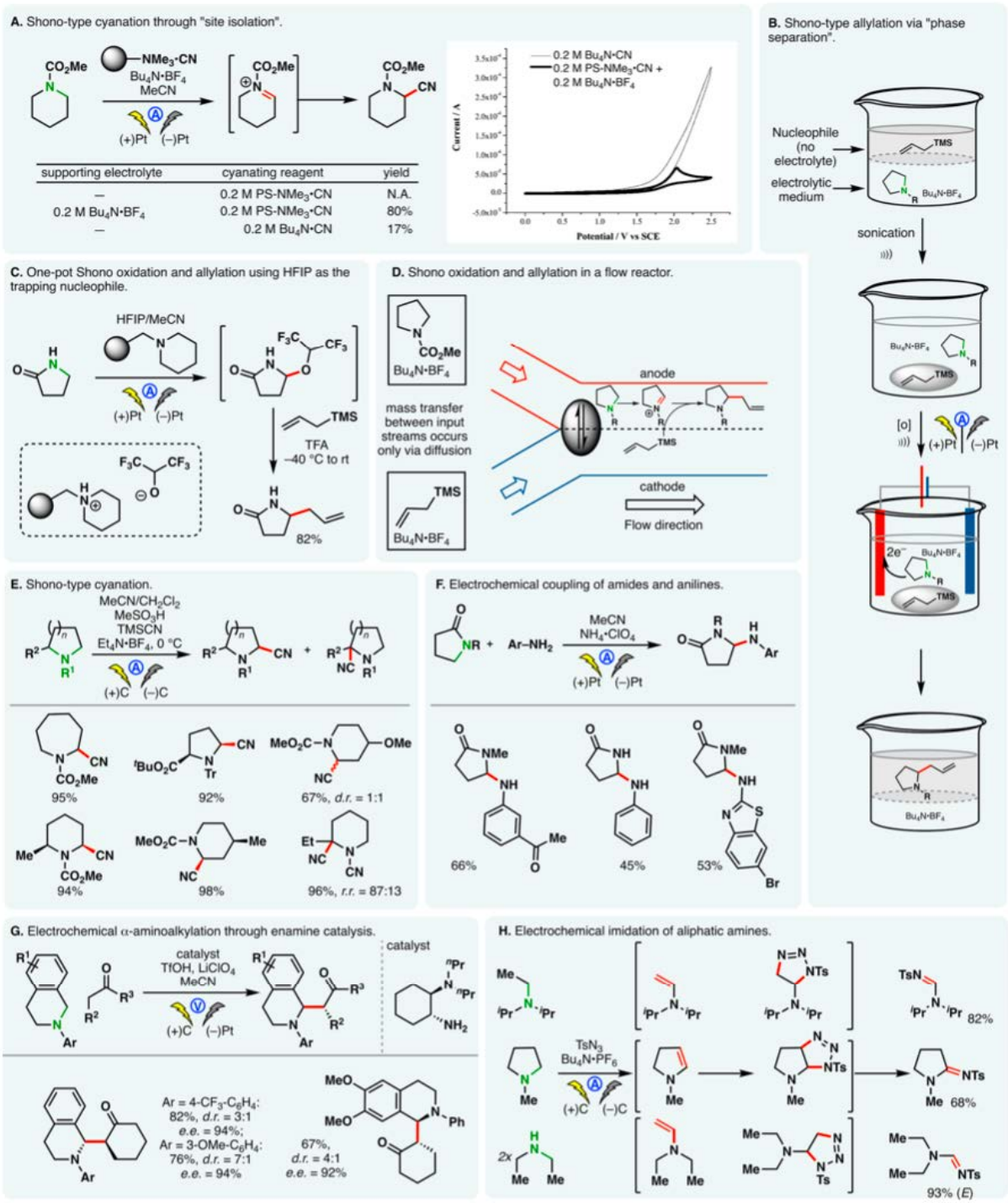

Figure 4.6 Shono oxidation: variation of trapping nucleophiles. [Reprinted/adapted with permission from: *Chem. Rev.* **2017**, *117*, 13230–13319, Copyright 2017 American Chemical Society].

4.5.3 Oxidation of Alcohols

A seemingly simple substrate to oxidize is an alcohol, yet advances were required to allow for this transformation to occur electrochemically without substrate degradation and over-oxidation. After all, alcohol oxidations that are reagent-based typically require stoichiometric oxidants that are toxic (e.g., Cr-based oxidations), explosive (e.g., iodine(V)-based oxidations), or impractical on a large scale (e.g., Swern oxidation), and are therefore not necessarily the most optimal from an atom economy or a green chemistry point of view. One advantage of electrochemical oxidation is the use of electricity as the stoichiometric oxidant, and therefore less by-products of reagents are produced. A seminal report in 1983 started the field's interest in the indirect anodic oxidation of alcohols by using TEMPO, a nitroxyl radical, as the mediator (Figure 4.7A, compound A).[71] Under electrochemical conditions, nitroxyl radicals can be oxidized into the corresponding oxoammonium species, which are the reactive oxidants. Related nitroxyl mediators bearing ionic tags (e.g., Figure 4.7A, compound C) have been developed, as their solubility in aqueous electrolyte solutions are increased.[72] Bicyclic nitroxyl mediators were found to be superior in the anodic oxidation of hindered secondary alcohols compared to TEMPO (Figure 4.7B).[73] At the time, this enhanced reactivity was attributed to steric effects, as these bicyclic structures are actually smaller and more likely to engage with the substrate.

Several years later, Stahl and co-workers reported that the catalytic activity of nitroxyl mediators is more strongly influenced by the nitroxyl/oxoammonium redox potential than steric effects.[74] Their study led to the identification of an acetamido-TEMPO nitroxyl (Figure 4.7A, compound B) as an effective and inexpensive mediator. These studies were further supported by computational models from Minteer, Sigman, and co-workers that identified structure–functional relationships of nitroxyl radicals to accurately predict their electrochemical potentials and catalytic activities (Figure 4.7C).[75] Despite these advantages, TEMPO and many other nitroxyl mediators are sparingly soluble in polar electrolytic media, limiting their synthetic utilities; this can be solved by a "double mediatory system", which is essentially a biphasic or emulsion system involving halides as a second mediator in addition to the nitroxyl mediator (Figure 4.7D).[76] Furthermore, an elegant method to resolve secondary benzyl alcohols was reported, wherein a double mediatory system with NaBr and a binaphthyl-based chiral mediator was used (Figure 4.7E, left).[77] To address further solubility concerns, nitroxyl mediators could be dispersed onto a polymer support or an emulsion,[78–83] or anchored onto the surface of an electrode.[84–86] For example, by attaching a chiral spirocyclic *N*-oxyl mediator onto a graphite anode, an electrocatalytic method to desymmetrize *meso*-diols was achieved (Figure 4.7E, right).[87] Other anode fixation examples include a pyrene-tethered TEMPO derivative with *in situ* noncovalent immobilization onto a carbon anode,[88] and a method to covalently immobilize TEMPO onto linear poly(ethylenimine) with cross-linking onto a glassy carbon electrode.[89] These modified electrodes exhibited significantly enhanced catalytic current density compared to the analogous systems employing TEMPO as the redox catalyst. On a slightly different substrate family of glycosides and disaccharides, the TEMPO-mediated electrochemical oxidation converted primary alcohols selectively, leaving secondary alcohols and other functional groups intact (Figure 4.7F).[90]

The alcohol oxidation methods described above all rely on the interconversion between nitroxyl and oxoammonium species (i.e., radical to cationic forms), which occurs at a relatively high potential compared to that between the hydroxylamine and nitroxyl (i.e., neutral to radical forms). Stahl and co-workers reported a "cooperative electrocatalytic system" using Cu(II) and TEMPO, which exploits the low-potential conversion between TEMPO and its hydroxylamine TEMPO-H (Figure 4.7G).[91] This dual system allows alcohol oxidations to occur at higher rates and at a significantly lower potential. Nitrate salts have been used as electrochemical mediators to oxidize secondary benzyl alcohols, wherein the nitrate radical serves as the reactive oxidant (Figure 4.7H).[92,93] Halides and oxyhalide anions could also serve as mediators in the electrochemical oxidation of alcohols (Figure 4.7I−K). For example, oxidative cleavage of diols have been reported, wherein sodium periodate is anodically generated in a biphasic system (Figure 4.7I).[94] Unmediated diol cleavage has also been described.[95] Interestingly, 1,2-diols can be efficiently oxidized into α-hydroxyketones under electrochemical conditions using $Et_4N{\cdot}Br$ as the mediator (Figure 4.7J).[96] In this reaction, Me_2SnCl_2 is an essential, catalytic additive since it converts the vicinal diol to the corresponding stannylene acetal, where the reversible cleavage of a Sn−O bond allows halide-mediated alcohol oxidation. The organotin reagent used in this reaction may be replaced by a copper salt with a chiral ligand, with which racemic substrates may be resolved.[97] A NaCl-mediated oxidation of cholic acid into dehydrocholic acid was reported (Figure 4.7K) [98] wherein the nature of the anode was found to play an important role in the selectivity of alcohol oxidation.[99] Other mediators for alcohol oxidation include Shvo's Ru catalyst [100] and *N*-aryl carbazole (Figure 4.7L).[101] For multiple oxidations, anodic oxidation of cholesterol led to the formation of cholesta-4,6,-diene-3-one (Figure 4.7M),[102] which was further optimized on larger scale with a flow cell.[103]

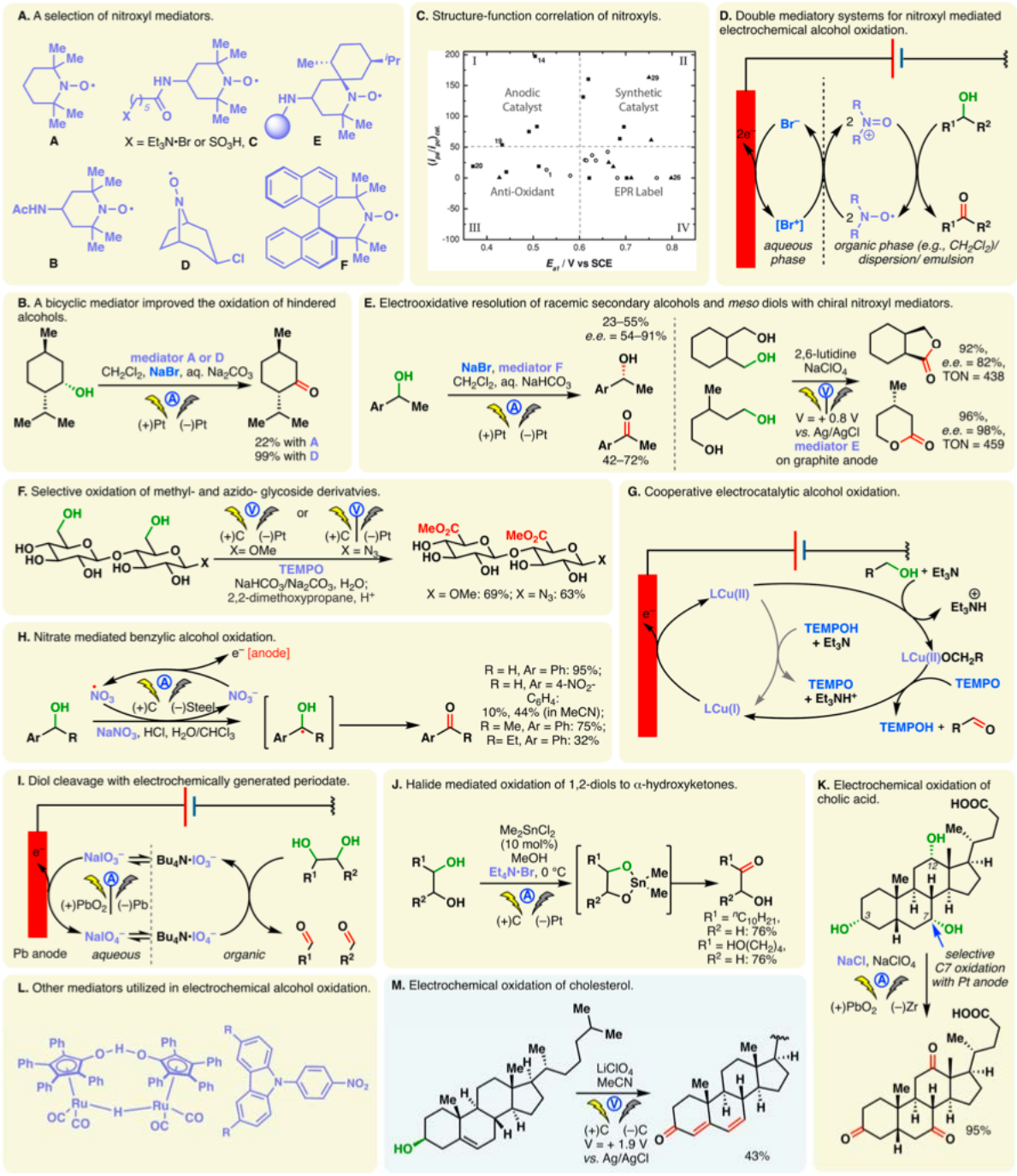

Figure 4.7 Electrochemical oxidation of alcohols. [Reprinted/adapted with permission from: *Chem. Rev.* **2017**, *117*, 13230–13319, Copyright 2017 American Chemical Society].

4.5.4 Benzylic Oxidation and Benzylic Functionalizations

With discoveries through Kolbe and Shono reactions, as well as alcohol oxidation, the field of electrochemistry accumulated enough collective knowledge to functionalize more difficult bonds in organic chemistry. C–H functionalization and C–H oxidation are the pinnacle of difficulty in organic synthesis because C–H bonds are nonpolar and their bond dissociation

energies are high. As a point of entry, the easiest C–H bond to functionalize from the perspective of bond strength is the benzylic C–H bond. Electron-rich and electron-neutral arenes exhibit relatively low redox potentials, and can undergo anodic oxidation to form the corresponding radical cations. When an arene is substituted with an alkyl side chain, the aryl radical cation can undergo further oxidation to a benzyl cation after losing a proton. This presents a convenient gateway to benzylic functionalization. One application of this electrochemical process is the oxidative cleavage of *para*-methoxybenzyl (PMB) ethers (Figure 4.8A).[104] This deprotection process compares favorably with common chemical methods involving strong oxidants such as CAN because stoichiometric waste of transition metal by-products are not generated.

Regarding benzylic oxidation, Wang and co-workers demonstrated that the benzyl cation intermediate formed after the first oxidation could be intercepted with water, after which further oxidation of the resulting benzyl alcohol furnishes the ketone (Figure 4.8B).[105] This process is most effective for methylene units substituted with two arenes. This type of benzylic oxidation could also access dihydroisoquinolinones, isochromanones, and xanthenones by using a dual mediator system comprising TEMPO and sodium bromide (Figure 4.8C).[106] This benzylic oxidation process compares favorably with the common chemical method of using stoichiometric DDQ, which presents stoichiometric waste that is often difficult to remove. Through electrochemistry, DDQ can be used in catalytic amounts to effect benzylic oxidation as well (Figure 4.8D).[107] Furthermore, *N*-hydroxyphthalimide (NHPI) could mediate benzylic oxidation reactions under aerobic and electrochemical conditions (Figure 4.8E). [108]

As mentioned previously, mediators are of critical importance in electrochemistry because they can tune the reactivity when the required potential is high enough to decompose the substrate. The structures of the mediators are directly related to their electronics, and in turn, correlate to the types of substrates they can mediate. For example, a series of triarylimidazoles were used as redox mediators, wherein electron-donating or electron-withdrawing groups modulated the oxidation potential (Figure 4.8F, left).[109,110] Electrochemical oxidation of these mediators occurs first to give imidazole radical cations, which subsequently facilitate benzylic oxidation reactions under mild conditions (Figure 4.8G).[109] This class of mediators were also used to induce the ring opening and Friedel–Crafts arylation of epoxides (Figure 4.8H).[111] In this example, the use of a mediator circumvented overoxidation of the product, even though it has a lower oxidation potential than the starting material and is therefore susceptible. This reaction can also be conducted using a polymeric ionic liquid and carbon black composite as the supporting electrolyte.[112] Further elaboration of these imidazole mediators led to 2-aryl-1-methylphenanthro[9,10-*d*]imidazoles, which showed higher radical cation stability and a broader range of accessible electrochemical potentials (Figure 4.8F, right).[113]

Diaryl carbenium cations obtained through electrochemical benzylic oxidation may, in some cases, be accumulated under cryogenic temperatures in a cation pool, which can then be trapped with carbon-centered nucleophiles such as heteroarenes, organozinc reagents, or silyl ketene

acetals (Figure 4.8I).[114,115] In an alternative reaction paradigm, they may be subjected to cathodic reduction where the ensuing radical undergoes homodimerization. This diarylcarbenium cation pool could also lead to the synthesis of dendritic molecules through iterative cation pool formation and nucleophile trapping (Figure 4.8J).[116–119]

Yoshida and co-workers reported that diarylcarbenium cations can be trapped with DMSO and treated with a base to furnish a ketone, resembling a Swern oxidation mechanism (Figure 4.8K).[120] Unlike diarylcarbeniums, other types of benzyl cations are generally unstable even at –78 °C, and direct formation of cation pools are typically unfeasible. Instead, Yoshida showed that these fleeting cations may be generated in the presence of a sulfilimine, leading to the formation of a stabilized benzylaminosulfonium cation pool (Figure 4.8L).[121] The resulting aminosulfonium group can be readily displaced by a variety of carbon-based nucleophiles to give rise to benzylic substitution products. Furthermore, treatment of the aminosulfonium group with iodide was found to cleave the N–S bond, resulting in benzylic amination products.[122]

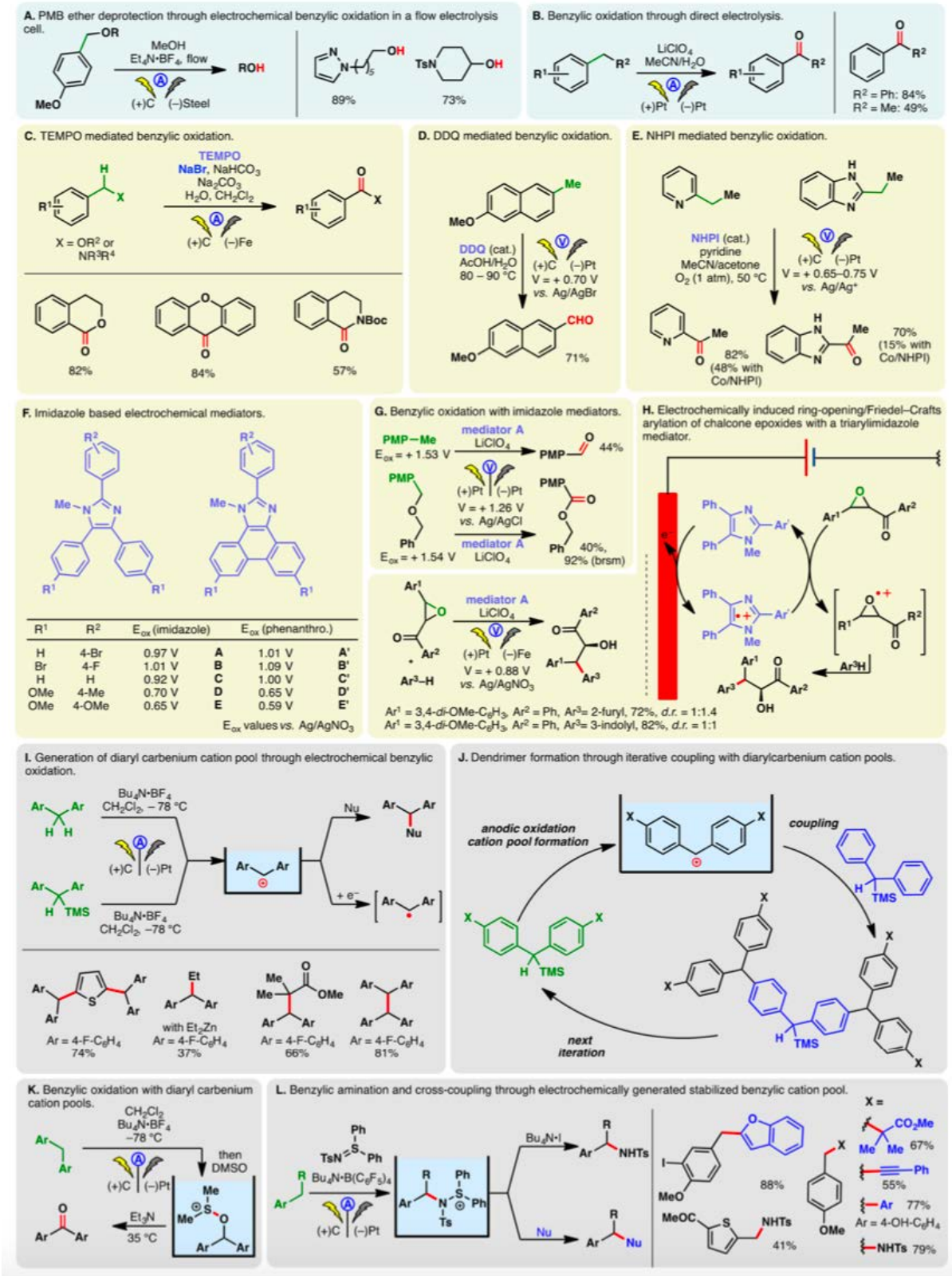

Figure 4.8 Electrochemical benzylic oxidation. [Reprinted/adapted with permission from: *Chem. Rev.* **2017**, *117*, 13230–13319, Copyright 2017 American Chemical Society].

4.5.5 Oxidation of Aliphatic C–H bonds

Although many methods for electrochemical benzylic C–H oxidation have been described, aliphatic C–H bonds in both allylic and unactivated systems have very high oxidation potentials, and as a result, examples of direct anodic oxidation of such systems are rare. In 2005, Sobkowiak reported that the allylic position of cholesterol can be electrochemically acetoxylated in modest yields (Figure 4.9A).[123]

Electrochemically oxidizing bonds that have high oxidation potentials requires high reaction potential to activate such bonds. However, such high reaction potentials tend to decompose the substrates in question. Thus, the challenge of oxidizing aliphatic C–H bonds can be overcome through indirect electrolysis, employing an appropriate mediator. To this end, Baran and co-workers have reported some of the only examples of allylic and unactivated C–H bond oxidation to date.[124, 125] For the former type of C–H bond, a scalable means for allylic oxidation was achieved using tetrachloro-*N*-hydroxyphthalimide (TCNHPI) as the mediator (Figure 4.9B).[124] Under basic conditions, the anion of the mediator is oxidized anodically, giving rise to a reactive *N*-oxyl radical, which can abstract the hydrogen from the allylic C−H bond. The electron-withdrawing chloride atoms enhance the reactivity of the nitroxyl species, as the use of non-chlorinated NHPI led to inferior results. This process utilizes inexpensive electrode materials and is amenable to large-scale synthesis. This reaction tolerates functional groups such as ketones and alcohols, with complex steroids, monoterpenoids, and triterpenoids being oxidized on 100 g scale.

In the most recent development, the most difficult electrochemical C–H oxidation has been achieved: the “unactivated” C–H bond, that is, a non-benzylic, non-allylic, and non-acidic C(sp^3)–H bond that is not adjacent to a heteroatom or a carbonyl group. [125] Attempts to adapt the TCNHPI mediatory system to oxidize unactivated methylene and methine C–H bonds were unsuccessful, presumably because the nitroxyl radical species is not strong enough to cleave these bonds. To overcome this problem, Baran and co-workers developed a quinuclidine-based mediator system that allowed the functionalization of unactivated methylene and methine units (Figure 4.9C).[125] Selectivity for methylene oxidation is dependent on both steric and electronic factors, for example, homolysis of an electron-rich C–H bond distal to electronegative functionalities is usually preferred. Oxidation of sclareolide was achieved on 50-g scale, affording the corresponding 2-oxo product selectively. The electrochemically generated quinuclidine radical cation is believed to be the reactive species in this reaction.

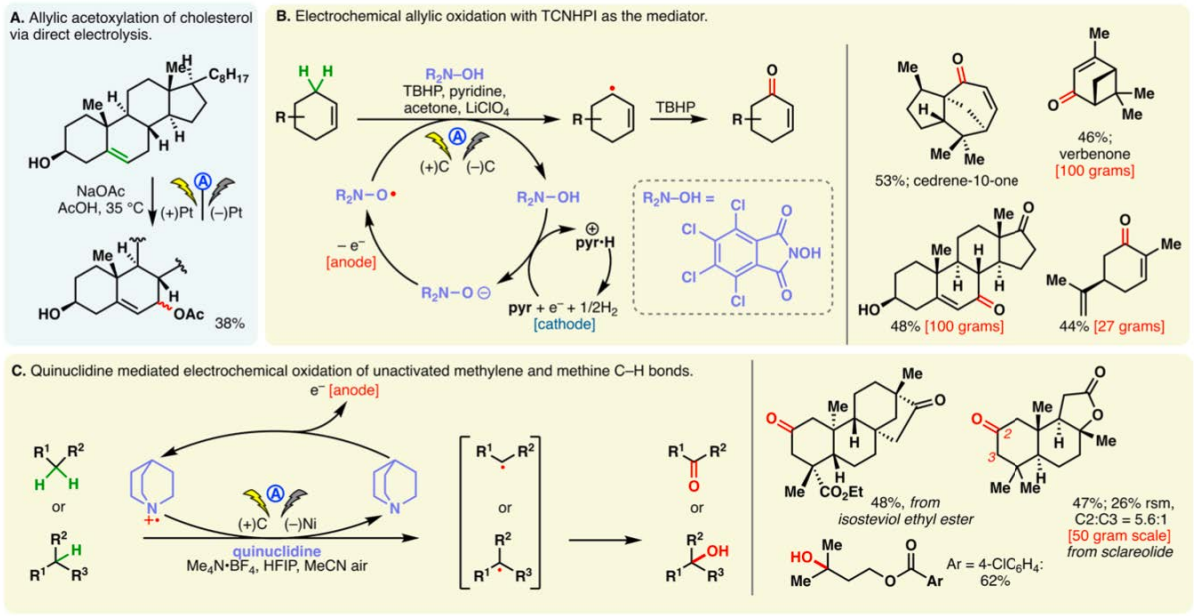

Figure 4.9 Electrochemical oxidation of allylic and unactivated C–H bonds. [Reprinted/adapted with permission from: *Chem. Rev.* **2017**, *117*, 13230–13319, Copyright 2017 American Chemical Society].

4.6 Outlook

As described in this Chapter, electrochemistry has the ability to oxidize many types of bonds at the anode, and has made significant advances as to even oxidize unactivated C–H bonds. Much like photochemistry often relies on photosensitizers to tune the reactivity, electrochemistry often relies on mediators to dial in the desired reactivity onto molecules of interest. (Electrochemical mediators are not always required for every transformation, however.) The opportunities for electrochemical discovery are seemingly endless, yet there is an equally daunting task of finding just the right mediator to achieve a certain transformation. This search for mediators has thus far been an empirical endeavor, but laboratories around the world are continuously developing new methods to streamline this trial-and-error process. This field is still in its infancy, with so many more systematic approaches to be uncovered. Finally, electrochemistry can also be designed as cathodic reduction and academic progress in this field is also being achieved, [1,2] however, reduction chemistry is beyond the scope of this thesis.

4.7 References

1. Yan, M.; Kawamata, Y.; Baran, P. S. *Chem. Rev.* **2017**, *117*, 13230.
2. Kingston, C.; Palkowitz, M. D.; Takahira, Y.; Vantourout, J. C.; Peters, B. K.; Kawamata, Y.; Baran, P. S. *Acc. Chem. Res.* **2020**, *53*, 72.
3. Shono, T., *Oxidation by Electrochemical Methods. In Comprehensive Organic Synthesis*; Trost, B. M., Fleming, I., Eds.; Pergamon: Oxford, pp 789−813, **1991**.

4. a) Lund, H.; Hammerich, O., *Organic Electrochemistry* Eds.; Marcel Dekker: New York, **2001**; b) Fuchigami, T., Inagi, S., Atobe, M. *Fundamentals and Applications of Organic Electrochemistry: Synthesis, Materials, Devices*, Eds.; Wiley-VCH: Chichester, West Sussex, **2015**, c) Luca, O. R.; Gustafson, J. L.; Maddox, S. M.; Fenwick, A. Q.; Smith, D. C. *Org. Chem. Front.* **2015**, *2*, 823; d) Mitsudo, K.; Kurimoto, Y.; Yoshioka, K.; Suga, S. *Chem.Rev.* **2018**, *118*, 5985.
5. Horn, E. J.; Rosen, B. R.; Baran, P. S. *ACS Cent. Sci.* **2016**, *2*, 302.
6. Yan, M.; Kawamata, Y.; Baran, P. S. *Angew. Chem., Int. Ed.* **2018**, *57*, 4149.
7. Pletcher, D.; Green, R. A.; Brown, R. C. D. *Chem. Rev.* **2018**, *118*, 4573.
8. Noël, T.;Cao,Y.; Laudadio, G. *Acc. Chem. Res.* **2019**, *52*, 2858.
9. Schäfer,H. *Top. Curr. Chem.* **1990**, *152*, 91.
10. Moeller, K. D. Tetrahedron **2000**, *56*, 9527.
11. Schäfer, H. J. *Chem. Phys. Lipids* **1979**, *24*, 321.
12. Lateef, S.; Reddy Krishna Mohan, S.; Reddy Jayarama Reddy, S. *Tetrahedron Lett.* **2007**, *48*, 77.
13. Sugiya, M.; Nohira, H. *Bull. Chem. Soc. Jpn.* **2000**, *73*, 705.
14. Brakha, L.; Becker, J. Y. *Electrochim. Acta* **2012**, *59*, 135.
15. Brakha, L.; Becker, J. Y. *Electrochim. Acta* **2012**, *77*, 143.
16. Shtelman, A. V.; Becker, J. Y. *J. Org. Chem.* **2011**, *76*, 4710.
17. Schäfer, H. J. *Eur.J. Lipid Sci. Technol.* **2012**, *114*, 2.
18. Behr, S.; Hegemann, K.; Schimanski, H.; Fröhlich, R.; Haufe, G. *Eur. J. Org. Chem.* **2004**, *2004*, 3884.
19. Brecht Forster, A.; Fitremann, J.; Renaud, P. *Helv. Chim. Acta* **2002**, *85*, 3965.
20. Ng'ang'a Wanyoik, G.; Onomura, O.; Maki, T.; Matsumura, Y. *Org. Lett.* **2002**, *4*, 1875.
21. Matsumura, Y.; Shirakawa, Y.; Satoh, Y.; Umino, M.; Tanaka, T.; Maki, T.; Onomura, O. *Org. Lett.* **2000**, *2*, 1689.
22. Onomura, O.; Ng'ang'a Wanyoike, G.; Matsumura, Y.; Kuriyama, M. *Heterocycles* **2010**, *80*, 1177.
23. Kurihara, H.; Fuchigami, T.; Tajima, T. *J. Org. Chem.* **2008**, *73*, 6888.
24. Kurihara, H.; Tajima, T.; Fuchigami, T. *Electrochemistry* **2006**, *74*, 615.
25. Tajima, T.; Kurihara, H.; Fuchigami, T. *J. Am. Chem. Soc.* **2007**, *129*, 6680.
26. Galicia, M.; Gonzaĺez-Fuentes, M.A.; Valencia, D.P.; Gonzaĺez, F. J. *J. Electroanal. Chem.* **2012**, *672*, 28.
27. Okada, Y.; Kamimura, K.; Chiba, K. *Tetrahedron* **2012**, *68*, 5857.
28. Wadhawan, J. D.; Marken, F.; Compton, R. G.; Bull, S. D.; Davies, S. G. *Chem. Commun.* **2001**, 87.
29. Becking, L.; Schäfer, H. J. *Tetrahedron Lett.* **1988**, *29*, 2797.
30. Lebreux, F. D. R.; Buzzo, F.; Marko, I. N. *Synlett* **2008**, *2008*, 2815.
31. Arai, K.; Watts, K.; Wirth, T. *Chemistry Open* **2014**, *3*, 23.
32. Uneyama, K.; Nanbu, H. *J. Org. Chem.* **1988**, *53*, 4598.
33. Ma, X.; Luo, X.; Dochain, S.; Mathot, C.; Marko, ́ I. E. *Org. Lett.* **2015**, *17*, 4690.
34. Jones, A. M.; Banks, C. E. *Beilstein J. Org. Chem.* **2014**, *10*, 3056.
35. Onomura, O. *Heterocycles* **2012**, *85*, 2111.

36. D'Oca, M. G. M.; Pilli, R. A.; Pardini, V. L.; Curi, D.; Comninos, F. C. M. *J. Braz. Chem. Soc.* **2001**, *12*, 507.
37. D'Oca, M.; Pilli, R. A.; Vencato, I. *Tetrahedron Lett*. **2000**, *41*, 9709.
38. Schierle Arndt, K.; Kolter, D.; Danielmeier, K.; Steckhan, E. *Eur. J. Org. Chem*. **2001**, *2001*, 2425.
39. Zelgert, M.; Nieger, M.; Lennartz, M.; Steckhan, E. *Tetrahedron* **2002**, *58*, 2641.
40. Sierecki, E.; Errasti, G.; Martens, T.; Royer, J. *Tetrahedron* **2010**, *66*, 10002.
41. Sierecki, E.; Turcaud, S.; Martens, T.; Royer, J. *Synthesis* **2006**, 3199.
42. Turcaud, S.; Martens, T.; Sierecki, E.; Peŕard-Viret, J.; Royer, J. *Tetrahedron Lett.* **2005**, *46*, 5131.
43. Lee, D.-S. *Tetrahedron: Asymmetry* **2009**, *20*, 2014.
44. Matsumura, Y.; Kanda, Y.; Shirai, K.; Onomura, O.; Maki, T. *Tetrahedron* **2000**, *56*, 7411.
45. Libendi, S. S.; Demizu, Y.; Matsumura, Y.; Onomura, O. *Tetrahedron* **2008**, *64*, 3935.
46. Onomura, O.; Ishida, Y.; Maki, T.; Minato, D.; Demizu, Y.; Matsumura, Y. *Electrochemistry* **2006**, *74*, 645.
47. Gallardo, I.; Vilà, N. *J. Org. Chem.* **2010**, *75*, 680.
48. Gallardo, I.; Vilà, N. *J. Org. Chem.* **2008**, *73*, 6647.
49. Okimoto, M.; Yoshida, T.; Hoshi, M.; Hattori, K.; Komata, M.; Numata, K.; Tomozawa, K. *Aust. J. Chem.* **2007**, *60*, 236.
50. Okimoto, M.; Ohashi, K.; Yamamori, H.; Nishikawa, S.; Hoshi, M.; Yoshida, T. *Synthesis* **2012**, *44*, 1315.
51. Baslé, O.; Borduas, N.; Dubois, P.; Chapuzet, J. M.; Chan, T.-H.; Lessard, J.; Li, C.-J. *Chem. Eur. J.* **2010**, *16*, 8162.
52. Kashiwagi, Y.; Anzai, J. *Chem. Pharm. Bull.* **2001**, *49*, 324.
53. Baba, D.; Fuchigami, T. *Tetrahedron Lett.* **2003**, *44*, 3133.
54. Kirira, P. G.; Kuriyama, M.; Onomura, O. *Chem. Eur. J.* **2010**, *16*, 3970.
55. Mazurkiewicz, R.; Adamek, J.; Pazd́ zierniok-Holewa, A.; Zielińska, K.; Simka,W.;Gajos,A.; Szymura, K.. *J. Org. Chem*. **2012**, *77*, 1952.
56. Adamek, J.; Mazurkiewicz, R.; Pazd́ zierniok-Holewa, A.; Grymel, M.; Kuzńik, A.; Zielińska, K. *J. Org. Chem.* **2014**, *79,* 2765.
57. Adamek, J.; Mazurkiewicz, R.; Pazd́zierniok-Holewa,A.; Kuzńik, A.; Grymel, M.; Zielińska, K.; Simka, W. *Tetrahedron* **2014**, *70*, 5725.
58. Tajima, T.; Nakajima, A. *J. Am. Chem. Soc*. **2008**, *130*, 10496.
59. Asami, R.; Fuchigami, T.; Atobe, M. *Chem. Commun.* **2008**, 244.
60. Kathiresan, M.; Velayutham, D. *Chem. Commun.* **2015**, *51*, 17499.
61. Tajima, T.; Kurihara, H.; Shimizu, S.; Tateno, H. *Electrochemistry* **2013**, *81*, 353.
62. Tajima, T.; Fuchigami, T. *J. Am. Chem. Soc*. **2005**, *127*, 2848.
63. Tajima, T.; Fuchigami, T. *Chem. Eur. J.* **2005**, *11*, 6192.
64. Tajima, T.; Kurihara, H. *Chem. Commun.* **2008**, *99*, 5167.
65. Horii, D.; Fuchigami, T.; Atobe, M. A *J. Am. Chem. Soc.* **2007**, *129*, 11692.
66. Horii, D.; Amemiya, F.; Fuchigami, T.; Atobe, M. *Chem. Eur. J.* **2008**, *14*, 10382.
67. Libendi, S. S.; Demizu, Y.; Onomura, O. *Org. Biomol. Chem*. **2009**, *7*, 351.
68. Gong, M.; Huang, J.-M. *Chem. Eur. J.* **2016**, *22*, 14293.

69. Fu, N.; Li, L.; Yang, Q.; Luo, S. *Org. Lett.* **2017**, *19*, 2122.
70. Zhang, L.; Su, J.-H.; Wang, S.; Wan, C.; Zha, Z.; Du, J.; Wang, Z. *Chem. Commun*. **2011**, *47*, 5488.
71. Semmelhack, M. F.; Chou, C. S.; Cortes, D. A *J. Am. Chem. Soc.* **1983**, *105*, 4492.
72. Kubota, J.; Shimizu, Y.; Mitsudo, K.; Tanaka, H. *Tetrahedron Lett*. **2005**, *46*, 8975.
73. Demizu, Y.; Shiigi, H.; Oda, T.; Matsumura, Y.; Onomura, O. *Tetrahedron Lett.* **2008**, *49*, 48.
74. Rafiee, M.; Miles, K. C.; Stahl, S. S. *J. Am. Chem. Soc.* **2015**, *137*, 14751.
75. Hickey, D. P.; Schiedler, D. A.; Matanovic, I.; Doan, P. V.; Atanassov, P.; Minteer, S. D.; Sigman, M. S. *J. Am. Chem. Soc.* **2015**, *137*, 16179.
76. Palma, A.; Caŕdenas, J.; Frontana-Uribe, B.A. *Green Chem*. **2009**, *11*, 283.
77. Kuroboshi, M.; Yoshihisa, H.; Cortona, M. N.; Kawakami, Y. *Tetrahedron Lett.* **2000**, *41*, 8131.
78. Tanaka, H.; Kawakami, Y.; Goto, K.; Kuroboshi, M. *Tetrahedron Lett*. **2001**, *42*, 445.
79. Tanaka, H.; Kubota, J.; Itogawa, S.-J.; Ido, T.; Kuroboshi, M.; Shimamura, K.; Uchida, T. *Synlett* **2003**, 951.
80. Yoshida, T.; Kuroboshi, M.; Oshitani, J.; Gotoh, K.; Tanaka, H. *Synlett* **2007**, *2007*, 2691.
81. Hill-Cousins, J. T.; Kuleshova, J.; Green, R. A.; Birkin, P. R.; Pletcher, D.; Underwood, T. J.; Leach, S. G.; Brown, R. C. D. *Chem. Sus. Chem.* **2012**, *5*, 326.
82. Kubota, J.; Ido, T.; Kuroboshi, M.; Tanaka, H.; Uchida, T.; Shimamura, K. *Tetrahedron* **2006**, *62*, 4769.
83. Tanaka, H.; Kubota, J.; Miyahara, S.; Kuroboshi, M. *Bull. Chem. Soc. Jpn*. **2005**, *78*, 1677.
84. Geneste, F.; Moinet, C.; Ababou-Girard, S.; Solal, F. *New J. Chem*. **2005**, *29*, 1520.
85. Belgsir, E. M.; Schäfer, H. J. *Electrochem. Commun.* **2001**, *3*, 32.
86. Palmisano, G.; Ciriminna, R.; Pagliaro, M. *Adv. Synth. Catal.* **2006**, *348*, 2033.
87. Kashiwagi, Y.; Kurashima, F.; Chiba, S.; Anzai, J.-I.; Osa, T.; Bobbitt, J. M. *Chem. Commun.* **2003**, 114.
88. Das, A.; Stahl, S. S. *Angew. Chem., Int. Ed.* **2017**, *56*, 8892.
89. Hickey, D. P.; Milton, R. D.; Chen, D.; Sigman, M. S.; Minteer, S. D. *ACS Catal.* **2015**, *5*, 5519.
90. Schaḿann, M.; Schaf̈er, H. J. *Eur. J. Org. Chem.* **2003**, *2003*, 351.
91. Badalyan, A.; Stahl, S. S. *Nature* **2016**, *535*, 406.
92. Christopher, C.; Lawrence, S.; Kulandainathan, M. A.; Kulangiappar, K.; Raja, M. E.; Xavier, N.; Raja, S. *Tetrahedron Lett.* **2012**, *53*, 2802.
93. Christopher, C.; Lawrence, S.; Bosco, A. J.; Xavier, N.; Raja, S. *Catal. Sci. Technol.* **2012**, *2*, 824.
94. Khan, F. N.; Jayakumar, R.; Pillai, C. N. *J. Mol. Catal. A: Chem.* **2003**, *195*, 139.
95. Blanco, M.; de Lima, D. P.; Maia, G. *J. Electroanal. Chem.* **2001**, *512*, 49.
96. Maki, T.; Iikawa, S.; Mogami, G.; Harasawa, H.; Matsumura, Y.; Onomura, O. *Chem. Eur. J.* **2009**, *15*, 5364.
97. Minato, D.; Arimoto, H.; Nagasue, Y.; Demizu, Y.; Onomura, O. *Tetrahedron* **2008**, *64*, 6675.

98. Medici, A.; Pedrini, P.; De Battisti, A.; Fantin, G. *Steroids* **2001**, *66*, 63.
99. Carr, J. P.; Hampson, N. A. *Chem. Rev.* **1972**, *72*, 679.
100. Lybaert, J.; Trashin, S.; Maes, B. U. W.; De Wael, K.; Abbaspour Tehrani, K. *Adv. Synth. Catal.* **2017**, *359*, 919.
101. Zhu, Y.; Zhang, J.; Chen, Z.; Zhang, A.; Ma, C. *Chin. J. Catal.* **2016**, *37*, 533.
102. Hosokawa, Y.-Y.; Hakamata, H.; Murakami, T.; Aoyagi, S.; Kuroda, M.; Mimaki, Y.; Ito, A.; Morosawa, S.; Kusu, F. *Electrochim. Acta* **2009**, *54*, 6412.
103. Hosokawa, Y.-Y.; Hakamata, H.; Murakami, T.; Kusu, F. *Tetrahedron Lett.* **2010**, *51*, 129.
104. Green, R. A.; Jolley, K. E.; Al-Hadedi, A. A. M.; Pletcher, D.; Harrowven, D.C.; DeFrutos, O.; Mateos, C.; Klauber, D.J.; Rincoń, J. A.; Brown, R. C. D. *Org. Lett.* **2017**, *19*, 2050.
105. Meng, L.; Su, J.; Zha, Z.; Zhang, L.; Zhang, Z.; Wang, Z. *Chem. Eur. J*. **2013**, *19*, 5542.
106. Li, C.; Zeng, C.-C.; Hu, L.-M.; Yang, F.-L.; Yoo, S. J.; Little, R. D. *Electrochim. Acta* **2013**, *114*, 560.
107. Utley, J. H. P.; Rozenberg, G. G. *J. Appl. Electrochem.* **2003**, *33*, 525.
108. Hruszkewycz, D. P.; Miles, K. C.; Thiel, O. R.; Stahl, S. S. *Chem. Sci.* **2017**, *8*, 1282.
109. Zeng, C.-C.; Zhang, N.-T.; Lam, C. M.; Little, R. D. *Org. Lett.* **2012**, *14*, 1314.
110. Lu, N.-N.; Yoo, S. J.; Li, L.-J.; Zeng, C.-C.; Little, R. D. *Electrochim. Acta* **2014**, *142*, 254.
111. Lu, N.-N.; Zhang, N.-T.; Zeng, C.-C.; Hu, L.-M.; Yoo, S. J.; Little, R. D. *J. Org. Chem.* **2015**, *80*, 781.
112. Yoo, S. J.; Li, L.-J.; Zeng, C.-C.; Little, R. D. *Angew. Chem., Int. Ed.* **2015**, *54*, 3744.
113. Francke, R.; Little, R. D. *J. Am. Chem. Soc*. **2014**, *136*, 427.
114. Okajima, M.; Soga, K.; Nokami, T.; Suga, S.; Yoshida, J.-I. *Org. Lett.* **2006**, *8*, 5005.
115. Nokami, T.; Watanabe, T.; Terao, K.; Soga, K.; Ohata, K.; Yoshida, J.-I. *Electrochemistry* **2013**, *81*, 399.
116. Nokami, T.; Ohata, K.; Inoue, M.; Tsuyama, H.; Shibuya, A.; Soga, K.; Okajima, M.; Suga, S.; Yoshida, J.-I. *J. Am. Chem. Soc.* **2008**, *130*, 10864.
117. Nokami, T.; Watanabe, T.; Musya, N.; Morofuji, T.; Tahara, K.; Tobe, Y.; Yoshida, J.-I. *Chem. Commun.* **2011**, *47*, 5575.
118. Nokami, T.; Watanabe, T.; Musya, N.; Suehiro, T.; Morofuji, T.; Yoshida, J.-I. *Tetrahedron* **2011**, *67*, 4664.
119. Nokami, T.; Musya, N.; Morofuji, T.; Takeda, K.; Takumi, M.; Shimizu, A.; Yoshida, J.-I. *Beilstein J. Org. Chem.* **2014**, *10*, 3097.
120. Ashikari, Y.; Nokami, T.; Yoshida, J.-I. *J. Am. Chem. Soc.* **2011**, *133*, 11840.
121. Hayashi, R.; Shimizu, A.; Yoshida, J.-I. *J. Am. Chem. Soc.* **2016**, *138*, 8400.
122. Hayashi, R.; Shimizu, A.; Song, Y.; Ashikari, Y.; Nokami, T.; Yoshida, J.-I. *Chem. Eur. J.* **2017**, *23*, 61.

123. Kowalski, J.; Płoszyńska, J.; Sobkowiak, A.; Morzycki, J.W.; Wilczewska, A. Z. *J. Electroanal. Chem.* **2005**, *585*, 275.
124. Horn, E. J.; Rosen, B. R.; Chen, Y.; Tang, J.; Chen, K.; Eastgate, M. D.; Baran, P. S. *Nature* **2016**, *533*, 77.
125. Kawamata, Y.; Yan, M.; Liu, Z.; Bao, D.-H.; Chen, J.; Starr, J. T.; Baran, P. S. *J. Am. Chem. Soc.* **2017**, *139*, 7448.

Chapter 5: N-Ammonium Ylide Mediators for Electrochemical C–H Oxidation

5.1 Chapter Abstract

The previous chapter described an overview of electrochemistry, specifically electrochemical C–H oxidation. There is a conundrum in that there is a large variety in the structures of substrates that need to be oxidized, yet there is only a small variety in the structure and reactivity of the reagents that are used. Achieving such a diversity in the employed reagents is difficult both for preparing the reagents themselves, and for ensuring orthogonality to existing reagents. A unique selectivity and reactivity was desired, with the further challenge that electrochemical oxidation of "unactivated" C–H bonds is rare. To this end, a large number of electrochemical mediators were conceived and computationally analyzed, leading to the identification of a class of easily synthesized mediators that spans a wide range of chemical space and reactivity. In this chapter, an electrochemically generated oxidant class, N-ammonium ylides, is shown to promote site-specific C(sp3)–H oxidation in a chemoselective fashion.

5.2 Copyright/disclaimers

 This article is the result of an extensive collaboration between many research groups, of which the Matthew Neurock group and Matthew S. Sigman were in charge of the computational work. This project was also done in collaboration with two companies: Syngenta Crop Protection and Bristol-Myers Squibb.

5.3 Introduction

The area of C–H oxidation has experienced a dramatic increase in attention from the organic chemistry community stemming from a strategic simplification of retrosynthesis,[1] a desire for late-stage functionalization in discovery settings,[2] and as a means to access valuable metabolites.[3] Methods to achieve such functionalizations, specifically C(sp^3)–H to C–O, have a rich history in organic synthesis.[4] In an industrial setting, biochemical approaches are the most oft-applied methods of achieving such transformations in a chemo- and position-selective manner using a toolkit of CYP-enzymes or whole cell approaches (Figure 5.1A).[5] These methods are popular due to their mild nature, catalyst-controlled selectivity (rather than substrate control), and their ability to tune and modulate selectivity through directed evolution.[6,7] In an effort to emulate these features, a myriad of reactive species have been

described for the direct conversion of C(sp^3)–H to C–O bonds. Among the tactics explored, direct hydrogen abstraction by reactive radicals[4,8,9] (including metal-oxo[10] and dioxirane[11] that are known to generate reactive radicals transiently) has been established as an effective approach for this purpose (Figure 5.1A). The mainstream approach for metabolite synthesis/late-stage oxidation involves a combination of trial-and-error together with a careful evaluation of critical chemical features such as sterics and electronics to control innate selectivity. This is illustrated in Figure 5.1B with three different commercially used pharmaceuticals (**1**[12,13], **3**[14] and **4**[15]) and one agrochemical (**2**)[16]. With the native metabolic sites highlighted in red,[17-20] one observes similar selectivities using metal-oxo species that can be tuned to some extent using engineered enzymes such as **5** for the oxidation of buspirone (**1**). Although the screening of chemical reagents such as **5**-**8** on these commercial products (**1**-**4**) can also furnish natural metabolites, this trial-and-error approach is limited. To be sure, each reagent or catalyst requires a separate laborious synthesis that makes rapid tunability challenging. In contrast, the extraordinary utility of directed evolution approaches is a consequence of the sheer number of enzymatic catalysts that can be empirically screened (hundreds to millions). Our attempts to improve electrochemical C–H oxidation using quinuclidine **11** as the hydrogen atom transfer (HAT) based mediator (Figure 5.1C) was emblematic of this problem.[21] Thus, several analogs of quinuclidine (**12**-**17**) were either prepared (4–6 steps)[22] or purchased, yet no improvement in efficiency or selectivity was observed in the oxidation of sclareolide **9**. Each designed quinuclidine analog generally required a de novo total synthesis requiring weeks or months of effort. To even begin to compete with any biochemical approach, a combinatorial array of simple, tunable, and easily accessed mediators/reagents/catalysts is needed so that synthesis is no longer a bottleneck. Herein we present such an approach using a new class of mediators that have rarely been employed in organic synthesis: *N*-alkyl ammonium ylides. These mediators, designed based on first principles and triaged through *in-silico* screening, form the basis of a simple chemical approach to C–H oxidation as they are easily prepared, stable, modular, and exhibit unique selectivity.

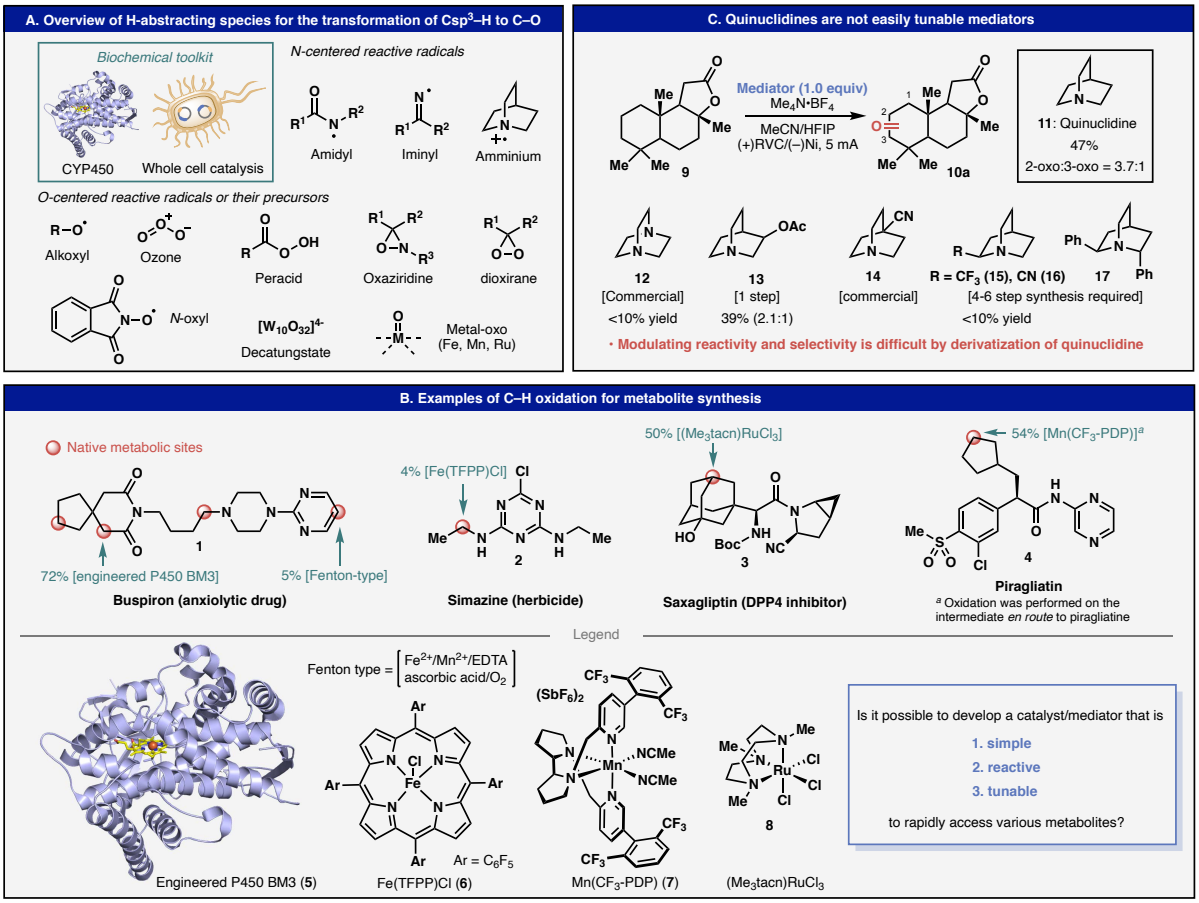

Figure 5.1 Overview of known reactive species for strong C(sp^3)–H bond oxidation, current state of the art in metabolite synthesis, and challenges for further innovation. (A). Summary of representative reactive species or precursors that were previously used for C(sp^3)–H oxidation. (B). Sophisticated reactive species are used in recent examples for metabolite synthesis, illustrating the potential of simple and tunable mediators to enable access to various metabolites. (C). Our attempt to develop tunable quinuclidine-based mediators were concluded difficult due to synthetic inefficiency for analog preparation and unsatisfactory change in reactivity/selectivity.

5.4 Results and Discussion

This study was launched with a structure-agnostic approach guided by a postulated mechanism. As such, instead of starting with a plausible mediator structure, the desired catalytic cycle was modeled, and thermodynamic descriptors were evaluated computationally. To perform such an *in-silico* screen logically, parameters were chosen to evaluate reactive radicals based on the cycle depicted in Figure 5.2A. This general catalytic cycle was modeled from the mechanism of quinuclidine-mediated C–H oxidation[21] and consists of three elementary steps: 1) hydrogen abstraction by the reactive mediator-centered radical $\mathbf{M}^{\bullet}$, 2) deprotonation of protonated species **MH** to regenerate the precursor to this radical $\mathbf{M}^{-}$, and 3) oxidative regeneration of $\mathbf{M}^{\bullet}$. Accordingly, three thermodynamic parameters were chosen to estimate the efficacy of each elementary step: hydrogen binding free energy ($\Delta G_{H\text{-}bind}$), deprotonation free

energy (DPFE) and oxidation potential (E_{ox}). The ideal reactive radical needs to have a large negative $\Delta G_{H\text{-}bind}$ (kJ/mol) to readily facilitate hydrogen abstraction, low DPFE (kJ/mol) for mild deprotonation, and low E_{ox} (V/SHE) for facile oxidation. We initially evaluated the oxidation potentials (E_{ox}) and hydrogen binding energies ($\Delta G_{H\text{-}bind}$) for numerous potential mediator structural classes (**11**, **12**, **18-24**) using first principle density functional theory (DFT) calculations along with chemical intuition and literature precedent[23-27] (see Chapter 7, pages 242–245 for details regarding the calculation methodology). This allows for a targeted search of effective mediator candidates. Boundaries for furthering the search ($\Delta G_{H\text{-}bind} \leq -180$ kJ/mol, $E_{ox} \leq 1.7$ V vs. SHE) were set based on the $\Delta G_{H\text{-}bind}$ for the quinuclidinium radical **11•** ($\Delta G_{H\text{-}bind} = -183$ kJ/mol) which has shown demonstrated reactivity for the desired transformation (Figure 5.2A), as well as readily achievable oxidation potential within common solvent electrochemical window ($E_{ox} \leq 1.7$ V). Within these boundaries (highlighted in blue), three promising mediator candidates (**11•**, **22•**, **23•**) were identified, effectively ruling out the unpromising ones. For example, the quinuclidine analog **12** (Figure 5.1C), which is not effective in C–H oxidation, lies far outside the promising area. Among the promising candidates, the imidazolium mediator **23** was considered less attractive due to its high DPFE values (673 kJ/mol, experimental pK_a = 23[28]), making regeneration of such species difficult under mild conditions. Quinuclidine scaffolds based on **11** were excluded due to low tunability demonstrated previously (Figure 5.1C). The result of this analysis thus led to the identification of the *N*-ammonium amminium radical **22•** as a possible candidate for experimental study: low DPFE (600 kJ/mol), highly negative hydrogen binding energy ($\Delta G_{H\text{-}bind} = -229$ kJ/mol), moderate oxidation potentials ($E_{ox} = 1.7$ V vs. SHE) and excellent tunability as discussed below. To our knowledge, *N*-ammonium ylides (the precursor to such radicals) have not been studied in the realm of C–H functionalization, with the closest example being a triazolium betaine for activated C–H bond functionalization.[29]

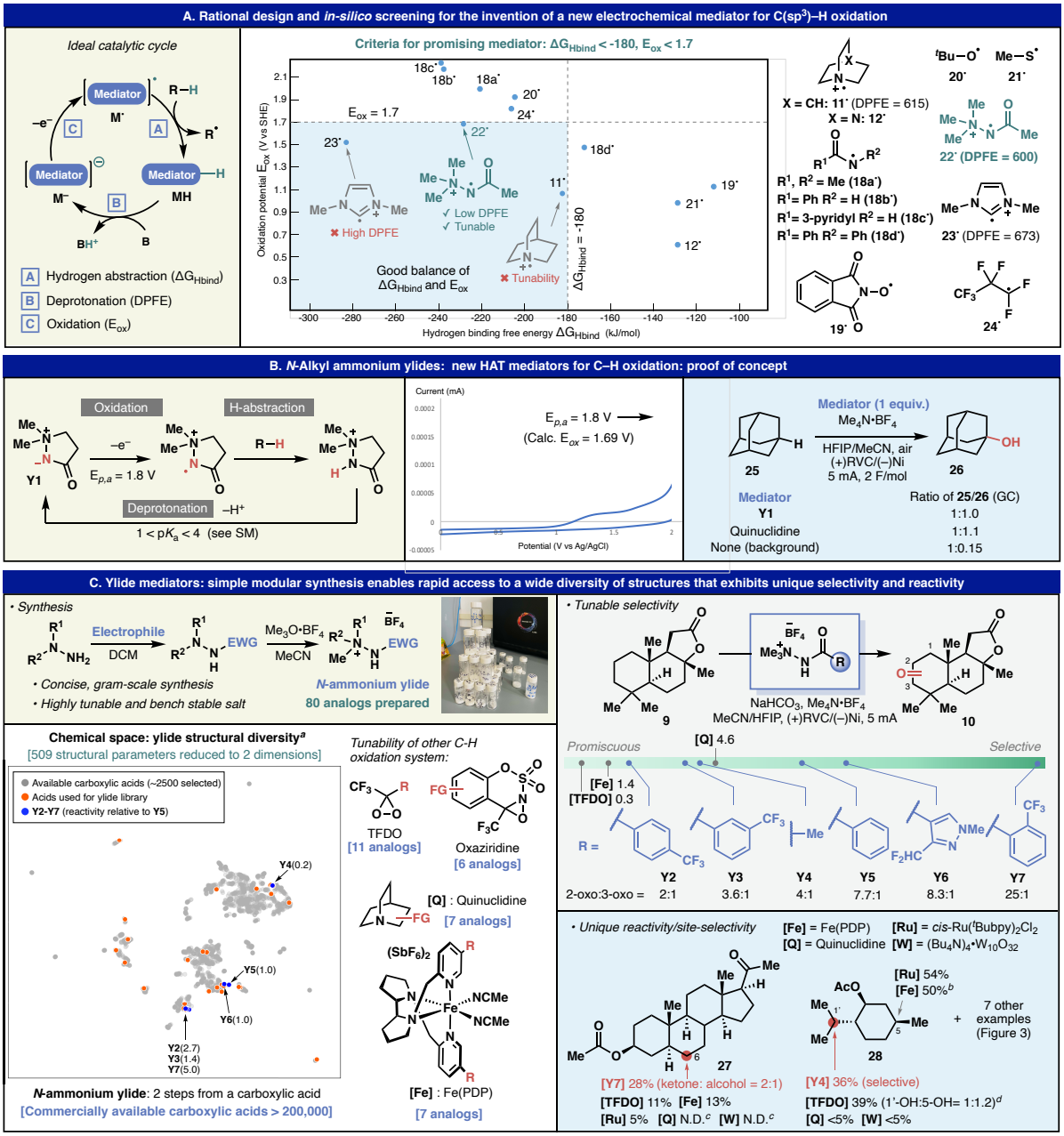

Figure 5.2 Design, proof of concept and library construction of new electrochemical mediator N-ammonium ylides (A). Design of ideal catalytic cycle and evaluation of thermodynamic parameters (E_{ox}, $\Delta G_{H\text{-}bind}$, DPFE) of reactive species in order to perform in-silico screening logically and efficiently. (B). The preliminary results to confirm predicted parameters, which were proven to be in good agreement with experimental results. (C). Synthesis of N-ammonium ylides, their unparalleled diversity and unique tunability to rapidly modulate their reactivity/selectivity. [a] Possible chemical space constructed by 2419 acids shown in grey, screened mediators are highlighted orange, and **Y2-Y7** are highlighted blue. [b] Reference 34. [c] Product distribution was too complex to analyze. [d] Reference 42.

The simple cyclic *N*-ammonium ylide **Y1** was synthesized to confirm these calculated results (Figure 5.2B). Indeed, the measured oxidation potential matched with the calculated value (reference electrode was added to the cyclic voltammetry in Figure 5.2), and the predicted basicity (less basic than quinuclidine) was experimentally confirmed (see Chapter 7, page 265 for basicity study). Most excitingly, it was experimentally proven that an *N*-ammonium ylide can be effective for unactivated C–H bond oxidation. This finding led to an extensive investigation of *N*-ammonium ylides as a new class of tunable and easily accessed mediators for electrochemical C–H bond oxidation. The simple, modular gram-scale synthesis of *N*-ammonium ylide salts enabled rapid construction of a library, carrying various electron-withdrawing groups (EWG) and alkyl groups (R^1, R^2) (Figure 5.2C). Most of the ylide salts are stable and handled without any precaution to atmospheric oxygen and moisture. The free ylides can be conveniently generated in situ with a mild base ($NaHCO_3$) or separately isolated and employed in the reaction. The tunability of *N*-ammonium ylides is unparalleled to other classes of reactive species; even if the EWG is limited to carboxylic acids, more than 200,000 carboxylic acids are commercially available, demonstrating a huge window of structural variation. With a small library of ylides in hand (80 members), a reactivity screening was performed across the entire library (see Chapter 7, page 120 for details), leading to the identification of ylides **Y2**-**Y7** as better mediators than **Y1** based on reactivity, ease of preparation and structural diversity. In particular, to highlight the remarkable structural diversity, visualization of the chemical space for readily available carboxylic acids, building unit for ylide mediators, was attempted.[30] In order to provide a reasonably sized dataset for the analysis of carboxylic acid chemical space (see Chapter 7, pages 249–253 for details), the list of acids from a Reaxys® substructure search (>2.78 million) was filtered based on commercial availability, functionality and available data, resulting in 2419 acids for which two- and three-dimensional Mordred descriptors were calculated.[31] Uniform Manifold Approximation and Projection (UMAP), a non-linear dimensionality reduction technique that preserves global structure, was applied to the data to enable visualization of the chemical space (Figure 5.2C, UMAP).[32,33] Qualitative analysis indicated that the preliminary screening campaign covered a large region of chemical space, but the possibilities for further exploration are vast. In contrast, other species known to be useful for direct C–H oxidation such as dioxirane, oxaziridine, quinuclidine, and iron-oxo complexes have much fewer derivatives reported in the literature to date despite many decades of precedent (see Chapter 7, pages 265–266 for detailed references used for counting derivatives). The tunable selectivity of these mediators was vividly demonstrated in the oxidation of sclareolide **9**, in which the ratio of 2-oxo and 3-oxo products varied from 2:1 to 25:1 simply by changing substituents on the ylides. Moreover, these ylides provided improved reactivity and differing site-selectivity in C–H oxidation relative to other methods. For example, isopregnanolone acetate (**27**) and menthol acetate (**28**) gave poor conversion when quinuclidine was used as a mediator, whereas ylides **Y4** and **Y7** afforded the oxidation products in synthetically useful yields in these cases. Notably, site-selectivity and reactivity for these substrates were either superior (in the case of **27**) or orthogonal (in the case of **28**) to known oxidation systems (Fe-[34], Ru-[35], and W-based[36], TFDO[37,38], and quinuclidine[21]) demonstrating that *N*-alkyl ammonium ylides are a distinct class of reactive species with high tunability. To aid the practitioner and

understand the contextual selectivity of ylides, all substrates in this study were subjected to this comparative panel of oxidants.

Figure 5.3 illustrates the scope of ylide-mediated electrochemical C–H oxidation with a broad range of substrates and unveils their unusual and often singularly selective nature. **Y7** was found to be the most effective across various substrates; in some cases, **Y4** and **Y6** were found superior to **Y7**, demonstrating rapid reaction optimization through this combinatorial approach. Two general protocols employing either hexafluoroisopropanol (HFIP)/CH_3CN or water/CH_3CN solvent mixtures. The latter solvent combination often resulted in a cleaner reaction, albeit with slower product formation. Although the oxidation of unactivated C–H bonds are routinely carried out in the presence of a large excess of substrates in the literature, all screening was performed with the substrate as limiting agent, to accurately represent real-world applications. Ylide-based C–H oxidations generally fell into two categories: unique selectivity and enhanced reactivity not readily achievable with other known chemical oxidants (Class I) and selectivity in line with that observed previously (Class II). In general, substrates falling into Class I are more complex and likely better representations of the types of molecules encountered in medicinal and natural product chemistry. The ability of ylide-mediators to oxidize unactivated methylene positions in these settings where all other commonly employed chemical reagents fail is notable (e.g., **27**, **29**–**32**). This selectivity stems from a strong affinity of the *N*-ammonium amidyl radical to hydrogen along with steric guidance of such radical, as corroborated by DFT calculations which model the transition state of the oxidation of **29** (see Chapter 7, pages 245–248 for details). The same calculations can rationalize why quinuclidine has unique methine selectivity on the same molecule. In fact, one of the only methine-oxidations observed in this work was on the isopropyl group of menthol acetate (**28**). In this case, the methylene positions are less sterically accessible by the bulky ylide mediator resulting in the tertiary alcohol product derived from C1 oxidation. This result is especially unusual given that, of the productive oxidants screened, all favored C5-oxidation. Another unique attribute of the ylide platform is its tendency to afford significant quantities of secondary alcohol rather than ketone products (**27**, **32**, **33**).[39] This stands in stark contrast to quinuclidine-mediated electrochemical oxidation, where only ketone products were observed. Although a precise reason for this observation remains elusive, the literature supports a Russell-type mechanism for disproportionation of the intermediate hydroperoxy radical leading to carbonyl and alcohol products.[24] Oxidation of an amide to an imide could also be achieved in good yield relative to other chemical oxidants screened (**34).** Dealkylation, a process that is often observed in drug metabolism, was observed when imide formation was structurally impossible (**35**).

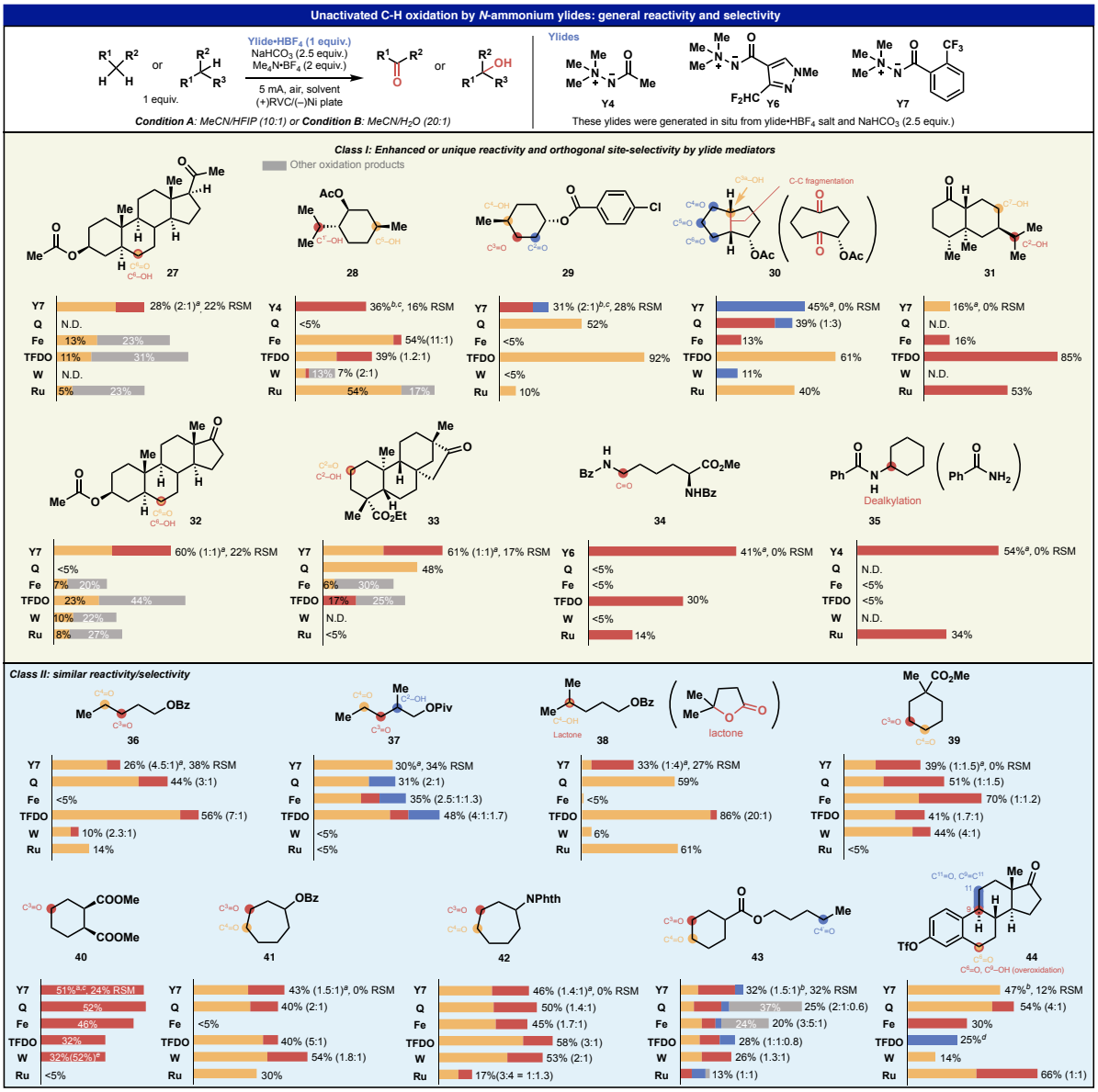

Figure 5.3 Ylide-mediated electrochemical C(sp^3)–H oxidation. See Chapter 7 for the detailed conditions for each reaction. N.D. indicates that product distribution was too complex to analyze. RSM: recovered starting material (%). [a] Condition A was used. [b] Condition B was used. [c] Recovered starting material was recycled once. [d] See Chapter 7 for detailed product distribution. [e] Yield with flow system (Reference 36).

Class II substrates are simpler systems that are often found within the scope tables of other methodologies and provide a good baseline comparison to existing protocols. In general, ylides delivered similar site-selectivity to other systems involving homolytic hydrogen abstraction. Namely, distal C–H bonds that are more than two carbon atoms away from an electron-withdrawing group are susceptible to oxidation, and C–H bonds in cyclic structures are more reactive than acyclic ones.[40] Estrone derivative **44** did display some unique reactivity using **Y7** as it cleanly furnished benzylic ketone (C6), whereas other oxidants gave mixtures of overoxidized products (C6 and C9) or the unusual olefin product (likely stemming from dehydration of C9–OH). As mentioned above, a subtle difference between ylides and other

oxidants was noticeable when a substrate contains tertiary C–H bond (**37** and **38**). Although low conversion or yield was indeed observed in some cases, this appears to be the trend for all oxidants screened and is a general challenge in this field.

Figure 5.4 depicts specific applications of the ylide-platform for the preparation of valuable metabolites and derivatives thereof. For instance, Penconazole **45** (Figure 5.4A) is a widely used fungicide with a primary metabolite profile in humans stemming from enzymatic oxidation on the propyl chain.[41] When this compound was subjected to ylide-mediated electrochemical C–H oxidation (**Y4**), the propyl group was successfully oxidized to afford the ketone products **46** in 26% yield in a 2:1 ratio (the alcohol corresponding to **46a** being the natural metabolite). Notably, other known oxidation conditions gave either poor conversion or different oxidation products, again demonstrating the unique chemoselectivity of the ylide protocol in the presence of the Lewis-basic triazole. In contrast, non-enzymatic routes to such derivatives required a de novo total synthesis (6 steps each from 2,4-dichlorophenylacetic acid). Another interesting application is the short synthesis of compound **50**, which is a common intermediate for metabolites of buspirone and tiospirone (Figure 5.4B).[42] In this case the remote oxidation of **52** to **53** was performed using **Y7** without affecting the alkyl bromide and imide functionality (The starting material was recycled three times). The success of this key oxidation allowed us to access **53** in two steps from readily available material as opposed to a known 8-step synthesis from expensive, pre-oxidized **54.**[42]

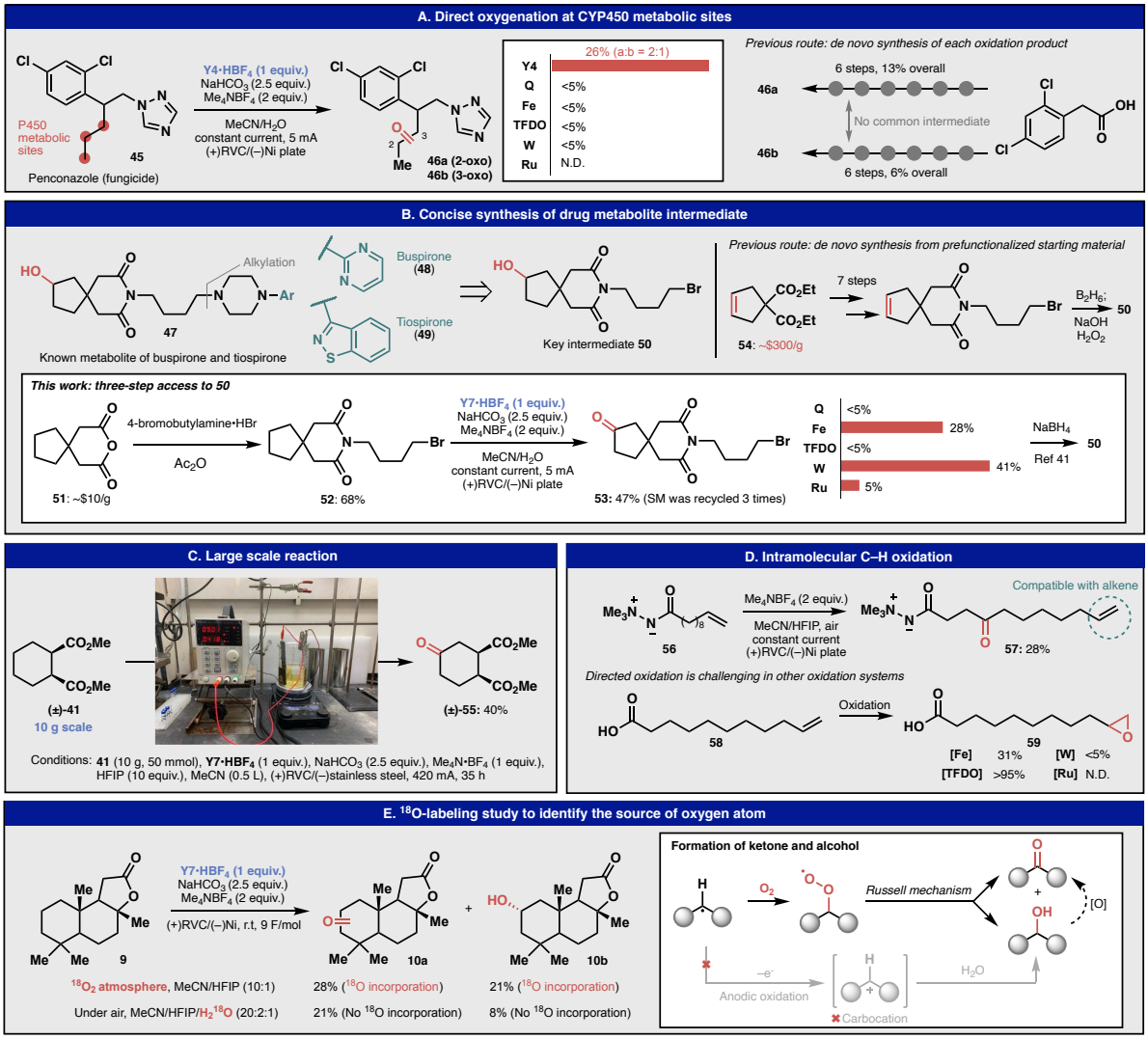

Figure 5.4 Practicality of ylide-mediated electrochemical C–H oxidation in various contexts and mechanistic study. (A). Ylide mediated oxidation as uniquely effective approach for direct oxidation of P450 metabolic sites on Penconazole. (B). Short synthesis of a key intermediate for drug metabolites without prefunctionalization. (C). 10 gram-scale reaction was performed without the need of expensive reagents. (D). Intramolecular C–H oxidation is directed and tolerates alkene. (E). ^{18}O-labelled experiments to identify the source of oxygen in the products.

The reaction was also robust enough for preparative scale as demonstrated with the 10-gram scale oxidation of **41** in batch, delivering 40% yield of ketone **55** (Figure 5.4C). For this larger scale run, a less expensive stainless steel cathode could be used in place of the Ni-plate.

Mechanistically, it is hypothesized that ylide mediators achieve C–H oxidation through the canonical electrochemical pathway outlined in Figure 5.2A (analogous to quinuclidine). The intramolecular experiment outlined in Figure 5.4D using ylide **56** demonstrates a clear directing effect that is unique to this system as most oxidants employed for sp^3 C–H oxidation will engage an olefin preferentially (see **58**). Further evidence for this mechanism (see Chapter 7,

pages 239–242 for an extensive discussion) stems from the use of both labeled $^{18}O_2$ and $H_2{}^{18}O$ showing conclusively that the source of oxygen comes from air (Figure 5.4E).[24]

5.5 Conclusion

A new class of reactive radicals with tunable reactivity and selectivity for unactivated C–H oxidation has been disclosed. Although the reactions presented in this work were performed under electrochemical conditions, the utility of *N*-ammonium ylides may not be limited to electrochemical oxidation; it is possible that such species can also be employed in other (photo)chemical C–H functionalization processes under suitable conditions. Since various ways to intercept the resulting carbon radical after C–H abstraction are known, the unique tunability of such ylides will have an impact on various aspects of C–H functionalization chemistry.

5.6 References

1. Gutekunst, W. R.; Baran, P. S. *Chem. Soc. Rev*. **2011**, *40*, 1976.
2. Börgel, J.; Ritter, T. *Chem*. **2020**, *6*, 1877.
3. Genovino, J.; Sames, D.; Hamann, L. G.; Touré B. B. *Angew. Chem. Int. Ed.* **2016**, *55*, 14218.
4. Newhouse, T. R.; Baran, P. S. *Angew. Chem. Int. Ed.* **2011**, *50*, 3362.
5. Lewis J. C.; Coelho, P. S.; Arnold, F. H. *Chem. Soc. Rev.* **2011**, *40*, 2003.
6. Arnold, F. H. *Angew. Chem. Int. Ed.* **2017**, *57*, 4143.
7. Meunier, B.; de Visser, S. P.; Shaik, S. *Chem. Rev.* **2004**, *104,* 3947.
8. Sterckx, H.; Morel, B.; Maes, B. U. W. *Angew. Chem. Int. Ed.* **2019**, *58*, 7946.
9. Stateman, L.; Nakafuku, K.; Nagib, D. *Synthesis* **2018**, *50*, 1569.
10. Gunay, A.; Theopold, K. H. *Chem. Rev.* **2010**, *110*, 1060.
11. Zou, L.; Paton, R. S.; Eschenmoser, A.; Newhouse, T. R.; Baran, P. S.; Houk, K. N. *J. Org. Chem.* **2013**, *78*, 4037.
12. Landwehr, M.; Hochrein, L.; Otey, C. R.; Kasrayan, A.; Bäckvall, J.-E.; Arnold, F. H. *J. Am. Chem. Soc.* **2006**, *128*, 6058.
13. Slavik, R.; Peters, J.-U.; Giger, R.; Bürkler, M.; Bald, E. *Tetrahedron Lett.* **2011**, *52*, 749.
14. McNeill, E.; Du Bois, J. *Chem. Sci.* **2012**, *3*, 1810.
15. Zhao, J.; Nanjo, T.; de Lucca, E. C.; White, M. C. *Nature Chem.* **2019**, *11*, 213.
16. Santos, dos, J. S.; Palaretti, V.; de Faria, A. L.; Crevelin, E. J.; de Moraes, L. A. B.; Dores Assis, das, M. *Appl. Catal. A: Gen.* **2011**, *408*, 163.
17. Zhu, M.; Zhao, W.; Jimenez, H.; Zhang, D.; Yeola, S.; Dai, R.; Vachharajani, N.; Mitroka, J. *Drug Metab Dispos*. **2005**, *33*, 500.
18. Behki, R. M.; Khan, S. U. *J. Agric. Food Chem.* **1994**, *42*, 1237.
19. Su, H.; Boulton, D. W.; Barros, A., Jr.; Wang, L.; Cao, K.; Bonacorsi, S. J., Jr.; Iyer, R. A.; Humphreys, W. G.; Christopher, L. J. *Drug Metab Dispos*. **2012**, *40*, 1345.

20. Sarabu, R.; Bizzarro, F. T.; Corbett, W. L.; Dvorozniak, M. T.; Geng, W.; Grippo, J. F.; Haynes, N.-E.; Hutchings, S.; Garofalo, L.; Guertin, K. R.; Hilliard, D. W.; Kabat, M.; Kester, R. F.; Ka, W.; Liang, Z.; Mahaney, P. E.; Marcus, L.; Matschinsky, F. M.; Moore, D.; Racha, J.; Radinov, R.; Ren, Y.; Qi, L.; Pignatello, M.; Spence, C. L.; Steele, T.; Tengi, J.; Grimsby, J. *J. Med. Chem.* **2012**, *55*, 7021.
21. Kawamata, Y.; Yan, M.; Liu, Z.; Bao, D.-H.; Chen, J.; Starr, J. T.; Baran, P. S. *J. Am. Chem. Soc.* **2017**, *139*, 7448.
22. Mi, Y.; Corey, E. J. *Tetrahedron Lett.* **2006**, *47*, 2515.
23. Tierney, M. M.; Crespi, S.; Ravelli, D.; Alexanian, E. J. *J. Org. Chem.* **2019**, *84*, 12983.
24. Recupero, F.; Punta, C. *Chem. Rev.* **2007**, *107*, 3800.
25. An, Q.; Wang, Z.; Chen, Y.; Wang, X.; Zhang, K.; Pan, H.; Liu, W.; Zuo, Z. *J. Am. Chem. Soc.* **2020**, *142*, 6216.
26. Cuthbertson, J. D.; MacMillan, D. W. C. *Nature* **2015**, *519*, 74.
27. Shtarev, A. B.; Tian, F.; Dolbier, W. R.; Smart, B. E. *J. Am. Chem. Soc.* **1999**, *121*, 7335.
28. Amyes, T. L.; Diver, S. T.; Richard, J. P.; Rivas, F. M.; Toth, K. *J. Am. Chem. Soc.* **2004,** *126*, 4366.
29. Ohmatsu, K.; Suzuki, R.; Furukawa, Y.; Sato, M.; Ooi, T. *ACS Catal.* **2020**, *10*, 2627.
30. Dobson, C. M. *Nature* **2004**, *432*, 824.
31. Moriwaki, H.; Tian, Y.-S.; Kawashita, N.; Takagi, T. *J Cheminform*. **2018**, *10*, 4.
32. McInnes, L.; Healy, J.; Melville, J. UMAP: Uniform Manifold Approximation and Projection for Dimension Reduction. arXiv, September 18, 2020, 1802.03426v3. https://arxiv.org/abs/1802.03426
33. Probst, D.; Reymond, J.-L. *J Cheminform.* **2020***, 12*, 1.
34. Vermeulen, N. A.; Chen, M. S.; White, M. C. *Tetrahedron* **2009**, ***65***, 3078.
35. Mack, J. B. C.; Gipson, J. D.; Bois, Du, J.; Sigman, M. S. *J. Am. Chem. Soc.* **2017**, *139*, 9503.
36. Laudadio, G.; Govaerts, S.; Wang, Y.; Ravelli, D.; Koolman, H. F.; Fagnoni, M.; Djuric, S. W.; Noël, T. *Angew. Chem. Int. Ed.* **2018**, *57*, 4078.
37. Asensio, G.; Castellano, G.; Mello, R.; González Núñez, M. E. *J. Org. Chem.* **1996**, *61*, 5564.
38. Lesieur, M.; Battilocchio, C.; Labes, R.; Jacq, J.; Genicot, C.; Ley, S. V.; Pasau, P. *Chem. Eur. J.* **2018**, *25*, 1203.
39. Howell, J. M.; Feng, K.; Clark, J. R.; Trzepkowski, L. J.; White, M. C. *J. Am. Chem. Soc.* **2015**, *137*, 14590.
40. White, M. C.; Zhao, J. *J. Am. Chem. Soc.* **2018**, *140*, 13988.
41. Mercadante, R.; Polledri, E.; Scurati, S.; Moretto, A.; Fustinoni, S. *Chem. Res. Toxicol.* **2016***, 29*, 1179.
42. Cipollina, J. A.; Ruediger, E. H.; New, J. S.; Wire, M. E.; Shepherd, T. A.; Smith, D. W.; Yevich, J. P. *J. Med. Chem.* **1991**, *34*, 3316.

Chapter 6: Experimental Data for Oxo-rhenium-promoted Biomimetic Cyclizations (University of Pavia)

(Compound numbers refer to numbers from Chapter 3)

Table of Contents for this Chapter

General experimental

All the reactions were performed in glassware which has been dried in an oven at 140 °C for at least 3 h prior to use and allowed to cool in a desiccator over self-indicating silica gel pellets. Anhydrous solvents were distilled from appropriate drying agents. The reactions were carried out under a slightly positive static pressure of argon. Routine monitoring of reactions was performed using GF- 254 Merck (0.25 mm) aluminum-supported TLC plates.
Compounds were visualized by UV irradiation at a wavelength of 254 nm or stained by exposure to a 0.5% solution of vanillin in H_2SO_4− EtOH followed by charring. Flash column chromatography was performed using Kieselgel 60 Merck (40−63 μm). Yields are reported for chromatographically and spectroscopically pure isolated compounds. NMR spectra were recorded on 200, 300, and 400 MHz spectrometers. Chemical shifts are reported in δ units relative to the employed solvent; the main abbreviations used have the following meaning: s = singlet, d = doublet, t = triplet, q = quartet, qu = quintuplet, m = multiplet, and br = broad. Coupling constants (J) are given in Hz.

General Procedure for Oxo-rhenium-catalyzed Biomimetic Cyclization

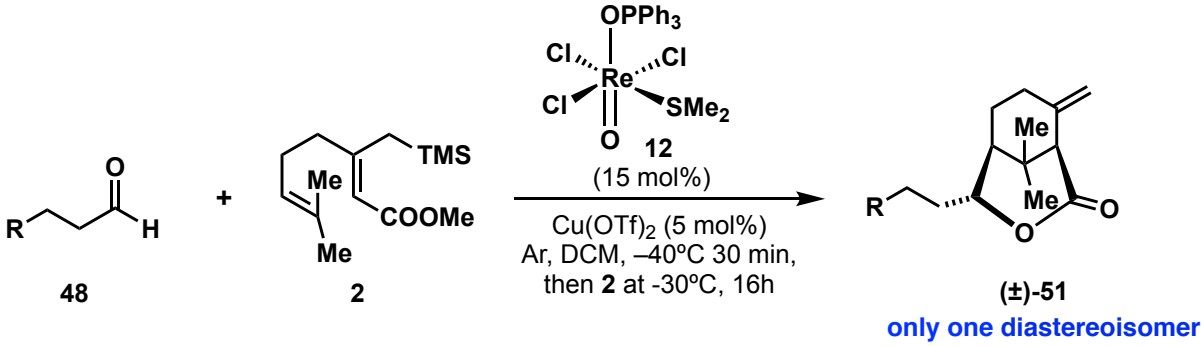

A two-necked round bottom flask was equipped with a magnetic stir bar, a desiccator and an Ar/ vacuum inlet for the central neck, and a rubber septum for the side neck. The entire system was evacuated then filled with Ar three times. Then, a solution of aldehyde (1 equiv, 0.35 mmol) in dry DCM (7 mL), under an Ar atmosphere, was cooled to –40 °C, and $[Re^{v}O(SMe_2)(OPPh_3)Cl_3]$ (34.4 mg, 15 mol %, 0.053 mmol) was added, followed by $Cu(OTf)_2$ (6.5 mg, 5 mol%, 0.018 mmol). The reaction was stirred at –40 ºC for 30 min, then a solution of compound **2** (178.2 mg, 2 equiv, 0.7 mmol) in dry DCM (1 mL) was added. The reaction temperature was warmed to –30 °C, and the reaction was stirred at that temperature for 16 h. After completion, the reaction was quenched with 10 mL of a 1:1 mixture of 5% aqueous $NaHCO_3$:brine and diluted with DCM (10 mL). The aqueous phase was extracted with DCM (3 × 20 mL) and the combined organic layers were dried over Na_2SO_4, filtered, and concentrated. The crude residue was purified by flash chromatography on silica gel using a gradient eluent of 1% to 30% EtOAc in hexanes to give the desired bicyclic lactone.

Procedure for Rhenium Complex Synthesis

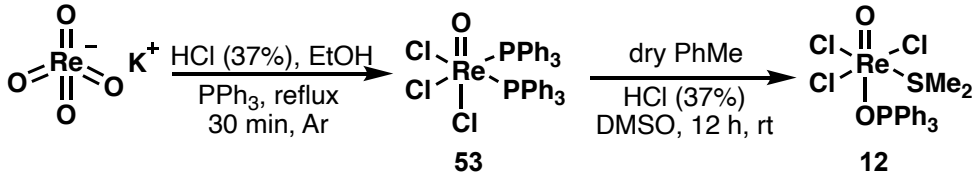

The procedure for the synthesis of **53** and **12** that are described in Abu-Omar, M. M.; Khan, S. I. *Inorg. Chem.* **1998***, 37,* 4979–4985 were modified as follows.

Compound 53. In a 250-mL round-bottomed flask, sodium perrhenate (1.65 g, 6.0 mmol, 1.00 equiv) and conc. HCl 37% (10 mL) was dissolved in EtOH (50 mL) and a solution of PPh_3 (9.0 g, 34.0 mmol, 5.7 equiv) in hot EtOH (50 mL) was added. The reaction was stirred under reflux (80 ºC bath temperature) and under Ar atmosphere for 30 min. Then the reaction was cooled down at room temperature and the resulting precipitate was filtrated with a Büchner under vacuum and washed with cold EtOH (3 × 15 mL). The resulting yellow-green solid was dried under high vacuum for 3 h and directly used in the next step.

Spectral data matched reported literature values (Abu-Omar, M. M.; Khan, S. *I. Inorg. chem.* ***1998****, 37, 4979–4985*).

Compound 12. In a 250-mL round-bottomed flask, compound **53** (5.0 g, 5.4 mmol, 1.00 equiv) was suspended in dry toluene (50 mL), then conc. HCl 37% (23 mL) and DMSO (4.6 mL, 64.0 mmol, 11.8 equiv) were added. The reaction was stirred at room temperature and under Ar atmosphere for 12 h. Then the resulting precipitate was filtrated with a Büchner under vacuum and washed with cold MeOH (3 × 15 mL) and Et_2O (3 × 15 mL). The resulting solid was suspended in DCM (200 mL) and stirred under reflux (40ºC bath temperature) for 5 min. The reaction was cooled down to room temperature, then the precipitate was filtrated with a Büchner under vacuum and the solid obtained was dried under high vacuum for 12h. After drying, a crystallin green solid was obtained (2.05 g) with 53% isolated yield.

Spectral data matched reported literature values (Abu-Omar, M. M.; Khan, S. I. *Inorg. Chem.* **1998***, 37,* 4979–4985).

Procedure for the Synthesis of Extended Diene Allyl Silane

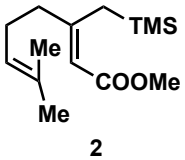

2

Compound 2. A solution of methyl acetoacetate (9.3 mL, 85.9 mmol) in dry THF (50 mL) was added dropwise to NaH (60% dispersion in mineral oil, 3.78 g, 1.1 equiv.) in dry THF (100 mL) at 0 °C. After complete addition, the solution was stirred at the same temperature for 15 min, then *n*-BuLi (2.5 M solution in hexanes, 36.1 mL, 1.05 equiv.) was added dropwise and the mixture was stirred at 0 °C for a further 15 min. 3,3-Dimethylallylbromide (10 mL, 85.9 mmol, 1 equiv.) was then added and the mixture was allowed to warm to room temperature over 45 min. The mixture was then cooled to 0 °C, diethylchlorophosphate (12.8 mL, 1.05 equiv.) was added dropwise, and the resulting enolphosphate was stirred for 1.5 h while warming to room temperature. In a separate flask, Me_3SiCH_2MgCl was prepared from Me_3SiCH_2Cl (1 M in THF, 21.6 mL, 1.8 equiv.) and Mg (3.86 g, 1.85 equiv.) in dry THF (160 mL) at 0 °C, and to it was

added $Ni(acac)_2$ (1.63 g, 0.07 equiv.), and after 15 min, the enolphosphate mixture was added dropwise. After complete addition, the mixture was kept at 0 °C for 1 h, and then poured into a mixture of 1 M aq. HCl and Et_2O at 0 °C. The phases were separated and the organic layer was washed with a further portion of 1 M aq. HCl. The aq. phase was extracted with Et_2O (×3) and the organic layer washed with brine (×3), dried over Na_2SO_4 and evaporated. The crude extract was purified by silica gel chromatography (hexane:EtOAc, 98:2) to give ester **2** as a pale yellow oil (11.1 g, 51% overall yield).
Spectral data matched reported literature values (Beszant, S.; Giannini, E.; Zanoni, G.; Vidari, G. *Tetrahedron: Asymmetry* **2002**, *13*, 1245–1255).

General Procedures for Aldehyde Synthesis

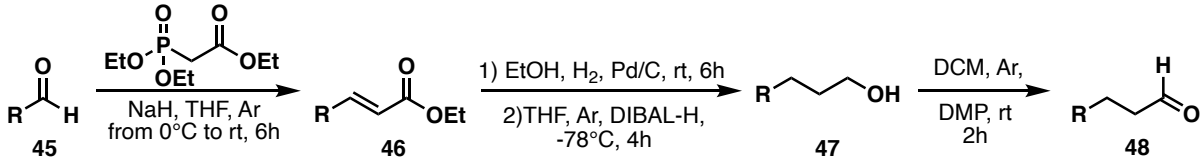

R = alkyl, aryl, hetero aryl

Compound 46. In a two-necked round bottom flask, under stirring and under argon, NaH (60% in mineral oil, 4.1 eq) was suspended in dry THF (0.1 M), then the reaction was cooled at 0 ºC and ethyl phosphonacetate (4.2 eq, d = 1.12 g / cm^3) was added. The reaction was stirred at 0 °C for 40 min, then aldehyde **45** (1 eq) was added, and the reaction was allowed to warm to room temperature. The reaction was stirred at room temperature for 6 h, and after completion, the reaction was quenched with sat. aq NH_4Cl (50–70 mL). This mixture was then diluted with Et_2O (30 mL). The organic phases were separated and the resulting aqueous phase was extracted with Et_2O (×3). The combined organic phases were dried over Na_2SO_4, filtrated, and concentrated under reduced pressure. The crude solid was purified column chromatography using as eluent 10% EtOAc in hexanes to give pure product **46**.

Compound 47.
Part A: In a round bottom flask, under magnetic stirring, compound **46** (1 equiv) was dissolved in EtOH (0.1 M), and Pd/C (10 mol %) was added. The resulting mixture was stirred under H_2 atmosphere at room temperature for 6 h. After completion, the reaction mixture was filtered and the resulting solution was evaporated under reduced pressure. The obtained crude material was used directly in the next step.
Part B: The crude product obtained in part A (1 eq) was dissolved in dry THF (0.1 M) under inert atmosphere and the reaction was cooled at –78 ºC. Then, DIBAL-H (1 M solution, 5 eq) was added dropwise. The reaction was stirred for 30 min and then quenched with MeOH. An aqueous solution of Rochelle salt was added and the resulting mixture was stirred overnight. The phases were separated and the aqueous phase was extracted with DCM (×3) and the combined organic phases were dried over anhydrous Na_2SO_4 and concentrated under reduced pressure. The crude solid was purified column chromatography using as eluent 30% EtOAc in hexanes to give pure product **47**.

Compound 48. Compound **47** (1 equiv) was dissolved in anhydrous DCM (0.1 M), then Dess–Martin periodinane (1.15 equiv) was added in a single portion. The reaction was stirred at room temperature for 1.5 h, and after completion, it was quenched with a 1:1 mixture of sat. aq. $NaHCO_3$ and sat. aq. $Na_2S_2O_3$. The aqueous phase was extracted with Et_2O (× 3). The combined organic phases were dried over anhydrous Na_2SO_4, filtered and concentrated under reduced pressure. The crude solid was purified by column chromatography using as eluent 20% EtOAc in hexanes to give pure product **48**.

With this general procedure, the following aldehydes were synthesized:

Products:	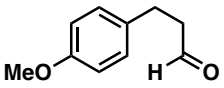 **22**	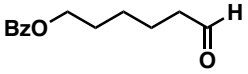 **31**	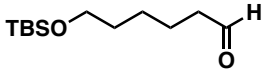 **33**
Step 1: HWE	91%	94%	97%
Step 2: hydrogenation + DIBAL-H red.	75%	84%	88%
Step 3: DMP ox.	84%	87%	93%

The obtained spectral data matched reported literature values (compound **22**: *J. Am. Chem. Soc.* **2012**, *134*, 9890–9893; compound **31**: *Bioorg. Chem*. **2021**, *111*, 104895; compound **33**: *J. Med. Chem.* **2020**, *63,* 2282–2291).

All the other aldehydes employed in this thesis are commercially available.

Characterization of Biomimetic Cyclization Products

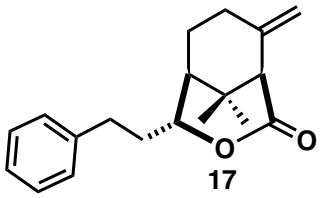

17

Compound 17.

^{1}H NMR (300 MHz, $CDCl_3$) δ 7.40 – 6.89 (m, 5H), 4.94 – 4.81 (m, 2H), 4.65 (dt, *J* = 8.8, 4.2 Hz, 1H), 3.06 – 2.87 (m, 2H), 2.73 (ddd, *J* = 13.7, 9.9, 6.4 Hz, 1H), 2.30 – 2.04 (m, 3H), 1.94 – 1.71 (m, 3H), 1.53 – 1.44 (m, 1H), 1.12 (s, 3H), 1.02 (s, 3H).

^{13}C NMR (75 MHz, $CDCl_3$) δ 171.9, 142.1, 141.1, 128.4, 128.3, 126.1, 113.2, 80.3, 59.3, 39.5, 34.8, 34.8, 32.0, 27.9, 26.9, 25.1, 21.3.

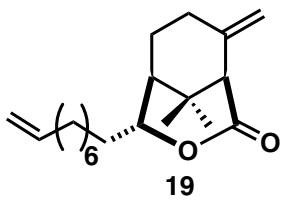

19

Compound 19.

^{1}H NMR (300 MHz, $CDCl_3$) δ 5.81 (ddt, *J* = 16.9, 10.1, 6.7 Hz, 1H), 5.05 – 4.91 (m, 2H), 4.90 – 4.87 (m, 2H), 4.61 (dt, *J* = 8.9, 4.2 Hz, 1H), 2.93 (d, *J* = 1.9 Hz, 1H), 2.24 – 1.98 (m, 4H), 1.83 (d, *J* = 7.5 Hz, 3H), 1.57 (s, 6H), 1.42 – 1.24 (m, 6H), 1.14 (s, 3H), 1.01 (s, 3H).

^{13}C NMR (75 MHz, $CDCl_3$) δ 172.3, 142.5, 139.3, 114.4, 113.3, 81.5, 59.6, 39.5, 35.0, 33.9, 32.9, 29.6, 29.5, 29.2, 29.0, 28.2, 27.2, 26.0, 25.4, 21.4.

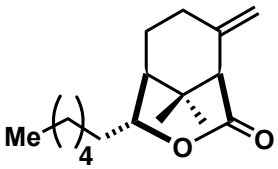

21

Compound 21.

^{1}H NMR (300 MHz, $CDCl_3$) δ 4.93 – 4.84 (m, 2H), 4.61 (dt, *J* = 8.9, 4.3 Hz, 1H), 2.93 (d, *J* = 1.9 Hz, 1H), 2.24 – 2.15 (m, 2H), 1.89 – 1.76 (m, 3H), 1.65 – 1.45 (m, 4H), 1.34 – 1.27 (m, 6H), 1.14 (s, 3H), 1.01 (s, 3H), 0.93 – 0.84 (m, 3H).

^{13}C NMR (75 MHz, $CDCl_3$) δ 172.3, 142.5, 113.2, 81.6, 59.6, 39.5, 35.0, 33.0, 31.9, 29.3, 28.2, 27.2, 25.9, 25.4, 22.7, 21.4, 14.2.

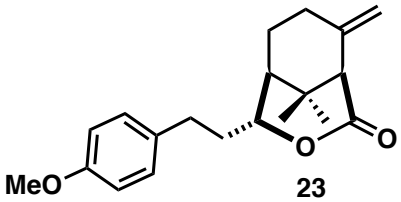

23

Compound 23.

^{1}H NMR (300 MHz, $CDCl_3$) δ 7.23 – 6.98 (d, *J* =8.5 Hz, 2H), 6.89 – 6.75 (d, *J* =8.6 Hz, 2H), 4.98 – 4.85 (m, 2H), 4.69 (dt, *J* = 8.7, 4.2 Hz, 1H), 3.76 (s, 3H), 2.98 (s, 1H), 2.92 (ddd, *J* = 16.2, 10.0, 5.3 Hz, 2H), 2.74 (ddd, *J* = 16.2, 9.5, 6.6 Hz, 1H), 2.35 – 2.10 (m, 3H), 1.90 – 1.75 (m, 3H), 1.50 – 1.47 (m, 1H), 1.13 (s, 3H), 1.03 (s, 3H).

^{13}C NMR (75 MHz, $CDCl_3$) δ 171.9, 157.9, 142.1, 133.1, 129.3, 113.8, 113.6, 113.1, 80.2, 59.3, 55.2, 39.5, 34.8, 31.1, 27.9, 26.9, 25.1, 21.3.

Cartesian Coordinates

Transition states:

TS_2 (see energetic profile in chapter 3, Figure 3.9)

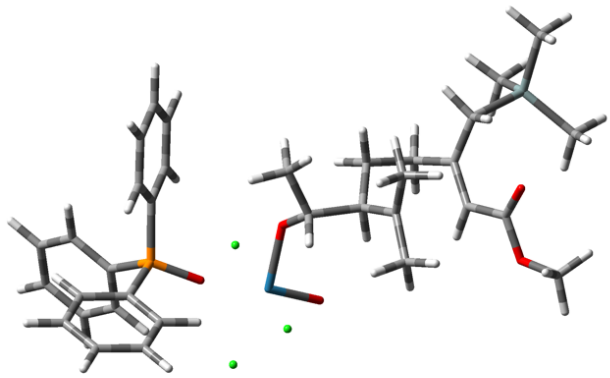

DFT B3LYP, (Si, P, Cl, O) 6-31+G(d,p)/(C, H) 6-31G(d,p)//Re LanL2DZ//DCM(PCM)
Energy = -3789.638533 (aU); Number of Imaginary Frequencies = 1 (-115.8)

C	2.85395600	1.34376100	-0.19378500
C	2.33903800	0.02075200	0.37706100
C	3.20686600	-0.65849500	1.37627400
C	5.18913500	-0.83196400	-0.03435200
C	5.21413200	0.54547100	-0.18197500
C	4.13908000	1.14356600	-1.04449500
C	3.75657000	0.06170300	2.56178500
C	3.03551800	-2.13398200	1.54382000
C	6.13747600	1.46189100	0.49471100
C	6.13510400	-1.62572000	0.77659000
O	6.80951200	-1.22217100	1.71670500
O	6.14065900	-2.90976000	0.36709500
C	7.00909900	-3.81535200	1.08550000
H	2.07537100	1.76575400	-0.83337800
H	3.05104300	2.07476300	0.59604900
H	2.17500300	-0.67852400	-0.44846400
H	4.61845200	-1.40989100	-0.75300300
H	3.90957300	0.49230800	-1.89301800
H	4.45171400	2.11592800	-1.43271200
H	4.72459100	-0.34978100	2.86203300
H	3.84037200	1.13914300	2.42993200

H	3.07309200	-0.13422100	3.40113000
H	3.83317600	-2.58632100	2.13548700
H	2.09989400	-2.27530100	2.10789900
H	2.91246400	-2.66087000	0.59723400
H	5.65997200	2.43045100	0.68479400
H	6.54665300	1.04867600	1.41772800
H	6.87281400	-4.78303600	0.60663600
H	8.04676000	-3.48695300	1.00311600
H	6.71967300	-3.86198800	2.13705600
Si	7.71208400	1.93005600	-0.57285200
C	7.17875400	2.79632900	-2.16144700
C	8.68867900	3.10760000	0.52962700
C	8.70448700	0.37744100	-0.96480100
H	8.06694000	3.15259200	-2.69645600
H	6.63480300	2.12651300	-2.83579900
H	6.54428800	3.66537200	-1.95570500
H	9.60054700	3.43476000	0.01704100
H	8.10255800	4.00006100	0.77486500
H	8.98405500	2.62454500	1.46723100
H	9.60784900	0.65102700	-1.52223300
H	9.01379100	-0.14244700	-0.05258300
H	8.13418600	-0.32411900	-1.58314000
C	0.83840700	0.19767000	0.97701600
O	0.01266300	0.38380800	-0.14119800
C	0.66772100	1.38417800	1.92125700
H	0.84000900	2.33157300	1.40550100
H	-0.36326500	1.38766400	2.28488400
H	1.33023100	1.32554700	2.78878000
H	0.59409700	-0.73175000	1.49807600
C	-4.75655400	-0.52311200	1.67356000
C	-6.05548400	-0.17886100	2.08178100
C	-4.12596300	-1.65319600	2.21577600
C	-6.71085100	-0.95408500	3.03802600
H	-6.55951200	0.68065500	1.65036300
C	-4.79145100	-2.42518400	3.16996100
H	-3.13357700	-1.93091600	1.87510200
C	-6.07845000	-2.07521800	3.58348300
H	-7.71598200	-0.68799700	3.35022800
H	-4.30518500	-3.30310800	3.58413900
H	-6.59356200	-2.67959300	4.32418500
C	-3.28072400	2.00116200	1.23217000
C	-2.61210400	2.94762400	0.43495100
C	-3.45918300	2.24478500	2.60205100
C	-2.13784300	4.12661900	1.00696100

H	-2.45391000	2.75539800	-0.62218200
C	-2.97855700	3.42809600	3.16818000
H	-3.97155400	1.51983900	3.22544400
C	-2.32211000	4.36830900	2.37210500
H	-1.62300900	4.85511700	0.38826500
H	-3.12099200	3.61324900	4.22835500
H	-1.95275700	5.28899800	2.81392900
C	-5.03421900	0.94072800	-0.85774500
C	-5.77263000	2.13250200	-0.77677700
C	-5.24813600	0.05496800	-1.92660900
C	-6.71893000	2.43298800	-1.75829600
H	-5.60758100	2.82929200	0.03864200
C	-6.19242600	0.36666300	-2.90475400
H	-4.66284300	-0.85590100	-2.00438000
C	-6.92857000	1.55167300	-2.82101700
H	-7.28518200	3.35701700	-1.69404700
H	-6.34775800	-0.31450400	-3.73569600
H	-7.66121300	1.79033100	-3.58622600
P	-3.86150000	0.47033400	0.44508500
O	-2.69460100	-0.37079300	-0.09757800
Re	-0.94253900	-1.01281700	-1.15637000
Cl	-0.77140000	-2.68390800	0.64383800
Cl	-1.46393600	0.83169800	-2.69344700
O	0.32159700	-1.60817200	-2.08543900
Cl	-2.59525400	-2.53161600	-2.28156300

TS_1 less thermodynamically stable version (see energetic profile in chapter 3, Figure 3.9)

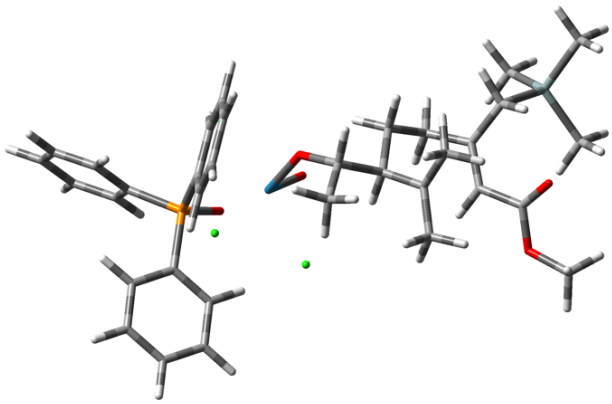

DFT B3LYP, (Si, P, Cl, O) 6-31+G(d,p)/(C, H) 6-31G(d,p)//Re LanL2DZ//DCM(PCM)

Energy = -3789.633873 (aU); Number of Imaginary Frequencies = 1 (-130.6)

C	-2.77665100	-0.90162800	0.84730400
C	-2.19788700	0.44307500	0.37613800
C	-3.08968400	1.62500500	0.55887400
C	-5.02729200	0.81541800	-0.59340000
C	-5.10592300	-0.30154300	0.22598700
C	-4.03032900	-1.32994700	0.04118000
C	-3.64425100	1.94033500	1.91033600
C	-2.92218600	2.79042300	-0.36719800
C	-6.09110100	-0.51516300	1.28804100
C	-5.97905900	1.94686100	-0.57871700
O	-6.66694700	2.31016800	0.36709500
O	-5.97536100	2.57930100	-1.76915800
C	-6.85501600	3.71952200	-1.89887700
H	-2.01053500	-1.66728800	0.72199600
H	-3.01542300	-0.86829400	1.91609900
H	-1.91925300	0.37647300	-0.67879200
H	-4.43827400	0.73484100	-1.50042800
H	-3.75748900	-1.43167900	-1.01300700
H	-4.35848100	-2.30578000	0.40771700
H	-4.55573200	2.53919300	1.84697100
H	-3.82325500	1.06250800	2.53009700
H	-2.89543200	2.56393600	2.42231300
H	-3.77001100	3.47659000	-0.33366800
H	-2.05127500	3.36010200	-0.01747600
H	-2.71683100	2.48778900	-1.39431300
H	-5.68218100	-1.13900500	2.09071700
H	-6.49822300	0.41427700	1.68962000
H	-6.70303500	4.08476200	-2.91269100
H	-7.89218700	3.41320700	-1.75103300
H	-6.58998000	4.48668400	-1.16894300
Si	-7.66396700	-1.51726800	0.67412300
C	-7.14236100	-3.24038700	0.11467000
C	-8.77968800	-1.61811000	2.19072700
C	-8.50129900	-0.58775400	-0.73363400
H	-8.03479800	-3.82597100	-0.13591100
H	-6.50670800	-3.21178600	-0.77647300
H	-6.60349900	-3.77725800	0.90293200
H	-9.69595100	-2.16801900	1.94674800
H	-8.28293600	-2.14121600	3.01507600
H	-9.06817200	-0.62175600	2.54225500
H	-9.38949400	-1.14063200	-1.06098100
H	-8.82104600	0.41140000	-0.42190700

H	-7.83979700	-0.48309900	-1.60034000
C	-0.79894000	0.63946100	1.16972300
O	0.03812100	-0.44455400	0.85181400
C	4.52674600	1.77967500	-0.67482800
C	5.88458000	2.13027400	-0.60422900
C	3.65492400	2.51018400	-1.49784900
C	6.36142200	3.21407900	-1.34214000
H	6.56985700	1.55623700	0.01177800
C	4.14183900	3.59095800	-2.23443900
H	2.61269700	2.21746100	-1.57499200
C	5.49057200	3.94526600	-2.15440400
H	7.41235200	3.48086800	-1.28880300
H	3.46812000	4.15061200	-2.87600500
H	5.86591500	4.78503600	-2.73153800
C	3.54346300	0.96705000	1.99058300
C	2.92116500	0.07514900	2.88291500
C	3.89444700	2.25526100	2.42031300
C	2.65731700	0.47595600	4.19158900
H	2.63115400	-0.91611100	2.54794200
C	3.62647100	2.64813800	3.73402200
H	4.37237600	2.94939700	1.73731600
C	3.01018700	1.76062600	4.61772400
H	2.17484400	-0.21327000	4.87771900
H	3.89963300	3.64594800	4.06312300
H	2.80317300	2.06872200	5.63826400
C	5.11703500	-0.90238400	0.38212700
C	6.05425900	-0.93147500	1.42765300
C	5.18283400	-1.85554300	-0.64706300
C	7.05429400	-1.90542400	1.43812000
H	6.00333200	-0.20685000	2.23417800
C	6.18297400	-2.82776100	-0.62439800
H	4.44386300	-1.84956700	-1.44205900
C	7.11867400	-2.85224300	0.41352600
H	7.77589100	-1.92673500	2.24891700
H	6.22609700	-3.57015200	-1.41535300
H	7.89404400	-3.61244900	0.42671300
P	3.85662000	0.39805600	0.29394400
O	2.56408000	-0.08739100	-0.38392300
Re	0.77276700	-1.16075600	-0.83618600
Cl	0.22643800	0.79299100	-2.23282000
Cl	1.69481500	-2.89133600	0.65146000
O	-0.53042900	-2.09693900	-1.32751400
Cl	2.15362700	-1.98127700	-2.76431700
C	-0.09646700	1.98851300	1.03341700

H	0.86662900	1.91083400	1.54294000
H	0.08587300	2.25454300	-0.00827900
H	-0.65658500	2.78901500	1.52675100
H	-1.05966200	0.50178400	2.22915600

TS_1 (see energetic profile in chapter 3, Figure 3.9)

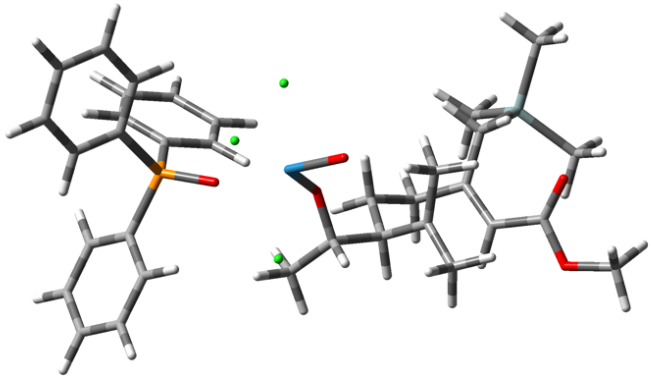

DFT B3LYP, (Si, P, Cl, O) 6-31+G(d,p)/(C, H) 6-31G(d,p)//Re LanL2DZ//DCM(PCM)
Energy = -3789.642195 (aU); Number of Imaginary Frequencies = 1 (-64.6)

C	-2.53315700	1.02643200	1.11702000
C	-2.38172700	-0.45492100	1.47936200
C	-3.16133700	-1.41236700	0.64617300
C	-5.40962000	-0.42969700	1.12368500
C	-4.96890800	0.75934600	0.57482200
C	-3.97200600	1.54529900	1.38359600
C	-3.11640900	-1.34728600	-0.83474400
C	-3.48954400	-2.74125000	1.24184900
C	-5.33415900	1.27506000	-0.75077700
C	-6.37272300	-1.36086700	0.50266600
O	-6.70712200	-1.39773900	-0.67433600
O	-6.84636800	-2.22580900	1.42614500
C	-7.80090200	-3.20686300	0.96133100
H	-1.85003500	1.61855200	1.72970600
H	-2.24190600	1.19606700	0.07833400
H	-2.66823600	-0.60737700	2.52513700
H	-5.23086600	-0.60608700	2.17886200
H	-4.18840400	1.45715600	2.45292700

H	-4.01171000	2.60442700	1.11608700
H	-3.91986700	-1.92404600	-1.29716400
H	-3.08982100	-0.33677000	-1.23693200
H	-2.16218500	-1.82084300	-1.12059000
H	-4.29683800	-3.25080800	0.71406800
H	-2.59314100	-3.36717800	1.10752800
H	-3.70004100	-2.69333500	2.31072700
H	-4.51167400	1.85397500	-1.18741500
H	-5.65275100	0.48819300	-1.43592000
H	-8.05762400	-3.79611900	1.83970700
H	-8.68568200	-2.71031900	0.55870300
H	-7.35167600	-3.83812400	0.19230400
Si	-6.82459100	2.54080700	-0.72902200
C	-6.30600000	4.11960600	0.16573500
C	-7.16945400	2.89502800	-2.54864100
C	-8.32329400	1.76947300	0.11286000
H	-7.09359000	4.87473700	0.05750400
H	-6.15187900	3.95690500	1.23769900
H	-5.38475200	4.53831100	-0.25401700
H	-7.98613600	3.61954200	-2.64533900
H	-6.28764000	3.31293000	-3.04644200
H	-7.46111800	1.98392200	-3.08200500
H	-9.16763700	2.46746700	0.07230600
H	-8.62689800	0.84154700	-0.38168900
H	-8.12693600	1.54769700	1.16744900
C	-0.83673000	-0.91849400	1.41615500
O	-0.30317700	-0.52706700	0.18088000
C	4.92437400	0.71840700	-0.83723200
C	6.22307400	0.37077800	-0.43701200
C	4.66094000	1.00574500	-2.18813300
C	7.25083700	0.31436800	-1.38110000
H	6.43439200	0.14418800	0.60249500
C	5.69184000	0.94818000	-3.12344600
H	3.65301500	1.25369600	-2.50666800
C	6.98634900	0.60344500	-2.72072400
H	8.25442900	0.04431200	-1.06758400
H	5.48443100	1.16552600	-4.16656000
H	7.78698000	0.55874300	-3.45298600
C	2.84426000	2.46016000	0.24754600
C	1.45458000	2.60932300	0.37332000
C	3.66003200	3.59131100	0.08259300
C	0.89174700	3.88651800	0.34846500
H	0.82579100	1.72948900	0.45786100
C	3.08840900	4.86429400	0.06235100

H	4.73328300	3.48437600	-0.04260300
C	1.70568700	5.01200600	0.19806600
H	-0.18452800	4.00091900	0.43578700
H	3.72138200	5.73666700	-0.06695100
H	1.26283700	6.00327400	0.17656600
C	4.21103600	0.51935700	2.01615500
C	4.77473200	1.56084800	2.76988800
C	4.15929500	-0.78073100	2.54533900
C	5.29086700	1.29961100	4.03962300
H	4.80340300	2.57257300	2.37852800
C	4.67853800	-1.03237400	3.81615200
H	3.70012100	-1.57959600	1.97162500
C	5.24555000	0.00411400	4.56135500
H	5.72244700	2.10816800	4.62148300
H	4.63603700	-2.03772500	4.22378000
H	5.64651400	-0.19527200	5.55064300
P	3.55126800	0.79133400	0.34507200
O	2.46031000	-0.26251900	0.09048500
Re	1.03164100	-1.51808600	-0.89635800
Cl	0.78894600	0.35173900	-2.47399400
Cl	1.54663900	-3.10640200	0.90896500
O	0.01321800	-2.54922800	-1.74539700
Cl	3.04602200	-2.34815400	-2.10119800
C	-0.07605300	-0.31061900	2.60002700
H	-0.52409700	-0.61785900	3.55036300
H	0.95326800	-0.67304200	2.56888500
H	-0.05552300	0.78098800	2.55732700
H	-0.81590800	-2.00734900	1.53124000
H	0.23273800	-1.56739200	2.38215900

TS_4 (see energetic profile in chapter 3, Figure 3.9)

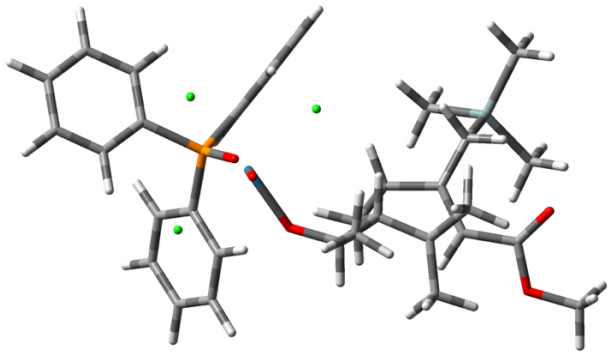

DFT B3LYP, (Si, P, Cl, O) 6-31+G(d,p)/(C, H) 6-31G(d,p)//Re LanL2DZ//DCM(PCM)
Energy = -3789.628318 (aU); Number of Imaginary Frequencies = 1 (-154.3)

C	-1.73097100	-0.41488300	1.04712400
C	-1.97937400	-1.68693600	0.21206300
C	-3.36995700	-2.23802800	0.36682100
C	-4.61542100	-0.34413900	0.93927500
C	-3.90690100	0.46218000	0.05531800
C	-2.48911600	0.78685900	0.44841700
C	-4.08665300	-2.67218200	-0.87237100
C	-3.72282300	-2.96830600	1.62993300
C	-4.41200100	0.96865600	-1.21556900
C	-6.03824000	-0.72460600	0.79249100
O	-6.70378400	-0.70293400	-0.23335300
O	-6.52934500	-1.14773400	1.97686900
C	-7.91333000	-1.56826300	1.98844100
H	-0.66304200	-0.20026000	1.02633900
H	-2.00585700	-0.58102300	2.09424900
H	-1.81168200	-1.43631300	-0.83901800
H	-4.24060500	-0.42518800	1.95245100
H	-1.94808900	1.17290700	-0.41904700
H	-2.51158500	1.59573000	1.19227600
H	-3.57649700	-3.57529000	-1.23696500
H	-4.02106200	-1.93340100	-1.67334900
H	-5.12928300	-2.93706900	-0.69153500
H	-3.33811900	-3.99302000	1.52238000
H	-3.26459100	-2.53893600	2.52215800
H	-4.80031200	-3.05355900	1.77462700
H	-5.25091600	0.38706400	-1.60148100
H	-3.61115600	1.05147900	-1.95761200

H	-8.55982600	-0.74268900	1.68592700
H	-8.11591400	-1.85826000	3.01767900
H	-8.05623100	-2.41459700	1.31412300
Si	-5.14743100	2.79105000	-1.11317900
C	-6.63297600	2.80743700	0.04458700
C	-5.65990200	3.17203800	-2.88601200
C	-3.83112800	3.99785700	-0.51251100
H	-7.08003200	3.80852000	0.04781900
H	-6.35162800	2.56854300	1.07590500
H	-7.39784000	2.09406800	-0.27634400
H	-6.09845700	4.17500700	-2.94113000
H	-6.40737500	2.45682200	-3.24568600
H	-4.80224100	3.14088700	-3.56632300
H	-4.22074000	5.02000900	-0.58988700
H	-2.91647800	3.94254000	-1.11101200
H	-3.56424300	3.82755500	0.53592700
C	-0.89296300	-2.80079400	0.59122900
O	0.41188300	-2.27052400	0.63694100
C	4.15390500	1.63420000	0.03134500
C	5.15884300	0.92797500	0.71568900
C	4.50788700	2.54498200	-0.97632000
C	6.49809500	1.13166400	0.38981200
H	4.89446800	0.21011000	1.48495500
C	5.85176600	2.74393200	-1.29699200
H	3.74283700	3.09622200	-1.51214200
C	6.84568100	2.03896600	-0.61554400
H	7.26948200	0.57983600	0.91776100
H	6.11889000	3.44952600	-2.07747700
H	7.89053400	2.19593700	-0.86618200
C	1.43091300	2.68868600	-0.25404500
C	0.91311200	2.50328400	-1.54729800
C	1.21746100	3.90306000	0.41571000
C	0.20619300	3.53527100	-2.16709500
H	1.05884700	1.55645200	-2.05757400
C	0.50461100	4.92757000	-0.20873000
H	1.59641400	4.05270800	1.42094500
C	0.00573200	4.74790000	-1.50158900
H	-0.18344100	3.39181700	-3.17029700
H	0.34059800	5.86450000	0.31451700
H	-0.53934200	5.55091100	-1.98863200
C	2.31121200	1.37804100	2.27527500
C	2.96597800	2.37246700	3.02198300
C	1.55822200	0.39256900	2.93167200
C	2.84217300	2.39442600	4.41127900

H	3.58514800	3.11640100	2.52971400
C	1.44473400	0.41920400	4.32318700
H	1.09915900	-0.40472400	2.35723200
C	2.07849600	1.42085700	5.06134800
H	3.34936600	3.16412200	4.98462000
H	0.87041700	-0.35045200	4.82962700
H	1.98939900	1.43670000	6.14344700
P	2.41459200	1.33640000	0.46281600
O	1.82031100	0.01420000	-0.06011600
Re	1.81127400	-2.02898000	-0.74785000
Cl	0.23514500	-1.23876500	-2.44515800
Cl	3.37801000	-2.38197100	1.12902300
O	1.99606000	-3.59711000	-1.30325200
Cl	3.64294000	-1.21271600	-2.24411700
C	-0.97791900	-4.04807700	-0.29152100
H	-0.91503400	-3.79638100	-1.35334600
H	-0.14548000	-4.71255300	-0.04702900
H	-1.90126800	-4.60863400	-0.11752800
H	-1.10423800	-3.09288600	1.62907200

TS_3 (see energetic profile in chapter 3, Figure 3.9)

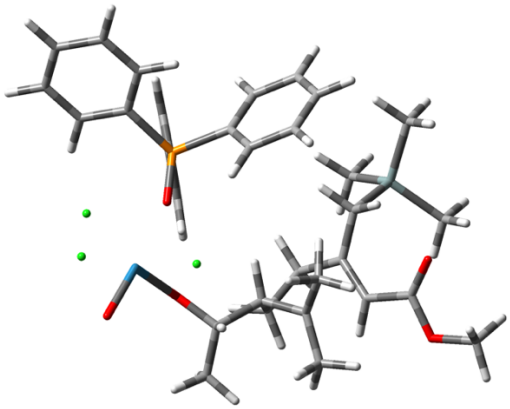

DFT B3LYP, (Si, P, Cl, O) 6-31+G(d,p)/(C, H) 6-31G(d,p)//Re LanL2DZ//DCM(PCM)
Energy = -3789.635678 (aU); Number of Imaginary Frequencies = 1 (-135.8)

C	-2.22145800	-1.46202700	2.03301000
C	-1.62520600	-1.83431300	0.66330800
C	-2.63057500	-2.31642200	-0.34226700
C	-4.57468600	-1.13789200	0.35025300
C	-3.82716200	-0.01862600	0.68757700
C	-2.98810800	-0.12483500	1.93707700

C	-2.45688800	-1.83529900	-1.74108200
C	-3.26906200	-3.66117700	-0.18325300
C	-3.76284500	1.21689600	-0.08826800
C	-5.52083000	-1.22434300	-0.78381600
O	-5.59222300	-0.47042800	-1.74456900
O	-6.32164000	-2.30160700	-0.63669800
C	-7.30248900	-2.52349600	-1.67613200
H	-1.41589000	-1.35138700	2.76247400
H	-2.87083800	-2.26085600	2.40343900
H	-1.14929000	-0.94076100	0.24848100
H	-4.73083300	-1.89038300	1.11432300
H	-2.28530300	0.71124700	1.97569200
H	-3.64518500	-0.02940400	2.81229400
H	-1.50518300	-2.27180800	-2.09118300
H	-2.32884600	-0.75247800	-1.80181800
H	-3.24997700	-2.16505900	-2.41333500
H	-2.54872100	-4.39299000	-0.58018900
H	-3.48042900	-3.92807900	0.85215500
H	-4.17484700	-3.76042500	-0.78302300
H	-4.09438800	1.08691400	-1.11907800
H	-2.76334200	1.66394500	-0.04890800
H	-7.98170600	-1.67153800	-1.73984200
H	-7.83931700	-3.42152100	-1.37640100
H	-6.80727700	-2.67285500	-2.63725600
Si	-4.92900500	2.63841500	0.60578200
C	-6.68819500	1.98976800	0.78676000
C	-4.83899100	3.99892700	-0.69475600
C	-4.26178000	3.24774100	2.26064200
H	-7.34615700	2.80447200	1.11113200
H	-6.75706800	1.19111500	1.53308600
H	-7.07075900	1.60571800	-0.16411000
H	-5.42400000	4.86651900	-0.36843800
H	-5.24548300	3.65817400	-1.65297600
H	-3.80781300	4.32810700	-0.85875400
H	-4.85489100	4.10609000	2.59758200
H	-3.21938300	3.57353100	2.17856400
H	-4.31983700	2.48121100	3.04023200
C	-0.41620800	-2.87529800	0.77750400
O	0.72465800	-2.12624600	1.13801700
C	3.40196000	2.30684900	-0.67061500
C	4.48759100	2.11249100	0.20169200
C	3.57584000	3.04806500	-1.84904000
C	5.73094600	2.66050100	-0.10581200
H	4.36362200	1.51978600	1.10274700

C	4.82556700	3.59416300	-2.14972600
H	2.74535100	3.19926100	-2.53012300
C	5.90002400	3.40211600	-1.27975500
H	6.56867200	2.50445100	0.56656400
H	4.95638900	4.16715400	-3.06238800
H	6.87079500	3.82774300	-1.51565600
C	0.56336000	2.14141200	-1.44039100
C	0.23138500	1.29072000	-2.50733200
C	-0.04030800	3.40504000	-1.34016100
C	-0.69160400	1.70867700	-3.46812000
H	0.68552600	0.30709900	-2.57254000
C	-0.95812300	3.81712600	-2.30775700
H	0.19660500	4.06622800	-0.51294200
C	-1.28285900	2.97073500	-3.37216700
H	-0.94449600	1.04890800	-4.29237500
H	-1.41676200	4.79824500	-2.23117600
H	-1.99586600	3.29525400	-4.12408000
C	1.35303700	2.18716900	1.40809000
C	1.60790300	3.51534600	1.78637700
C	0.70992900	1.31476600	2.29985400
C	1.20021800	3.97208000	3.04058700
H	2.13477500	4.18934000	1.11765100
C	0.31115200	1.77886500	3.55511600
H	0.56388000	0.27609400	2.02100400
C	0.54942800	3.10583600	3.92291000
H	1.40033400	4.99881200	3.33073400
H	-0.17238100	1.09977700	4.25083800
H	0.24072400	3.46153800	4.90131100
P	1.80313600	1.56728700	-0.23857600
O	1.79212300	0.03084400	-0.24947900
Re	2.39496500	-2.02138500	0.08959300
Cl	1.25794800	-2.41169400	-2.05744900
Cl	3.37154700	-1.15664900	2.16688300
O	2.97932400	-3.57778500	0.30167600
Cl	4.40770000	-1.32814100	-1.21386500
C	-0.60278300	-3.97927000	1.82188900
H	0.28099600	-4.62347200	1.80120200
H	-0.68871400	-3.56105600	2.82758700
H	-1.47649900	-4.60421100	1.62322600
H	-0.27881000	-3.33344600	-0.20693600

Products:

Compound 50a (see energetic profile in chapter 3, Figure 3.9)

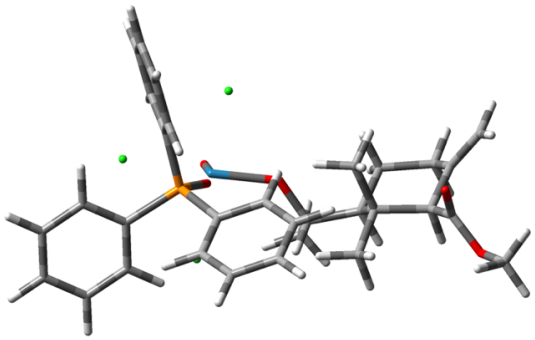

DFT B3LYP, (P, Cl, O) 6-31+G(d,p)/(C, H) 6-31G(d,p)//Re LanL2DZ//DCM(PCM)
Energy = -3380.534254 (aU); Number of Imaginary Frequencies = 0; Total charge = -1

C	-3.96461200	-2.29996600	0.51973600
C	-3.42436700	-1.41380100	-0.61909100
C	-3.63548300	0.11027100	-0.30441200
C	-5.20047200	0.29300400	-0.13539000
C	-5.75079100	-0.56671700	0.99659600
C	-5.45650400	-2.03475000	0.79443800
C	-2.88785900	0.55812100	0.96542600
C	-3.17900500	0.96678400	-1.50173700
C	-5.64177200	1.74308500	-0.03697600
O	-5.28414500	2.56242700	0.79305600
O	-6.53203500	2.04530500	-1.00960500
C	-7.05214700	3.39246200	-1.01093200
H	-3.84408800	-3.35628500	0.26258100
H	-3.37745700	-2.13435200	1.42769000
H	-4.05356000	-1.60863300	-1.50254200
H	-5.64778200	-0.08666100	-1.06296800
H	-6.03539800	-2.39209200	-0.07122900
H	-5.79641200	-2.60943700	1.66230300
H	-2.97895600	1.63833600	1.10267500
H	-3.28859100	0.08350500	1.86453100
H	-1.83489000	0.28488600	0.88686800
H	-3.42749100	2.02262400	-1.35100600
H	-2.09547600	0.91649200	-1.63383000
H	-3.65125900	0.63658800	-2.43473100
H	-7.74528000	3.43413400	-1.84961200
H	-7.57185100	3.59942800	-0.07329200

H	-6.24211300	4.11174600	-1.14714300
C	-2.00131000	-1.83869300	-1.08875300
O	-1.08454700	-1.78637800	0.00943200
C	2.71200600	1.65928600	1.72367400
C	2.83779400	2.99381500	2.14499300
C	3.10587500	0.61816100	2.58018900
C	3.35212600	3.28216200	3.40990100
H	2.53375200	3.80648500	1.49353400
C	3.61770200	0.91631600	3.84399100
H	3.00603100	-0.41251100	2.26031400
C	3.74154700	2.24420900	4.25967600
H	3.44334600	4.31550600	3.73042500
H	3.91714200	0.10757600	4.50357600
H	4.13828300	2.47032900	5.24508200
C	3.53003000	1.17399300	-1.05778700
C	3.32317800	0.89946800	-2.42053700
C	4.83173200	1.40735700	-0.58943300
C	4.40550000	0.86041200	-3.29786700
H	2.32406200	0.69691200	-2.78965500
C	5.91211400	1.36487300	-1.47323700
H	5.00726000	1.61420700	0.46043600
C	5.70058100	1.09252800	-2.82588900
H	4.23759000	0.64343900	-4.34830900
H	6.91671600	1.54181200	-1.10156600
H	6.54220600	1.05919500	-3.51138100
C	1.11235600	2.70779500	-0.47876500
C	1.59688000	3.64538500	-1.40363500
C	-0.15210800	2.90010600	0.10249500
C	0.82045300	4.75445100	-1.74838900
H	2.57265000	3.51350400	-1.85722200
C	-0.92122400	4.01031400	-0.24303700
H	-0.53479500	2.18039600	0.81701200
C	-0.43622900	4.93787300	-1.16951500
H	1.20037200	5.47234300	-2.46885800
H	-1.89747700	4.15088300	0.21059500
H	-1.03732100	5.80138100	-1.43853700
P	2.09397900	1.26880500	0.05650800
O	1.19275900	0.01723900	0.05324200
Re	0.82933300	-2.14949300	0.00205400
Cl	1.04548800	-1.82027400	-2.42405200
Cl	0.58833100	-1.95100400	2.43791600
O	0.84480900	-3.82687200	-0.01568800
Cl	3.37544800	-2.21409100	0.20997800
C	-2.03565800	-3.24642700	-1.70582500

H	-2.81845800	-3.30971500	-2.47007700
H	-1.07989700	-3.47373200	-2.17894100
H	-2.23154100	-4.01056500	-0.94821600
H	-1.66882200	-1.14563400	-1.87018000
C	-6.42904700	-0.11016900	2.05447300
H	-6.63793200	0.94264600	2.21114700
H	-6.79220900	-0.79758900	2.81375900

Compound 50b (see energetic profile in chapter 3, Figure 3.9)

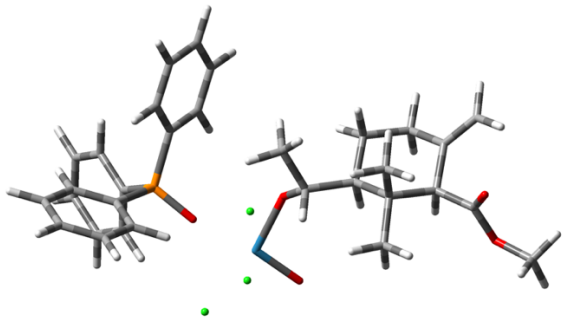

DFT B3LYP, (P, Cl, O) 6-31+G(d,p)/(C, H) 6-31G(d,p)//Re LanL2DZ//DCM(PCM)
Energy = -3380.539012 (aU); Number of Imaginary Frequencies = 0, Total charge = -1

C	3.26270000	1.80129600	-1.25691500
C	3.15085100	0.66043300	-0.22978600
C	4.42241700	0.54253700	0.68918300
C	5.65121600	0.38783200	-0.30169200
C	5.76089200	1.54631200	-1.28592300
C	4.51914000	1.67848600	-2.13495000
C	4.60095300	1.75123600	1.62647700
C	4.35080500	-0.74514600	1.53708700
C	6.96618400	0.08328200	0.39603200
O	7.54377100	0.79036800	1.20605300
O	7.46478500	-1.10585900	-0.00654200
C	8.72453700	-1.50760700	0.57490000
H	2.36938100	1.79292100	-1.88987400
H	3.28167800	2.77215000	-0.74844000
H	3.12706800	-0.27940300	-0.80011400
H	5.42508400	-0.50290400	-0.90095600
H	4.42125200	0.78409100	-2.76824200
H	4.60709000	2.53921000	-2.80615700
H	5.52523600	1.66034100	2.20084200
H	4.64543000	2.69667500	1.07888600

H	3.77232200	1.80562100	2.33778300
H	5.26949300	-0.88599900	2.11732600
H	3.52784000	-0.70974300	2.25500800
H	4.20781400	-1.63009400	0.90707700
H	8.95276700	-2.47449200	0.12947400
H	9.50255600	-0.78045900	0.33402600
H	8.62972900	-1.59770000	1.65887100
C	1.77357400	0.67316900	0.50369700
O	0.82854400	0.10172700	-0.41656200
C	1.23306900	2.04222700	0.92531500
H	1.00367400	2.66048900	0.05342500
H	0.30607100	1.90320100	1.48948100
H	1.93836800	2.58591600	1.55956000
H	1.84200800	0.04092700	1.38998300
C	-3.86384400	0.64500700	1.78824600
C	-5.18661800	1.09287200	1.93363600
C	-3.12732000	0.25641200	2.91792900
C	-5.76185900	1.16263600	3.20253900
H	-5.77081100	1.37499200	1.06301700
C	-3.71141000	0.32822400	4.18382600
H	-2.11519800	-0.11690000	2.79866100
C	-5.02398800	0.78317700	4.32733000
H	-6.78620800	1.50566000	3.31130900
H	-3.14158800	0.02246400	5.05597600
H	-5.47572900	0.83489700	5.31356500
C	-2.54038700	2.24422600	-0.30478600
C	-1.94791100	2.44156300	-1.56512000
C	-2.70019900	3.33265200	0.56576300
C	-1.52721700	3.71478500	-1.94508000
H	-1.80056800	1.60013100	-2.23540300
C	-2.27570100	4.60584000	0.17800900
H	-3.15267700	3.19128700	1.54139300
C	-1.69267500	4.79759900	-1.07565100
H	-1.06800300	3.86082300	-2.91788500
H	-2.40244500	5.44434100	0.85592300
H	-1.36487800	5.78853000	-1.37568700
C	-4.31189300	0.04072200	-1.05121800
C	-5.12750600	0.97711500	-1.70695400
C	-4.50195600	-1.33227400	-1.27545800
C	-6.12774800	0.54087600	-2.57769200
H	-4.98128800	2.04094800	-1.54914700
C	-5.50138200	-1.75830300	-2.15086800
H	-3.85703800	-2.05620600	-0.78714700
C	-6.31482100	-0.82531300	-2.79944100

H	-6.75390000	1.26817300	-3.08540500
H	-5.63898100	-2.82022300	-2.33033400
H	-7.09010400	-1.16232000	-3.48123100
P	-3.06159800	0.56306400	0.15860700
O	-1.88674700	-0.41781800	0.24969700
Re	-0.11653900	-1.58400900	-0.24917600
Cl	0.16600800	-1.69177300	2.19055200
Cl	-0.78377200	-1.14260400	-2.58788500
O	1.07850100	-2.68919200	-0.66310400
Cl	-1.78979000	-3.49639400	-0.02151800
C	6.81196700	2.36303400	-1.41349300
H	7.69950400	2.28097600	-0.79561100
H	6.80386700	3.15627000	-2.15635300

Compound 50a diaxial (see energetic profile in chapter 3, Figure 3.9)

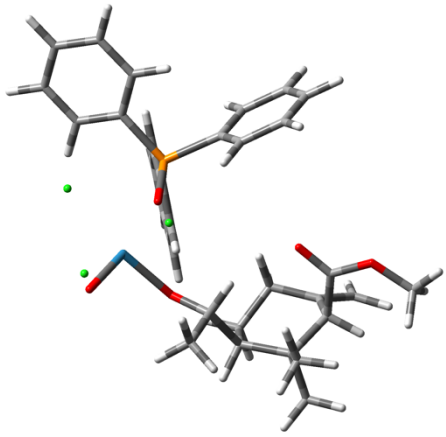

DFT B3LYP, (P, Cl, O) 6-31+G(d,p)/(C, H) 6-31G(d,p)//Re LanL2DZ//DCM(PCM)
Energy = -3380.514485 (aU); Number of Imaginary Frequencies = 0, Total charge = -1

C	-4.70380200	0.93818000	0.21638000
C	-4.65700900	-0.52902100	0.81552600
C	-3.21058100	-1.02530000	1.23181700
C	-2.47859000	0.09387600	2.00792400
C	-2.40590600	1.42330800	1.23723700
H	-5.73007600	1.27425000	0.36625700
H	-1.85513900	2.17100600	1.81809300
H	-3.39028500	-1.83193800	1.95637900
H	-2.98384400	0.26942700	2.96412600
H	-1.47473100	-0.26046700	2.23868600
H	-1.86012700	1.27000600	0.29824900

C	-5.50600500	-0.46904700	2.11433200
H	-5.50962600	-1.44406500	2.61163100
H	-6.54497300	-0.21073400	1.88163700
H	-5.13426500	0.27289400	2.82506000
C	-5.41230900	-1.46334900	-0.14962700
H	-6.43025000	-1.08709100	-0.30828400
H	-5.50391200	-2.46954900	0.26910900
H	-4.93189600	-1.54432400	-1.12716900
C	-4.39167900	1.02256900	-1.27938200
O	-3.32647200	0.70121800	-1.77147800
C	-3.79371800	1.92396900	0.94598800
O	-0.97000900	-1.79714100	0.75750800
C	3.65373600	1.10795700	-0.63159800
C	3.97127900	1.54991600	-1.92492600
C	4.65929600	0.55323400	0.17806500
C	5.27907200	1.43961600	-2.40101800
H	3.20416000	1.97865100	-2.56096400
C	5.96376200	0.45018800	-0.30022500
H	4.42366800	0.19484700	1.17473700
C	6.27481200	0.89276000	-1.58974900
H	5.51698200	1.78291500	-3.40309000
H	6.73571900	0.02035700	0.33049000
H	7.29237800	0.81093400	-1.96021700
C	2.07498200	1.85370500	1.69722300
C	1.16743300	1.38813300	2.65944400
C	3.02322300	2.82905600	2.04939700
C	1.20397800	1.89817300	3.95824800
H	0.45887600	0.61375000	2.39299500
C	3.05111200	3.33840000	3.34831900
H	3.74763200	3.18171500	1.32188800
C	2.14165100	2.87431400	4.30225800
H	0.50481900	1.52639000	4.70094300
H	3.78769800	4.08993500	3.61547900
H	2.16985900	3.26777800	5.31404700
C	1.06985500	2.43185900	-1.01917900
C	1.17484800	3.81085700	-0.77653500
C	0.29761000	1.96853000	-2.09587600
C	0.51833600	4.71702400	-1.60985900
H	1.75514200	4.18062000	0.06245200
C	-0.35084700	2.88309000	-2.92856600
H	0.19736600	0.90187400	-2.26975400
C	-0.24099500	4.25426500	-2.68791900
H	0.59671800	5.78211300	-1.41377900
H	-0.94762900	2.52012800	-3.75953100

H	-0.75126000	4.96187400	-3.33471800
P	1.95181700	1.20932400	0.00053000
O	1.16249600	-0.10785900	-0.01978500
Re	0.71897600	-2.25619800	-0.09193100
Cl	1.59862000	-2.27014600	2.21765700
Cl	-0.09810800	-1.76925200	-2.35348600
O	0.61045800	-3.92761700	-0.19846200
Cl	3.06531100	-2.37414500	-1.03986000
O	-5.32951900	1.51800800	-2.13054400
C	-6.63707000	1.96245300	-1.71922100
H	-7.21178400	1.14936100	-1.26975100
H	-7.12714500	2.28316200	-2.63809400
H	-6.56894500	2.80824900	-1.03148100
C	-4.24523600	3.12101500	1.33746000
H	-3.60038300	3.82078200	1.86257000
H	-5.26636800	3.44456900	1.15220400
C	-2.27567800	-1.68143400	0.15260500
C	-2.70661900	-3.10197600	-0.23483700
H	-1.94051800	-3.55680800	-0.86575800
H	-2.81937700	-3.71984500	0.66420600
H	-3.64406800	-3.12737700	-0.78891700
H	-2.21319900	-1.05096600	-0.73630100

Compound 2 (see energetic profile in chapter 3, Figure 3.9)

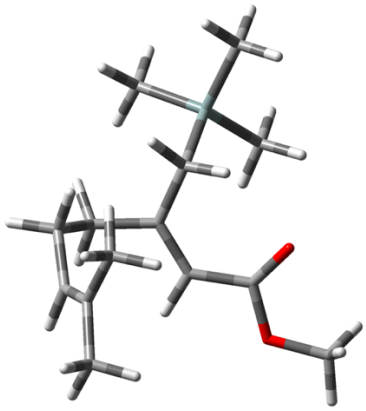

DFT B3LYP, (Si, O) 6-31+G(d,p)/(C, H) 6-31G(d,p)//DCM(PCM)
Energy = -989.163824 (aU); Number of Imaginary Frequencies = 0, Total charge = 0

C	1.63305600	-2.21666900	-0.83402200
C	2.90828800	-1.42388900	-0.73859300
C	3.62262600	-1.11029600	0.35465200

C	0.33305100	0.96964900	-0.85724000
C	-0.05017900	-0.30077500	-0.56789900
C	0.45091700	-1.41911000	-1.45836900
C	3.26370400	-1.50429300	1.76677400
C	4.89934600	-0.31085100	0.23738300
C	-0.91950200	-0.70492200	0.57630100
C	0.05730100	2.16855300	-0.06503500
O	-0.55711900	2.25510700	0.99459300
O	0.61035900	3.26379800	-0.65986400
C	0.43488000	4.51922900	0.02221600
H	1.80179800	-3.08761900	-1.48249500
H	1.33296900	-2.61623200	0.13902600
H	3.28677500	-1.06807400	-1.69885500
H	0.94251900	1.14311200	-1.73826200
H	0.77048800	-1.01505300	-2.42499100
H	-0.36459800	-2.12428900	-1.65360500
H	3.17107300	-0.61317000	2.40097200
H	2.32966900	-2.06416400	1.83838100
H	4.05953800	-2.11703700	2.21033800
H	4.83735100	0.61768300	0.82023800
H	5.75329500	-0.87149900	0.64066500
H	5.12398200	-0.04776500	-0.80004400
H	-0.63483000	-1.70435200	0.92961400
H	-0.83426900	-0.00195600	1.40855800
H	0.92872600	5.26156000	-0.60359100
H	-0.62655000	4.75506600	0.12653900
H	0.89814900	4.48756100	1.01098800
Si	-2.80772700	-0.81781700	0.19949500
C	-3.16739500	-2.15004600	-1.09635200
C	-3.63101500	-1.30276300	1.83225000
C	-3.47753000	0.83940300	-0.40686000
H	-4.25145700	-2.27403500	-1.20699600
H	-2.76437600	-1.88713800	-2.08051600
H	-2.74943000	-3.12083600	-0.80677300
H	-4.71642500	-1.39189800	1.70741200
H	-3.25492000	-2.26680200	2.19353200
H	-3.44232400	-0.55451700	2.61028400
H	-4.54675400	0.75431100	-0.63385400
H	-3.34752700	1.61904700	0.34990100
H	-2.96590700	1.16697900	-1.31847500

Compound 51a (see energetic profile in chapter 3, Figure 3.9)

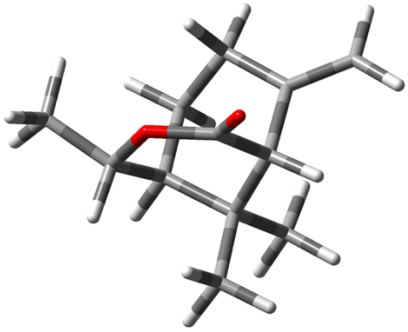

DFT B3LYP, (O) 6-31+G(d,p)/(C, H) 6-31G(d,p)//DCM(PCM)
Energy = -618.597166 (aU); Number of Imaginary Frequencies = 0, Total charge = 0

C	0.95576600	0.23970200	0.67396800
C	0.33173400	-1.18269000	0.58229500
C	-0.78488900	-1.06138100	-0.49604100
C	-0.19912500	-0.67193500	-1.87234100
C	0.62801300	0.63079900	-1.83414400
H	1.71908000	0.27545300	1.45708600
H	1.18448100	0.75562800	-2.76923700
H	-1.27774700	-2.03769200	-0.60317900
H	0.43257700	-1.49266300	-2.22696700
H	-1.00344200	-0.57525200	-2.60879100
H	-0.05899800	1.48664600	-1.76579900
C	1.39773100	-2.22540600	0.19456900
H	0.93694600	-3.21370900	0.07769400
H	2.15392200	-2.30114400	0.98476900
H	1.92116900	-1.98164100	-0.73230600
C	-0.22963300	-1.59989800	1.95935400
H	0.59285000	-1.74238500	2.66929700
H	-0.77323100	-2.54918900	1.88337800
H	-0.90757100	-0.86029300	2.39708100
C	-1.87922800	-0.10599800	0.01632700
H	-2.39134400	-0.59741100	0.84980400
C	-0.09408800	1.28316600	1.06193900
O	-1.35178200	1.14019100	0.58683100
O	0.17145900	2.27381200	1.71182300
C	1.57431900	0.66613700	-0.65418400
C	2.85617300	1.03101900	-0.74698100

H	3.29630000	1.31716300	-1.69949100
H	3.50923200	1.05967600	0.12173300
C	-2.93443600	0.31306900	-0.99814900
H	-3.70318100	0.91712200	-0.50675600
H	-3.41517200	-0.57461100	-1.42319900
H	-2.50731400	0.90277600	-1.81402100

Chapter 7: Experimental Data for *N*-Ammonium Ylide Mediators for Electrochemical C–H Oxidation (Internship in the Baran Laboratory)

(Compound numbers refer to numbers from Chapter 5)

Table of Contents for this Chapter

General Experimental

Dry tetrahydrofuran (THF), *N*,*N*-dimethylformamide (DMF), acetonitrile (MeCN), and dichloromethane (CH_2Cl_2) were obtained by passing the previously degassed solvents through an activated alumina column. Reagents were purchased at the highest commercial quality and used without further purification, unless otherwise stated. Yields refer to chromatographically and spectroscopically (^{1}H NMR) homogeneous material, unless otherwise stated. Reactions were monitored by GC/MS, LC/MS, and thin layer chromatography (TLC). TLC was performed using 0.25 mm E. Merck silica plates (60F-254), using short-wave UV light as the visualizing agent, and Hanessian's Stain, acidic ethanolic anisaldehyde, Vanillin, or $KMnO_4$ and heat as developing agents. NMR spectra were recorded on Bruker DRX-600, DRX-500, and AMX-400 instruments and were calibrated using residual undeuterated solvent ($CHCl_3$ at 7.26 ppm ^{1}H NMR, 77.16 ppm ^{13}C NMR; CH_3CN at 1.94 ppm ^{1}H NMR, 1.32 and 118.26 ppm ^{13}C NMR; CH_3OH at 3.31 ppm ^{1}H NMR, 49.0 ppm ^{13}C NMR; DMSO at 2.50 ppm ^{1}H NMR, 39.52 ppm ^{13}C NMR). The following abbreviations were used to explain multiplicities: s = singlet, d = doublet, t = triplet, q = quartet, m = multiplet, br = broad. Column chromatography was performed using E. Merck silica (60, particle size 0.043–0.063 mm), and pTLC was performed on Merck silica plates (60F-254). High- resolution mass spectra (HRMS) were recorded on an Agilent LC/MSD TOF mass spectrometer by electrospray ionization time of flight reflectron experiments. Optical rotations were recorded on a Rudolph Research Analytical Autopol III Automatic Polarimeter.

Ylide library

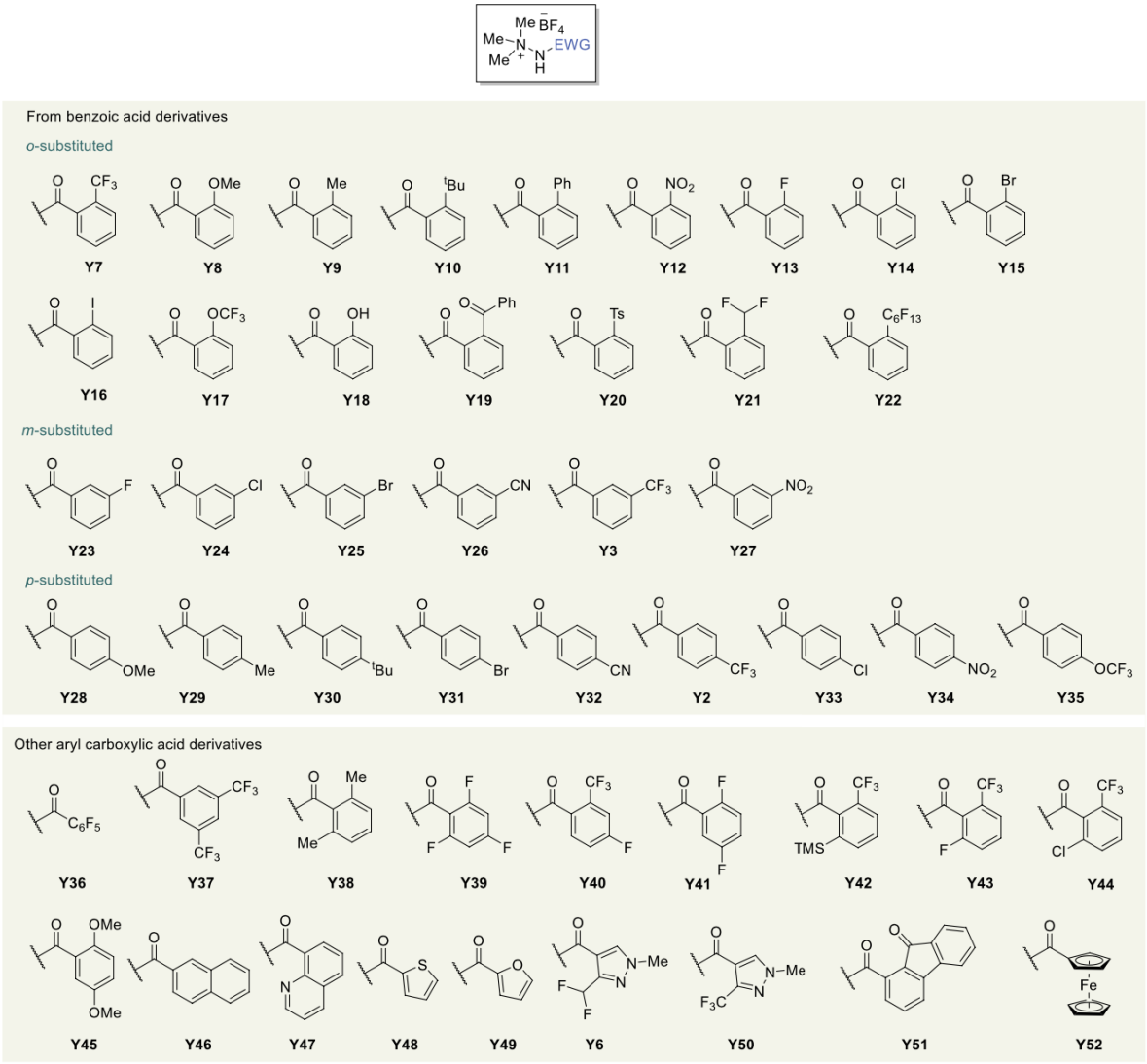

Figure S1. Ylide Mediator Library Part 1.

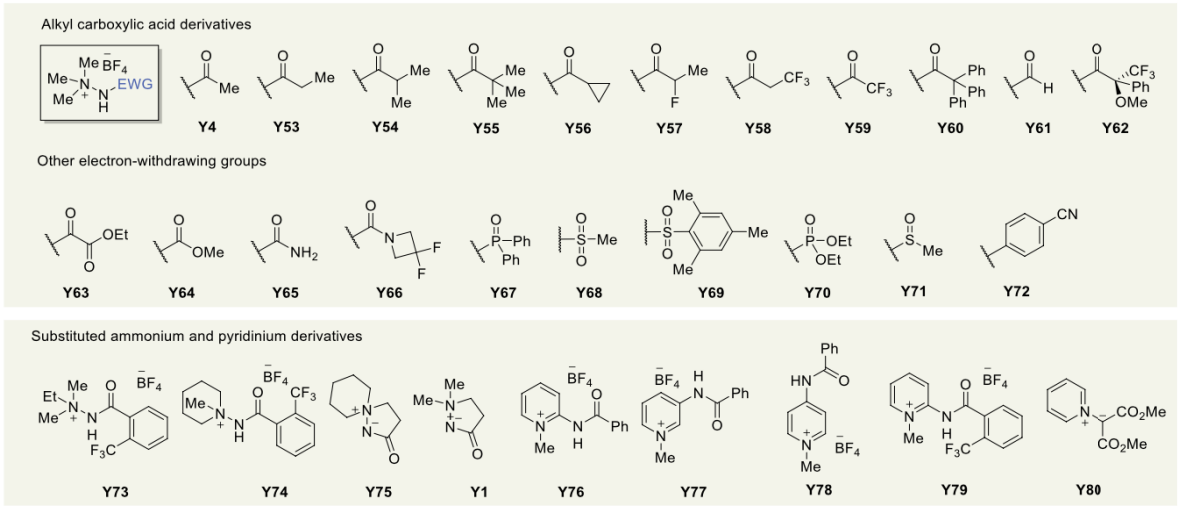

Figure S2. Ylide Mediator Library Part 2.

Mediator Synthesis

General Procedure A (from Acyl Chlorides)

Step 1: N-acyl-N',N'-dimethylhydrazide formation

A round-bottom flask charged with a magnetic stir bar was evacuated and backfilled with argon twice. The flask was charged with *N*,*N*-dimethyl hydrazine (2.1 – 3.0 equiv.) and dry CH_2Cl_2 (0.2 – 0.3 M) and the resulting solution was cooled to 0 °C. To this solution, acyl chloride (1 equiv.) was added dropwise over 15 min and the reaction was stirred for 30 min at 0 °C and 3 h at laboratory temperature. The reaction mixture was diluted with CH_2Cl_2 (10 – 50 mL) and 1 M aq. NaOH (20 – 50 mL), the organic phase was separated, and the aqueous phase was extracted with CH_2Cl_2 twice. Combined organic phases were dried over $MgSO_4$, filtered, and concentrated under reduced pressure. The crude hydrazide was used directly in the following transformation with no further purification.

Step 2: N-methylation of hydrazide

A round-bottom flask charged with a hydrazide (1.0 equiv.) and a magnetic stir bar was evacuated and backfilled with argon twice. Dry MeCN (0.10 – 0.25 M) was added, followed by the addition of trimethyloxonium tetrafluoroborate (1.1 equiv.) in one portion. The resulting homogeneous solution was stirred at laboratory temperature for 30 min. Then the reaction mixture was concentrated under reduced pressure to afford a solid residue. The crude ylide salt was recrystallized from refluxing EtOH then washed with Et_2O and EtOH to afford pure ylide salt.

NOTE: N-methylation on larger scales (> 2 g of hydrazide) was done with minor modifications. Trimethyloxonium tetrafluoroborate (1.05 equiv.) was added in ~2 gram portions over 1 min to the solution of hydrazide cooled at −10 °C (ice/NaCl bath). The reaction mixture was stirred for 20 min at −10 °C and 20 min at laboratory temperature. Then MeOH (~ 1 mL) was added to quench excess of Me_3OBF_4 and the reaction mixture was concentrated under reduced pressure to afford a solid residue. The crude ylide salt was recrystallized from EtOH, washed with Et_2O and EtOH to afford the desired ylide salt.

General Procedure B (from Carboxylic Acids)

Step 1: Acyl chloride formation

A round-bottom flask was charged with carboxylic acid (1.0 equiv.) and a magnetic stirring bar. The flask was then evacuated and backfilled with argon. Depending on the carboxylic acid solubility, either dry CH_2Cl_2 or dry THF (0.2 – 0.3 M) was used and the resulting solution was cooled to 0 °C. DMF (3 – 5 drops) was added and oxalyl chloride (1.5 – 2.0 equiv.) was added dropwise over 10 min to the reaction mixture. Following addition, the reaction mixture was stirred for 1 h at 0 °C and 2 h at laboratory temperature. Then the reaction mixture was concentrated under reduced pressure to remove excess of oxalyl chloride and afforded the desired acyl chloride. The crude acyl chloride was used directly in the following step without further purification.

Step 1: N-acyl-N',N'-dimethylhydrazide formation

A round-bottom flask charged with a magnetic stir bar was evacuated and backfilled with argon twice. The flask was charged with *N*,*N*-dimethyl hydrazine (2.1 – 3.0 equiv.) and dry CH_2Cl_2 (0.2 – 0.3 M) and the resulting solution was cooled to 0 °C. To this solution, acyl chloride (1 equiv.) was added dropwise over 15 min and the reaction was stirred for 30 min at 0 °C and 3 h at laboratory temperature. The reaction mixture was diluted with CH_2Cl_2 (10 – 50 mL) and 1 M aq. NaOH (20 – 50 mL), the organic phase was separated, and the aqueous phase was extracted with CH_2Cl_2 twice. Combined organic phases were dried over $MgSO_4$, filtered, and concentrated under reduced pressure. The crude hydrazide was used directly in the following transformation with no further purification.

Step 2: N-methylation of hydrazide

A round-bottom flask charged with a hydrazide (1.0 equiv.) and a magnetic stir bar was evacuated and backfilled with argon twice. Dry MeCN (0.10 – 0.25 M) was added, followed by the addition of trimethyloxonium tetrafluoroborate (1.1 equiv.) in one portion. The resulting homogeneous solution was stirred at laboratory temperature for 30 min. Then the reaction mixture was concentrated under reduced pressure to afford a solid residue. The crude ylide salt was recrystallized from refluxing EtOH then washed with Et_2O and EtOH to afford pure ylide salt.

NOTE: N-methylation on larger scales (> 2 g of hydrazide) was done with minor modifications. Trimethyloxonium tetrafluoroborate (1.05 equiv.) was added in ~2 gram portions over 1 min to the solution of hydrazide cooled at −10 °C (ice/NaCl bath). The reaction mixture was stirred for 20 min at −10 °C and 20 min at laboratory temperature. Then MeOH (~ 1 mL) was added to quench excess of Me_3OBF_4 and the reaction mixture was concentrated under reduced pressure to afford a solid residue. The crude ylide salt was recrystallized from EtOH, washed with Et_2O and EtOH to afford the desired ylide salt.

General Procedure C (from *N*-Acyl-*N'*, *N'*-dimethylhydrazides)

Step 1: Ortho-lithiation of aroyl hydrazides

Hydrazides were functionalized following literature procedure.[1] A round-bottom flask charged with hydrazide (1.0 equiv.) and a magnetic stir bar was evacuated and backfilled with argon twice. Dry THF (0.30 M) was added and the reaction mixture was cooled to −78 °C (dry ice/acetone bath). To this solution, *s*-BuLi (1.4 M in cyclohexane, 2.1 equiv.) was added dropwise over 10 min and the resulting reaction mixture was stirred for 30 min at −78 °C. Then a solution of electrophile (1.2 – 3.0 equiv.) in THF (1 mL) was added dropwise over 5 min at −78 °C. The resulting reaction mixture was gradually warmed to laboratory temperature and stirred overnight. The reaction mixture was diluted with sat. aq. $NaHCO_3$ and EtOAc. The organic phase was separated and the aqueous phase was extracted with EtOAc. Combined organic phases were dried over $MgSO_4$, filtered, and concentrated under reduced pressure. The crude product was purified by flash column chromatography as indicated and directly used in the next step.

Step 2: N-methylation of hydrazide

A round-bottom flask charged with a hydrazide (1.0 equiv.) and a magnetic stir bar was evacuated and backfilled with argon twice. Dry MeCN (0.10 – 0.25 M) was added, followed by the addition of trimethyloxonium tetrafluoroborate (1.1 equiv.) in one portion. The resulting homogeneous solution was stirred at laboratory temperature for 30 min. Then the reaction mixture was concentrated under reduced pressure to afford a solid residue. The crude ylide salt was recrystallized from refluxing EtOH then washed with Et_2O and EtOH to afford pure ylide salt.

Ylide C-H Oxidation: General Procedures

Condition A

To an ElectraSyn reaction vial charged with substrate (1 equiv) in 2.00 mL of MeCN (0.05 – 0.15 M, previously saturated with O_2 for 30 min) was added HFIP (1.9 mmol, 0.2 mL, 19 equiv.), tetramethylammonium tetrafluoroborate (Me_4NBF_4) (1.0 equiv.), ylide mediator (1.0 equiv.), and $NaHCO_3$ (2.5 equiv.). As depicted in the graphical guide (see page 124, using a RVC anode (pore size = 80 ppl) and a Ni plate cathode the resulting reaction mixture was electrolyzed under a constant current of 5 mA until complete consumption of the starting material as judged by TLC analysis or by spectroscopic analysis of an ^1H NMR aliquot. The reaction mixture was then concentrated under reduced pressure. The crude reaction mixture was then redissolved in either CH_2Cl_2 or EtOAc and filtered through a short silica plug and concentrated under reduced pressure. The crude reaction mixture was purified by either flash column chromatography or preparative thin-layer chromatography (pTLC) to furnish the desired product.

Condition B

To an ElectraSyn reaction vial charged with substrate (1 equiv) in 2.00 mL of MeCN (0.05 – 0.15 M, previously saturated with O_2 for 30 min) was added H_2O (0.10 mL), tetramethylammonium tetrafluoroborate (Me_4NBF_4) (1.0 equiv.), ylide mediator (1.0 equiv.), and $NaHCO_3$ (2.5 equiv.). As depicted in the graphical guide (see page 124), using an RVC anode (pore size = 80 ppl) and a Ni plate cathode the resulting reaction mixture was electrolyzed under a constant current of 5 mA until complete consumption of the starting material as judged by TLC analysis or by spectroscopic analysis of an ^1H NMR aliquot. The reaction mixture was then filtered and concentrated under reduced pressure. The crude reaction mixture was purified by either flash column chromatography or preparative thin-layer chromatography (pTLC) to furnish the desired product.

Graphical Guide

Ylide Mediator Synthesis — Methylation of Hydrazide with Me_3OBF_4

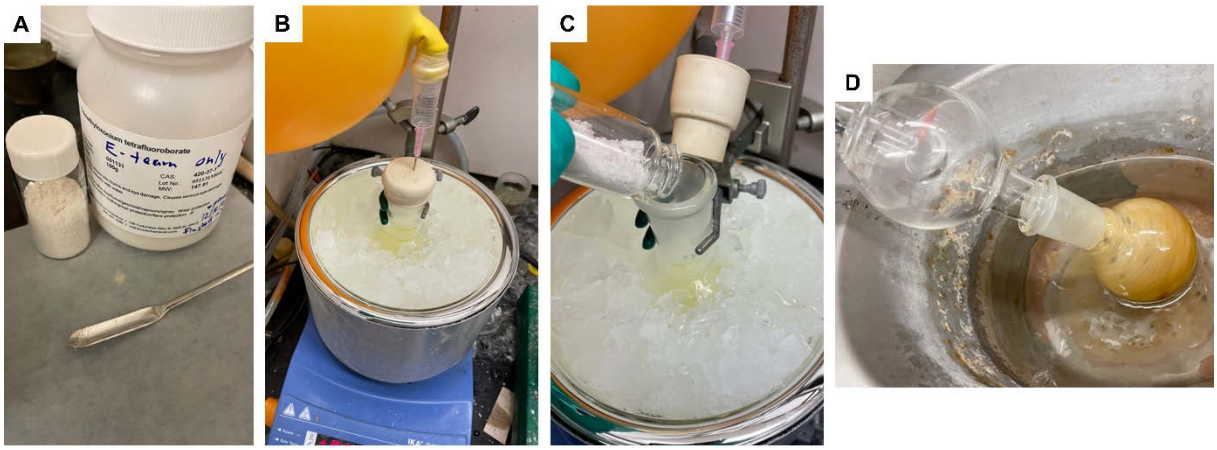

Figure S3. **A)** Me_3OBF_4 is quickly weighted into an argon-flushed vial. *NOTE: Me_3OBF_4 is a strong methylation agent, which hydrolyses to corrosive HBF_4; hence, personal protective equipment must be worn and appropriate safety measures must be taken when working with Me_3OBF_4.* **B)** Hydrazide is dissolved in dry MeCN and cooled to -10 °C (ice/NaCl bath) under argon atmosphere (cooling can be omitted while performing the on < 2g scale). **C)** Me_3OBF_4 is added in ca. 2-gram portions over 1 minute (Me_3OBF_4 can be added in a single portion when working on < 2g scale). Reaction mixture is stirred for 20 min. at -10 °C and 20 min. at laboratory temperature. **D)** Excess of Me_3OBF_4 is quenched by adding MeOH (~ 1 mL) and the reaction is evaporated to dryness and further dried on high vacuum for 30 minutes.

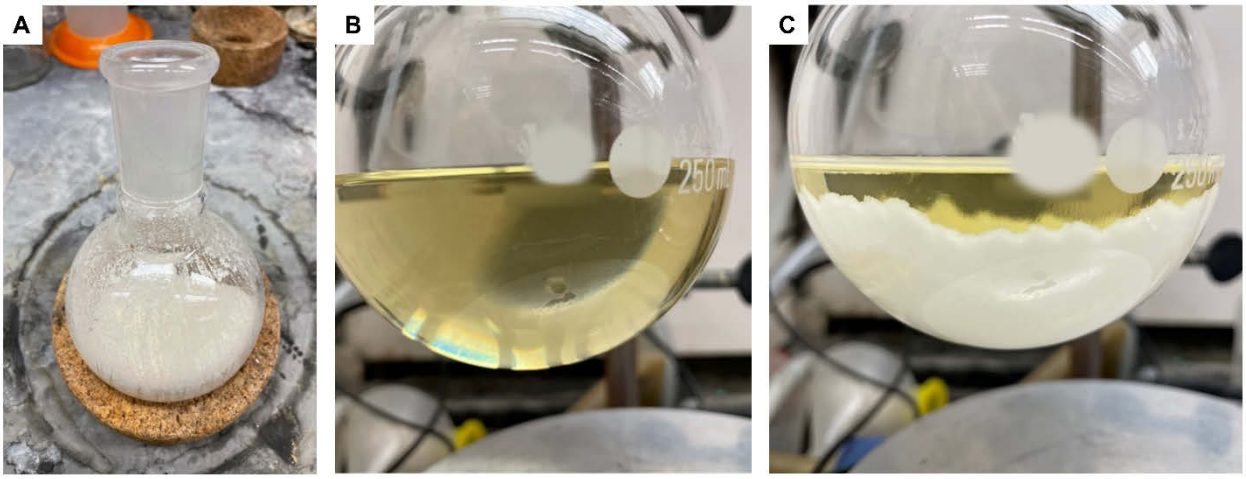

Figure S4. A) Dried reaction mixture (off-white to yellow color is normal). **B)** Crude ylide is recrystallized from refluxing EtOH. **C)** Ylide precipitates upon cooling.

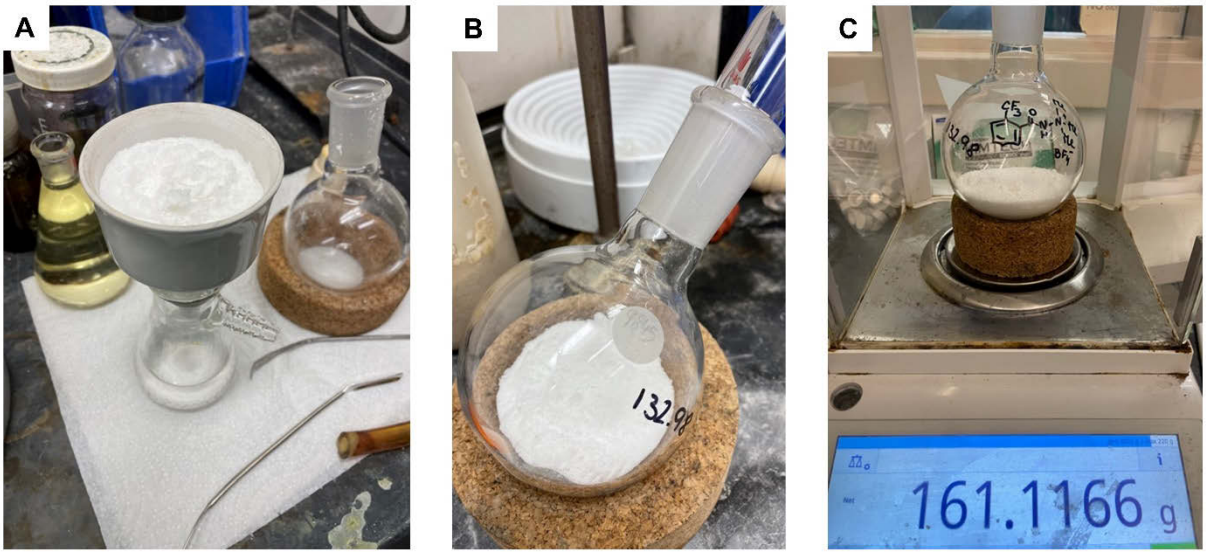

Figure S5. A) Recrystallized ylide is collected by filtration using a Büchner funnel and washed with EtOH and Et_2O, furnishing a white solid. **B)** Ylide is dried on high-vacuum overnight. **C)** 28 grams of *o*-CF_3Bz ylide **Y7** prepared in a single batch.

Ylide-mediated Oxidation Setup

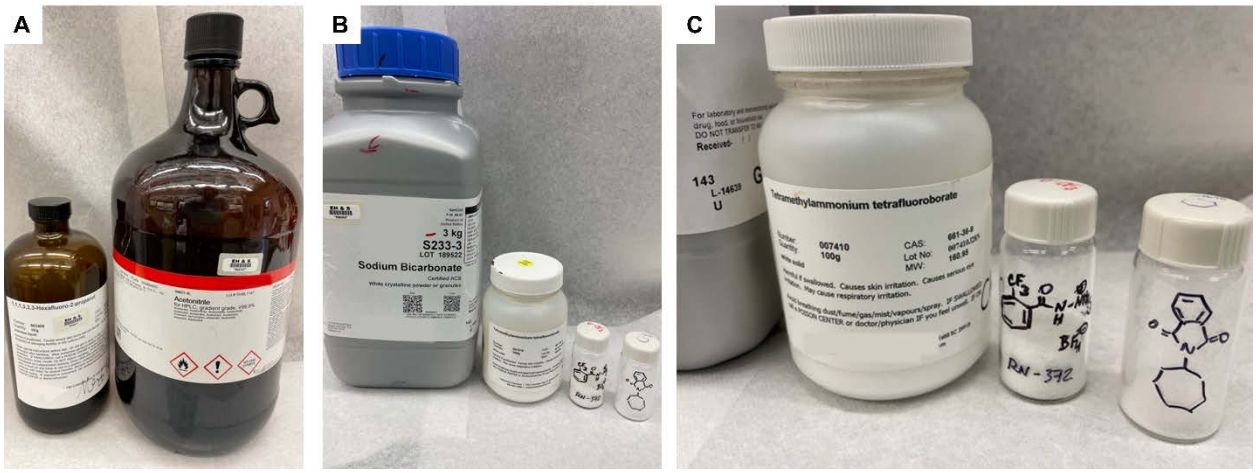

Figure S6. A) Solvents – 1,1,1,3,3,3-hexafluoropropan-2-ol and MeCN. **B)** Reagents – $NaHCO_3$, Me_4NBF_4, ylide salt, substrate. **C)** Reagents.

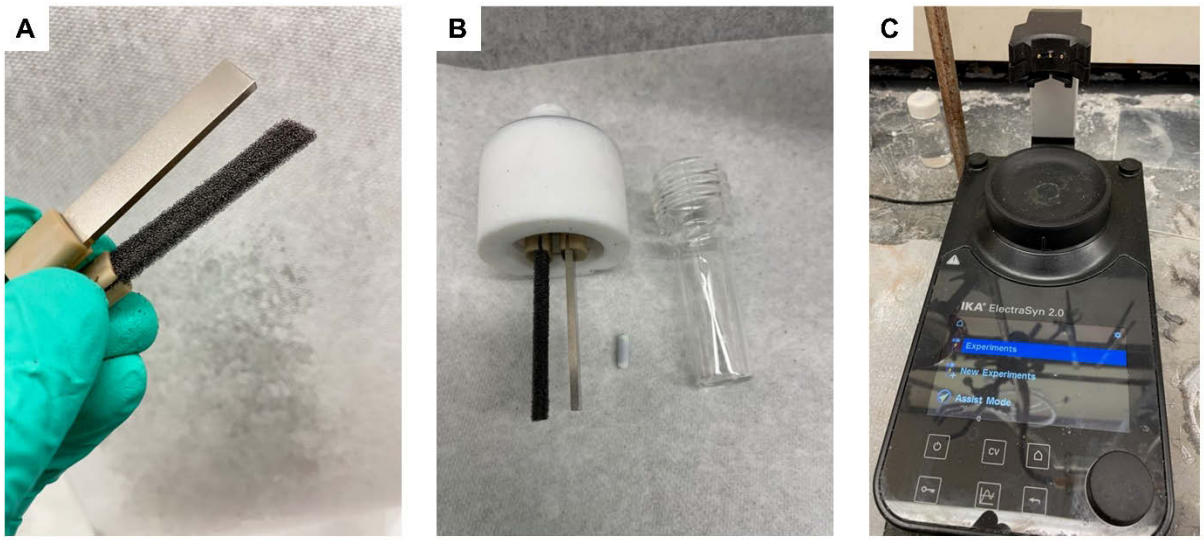

Figure S7. Equipment for electrolysis. **A)** IKA nickel plate and non-IKA (Ultramet) RVC electrodes. Note that non-IKA RVC electrode is cut to match the size of IKA nickel-plate electrode. **B)** Both electrodes attached to an IKA ElectraSyn cap (RVC anode on the left, Ni cathode on the right), small Teflon-coated magnetic stirring bar, IKA 5-mL ElectraSyn vial. **C)** IKA ElectraSyn 2.0 device equipped with a single vial holder. Permission granted by IKA (Figure 7C).

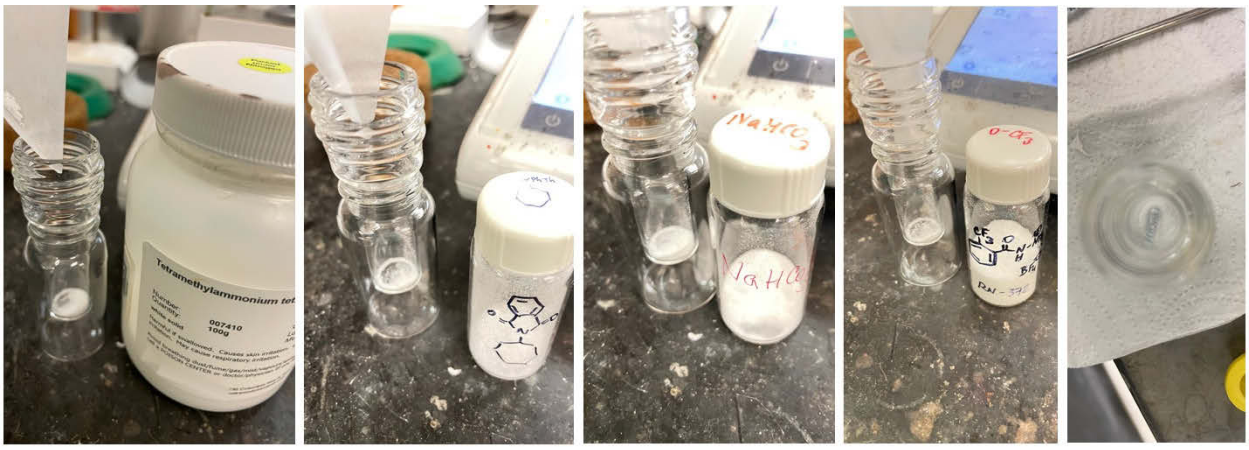

Figure S8. A 5-mL IKA ElectraSyn vial is charged with electrolyte, substrate, base, ylide and a magnetic stirring bar. All operations are done open to air.

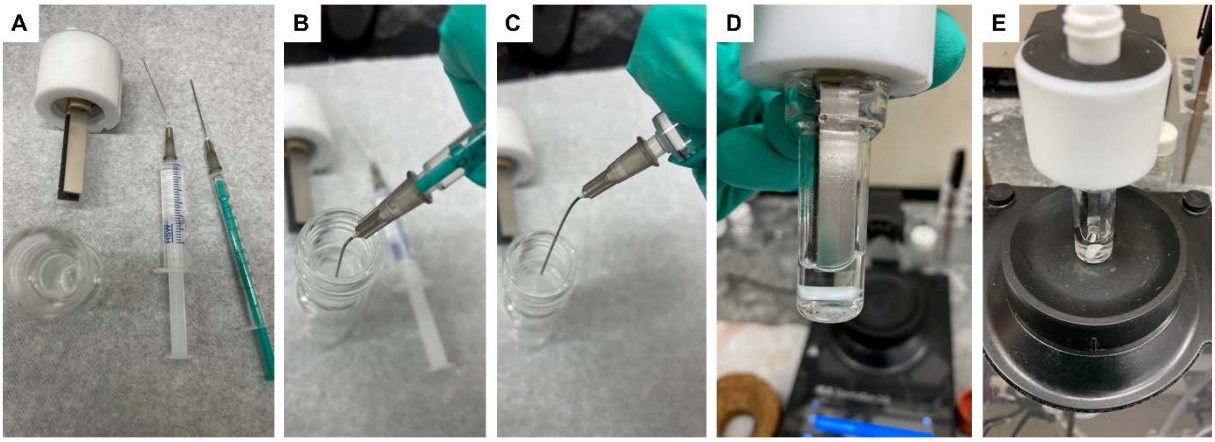

Figure S9. A) ElectraSyn vial charged with reagents, ElectraSyn cap with mounted electrodes, and appropriate amounts of MeCN and HFIP in syringes. **B)** and **C)** HFIP and MeCN are added into the vial. **D)** Vial and ElectraSyn cap with electrodes are assembled together (make sure that electrodes are immersed in solvent). **E)** Whole assembly is attached to ElectraSyn 2.0 (make sure that RVC anode is on the left and Ni cathode on the right). Note that the reaction mixture remains open to air during the reaction.

ElectraSyn 2.0 Settings

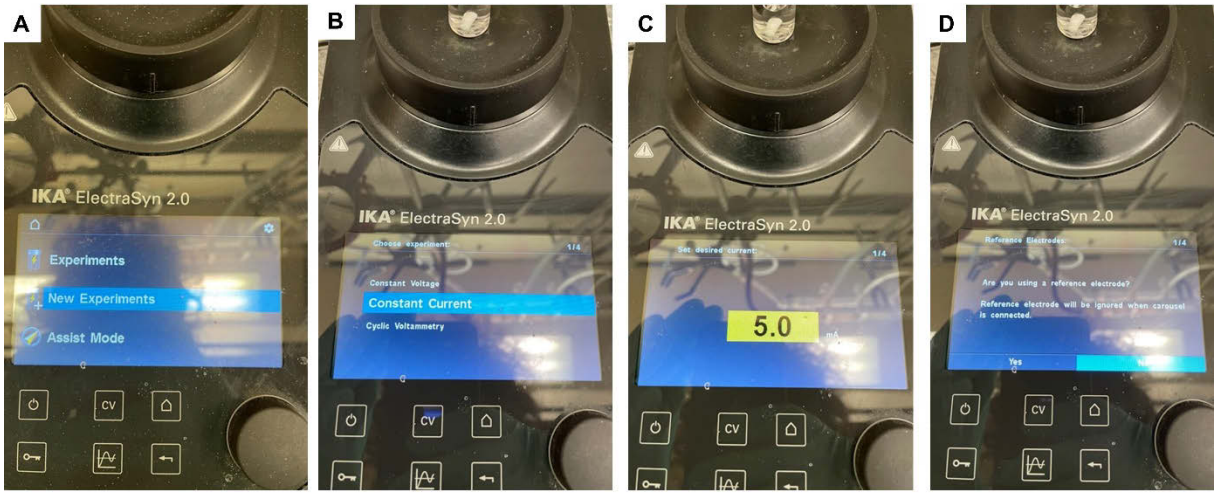

Figure S10. A) Select "*New Experiments*". **B)** Select "*Constant Current*". **C)** Select "*5.0 mA*" by turning the knob. **D)** Select "*No*" (no reference electrode is used for this reaction). Permission granted by IKA.

Figure S11. E) Select "*Total charge*". **F)** Select the number of mmol of substrate, in this case "*0.1*", and the number of equivalents of electrons, typically "*5.0 – 9.0* ". We recommend monitoring the reaction progress by TLC analysis every 2-3 F/mol and to adjust accordingly. **G)** Select "*No*" (the electrode polarity is not altered). **H)** Please check if the selected options and values are correct. If yes, then press "*Start*". **I)** ElectraSyn 2.0 screen showing experimental parameters while the reaction is running. You can also adjust the stirring to 600–700 rpm by turning the knob on the right (400 rpm is the default); make sure that the stirring bar does not hit the electrodes. Permission granted by IKA.

Reaction Workup

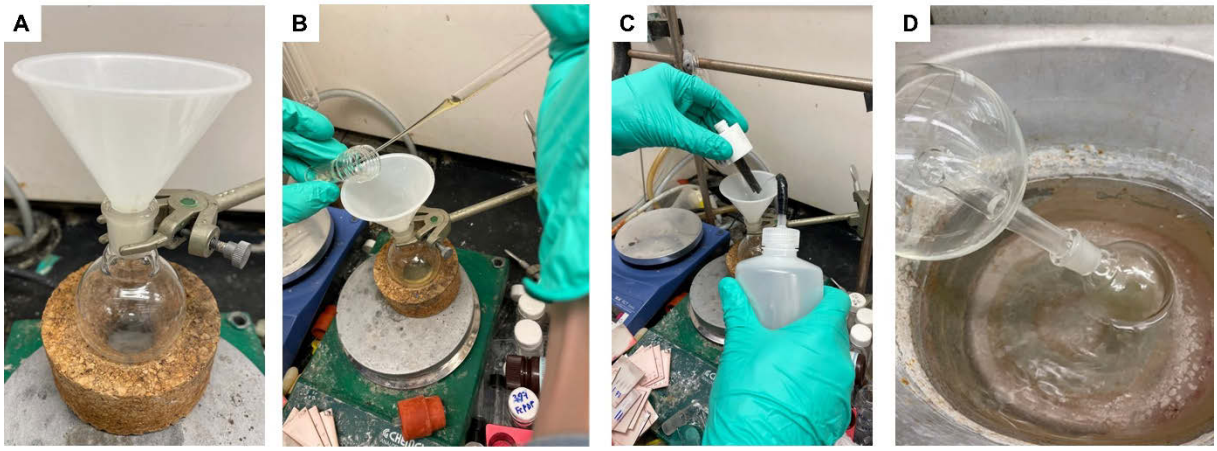

Figure S12. A) A round-bottomed flask with a funnel. **B)** Electrolyzed reaction mixture is transferred into the round-bottom flask using a Pasteur pipette and the vial is washed with CH_2Cl_2 or EtOAc. **C)** Both electrodes (especially the porous RVC) are also washed thoroughly with solvent into the round-bottomed flask. **D)** Crude reaction mixture is concentrated in vacuo to remove MeCN and HFIP.

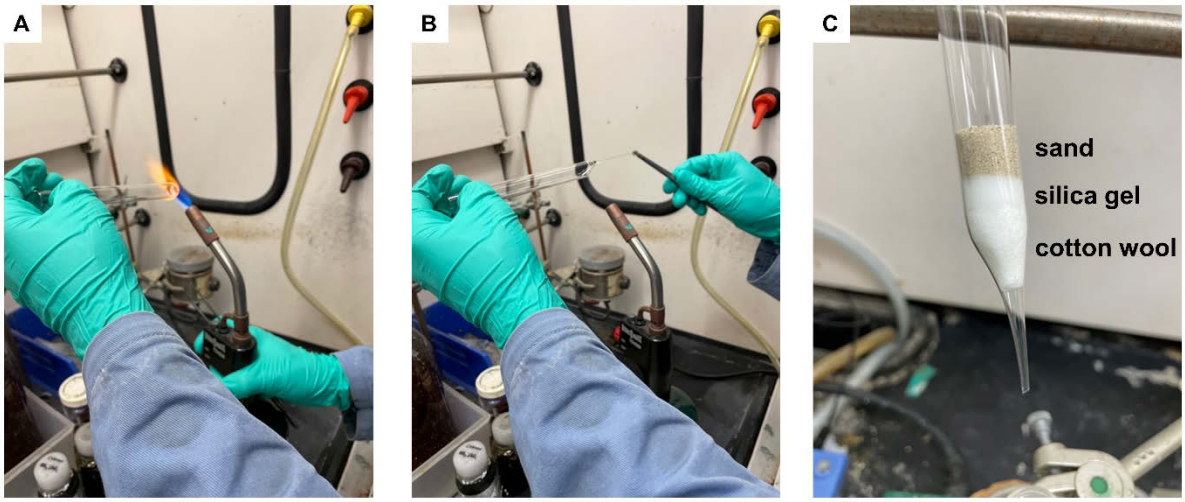

Figure S13. A) The bottom of a test tube is heated with a torch. **B)** Hot tube is pulled by a pair of tweezers to make a long stem. **C)** After cooling, pulled stem is shortened and the test tube is packed with cotton wool, ca. 0.5 cm of silica gel, and sand.

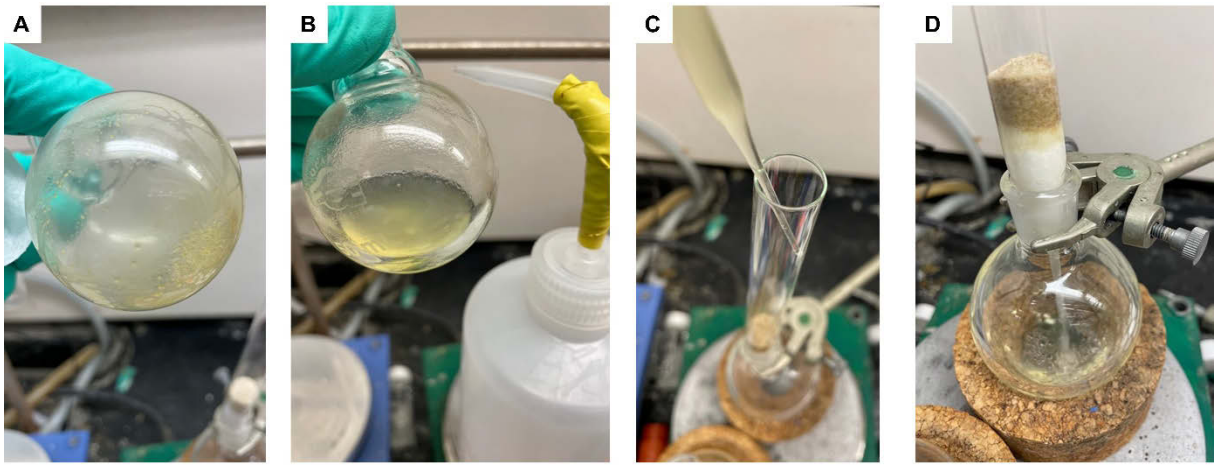

Figure S14. A) Evaporated reaction mixture. **B)** Reaction mixture is redissolved in EtOAc or CH_2Cl_2. **C)** and **D)** Re-dissolved reaction mixture is filtered through a pad of silica gel and cotton wool using the prepared packed test tube (alternatively, a funnel with silica gel pad can be used). This filtration step removes the electrolyte. Furthermore, the filtrate is concentrated in vacuo and crude NMR spectrum is typically measured at this point. Finally, the crude reaction mixture is purified by column chromatography or pTLC.

Experimental Procedures and Characterization Data

CHARACTERIZATION OF MEDIATORS

Preparation of mediator Y1

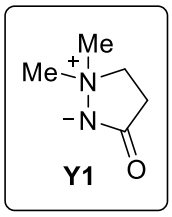

Dimethyl hydrazine (760 µL, 10.00 mmol) was added dropwise to a solution of ethyl acrylate (1.07 mL, 10.00 mmol) in MeOH (5 mL) at 0 °C over 1 min. After addition, the reaction was stirred for 1 h at 0 °C and 3 h at laboratory temperature. Then the reaction mixture was concentrated under reduced pressure to afford an off-white solid. The crude ylide was recrystalized from refluxing acetone (5 mL), then washed with hexanes to afford ylide **Y1** as a white solid (200 mg, 18% yield)

Data for mediator **Y1**:

^{1}H NMR (600 MHz, DMSO-d_6): δ 3.65 (t, J = 8.1 Hz, 2H), 3.04 (s, 6H), 2.50 (t, J = 8.1 Hz, 2H).

^{13}C NMR (151 MHz, DMSO-d_6): δ 177.0, 63.0, 56.1, 32.9.

HRMS (ESI-TOF, m/z): LRMS (ESI) Calcd for $[M+H]^+$ 115.08; Found 115.10.

Preparation of mediator Y2

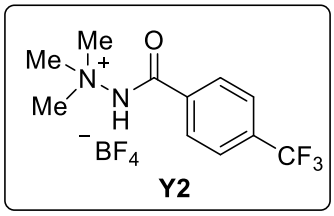

Y2

Following General Procedure A, 4-(trifluoromethyl) benzoyl chloride (1.47 mL, 10.00 mmol) was added to a solution of *N*,*N*-dimethylhydrazine (2.28 mL, 30.00 mmol) in CH_2Cl_2 (15 mL) at 0 °C under argon over 15 min and the reaction was stirred for 30 min at 0 °C and 3 h at laboratory temperature. The reaction mixture was diluted with CH_2Cl_2 (40 mL) and 1 M aq. NaOH (30 mL), the organic phase was separated, and the aqueous phase was extracted with CH_2Cl_2 (2 × 40 mL). Combined organic phases were dried over $MgSO_4$, filtered, and concentrated under reduced pressure to afford a white solid. A round-bottom flask charged with the crude hydrazide (1.48 g, 6.37 mmol) and a magnetic stir bar was evacuated and backfilled with argon twice. Dry MeCN (15 mL) was added, followed by the addition of trimethyloxonium tetrafluoroborate (1.04 g, 7.01 mmol) in one portion. The resulting homogeneous solution was stirred at laboratory temperature for 30 min. Then the reaction mixture was concentrated under reduced pressure to afford a solid residue. The crude ylide salt was recrystallized from a mixture of MeOH and Et_2O, then washed with Et_2O to afford ylide salt **Y2** as a white solid (1.90 g, 89% yield).

Data for mediator **Y2**:

^{1}H NMR (600 MHz, MeOH-*d*$_4$): δ 8.03 (d, *J* = 8.2 Hz, 2H), 7.84 (d, *J* = 8.2 Hz, 2H), 3.83 (s, 9H).

^{13}C NMR (151 MHz, MeOH-*d*$_4$): δ 165.4, 135.0, 134.1 (q, $^2J_{C\text{-}F}$ = 32.7 Hz), 130.1, 126.7 (q, $^3J_{C\text{-}F}$ = 3.8 Hz), 125.0 (q, $^1J_{C\text{-}F}$ = 273 Hz), 57.7.

^{19}F NMR (376 MHz, MeOH-*d*$_4$): δ −67.3, −156.0.

HRMS (ESI-TOF, m/z): HRMS (ESI) Calcd for $[M–BF_4]^+$ 247.1053; Found 247.1059.

Preparation of mediator Y3

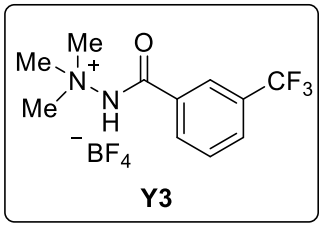

Y3

Following General Procedure A, 3-(trifluoromethyl) benzoyl chloride (1.51 mL, 10.00 mmol) was added to a solution of *N*,*N*-dimethylhydrazine (2.28 mL, 30.00 mmol) in CH_2Cl_2 (15 mL) at 0 °C under argon over 15 min and the reaction was stirred for 30 min at 0 °C and 3 h at laboratory temperature. The reaction mixture was diluted with CH_2Cl_2 (30 mL) and 1 M aq. NaOH (30 mL), the organic phase was separated, and the aqueous phase was extracted with CH_2Cl_2 (2 × 40 mL). Combined organic phases were dried over $MgSO_4$, filtered, and concentrated under reduced pressure to afford a white solid. A round-bottom flask charged with the crude hydrazide (1.38 g, 5.94 mmol) and a magnetic stir bar was evacuated and backfilled with argon twice. Dry MeCN (15 mL) was added, followed by the addition of trimethyloxonium tetrafluoroborate (966 mg, 6.53 mmol) in one portion. The resulting homogeneous solution was stirred at laboratory temperature for 30 min. Then the reaction mixture was concentrated under reduced pressure to afford a solid residue. The crude ylide salt was recrystallized from a mixture of MeOH and Et_2O, then washed with Et_2O to afford ylide salt **Y3** as a white solid (1.44 g, 68% yield).

Data for mediator **Y3**:
^{1}H NMR (600 MHz, MeOH-*d*$_4$): δ 8.17 (d, *J* = 2.0 Hz, 1H), 8.12 (dt, *J* = 7.9, 1.4 Hz, 1H), 7.97 – 7.94 (m, 1H), 7.75 (t, *J* = 7.8 Hz, 1H), 3.83 (s, 9H).
^{13}C NMR (151 MHz, MeOH-*d*$_4$): δ 166.5, 133.7, 133.0, 132.1 (q, $^{2}J_{C\text{-}F}$ = 33.3 Hz), 130.9, 130.7 (q, $^{3}J_{C\text{-}F}$ = 3.7 Hz), 126.1 (q, $^{3}J_{C\text{-}F}$ = 3.9 Hz), 125.1 (q, $^{1}J_{C\text{-}F}$ = 273.0 Hz), 57.7.
^{19}F NMR (376 MHz, MeOH-*d*$_4$): δ −66.9, −155.9.
HRMS (ESI-TOF, m/z): HRMS (ESI) Calcd for $[M–BF_4]^+$ 247.1053; Found 247.1057.

Preparation of mediator Y4

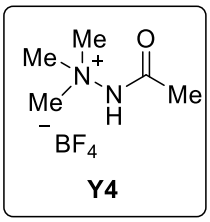

Y4

Following a modified General Procedure A, acetyl chloride (9.0 mL, 127.39 mmol) was added to a solution of *N*,*N*-dimethylhydrazine (24.0 mL, 318.48 mmol) in CH_2Cl_2 (100 mL) at −78 °C under argon over 15 min. The reaction mixture was stirred 30 min at −78 °C and then gradually warmed to laboratory temperature and stirred for 3 h. The reaction mixture was diluted with CH_2Cl_2 (200 mL) and dist. water (100 mL), the organic phase was separated, and the aqueous phase was extracted with CH_2Cl_2 (3 × 200 mL). Combined organic phases were washed with sat. aq. $NaHCO_3$ (200 mL), separated and dried over $MgSO_4$, filtered, and concentrated under reduced pressure to afford an off-white solid, crude hydrazide (4.10 g, 32% yield). A round-bottom flask charged with the crude hydrazide (4.10 g, 40.14 mmol) and a magnetic stir bar was evacuated and backfilled with argon twice. Dry MeCN (40 mL) was added and the solution was cooled to 0 °C, trimethyloxonium tetrafluoroborate (6.23 g, 42.15 mmol) was then added in one portion. The resulting homogeneous solution was stirred at 0 °C for 20 min and at laboratory temperature for 20 min. Then the reaction mixture was concentrated under reduced pressure to afford a solid residue. The crude product was recrystallized from refluxing EtOH (25 mL), then washed with Et_2O and EtOH to afford ylide salt **Y4** as colorless crystalline solid (4.34 g, 53% yield) which was kept at 5 °C for prolonged storage.

Data for mediator **Y4**:
^{1}H NMR (600 MHz, DMSO-*d*$_6$): δ 11.43 (s, 1H), 3.57 (s, 9H), 1.96 (s, 3H).
^{13}C NMR (151 MHz, DMSO-*d*$_6$): δ 167.9, 56.3, 21.8.
MS (ESI, m/z): MS (ESI) Calcd for $[M–BF_4]^+$ 117.10; Found 117.10.

Preparation of mediator Y5

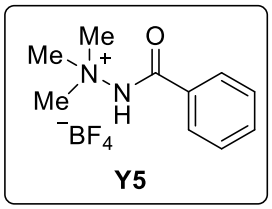

Y5

Following General Procedure A, benzoyl chloride (5.00 mL, 43.04 mmol) was added to a solution of *N*,*N*-dimethylhydrazine (6.88 mL, 90.38 mmol) in CH_2Cl_2 (50 mL) at 0 °C under argon over 15 min. The resulting reaction mixture was stirred for 30 min at 0 °C and 3 h at laboratory temperature. The reaction mixture was diluted with CH_2Cl_2 (40 mL) and 1 M aq. NaOH (50 mL), the organic phase was separated, and the aqueous phase was extracted with CH_2Cl_2 (2 × 100 mL). Combined organic phases were dried over $MgSO_4$, filtered, and concentrated under reduced pressure to afford a white solid, crude hydrazide (6.22 g, 88% yield). A round-bottom flask charged with the crude hydrazide (6.22 g, 37.88 mmol) and a magnetic stir bar was evacuated and backfilled with argon twice. Dry MeCN (20 mL) was added, followed by the addition of trimethyloxonium tetrafluoroborate (6.17 g, 41.70 mmol) over 1 min. The resulting homogeneous solution was stirred at laboratory temperature for 30 min. Then the reaction mixture was concentrated under reduced pressure to afford a solid residue. The crude ylide salt was recrystallized from refluxing EtOH, then washed with Et_2O and EtOH to afford ylide salt **Y5** as a white crystalline solid (7.50 g, 74% yield).

Data for mediator **Y5**:
^{1}H NMR (600 MHz, DMSO-d_6): δ 11.81 (s, 1H), 7.83 (d, *J* = 7.5 Hz, 2H), 7.68 (t, *J* = 7.5 Hz, 1H), 7.57 (t, *J* = 7.8 Hz, 2H), 3.73 (s, 9H).
^{13}C NMR (151 MHz, DMSO-d_6): δ 165.9, 133.2, 131.4, 128.7, 128.2, 56.5.
HRMS (ESI-TOF, m/z): HRMS (ESI) Calcd for $[M–BF_4]^+$ 179.1179; Found 179.1188.

Preparation of mediator Y6

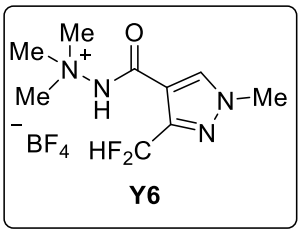

Y6

Following General Procedure B, oxalyl chloride (1.46 mL, 17.04 mmol) was added dropwise to a solution of 3-(difluoromethyl)-1-methyl-1*H*-pyrazole-4-carboxylic acid (1.50 g, 8.52 mmol), DMF (4 drops) in CH_2Cl_2 (15 mL) at 0 °C under argon over 10 min. After the addition, the reaction was stirred for 1 h at 0 °C and 2 h at laboratory temperature. The reaction mixture was concentrated under reduced pressure to remove excess of oxalyl chloride and afforded crude acyl chloride. A solution of the crude acyl chloride in CH_2Cl_2 (2 mL) was added to a solution of *N*,*N*-dimethylhydrazine (1.94 mL, 25.56 mmol) in CH_2Cl_2 (10 mL) at 0 °C under argon over 15 min and the reaction was stirred for 30 min at 0 °C and 3 h at laboratory temperature. The reaction mixture was diluted with CH_2Cl_2 (20 mL) and 1 M aq. NaOH (20 mL), the organic phase was separated, and the aqueous phase was extracted with CH_2Cl_2 (2 × 20 mL). Combined organic phases were dried over Na_2SO_4, filtered, and concentrated under reduced pressure to afford a white solid (1.51 g). A round-bottom flask charged with the crude hydrazide and a magnetic stir bar was evacuated and backfilled with argon twice. Dry MeCN (10 mL) was added, followed by the addition of trimethyloxonium tetrafluoroborate (1.26 g, 8.52 mmol) in one portion. The resulting homogeneous solution was stirred at laboratory temperature for 30 min. Then the reaction mixture was concentrated under reduced pressure to afford a solid residue. The crude

ylide salt was recrystallized from refluxing EtOH, then washed with Et_2O and EtOH to afford ylide salt **Y6** as a white crystalline solid (1.80 g, 66% yield).

Data for mediator **Y6**:
^{1}H NMR (600 MHz, DMSO-d_6): δ 11.51 (s, 1H), 8.35 (s, 1H), 7.19 (t, J = 53.6 Hz, 1H), 3.97 (s, 3H), 3.67 (s, 9H).
^{13}C NMR (151 MHz, DMSO-d_6): δ 160.0, 145.5 (t, $^2J_{C\text{-}F}$ = 24.2 Hz), 135.4, 112.1, 109.7 (t, $^1J_{C\text{-}F}$ = 235.5 Hz), 56.7.
^{19}F NMR (376 MHz, DMSO-d_6): δ -117.1, -150.9.
HRMS (ESI-TOF, m/z): HRMS (ESI) Calcd for $[M–BF_4]^+$ 233.1208; Found 233.1217.

Large scale Preparation of mediator Y7

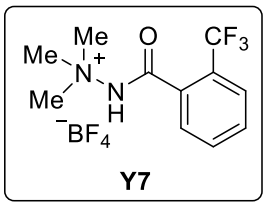

Y7

Following General Procedure B, oxalyl chloride (11.91 mL, 138.88 mmol) was added dropwise to a solution of 2-(trifluoromethyl)benzoic acid (22.00 g, 115.73 mmol) and DMF (0.3 mL) in THF (60 mL) at 0 °C under argon over 30 min. After the addition, the reaction was stirred for 1 h at 0 °C and 3 h at laboratory temperature. The reaction mixture was concentrated under reduced pressure to remove excess oxalyl chloride and afforded crude acyl chloride.
A solution of the crude acyl chloride in CH_2Cl_2 (50 mL) was added to a solution of *N*,*N*-dimethylhydrazine (18.47 mL, 243.03 mmol) in CH_2Cl_2 (100 mL) at −78 °C under argon over 30 min and the reaction was stirred 30 min at −78 °C and 3 h at laboratory temperature. The reaction mixture was diluted with CH_2Cl_2 (200 mL) and 1 M aq NaOH (200 mL), the organic phase was separated, and the aqueous phase was extracted with CH_2Cl_2 (2 × 250 mL). Combined organic phases were dried over $MgSO_4$, filtered, and concentrated under reduced pressure to afford hydrazide **Y7-H** as a white solid (24.01 g, 89 % yield). A round-bottom flask charged with the crude hydrazide **Y7-H** (22.00 g, 94.74 mmol) and a magnetic stir bar was evacuated and backfilled with argon twice. Dry MeCN (150 mL) was added and the reaction mixture was cooled to −10 °C (ice/NaCl bath). To this vigorously stirred solution, trimethyloxonium tetrafluoroborate (14.72 g, 4.76 mmol) was added in ~ 2 g portions over 1 min. The resulting yellow homogeneous solution was stirred at –10 °C for 20 min and at laboratory temperature for 20 min. Then MeOH (~ 1 mL) was added to quench excess Me_3OBF_4 and the reaction mixture was concentrated under reduced pressure to afford an off-white solid. The crude ylide salt was recrystallized from refluxing EtOH (80 mL), then washed with Et_2O and EtOH to afford ylide salt **Y7** as a white solid (28.14 g, 90% yield).

Data for mediator **Y7**:
^{1}H NMR (600 MHz, MeOH-d_4): δ 7.85 (d, J = 8.5 Hz, 1H), 7.80 – 7.74 (m, 3H), 3.81 (s, 9H).
^{13}C NMR (151 MHz, MeOH-d_4): δ 166.8, 133.7, 132.7, 132.60 (q, $^3J_{C\text{-}F}$ = 2.2 Hz), 130.3, 128.7 (q, $^2J_{C\text{-}F}$ = 32.1 Hz), 127.9 (q, $^3J_{C\text{-}F}$ = 4.9 Hz), 125.0 (q, $^1J_{C\text{-}F}$ = 272.5 Hz), 57.5.
^{19}F NMR (376 MHz, MeOH-d_4): δ -62.7, -155.9.
HRMS (ESI-TOF, m/z): HRMS (ESI) Calcd for $[M–BF_4]^+$ 247.1053; Found 247.1063.

Preparation of mediator Y7 ylide

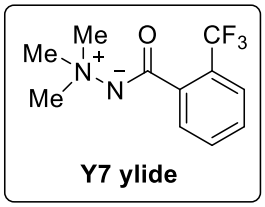

Y7 ylide

Methyl iodide (7.20 mL, 114.98 mmol) was added dropwise over 20 min to a vigorously stirred solution *N'*,*N'*-dimethyl-2-(trifluoromethyl)benzo-hydrazide **Y7-H** (17.80 g, 76.65 mmol) in dry MeCN (50 mL) at 0 °C under argon. The resulting orange solution was stirred for 30 min at 0 °C and 12 hours at laboratory temperature. Then the reaction mixture was concentrated under reduced pressure to afford a yellow-orange solid which was triturated with Et_2O (50 mL). The solid was washed with Et_2O (50 mL), hexanes (50 mL) and minimal amount of cold EtOH on a Büchner funnel. The remaining white solid was dried under high vacuum overnight to afford a hydroiodide salt as a white solid (24.18 g, 84 % yield). The hydroiodide salt was added to vigorously stirred 2 M aq. NaOH (250 mL) at laboratory temperature. The mixture was stirred for 20 min, then CH_2Cl_2 (50 mL) was added and the heterogenous mixture was stirred for an additional 15 min. The mixture was extracted with CH_2Cl_2 (4 × 250 mL), dried over $MgSO_4$, filtered, and concentrated under reduced pressure to afford ylide **Y7 ylide** as a white solid (15.75 g, 99% yield)

Data for mediator **Y7 ylide**:
^{1}H NMR (600 MHz, $CDCl_3$): δ 7.55 (d, *J* = 8.0 Hz, 1H), 7.49 (d, *J* = 7.7 Hz, 1H), 7.43 (t, *J* = 7.3 Hz, 1H), 7.31 (t, *J* = 7.7 Hz, 1H), 3.40 (s, 9H).
^{13}C NMR (151 MHz, $CDCl_3$): δ 172.0, 139.5 (q, $^3J_{C\text{-}F}$ = 2.2 Hz), 131.5, 129.3, 127.8, 127.3 (q, $^2J_{C\text{-}F}$ = 31.0 Hz), 126.0 (q, $^3J_{C\text{-}F}$ = 5.0 Hz), 124.4 (q, $^1J_{C\text{-}F}$ = 273.7 Hz), 55.2.
^{19}F NMR (376 MHz, $CDCl_3$): δ −61.6.
HRMS (ESI-TOF, m/z): HRMS (ESI) Calcd for $[M+H]^+$ 247.1053; Found 247.1061.

Preparation of mediator Y8

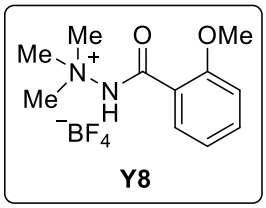

Y8

Following General Procedure A, 2-methyxybenzoyl chloride (740 µL, 4.97 mmol) was added to a solution of *N*,*N*-dimethylhydrazine (378 µL, 14.91 mmol) in CH_2Cl_2 (10 mL) at 0 °C under argon over 15 min and the reaction was stirred for 30 min at 0 °C and 3 h at laboratory temperature. The reaction mixture was diluted with CH_2Cl_2 (30 mL) and 1 M aq. NaOH (30 mL), the organic phase was separated, and the aqueous phase was extracted with CH_2Cl_2 (2 × 30 mL). Combined organic phases were dried over $MgSO_4$, filtered, and concentrated under reduced pressure to afford an oil, crude hydrazide. A round-bottom flask charged with the crude hydrazide (1.02 g, 5.25 mmol) and a magnetic stir bar was evacuated and backfilled with argon twice. Dry MeCN (10 mL) was added, followed by the addition of trimethyloxonium tetrafluoroborate (851 mg, 5.78 mmol) in one portion. The resulting homogeneous solution was stirred at laboratory temperature for 30 min. Then the reaction mixture was concentrated under reduced pressure to afford a solid residue. The crude ylide salt was recrystallized from a mixture of MeOH and Et_2O mixture, then washed with Et_2O to afford ylide salt **Y8** as a white solid (924 mg, 60% yield).

Data for mediator **Y8**:
^{1}H NMR (600 MHz, MeOH-d_4): δ 7.76 (d, *J* = 7.7 Hz, 1H), 7.58 (t, *J* = 7.9 Hz, 1H), 7.18 (d, *J* = 8.4 Hz, 1H), 7.09 (t, *J* = 7.5 Hz, 1H), 3.98 (s, 3H), 3.81 (s, 9H).
^{13}C NMR (151 MHz, MeOH-d_4): δ 164.7, 157.5, 134.1, 130.1, 120.7, 119.9, 111.7, 56.4, 55.4.
HRMS (ESI-TOF, m/z): HRMS (ESI) Calcd for $[M–BF_4]^+$ 209.1285; Found 209.1290.

Preparation of mediator Y9

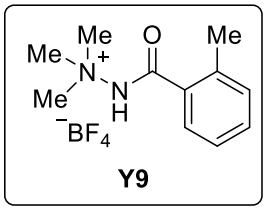

Y9

Following General Procedure B, oxalyl chloride (1.00 mL, 11.74 mmol) was added dropwise to a solution of 2-methylbenzoic acid (800 mg, 5.87 mmol) and DMF (4 drops) in CH_2Cl_2 (10 mL) at 0 °C under argon over 10 min. After the addition, the reaction was stirred for 1 h at 0 °C and 2 h at laboratory temperature. The reaction mixture was concentrated under reduced pressure to remove excess of oxalyl chloride and afforded crude acyl chloride. A solution of the crude acyl chloride in CH_2Cl_2 (2 mL) was added to a solution of *N*,*N*-dimethylhydrazine (936 µL, 12.33 mmol) in CH_2Cl_2 (10 mL) at 0 °C under argon over 15 min and the reaction was stirred for 30 min at 0 °C and 3 h at laboratory temperature. The reaction mixture was diluted with CH_2Cl_2 (20 mL) and 1 M aq. NaOH (50 mL), the organic phase was separated, and the aqueous phase was extracted with CH_2Cl_2 (2 × 50 mL). Combined organic phases were dried over $MgSO_4$, filtered, and concentrated under reduced pressure to afford a white solid, crude hydrazide (1.03 g, 98% yield). A round-bottom flask charged with the crude hydrazide (771 mg, 4.33 mmol) and a magnetic stir bar was evacuated and backfilled with argon twice. Dry MeCN (10 mL) was added, followed by the addition of trimethyloxonium tetrafluoroborate (705 mg, 4.76 mmol) in one portion. The resulting homogeneous solution was stirred at laboratory temperature for 30 min. Then the reaction mixture was concentrated under reduced pressure to afford a solid residue. The crude ylide salt was recrystallized from refluxing EtOH, then washed with Et_2O and EtOH to afford ylide salt **Y9** as a white crystalline solid (876 mg, 72% yield).

Data for mediator **Y9**:
^{1}H NMR (600 MHz, DMSO-d_6): δ 12.06 (s, 1H), 7.48 – 7.44 (m, 2H), 7.35 – 7.29 (m, 2H), 3.70 (s, 9H), 2.36 (s, 3H).
^{13}C NMR (151 MHz, DMSO-d_6): δ 166.9, 136.1, 132.7, 131.1, 130.8, 128.0, 125.7, 56.4, 19.0.
HRMS (ESI-TOF, m/z): HRMS (ESI) Calcd for $[M–BF_4]^+$ 193.1335; Found 193.1345.

Preparation of mediator Y10

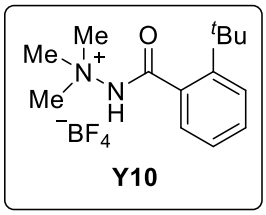

Following General Procedure B, oxalyl chloride (1.25 mL, 14.52 mmol) was added dropwise to a solution of 2-*t*-butylcarboxylic acid (647 mg, 3.63 mmol) and DMF (5 drops) in CH_2Cl_2 (40 mL) at 0 °C under argon over 10 min. After the addition, the reaction was stirred for 1 h at 0 °C and 2 h at laboratory temperature. The reaction mixture was concentrated under reduced pressure to remove excess oxalyl chloride and afforded crude acyl chloride. A solution of the crude acyl chloride in CH_2Cl_2 (2 mL) was added to a solution of *N*,*N*-dimethylhydrazine (827 µL, 10.89 mmol) in CH_2Cl_2 (10 mL) at 0 °C under argon over 15 min and the reaction was stirred for 30 min at 0 °C and 3 h at laboratory temperature. The reaction mixture was diluted with CH_2Cl_2 (30 mL) and 1 M aq. NaOH (30 mL), the organic phase was separated, and the aqueous phase was extracted with CH_2Cl_2 (2 × 30 mL). Combined organic phases were dried over $MgSO_4$, filtered, and concentrated under reduced pressure to afford crude hydrazide.
A round-bottom flask charged with the crude hydrazide and a magnetic stir bar was evacuated and backfilled with argon twice. Dry MeCN (10 mL) was added, followed by the addition of trimethyloxonium tetrafluoroborate (590 mg, 3.99 mmol) in one portion. The resulting homogeneous solution was stirred at laboratory temperature for 30 min. Then the reaction mixture was concentrated under reduced pressure to afford a solid residue. The crude ylide salt was recrystallized from a mixture of methanol and Et_2O to afford ylide **Y10** (420 mg, 39% yield) as a white solid.

Data for mediator **Y10**:
^{1}H NMR (600 MHz, DMSO-*d*$_6$): δ 12.26 (s, 1H), 7.59 (d, *J* = 8.1 Hz, 1H), 7.52 – 7.47 (m, 1H), 7.42 (dd, *J* = 7.6, 1.5 Hz, 1H), 7.34 (td, *J* = 7.5, 1.1 Hz, 1H), 3.72 (s, 9H), 1.40 (s, 9H).
^{13}C NMR (151 MHz, DMSO-*d*$_6$): δ 168.9, 147.9, 132.4, 130.6, 129.8, 127.5, 125.5, 56.0, 36.0, 31.4.
HRMS (ESI-TOF, m/z): HRMS (ESI) Calcd for $[M–BF_4]^+$ 235.1805; Found 235.1816.

Preparation of mediator Y11

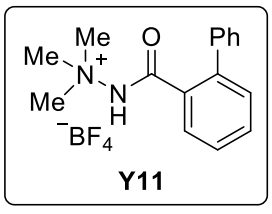

Following General Procedure B, oxalyl chloride (700 mL, 8.16 mmol) was added dropwise to a solution of biphenyl-2-carboxylic acid (540 mg, 2.72 mmol) and DMF (5 drops) in CH_2Cl_2 (15 mL) at 0 °C under argon over 10 min. After the addition, the reaction was stirred for 1 h at 0 °C and 2 h at laboratory temperature. The reaction mixture was concentrated under reduced pressure to remove excess oxalyl chloride and afforded crude acyl chloride. A solution of the crude acyl chloride in CH_2Cl_2 (2 mL) was added to a solution of *N*,*N*-dimethylhydrazine (520 µL, 6.80 mmol) in CH_2Cl_2 (10 mL) at 0 °C under argon over 15 min and the reaction was stirred for 30 min at 0 °C and 3 h at laboratory temperature. The reaction mixture was diluted with CH_2Cl_2 (20 mL) and 1 M aq. NaOH (50 mL), the organic

phase was separated, and the aqueous phase was extracted with CH_2Cl_2 (2 × 50 mL). Combined organic phases were dried over $MgSO_4$, filtered, and concentrated under reduced pressure to afford a white solid, crude hydrazide (653 mg, 99% yield). A round-bottom flask charged with the crude hydrazide (644 mg, 2.68 mmol) and a magnetic stir bar was evacuated and backfilled with argon twice. Dry MeCN (10 mL) was added, followed by the addition of trimethyloxonium tetrafluoroborate (436 mg, 2.95 mmol) in one portion. The resulting homogeneous solution was stirred at laboratory temperature for 30 min. Then the reaction mixture was concentrated under reduced pressure to afford a solid residue. The crude ylide salt was recrystallized from refluxing EtOH, washed with Et_2O and EtOH to afford ylide salt **Y11** as a white crystalline solid (550 mg, 60% yield).

Data for mediator **Y11**:
^{1}H NMR (500 MHz, DMSO-*d*$_6$): δ 12.27 (s, 1H), 7.69 – 7.61 (m, 2H), 7.53 (m, 2H), 7.49 – 7.44 (m, 2H), 7.44 – 7.38 (m, 3H), 3.58 (s, 9H).
^{13}C NMR (126 MHz, DMSO-*d*$_6$): δ 166.7, 140.3, 139.3, 132.6, 131.3, 130.2, 128.6, 128.5, 128.4, 127.8, 127.3, 56.1.
HRMS (ESI-TOF, m/z): HRMS (ESI) Calcd for $[M–BF_4]^+$ 255.1492; Found 255.1500.

Preparation of mediator Y12

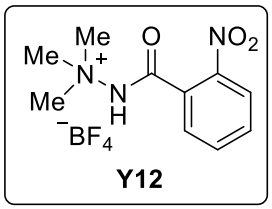

Y12

Following General Procedure B, oxalyl chloride (750 µL, 8.74 mmol) was added dropwise to a solution of 2-nitrobenzoic acid (730 mg, 4.37 mmol) and DMF (5 drops) in CH_2Cl_2 (15 mL) at 0 °C under argon over 10 min. After the addition, the reaction was stirred for 1 h at 0 °C and 2 h at laboratory temperature. The reaction mixture was concentrated under reduced pressure to remove excess oxalyl chloride and afforded crude acyl chloride. A solution of the crude acyl chloride in CH_2Cl_2 (2 mL) was added to a solution of *N*,*N*-dimethylhydrazine (697 µL, 9.18 mmol) in CH_2Cl_2 (10 mL) at 0 °C under argon over 15 min and the reaction was stirred for 30 min at 0 °C and 3 h at laboratory temperature. The reaction mixture was diluted with CH_2Cl_2 (20 mL) and 1 M aq. NaOH (50 mL), the organic phase was separated, and the aqueous phase was extracted with CH_2Cl_2 (2 × 50 mL). Combined organic phases were dried over $MgSO_4$, filtered, and concentrated under reduced pressure to afford a white solid, crude hydrazide (741 mg, 81 % yield). A round-bottom flask charged with the crude hydrazide (741 mg, 3.54 mmol) and a magnetic stir bar was evacuated and backfilled with argon twice. Dry MeCN (10 mL) was added, followed by the addition of trimethyloxonium tetrafluoroborate (576 mg, 3.90 mmol) in one portion. The resulting homogeneous solution was stirred at laboratory temperature for 30 min. Then the reaction mixture was concentrated under reduced pressure to afford a solid residue. The crude ylide salt was recrystallized from refluxing EtOH, then washed with Et_2O and EtOH to afford ylide salt **Y12** as a white crystalline solid (751 mg, 68% yield).

Data for mediator **Y12**:
^{1}H NMR (600 MHz, DMSO-*d*$_6$): δ 12.46 (br s, 1H), 8.25 (dd, *J* = 8.2, 1.2 Hz, 1H), 7.94 (td, *J* = 7.5, 1.2 Hz, 1H), 7.84 (td, *J* = 7.8, 1.5 Hz, 1H), 7.78 (dd, *J* = 7.5, 1.4 Hz, 1H), 3.70 (s, 9H).

^{13}C NMR (151 MHz, DMSO-d_6): δ 163.8, 145.6, 134.9, 132.3, 129.9, 129.0, 124.7, 56.2.
HRMS (ESI-TOF, m/z): HRMS (ESI) Calcd for $[M–BF_4]^+$ 224.1030; Found 224.1038.

Preparation of mediator Y13

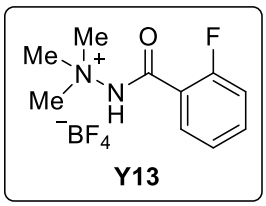

Y13

Following General Procedure A, 2-fluorobenzoyl chloride (600 µL, 5.03 mmol) was added to a solution of *N*,*N*-dimethylhydrazine (1.15 mL, 15.09 mmol) in CH_2Cl_2 (15 mL) at 0 °C under argon over 15 min and the reaction was stirred for 30 min at 0 °C and 3 h at laboratory temperature. The reaction mixture was diluted with CH_2Cl_2 (30 mL) and 1 M aq. NaOH (30 mL), the organic phase was separated, and the aqueous phase was extracted with CH_2Cl_2 (2 × 30 mL). Combined organic phases were dried over $MgSO_4$, filtered, and concentrated under reduced pressure to afford a white solid, crude hydrazide. A round-bottom flask charged with the crude hydrazide (710 mg, 3.90 mmol) and a magnetic stir bar was evacuated and backfilled with argon twice. Dry MeCN (10 mL) was added, followed by the addition of trimethyloxonium tetrafluoroborate (635 mg, 4.29 mmol) in one portion. The resulting homogeneous solution was stirred at laboratory temperature for 30 min. Then the reaction mixture was concentrated under reduced pressure to afford a solid residue. The crude ylide salt was recrystallized from a mixture of MeOH and Et_2O, then washed with Et_2O to afford ylide salt **Y13** as a white solid (835 mg, 75% yield).

Data for mediator **Y13**:
^{1}H NMR (600 MHz, MeOH-d_4): δ 7.74 (td, J = 7.4, 1.8 Hz, 1H), 7.64 (dddd, J = 8.8, 7.2, 5.2, 1.8 Hz, 1H), 7.34 (td, J = 7.6, 1.0 Hz, 1H), 7.30 – 7.26 (m, 1H), 3.82 (s, 9H).
^{13}C NMR (151 MHz, MeOH-d_4): δ 164.4, 161.2 (d, $^1J_{C\text{-}F}$ = 253.2 Hz), 135.7 (d, $^3J_{C\text{-}F}$ = 8.3 Hz), 131.5 (d, $^4J_{C\text{-}F}$ = 1.3 Hz), 125.9 (d, $^3J_{C\text{-}F}$ = 3.6 Hz), 121.6 (d, $^2J_{C\text{-}F}$ = 14.7 Hz), 117.5 (d, $^2J_{C\text{-}F}$ = 22.3 Hz), 57.7.
^{19}F NMR (376 MHz, MeOH-d_4): δ −117.5, −156.2.
HRMS (ESI-TOF, m/z): HRMS (ESI) Calcd for $[M–BF_4]^+$ 197.1085; Found 197.1090.

Preparation of mediator Y14

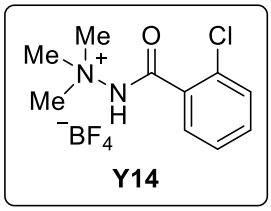

Y14

Following General Procedure A, 2-chlorobenzoyl chloride (1.27 mL, 10.03 mmol) was added to a solution of *N*,*N*-dimethylhydrazine (2.29 mL, 30.09 mmol) in CH_2Cl_2 (20 mL) at 0 °C under argon over 15 min and the reaction was stirred for 30 min at 0 °C and 3 h at laboratory temperature. The reaction mixture was diluted with CH_2Cl_2 (40 mL) and 1 M aq. NaOH (40 mL), the organic phase was separated, and the aqueous phase was extracted with CH_2Cl_2 (2 × 50 mL). Combined organic phases were dried over $MgSO_4$, filtered, and concentrated under reduced pressure to afford a white solid, crude hydrazide. A round-bottom flask charged with the crude hydrazide (1.36 g, 6.85 mmol) and a magnetic stir bar was evacuated and backfilled

with argon twice. Dry MeCN (10 mL) was added, followed by the addition of trimethyloxonium tetrafluoroborate (1.12 g, 7.54 mmol) in one portion. The resulting homogeneous solution was stirred at laboratory temperature for 30 min. Then the reaction mixture was concentrated under reduced pressure to afford a solid residue. The crude ylide salt was recrystallized from a mixture of MeOH and Et_2O, then washed with Et_2O to afford ylide salt **Y14** as a white solid (1.80 g, 87% yield).

Data for mediator **Y14**:
^{1}H NMR (600 MHz, DMSO-*d*$_6$): δ 12.45 (s, 1H), 7.66 – 7.57 (m, 3H), 7.51 (t, *J* = 7.3 Hz, 1H), 3.72 (s, 9H).
^{13}C NMR (151 MHz, DMSO-*d*$_6$): δ 163.8, 132.6, 132.6, 130.4, 129.9, 129.5, 127.4, 56.5.
HRMS (ESI-TOF, m/z): HRMS (ESI) Calcd for $[M–BF_4]^+$ 213.0789; Found 213.0792.

Preparation of mediator Y15

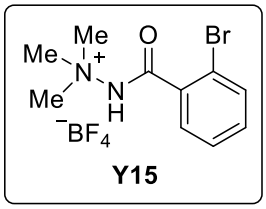

Y15

Following General Procedure A, 2-bromobenzoyl chloride (890 µL, 6.80 mmol) was added to a solution of *N*,*N*-dimethylhydrazine (1.55 mL, 20.40 mmol) in CH_2Cl_2 (15 mL) at 0 °C under argon over 15 min and the reaction was stirred for 30 min at 0 °C and 3 h at laboratory temperature. The reaction mixture was diluted with CH_2Cl_2 (10 mL) and 1 M aq. NaOH (20 mL), the organic phase was separated, and the aqueous phase was extracted with CH_2Cl_2 (2 × 10 mL). Combined organic phases were dried over Na_2SO_4, filtered, and concentrated under reduced pressure to afford as a white solid, crude hydrazide (1.56 g). A round-bottom flask charged with the crude hydrazide and a magnetic stir bar was evacuated and backfilled with argon twice. Dry MeCN (7 mL) was added, followed by the addition of trimethyloxonium tetrafluoroborate (1.01 g, 6.80 mmol) in one portion. The resulting homogeneous solution was stirred at laboratory temperature for 30 min. Then the reaction mixture was concentrated under reduced pressure to afford a solid residue. This crude ylide salt was recrystallized from refluxing EtOH, then washed with Et_2O and EtOH to afford ylide salt **Y15** as a white crystalline solid (1.38 g, 59% yield).

Data for mediator **Y15**:
^{1}H NMR (600 MHz, DMSO-*d*$_6$): δ 12.61 – 12.28 (m, 1H), 7.76 (dd, *J* = 7.9, 1.2 Hz, 1H), 7.61 (dd, *J* = 7.4, 1.9 Hz, 1H), 7.54 (td, *J* = 7.5, 1.3 Hz, 1H), 7.50 (td, *J* = 7.7, 1.9 Hz, 1H), 3.72 (s, 9H).
^{13}C NMR (151 MHz, DMSO-*d*$_6$): δ 164.6, 134.7, 133.0, 132.6, 129.5, 127.8, 119.2, 56.4.
HRMS (ESI-TOF, m/z): HRMS (ESI) Calcd for $[M–BF_4]^+$ 257.0284; Found 257.0293.

Preparation of mediator Y16

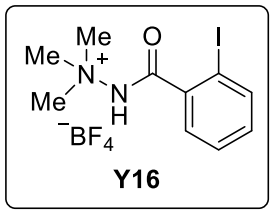

Y16

Following General Procedure A, 2-iodobenzoyl chloride (1.33 g, 5.00 mmol) was added to a solution of *N*,*N*-dimethylhydrazine (1.14 mL, 15.00 mmol) in CH_2Cl_2 (50 mL) at 0 °C under argon over 30 min and the reaction was stirred for 30 min at 0 °C and 3 h at laboratory temperature. The reaction mixture was diluted with CH_2Cl_2 (30 mL) and 1 M aq. NaOH (40 mL), the organic phase was separated, and the aqueous phase was extracted with CH_2Cl_2 (2 × 50 mL). Combined organic phases were dried over $MgSO_4$, filtered, and concentrated under reduced pressure to afford as crude hydrazide. A round-bottom flask charged with the crude hydrazide (580 mg, 2.00 mmol) and a magnetic stir bar was evacuated and backfilled with argon twice. Dry MeCN (10 mL) was added, followed by the addition of trimethyloxonium tetrafluoroborate (325 mg, 2.2 mmol) in one portion. The resulting homogeneous solution was stirred at room temperature for 30 min. Then the reaction mixture was concentrated under reduced pressure to afford a solid residue. The crude ylide salt was recrystallized from a mixture of MeOH and Et_2O to afford ylide salt **Y16** as a white solid (595 mg, 76% yield).

Data for mediator **Y16**:
^{1}H NMR (600 MHz, DMSO-d_6): δ 12.41 (s, 1H), 7.99 (s, 1H), 7.55 (m, 2H), 7.32 (m, 1H), 3.73 (s, 9H).
^{13}C NMR (151 MHz, DMSO-d_6): δ 166.2 , 139.3, 138.4, 132.4, 128.9, 128.2, 93.7, 56.4.
HRMS (ESI-TOF, m/z): HRMS (ESI) Calcd for $[M–BF_4]^+$ 305.0145; Found 305.0154.

Preparation of mediator Y17

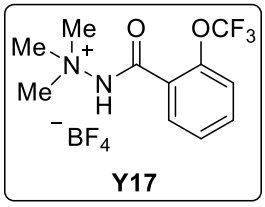

Y17

Following General Procedure A, 2-trifluoromethoxybenzoyl chloride (984 µL, 6.68 mmol) was added to a solution of *N*,*N*-dimethylhydrazine (1.52 mL, 20.04 mmol) in CH_2Cl_2 (15 mL) at 0˚C under argon over 15 min and the reaction was stirred for 30 min at 0 °C and 3 h at room temperature. The reaction mixture was diluted with CH_2Cl_2 (10 mL) and 1 M aq NaOH (20 mL), the organic phase was separated, and the aqueous phase was extracted with CH_2Cl_2 (2 × 10 mL). Combined organic phases were dried over Na_2SO_4, filtered, and concentrated under reduced pressure to afford a white solid, crude hydrazide (1.51 g). This material was used directly in the next step. A round-bottom flask charged with the crude hydrazide and a magnetic stir bar was evacuated and backfilled with argon twice. Dry MeCN (10 mL) was added, followed by the addition of trimethyloxonium tetrafluoroborate (988 mg, 6.68 mmol) in one portion. The resulting homogeneous solution was stirred at room temperature for 30 min. Then the reaction mixture was concentrated under reduced pressure to afford a solid residue. The crude ylide salt was recrystallized from refluxing EtOH, then washed with Et_2O and EtOH to afford ylide salt **Y17** as a white crystalline solid (1.66 g, 71% yield).

Data for mediator **Y17**:
^{1}H NMR (600 MHz, DMSO-d_6): δ 12.42 (br s, 1H), 7.78 – 7.72 (m, 2H), 7.61 – 7.54 (m, 2H), 3.71 (s, 9H).
^{13}C NMR (151 MHz, DMSO-d_6): δ 162.6, 145.1, 130.3, 127.8, 126.9, 122.0, 120.0 (q, $^{1}J_{C-F}$ = 258.0 Hz), 56.4.
^{19}F NMR (376 MHz, DMSO-d_6): δ −59.2, −150.8
HRMS (ESI-TOF, m/z): HRMS (ESI) Calcd for $[M–BF_4]^+$ 263.1002; Found 263.1010.

Preparation of mediator Y18

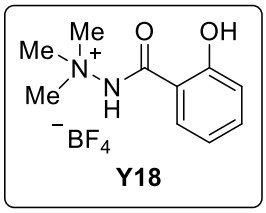

Y18

Following General Procedure B, oxalyl chloride (1.43 mL, 16.66 mmol) was added dropwise to a solution of acetylsalicylic acid (1.50 g, 8.33 mmol) and DMF (4 drops) in CH_2Cl_2 (15 mL) at 0 °C under argon over 10 min. After the addition, the reaction was stirred for 2 h at laboratory temperature. The reaction mixture was concentrated under reduced pressure to remove excess of oxalyl chloride and afforded crude acyl chloride. A solution of the crude acyl chloride in CH_2Cl_2 (2 mL) was added to a solution of *N*,*N*-dimethylhydrazine (1.90 mL, 25.00 mmol) in CH_2Cl_2 (10 mL) at 0 °C under argon over 15 min and the reaction was stirred for 30 min at 0 °C and 3 h at laboratory temperature. The reaction mixture was diluted with CH_2Cl_2 (20 mL) and 1 M aq. NaOH (20 mL), the organic phase was separated, and the aqueous phase was extracted with CH_2Cl_2 (2 × 20 mL). Combined organic phases were dried over Na_2SO_4, filtered, and concentrated under reduced pressure to afford a white solid. A round-bottom flask charged with the crude hydrazide and a magnetic stir bar was evacuated and backfilled with argon twice. Dry MeCN (10 mL) was added, followed by the addition of trimethyloxonium tetrafluoroborate (1.35 g, 9.16 mmol) in one portion. The resulting homogeneous solution was stirred at laboratory temperature for 30 min. Then the reaction mixture was concentrated under reduced pressure to afford a solid residue. The crude ylide salt was recrystallized from refluxing EtOH, then washed with Et_2O and EtOH to afford ylide salt **Y18** as a white crystalline solid (1.10 g, 43% yield). *NOTE: Acetyl group spontaneously hydrolyzed to hydroxyl group during the methylation step.*

Data for mediator **Y18**:
^{1}H NMR (600 MHz, DMSO-d_6): δ δ 7.66 (dd, *J* = 7.8, 1.8 Hz, 1H), 7.42 (ddd, *J* = 8.6, 7.2, 1.8 Hz, 1H), 6.97 (dd, *J* = 8.3, 1.1 Hz, 1H), 6.93 (td, *J* = 7.5, 1.1 Hz, 1H), 3.69 (s, 9H).
^{13}C NMR (151 MHz, DMSO-d_6): δ 165.1, 156.4, 133.7, 129.7, 119.1, 118.2, 116.7, 56.3.
HRMS (ESI-TOF, m/z): HRMS (ESI) Calcd for $[M–BF_4]^+$ 195.1128; Found 195.1140.

Preparation of mediator Y19

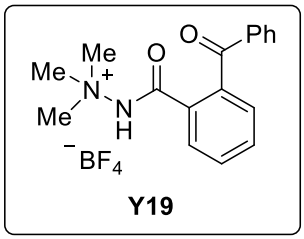

Y19

Following General Procedure B, oxalyl chloride (570 µL, 6.63 mmol) was added dropwise to a solution of 2-benzoylbenzoic acid (1.00 g, 4.42 mmol) and DMF (4 drops) in CH_2Cl_2 (15 mL) and THF (5 mL) at 0 °C under argon over 10 min. After the addition, the reaction was stirred for 1 h at 0 °C and 2 h at laboratory temperature. Then the reaction mixture was concentrated under reduced pressure to remove excess of oxalyl chloride and afforded crude acyl chloride. A solution of the crude acyl chloride in CH_2Cl_2 (5 mL) was added to a solution of *N*,*N*-dimethylhydrazine (705 µL, 9.28 mmol) in CH_2Cl_2 (10 mL) at 0 °C under argon over 15 min and the reaction was stirred for 30 min at 0 °C and 3 h at laboratory temperature. The reaction mixture was diluted with CH_2Cl_2 (40 mL) and 1 M aq. NaOH (50 mL), the organic phase was separated, and the aqueous phase was extracted with CH_2Cl_2 (2 × 50 mL). Combined organic phases were dried over $MgSO_4$, filtered, and concentrated under reduced pressure to afford a white solid, crude hydrazide (985 mg, 83 % yield). A round-bottom flask charged with the crude hydrazide (985 mg, 3.67 mmol) and a magnetic stir bar was evacuated and backfilled with argon twice. Dry MeCN (15 mL) was added, followed by the addition of trimethyloxonium tetrafluoroborate (597 mg, 4.04 mmol) in one portion. The resulting homogeneous solution was stirred at laboratory temperature for 30 min. Then the reaction mixture was concentrated under reduced pressure to afford a solid residue. The crude ylide salt was recrystallized from refluxing EtOH, then washed with Et_2O and EtOH to afford ylide salt **Y19** as an off- white crystalline solid (801 mg, 59% yield).

Data for mediator **Y19**:

^{1}H NMR (600 MHz, DMSO-*d*$_6$): δ 12.29 (br s, 1H), 7.82 – 7.78 (m, 1H), 7.76 (m, 2H), 7.72 – 7.66 (m, 3H), 7.62 (m, 1H), 7.56 (dd, *J* = 8.3, 7.3 Hz, 2H), 3.50 (s, 9H).

^{13}C NMR (151 MHz, DMSO-*d*$_6$): δ 195.7, 166.0, 138.7, 136.6, 133.5, 133.1, 131.7, 130.8, 129.4, 128.8, 56.0.

HRMS (ESI-TOF, m/z): HRMS (ESI) Calcd for $[M–BF_4]^+$ 283.1441; Found 283.1453.

Preparation of mediator Y20

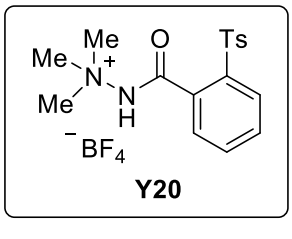

Y20

Following General Procedure C, a round-bottom flask was charged with *N'*,*N'*-dimethylbenzohydrazide (500 mg, 3.04 mmol, prepared in General method A) and a magnetic stir bar and the flask was evacuated and backfilled with argon three times. Dry THF (10 mL) was added and the solution was cooled to −78 °C. To this solution, *s*-BuLi (1.4 M in cyclohexane, 4.56 mL, 6.38 mmol) was added dropwise over 10 min; the reaction mixture color changed to orange/red and was stirred for 30 min at −78 °C. A solution of *p*-toluenesulfonyl fluoride (636 mg, 3.65 mmol) in dry THF (1 mL) was added dropwise over 5 min at −78 °C. The reaction mixture was gradually warmed up to laboratory temperature and stirred overnight. The resulting mixture was diluted with sat. aq. $NaHCO_3$ (50 mL) and EtOAc (40 mL), the organic phase was separated, and the aqueous phase was extracted with EtOAc (3 × 50 mL). Combined organic phases were dried over $MgSO_4$, filtered, and concentrated under reduced pressure. The crude product was purified by a flash column

chromatography (CH_2Cl_2/MeOH 100:5) and was directly used in the next step. A round-bottom flask charged with the hydrazide (985 mg, 3.67 mmol) and a magnetic stir bar was evacuated and backfilled with argon twice. Dry MeCN (15 mL) was added, followed by the addition of trimethyloxonium tetrafluoroborate (632 mg, 1.98 mmol) in one portion. The resulting homogeneous solution was stirred at laboratory temperature for 30 min. Then the reaction mixture was concentrated under reduced pressure to afford a solid residue. The crude product was recrystallized from a mixture of MeCN and PhMe, then washed with Et_2O and EtOH to afford ylide salt **Y20** as an off-white solid (368 mg, 46% yield).

Data for mediator **Y20**:
^{1}H NMR (500 MHz, DMSO-*d*$_6$): δ 12.46 (br s, 1H), 8.15 (dd, *J* = 7.7, 1.5 Hz, 1H), 7.93 – 7.87 (m, 2H), 7.86 – 7.76 (m, 2H), 7.67 (dd, *J* = 7.2, 1.7 Hz, 1H), 7.45 (d, *J* = 8.2 Hz, 2H), 3.76 (s, 9H), 2.38 (s, 3H).
^{13}C NMR (126 MHz, DMSO-*d*$_6$): δ 165.0, 144.8, 138.6, 137.8, 133.9, 132.4, 131.9, 130.1, 130.0, 129.4, 127.9, 56.4, 21.1.
HRMS (ESI-TOF, m/z): HRMS (ESI) Calcd for $[M–BF_4]^+$ 333.1267; Found 333.1274.

Preparation of mediator Y21

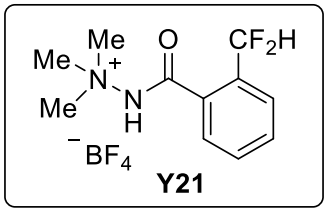

Following a literature procedure, 2-methylbenzoic acid was converted into 2-(difluoromethyl)benzoic acid.[2] A round-bottom flask was charged with 2-methylbenzoic acid (768 mg, 5.64 mmol), $Na_2S_2O_8$ (671 mg, 2.82 mmol), SelectFluor (5.00 g, 14.10 mmol), MeCN (15 mL) and dist. H_2O (15 mL). The mixture was degassed by passing argon through the mixture for 30 min. Then $AgNO_3$ (92 mg, 0.54 mmol) was added in one portion and the reaction mixture was heated to 80 °C for 4 h. After cooling to laboratory temperature, the reaction mixture was filtered through a pad of Celite, eluting with EtOAc. The filtrate was washed with sat. aq. $NaHCO_3$ (2 × 30 mL). The aqueous phase was acidified by adding 1 M aq. HCl, and extracted with EtOAc (3 × 30 mL). Combined organic extracts were washed with brine, dried over Na_2SO_4, filtered and concentrated under reduced pressure. The crude product was purified by flash chromatography (R_f = 0.45 in CH_2Cl_2/MeOH/AcOH 100:5:0.1) to afford 2-(difluoro-methyl)benzoic acid as a white solid (717 mg, 75 % yield). In the next step, a round-bottom flask was charged with 2-(difluoromethyl)benzoic acid (717 mg, 4.17 mmol), *N*,*N'*-dicyclohexyldiimide (1.03 g, 5.00 mmol), a catalytic amount of 4-dimethylaminopyridine and dry CH_2Cl_2 (10 mL). The mixture was cooled to 0 °C under argon and stirred for 20 min. Then, *N*,*N*-dimethylhydrazine (380 µL, 5.00 mmol) was added dropwise at 0 °C. The reaction mixture was gradually warmed to laboratory temperature and stirred overnight. The reaction mixture was filtered and the filtrate was diluted with CH_2Cl_2 (30 mL) and dist. H_2O (50 mL). The phases were separated, the aqueous phase was extracted with (2 × 30 mL). Combined organic extracts were washed with brine (100 mL), dried over $MgSO_4$, filtered, and concentrated under reduced pressure. The crude product was purified by flash chromatography (R_f = 0.5 in EtOAc/CH_2Cl_2/MeOH 10:1:1) to afford hydrazide as an off-white solid which was used directly in the next step. A

round-bottom flask charged with the crude hydrazide (282 mg, 1.32 mmol) and a magnetic stir bar was evacuated and backfilled with argon twice. Dry MeCN (10 mL) was added, followed by the addition of trimethyloxonium tetrafluoroborate (214 mg, 1.45 mmol) in one portion. The resulting homogeneous solution was stirred at laboratory temperature for 30 min. Then the reaction mixture was concentrated under reduced pressure to afford a solid residue. The crude ylide salt was recrystallized from a mixture of MeCN and PhMe (it is best to avoid protic solvents), then washed with PhMe, CH_2Cl_2 and Et_2O to afford ylide salt **Y21** as a white solid (307 mg, 74% yield).

Data for mediator **Y21**:
^{1}H NMR (600 MHz, DMSO-*d*$_6$): δ 7.89 – 7.63 (m, 4H), 7.28 (t, *J* = 55.0 Hz, 1H), 3.72 (s, 9H).
^{13}C NMR (151 MHz, DMSO-*d*$_6$): δ 165.2, 132.5 (t, $^2J_{C\text{-}F}$ = 23.3 Hz), 132.1, 131.4 (t, $^3J_{C\text{-}F}$ = 4.6 Hz), 130.8, 129.1, 126.1 (t, $^3J_{C\text{-}F}$ = 7.1 Hz), 112.8 (t, $^1J_{C\text{-}F}$ = 239.1 Hz), 56.4.
^{19}F NMR (376 MHz, DMSO-*d*$_6$): δ −114.0, −150.9.
HRMS (ESI-TOF, m/z): HRMS (ESI) Calcd for $[M–BF_4]^+$ 229.1147; Found 229.1156
Preparation of mediator Y22

The ylide salt was prepared by in five steps starting from methyl 2-iodobenzoate and 1-iodoperfluorohexan. A literature procedure was followed for the first step with a minor modification (DMF was used instead of DMPU).[3]

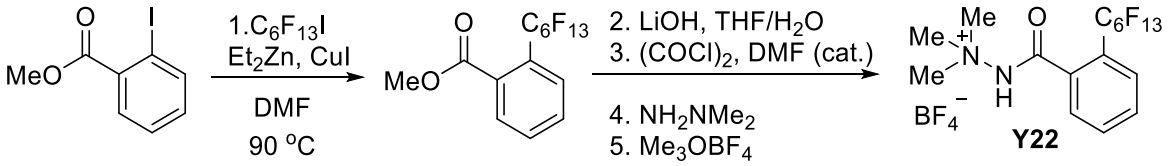

Scheme S1. Synthesis of **Y22** from methyl 2-iodobenzoate.

Step 1. A flame dried round-bottom flask equipped with a magnetic stir bar and a rubber septum was evacuated and backfilled with argon three times. Then the flask was charged with Et_2Zn (1.0 M in hexane, 2.25 mL), dry DMF (1.5 mL) and $C_6F_{13}I$ (730 µL, 3.38 mmol) were added dropwise to the flask at laboratory temperature. Subsequently, methyl 2-iodobenzoate (220 µg, 1.50 mmol) and CuI (28.6 mg, 0.15 mmol) were added. The flask was immersed in an oil bath and heated to 90 °C for 19 h with stirring under argon. The reaction mixture was cooled to laboratory temperature and the reaction was quenched by adding 1 M aq. HCl (5 mL). The crude products were extracted with Et_2O (3 × 50 mL), combined organic phases were washed with brine, dried over $MgSO_4$, filtered, and concentrated under reduced pressure. The crude product was purified by column chromatography (R_f = 0.2 in CH_2Cl_2/hexanes 1:5) using CH_2Cl_2/hexanes 1:5 → 1:1 mobile phase to afford as an oil (636 mg, 93 % yield), which was used directly in the next step.
Step 2. A round-bottom flask was charged with the product of the previous step (524 mg, 1.15 mmol), $LiOH·H_2O$ (483 mg, 11.50 mmol), dist. H_2O (2.5 mL), THF (2.5 mL) and a magnetic stir bar. After the reaction mixture was refluxed overnight, TLC showed no remaining

starting material. The solution was adjusted to pH 1 by adding 1 M aq HCl and the contents of the flask were extracted with CH_2Cl_2 (4 × 50 mL), dried over $MgSO_4$, filtered, and concentrated under reduced pressure. The crude acid was used directly in the next step. Oxalyl chloride (175 µL, 2.04 mmol) was added dropwise to a solution of the crude acid from the previous step (450 mg, 1.02 mmol) and DMF (3 drops) in dry CH_2Cl_2 (10 mL) and dry THF (5 mL) at 0 °C under argon over 10 min. After the addition, the reaction was stirred 3 h at laboratory temperature. The reaction mixture was concentrated under reduced pressure to remove excess of oxalyl chloride and afforded crude acyl chloride. A solution of the crude acyl chloride in CH_2Cl_2 (2 mL) was added to a solution of *N*, *N* - dimethylhydrazine (232 µL, 3.06 mmol) in CH_2Cl_2 (15 mL) at 0 °C under argon over 15 min and the reaction was stirred for 30 min at 0 °C and 3 h at laboratory temperature. The reaction mixture was diluted with CH_2Cl_2 (40 mL) and 1 M aq. NaOH (20 mL), the organic phase was separated, and the aqueous phase was extracted with CH_2Cl_2 (2 × 20 mL). Combined organic phases were dried over Na_2SO_4, filtered, and concentrated under reduced pressure to afford crude hydrazide. A round-bottom flask charged with the crude hydrazide (429 mg, 0.89 mmol) and a magnetic stir bar was evacuated and backfilled with argon twice. Dry MeCN (8 mL) was added, followed by the addition of trimethyloxonium tetrafluoroborate (145 mg, 0.98 mmol) in one portion. The resulting homogeneous solution was stirred at laboratory temperature for 30 min. Then the reaction mixture was concentrated under reduced pressure to afford a solid residue. The crude ylide salt was recrystallized from a mixture of EtOH (2 mL) and Et_2O (30 mL) and kept at 5 °C overnight. This afforded ylide salt **Y22** as a beige crystalline solid (376 mg, 72% yield for the methylation step).

Data for mediator **Y22**:
^{1}H NMR (600 MHz, DMSO-*d*$_6$): δ 12.47 (s, 1H), 7.89 (t, *J* = 8.1 Hz, 1H), 7.83 (t, *J* = 7.6 Hz, 1H), 7.79 (t, *J* = 6.9 Hz, 2H), 3.70 (s, 9H).
^{13}C NMR {H,F decoupled} (100 MHz, DMSO-*d*$_6$): δ 164.6, 133.1, 133.0, 131.4, 129.8, 128.7, 124.4, 116.7, 116.6, 110.9, 110.1, 109.9, 108.0, 56.1.
^{19}F NMR (376 MHz, MeCN-*d*$_3$): δ −84.2, −108.4, −122.7, −124.7, −125.8, −129.2, −154.3.
HRMS (ESI-TOF, m/z): HRMS (ESI) Calcd for $[M–BF_4]^+$ 497.0893; Found 497.0902.

Preparation of mediator Y23

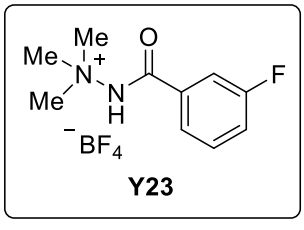

Y23

Following General Procedure A, 3-fluorobenzoyl chloride (610 µL, 5.02 mmol) was added to a solution of *N*,*N*-dimethylhydrazine (1.14 mL, 15.06 mmol) in CH_2Cl_2 (15 mL) at 0 °C under argon over 15 min and the reaction was stirred for 30 min at 0 °C and 3 h at laboratory temperature. The reaction mixture was diluted with CH_2Cl_2 (20 mL) and 1 M aq. NaOH (20 mL), the organic phase was separated, and the aqueous phase was extracted with CH_2Cl_2 (2 × 30 mL). Combined organic phases were dried over $MgSO_4$, filtered, and concentrated under reduced pressure to afford a white solid, crude hydrazide. A round-bottom flask charged with the crude hydrazide (860 mg, 4.72 mmol) and a magnetic stir bar was evacuated and backfilled with argon twice. Dry MeCN (10 mL) was added, followed by the addition of trimethyloxonium tetrafluoroborate (768 mg,

5.19 mmol) in one portion. The resulting homogeneous solution was stirred at laboratory temperature for 30 min. Then the reaction mixture was concentrated under reduced pressure to afford a solid residue. The crude ylide salt was recrystallized from a mixture of MeOH and Et_2O, then washed with Et_2O to afford ylide salt **Y23** as a white solid (864 mg, 64% yield).

Data for mediator **Y23**:
^{1}H NMR (600 MHz, MeOH-d_4): δ 7.68 (dt, J = 7.7, 1.3 Hz, 1H), 7.61 (ddd, J = 9.3, 2.7, 1.7 Hz, 1H), 7.57 (td, J = 8.0, 5.5 Hz, 1H), 7.41 (tdd, J = 8.4, 2.6, 1.0 Hz, 1H), 3.81 (s, 9H).
^{13}C NMR (151 MHz, MeOH-d_4): δ 166.7 (d, J = 2.7 Hz), 163.9 (d, $^1J_{C\text{-}F}$ = 247.0 Hz), 134.8 (d, $^3J_{C\text{-}F}$ = 8.3 Hz), 132.0 (d, $^3J_{C\text{-}F}$ = 7.9 Hz), 125.2 (d, $^4J_{C\text{-}F}$ = 3.3 Hz), 121.3 (d, $^2J_{C\text{-}F}$ = 21.3 Hz), 116.2 (d, $^2J_{C\text{-}F}$ = 24.5 Hz), 57.6.
^{19}F NMR (376 MHz, MeOH-d_4): δ −116.3, −156.5.
HRMS (ESI-TOF, m/z): HRMS (ESI) Calcd for $[M–BF_4]^+$ 197.1085; Found 197.1090.

Preparation of mediator Y24

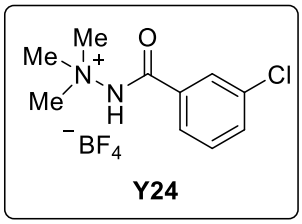

Y24

Following General Procedure A, 3-chlorobenzoyl chloride (600 µL, 4.69 mmol) was added to a solution of *N*,*N*-dimethylhydrazine (748 µL, 9.85 mmol) in CH_2Cl_2 (10 mL) at 0 °C under argon over 15 min and the reaction was stirred for 30 min at 0 °C and 3 h at laboratory temperature. The reaction mixture was diluted with CH_2Cl_2 (40 mL) and 1 M aq. NaOH (50 mL), the organic phase was separated, and the aqueous phase was extracted with CH_2Cl_2 (2 × 50 mL). Combined organic phases were dried over $MgSO_4$, filtered, and concentrated under reduced pressure to afford a white solid (903 mg, 97 % yield).
A round-bottom flask charged with the crude hydrazide (903 mg, 4.55 mmol) and a magnetic stir bar was evacuated and backfilled with argon twice. Dry MeCN (10 mL) was added, followed by the addition of trimethyloxonium tetrafluoroborate (740 mg, 5.01 mmol) in one portion.
The resulting homogeneous solution was stirred at laboratory temperature for 30 min. Then the reaction mixture was concentrated under reduced pressure to afford a solid residue. The crude ylide salt was recrystallized from refluxing EtOH, then washed with Et_2O and EtOH to afford ylide salt **Y24** as a white crystalline solid (998 mg, 73% yield).

Data for mediator **Y24**:
^{1}H NMR (600 MHz, DMSO-d_6): δ 11.95 (s, 1H), 7.87 (dd, J = 1.9 Hz, 1H), 7.78 – 7.75 (m, 1H), 7.73 (ddd, J = 8.1, 2.2, 1.1 Hz, 1H), 7.59 (t, J = 7.9 Hz, 1H), 3.70 (s, 9H).
^{13}C NMR (151 MHz, DMSO-d_6): δ 164.3, 133.6, 133.2, 132.8, 130.8, 128.0, 127.0, 56.5.
HRMS (ESI-TOF, m/z): HRMS (ESI) Calcd for $[M–BF_4]^+$ 213.0789; Found 213.0799.

Preparation of mediator Y25

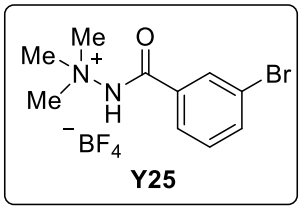

Y25

Following General Procedure A, 3-bromobenzoyl chloride (902 µL, 6.83 mmol) was added to a solution of *N*,*N*-dimethylhydrazine (1.56 mL, 20.49 mmol) in CH_2Cl_2 (15 mL) at 0 °C under argon over 15 min and the reaction was stirred for 30 min at 0 °C and 3 h at laboratory temperature. The reaction mixture was diluted with CH_2Cl_2 (10 mL) and 1 M aq NaOH (20 mL), the organic phase was separated, and the aqueous phase was extracted with CH_2Cl_2 (2 × 10 mL). Combined organic phases were dried over Na_2SO_4, filtered, and concentrated under reduced pressure to afford crude hydrazide (1.50 g) as a white solid. A round-bottom flask charged with the crude hydrazide and a magnetic stir bar was evacuated and backfilled with argon twice. Dry MeCN (7 mL) was added, followed by the addition of trimethyloxonium tetrafluoroborate (1.01 g, 6.83 mmol) in one portion. The resulting homogeneous solution was stirred at laboratory temperature for 30 min. Then the reaction mixture was concentrated under reduced pressure to afford a solid residue. This crude ylide salt was recrystallized from refluxing EtOH, then washed with Et_2O and EtOH to afford ylide salt **Y25** as a white crystalline solid (1.77 g, 75 % yield).

Data for mediator **Y25**:

^{1}H NMR (600 MHz, DMSO-d_6): δ 8.01 (t, *J* = 1.9 Hz, 1H), 7.88 (d, *J* = 8.1 Hz, 1H), 7.81 (dt, *J* = 7.8, 1.4 Hz, 1H), 7.54 (t, *J* = 7.9 Hz, 1H), 3.71 (s, 9H).

^{13}C NMR (151 MHz, DMSO-d_6): δ 164.2, 135.7, 133.7, 131.0, 130.8, 127.4, 121.6, 56.5.

HRMS (ESI-TOF, m/z): HRMS (ESI) Calcd for $[M–BF_4]^+$ 257.0284; Found 257.0294.

Preparation of mediator Y26

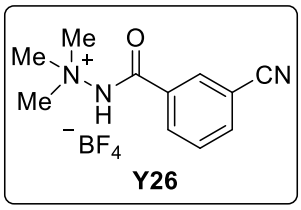

Y26

Following General Procedure A, 3-cyanobenzoyl chloride (1.00 g, 6.04 mmol) was added to a solution of *N*,*N*-dimethylhydrazine (1.38 mL, 18.12 mmol) in CH_2Cl_2 (15 mL) at 0 °C under argon over 15 min and the reaction was stirred for 30 min at 0 °C and 3 h at laboratory temperature. The reaction mixture was diluted with CH_2Cl_2 (10 mL) and 1 M aq. NaOH (20 mL), the organic phase was separated, and the aqueous phase was extracted with CH_2Cl_2 (2 × 10 mL). Combined organic phases were dried over Na_2SO_4, filtered, and concentrated under reduced pressure to afford a white solid (968 mg). A round-bottom flask charged with the crude hydrazide and a magnetic stir bar was evacuated and backfilled with argon twice. Dry MeCN (5 mL) was added, followed by the addition of trimethyloxonium tetrafluoroborate (893 mg, 6.04 mmol) in one portion. The resulting homogeneous solution was stirred at laboratory temperature for 30 min. Then the reaction mixture was concentrated under reduced pressure to afford a solid residue. This crude ylide salt was recrystallized from refluxing EtOH, then washed with Et_2O and EtOH to afford ylide salt **Y26** as a white crystalline solid (1.10 g, 63% yield).

Data for mediator **Y26**:

^{1}H NMR (600 MHz, DMSO-d_6): δ 8.28 (t, *J* = 1.8 Hz, 1H), 8.14 (dt, *J* = 7.8, 1.4 Hz, 1H), 8.11 (dt, *J* = 7.9, 1.5 Hz, 1H), 7.78 (t, *J* = 7.9 Hz, 1H), 3.71 (s, 9H).

^{13}C NMR (100 MHz, DMSO-d_6): δ 163.9, 136.3, 133.0, 132.8, 132.1, 130.2, 118.0, 111.6, 56.6.
HRMS (ESI-TOF, m/z): HRMS (ESI) Calcd for $[M–BF_4]^+$ 204.1131; Found 204.1139.

Preparation of mediator Y27

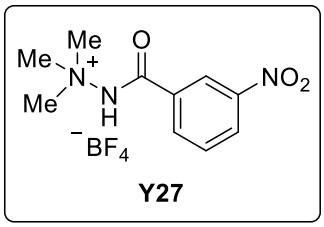

Y27

Following General Procedure A, 3-nitrobenzoyl chloride (1.50 g, 8.08 mmol) was added to a solution of *N*,*N*-dimethylhydrazine (1.84 mL, 24.24 mmol) in CH_2Cl_2 (15 mL) at 0 °C under argon over 15 min and the reaction was stirred for 30 min at 0 °C and 3 h at laboratory temperature. The reaction mixture was diluted with CH_2Cl_2 (10 mL) and 1 M aq. NaOH (20 mL), the organic phase was separated, and the aqueous phase was extracted with CH_2Cl_2 (2 × 10 mL). Combined organic phases were dried over Na_2SO_4, filtered, and concentrated under reduced pressure to afford crude hydrazide (1.60 g) as a white solid. A round-bottom flask charged with the crude hydrazide and a magnetic stir bar was evacuated and backfilled with argon twice. Dry MeCN (7 mL) was added, followed by the addition of trimethyloxonium tetrafluoroborate (1.20 g, 8.08 mmol) in one portion. The resulting homogeneous solution was stirred at laboratory temperature for 30 min. Then the reaction mixture was concentrated under reduced pressure to afford a solid residue. This crude ylide salt was recrystallized from refluxing EtOH, then washed with Et_2O and EtOH to afford ylide salt **Y27** as a white crystalline solid (1.75 g, 70 % yield).

Data for mediator **Y27**:
^{1}H NMR (600 MHz, DMSO-d_6): δ 8.65 (t, *J* = 2.0 Hz, 1H), 8.50 (dd, *J* = 8.5, 2.4 Hz, 1H), 8.25 (dt, *J* = 7.7, 1.4 Hz, 1H), 7.87 (t, *J* = 8.0 Hz, 1H), 3.73 (s, 9H).
^{13}C NMR (151 MHz, DMSO-d_6): δ 163.7, 147.6, 134.7, 133.3, 130.6, 127.5, 123.0, 56.5.
HRMS (ESI-TOF, m/z): HRMS (ESI) Calcd for $[M–BF_4]^+$ 224.1030; Found 224.1033.

Preparation of mediator Y28

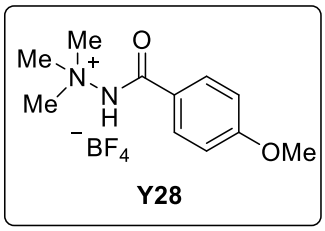

Y28

Following General Procedure A, 4-methoxybenzoyl chloride (872 mg, 5.11 mmol) was added to a solution of *N*,*N*-dimethylhydrazine (815 µL, 10.73 mmol) in CH_2Cl_2 (10 mL) at 0 °C under argon over 15 min and the reaction was stirred for 30 min at 0 °C and 3 h at laboratory temperature. The reaction mixture was diluted with CH_2Cl_2 (40 mL) and 1 M aq. NaOH (50 mL), the organic phase was separated, and the aqueous phase was extracted with CH_2Cl_2 (2 × 50 mL). Combined organic phases were dried over $MgSO_4$, filtered, and concentrated under reduced pressure to afford a white solid (787 mg, 79 % yield). A round-bottom flask charged with the crude hydrazide (675 mg, 3.48 mmol) and a magnetic stir bar was evacuated and backfilled with argon twice. Dry MeCN (10 mL) was added, followed by the addition of trimethyloxonium tetrafluoroborate (566 mg, 3.82 mmol) in one portion. The resulting homogeneous solution was stirred at laboratory temperature for 30 min. Then the reaction mixture was concentrated under reduced

pressure to afford a solid residue. The crude product was recrystallized from refluxing EtOH, then washed with Et_2O and EtOH to afford ylide salt **Y28** as a white crystalline solid (756 mg, 73% yield).

Data for mediator **Y28**:
^{1}H NMR (600 MHz, DMSO-d_6): δ 11.54 (s, 1H), 7.81 (d, J = 8.9 Hz, 2H), 7.10 (d, J = 8.9 Hz, 2H), 3.85 (s, 3H), 3.70 (s, 9H).
^{13}C NMR (151 MHz, DMSO-d_6): δ 165.4, 163.2, 130.4, 123.3, 114.0, 56.5, 55.7.
HRMS (ESI-TOF, m/z): HRMS (ESI) Calcd for $[M–BF_4]^+$ 209.1285; Found 209.1290.

Preparation of mediator Y29

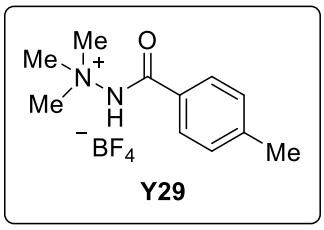

Y29

Following General Procedure A, 4-methylbenzoyl chloride (1.49 µL, 11.30 mmol) was added to a solution of *N*,*N*-dimethylhydrazine (2.58 mL, 33.90 mmol) in CH_2Cl_2 (15 mL) at 0 °C under argon over 15 min and the reaction was stirred for 30 min at 0 °C and 3 h at laboratory temperature. The reaction mixture was diluted with CH_2Cl_2 (10 mL) and 1 M aq. NaOH (20 mL), the organic phase was separated, and the aqueous phase was extracted with CH_2Cl_2 (2 × 10 mL). Combined organic phases were dried over Na_2SO_4, filtered, and concentrated under reduced pressure to afford a white solid (1.98 g). A round-bottom flask charged with the crude hydrazide and a magnetic stir bar was evacuated and backfilled with argon twice. Dry MeCN (10 mL) was added, followed by the addition of trimethyloxonium tetrafluoroborate (1.67 g, 11.30 mmol) in one portion. The resulting homogeneous solution was stirred at laboratory temperature for 30 min. Then the reaction mixture was concentrated under reduced pressure to afford a solid residue. This crude ylide salt was recrystallized from refluxing EtOH, then washed with Et_2O and EtOH to afford ylide salt **Y29** as a white crystalline solid (2.25 g, 71% yield).

Data for mediator **Y29**:
^{1}H NMR (600 MHz, DMSO-d_6): δ 11.66 (s, 1H), 7.73 (d, J = 8.3 Hz, 2H), 7.38 (d, J = 8.0 Hz, 2H), 3.71 (s, 9H), 2.39 (s, 3H).
^{13}C NMR (151 MHz, DMSO-d_6): δ 165.7, 143.6, 129.2, 128.5, 128.2, 56.45, 21.1.
HRMS (ESI-TOF, m/z): HRMS (ESI) Calcd for $[M–BF_4]^+$ 193.1335; Found 193.1346.

Preparation of mediator Y30

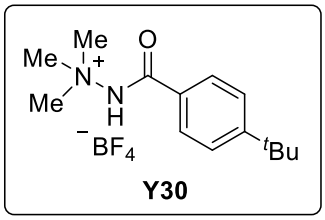

Y30

Following General Procedure B, oxalyl chloride (650 µL, 7.58 mmol) was added dropwise to a solution of 4-*t*-butylbenzoic acid (675 mg, 3.79 mmol) and DMF (5 drops) in CH_2Cl_2 (20 mL) at 0 °C under argon over 10 min. After the addition, the reaction was stirred for 1 h at 0 °C and 2 h at laboratory temperature. Then the reaction mixture was concentrated under reduced pressure to remove excess oxalyl chloride and afforded crude acyl chloride. A solution of the crude acyl chloride in CH_2Cl_2 (5 mL) was added to a solution of *N*,*N*-dimethylhydrazine (605 µL, 7.96 mmol) in CH_2Cl_2 (15 mL) at 0 °C under argon over 15 min and the reaction was stirred for 30

min at 0 °C and 3 h at laboratory temperature. The reaction mixture was diluted with CH_2Cl_2 (40 mL) and 1 M aq. NaOH (50 mL), the organic phase was separated, and the aqueous phase was extracted with CH_2Cl_2 (2 × 50 mL). Combined organic phases were dried over $MgSO_4$, filtered, and concentrated under reduced pressure to afford a white solid, crude hydrazide (835 mg, 99 % yield). A round-bottom flask charged with the crude hydrazide (835 mg, 3.79 mmol) and a magnetic stir bar was evacuated and backfilled with argon twice. Dry MeCN (10 mL) was added, followed by the addition of trimethyloxonium tetrafluoroborate (617 mg, 4.17 mmol) in one portion. The resulting homogeneous solution was stirred at laboratory temperature for 30 min. Then the reaction mixture was concentrated under reduced pressure to afford a solid residue. The crude ylide salt was recrystallized from refluxing EtOH, then washed with Et_2O and EtOH to afford ylide salt **Y30** as a white crystalline solid (892 mg, 73 % yield).

Data for mediator **Y30**:
^{1}H NMR (600 MHz, DMSO-d_6): δ 11.68 (s, 1H), 7.75 (d, J = 8.5 Hz, 2H), 7.59 (d, J = 8.5 Hz, 2H), 3.71 (s, 9H), 1.31 (s, 9H).
^{13}C NMR (126 MHz, DMSO-d_6): δ 166.0, 156.4, 128.7, 128.1, 125.5, 56.5, 34.9, 30.8.
HRMS (ESI-TOF, m/z): HRMS (ESI) Calcd for $[M–BF_4]^+$ 235.1805; Found 235.1809.

Preparation of mediator Y31

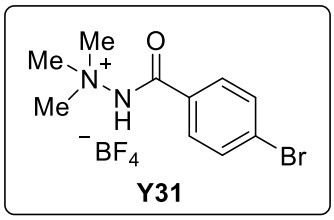

Y31

Following General Procedure B, oxalyl chloride (1.28 mL, 14.92 mmol) was added dropwise to a solution of 4-bromobenzoic acid (1.50 g, 7.46 mmol) and DMF (4 drops) in CH_2Cl_2 (15 mL) at 0 °C under argon over 10 min. After the addition, the reaction was stirred for 2 h at laboratory temperature. Then the reaction mixture was concentrated under reduced pressure to remove excess of oxalyl chloride and afforded crude acyl chloride. A solution of the crude acyl chloride in CH_2Cl_2 (2 mL) was added to a solution of *N*,*N*-dimethylhydrazine (1.70 mL, 22.38 mmol) in CH_2Cl_2 (10 mL) at 0 °C under argon over 15 min and the reaction was stirred for 30 min at 0 °C and 3 h at laboratory temperature. The reaction mixture was diluted with CH_2Cl_2 (20 mL) and 1 M aq. NaOH (20 mL), the organic phase was separated, and the aqueous phase was extracted with CH_2Cl_2 (2 × 20 mL). Combined organic phases were dried over Na_2SO_4, filtered, and concentrated under reduced pressure to afford a white solid. A round-bottom flask charged with the crude hydrazide and a magnetic stir bar was evacuated and backfilled with argon twice. Dry MeCN (7 mL) was added, followed by the addition of trimethyloxonium tetrafluoroborate (1.10 g, 7.46 mmol) in one portion. The resulting homogeneous solution was stirred at laboratory temperature for 30 min. Then the reaction mixture was concentrated under reduced pressure to afford a solid residue. The crude ylide salt was recrystallized from refluxing EtOH to afford ylide salt **Y31** as a white crystalline solid (1.13 g, 44% yield).

Data for mediator **Y31**:
^{1}H NMR (600 MHz, DMSO-d_6): δ 7.81 (d, J = 8.6 Hz, 2H), 7.77 (d, J = 8.6 Hz, 2H), 3.70 (s, 9H).

^{13}C NMR (151 MHz, DMSO-d_6): δ 165.4, 132.2, 131.1, 130.8, 127.5, 57.0.
HRMS (ESI-TOF, m/z): HRMS (ESI) Calcd for $[M–BF_4]^+$ 257.0284; Found 257.0295.

Preparation of mediator Y32

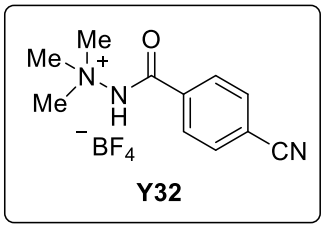

Y32

Following General Procedure A, 4-cyanobenzoyl chloride (917 mg, 5.54 mmol) was added to a solution of *N*,*N*-dimethylhydrazine (884 μL, 11.63 mmol) in CH_2Cl_2 (10 mL) at 0 °C under argon over 15 min and the reaction was stirred for 30 min at 0 °C and 3 h at laboratory temperature. The reaction mixture was diluted with CH_2Cl_2 (40 mL) and 1 M aq. NaOH (50 mL), the organic phase was separated, and the aqueous phase was extracted with CH_2Cl_2 (2 × 50 mL). Combined organic phases were dried over $MgSO_4$, filtered, and concentrated under reduced pressure to afford a white solid (998 mg, 91 % yield). A round-bottom flask charged with the crude hydrazide (998 mg, 5.03 mmol) and a magnetic stir bar was evacuated and backfilled with argon twice. Dry MeCN (10 mL) was added, followed by the addition of trimethyloxonium tetrafluoroborate (818 mg, 5.53 mmol) in one portion. The resulting homogeneous solution was stirred at laboratory temperature for 30 min. Then the reaction mixture was concentrated under reduced pressure to afford a solid residue. The crude product was recrystallized from refluxing EtOH, then washed with Et_2O and EtOH to afford ylide salt **Y32** as white needles (887 mg, 61% yield).

Data for mediator **Y32**:
^{1}H NMR (500 MHz, DMSO-d_6): δ 8.04 (d, J = 8.4 Hz, 2H), 7.95 (d, J = 8.6 Hz, 2H), 3.69 (s, 9H).
^{13}C NMR (151 MHz, DMSO-d_6): δ 164.4, 135.7, 132.6, 129.1, 118.1, 115.2, 56.5.
HRMS (ESI-TOF, m/z): HRMS (ESI) Calcd for $[M–BF_4]^+$ 204.1131; Found 204.1142.

Preparation of mediator Y33

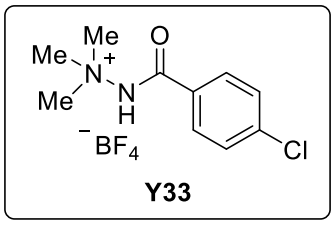

Y33

Following General procedure A, 4-chlorobenzoylchloride (641 μL, 5.00 mmol) was added into a solution of *N*,*N*-dimethylhydrazine (1.14 mL, 15.00 mmol) in CH_2Cl_2 (50 mL) at 0 °C under argon and the reaction mixture was stirred for 30 min. The reaction mixture was diluted with CH_2Cl_2 (30 mL) and 1 M aq. NaOH (40 mL), the organic phase was separated, and the aqueous phase was extracted with CH_2Cl_2 (2 × 30 mL). Combined organic phases were dried over Na_2SO_4, filtered, and concentrated under reduced pressure to afford crude hydrazide. A round-bottom flask charged with the crude hydrazide and a magnetic stir bar was evacuated and backfilled with argon twice. Dry MeCN (10 mL) was added, followed by the addition of trimethyloxonium tetrafluoroborate (814 mg, 5.5 mmol) in one portion. The resulting homogeneous solution was stirred at room temperature for 30 min. Then the reaction mixture was concentrated under reduced pressure to afford a solid residue. The crude ylide salt was recrystallized from a mixture of methanol and Et_2O, then washed with Et_2O to afford ylide (1.08 g, 36% yield) as a white solid.

Data for mediator **Y33**:
^{1}H NMR (600 MHz, DMSO-d_6): δ 11.89 (s, 1H), 7.85 (d, J = 8.6 Hz, 2H), 7.67 (d, J = 8.6 Hz, 2H), 3.72 (s, 9H).
^{13}C NMR (151 MHz, DMSO-d_6): δ 164.8, 138.0, 130.3, 130.2, 128.8, 56.5.
HRMS (ESI-TOF, m/z): HRMS (ESI) Calcd for $[M–BF_4]^+$ 213.0789; Found 213.0800.

Preparation of mediator Y34

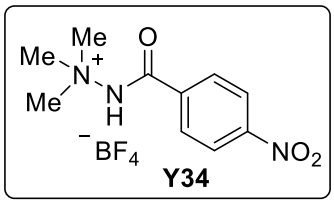

Y34

Following General Procedure A, 4-nitrobenzoyl chloride (1.00 g, 5.39 mmol) was added to a solution of *N*,*N*-dimethylhydrazine (1.23 mL, 16.17 mmol) in CH_2Cl_2 (15 mL) at 0˚C under argon over 15 min and the reaction was stirred for 30 min at 0 °C and 3 h at room temperature. The reaction mixture was diluted with CH_2Cl_2 (10 mL) and 1 M aq. NaOH (20 mL), the organic phase was separated, and the aqueous phase was extracted with CH_2Cl_2 (2 × 10 mL). Combined organic phases were dried over Na_2SO_4, filtered, and concentrated under reduced pressure to afford crude hydrazide (875 mg) as a white solid. This material was used directly in the next step. A round-bottom flask charged with the crude hydrazide and a magnetic stir bar was evacuated and backfilled with argon twice. Dry MeCN (5 mL) was added, followed by the addition of trimethyloxonium tetrafluoroborate (797 mg, 5.39 mmol) in one portion. The resulting homogeneous solution was stirred at room temperature for 30 min. Then the reaction mixture was concentrated under reduced pressure to afford a solid residue. This crude ylide salt was recrystallized from refluxing EtOH, then washed with EtOH and Et_2O to afford ylide salt **Y34** as a white crystalline solid (880 mg, 52% yield).

Data for mediator **Y34**:
^{1}H NMR (600 MHz, DMSO-d_6): δ 8.39 (d, J = 8.7 Hz, 2H), 8.06 (d, J = 8.9 Hz, 2H), 3.71 (s, 9H).
^{13}C NMR (151 MHz, DMSO-d_6): δ 164.3, 150.0, 137.5, 129.9, 123.8, 56.6.
HRMS (ESI-TOF, m/z): HRMS (ESI) Calcd for $[M–BF_4]^+$ 224.1030; Found 224.1039.

Preparation of mediator Y35

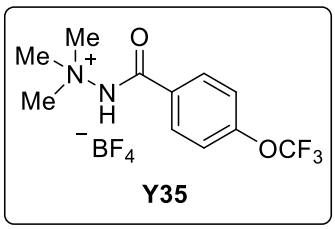

Y35

Following General Procedure A, 4-(trifluoromethoxy)benzoyl chloride (702 µL, 4.45 mmol) was added to a solution of *N*,*N*-dimethylhydrazine (710 µL, 9.35 mmol) in CH_2Cl_2 (15 mL) at 0 °C under argon over 15 min and the reaction was stirred for 30 min at 0 °C and 3 h at laboratory temperature. The reaction mixture was diluted with CH_2Cl_2 (50 mL) and 1 M aq. NaOH (50 mL), the organic phase was separated, and the aqueous phase was extracted with CH_2Cl_2 (2 × 50 mL). Combined organic phases were dried over $MgSO_4$, filtered, and concentrated under reduced pressure to afford a white solid, crude hydrazide (800 mg, 72% yield). A round-bottom flask charged with the crude hydrazide (715 mg, 2.88 mmol) and a magnetic stir bar was evacuated and backfilled with argon twice.

Dry MeCN (10 mL) was added, followed by the addition of trimethyloxonium tetrafluoroborate (469 mg, 3.17 mmol) in one portion. The resulting homogeneous solution was stirred at laboratory temperature for 30 min. Then the reaction mixture was concentrated under reduced pressure to afford a solid residue, crude ylide salt. The crude product was recrystallized from refluxing EtOH, then washed with Et_2O and EtOH to afford ylide salt **Y35** as a white solid (681 mg, 68% yield).

Data for mediator **Y35**:
^{1}H NMR (600 MHz, DMSO-*d*$_6$): δ 11.93 (s, 1H), 7.95 (d, *J* = 8.9 Hz, 2H), 7.58 (d, *J* = 7.7 Hz, 2H), 3.71 (s, 9H).
^{13}C NMR (151 MHz, DMSO-*d*$_6$): δ 164.6, 151.4, 130.8, 130.70, 120.94, 120.79 (q, $^1J_{C\text{-}F}$ = 258 Hz), 56.5.
^{19}F NMR (376 MHz, DMSO-*d*$_6$): δ −56.7, −148.1.
HRMS (ESI-TOF, m/z): HRMS (ESI) Calcd for $[M–BF_4]^+$ 263.1002; Found 263.1006.

Preparation of mediator Y36

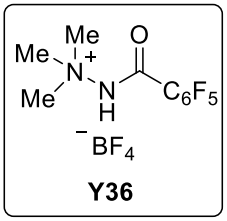

Following General Procedure A, 2,3,4,5,6-pentafluorobenzoyl chloride (1.00 mL, 6.95 mmol) was added to a solution of *N*,*N*-dimethylhydrazine (1.11 mL, 14.60 mmol) in CH_2Cl_2 (10 mL) at 0 °C under argon over 15 min and the reaction was stirred for 30 min at 0 °C and 3 h at laboratory temperature. The reaction mixture was diluted with EtOAc (25 mL) and 1 M aq. NaOH (30 mL), the organic phase was separated, and the aqueous phase was extracted with EtOAc (2 × 25 mL). Combined organic extracts were dried over $MgSO_4$, filtered, and concentrated under reduced pressure to afford a white solid, crude hydrazide (1.63 g, 93 % yield). A round-bottom flask charged with the crude hydrazide (1.12 g, 4.41 mmol) and a magnetic stir bar was evacuated and backfilled with argon twice. Dry MeCN (10 mL) was added, followed by the addition of trimethyloxonium tetrafluoroborate (717 mg, 4.85 mmol) in one portion. The resulting homogeneous solution was stirred at laboratory temperature for 30 min. Then the reaction mixture was concentrated under reduced pressure to afford a solid residue, crude ylide salt. The crude product was recrystallized from refluxing EtOH, then washed with Et_2O and EtOH to afford ylide salt **Y36** as white crystalline solid (946 mg, 60% yield).

Data for mediator **Y36**:
^{1}H NMR (600 MHz, DMSO-*d*$_6$): δ 3.60 (s, 9H).
^{13}C NMR {H,F}-decoupled (100 MHz, DMSO-*d*$_6$): δ 155.7, 143.5, 142.1, 137.2, 110.3, 56.3.
^{19}F NMR (376 MHz, DMSO-*d*$_6$): δ −144.7, −150.9, −154.9, −163.7.
HRMS (ESI-TOF, m/z): HRMS (ESI) Calcd for $[M–BF_4]^+$ 269.0708; Found 269.0718.

Preparation of mediator Y37

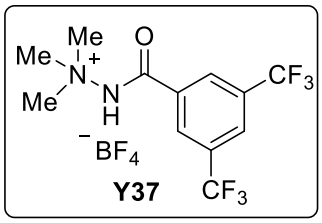

Y37

Following General Procedure A, 3,5-bis(trifluoromethyl)benzoyl chloride (905 μL, 5.00 mmol) was added dropwise to a solution of *N*,*N*-dimethylhydrazine (1.14 ml, 15.00 mmol) in CH_2Cl_2 (50 ml) at 0 °C under argon and the reaction mixture was stirred at 0 °C for 30 min.

The reaction mixture was diluted with CH_2Cl_2 (30 mL) and 1 M aq. NaOH (30 mL), the organic phase was separated, and the aqueous phase was extracted with CH_2Cl_2 (2 × 30 mL). Combined organic extracts were dried over $MgSO_4$, filtered, and concentrated under reduced pressure to afford crude hydrazide. A round-bottom flask charged with the crude hydrazide (565 mg, 1.88 mmol) and a magnetic stir bar was evacuated and backfilled with argon twice. Dry MeCN (10 mL) was added, followed by the addition of trimethyloxonium tetrafluoroborate (306 mg, 2.07 mmol) in one portion. The resulting homogeneous solution was stirred at laboratory temperature for 30 min. Then the reaction mixture was concentrated under reduced pressure to afford a solid residue. The crude product was recrystallized from a mixture of MeOH and Et_2O, then washed with Et_2O to afford ylide **Y37** as a white solid (542 mg, 67% yield).

Data for mediator **Y37**:

^{1}H NMR (500 MHz, DMSO-d_6): δ 8.40 (s, 1H), 8.38 (s, 1H), 3.69 (s, 9H).

^{13}C NMR (126 MHz, DMSO-d_6): δ 163.0, 134.6, 130.5 (q, $^2J_{C\text{-}F}$ = 33.1 Hz), 129.2, 126.2, 123.0 (q, $^1J_{C\text{-}F}$ = 273.8 Hz), 56.6.

^{19}F NMR (376 MHz, DMSO-d_6): δ −64.14, −150.9.

HRMS (ESI-TOF, m/z): HRMS (ESI) Calcd for $[M–BF_4]^+$ 315.0932; Found 315.0939.

Preparation of mediator Y38

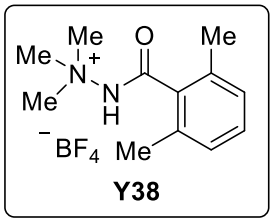

Y38

Following General Procedure B, oxalyl chloride (858 μL, 10.00 mmol) was added dropwise to a solution of 2,6-dimethylbenzoic acid (751 mg, 5.00 mmol) and DMF (2 drops) in CH_2Cl_2 (40 mL) at 0 °C under argon over 10 min. After the addition, the reaction was stirred for 1 h at 0 °C and 3 h at laboratory temperature. Then the reaction mixture was concentrated under reduced pressure to remove excess of oxalyl chloride and afforded crude acyl chloride. A solution of the crude acyl chloride in CH_2Cl_2 (2 mL) was added to a solution of *N*,*N*-dimethylhydrazine (760 μL, 10.00 mmol) in CH_2Cl_2 (20 mL) at 0 °C under argon over 15 min and the reaction was stirred for 30 min at 0 °C and 3 h at laboratory temperature. The reaction mixture was diluted with CH_2Cl_2 (40 mL) and 1 M aq. NaOH (50 mL), the organic phase was separated, and the aqueous phase was extracted with CH_2Cl_2 (2 × 50 mL). Combined organic phases were dried over $MgSO_4$, filtered, and concentrated under reduced pressure to afford crude hydrazine. A round-bottom flask charged with the crude hydrazide and a magnetic stir bar was evacuated and backfilled with argon twice. Dry MeCN (10 mL) was added, followed by the addition of trimethyloxonium tetrafluoroborate (740 mg, 5.00 mmol) in one portion. The resulting homogeneous solution was stirred at laboratory temperature for 30 min. Then the reaction mixture was concentrated under reduced

pressure to afford a solid residue. The crude ylide salt was recrystallized from a mixture of MeOH and Et_2O, then washed with Et_2O to afford ylide salt **Y38** as a white solid (765 mg, 52% yield).

Data for mediator **Y38**:
^{1}H NMR (500 MHz, MeCN-d_3): δ 9.90 (s, 1H), 7.32 (t, J = 7.7 Hz, 1H), 7.14 (d, J = 7.7 Hz, 2H), 3.76 (s, 9H), 2.35 (s, 6H).
^{13}C NMR (126 MHz, MeCN-d_3): δ 168.2, 136.1, 131.4, 128.6, 118.4, 57.8, 19.0.
HRMS (ESI-TOF, m/z): HRMS (ESI) Calcd for $[M–BF_4]^+$ 207.1492; Found 207.1504.

Preparation of mediator Y39

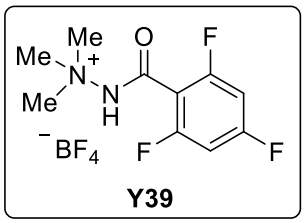

Y39

Following General Procedure A, 2,4,6-trifluorobenzoyl chloride (973 mg, 5.0 mmol) was added to a solution of *N*,*N*-dimethylhydrazine (1.14 mL, 15.00 mmol) in CH_2Cl_2 (50 mL) at 0 °C under argon over 15 min and the reaction was stirred for 30 min at 0 °C and 3 h at laboratory temperature. The reaction mixture was diluted with CH_2Cl_2 (50 mL) and 1 M aq. NaOH (50 mL), the organic phase was separated, and the aqueous phase was extracted with CH_2Cl_2 (2 × 50 mL). Combined organic phases were dried over $MgSO_4$, filtered, and concentrated under reduced pressure to afford crude hydrazide. A round-bottom flask charged with the crude hydrazide and a magnetic stir bar was evacuated and backfilled with argon twice. Dry MeCN (10 mL) was added, followed by the addition of trimethyloxonium tetrafluoroborate (814 mg, 5.5 mmol) in one portion. The resulting homogeneous solution was stirred at laboratory temperature for 30 min. Then the reaction mixture was concentrated under reduced pressure to afford a solid residue. The crude product was recrystallized from a mixture of methanol and Et_2O, then washed with Et_2O to afford ylide **Y39** as a yellowish solid (1.00 g, 67% yield).

Data for mediator **Y39**:
^{1}H NMR (600 MHz, MeCN-d_3): δ 10.09 (s, 1H), 7.04 – 6.97 (m, 2H), 3.72 (s, 9H).
^{13}C NMR (151 MHz, MeCN-d_3): δ 165.5 (td, J = 257.0, 15.2 Hz), 161.1 (ddd, J = 253.0, 15.0, 9.0 Hz), 157.7, 108.2 (td, J = 21.0, 4.7 Hz), 102.1 (td, J = 26.6, 3.9 Hz), 57.8 (m).
^{19}F NMR (376 MHz, MeCN-d_3): δ −106.2, −113.0, −153.7.
HRMS (ESI-TOF, m/z): HRMS (ESI) Calcd for $[M–BF_4]^+$ 233.0902; Found 233.0908.

Preparation of mediator Y40

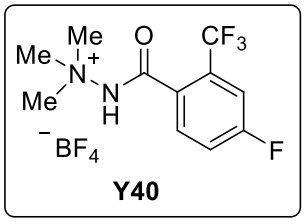

Y40

Following General Procedure A, 4-fluoro-2-(trifluoromethyl)benzoyl chloride (1.00 mL, 6.60 mmol) was added to a solution of *N*,*N*-dimethylhydrazine (1.05 mL, 13.86 mmol) in CH_2Cl_2 (10 mL) at 0 °C under argon over 15 min and the reaction was stirred for 30 min at 0 °C and 3 h at laboratory temperature. The reaction mixture was diluted with CH_2Cl_2 (50 mL) and 1 M aq.

NaOH (50 mL), the organic phase was separated, and the aqueous phase was extracted with CH_2Cl_2 (2 × 50 mL). Combined organic phases were dried over $MgSO_4$, filtered, and concentrated under reduced pressure to afford a white solid (1.64 g, 99 % yield). A round-bottom flask charged with the crude hydrazide (1.38 g, 5.52 mmol) and a magnetic stir bar was evacuated and backfilled with argon twice. Dry MeCN (10 mL) was added, followed by the addition of trimethyloxonium tetrafluoroborate (898 mg, 6.07 mmol) in one portion. The resulting homogeneous solution was stirred at laboratory temperature for 30 min. Then the reaction mixture was concentrated under reduced pressure to afford a solid residue, crude ylide salt. The crude product was recrystallized from refluxing EtOH, then washed with Et_2O and EtOH to afford ylide salt **Y40** as white solid (1.31 g, 67% yield).

Data for mediator **Y40**:
^{1}H NMR (600 MHz, DMSO-d_6): δ 12.54 (s, 1H), 7.89 (m, 2H), 7.77 (m, 1H), 3.70 (s, 9H).
^{13}C NMR (151 MHz, DMSO-d_6): δ 163.8, 162.8 (d, *J* = 251.1 Hz), 132.5 (d, *J* = 8.9 Hz), 129.0 (qd, *J* = 32.9, 8.3 Hz), 128.3, 122.6 (qd, *J* = 274.1, 2.6 Hz), 119.8 (d, *J* = 21.5 Hz), 114.9 (dt, *J* = 25.6, 4.8 Hz), 56.2.
^{19}F NMR (376 MHz, DMSO-d_6): δ −60.7, −109.2, −150.8.
HRMS (ESI-TOF, m/z): HRMS (ESI) Calcd for $[M–BF_4]^+$ 265.0959; Found 265.0968.

Preparation of mediator Y41

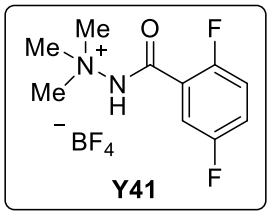

Y41

Following General Procedure A, 2,5-difluorobenzoyl chloride (1.00 mL, 8.07 mmol) was added to a solution of *N*,*N*-dimethylhydrazine (1.84 mL, 24.21 mmol) in CH_2Cl_2 (15 mL) at 0 °C under argon over 15 min and the reaction was stirred for 30 min at 0 °C and 3 h at laboratory temperature. The reaction mixture was diluted with CH_2Cl_2 (50 mL) and 1 M aq. NaOH (50 mL), the organic phase was separated, and the aqueous phase was extracted with CH_2Cl_2 (2 × 50 mL). Combined organic phases were dried over $MgSO_4$, filtered, and concentrated under reduced pressure to afford a white solid, crude hydrazide (1.57 g, 97% yield). A round-bottom flask charged with the crude hydrazide (684 mg, 3.42 mmol) and a magnetic stir bar was evacuated and backfilled with argon twice. Dry MeCN (15 mL) was added, followed by the addition of trimethyloxonium tetrafluoroborate (556 mg, 3.76 mmol) in one portion. The resulting homogeneous solution was stirred at laboratory temperature for 30 min. Then the reaction mixture was concentrated under reduced pressure to afford a solid residue. The crude product was recrystallized from refluxing EtOH, then washed with Et_2O and EtOH to afford ylide salt **Y41** as a white crystalline solid (361 mg, 35% yield).

Data for mediator **Y41**:
^{1}H NMR (600 MHz, DMSO-d_6): δ 7.61 (ddd, *J* = 8.4, 5.2, 3.2 Hz, 1H), 7.53 (tt, *J* = 7.5, 3.7 Hz, 1H), 7.47 (td, *J* = 9.2, 4.2 Hz, 1H), 3.71 (s, 9H).
^{13}C NMR {H,F}-decoupled (151 MHz, DMSO-d_6): δ 161.0, 157.5, 155.5, 122.2, 120.7, 118.4, 117.0, 56.5.
^{19}F NMR (376 MHz, DMSO-d_6): δ −120.5, −122.4, −150.8.

HRMS (ESI-TOF, m/z): HRMS (ESI) Calcd for $[M–BF_4]^+$ 215.0990; Found 215.0998.

Preparation of mediator Y42

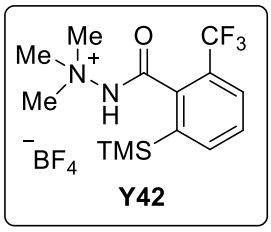

Y42

Following General Procedure C, a round-bottom flask was charged with *N,N*-dimethyl-2-(trifluoromethyl)benzohydrazide **Y7-H** (706 mg, 3.04 mmol) and a magnetic stir bar and the flask was evacuated and backfilled with argon three times. Dry THF (10 mL) was added and the solution was cooled to −78 °C. To this solution, *s*-BuLi (1.4 M in cyclohexane, 4.56 mL, 6.38 mmol) was added dropwise over 10 min, the reaction mixture color changed to red and was stirred 1 hour at −78 °C. Then a solution of trimethylsilyl chloride (1.2 mL, 9.12 mmol) in dry THF (2 mL) was added dropwise over 5 min at −78 °C. The reaction mixture was gradually warmed to laboratory temperature and stirred overnight. The reaction mixture was diluted with sat. aq. $NaHCO_3$ (50 mL) and EtOAc (40 mL), the organic phase was separated, and the aqueous phase was extracted with EtOAc (3 × 50 mL). Combined organic phases were dried over $MgSO_4$, filtered, and concentrated under reduced pressure. The crude product was purified by a short column chromatography (EtOAc/CH_2Cl_2/MeOH 10:1:1) and was directly used in the next step. A round-bottom flask charged with the hydrazide (560 mg, 1.84 mmol) and a magnetic stir bar was evacuated and backfilled with argon twice. Dry MeCN (10 mL) was added, followed by the addition of trimethyloxonium tetrafluoroborate (299 mg, 2.02 mmol) in one portion. The resulting homogeneous solution was stirred at laboratory temperature for 30 min. Then the reaction mixture was concentrated under reduced pressure to afford a solid residue. The crude product was recrystallized from a mixture of MeOH and Et_2O, then washed with Et_2O mixture to afford ylide salt **Y42** as a white foamy solid (116 mg, 16% yield).

Data for mediator **Y42**:
^{1}H NMR (600 MHz, DMSO-*d*$_6$): δ 12.56 (s, 1H), 7.96 (d, *J* = 7.8 Hz, 1H), 7.90 (d, *J* = 7.9 Hz, 1H), 7.77 (d, *J* = 8.3 Hz, 1H), 3.69 (s, 9H), 0.36 (s, 9H).
^{13}C NMR (150 MHz, DMSO-*d*$_6$): δ 165.4, 140.0, 139.1, 136.5, 130.2, 127.3 (q, $^3J_{C\text{-}F}$ = 4.2 Hz), 126.5 (q, $^2J_{C\text{-}F}$ = 30.5 Hz), 123.9 (q, $^1J_{C\text{-}F}$ = 274.8 Hz), 56.4, 0.3.
^{19}F NMR (376 MHz, DMSO-*d*$_6$): δ −59.1, −150.9.
HRMS (ESI-TOF, m/z): HRMS (ESI) Calcd for $[M–BF_4]^+$ 319.1448; Found 319.1456.

Preparation of mediator Y43

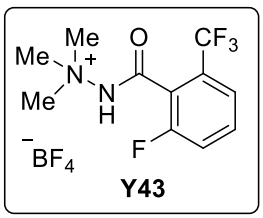

Y43

Following General Procedure A, 2-fluoro-6-(trifluoromethyl)benzoyl chloride (700 µL, 4.53 mmol) was added to a solution of *N,N*-dimethylhydrazine (860 µL, 11.33 mmol) in CH_2Cl_2 (15 mL) at 0 °C under argon over 15 min and the reaction was stirred for 30 min at 0 °C and 3 h at laboratory temperature. The reaction mixture was diluted with CH_2Cl_2 (50 mL) and 1 M aq NaOH (50 mL), the organic phase was separated, and the aqueous phase was extracted with CH_2Cl_2 (2 × 50 mL). Combined organic phases were dried over $MgSO_4$, filtered, and concentrated under reduced pressure to afford a

white solid, crude hydrazide (883 mg, 78% yield). A round-bottom flask charged with the crude hydrazide (883 mg, 3.53 mmol) and a magnetic stir bar was evacuated and backfilled with argon twice. Dry MeCN (15 mL) was added, followed by the addition of trimethyloxonium tetrafluoroborate (574 mg, 3.88 mmol) in one portion. The resulting homogeneous solution was stirred at laboratory temperature for 30 min. Then the reaction mixture was concentrated under reduced pressure to afford a solid residue. The crude product was recrystallized from refluxing EtOH, then washed with Et_2O and EtOH to afford ylide salt **Y43** as a white solid (740 mg, 60% yield).

Data for mediator **Y43**:
^{1}H NMR (400 MHz, DMSO-*d*$_6$): δ 7.85 (m, 1H), 7.82 – 7.73 (m, 2H), 3.70 (s, 9H).
^{13}C NMR (126 MHz, DMSO-*d*$_6$): δ 159.7, 158.3 (d, *J* = 248.5 Hz), 133.7 (d, *J* = 8.8 Hz), 127.9 (qd, *J* = 32.2, 3.5 Hz), 122.9, 122.8 (qd, *J* = 123.2, 2.8 Hz), 120.7 (d, *J* = 21.5 Hz), 120.3, 56.3.
^{19}F NMR (376 MHz, DMSO-*d*$_6$): δ −60.5, −117.1, −150.9.
HRMS (ESI-TOF, m/z): HRMS (ESI) Calcd for $[M–BF_4]^+$ 265.0959; Found 265.0968.

Preparation of mediator Y44

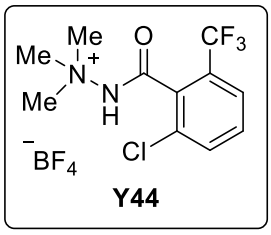

Y44

Following General Procedure A, 2-chloro-6-(trifluoromethyl)benzoyl chloride (1.00 g, 4.12 mmol) was added to a solution of *N*,*N*-dimethylhydrazine (939 µL, 12.36 mmol) in CH_2Cl_2 (15 mL) at 0 °C under argon over 15 min and the reaction was stirred for 30 min at 0 °C and 3 h at laboratory temperature. The reaction mixture was diluted with CH_2Cl_2 (50 mL) and 1 M aq. NaOH (50 mL), the organic phase was separated, and the aqueous phase was extracted with CH_2Cl_2 (2 × 50 mL). Combined organic phases were dried over $MgSO_4$, filtered, and concentrated under reduced pressure to afford a white solid, crude hydrazide (851 mg, 77% yield). A round-bottom flask charged with the crude hydrazide (851 mg, 3.19 mmol) and a magnetic stir bar was evacuated and backfilled with argon twice. Dry MeCN (15 mL) was added, followed by the addition of trimethyloxonium tetrafluoroborate (519 mg, 3.51 mmol) in one portion. The resulting homogeneous solution was stirred at laboratory temperature for 30 min. Then the reaction mixture was concentrated under reduced pressure to afford a solid residue. The crude product was recrystallized from a mixture of MeOH and Et_2O, then washed with Et_2O to afford ylide salt **Y44** as a white solid (633 mg, 54% yield).

Data for mediator **Y44**:
^{1}H NMR (600 MHz, DMSO-*d*$_6$): δ 7.98 (d, *J* = 8.1 Hz, 1H), 7.90 (d, *J* = 7.9 Hz, 1H), 7.81 (t, *J* = 8.0 Hz, 1H), 3.72 (s, 9H).
^{13}C NMR (151 MHz, DMSO-*d*$_6$): δ 161.3, 134.1, 132.7, 132.4, 130.6, 128.0 (q, $^2J_{C\text{-}F}$ = 32.1 Hz), 125.6 (q, $^3J_{C\text{-}F}$ = 4.2 Hz), 122.9 (q, $^1J_{C\text{-}F}$ = 274.3 Hz), 56.2.
^{19}F NMR (376 MHz, DMSO-*d*$_6$): δ −60.6, −150.9.
HRMS (ESI-TOF, m/z): HRMS (ESI) Calcd for $[M–BF_4]^+$ 281.0663; Found 281.1295.

Preparation of mediator Y45

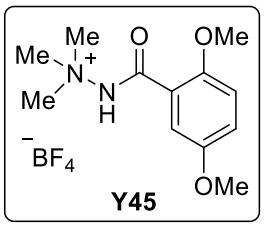

Y45

Following General Procedure B, oxalyl chloride (801 μL, 9.34 mmol) was added dropwise to a solution of 2,5-dimethoxybenzoic acid (850 mg, 4.67 mmol) and DMF (5 drops) in CH_2Cl_2 (20 mL) at 0 °C under argon over 10 min. After the addition, the reaction was stirred for 1 h at 0 °C and 2 h at laboratory temperature. Then the reaction mixture was concentrated under reduced pressure to remove excess oxalyl chloride and afforded crude acyl chloride. A solution of the crude acyl chloride in CH_2Cl_2 (5 mL) was added to a solution of *N*,*N*-dimethylhydrazine (1.1 mL, 14.01 mmol) in CH_2Cl_2 (20 mL) at 0 °C under argon over 15 min and the reaction was stirred for 30 min at 0 °C and 3 h at laboratory temperature. The reaction mixture was diluted with CH_2Cl_2 (40 mL) and 1 M aq. NaOH (50 mL), the organic phase was separated, and the aqueous phase was extracted with CH_2Cl_2 (2 × 50 mL). Combined organic phases were dried over $MgSO_4$, filtered, and concentrated under reduced pressure to afford a white solid (971 mg, 93% yield). A round-bottom flask charged with the crude hydrazide (971 mg, 4.33 mmol) and a magnetic stir bar was evacuated and backfilled with argon twice. Dry MeCN (10 mL) was added, followed by the addition of trimethyloxonium tetrafluoroborate (704 mg, 4.76 mmol) in one portion. The resulting homogeneous solution was stirred at laboratory temperature for 30 min. Then the reaction mixture was concentrated under reduced pressure to afford a solid residue. The crude ylide salt was recrystallized from refluxing EtOH, then washed with Et_2O and EtOH to afford ylide salt **Y45** as a colorless crystalline solid (915 mg, 65% yield).

Data for mediator **Y45**:

^{1}H NMR (500 MHz, DMSO-*d*$_6$): δ 11.66 (s, 1H), 7.13 (m, 3H), 3.81 (s, 3H), 3.75 (s, 3H), 3.69 (s, 9H).

^{13}C NMR (126 MHz, DMSO-*d*$_6$): δ 163.9, 152.8, 150.8, 122.0, 118.3, 114.6, 113.7, 56.5, 56.4, 55.8.

HRMS (ESI-TOF, m/z): HRMS (ESI) Calcd for $[M–BF_4]^+$ 239.1390; Found 239.1399.

Preparation of mediator Y46

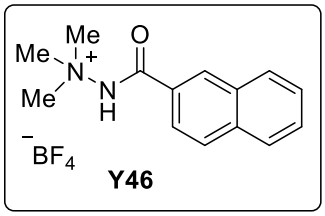

Y46

Following General Procedure A, 2-naphthoyl chloride (1.33 g, 7.00 mmol) was added to a solution of *N*,*N*-dimethylhydrazine (1.60 mL, 21.00 mmol) in CH_2Cl_2 (15 mL) at 0 °C under argon over 15 min and the reaction was stirred for 30 min at 0 °C and 3 h at laboratory temperature. The reaction mixture was diluted with CH_2Cl_2 (10 mL) and 1 M aq. NaOH (20 mL), the organic phase was separated, and the aqueous phase was extracted with CH_2Cl_2 (2 × 10 mL). Combined organic phases were dried over Na_2SO_4, filtered, and concentrated under reduced pressure to afford crude hydrazide (1.2 g) as a white solid. A round-bottom flask charged with the crude hydrazide and a magnetic stir bar was evacuated and backfilled with argon twice. Dry MeCN

(5 mL) was added, followed by the addition of trimethyloxonium tetrafluoroborate (1.04 g, 7.00 mmol) in one portion. The resulting homogeneous solution was stirred at laboratory temperature for 30 min. Then the reaction mixture was concentrated under reduced pressure to afford a solid residue. This crude ylide salt was recrystallized from refluxing EtOH, then washed with Et_2O and EtOH to afford ylide salt **Y46** as a white crystalline solid (1.73 g, 78% yield).

Data for mediator **Y46**:
^{1}H NMR (600 MHz, DMSO-d_6): δ 11.96 (s, 1H), 8.48 (s, 1H), 8.10 (d, J = 8.2 Hz, 2H), 8.05 (d, J = 7.6 Hz, 1H), 7.87 (dd, J = 8.5, 1.9 Hz, 1H), 7.73 – 7.64 (m, 2H), 3.77 (s, 9H).
^{13}C NMR (100 MHz, DMSO-d_6): δ 166.0, 134.9, 131.8, 129.3, 129.1, 128.7, 128.7, 128.5, 127.9, 127.4, 124.1, 56.6.
RMS (ESI-TOF, m/z): HRMS (ESI) Calcd for $[M–BF_4]^+$ 229.1335; Found 229.1345.

Preparation of mediator Y47

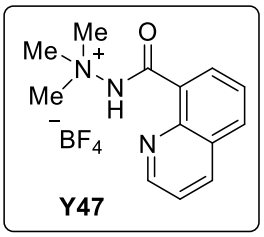

Y47

Following General Procedure B, oxalyl chloride (509 µL, 5.93 mmol) was added dropwise to a solution of quinoline-8-carboxylic acid (604 mg, 3.49 mmol) and DMF (5 drops) in CH_2Cl_2 (20 mL) at 0 °C under argon over 10 min. After the addition, the reaction was stirred 1 h at 0 °C and 2 h at laboratory temperature. Then the reaction mixture was concentrated under reduced pressure to remove excess oxalyl chloride and afforded crude acyl chloride. A solution of the crude acyl chloride in CH_2Cl_2 (5 mL) was added to a solution of *N*,*N*-dimethylhydrazine (796 µL, 10.47 mmol) in CH_2Cl_2 (20 mL) at 0 °C under argon over 15 min and the reaction was stirred for 30 min at 0 °C and 3 h at laboratory temperature. The reaction mixture was diluted with CH_2Cl_2 (40 mL) and 1 M aq. NaOH (50 mL), the organic phase was separated, and the aqueous phase was extracted with CH_2Cl_2 (2 × 50 mL). Combined organic phases were dried over $MgSO_4$, filtered, and concentrated under reduced pressure. The crude product was purified by a short column chromatography (CH_2Cl_2/MeOH 95:5) and was directly used in the next step. A round-bottom flask charged with the crude hydrazide (322 mg, 1.50 mmol) and a magnetic stir bar was evacuated and backfilled with argon twice. Dry MeCN (5 mL) was added, followed by the addition of trimethyloxonium tetrafluoroborate (244 mg, 1.65 mmol) in one portion. The resulting homogeneous solution was stirred at laboratory temperature for 30 min. Then the reaction mixture was concentrated under reduced pressure to afford a solid residue. The crude ylide salt was recrystallized from refluxing EtOH, then washed with Et_2O and EtOH to afford ylide salt **Y47** as a light orange solid (180 mg, 38% yield).

Data for mediator **Y47**:
^{1}H NMR (600 MHz, DMSO-d_6): δ 9.16 – 9.12 (m, 1H), 8.73 (dd, J = 8.4, 1.7 Hz, 1H), 8.56 (d, J = 7.3 Hz, 1H), 8.37 (d, J = 8.1 Hz, 1H), 7.89 – 7.81 (m, 2H), 3.86 (s, 9H).
^{13}C NMR (151 MHz, DMSO-d_6): δ 163.4, 150.1, 143.0, 139.4, 133.7, 132.9, 128.3, 126.9, 126.4, 122.3, 56.6.
HRMS (ESI-TOF, m/z): HRMS (ESI) Calcd for $[M–BF_4]^+$ 230.1288; Found 230.1295.

Preparation of mediator Y48

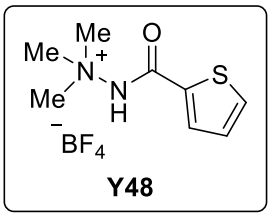

Y48

Following General Procedure A, 2-thiophenecarbonyl chloride (600 µL, 5.61 mmol) was added to a solution of *N*,*N*-dimethylhydrazine (895 µL, 11.78 mmol) in CH_2Cl_2 (10 mL) at 0 °C under argon over 15 min and the reaction was stirred for 30 min at 0 °C and 3 h at laboratory temperature. The reaction mixture was diluted with CH_2Cl_2 (50 mL) and 1 M aq. NaOH (50 mL), the organic phase was separated, and the aqueous phase was extracted with CH_2Cl_2 (2 × 50 mL). Combined organic phases were dried over $MgSO_4$, filtered, and concentrated under reduced pressure to afford an off-white solid, crude hydrazide (932 mg, 98 % yield). A round-bottom flask charged with the crude hydrazide (851 mg, 5.00 mmol) and a magnetic stir bar was evacuated and backfilled with argon twice. Dry MeCN (10 mL) was added, followed by the addition of trimethyloxonium tetrafluoroborate (814 mg, 5.50 mmol) in one portion. The resulting homogeneous solution was stirred at laboratory temperature for 30 min. Then the reaction mixture was concentrated under reduced pressure to afford a solid residue. The crude product was recrystallized from refluxing EtOH, then washed with Et_2O and EtOH to afford ylide salt **Y48** as white solid (974 mg, 66% yield).

Data for mediator **Y48**:
^{1}H NMR (600 MHz, DMSO-d_6): δ 11.70 (s, 1H), 8.01 (dd, *J* = 5.0, 1.2 Hz, 1H), 7.86 (dd, *J* = 3.8, 1.2 Hz, 1H), 7.27 (dd, *J* = 5.0, 3.8 Hz, 1H), 3.71 (s, 9H).
^{13}C NMR (151 MHz, DMSO-d_6): δ 160.3, 134.7, 134.0, 131.9, 128.4, 56.7.
HRMS (ESI-TOF, m/z): HRMS (ESI) Calcd for $[M–BF_4]^+$ 185.0743; Found 185.0751.

Preparation of mediator Y49

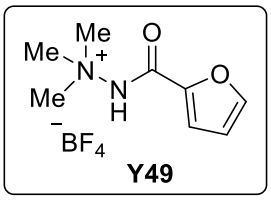

Y49

Following General Procedure A, 2-furoyl chloride (1.09 mL, 11.04 mmol) was added to a solution of *N*,*N*-dimethylhydrazine (2.52 mL, 33.12 mmol) in CH_2Cl_2 (15 mL) at 0 °C under argon over 15 min and the reaction was stirred for 30 min at 0 °C and 3 h at laboratory temperature. The reaction mixture was diluted with CH_2Cl_2 (10 mL) and 1 M aq. NaOH (20 mL), the organic phase was separated, and the aqueous phase was extracted with CH_2Cl_2 (2 × 10 mL). Combined organic phases were dried over Na_2SO_4, filtered, and concentrated under reduced pressure to afford a white solid (1.64 g). A round-bottom flask charged with the crude hydrazide and a magnetic stir bar was evacuated and backfilled with argon twice. Dry MeCN (10 mL) was added, followed by the addition of trimethyloxonium tetrafluoroborate (1.63 g, 11.04 mmol) in one portion. The resulting homogeneous solution was stirred at laboratory temperature for 30 min. Then the reaction mixture was concentrated under reduced pressure to afford a solid residue. This crude ylide salt was recrystallized from refluxing EtOH, then washed with Et_2O and EtOH to afford ylide salt **Y49** as a white crystalline solid (1.61 g, 57% yield).
Data for mediator **Y49**:

^{1}H NMR (600 MHz, DMSO-d_6): δ 11.78 (s, 1H), 8.05 (dd, J = 1.8, 0.8 Hz, 1H), 7.40 (dd, J = 3.6, 0.8 Hz, 1H), 6.76 (dd, J = 3.6, 1.7 Hz, 1H), 3.70 (s, 9H).
^{13}C NMR (151 MHz, DMSO-d_6): δ 156.3, 147.5, 144.2, 118.0, 112.7, 56.9.
HRMS (ESI-TOF, m/z): HRMS (ESI) Calcd for $[M–BF_4]^+$ 169.0972; Found 169.0977.

Preparation of mediator Y50

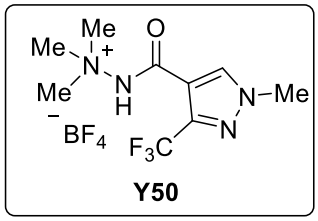

Y50

Following General Procedure B, oxalyl chloride (663 μL, 7.73 mmol) was added dropwise to a solution of 1-methyl-3-(trifluoromethyl)-1*H*-pyrazole-4-carboxylic acid (1.0 g, 5.15 mmol) and DMF (4 drops) in CH_2Cl_2 (10 mL) and THF (10 mL) at 0 °C under argon over 10 min. After the addition, the reaction was stirred for 1 h at 0 °C and 2 h at laboratory temperature. The reaction mixture was concentrated under reduced pressure to remove excess oxalyl chloride and afforded crude acyl chloride. A solution of the crude acyl chloride in CH_2Cl_2 (5 mL) was added to a solution of *N*,*N*-dimethylhydrazine (822 μL, 10.82 mmol) in CH_2Cl_2 (15 mL) at 0 °C under argon over 15 min and the reaction was stirred for 30 min at 0 °C and 3 h at laboratory temperature. The reaction mixture was diluted with CH_2Cl_2 (20 mL) and 1 M aq. NaOH (40 mL), the organic phase was separated, and the aqueous phase was extracted with CH_2Cl_2 (2 × 50 mL). Combined organic phases were dried over $MgSO_4$, filtered, and concentrated under reduced pressure to afford a yellow solid, crude hydrazide (624 mg, 51% yield). A round-bottom flask charged with the crude hydrazide (624 mg, 2.64 mmol) and a magnetic stir bar was evacuated and backfilled with argon twice. Dry MeCN (10 mL) was added, followed by the addition of trimethyloxonium tetrafluoroborate (430 mg, 2.90 mmol) in one portion. The resulting homogeneous solution was stirred at laboratory temperature for 30 min. Then the reaction mixture was concentrated under reduced pressure to afford a solid residue. The crude ylide salt was recrystallized from refluxing EtOH, then washed with Et_2O and EtOH to afford ylide salt **Y50** as a light yellow solid (567 mg, 64% yield).

Data for mediator **Y50**:
^{1}H NMR (600 MHz, MeCN-d_3): δ 9.50 (s, 1H), 8.15 (s, 1H), 3.95 (s, 3H), 3.68 (s, 9H).
^{13}C NMR (151 MHz, MeCN-d_3): δ 159.7, 141.5 (q, $^2J_{C\text{-}F}$ = 38.4 Hz), 135.9, 121.5 (q, $^1J_{C\text{-}F}$ = 270.8 Hz), 112.5, 58.0, 40.4.
^{19}F NMR (376 MHz, DMSO-d_6): δ −62.8, −150.8.
HRMS (ESI-TOF, m/z): HRMS (ESI) Calcd for $[M–BF_4]^+$ 251.1114; Found 251.1122.

Preparation of mediator Y51

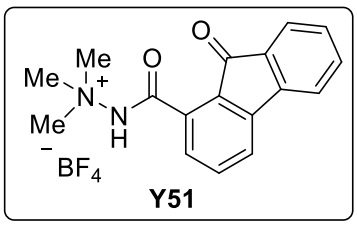

Y51

Following General Procedure B, oxalyl chloride (306 μL, 3.56 mmol) was added dropwise to a solution of 9-fluorenone-1-carboxylic acid (400 mg, 1.78 mmol) and DMF (4 drops) in CH_2Cl_2 (10 mL) at 0 °C under argon over 10 min. After the addition, the reaction was stirred for 1 h at 0 °C and 2 h at laboratory temperature. Then the reaction mixture was

concentrated under reduced pressure to remove excess oxalyl chloride and afforded crude acyl chloride. A solution of the crude acyl chloride in CH_2Cl_2 (5 mL) was added to a solution of *N*,*N*-dimethylhydrazine (297 μL, 3.92 mmol) in CH_2Cl_2 (10 mL) at 0 °C under argon over 15 min and the reaction was stirred for 30 min at 0 °C and 3 h at laboratory temperature. The reaction mixture was diluted with CH_2Cl_2 (40 mL) and 1 M aq. NaOH (40 mL), the organic phase was separated, and the aqueous phase was extracted with CH_2Cl_2 (2 × 50 mL). Combined organic phases were dried over $MgSO_4$, filtered, and concentrated under reduced pressure to afford a bright yellow solid, crude hydrazide (454 mg, 96% yield). A round-bottom flask charged with the crude hydrazide (454 mg, 1.70 mmol) and a magnetic stir bar was evacuated and backfilled with argon twice. Dry MeCN (10 mL) was added, followed by the addition of trimethyloxonium tetrafluoroborate (277 mg, 1.87 mmol) in one portion. The resulting homogeneous solution was stirred at laboratory temperature for 30 min. Then the reaction mixture was concentrated under reduced pressure to afford a solid residue. The crude ylide salt was recrystallized from refluxing EtOH, then washed with Et_2O and EtOH to afford ylide salt **Y51** as a yellow-orange solid (511 mg, 82% yield).

Data for mediator **Y51**:

^{1}H NMR (500 MHz, DMSO-d_6): δ 12.26 (s, 1H), 8.01 (dd, *J* = 7.6, 0.9 Hz, 1H), 7.89 (dt, *J* = 7.5, 0.9 Hz, 1H), 7.75 (t, *J* = 7.6 Hz, 1H), 7.68 (td, *J* = 7.5, 1.2 Hz, 1H), 7.65 (dt, *J* = 7.4, 1.0 Hz, 1H), 7.48 – 7.42 (m, 2H), 3.76 (s, 9H).

^{13}C NMR (151 MHz, DMSO-d_6): δ 191.9, 164.0, 143.9, 143.1, 135.95, 136.0, 132.7, 130.2, 130.2, 128.2, 124.4, 123.4, 121.7, 56.4.

HRMS (ESI-TOF, m/z): HRMS (ESI) Calcd for $[M–BF_4]^+$ 281.1285; Found 281.1295.

Preparation of mediator Y52

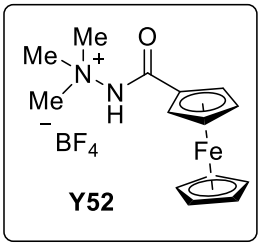

Y52

Following a modified General Procedure B, oxalyl chloride (2.24 mL, 26.10 mmol) was added dropwise to a solution of ferrocenecarboxylic acid (600 mg, 2.61 mmol) and DMF (5 drops) in THF (15 mL) at 0 °C under argon over 10 min. After the addition, the reaction was stirred for 30 min at 0 °C and 3 h at laboratory temperature. Then the reaction mixture was concentrated under reduced pressure ($T < 30$ °C) to remove excess oxalyl chloride and afforded crude acyl chloride. A solution of the crude acyl chloride in CH_2Cl_2 (5 mL) was added to a solution of *N*,*N*-dimethylhydrazine (258 μL, 3.39 mmol) and dry Et_3N (473 μL, 3.39 mmol) in CH_2Cl_2 (15 mL) at −78 °C under argon over 15 min and the reaction was stirred 30 min at −78 °C, then gradually warmed to laboratory temperature and stirred for 3 h. The reaction mixture was diluted with CH_2Cl_2 (40 mL) and 1 M aq. NaOH (40 mL), the organic phase was separated, and the aqueous phase was extracted with CH_2Cl_2 (3 × 50 mL). Combined organic phases were dried over $MgSO_4$, filtered, and concentrated under reduced pressure to afford a dark red solid (632 mg, 89% yield). A round-bottom flask charged with the crude hydrazide (632 mg, 2.32 mmol) and a magnetic stir bar was evacuated and backfilled with argon twice. Dry MeCN (15 mL) was added, followed by the addition of trimethyloxonium tetrafluoroborate (377 mg, 2.55 mmol) in one portion. The resulting homogeneous solution was stirred at laboratory temperature for 30 min. Then the reaction mixture was concentrated under reduced pressure to afford an orange solid residue,

crude ylide salt. The crude ylide salt was recrystallized from refluxing EtOH, then washed with Et_2O and EtOH to afford ylide salt **Y52** as an orange crystalline solid (542 mg, 62% yield).

Data for mediator **Y52**:
^{1}H NMR (600 MHz, DMSO-d_6): δ 10.77 (s, 1H), 4.91 (s, 2H), 4.55 (s, 2H), 4.28 (s, 5H), 3.69 (s, 9H).
^{13}C NMR (151 MHz, DMSO-d_6): δ 169.1, 71.8, 71.5, 71.0, 69.0, 56.5.
HRMS (ESI-TOF, m/z): HRMS (ESI) Calcd for $[M–BF4]^+$ 285.0888; Found 287.0898.

Preparation of mediator Y53

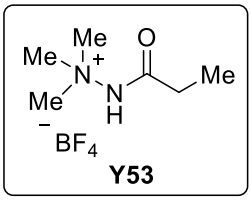

Y53

Following General Procedure A, propionyl chloride (874 µL, 10.00 mmol) was added to a solution of *N*,*N*-dimethylhydrazine (2.28 mL, 30.00 mmol) in CH_2Cl_2 (20 mL) at 0 °C under argon over 15 min and the reaction was stirred for 30 min at 0 °C and 3 h at laboratory temperature. The reaction mixture was diluted with CH_2Cl_2 (40 mL) and 1 M aq. NaOH (40 mL), the organic phase was separated, and the aqueous phase was extracted with CH_2Cl_2 (2 × 50 mL). Combined organic phases were dried over $MgSO_4$, filtered, and concentrated under reduced pressure to afford a white solid, crude hydrazide. A round-bottom flask charged with the crude hydrazide (470 mg, 4.05 mmol) and a magnetic stir bar was evacuated and backfilled with argon twice. Dry MeCN (10 mL) was added, followed by the addition of trimethyloxonium tetrafluoroborate (660 mg, 4.46 mmol) in one portion. The resulting homogeneous solution was stirred at laboratory temperature for 30 min. Then the reaction mixture was concentrated under reduced pressure to afford a solid residue. The crude ylide salt was recrystallized from a mixture of MeOH and Et_2O, then washed with Et_2O to afford ylide salt **Y53** as a white crystalline solid (689 mg, 78% yield).

Data for mediator **Y53**:
^{1}H NMR (600 MHz, DMSO-d_6): δ 11.38 (s, 1H), 3.57 (s, 9H), 2.21 (q, J = 7.5 Hz, 2H), 1.03 (t, J = 7.5 Hz, 3H).
^{13}C NMR (151 MHz, DMSO-d_6): δ 171.5, 56.2, 27.2, 8.7.
HRMS (ESI-TOF, m/z): LRMS (ESI) Calcd for $[M–BF_4]^+$ 131.11; Found 131.10.

Preparation of mediator Y54

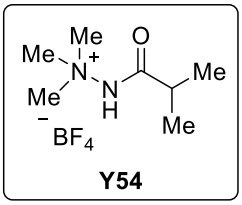

Y54

Following General Procedure A, isobutyryl chloride (1.17 mL, 11.11 mmol) was added to a solution of *N*,*N*-dimethylhydrazine (2.53 mL, 33.33 mmol) in CH_2Cl_2 (15 mL) at 0 °C under argon over 15 min and the reaction was stirred for 30 min at 0 °C and 3 h at laboratory temperature. The reaction mixture was diluted with CH_2Cl_2 (10 mL) and 1 M aq. NaOH (20 mL), the organic phase was separated, and the aqueous phase was extracted with CH_2Cl_2 (2 × 10 mL). Combined organic phases were dried over

Na_2SO_4, filtered, and concentrated under reduced pressure to afford crude hydrazide (536 mg) as a white solid. A round-bottom flask charged with the crude hydrazide and a magnetic stir bar was evacuated and backfilled with argon twice. Dry MeCN (5 mL) was added, followed by the addition of trimethyloxonium tetrafluoroborate (1.64 g, 11.11 mmol) in one portion. The resulting homogeneous solution was stirred at laboratory temperature for 30 min. Then the reaction mixture was concentrated under reduced pressure to afford a solid residue. This crude ylide salt was recrystallized from refluxing EtOH, then washed with Et_2O and EtOH to afford ylide salt **Y54** as a white crystalline solid (1.12 g, 43% yield).

Data for mediator **Y54**:
^{1}H NMR (600 MHz, DMSO-d_6): δ 11.40 (s, 1H), 3.58 (s, 9H), 2.44 (sextet, J = 6.8 Hz, 1H), 1.06 (d, J = 6.9 Hz, 6H).
^{13}C NMR (151 MHz, DMSO-d_6): δ 174.6, 56.2, 32.9, 18.7.
HRMS (ESI-TOF, m/z): HRMS (ESI) Calcd for $[M–BF_4]^+$ 145.1335; Found 145.1341.

Preparation of mediator Y55

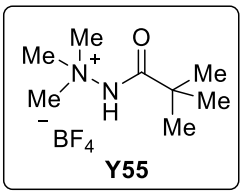

Y55

Following General Procedure A, pivaloyl chloride (1.36 mL, 11.11 mmol) was added to a solution of *N*,*N*-dimethylhydrazine (2.53 mL, 33.33 mmol) in CH_2Cl_2 (15 mL) at 0 °C under argon over 15 min and the reaction was stirred for 30 min at 0 °C and 3 h at laboratory temperature. The reaction mixture was diluted with CH_2Cl_2 (10 mL) and 1 M aq. NaOH (20 mL), the organic phase was separated, and the aqueous phase was extracted with CH_2Cl_2 (2 × 10 mL). Combined organic phases were dried over Na_2SO_4, filtered, and concentrated under reduced pressure to afford crude hydrazide (1.30 g) as a white solid. A round-bottom flask charged with the crude hydrazide and a magnetic stir bar was evacuated and backfilled with argon twice. Dry MeCN (7 mL) was added, followed by the addition of trimethyloxonium tetrafluoroborate (1.64 g, 11.11 mmol) in one portion. The resulting homogeneous solution was stirred at laboratory temperature for 30 min. Then the reaction mixture was concentrated under reduced pressure to afford a solid residue. This crude ylide salt was recrystallized from refluxing EtOH to afford ylide salt **Y55** as a white crystalline solid (2.08 g, 76% yield).

Data for mediator **Y55**:
^{1}H NMR (600 MHz, DMSO-d_6): δ 10.47 (s, 1H), 3.59 (s, 9H), 1.17 (s, 9H).
^{13}C NMR (151 MHz, DMSO-d_6): δ 176.4, 56.3, 39.1, 26.4.
HRMS (ESI-TOF, m/z): HRMS (ESI) Calcd for $[M–BF_4]^+$ 159.1492; Found 159.1500.

Preparation of mediator Y56

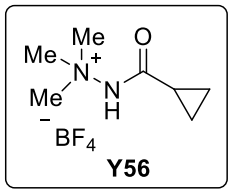

Following General Procedure A, cyclopropanecarbonyl chloride (1.27 mL, 14.00 mmol) was added to a solution of *N*,*N*-dimethylhydrazine (3.19 mL, 42.0 mmol) in CH_2Cl_2 (15 mL) at 0 °C under argon over 15 min and the reaction was stirred 30 min at 0 °C and 3 h at laboratory temperature. The reaction mixture was diluted with CH_2Cl_2 (10 mL) and 1 M aq. NaOH (20 mL), the organic phase was separated, and the aqueous phase was extracted with CH_2Cl_2 (2 × 10 mL). Combined organic phases were dried over Na_2SO_4, filtered, and concentrated under reduced pressure to afford a white solid (730 mg). A round-bottom flask charged with the crude hydrazide and a magnetic stir bar was evacuated and backfilled with argon twice. Dry MeCN (10 mL) was added, followed by the addition of trimethyloxonium tetrafluoroborate (2.07 g, 14.00 mmol) in one portion. The resulting homogeneous solution was stirred at laboratory temperature for 30 min. Then the reaction mixture was concentrated under reduced pressure to afford a solid residue. This crude ylide salt was recrystallized from refluxing EtOH, then washed with Et_2O and EtOH to afford ylide salt **Y56** as a white crystalline solid (1.32 g, 41% yield).

Data for mediator **Y56**:
^{1}H NMR (600 MHz, DMSO-d_6): δ 11.66 (s, 1H), 3.59 (s, 9H), 1.66 (tt, *J* = 7.8, 4.6 Hz, 1H), 0.89 (dt, *J* = 7.9, 3.1 Hz, 2H), 0.85 – 0.81 (m, 2H).
^{13}C NMR (151 MHz, DMSO-d_6): δ 171.3, 56.3, 12.9, 7.8.
HRMS (ESI-TOF, m/z): HRMS (ESI) Calcd for $[M–BF_4]^+$ 143.1179; Found 143.1185.

Preparation of mediator Y57

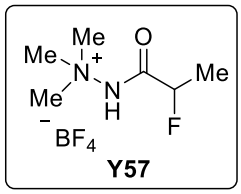

Following General Procedure B, oxalyl chloride (172 µL, 2.00 mmol) was added dropwise over 30 min to a solution of 2-fluoropropanoic acid (156 µL, 2.00 mmol) and DMF (3 drops) in CH_2Cl_2 (3 mL) at 0 °C under argon. After the addition, the reaction was stirred for 1 h at 0 °C and 3 h at laboratory temperature. Then the reaction mixture was concentrated under reduced pressure to remove excess oxalyl chloride and afforded crude acyl chloride. A solution of the crude acyl chloride in CH_2Cl_2 (2 mL) was added to a solution of *N*,*N*-dimethylhydrazine (608 µL, 8.00 mmol) in CH_2Cl_2 (3 mL) at 0 °C under argon over 30 min and the reaction was stirred for 30 min at 0 °C and 3 h at laboratory temperature. The reaction mixture was diluted with CH_2Cl_2 (10 mL) and 1 M aq. NaOH (10 mL), the organic phase was separated, and the aqueous phase was extracted with CH_2Cl_2 (2 × 15 mL). Combined organic extracts were dried over $MgSO_4$, filtered, and concentrated under reduced pressure to afford a crude hydrazide (260 mg, 97% yield).
A round-bottom flask charged with the crude hydrazide (260 mg, 1.94 mmol) and a magnetic stir bar was evacuated and backfilled with argon twice. Dry MeCN (5 mL) was added, followed by the addition of trimethyloxonium tetrafluoroborate (410 mg, 3.00 mmol) in one portion. The resulting homogeneous solution was stirred at laboratory temperature for 30 min. Then the reaction mixture was concentrated under reduced pressure to afford a solid residue. The crude ylide salt was recrystallized from refluxing EtOH, then washed with Et_2O and EtOH to afford ylide salt **Y57** as a white solid (381 mg, 83% yield).

Data for mediator **Y57**:
^{1}H NMR (600 MHz, DMSO-*d*$_6$): δ 11.96 (s, 1H), 5.13 (dq, *J* = 47.8, 6.7 Hz, 1H), 3.63 (s, 9H), 1.49 (dd, *J* = 24.7, 6.7 Hz, 3H).
^{13}C NMR (151 MHz, DMSO-*d*$_6$): δ 167.8, 86.6 (d, $^{1}J_{C\text{-}F}$ = 178.4 Hz), 56.4, 17.9 (d, $^{2}J_{C\text{-}F}$ = 21.7 Hz).
^{19}F NMR (396 MHz, DMSO-*d*$_6$): δ −150.9, −185.9.
HRMS (ESI-TOF, m/z): HRMS (ESI) Calcd for $[M–BF_4]^+$ 149.1085; Found 149.1092.

Preparation of mediator Y58

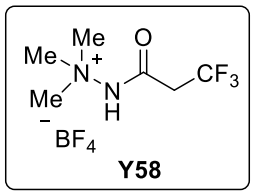

Y58

Following a modified General Procedure A, 3,3,3-trifluoropropionyl chloride (4.22 mL, 40.96 mmol) was added to a solution of *N*,*N*-dimethylhydrazine (4.67 mL, 61.44 mmol) in CH_2Cl_2 (50 mL) at −78 °C under argon over 15 min. The reaction was stirred for 30 min at −78 °C and then gradually warmed to laboratory temperature and stirred for 3 h. The reaction mixture was diluted with CH_2Cl_2 (150 mL) and H_2O (80 mL), the organic phase was separated, and the aqueous phase was extracted with CH_2Cl_2 (2 × 100 mL). Combined organic phases were washed with sat. aq. $NaHCO_3$ (100 mL), dried over $MgSO_4$, filtered, and concentrated under reduced pressure to afford a white solid (4.94 g, 71% yield). A round-bottom flask charged with the crude hydrazide (4.92 g, 28.92 mmol) and a magnetic stir bar was evacuated and backfilled with argon twice. Dry MeCN (50 mL) was added, followed by the addition of trimethyloxonium tetrafluoroborate (4.71 g, 31.81 mmol) in one portion. The resulting homogeneous solution was stirred at laboratory temperature for 30 min. Then the reaction mixture was concentrated under reduced pressure to afford a solid residue. The crude product was recrystallized from refluxing EtOH, then washed with Et_2O and EtOH to afford ylide salt **Y58** as white crystalline solid (5.55 g, 71% yield).

Data for mediator **Y58**:
^{1}H NMR (600 MHz, DMSO-*d*$_6$): δ 3.61 (s, 9H), 3.47 (q, *J* = 10.8 Hz, 2H).
^{13}C NMR (151 MHz, DMSO-*d*$_6$): δ 161.3 (q, $^{3}J_{C\text{-}F}$ = 3.9 Hz), 124.0 (q, $^{1}J_{C\text{-}F}$ = 276.5 Hz), 56.4, 38.6 (q, $^{2}J_{C\text{-}F}$ = 29.2 Hz).
^{19}F NMR (376 MHz, DMSO-*d*$_6$): δ −64.0, −150.9.
HRMS (ESI-TOF, m/z): HRMS (ESI) Calcd for $[M–BF_4]^+$ 185.0896; Found 185.0904.

Preparation of mediator Y59

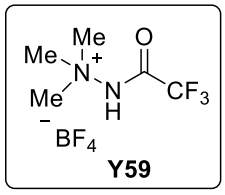

Y59

A round-bottom flask was charged with a magnetic stir bar, ethyl trifluoroacetate (1.07 mL, 9.00 mmol), and dry Et_3N (2.51 mL, 18.00 mmol) in dry MeOH (15 mL) under argon. The solution was cooled to 0°C and subsequently *N*,*N*-dimethylhydrazine (1.37 mL, 18.00 mmol) was added dropwise. Then, the reaction mixture was warmed to laboratory temperature and stirred for an additional 12 h. The reaction mixture was diluted with CH_2Cl_2 (10 mL) and sat. aq. NH_4Cl (20 mL), the organic phase was separated, and the aqueous phase

was extracted with CH_2Cl_2 (2 × 10 mL). Combined organic extracts were dried over Na_2SO_4, filtered, and concentrated under reduced pressure to afford crude hydrazide as a white solid. A round-bottom flask charged with the crude hydrazide and a magnetic stir bar was evacuated and backfilled with argon twice. Dry MeCN (10 mL) was added, followed by the addition of trimethyloxonium tetrafluoroborate (1.33 g, 9.00 mmol) over 1 min. The resulting homogeneous solution was stirred at room temperature for 30 min. Then the reaction mixture was concentrated under reduced pressure to afford a solid residue. This crude ylide salt was recrystallized from hot EtOH to afford ylide salt **Y59** as a white crystalline solid (1.20 g, 52% yield).

Data for mediator **Y59**:
^{1}H NMR (600 MHz, DMSO-*d*$_6$): δ 3.30 (s, 9H).
^{13}C NMR (151 MHz, DMSO-*d*$_6$): δ 159.3 (q, $^2J_{C\text{-}F}$ = 31.6 Hz), 118.3 (q, $^1J_{C\text{-}F}$ = 291.2 Hz), 54.5.
^{19}F NMR (376 MHz, DMSO-*d*$_6$): δ −75.0, −150.9.
HRMS (ESI-TOF, m/z): HRMS (ESI) Calcd for $[M–BF_4]^+$ 171.0740; Found 171.0746.

Preparation of mediator Y60

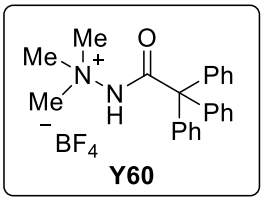

Y60

Following General Procedure B, oxalyl chloride (540 μL, 6.24 mmol) was added dropwise to a solution of triphenylacetic acid (900 mg, 2.61 mmol) and DMF (4 drops) in CH_2Cl_2 (10 mL) at 0 °C under argon over 10 min. After the addition, the reaction was stirred for 30 min at 0 °C and 3 h at laboratory temperature. Then the reaction mixture was concentrated under reduced pressure to remove excess of oxalyl chloride and afforded crude acyl chloride. A solution of the crude acyl chloride in CH_2Cl_2 (5 mL) was added to a solution of *N*,*N*-dimethylhydrazine (521 μL, 6.86 mmol) in CH_2Cl_2 (15 mL) at 0 °C under argon over 15 min and the reaction was stirred for 30 min at 0 °C and 3 h at laboratory temperature. The reaction mixture was diluted with CH_2Cl_2 (30 mL) and 1 M aq. NaOH (30 mL), the organic phase was separated, and the aqueous phase was extracted with CH_2Cl_2 (2 × 40 mL). Combined organic phases were dried over $MgSO_4$, filtered, and concentrated under reduced pressure to afford a solid, crude hydrazide (787 mg, 76% yield). A round-bottom flask charged with the crude hydrazide (787 mg, 2.38 mmol) and a magnetic stir bar was evacuated and backfilled with argon twice. Dry MeCN (15 mL) was added, followed by the addition of trimethyloxonium tetrafluoroborate (388 mg, 2.62 mmol) in one portion. The resulting homogeneous solution was stirred at laboratory temperature for 30 min. Then the reaction mixture was concentrated under reduced pressure to afford an orange solid residue. The crude ylide salt was recrystallized from refluxing EtOH, then washed with Et_2O and EtOH to afford ylide salt **Y60** as a white solid (613 mg, 60% yield).

Data for mediator **Y60**:

^{1}H NMR (600 MHz, DMSO-d_6): δ 10.81 (s, 1H), 7.36 (t, J = 7.6 Hz, 6H), 7.30 (t, J = 7.3 Hz, 3H), 7.24 (d, J = 7.3 Hz, 6H), 3.59 (s, 9H).
^{13}C NMR (151 MHz, DMSO-d_6): δ 171.1, 141.7, 130.1, 128.1, 127.2, 67.9, 56.4.
HRMS (ESI-TOF, m/z): HRMS (ESI) Calcd for $[M–BF_4]^+$ 345.1961; Found 345.1970.

Preparation of mediator Y61

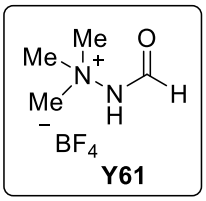

Y61

A round-bottom flask was charged with ethyl formate (5.38 mL, 66.65 mmol) and *N*,*N*-dimethylhydrazine (1.01 mL, 13.31 mmol) and a magnetic stir bar. The mixture was refluxed for 12 h and then stirred 12 h at laboratory temperature. Then, the reaction mixture was concentrated under reduced pressure to afford crude hydrazide which was directly used in the next step. A round-bottom flask charged with the crude hydrazide (486 mg, 5.52 mmol) and a magnetic stir bar was evacuated and backfilled with argon twice. Dry MeCN (10 mL) was added, followed by the addition of trimethyloxonium tetrafluoroborate (898 mg, 6.07 mmol) in one portion. The resulting homogeneous solution was stirred at laboratory temperature for 30 min. Then the reaction mixture was concentrated under reduced pressure to afford a white solid residue, crude ylide salt. The crude ylide salt was recrystallized from refluxing EtOH, then washed with Et_2O and EtOH to afford ylide salt **Y61** as an opaque crystalline solid (675 mg, 64% yield).

Data for mediator **Y61**:
^{1}H NMR (600 MHz, DMSO-d_6): δ 12.01 (br s, 1H), 8.12 (s, 1H), 3.60 (s, 9H).
^{13}C NMR (151 MHz, DMSO-d_6): δ 158.9, 56.5.
MS (ESI, m/z): MS (ESI) Calcd for $[M–BF_4]^+$103.09; Found 103.10.

Preparation of mediator Y62

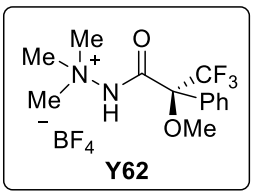

Y62

Following General Procedure B, oxalyl chloride (1.11 mL, 12.98 mmol) was added dropwise to a solution of (*R*)-(+)-α-methoxy-α-trifluoromethylphenylacetic acid (1.52 g, 6.49 mmol) and DMF (4 drops) in CH_2Cl_2 (15 mL) at 0 °C under argon over 10 min. After the addition, the reaction was stirred for 2 h at laboratory temperature. Then the reaction mixture was concentrated under reduced pressure to remove excess of oxalyl chloride and afforded crude acyl chloride. A solution of the crude acyl chloride in CH_2Cl_2 (2 mL) was added to a solution of *N*,*N*-dimethylhydrazine (1.48 mL, 19.47 mmol) in CH_2Cl_2 (10 mL) at 0 °C under argon over 15 min and the reaction was stirred for 30 min at 0 °C and 3 h at laboratory temperature. The reaction mixture was diluted with CH_2Cl_2 (20 mL) and 1 M aq. NaOH (20 mL), the organic phase was separated, and the aqueous phase was extracted with CH_2Cl_2 (2 × 20 mL). Combined organic phases were dried over Na_2SO_4, filtered, and concentrated under reduced pressure to afford a white solid, crude hydrazide (1.56 g). A round-bottom flask charged with the crude hydrazide and a magnetic stir bar was evacuated and backfilled with argon twice. Dry MeCN (10 mL) was added, followed by the addition of trimethyloxonium tetrafluoroborate (960 mg, 6.49 mmol) in one portion. The resulting homogeneous solution was stirred at laboratory temperature for 30 min. Then the reaction mixture was concentrated under

reduced pressure to afford a solid residue. The crude ylide salt was recrystallized from refluxing EtOH, then washed with Et_2O and EtOH to afford ylide salt **Y62** as a white crystalline solid (1.40 g, 57% yield).

Data for mediator **Y62**:
^{1}H NMR (400 MHz, DMSO-d_6): δ 7.64 – 7.37 (m, 5H), 3.62 (s, 9H), 3.51 (d, J = 1.6 Hz, 3H).
^{13}C NMR (100 MHz, DMSO-d_6): δ 165.3, 130.4, 129.2, 127.6, 84.5, 56.8, 55.8.
^{19}F NMR (376 MHz, DMSO-d_6): δ −71.3, −150.9.
HRMS (ESI-TOF, m/z): HRMS (ESI) Calcd for $[M–BF_4]^+$ 291.1315; Found 291.1324.

Preparation of mediator Y63

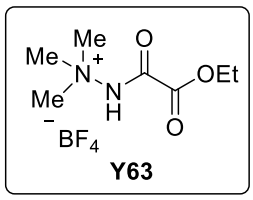

Following General Procedure A, ethyl chlorooxoacetate (1.00 mL, 8.94 mmol) was added to a solution of *N*,*N*-dimethylhydrazine (4.67 mL, 18.77 mmol) in CH_2Cl_2 (10 mL) at –78 °C under argon over 15 min. The reaction was stirred for 30 min at –78 °C and then gradually warmed to laboratory temperature and stirred for 3 h. The reaction mixture was diluted with CH_2Cl_2 (50 mL) and distd. water (50 mL), the organic phase was separated, and the aqueous phase was extracted with CH_2Cl_2 (3 × 50 mL). Combined organic phases were dried over $MgSO_4$, filtered, and concentrated under reduced pressure to afford a colorless oil, crude hydrazide (1.35 g, 94% yield). A round-bottom flask charged with the crude hydrazide (1.13 g, 7.06 mmol) and a magnetic stir bar was evacuated and backfilled with argon twice. Dry MeCN (10 mL) was added, followed by the addition of trimethyloxonium tetrafluoroborate (1.15 g, 7.77 mmol) in one portion. The resulting homogeneous solution was stirred at laboratory temperature for 30 min. Then the reaction mixture was concentrated under reduced pressure to afford a solid residue. The crude product was recrystallized from refluxing EtOH, then washed with Et_2O and EtOH to afford ylide salt **Y63** as a white solid (1.26 g, 68% yield).

Data for mediator **Y63**:
^{1}H NMR (600 MHz, DMSO-d_6): δ 4.27 (q, J = 7.1 Hz, 2H), 3.60 (s, 9H), 1.28 (t, J = 7.2 Hz, 3H).
^{13}C NMR (151 MHz, DMSO-d_6): δ 158.7, 156.0, 62.9, 56.3, 13.8.
HRMS (ESI-TOF, m/z): HRMS (ESI) Calcd for $[M–BF_4]^+$ 175.1077; Found 175.1086.

Preparation of mediator Y64

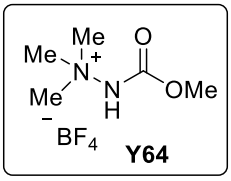

Y64

A round-bottom flask was charged with *N*,*N*-dimethylhydrazine (1.14 mL, 15.00 mmol) was added to a solution of methyl chloroformate (390 μL, 5.00 mmol) dissolved in CH_2Cl_2 (15 mL) and stirred at 0 °C under argon. The reaction mixture was stirred for 30 min at 0 °C and 3 h at laboratory temperature. The reaction mixture was diluted with CH_2Cl_2 (50 mL) and distd. water (50 mL), the organic phase was separated, and the aqueous phase was extracted with CH_2Cl_2 (2 × 50 mL). Combined organic phases were dried over $MgSO_4$, filtered, and concentrated under reduced pressure to afford crude hydrazide. A round-bottom flask charged with the crude hydrazide and a magnetic stir bar was evacuated and backfilled with argon twice. Dry MeCN (15 mL) was added, followed by the addition of trimethyloxonium tetrafluoroborate (740 mg, 5.00 mmol) in one portion. The resulting homogeneous solution was stirred at laboratory temperature for 30 min. Then the reaction mixture was concentrated under reduced pressure to afford a solid residue. The crude ylide salt was recrystallized from a mixture of MeCN, CH_2Cl_2, and Et_2O to afford ylide **Y64** as a white solid (1.05 g, 95% yield).

Data for mediator **Y64**:
^{1}H NMR (600 MHz, DMSO-d_6): δ 11.34 (s, 1H), 3.75 (s, 3H), 3.56 (s, 9H).
^{13}C NMR (151 MHz, DMSO-d_6): δ 153.3, 56.5, 53.2.
HRMS (ESI-TOF, m/z): HRMS (ESI) Calcd for $[M–BF_4+Na]^+$ 155.0791; Found 155.0800.

Preparation of mediator Y65

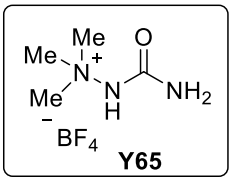

Y65

A flame dried 100-mL round-bottom flask was charged with (trimethylsilyl)isocyanate (1.35 mL, 10.00 mmol), dry hexane (12.5 mL), *N*,*N*-dimethylhydrazine (2.28 mL, 30.00 mmol) and a magnetic stir bar under argon. The reaction mixture was refluxed for 1 h. Then, the reaction mixture was cooled to laboratory temperature and concentrated under reduced pressure to afford crude hydrazide as a white solid, which was used directly in the next step. A round-bottom flask charged with the crude hydrazide and a magnetic stir bar was evacuated and backfilled with argon twice. Dry MeCN (5 mL) was added, followed by the addition of trimethyloxonium tetrafluoroborate (1.48 g, 10.00 mmol) in one portion. The resulting homogeneous solution was stirred at laboratory temperature for 30 min. Then the reaction mixture was concentrated under reduced pressure to afford ylide salt **Y65** as a white solid (755 mg, 37% yield).

Data for mediator **Y65**:
^{1}H NMR (600 MHz, DMSO-d_6): δ 9.43 (s, 1H), 6.68 (s, 2H), 3.52 (s, 9H).
^{13}C NMR (150 MHz, DMSO-d_6): δ 155.8, 56.3.
MS (ESI, m/z): MS (ESI) Calcd for $[M–BF_4]^+$ 118.10; Found 118.10
Preparation of mediator Y66

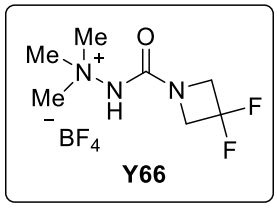

Y66

Following General Procedure A, 3,3-difluoroazetidine-1-carbonyl chloride (780 mg, 5.00 mmol), was added to a solution of *N*,*N*-dimethylhydrazine (1.14 mL, 15.00 mmol) in CH_2Cl_2 (50 mL) at 0 °C under argon over 15 min and the reaction was stirred for 30 min at 0 °C and 3 h at laboratory temperature. The reaction mixture was diluted with CH_2Cl_2 (30 mL) and distd. water (30 mL), the organic phase was separated, and the aqueous phase was extracted with CH_2Cl_2 (2 × 20 mL). Combined organic phases were dried over $MgSO_4$, filtered, and concentrated under reduced pressure to afford crude hydrazide. A round-bottom flask charged with the crude hydrazide and a magnetic stir bar was evacuated and backfilled with argon twice. Dry MeCN (10 mL) was added, followed by the addition of trimethyloxonium tetrafluoroborate (814 mg, 5.50 mmol) in one portion. The resulting homogeneous solution was stirred at laboratory temperature for 30 min. Then the reaction mixture was concentrated under reduced pressure to afford a solid residue. The crude product was recrystallized from a mixture of MeOH and Et_2O, then washed with Et_2O to afford ylide as a yellowish solid (313 mg, 22% yield).

Data for mediator **Y66**:
^{1}H NMR (600 MHz, DMSO-*d*$_6$): δ 10.10 (s, 1H), 4.38 (t, *J* = 12.6 Hz, 4H), 3.56 (s, 9H).
^{13}C NMR (151 MHz, DMSO-*d*$_6$): δ 155.2 (t, $^3J_{C\text{-}F}$ = 4.1 Hz), 115.9 (t, $^1J_{C\text{-}F}$ = 272.3 Hz), 61.4 (t, $^2J_{C\text{-}F}$ = 27.9 Hz), 56.6.
^{19}F NMR (376 MHz, DMSO-*d*$_6$): δ −102.0, −150.9.
HRMS (ESI-TOF, m/z): HRMS (ESI) Calcd for $[M–BF_4]^+$ 194.1099; Found 194.1110.

Preparation of mediator 67

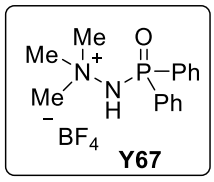

Y67

A round-bottom flask was charged with *N*,*N*-dimethylhydrazine (836 µL, 11.00 mmol), CH_2Cl_2 (15 mL) and a magnetic stir bar under argon. The solution was cooled to 0 °C and diphenylphosphinic chloride (1.00 mL, 5.24 mmol) was added dropwise over 5 min. The reaction mixture was stirred for 30 min at 0 °C and 3 h at laboratory temperature. The reaction mixture was diluted with CH_2Cl_2 (30 mL) and 1 M aq. NaOH (50 mL), the organic phase was separated, and the aqueous phase was extracted with CH_2Cl_2 (3 × 50 mL). Combined organic phases were dried over $MgSO_4$, filtered, and concentrated under reduced pressure to afford an off-white solid (1.32 g, 97% yield). A round-bottom flask charged with the crude hydrazide (1.32 g, 5.07 mmol) and a magnetic stir bar was evacuated and backfilled with argon twice. Dry MeCN (20 mL) was added, followed by the addition of trimethyloxonium tetrafluoroborate (823 mg, 5.57 mmol) in one portion. The resulting homogeneous solution was stirred at laboratory temperature for 30 min. Then the reaction mixture was concentrated under reduced pressure to afford a solid residue. The crude product was recrystallized from refluxing EtOH, then washed with Et_2O and EtOH to afford ylide salt **Y67** as an opaque crystalline solid (1.10 g, 60% yield).

Data for mediator **Y67**:

^{1}H NMR (600 MHz, DMSO-d_6): δ 9.30 (d, *J* = 7.6 Hz, 1H), 7.95 – 7.83 (m, 4H), 7.70 (td, *J* = 7.5, 1.6 Hz, 2H), 7.62 (td, *J* = 7.7, 3.5 Hz, 4H), 3.54 (s, 9H).
^{13}C NMR (151 MHz, DMSO-d_6): δ 133.3 (d, *J* = 2.7 Hz), 131.8 (d, *J* = 10.2 Hz), 130.5 (d, *J* = 127.0 Hz), 129.2 (d, *J* = 13.0 Hz), 59.0.
^{31}P NMR (162 MHz, DMSO-d_6): δ 22.7.
HRMS (ESI-TOF, m/z): HRMS (ESI) Calcd for $[M–BF_4]^+$ 275.1308; Found 275.1319.

Preparation of mediator Y68

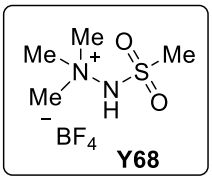

Y68

A round-bottom flask was charged with ethyl trifluoroacetate (1.07 mL, 9.00 mmol) was dissolved in dry MeOH (15 mL). The mixture was cooled to 0 °C and Et_3N (2.51 mL, 18.00 mmol) and subsequently *N*,*N*-dimethylhydrazine (1.37 mL, 18.0 mmol) were added dropwise. Then the reaction was warmed to laboratory temperature and stirred for an additional 12 h. The reaction mixture was diluted with CH_2Cl_2 (10 mL) and sat. aq. NH_4Cl (20 mL), the organic phase was separated, and the aqueous phase was extracted with CH_2Cl_2 (2 × 10 mL). Combined organic phases were dried over Na_2SO_4, filtered, and concentrated under reduced pressure to afford a white solid. A round-bottom flask charged with the crude hydrazide and a magnetic stir bar was evacuated and backfilled with argon twice. Dry MeCN (10 mL) was added, followed by the addition of trimethyloxonium tetrafluoroborate (1.33 g, 9.00 mmol) in one portion. The resulting homogeneous solution was stirred at laboratory temperature for 30 min. Then the reaction mixture was concentrated under reduced pressure to afford a solid residue. This crude ylide salt was recrystallized from refluxing EtOH, then washed with Et_2O and EtOH to afford ylide salt **Y68** as a white crystalline solid (1.20 g, 52% yield).

Data for mediator **Y68**:
^{1}H NMR (600 MHz, DMSO-d_6): δ 3.59 (s, 9H), 3.47 (s, 3H).
^{13}C NMR (151 MHz, DMSO-d_6): δ 57.6, 44.2.
HRMS (ESI-TOF, m/z): HRMS (ESI) Calcd for $[M–BF_4]^+$ 153.0692; Found 153.0701.

Preparation of mediator Y69

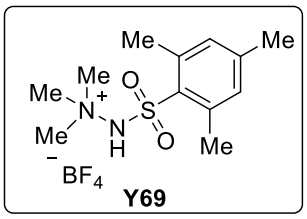

Y69

A round-bottom flask was charged with 2-mesitylenesulfonyl chloride (1.75 g, 8.00 mmol), Et_3N (3.35 mL, 24.00 mmol), dry CH_2Cl_2 (15 mL) and a magnetic a stir bar under argon. The mixture was cooled to 0 °C and *N*,*N*-dimethylhydrazine (1.82 mL, 24.00 mmol) was then added dropwise. Then the reaction was warmed to laboratory temperature and stirred for additional 3 h. The reaction mixture was diluted with CH_2Cl_2 (10 mL) and 1 M aq NaOH (20 mL), the organic phase was separated, and the aqueous phase was extracted with CH_2Cl_2 (2 × 10 mL). Combined organic phases were dried over Na_2SO_4, filtered, and concentrated under reduced pressure to afford a white solid (1.53 g). A round-bottom flask charged with the crude hydrazide and a magnetic stir bar was evacuated and backfilled with argon twice. Dry MeCN (10 mL) was added, followed by the addition of trimethyloxonium tetrafluoroborate (1.18 g, 8.00 mmol) in one portion. The resulting homogeneous solution was stirred at laboratory temperature for 30 min. Then the reaction mixture was concentrated under reduced pressure to afford a solid residue. The crude ylide salt was recrystallized from refluxing EtOH, then washed with Et_2O and EtOH to afford ylide salt **Y69** as a white crystalline solid (2.00 g, 73% yield).

Data for mediator **Y69**:
^{1}H NMR (600 MHz, DMSO-*d*$_6$): δ 7.18 (s, 2H), 3.47 (s, 9H), 2.62 (s, 6H), 2.31 (s, 3H).
^{13}C NMR (151 MHz, DMSO-*d*$_6$): δ 144.4, 139.7, 132.9, 132.5, 57.5, 22.4, 20.7.
HRMS (ESI-TOF, m/z): HRMS (ESI) Calcd for $[M–BF_4]^+$ 257.1318; Found 257.0293.

Preparation of mediator Y70

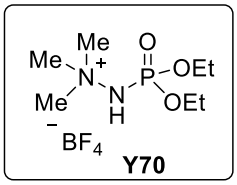

Y70

A round-bottom flask was charged with *N*,*N*-dimethylhydrazine (1.10 mL, 14.51 mmol), CH_2Cl_2 (5 mL) and a magnetic stir bar under argon. The solution was cooled to −78 °C and diphenylphosphinic chloride (1.00 mL, 6.91 mmol) was added dropwise over 5 min. The reaction mixture was stirred for 20 min at −78 °C and it was then gradually warmed to laboratory temperature and stirred for an additional 4 h. The reaction mixture was diluted with CH_2Cl_2 (50 mL) and distd. water (50 mL), the organic phase was separated, and the aqueous phase was extracted with CH_2Cl_2 (3 × 50 mL). Combined organic phases were dried over $MgSO_4$, filtered, and concentrated under reduced pressure to afford a colorless liquid, 2-ethoxyphosphinyl-1,1-dimethylhydrazide (1.30 g, 96% yield). A round-bottom flask charged with the crude hydrazide (1.30 g, 6.63 mmol) and a magnetic stir bar was evacuated and backfilled with argon twice. Dry MeCN (5 mL) was added, followed by the addition of trimethyloxonium tetrafluoroborate (1.08 g, 7.29 mmol) in one portion. The resulting homogeneous solution was stirred at laboratory temperature for 30 min. Then the reaction mixture was concentrated under reduced pressure to afford a solid residue. The crude product was recrystallized from refluxing EtOH, then washed with Et_2O and EtOH to afford ylide salt **Y70** a white solid (523 mg, 26% yield).

Data for mediator **Y70**:

^{1}H NMR (600 MHz, DMSO-d_6): δ 9.23 (d, J = 10.0 Hz, 1H), 4.23 – 4.04 (m, 4H), 3.50 (s, 9H), 1.29 (td, J = 7.0, 0.9 Hz, 6H).
^{13}C NMR (126 MHz, DMSO-d_6): δ 64.3 (d, J = 6.2 Hz), 58.3 (d, J = 2.6 Hz), 15.9 (d, J = 6.6 Hz).
^{31}P NMR (162 MHz, DMSO-d_6): δ 1.2.
HRMS (ESI-TOF, m/z): HRMS (ESI) Calcd for $[M–BF_4]^+$ 211.1206; Found 211.1216.

Preparation of mediator Y71

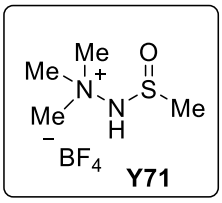

Y71

A round-bottom flask was charged with Me_2S_2 (1.00 mL 22.50 mmol), glacial AcOH (1.27 mL, 45.00 mmol) and a magnetic stir bar and the reaction mixture was cooled to −20 °C under argon. To this partially frozen solution, SO_2Cl_2 (2.78 mL, 69.75 mmol) was carefully (gas evolution) added dropwise over 15 min. After addition, the reaction mixture was stirred for 30 min at −20 °C and then it was slowly warmed to laboratory temperature (gas evolution) and stirred for additional 2 h. Acetyl chloride was subsequently carefully removed under reduced pressure (T < 20 °C, <u>*explosion risk*</u>). NMR aliquot confirmed successful generation of methanesulfinyl chloride and no presence of acetyl chloride. The resulting pale-yellow oil was dissolved in dry CH_2Cl_2 (20 mL) and cooled to −78 °C under argon. To this vigorously stirred mixture, a solution of *N*,*N*-dimethylhydrazine (6.84 mL, 90.00 mmol) in dry CH_2Cl_2 (10 mL) was added dropwise over 20 min at −78 °C. The reaction mixture was stirred overnight while it gradually warmed to laboratory temperature. The reaction mixture was concentrated under reduced pressure and the crude product was filtered over short silica gel column (R_f = 0.2 in EtOAc/hexanes 1:1, permanganate stain) using a gradient EtOAc/hexanes 1:3 → 1:1 → 100% EtOAc and finally EtOAc/MeOH 100:2 to afford a yellowish oil (726 mg) which solidified upon standing and was used directly in the next step. A round-bottom flask charged with the crude product (653 mg, 5.34 mmol) and a magnetic stir bar was evacuated and backfilled with argon twice. Dry MeCN (10 mL) was added, followed by the addition of trimethyloxonium tetrafluoroborate (868 mg, 5.87 mmol) in one portion. The resulting homogeneous solution was stirred at laboratory temperature for 30 min. Then the reaction mixture was concentrated under reduced pressure to afford a solid residue. The crude product was recrystallized from refluxing EtOH, then washed with Et_2O and EtOH to afford ylide salt **Y71** as white needles (778 mg, 65% yield).

Data for mediator **Y71**:
^{1}H NMR (600 MHz, DMSO-d_6): δ 3.58 (s, 9H), 3.45 (s, 3H).
^{13}C NMR (151 MHz, DMSO-d_6): δ 57.5, 44.1.
MS (ESI, m/z): MS (ESI) Calcd for $[M–BF_4]^+$ 137.07; Found 137.10.

Preparation of ylide Y72

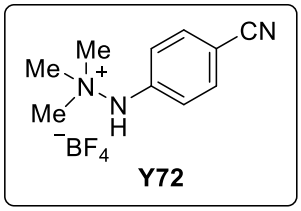

Y72

A round-bottom flask charged with *N*-(4-cyanophenyl)-*N*,*N*'-dimethylhydrazine (594 mg, 3.68 mmol) and a magnetic stir bar was evacuated and backfilled with argon twice. Dry MeCN (5 mL) was added, followed by the addition of trimethyloxonium tetrafluoroborate (599 mg, 4.05 mmol) in one portion. The resulting homogeneous solution was stirred at laboratory temperature for 30 min. Then the reaction mixture was concentrated under reduced pressure to afford a solid residue. The crude product was recrystallized from EtOH, then washed with EtOH and Et2O to afford ylide salt **Y72** as off-white needles (649 mg, 67% yield).

Data for mediator **Y72**:
^{1}H NMR (600 MHz, DMSO-*d*$_6$): δ 8.55 (s, 1H), 7.98 (d, *J* = 8.6 Hz, 2H), 7.61 (d, *J* = 8.6 Hz, 2H), 3.35 (s, 9H).
^{13}C NMR (151 MHz, DMSO-*d*$_6$): δ 141.5, 133.8, 129.5, 118.3, 111.3, 54.9.
HRMS (ESI-TOF, m/z): HRMS (ESI) Calcd for $[M–BF_4]^+$ 176.1182; Found 176.1189.

Preparation of mediator Y73

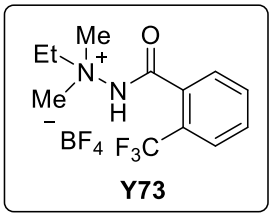

Y73

A round-bottom flask charged with *N,N*-dimethyl-2-(trifluoromethyl)benzohydrazide **Y7-H** (232 mg, 1.00 mmol) and a magnetic stir bar was evacuated and backfilled with argon two times. Dry MeCN (10 mL) was added, followed by the addition of trimethyloxonium tetrafluoroborate (209 mg, 1.1 mmol) in one portion. The resulting homogeneous solution was stirred at laboratory temperature for 30 min. Then the reaction mixture was concentrated under reduced pressure to afford a crude ylide salt. The crude ylide salt was recrystallized from a mixture of MeOH and Et_2O to afford ylide salt as a white solid (202 mg, 58% yield).

Data for mediator **Y73**:
^{1}H NMR (600 MHz, DMSO-*d*$_6$): δ 12.25 (s, 1H), 7.92 (d, *J* = 7.8 Hz, 1H), 7.89 – 7.84 (m, 1H), 7.82 (t, *J* = 7.2 Hz, 2H), 4.04 (q, *J* = 7.2 Hz, 2H), 3.63 (s, 6H), 1.34 (t, *J* = 7.1 Hz, 3H).
^{13}C NMR (151 MHz, DMSO-*d*$_6$): δ 164.7, 132.8, 131.8, 131.5, 129.7, 126.9, 126.3 (q, $^{2}J_{C\text{-}F}$ = 32.2 Hz), 123.5 (q, $^{1}J_{C\text{-}F}$ = 274.5 Hz), 62.4, 54.0, 8.00.
^{19}F NMR (376 MHz, DMSO-*d*$_6$): δ −60.3, −150.9.
HRMS (ESI-TOF, m/z): HRMS (ESI) Calcd for $[M–BF_4]^+$ 261.1209; Found 261.1220.

Preparation of mediator Y74

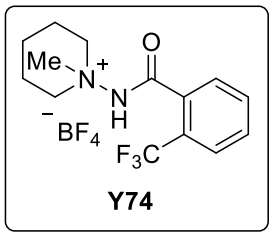

Y74

Following General Procedure A, piperidin-1-ylamine (1.18 mL, 11.00 mmol) was added dropwise to a solution of 2-(trifluoromethyl)benzoyl chloride (1.04 g, 5.00 mmol) in CH_2Cl_2 (50 ml) at 0 °C under argon and the reaction mixture was stirred for 30 min at 0 °C. The reaction mixture was diluted with CH_2Cl_2 (50 mL) and distd. water (50 mL), the organic phase was separated, and the aqueous phase was extracted with CH_2Cl_2 (3 × 50 mL). Combined organic phases were dried over $MgSO_4$, filtered, and concentrated under reduced pressure to afford crude hydrazide. A round-bottom flask charged with the crude hydrazide (544 mg, 2.00 mmol) and a magnetic stir bar was evacuated and backfilled with argon twice. Dry MeCN (10 mL) was added, followed by the addition of trimethyloxonium tetrafluoroborate (325 mg, 2.20 mmol) in one portion. The resulting homogeneous solution was stirred at laboratory temperature for 30 min. Then the reaction mixture was concentrated under reduced pressure to afford a solid residue. The crude ylide salt was recrystallized from a mixture of MeOH and Et_2O, then washed with Et_2O to afford ylide salt **Y74** as a white solid (612 mg, 82% yield).

Data for mediator **Y74**:
^{1}H NMR (600 MHz, DMSO-d_6): δ 12.06 (s, 1H), 7.93 (d, J = 7.7 Hz, 1H), 7.90 – 7.80 (m, 3H), 4.30 (d, J = 12.6 Hz, 2H), 3.83 – 3.72 (m, 2H), 3.68 (s, 3H), 1.93 (m, 4H), 1.79 – 1.70 (m, 1H), 1.57 – 1.45 (m, 1H).
^{13}C NMR (151 MHz, DMSO-d_6): δ 165.1, 132.9, 131.7, 129.6, 126.8 (q, $^3J_{C\text{-}F}$ = 4.2 Hz), 126.2 (q, $^2J_{C\text{-}F}$ = 31.2 Hz), 123.5 (q, $^1J_{C\text{-}F}$ = 274.5 Hz), 64.4, 54.2, 20.1, 20.0.
^{19}F NMR (376 MHz, DMSO-d_6): δ -60.3, -150.9.
HRMS (ESI-TOF, m/z): HRMS (ESI) Calcd for $C_{14}H_{18}F_3N_2O$ $[M]^+$ 288.1449; Found 288.1450.

Preparation of mediator Y75

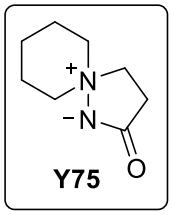

Y75

1-Aminopiperidine (1.08 mL, 10.00 mmol) was added dropwise over 1 min to a solution of ethyl acrylate (1.05 mL, 10.00 mmol) in MeOH (5 mL) at 0 °C. The reaction mixture was stirred at 0 °C for 1 h and at laboratory temperature 3 h. Then the reaction mixture was concentrated under reduced pressure to afford an off-white solid. The crude ylide was recrystalized from refluxing acetone (5 mL), washed with hexanes to afford ylide **Y75** as a white solid (196 mg, 13% yield).

Data for mediator **Y75**:
^{1}H NMR (600 MHz, DMSO-d_6): δ 4.93 (s, 1H), 3.65 (t, J = 8.2 Hz, 2H), 3.37 (m, 2H), 3.23 (m, 2H), 2.76 (t, J = 8.2 Hz, 2H), 2.23 (dp, J = 13.2, 4.6 Hz, 2H), 1.74 (m, 2H), 1.71 – 1.65 (m, 1H), 1.61 (m, 1H).
^{13}C NMR (151 MHz, DMSO-d_6): δ 178.0, 65.6, 62.0, 31.6, 21.9, 21.6.
HRMS (ESI-TOF, m/z): HRMS (ESI) Calcd for $[M+H]^+$ 155.1179; Found 155.1188.

Preparation of mediator Y76

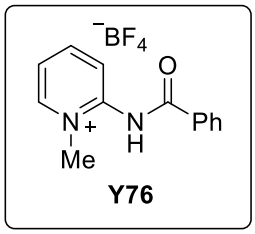

Y76

A round-bottom flask was charged with 2-aminopyridine (819 mg, 8.70 mmol), dry Et_3N (1.82 mL, 13.05 mmol), CH_2Cl_2 (8 mL), and a magnetic stir bar. The solution was cooled to −20 °C under argon and benzoyl chloride (1.52 mL, 13.05 mmol) was added dropwise over 20 min. The reaction mixture was stirred 1 h at −20 °C and 3 h at laboratory temperature. After that, the reaction was quenched by addition of sat. aq. NH_4Cl (10 mL) and extracted with CH_2Cl_2 (3 × 80 mL). Combined organic extracts were washed with brine, dried over $MgSO_4$, filtered, and concentrated under reduced pressure. ^1H NMR analysis of the crude product revealed presence of diacylated product, which was hydrolyzed by mixing the crude reaction mixture with NaOH (2 g) in dioxane (20 mL) and MeOH (40 mL) at laboratory temperature overnight. Subsequent extraction with CH_2Cl_2 (3 × 100 mL), drying over $MgSO_4$, concentration under reduced pressure and a short column chromatography (EtOAc/hexanes 1:2 → 2:1) afforded *N*-(pyrid-2-yl)benzamide (1.06 g, 61% yield) which was used directly in the next step. A round-bottom flask charged with *N*-(pyrid-2-yl)benzamide (1.06 g, 5.35 mmol) and a magnetic stir bar was evacuated and backfilled with argon twice. Dry MeCN (8 mL) was added, followed by the addition of trimethyloxonium tetrafluoroborate (871 mg, 5.89 mmol) in one portion. The resulting homogeneous solution was stirred at laboratory temperature for 30 min. Then the reaction mixture was concentrated under reduced pressure to afford a solid residue. The crude product was recrystallized from refluxing EtOH, then washed with Et_2O and EtOH to afford ylide salt **Y76** as a white crystalline solid (1.01 g, 63% yield).

Data for mediator **Y76**:

^{1}H NMR (500 MHz, DMSO-*d*$_6$): δ 11.35 (s, 1H), 8.93 (d, *J* = 6.0 Hz, 1H), 8.57 (dd, *J* = 7.7 Hz, 1H), 8.28 (dd, *J* = 8.5, 1.4 Hz, 1H), 8.07 – 8.01 (m, 2H), 7.89 (t, *J* = 7.1 Hz, 1H), 7.72 (m, 1H), 7.63 (t, *J* = 7.8 Hz, 2H), 4.28 (s, 3H).

^{13}C NMR (126 MHz, DMSO-*d*$_6$): δ 166.6, 148.0, 146.1, 145.7, 133.3, 132.5, 128.7, 128.6, 124.2, 123.4, 44.4.

HRMS (ESI-TOF, m/z): HRMS (ESI) Calcd for $[M–BF_4]^+$ 213.1022; Found 213.1033.

Preparation of mediator Y77

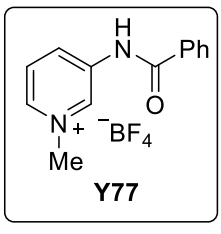

Y77

A round-bottom flask was charged with 3-aminopyridine (836 mg, 8.88 mmol), dry Et_3N (1.86 mL, 13.32 mmol), CH_2Cl_2 (8 mL) and a magnetic stir bar. The solution was cooled to −20 °C under argon and benzoyl chloride (1.55 mL, 13.32 mmol) was added dropwise over 20 min. The reaction mixture was stirred for 1 h at −20 °C and 3 h at laboratory temperature. After that, the reaction was quenched by addition of sat. aq

NH_4Cl (10 mL) and extracted with CH_2Cl_2 (3 × 80 mL). Combined organic extracts were washed with brine, dried over $MgSO_4$, filtered, and concentrated under reduced pressure. ^1H NMR analysis of the crude product revealed presence of diacylated product, which was hydrolyzed by mixing the crude reaction mixture with NaOH (2 g) in dioxane (20 mL) and MeOH (40 mL) at laboratory temperature overnight. Subsequent extraction with CH_2Cl_2 (3 × 100 mL), drying over $MgSO_4$, concentration under reduced pressure and a short column chromatography (EtOAc/hexanes 1:2 → 2:1) afforded *N*-(pyrid-3-yl)benzamide (1.60 g, 91% yield) which was used directly in the next step. A round-bottom flask charged with *N*-(pyrid-3-yl)benzamide (1.03 g, 5.20 mmol) and a magnetic stir bar was evacuated and backfilled with argon twice. Dry MeCN (8 mL) was added, followed by the addition of trimethyloxonium tetrafluoroborate (846 mg, 5.72 mmol) in one portion. The resulting homogeneous solution was stirred at laboratory temperature for 30 min. Then the reaction mixture was concentrated under reduced pressure to afford a solid residue, crude ylide salt. The crude product was recrystallized from refluxing EtOH, then washed with Et_2O and EtOH to afford ylide salt **Y77** as a beige solid (806 mg, 52% yield).

Data for mediator **Y77**:

^{1}H NMR (500 MHz, DMSO-*d*$_6$): δ 11.18 (s, 1H), 9.52 (t, *J* = 1.7 Hz, 1H), 8.73 (d, *J* = 5.9 Hz, 1H), 8.64 (d, *J* = 8.8 Hz, 1H), 8.11 (dd, *J* = 8.7, 5.9 Hz, 1H), 8.05 – 7.99 (m, 2H), 7.69 (m, 1H), 7.62 (dd, *J* = 8.4, 7.0 Hz, 2H), 4.41 (s, 3H).

^{13}C NMR (126 MHz, DMSO-*d*$_6$): δ 166.4, 140.4, 139.0, 136.4, 134.7, 133.0, 132.8, 128.8, 128.0, 127.8, 48.6.

HRMS (ESI-TOF, m/z): HRMS (ESI) Calcd for $[M–BF_4]^+$ 213.1022; Found 213.1030.

Preparation of mediator Y78

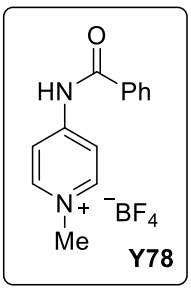

A round-bottom flask was charged with 4-aminopyridine (900 mg, 9.56 mmol), dry Et_3N (2.00 mL, 14.34 mmol), CH_2Cl_2 (10 mL) and a magnetic stir bar. The solution was cooled to −20 °C under argon and benzoyl chloride (1.11 mL, 9.56 mmol) was added dropwise over 20 min. The reaction mixture was stirred for 1 h at –20 °C and 3 h at laboratory temperature. After that, the reaction was quenched by addition of sat. aq NH_4Cl (10 mL) and extracted with CH_2Cl_2 (3 × 80 mL). Combined organic extracts were washed with brine, dried over $MgSO_4$, filtered and concentrated under reduced pressure to afford *N*-(pyrid-4-yl)benzamide (1.34 g, 71% yield) which was used directly in the next step. A round-bottom flask charged with *N*-(pyrid-4-yl)benzamide (1.34 g, 6.76 mmol) and a magnetic stir bar was evacuated and backfilled with argon twice. Dry MeCN (5 mL) was added, followed by the addition of trimethyloxonium tetrafluoroborate (1.10 g, 7.44 mmol) in one portion. The resulting homogeneous solution was stirred at laboratory temperature for 30 min. Then the reaction mixture was concentrated under reduced pressure to afford a solid residue. The crude product was recrystallized from refluxing EtOH, then washed with Et_2O and EtOH to afford ylide salt **Y78** as a white crystalline solid (1.40 g, 69% yield).

Data for mediator **Y78**:

^{1}H NMR (600 MHz, DMSO-d_6): δ 11.52 (s, 1H), 8.75 (d, J = 7.4 Hz, 2H), 8.28 (d, J = 7.3 Hz, 2H), 8.02 (dd, J = 8.3, 1.3 Hz, 2H), 7.74 – 7.68 (m, 1H), 7.62 (t, J = 7.7 Hz, 2H), 4.20 (s, 3H).
^{13}C NMR (126 MHz, DMSO-d_6): δ 167.3, 152.0, 145.9, 133.2, 133.0, 128.8, 128.3, 115.5, 46.4.
HRMS (ESI-TOF, m/z): HRMS (ESI) Calcd for $[M–BF_4]^+$ 213.1022; Found 213.1033.

Preparation of mediator Y79

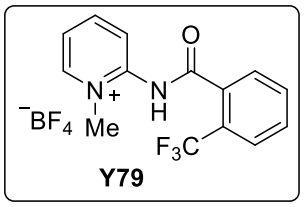

Y79

A round-bottom flask was charged with 2-aminopyridine (755 mg, 8.02 mmol), dry Et_3N (1.68 mL, 12.03 mmol), CH_2Cl_2 (10 mL) and a magnetic stir bar. The solution was cooled to −20 °C under argon and 2-(trifluoromethyl)benzoyl chloride (1.77 mL, 12.03 mmol) was added dropwise over 20 min. The reaction mixture was stirred for 1 h at −20 °C and 3 h at laboratory temperature. After that, the reaction was quenched by addition of sat. aq. NH_4Cl (10 mL) and extracted with CH_2Cl_2 (3 × 80 mL). Combined organic extracts were washed with brine, dried over $MgSO_4$, filtered, and concentrated under reduced pressure. ^{1}H NMR analysis of the crude product revealed presence of diacylated product, which was hydrolyzed by mixing the crude reaction mixture with NaOH (2 g) in dioxane (20 mL) and MeOH (40 mL) at laboratory temperature overnight. Subsequent extraction with CH_2Cl_2 (3 × 100 mL), drying over $MgSO_4$, concentration under reduced pressure and a short column chromatography (EtOAc/hexanes 1:2 → 2:1) afforded *N*-(pyrid-2-yl)-2-(trifluoromethyl)-benzamide (1.68 g, 79% yield) which was used directly in the next step. A round-bottom flask charged with *N*-(pyrid-2-yl)-2-(trifluoromethyl)benzamide (1.10 g, 4.13 mmol) and a magnetic stir bar was evacuated and backfilled with argon twice. Dry MeCN (5 mL) was added, followed by the addition of trimethyloxonium tetrafluoroborate (672 mg, 4.54 mmol) in one portion. The resulting homogeneous solution was stirred at laboratory temperature for 30 min. Then the reaction mixture was concentrated under reduced pressure to afford a solid residue. The crude product was recrystallized from refluxing EtOH, then washed with Et_2O and EtOH to afford ylide salt **Y79** as an off-white crystalline solid (218 mg, 14% yield).

Data for mediator **Y79**:
^{1}H NMR (600 MHz, DMSO-d_6): δ 11.85 (s, 1H), 8.90 (dd, J = 6.4, 1.8 Hz, 1H), 8.58 (td, J = 8.0, 1.7 Hz, 1H), 8.34 (dd, J = 8.6, 1.4 Hz, 1H), 7.96 (ddd, J = 13.3, 7.7, 1.2 Hz, 2H), 7.92 – 7.85 (m, 2H), 7.83 (t, J = 7.7 Hz, 1H), 4.24 (s, 3H).
^{13}C NMR (151 MHz, DMSO-d_6): δ 166.7, 147.0, 146.2, 145.7, 133.8, 132.8, 131.3, 129.0, 126.7 (q, J = 4.7 Hz), 126.1 (q, $^2J_{C\text{-}F}$ = 32.4 Hz), 123.7 (q, $^1J_{C\text{-}F}$ = 273.8 Hz), 123.2, 123.1, 44.4.
^{19}F NMR (376 MHz, DMSO-d_6): δ −60.3, −151.0.
HRMS (ESI-TOF, m/z): HRMS (ESI) Calcd for $[M–BF_4]^+$ 281.0896; Found 281.0907.

Preparation of mediator Y80

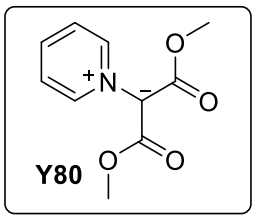

Mediator **Y80** was prepared following literature protocol. Spectral data matched reported values therein.[4]

Data for mediator **Y80**:
^{1}H NMR (600 MHz, $CDCl_3$): δ 8.60 (s, 2H), 8.14 (s, 1H), 7.73 (s, 2H), 3.73 (s, 6H).

PREPARATION OF STARTING MATERIALS

Preparation of compound 29

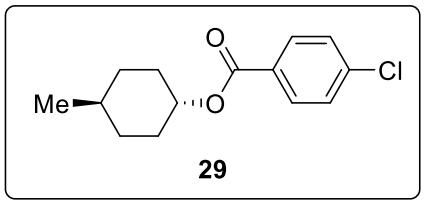

Prepared by following literature protocol.[43] Spectral data matched reported values therein.

Preparation of compound 30

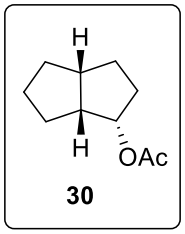

To a solution of octahydropentalen-1-ol (630 mg, 5 mmol) in Ac_2O was added one portion of DMAP. After the completion of the reaction, the mixture was concentrated in-vacuo followed by the purification by silica gel column chromatography to afforded (860 mg, >99%) of desired ester.

Data for compound **30**:
^{1}H NMR (600 MHz, $CDCl_3$): δ 5.06 – 5.00 (m, 1H), 2.61 (p, J = 8.1 Hz, 1H), 2.43 (qt, J = 8.6, 5.2 Hz, 1H), 2.02 (m, 3H), 1.82 – 1.62 (m, 4H), 1.59 (m, 1H), 1.52 – 1.39 (m, 3H), 1.35 – 1.27 (m, 1H), 1.24 (dt, J = 13.0, 6.4 Hz, 1H).
^{13}C NMR (151 MHz, $CDCl_3$): δ 170.9, 77.8, 45.6, 42.5, 34.6, 31.3, 29.3, 27.6, 27.4, 21.2.
HRMS (m/z): HRMS (ESI and APCI) calcd for $[M+H]^+$; Not detected.
R_f = 0.8 (20% EtOAc in hexanes); Stain: Hanessian's Stain.

Preparation of compound 31

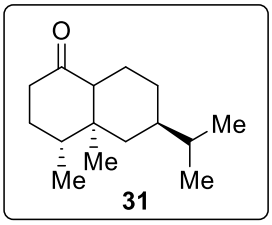

Prepared by following literature protocol.[5] Spectral data matched reported values therein.

Preparation of compound 34

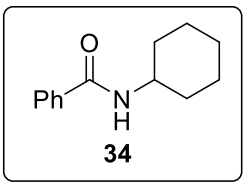

34

Prepared by following literature protocol.[6] Spectral data matched reported values therein.

Preparation of compound 35

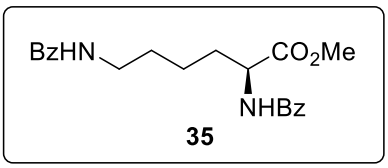

35

To a solution of Boc-Lys(Bz)-OMe (364 mg, 1.0 mmol) in CH_2Cl_2 (2 ml) was added TFA (5 ml). After the stirring for 3 hours at laboratory temperature, the rection mixture was concentrated in-vacuo and dissolved in CH_2Cl_2. Then, benzoyl chloride (168 mg, 1.2 mmol) and DIPEA (0.5 ml, 3 mmol) were added to the solution. After the completion of the reaction, the reaction mixture was extracted by CH_2Cl_2 and washed with 1N HCl once. Purification by silica gel column chromatography afforded Bz-Lys(Bz)-OMe (221.0 mg, 60% yield). All spectra matched the reported data.[7]

Data for compound **35**:
^{1}H NMR (600 MHz, $CDCl_3$): δ 7.86 – 7.77 (m, 2H), 7.77 – 7.68 (m, 2H), 7.50 – 7.42 (m, 2H), 7.40 – 7.36 (m, 2H), 7.36 – 7.32 (m, 2H), 6.59 (t, *J* = 5.7 Hz, 1H), 4.78 (ddd, *J* = 8.7, 7.5, 4.5 Hz, 1H), 3.75 (s, 3H), 3.49 (ddt, *J* = 14.1, 8.0, 6.2 Hz, 1H), 3.41 (dq, *J* = 13.5, 6.0 Hz, 1H), 1.98 (dddd, *J* = 14.0, 9.6, 6.8, 4.5 Hz, 1H), 1.88 (dtd, *J* = 13.9, 9.1, 5.1 Hz, 1H), 1.73 (dtt, *J* = 14.0, 8.2, 5.9 Hz, 1H), 1.64 (ddt, *J* = 13.6, 8.4, 6.6 Hz, 1H), 1.57 – 1.35 (m, 2H).
^{13}C NMR (151 MHz, $CDCl_3$): δ 173.2, 168.1, 167.6, 134.6, 133.8, 131.8, 131.4, 128.6, 128.5, 127.3, 127.1, 52.6, 52.4, 39.3, 32.1, 28.9, 22.6.
HRMS (ESI-TOF, m/z): HRMS (ESI) Calcd for $[M+H]^+$ 369.1809; Found 369.1812.
$[\alpha]_D^{20}$ = −8.0 (*c*.0.88 in $CHCl_3$).

Preparation of compound 36

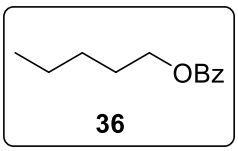

36

To a solution of 2-methylpentan-1-ol (1.00 mL, 9.23 mmol, 1.0 equiv.) in CH_2Cl_2 (15.4 mL), was added Et_3N (2.70 mL, 19.4 mmol, 2.1 equiv.) and benzoyl chloride (1.07 mL, 9.23 mmol, 1.0 equiv.). The resulting reaction mixture was stirred for 6 h, then diluted with CH_2Cl_2, and washed with 1M HCl. Subsequently, the organic layer was dried over $MgSO_4$, filtered, and concentrated under reduced pressure. The crude reaction mixture was purified by flash column chromatography (EtOAc/hexanes-5:95) to afford **36** (0.83 g, 47% yield) as a colorless oil. All spectra matched reported data.[8]

Preparation of compound 37

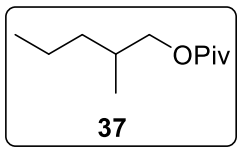

37

To a solution of 2-methylpentan-1-ol (0.500 mL, 4.04 mmol, 1.0 equiv.) in CH_2Cl_2 (6.8 mL), was added Et_3N (1.18 mL, 8.08 mmol, 2.1 equiv.) and pivaloyl chloride (0.495 mL, 4.04 mmol, 1.0 equiv.). The resulting reaction mixture was stirred for 6 h, then diluted with CH_2Cl_2, and washed with 1 M aq. HCl. Subsequently, the organic layer was dried over $MgSO_4$, filtered, and concentrated under reduced pressure. The crude reaction mixture was purified by flash column chromatography (EtOAc/hexanes-5:95) to afford **37** (0.47 g, 62% yield) as a colorless oil.

Data for compound **37**:
^{1}H NMR (500 MHz, $CDCl_3$): δ 3.93 (ddd, *J* = 10.7, 5.7, 0.8 Hz, 1H), 3.83 (ddd, *J* = 10.6, 6.7, 0.8 Hz, 1H), 1.80 (dddd, *J* = 12.3, 11.0, 6.3, 3.2 Hz, 1H), 1.44 – 1.28 (m, 3H), 1.20 (d, *J* = 0.9 Hz, 9H), 1.17 – 1.10 (m, 1H), 0.94 – 0.85 (m, 6H).
^{13}C NMR (126 MHz, $CDCl_3$): δ 69.4, 39.0, 35.8, 32.5, 27.4, 27.4, 20.1, 17.0, 14.4.
HRMS (m/z): HRMS (ESI and APCI) Calcd for $[M+H]^+$ 187.1693; Not detected..
R_f = 0.5 (2% EtOAc in hexanes); Stain: $KMnO_4$.

Preparation of compound 38

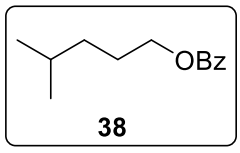

38

To a solution of 2-methylpentan-1-ol (1.500 mL, 11.95 mmol, 1.0 equiv.) in CH_2Cl_2 (19.9 mL), was added Et_3N (3.50 mL, 25.1 mmol, 2.1 equiv.) and benzoyl chloride (1.39 mL, 11.95 mmol, 1.0 equiv.). The resulting reaction mixture was stirred for 6 h, then diluted with CH_2Cl_2, and washed with 1 M aq. HCl. Subsequently, the organic layer was dried over $MgSO_4$, filtered, and concentrated under reduced pressure. The crude reaction mixture was purified by flash column chromatography (EtOAc/hexanes-5:95) to afford **38** (1.98 g, 78% yield) as a colorless oil. All spectra matched reported data.[9]

Preparation of compound 40

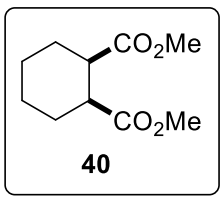

40

Prepared by following literature protocol.[43] Spectral data matched reported values therein.

Preparation of compound 41

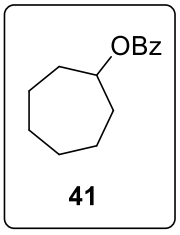

41

To a solution of cycloheptanol (1.14 g, 10 mmol) in CH_2Cl_2 was added benzoyl chloride (1.4 mL, 12 mmol), Et_3N (4 mL, 30 mmol) and one portion of DMAP. After the stirring for 3 h at laboratory temperature, the rection mixture was extracted by CH_2Cl_2 and 1N HCl. Purification by silica gel column chromatography afforded the desired ester **41** (1.1 g, 50% yield). All spectra matched the reported data.[10]

Preparation of compound 42

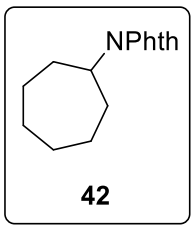

42

Prepared by following literature protocol.[43] Spectral data matched reported values therein.

Preparation of compound 43

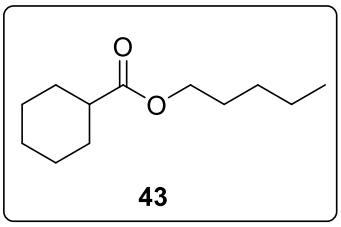

43

To a solution of 2-methylpentan-1-ol (1.00 mL, 9.23 mmol, 1.0 equiv.) in CH_2Cl_2 (15.4 mL), was added Et_3N (2.70 mL, 19.4 mmol, 2.1 equiv.) and cyclohexanecarbonyl chloride (1.23 mL, 9.23 mmol, 1.0 equiv.). The resulting reaction mixture was stirred for 6 h, then diluted with CH_2Cl_2, and washed with 1 M aq. HCl. Subsequently, the organic layer was dried over $MgSO_4$, filtered, and concentrated under reduced pressure. The crude reaction mixture was purified by flash column chromatography (EtOAc/hexanes-2:98) to afford **43** (1.50 g, 82% yield) as a colorless oil. Spectral data matched reported literature values.[11]

Preparation of compound 44

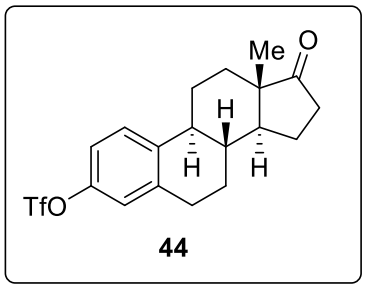

44

Prepared by following literature protocol.[12] Spectral data matched reported values therein.

Preparation of compound 52

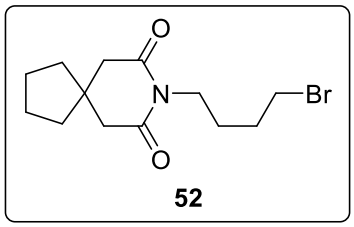

52

To a solution of 3,3-tetramethyleneglutaric anhydride (1.68 g, 10 mmol) in CH_2Cl_2 (20 mL) were added 4-bromobutylamine hydrobromide (2.3 g, 10 mmol) and iPr_2NEt (15 mmol, 2.1 mL) in one portion at 0 °C. The reaction mixture was stirred for 30 min at laboratory temperature, and then poured into 1 M aq. HCl. The organic layer was collected, and aqueous layer was further washed twice with CH_2Cl_2. The combined organic layer was dried over Na_2SO_4, then solvent was removed with a rotary evaporator. To this crude mixture were added Ac_2O (15 mL) and AcOH (10 mL), and the reaction mixture was stirred at 110 °C for 6 h. After cooling, the brown solution was poured into water, and organic compounds were extracted with hexane/EtOAc (5:1) three times. The crude mixture was purified by flash column chromatography (hexane/EtOAc-5:1) to afford the desired imide in 68% yield (2.04 g). Spectral data matched reported literature values.[53]

Preparation of compound 61

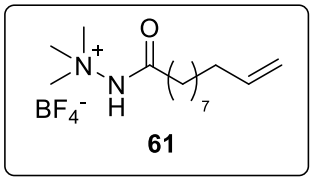

61

Prepared by following literature protocol.[13] Spectral data matched reported values therein.

CHARACTERIZATION OF OXIDATION PRODUCTS

Ylide oxidation of compound 9

Following Condition A, **9** (75.1 mg, 0.3 mmol), HFIP (600 μL, 5.7 mmol, 19 equiv), Me_4NBF_4 (48.3 mg, 0.3 mmol), ylide **Y7** (100.2 mg, 0.3 mmol), and $NaHCO_3$ (63 mg, 0.75 mmol, 2.5 equiv) were added to O_2 saturated MeCN (2.00 mL). The reaction mixture was electrolyzed for 6 F/mol. Purification by pTLC (CH_2Cl_2/Et_2O-5:2) afforded **10a** and **10c** (26.2 mg, 33% yield) as inseparable mixture of isomers (**10a/10c** = 25:1) as a white solid and **10b** (22 mg, 28% yield) as a colorless oil. Spectral data matched reported values.[14] **10c** = 3-oxo-sclareolide.

Data for **10a**:

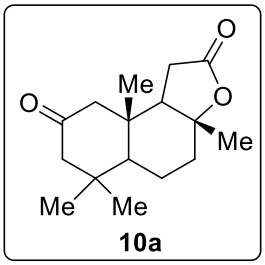

10a

^{1}H NMR (400 MHz, $CDCl_3$): δ 2.49 – 2.41 (m, 1H), 2.32 – 2.13 (m, 7H), 2.05 – 1.99 (m, 1H), 1.79 (td, *J* = 12.3, 4.0 Hz, 1H), 1.69 (dd, *J* = 12.6, 2.9 Hz, 1H), 1.54 – 1.43 (m, 1H), 1.35 (s, 3H), 1.09 (s, 3H), 0.92 (s, 6H).

^{13}C NMR (100 MHz, $CDCl_3$): δ 209.4, 175.8, 85.8, 58.3, 56.7, 55.7, 55.0, 40.4, 38.8, 38.2, 33.4, 28.7, 22.7, 21.2, 16.3.

R_f = 0.6 (CH_2Cl_2/Et_2O-5:1); Stain: Hanessian's Stain

$[\alpha]_D^{20} = -12.3$ (*c*.2.0 in $CHCl_3$).

Data for **10b**:

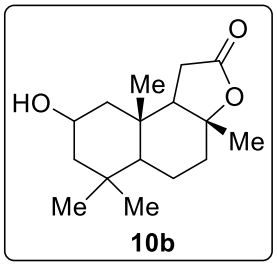

10b

^{1}H NMR (400 MHz, $CDCl_3$): δ 4.02 – 3.97 (m, 1H), 2.45 (dd, *J* = 16.2, 14.7 Hz, 1H), 2.27 (dd, *J* = 16.2, 6.6 Hz, 1H), 2.10 (dt, *J* = 11.9, 3.4 Hz, 1H), 2.01 (dd, *J* = 14.8, 6.6 Hz, 1H), 1.92 – 1.89 (m, 1H), 1.86 – 1.83 (m, 1H), 1.81 – 1.83 (m, 1H), 1.70 (td, *J* = 12.5, 4.5 Hz, 1H), 1.61 – 1.53 (m, 1H), 1.40 – 1.43 (m, 1H), 1.36 – 1.39 (m, 1H), 1.33 (s, 3H), 1.10 – 1.7 (m, 1H), 0.97 (s, 3H), 0.96 (s, 3H), 0.89 (s, 3H).
^{13}C NMR (100 MHz, $CDCl_3$): δ 209.4, 175.7, 85.8, 58.3, 56.7, 55.7, 55.0, 40.4, 38.8, 38.2, 33.4, 28.7, 22.7, 21.2, 20.8, 16.3.
$\mathbf{R}_f$ = 0.2 (CH_2Cl_2/Et_2O-5:1); Stain: Hanessian's Stain.
$[\alpha]_D^{20}$ = 10.4 (*c*.0.52 in $CHCl_3$).

Ylide oxidation of compound 27

Following Condition A, **27** (99.7 mg, 0.3 mmol), HFIP (0.2 mL), Me_4NBF_4 (16.0 mg, 0.1 mmol), ylide **Y7** (99.7 mg, 0.3 mmol) and $NaHCO_3$ (63.2 mg, 0.75 mmol) were added to O_2 saturated MeCN (2.00 mL). The reaction mixture was electrolyzed for 9 F/mol. Purification by flash choromatography on silica eluting with 10–30% EtOAc/hexane afforded **27-P1** (22.5 mg, 20% yield) as a colorless oil and **27-P2** (9.0 mg, 8% yield) as a colorless amorphous solid.

Data for **27-P1**:

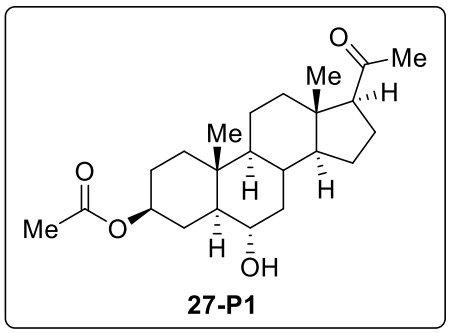

27-P1

^{1}H NMR (600 MHz, $CDCl_3$): δ 4.71 (ddd, *J* = 16.3, 11.5, 4.9 Hz, 1H), 3.44 (td, *J* = 10.8, 4.6 Hz,1H), 2.56 (t, *J* = 8.9 Hz, 1H), 2.27 – 2.16 (m, 2H), 2.14 (s, 3H), 2.05 (s, 3H), 2.05 – 1.99 (m, 2H), 1.91 – 0.89 (m, 15H), 0.96 (s, 3H), 0.77 (ddd, *J* = 12.3, 10.7, 4.1 Hz, 1H), 0.63 (s, 3H).
^{13}C NMR (151 MHz, $CDCl_3$): δ 209.0, 170.2, 73.0, 68.8, 63.2, 55.8, 53.1, 51.1, 43.7, 41.1, 38.3, 36.6, 35.9, 33.8, 31.1, 27.8, 26.7, 23.9, 22.3, 21.0, 20.6, 13.1, 12.9.
HRMS (ESI-TOF, m/z): HRMS (ESI) Calcd for $[M-OH]^+$ 359.2581; Found 359.2589. $\mathbf{R}_f$ = 0.2 (50% EtOAc in hexanes); Stain: Hanessian's Stain.

Data for **27-P2**:

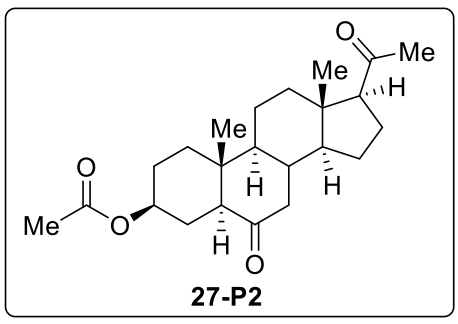

27-P2

^{1}H NMR (600 MHz, $CDCl_3$): δ 4.67 (tt, *J* = 11.6, 4.8 Hz, 1H), 2.55 (t, *J* = 9.1 Hz, 1H), 2.34 (dd, *J* = 13.3, 4.6 Hz, 1H), 2.30 – 2.24 (m, 1H), 2.22 – 2.15 (m, 1H), 2.13 (s, 3H), 2.08 (dt, *J* = 12.5, 3.3 Hz, 1H), 2.04 – 1.14 (m, 19H), 0.77 (s, 3H), 0.62 (s, 3H).
^{13}C NMR (151 MHz, $CDCl_3$): δ 209.8, 209.2, 170.8, 72.9, 63.5, 57.0, 56.6, 53.8, 46.6, 44.5, 41.0, 38.6, 37.9, 36.6, 31.6, 27.0, 26.2, 24.3, 22.9, 21.6, 21.5, 13.5, 13.2.

HRMS (ESI-TOF, m/z): HRMS (ESI) Calcd for $[M+H]^+$ 375.2530; Found 375.2532. $\mathbf{R_f}$ = 0.5 (50% EtOAc in hexanes); Stain: Hanessian's Stain.
$\mathbf{[\alpha]_D^{20}}$ = 13.3 (*c*.0.63 in $CHCl_3$).

Ylide oxidation of compound 28

Following Condition B, **28** (59.5 mg, 0.3 mmol), H_2O (0.1 ml), Me_4NBF_4 (16.0 mg, 0.1 mmol), ylide **Y7** (61.4 mg, 0.3 mmol) and $NaHCO_3$ (63.2 mg, 0.75 mmol) were added to O_2 saturated MeCN (2.0 ml). The reaction mixture was electrolyzed for 20 F/mol. Purification by flash choromatography on silica eluting with 10% EtOAc /hexane afforded **28-P1** (15.4 mg) and **28** (37.6 mg). To the recovered **28**, H_2O (0.1 ml), Me_4NBF_4 (16.0 mg, 0.1 mmol), ylide **Y7** (38.6 mg, 0.19 mmol), $NaHCO_3$ (40.3 mg, 0.48 mmol) and O_2 saturated MeCN (2.0 mL) were added followed by the electrolysis again. The reaction mixture was electrolyzed for 20 F/mol. After the completion of the reaction, the crude mixture was purified by flash chromatography on silica gel to afford **28-P1** (7.7 mg) and **28** (18.0 mg). Two runs of products were combined for a total of 36% yield.

Data for **28-P1**:

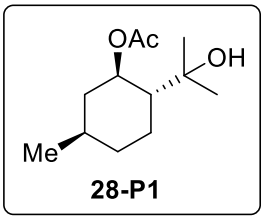

28-P1

^{1}H NMR (600 MHz, $CDCl_3$): δ 4.81 (td, *J* = 10.9, 4.2 Hz, 1H), 2.06 (s, 3H), 2.05 – 2.02 (m, 1H), 1.89 (dq, *J* = 13.2, 3.4 Hz, 1H), 1.75 – 1.67 (m, 1H), 1.67 – 1.60 (m, 1H), 1.61 – 1.43 (m, 1H), 1.15 (s, 3H), 1.13 (s, 3H), 1.08 – 0.92 (m, 3H), 0.90 (d, *J* = 6.5 Hz, 3H).
^{13}C NMR (151 MHz, $CDCl_3$): δ 169.9, 76.4, 73.2, 51.7, 34.4, 31.4, 28.8, 27.3, 25.8, 21.9, 21.9.
HRMS (ESI-TOF, m/z): HRMS (ESI) Calcd for $[M+Na]^+$ 237.1461; Found 237.1468.
$\mathbf{R_f}$ = 0.3 (20% EtOAc in hexanes); Stain: Hanessian's Stain.

Ylide oxidation of compound 29

Following Condition B, **29** (75.5 mg, 0.3 mmol), H_2O (0.2 mL), Me_4NBF_4 (16.0 mg, 0.1 mmol), ylide **Y7** (99.7 mg, 0.3 mmol) and $NaHCO_3$ (63.2 mg, 0.75 mmol) were added to O_2 saturated MeCN (2.0 mL). The reaction mixture was electrolyzed for 20 F/mol. Purification by flash chromatography on silica eluting with 30% CH_2Cl_2 /hexane afforded **29-2** (12.8 mg), **29-1** (6.3 mg) and **29** (25.2 mg) as a colorless amorphous solid. To the recovered **29**, H_2O (0.1 mL), Me_4NBF_4 (16.0 mg, 0.1 mmol), ylide **Y7** (33.6 mg, 0.1 mmol), $NaHCO_3$ (21.0 mg, 0.25 mmol) and O_2 saturated MeCN (2.00 ml) were added followed by the electrolysis again. The reaction mixture was electrolyzed for 20 F/mol. After the completion of the reaction, the crude mixture was purified by flash chromatography on silica gel to afford **29-2** (3.3 mg), **29-1** (2.4 mg) and **29** (7.2 mg). Two runs of products were combined for a total of 31% yield.

Data for **29-P1**:

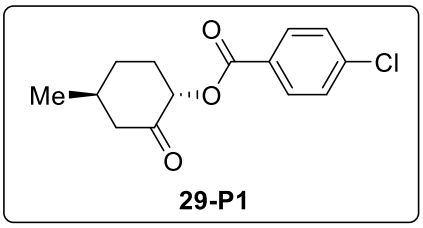

29-P1

^{1}H NMR (600 MHz, $CDCl_3$): δ 8.03 (d, *J* = 8.5 Hz, 2H), 7.43 (d, *J* = 8.5 Hz, 2H), 5.39 (dd, *J* = 12.6, 6.6 Hz, 1H), 2.54 (ddd, *J* = 13.4, 3.9, 2.6 Hz, 1H), 2.40 (ddt, *J* = 12.9, 6.6, 3.4 Hz, 1H), 2.25 – 2.19 (m, 1H), 2.09 – 1.78 (m, 3H), 1.69 – 1.58 (m, 1H), 1.10 (d, *J* = 6.5 Hz, 3H).
^{13}C NMR (151 MHz, $CDCl_3$): δ 203.1, 164.4, 139.2, 130.8, 128.2, 127.7, 76.4, 48.2, 34.6, 31.8, 31.2, 21.6.
HRMS (ESI-TOF, m/z): HRMS (ESI) Calcd for $[M+H]^+$ 267.0782; Found 267.0789.
R_f = 0.4 (20% EtOAc in hexanes); Stain: Hanessian's Stain.

Data for **29-P2**:

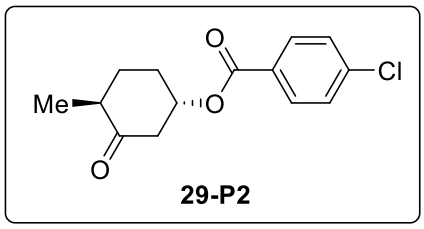

29-P2

^{1}H NMR (600 MHz, $CDCl_3$): δ 7.98 (d, *J* = 8.5 Hz, 2H), 7.44 (d, *J* = 8.5 Hz, 2H), 5.23 (tt, *J* = 10.1, 4.7 Hz, 1H), 2.94 (ddd, *J* = 13.6, 5.0, 1.8 Hz, 1H), 2.63 – 2.55 (m, 1H), 2.43 (dp, *J* = 12.9, 6.5 Hz, 1H), 2.40 – 2.33 (m, 1H), 2.16 (dq, *J* = 14.2, 4.7 Hz, 1H), 1.99 – 1.88 (m, 1H), 1.50 – 1.40 (m, 1H), 1.13 (d, *J* = 6.6 Hz, 2H).
^{13}C NMR (151 MHz, $CDCl_3$): δ 208.6, 164.6, 139.6, 131.0, 128.7, 128.5, 72.5, 46.8, 44.3, 30.2, 29.1, 14.3.
HRMS (ESI-TOF, m/z): HRMS (ESI) Calcd for $[M+H]^+$ 267.0782; Found 267.0782.
R_f = 0.4 (20% EtOAc in hexanes); Stain: Hanessian's Stain.

Ylide oxidation of compound 30

Following Condition A, **30** (55.9 mg, 0.3 mmol), HFIP (0.2 mL), Me_4NBF_4 (16.0 mg, 0.1 mmol), ylide **Y7** (99.7 mg, 0.3 mmol) and $NaHCO_3$ (63.2 mg, 0.75 mmol) were added to O_2 saturated MeCN (2.0 mL). The reaction mixture was electrolyzed for 9 F/mol. Purification by pTLC on silica eluting with 15% Et_2O/hexane afforded **30-P1** (9.8 mg, 18% yield) and an inseparable mixture of **30-P2** and **30-P3** (15.3 mg, 27% yield) as a colorless oil.

Data for **30-P1**:

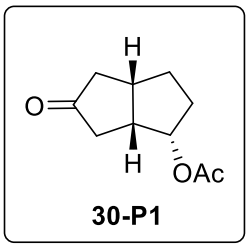

30-P1

^{1}H NMR (600 MHz, $CDCl_3$): δ 5.30 – 5.25 (m, 1H), 2.86 (m, 3H), 2.56 (dd, *J* = 19.0, 9.2 Hz, 1H), 2.38 – 2.26 (m, 2H), 2.18 – 2.04 (m, 3H), 2.03 (s, 4H), 2.00 – 1.85 (m, 3H).
^{13}C NMR (151 MHz, $CDCl_3$): δ 219.4, 170.5, 77.5, 45.4, 43.5, 38.5, 38.0, 32.4, 30.7, 21.1.
HRMS (APCI-TOF, m/z): HRMS (APCI) Calcd for $[M+H]^+$ 183.1016; Found 183.1017.
R_f = 0.6 (50% EtOAc in hexanes); Stain: Hanessian's Stain.

Data for **30-P2**:

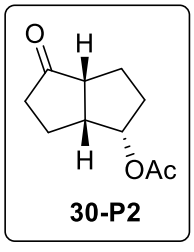

30-P2

8% yield based on the NMR mixture.
^{1}H NMR (600 MHz, $CDCl_3$): δ 5.24 (dt, *J* = 6.3, 4.8 Hz, 1H), 2.99 (dddd, *J* = 10.1, 8.7, 6.2, 4.1 Hz, 1H), 2.69 (td, *J* = 9.1, 3.9 Hz, 1H), 2.32 – 2.27 (m, 2H), 2.03 (s, 3H), 2.02 – 1.72 (m, 6H).
^{13}C NMR (151 MHz, $CDCl_3$): δ 222.1, 170.7, 78.3, 50.7, 43.9, 38.4, 32.0, 25.3, 21.3, 20.6.

HRMS (APCI-TOF, m/z): HRMS (APCI) Calcd for $[M+H]^+$ 183.1016; Found 183.1022. $\mathbf{R_f}$ = 0.3 (30% EtOAc in Hexane); Stain: Hanessian's Stain.

Data for **30-P3**:

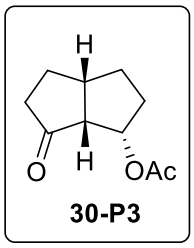

30-P3

19% yield based on the NMR mixture.
^{1}H NMR (600 MHz, $CDCl_3$): δ 5.42 (dt, *J* = 7.5, 4.9 Hz, 1H), 2.93 – 2.81 (m, 2H), 2.41 – 2.24 (m, 2H), 2.18 – 2.12 (m, 1H), 2.04 – 2.01 (m, 1H), 2.02 (s, 3H), 1.90 – 1.86 (m, 2H), 1.82 – 1.66 (m, 2H).
^{13}C NMR (151 MHz, $CDCl_3$): δ 217.4, 170.4, 76.7, 54.5, 41.0, 39.8, 33.9, 30.7, 27.4, 21.2.
HRMS (APCI-TOF, m/z): HRMS (APCI) Calcd for $[M+H]^+$ 183.1016; Found 183.1022. $\mathbf{R_f}$ = 0.6 (50% EtOAc in Hexane); Stain: Hanessian's Stain.

Ylide oxidation of compound 31

Following Condition A, **31** (55.9 mg, 0.3 mmol), HFIP (0.2 ml), Me_4NBF_4 (16.0 mg, 0.1 mmol), ylide **Y7** (99.7 mg, 0.3 mmol) and $NaHCO_3$ (63.2 mg, 0.75 mmol) were added to O_2 saturated MeCN (2.0 ml). The reaction mixture was electrolyzed for 9 F/mol. Purification by pTLC on silica gel eluting with 25% EtOAc in hexanes afforded **31-P1** (11.4 mg, 16% yield) as a colorless oil.

Data for **31-P1**:

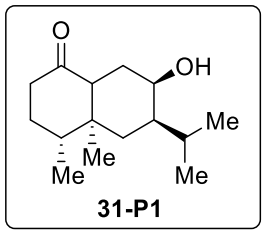

31-P1

^{1}H NMR (600 MHz, $CDCl_3$): δ 4.04 (ddd, *J* = 11.4, 9.8, 4.5 Hz, 1H), 2.36 (m, 2H), 2.06 (d, *J* = 9.8 Hz, 1H), 2.01 (dd, *J* = 10.7, 6.2 Hz, 1H), 1.92 – 1.84 (m, 1H), 1.79 (m, 1H), 1.71 – 1.59 (m, 2H), 1.47 (dp, *J* = 13.2, 6.8 Hz, 1H), 1.37 (m, 1H), 1.01 – 0.82 (m, 11H), 0.67 (s, 3H).
^{13}C NMR (151 MHz, $CDCl_3$): δ 215.0, 66.1, 65.4, 42.8, 42.6, 41.7, 41.6, 37.2, 35.9, 32.8, 31.3, 20.2, 19.5, 14.6, 13.3.
HRMS (ESI-TOF, m/z): HRMS (ESI) Calcd for $[M+H]^+$ 239.2006; Found 239.2018.
$\mathbf{R_f}$ = 0.39 (25% EtOAc in hexanes); Stain: Anisaldehyde.

Ylide oxidation of compound 32

Following Condition A, **32** (33.3 mg, 0.1 mmol), HFIP (200 μL), Me_4NBF_4 (16.1 mg, 0.1 mmol), ylide **Y7** (33.4 mg, 0.1 mmol), and $NaHCO_3$ (21 mg, 0.25 mmol) were added to O_2 saturated MeCN (2.00 mL). The reaction mixture was electrolyzed for 6 F/mol. Purification by pTLC (EtOAc/hexanes-1:1) afforded **32-P1** (10.4 mg, 30% yield) as white solid and **32-P2** (10.5 mg, 30% yield) as a colorless oil. Spectral data matched reported values.[14]

Data for **32-P1**:

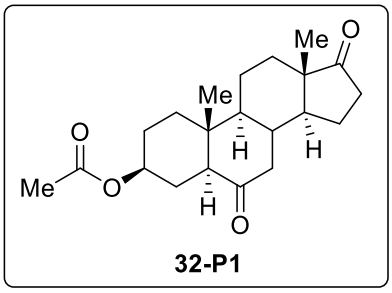

32-P1

^{1}H NMR (600 MHz, $CDCl_3$): δ 4.69 – 4.65 (m, 1H), 2.50 – 2.43 (m, 2H), 2.31 (dd, *J* = 12.7, 3.0 Hz, 1H), 2.15 – 2.09 (m, 1H), 2.03 (s, 3H), 1.96 – 1.77 (m, 6H), 1.60 – 1.47 (m, 4H), 1.41 – 1.29 (m, 6H), 0.88 (s, 3H), 0.80 (s, 3H).
^{13}C NMR (151 MHz, $CDCl_3$): δ 219.8, 209.3, 170.6, 72.6, 56.5, 53.9, 51.6, 48.1, 45.4, 40.9, 37.4, 36.4, 35.6, 31.1, 26.8, 26.1, 21.6, 21.3, 20.7, 14.2, 13.1.
HRMS (ESI-TOF, m/z): HRMS (ESI) Calcd for $[M+H]^+$ 347.2217; Found 347.2220.
R_f = 0.60 (50% EtOAc in hexanes); Stain: Hanessian's Stain.
$[\alpha]_D^{20}$ = 13.3 (*c*.0.63 in $CHCl_3$).

Data for **32-P2**:

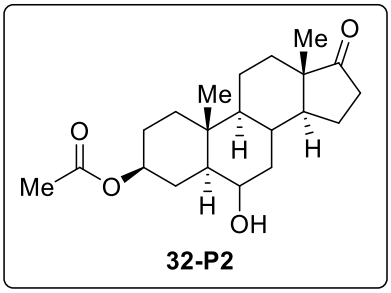

32-P2

^{1}H NMR (600 MHz, $CDCl_3$): δ 4.71 – 4.66 (m, 1H), 3.45 (td, *J* = 10.8, 4.7 Hz, 1H), 2.46 (dd, *J* = 19.6, 8.3 Hz, 1H), 2.25 – 2.22 (m, 1H), 2.17 – 2.10 (m, 2H), 2.03 (s, 3H), 1.98 – 1.93 (m, 1H), 1.86 – 1.80 (m, 2H), 1.74 (dt, *J* = 13.4, 3.6 Hz, 1H), 1.68 – 1.62 (m, 2H), 1.55 – 1.50 (m, 2H), 1.38 – 1.25 (m, 4H), 1.13 – 1.06 (m. 2H), 1.01 – 0.93 (m, 1H), 0.86 (s, 6H), 0.78 – 0.73 (m, 1H).
^{13}C NMR (151 MHz, $CDCl_3$): δ 220.7, 170.6, 73.3, 69.2, 53.8, 51.7, 51.1, 47.8, 40.5, 37.0, 36.4, 35.8, 33.9, 31.4, 28.3, 27.2, 21.8, 21.4, 20.4, 13.8, 13.3.
HRMS (ESI-TOF, m/z): HRMS (ESI) Calcd for $[M–OH]^+$ 331.2268; Found 331.2273.
R_f = 0.35 (50% EtOAc in hexanes); Stain: Hanessian's Stain.
$[\alpha]_D^{20}$ = 5.7 (*c*.0.35 in $CHCl_3$).

Ylide oxidation of compound 33

Following Condition A, **33** (34.6 mg, 0.1 mmol), HFIP (200 μL), Me_4NBF_4 (16.1 mg, 0.1 mmol), ylide **Y7** (33.4 mg, 0.1 mmol), and $NaHCO_3$ (21 mg, 0.25 mmol) were added to O_2 saturated MeCN (2.00 mL). The reaction mixture was electrolyzed for 6 F/mol. Purification by pTLC (EtOAc/hexanes-3:7) afforded **33-P1** (10.8 mg, 30% yield) as a white solid and **33-P2** (11.4 mg, 31% yield) as a colorless oil. Spectral data for 33-P1 matched reported values.[43]

Data for **33-P1**:

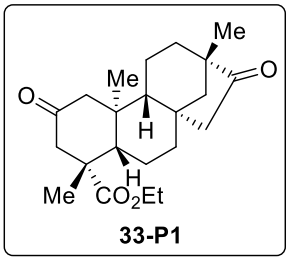

33-P1

^{1}H NMR (600 MHz, $CDCl_3$): δ 4.10 (dq, *J* = 11.0, 7.2 Hz, 1H), 4.04 (dq, *J* = 11.0, 7.2 Hz, 1H), 2.92 (dd, *J* = 14.1, 2.3 Hz, 1H), 2.54 (dd, *J* = 18.6, 3.8 Hz, 1H), 2.45 (dd, *J* = 13.7, 2.4 Hz, 1H), 2.09 – 2.04 (m, 2H), 1.94 (d, *J* = 13.9 Hz, 1H), 1.82 (d, *J* = 18.5 Hz, 1H), 1.75 – 1.54 (m, 7H), 1.46 – 1.39 (m, 3H),1.37 (s, 3H), 1.28 – 1.22 (m, 4H), 0.99 (s, 3H), 0.73 (s, 3H).

^{13}C NMR (151 MHz, $CDCl_3$): δ 221.5, 207.8, 175.3, 61.0, 56.1, 55.3, 54.19, 54.1, 53.9, 51.3, 48.6, 47.8, 47.8, 42.1, 40.8, 39.5, 37.0, 28.5, 21.5, 20.3, 19.8, 14.6, 14.0.

HRMS (ESI-TOF, m/z): HRMS (ESI) Calcd for $[M+H]^+$ 361.2373; Found 361.2382.

R_f = 0.5 (30% EtOAc in hexanes); Stain: Hanessian's Stain.

$[\alpha]_D^{20}$ = 43.3 (*c*.0.72 in $CHCl_3$).

Data for **33-P2**:

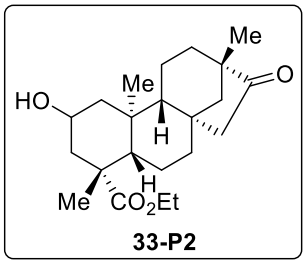

33-P2

^{1}H NMR (600 MHz, $CDCl_3$): 4.19 – 4.09 (m, 3H), 2.63 (dd, *J* = 18.6, 3.9 Hz, 1H), 2.52 – 2.45 (m, 1H), 2.13 – 2.08 (m, 1H), 1.98 – 1.91 (m, 1H), 1.84 (d, *J* = 18.6 Hz, 1H), 1.78 – 1.62 (m, 4H), 1.59 (dd, *J* = 11.6, 2.9 Hz, 1H), 1.51 (td, *J* = 13.9, 4.3 Hz, 1H), 1.44 (dd, *J* = 11.6, 3.9 Hz, 1H), 1.42 – 1.37 (m, 1H), 1.28 (s, 3H), 1.27 (s, 3H), 1.26 (s, 3H), 1.14 (dd, *J* = 12.0, 2.4 Hz, 1H), 1.03 (t, *J* = 11.6 Hz, 1H), 1.00 (s, 3H), 0.83 (t, *J* = 11.8 Hz, 1H), 0.75 (s, 3H).

^{13}C NMR (151 MHz, $CDCl_3$): 222.2, 176.8, 64.1, 60.4, 56.4, 54.6, 54.2, 48.8, 48.6, 48.5, 46.8, 45.1, 41.4, 39.4, 39.3, 37.1, 28.8, 21.4, 20.4, 19.8, 14.5, 14.1.

HRMS (ESI-TOF, m/z): HRMS (ESI) Calcd for $[M+H]^+$ 363.2530; Found 363.2541.

R_f = 0.25 (30% EtOAc in hexanes); Stain: Hanessian's Stain.

$[\alpha]_D^{20}$ = -43.3 (*c*.0.90 in $CHCl_3$).

Ylide oxidation of compound 34

Following Condition A, compound **34** (110.5 mg, 0.3 mmol), HFIP (0.2 mL), Me_4NBF_4 (48.0 mg, 0.3 mmol), ylide **Y6** (96.0 mg, 0.3 mmol), and $NaHCO_3$ (63.0 mg, 0.75 mmol) were added MeCN (2.00 mL). The reaction mixture was electrolyzed for 5 F/mol. Purification by flash chromatography (EtOAc/hexanes - 1:1) afforded **34-P1** (53.9 mg, 47% yield) as a white solid.

Data for **34-P1**:

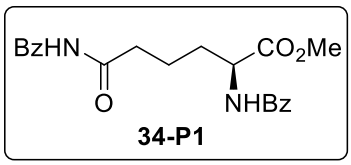

34-P1

^{1}H NMR (600 MHz, $CDCl_3$): δ 8.91 (s, 1H), 7.91 – 7.77 (m, 4H), 7.58 (t, *J* = 7.4 Hz, 1H), 7.48 (dt, *J* = 12.3, 7.5 Hz, 3H), 7.41 (t, *J* = 7.6 Hz, 2H), 6.99 (d, *J* = 7.7 Hz, 1H), 4.85 (td, *J* = 7.6, 4.8 Hz, 1H), 3.77 (s, 3H), 3.10 – 2.94 (m, 2H), 2.12 – 2.01 (m, 1H), 1.92 (dq, *J* = 14.4, 7.5 Hz, 1H), 1.83 (p, *J* = 7.4 Hz, 2H).

^{13}C NMR (151 MHz, $CDCl_3$): δ 175.5, 173.1, 133.9, 133.3, 132.8, 131.9, 129.1, 128.7, 127.8, 127.3, 52.7, 52.5, 37.1, 31.9, 20.1.

HRMS (ESI-TOF, m/z): HRMS (ESI) Calcd for $[M+H]^+$ 383.1601; Found 383.1607.

$\mathbf{R_f}$ = 0.45 (50% EtOAc in hexanes); UV detection.
$\mathbf{[\alpha]_D^{20}}$ = 4.4 (*c*.0.23 in $CHCl_3$).

Under the same reaction conditions, different ylides for oxidation of **34** leads to different yields for **34-P1** (**Y7** – 16% yield, **Y4** – 28% yield, **Y50** – 41% yield).

Ylide oxidation of compound 35

Following condition A, 34 (60.9 mg, 0.3 mmol), HFIP (0.2 mL), Me_4NBF_4 (16.0 mg, 0.1 mmol), ylide **Y4** (61.4 mg, 0.3 mmol) and $NaHCO_3$ (63.2 mg, 0.75 mmol) were added to O_2 saturated MeCN (2.0 mL). The reaction mixture was electrolyzed for 9 F/mol. After the electrolysis, 12 M aq. HCl (1 mL) was added to the reaction mixture followed by the stirring at laboratory temperature for 2 h. The resulting reaction mixture was concentrated in-vacuo and then purified by pTLC on silica gel eluting with 10% MeOH/CH_2Cl_2 to afford benzamide **35-P1** (19.6 mg, 54% yield) as a white solid. Spectral data matched reported literature values.[15]

Data for **35-P1**:

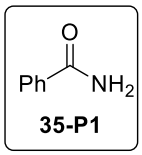

35-P1

^{1}H NMR (600 MHz, DMSO-d_6): δ 7.98 (s, 1H), 7.90 – 7.86 (m, 2H), 7.52 (td, *J* = 7.0, 1.3 Hz, 1H), 7.45 (td, *J* = 7.5, 1.7 Hz, 2H), 7.37 (s, 1H).

Ylide oxidation of compound 36

Following Condition A, **36** (57.7 mg, 0.30 mmol), HFIP (0.315 mL), Me_4NBF_4 (48.3 mg, 0.30 mmol), ylide **Y7** (0.100 g, 0.30 mmol), and $NaHCO_3$ (63.0 mg, 0.75 mmol) were added to O_2 saturated MeCN (2.00 mL). The reaction mixture was electrolyzed for 9 F/mol. Purification by flash chromatography (EtOAc/hexanes-20:80) afforded **36-P1** (13.2 mg, 21% yield) and **36-P2** (2.9 mg, 5%) as colorless oils. Spectral data matched reported values.[16]

Data for **36-P1**:

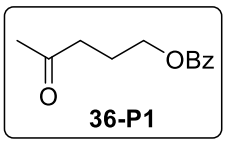

36-P1

^{1}H NMR (400 MHz, $CDCl_3$): δ 8.03 (dd, *J* = 8.4, 1.3 Hz, 2H), 7.60 – 7.53 (m, 1H), 7.49 – 7.40 (m, 2H), 4.34 (t, *J* = 6.4 Hz, 2H), 2.61 (t, *J* = 7.2 Hz, 2H), 2.18 (s, 3H), 2.06 (tt, *J* = 7.2, 6.3 Hz, 2H).
^{13}C NMR (126 MHz, $CDCl_3$): δ 207.8, 166.7, 133.1, 130.3, 129.7, 128.5, 64.3, 40.1, 30.2, 23.1.
$\mathbf{R_f}$ = 0.15 (15% EtOAc in hexanes); Stain: PMA
Data for **36-P2**:

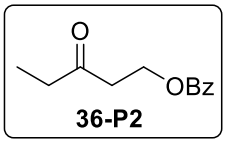

36-P2

^{1}H NMR (400 MHz, $CDCl_3$): δ 8.03 – 7.96 (m, 2H), 7.59 – 7.53 (m, 1H), 7.46 – 7.39 (m, 2H), 4.60 (t, *J* = 6.4 Hz, 2H), 2.88 (t, *J* = 6.4 Hz, 2H), 2.51 (q, *J* = 7.3 Hz, 2H), 1.10 (t, *J* = 7.3 Hz, 3H).

$\mathbf{R_f}$ = 0.25 (15% EtOAc in hexanes); Stain: PMA

Ylide oxidation of compound 37

Following Condition A, **37** (55.9 mg, 0.30 mmol), HFIP (0.315 mL), Me_4NBF_4 (48.3 mg, 0.30 mmol), ylide **Y7** (0.100 g, 0.30 mmol), and $NaHCO_3$ (63.0 mg, 0.75 mmol) were added to O_2 saturated MeCN (2.00 mL). The reaction mixture was electrolyzed for 9 F/mol. Purification by flash chromatography (EtOAc/hexanes-20:80) afforded **37-P1** (18.1 mg, 30% yield) as a colorless oil.

Data for **37-P1**:

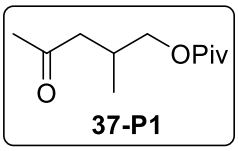

37-P1

^{1}H NMR (400 MHz, $CDCl_3$): δ 3.94 (dd, *J* = 10.8, 5.7 Hz, 1H), 3.89 (dd, *J* = 10.8, 6.0 Hz, 1H), 2.52 (dd, *J* = 16.2, 5.3 Hz, 1H), 2.40 (dq, *J* = 12.3, 6.1 Hz, 1H), 2.30 (dd, *J* = 16.2, 7.6 Hz, 1H), 2.15 (s, 3H), 1.20 (s, 9H), 0.96 (d, *J* = 6.6 Hz, 3H).
^{13}C NMR (126 MHz, $CDCl_3$): δ 207.7, 178.6, 68.5, 47.5, 39.0, 30.6, 29.0, 27.4, 17.1.
HRMS (ESI-TOF, m/z): HRMS (ESI) Calcd for $[M+Na]^+$ 223.1305; Found 223.1310.
R_f = 0.20 (20% EtOAc in hexanes); Stain: $KMnO_4$.

Ylide oxidation of compound 38

Following Condition A, **38** (61.9 mg, 0.30 mmol), HFIP (0.315 mL), Me_4NBF_4 (48.3 mg, 0.30 mmol), **Y7** (0.100 g, 0.30 mmol), and $NaHCO_3$ (63.0 mg, 0.75 mmol) were added to O_2 saturated MeCN (2.00 mL). The reaction mixture was electrolyzed for 9 F/mol. Purification by flash chromatography (EtOAc/hexanes-25:75) afforded an inseparable mixture of **38-P1** and **38-P2** lactone (21.8 mg, 26% yield, **38-P1**:**38-P2** = 1:4) as a colorless oil. Spectral data matched reported values.[17]

Data for **38-P1**:

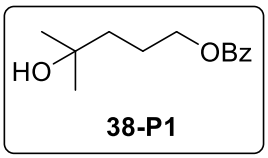

38-P1

^{1}H NMR (500 MHz, $CDCl_3$): δ 7.79 – 7.74 (m, 1H), 7.65 (t, *J* = 7.8 Hz, 2H), 4.56 (t, *J* = 6.6 Hz, 2H), 2.13 – 2.05 (m, 2H), 1.86 – 1.81 (m, 2H), 1.48 (s, 6H).
^{13}C NMR (126 MHz, $CDCl_3$): δ 166.8, 133.0, 130.5, 129.7, 128.5, 70.8, 65.5, 40.2, 29.5, 24.0.
R_f = 0.15 (25% EtOAc in hexanes); Stain: UV active.

Ylide oxidation of compound 39

Following Condition A, **39** (46.9 mg, 0.30 mmol), HFIP (0.315 mL), Me_4NBF_4 (48.3 mg, 0.30 mmol), **Y7** (0.100 g, 0.30 mmol), and $NaHCO_3$ (63.0 mg, 0.75 mmol) were added to O_2 saturated MeCN (2.00 mL). The reaction mixture was electrolyzed for 9 F/mol. Purification by flash chromatography (EtOAc/hexanes-25:75) afforded **39-P1** (12.0 mg, 24% yield) and **39-P2** (8.0 mg, 16% yield) as colorless oils. Spectral data matched reported values.[18]

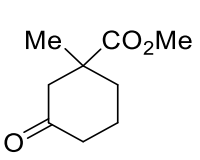

39-P1

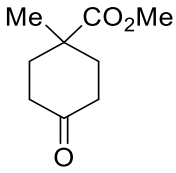

39-P2

Ylide oxidation of compound 40

Following Condition A, **40** (60.3 mg, 0.3 mmol), HFIP (0.2 mL), Me_4NBF_4 (16.0 mg, 0.1 mmol), ylide **Y7** (61.4 mg, 0.3 mmol), and $NaHCO_3$ (63.2 mg, 0.75 mmol) were added to O_2 saturated MeCN (2.00 mL). The reaction mixture was electrolyzed for 9 F/mol. Purification by flash chromatography on silica gel eluting with 20% EtOAc/hexane afforded **55** (24.4 mg) and **40** (24.7 mg). To the recovered **40**, H_2O (0.1 mL), Me_4NBF_4 (16.0 mg, 0.1 mmol), ylide **Y7** (43.4 mg, 0.13 mmol), $NaHCO_3$ (27.3 mg, 0.33 mmol), and O_2 saturated MeCN (2.00 mL) were added followed by the electrolysis again. The reaction mixture was electrolyzed for 9 F/mol. After the completion of the reaction, the crude mixture was purified by flash chromatography on silica gel to afford **55** (8.3 mg) and **40** (9.1 mg). Two runs of products were combined for a total of 51%. Spectral data matched reported values.[43]

Data for **55**:

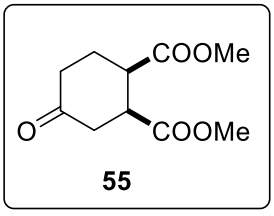

55

^{1}H NMR (600 MHz, $CDCl_3$): δ 3.77 (s, 3H), 3.73 (s, 3H), 3.28 (dt, *J* = 6.2, 4.4 Hz, 1H), 3.14 (dt, *J* = 9.6, 4.9 Hz, 1H), 2.90 (ddd, *J* = 15.4, 9.4, 1.2 Hz, 1H), 2.66 (dd, *J* = 15.4, 5.5 Hz, 1H), 2.51 – 2.25 (m, 3H), 2.15 – 1.99 (m, 1H).

Ylide oxidation of compound 41

Following Condition A, **41** (65.4 mg, 0.3 mmol), HFIP (0.2 mL), Me_4NBF_4 (16.0 mg, 0.1 mmol), ylide **Y7** (99.7 mg, 0.3 mmol) and $NaHCO_3$ (63.2 mg, 0.75 mmol) were added to O_2 saturated MeCN (2.00 mL). The reaction mixture was electrolyzed for 9 F/mol. Purification by flash chromatography on silica gel eluting with 15% EtOAc /hexane afforded **41-P1** (18.1 mg, 26% yield) and **41-P2** (11.8 mg, 17% yield) as colorless oils. Spectral data matched reported values for **41-P2**.[19]

Data for **41-P1**:

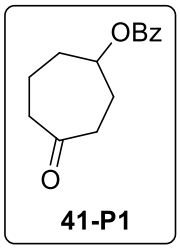

41-P1

^{1}H NMR (600 MHz, $CDCl_3$): δ 8.06 (d, *J* = 7.9, 2H), 7.59 (t, *J* = 7.5 Hz, 1H), 7.47 (t, *J* = 7.7 Hz, 2H), 5.32 (m, , 1H), 2.77 (ddd, *J* = 15.8, 9.2, 3.5 Hz, 1H), 2.60 (m, 2H), 2.54 (ddd, *J* = 15.7, 8.6, 3.5 Hz, 1H), 2.23 – 2.10 (m, 2H), 2.09 – 2.00 (m, 3H), 1.80 (m, *J* = 9.2, 2.5 Hz, 1H).
^{13}C NMR (151 MHz, $CDCl_3$) δ 213.0, 165.1, 132.6, 129.9, 129.1, 128.0, 73.0, 43.1, 37.3, 34.4, 28.4, 18.5.
HRMS (ESI-TOF, m/z): HRMS (ESI) Calcd for $[M+H]^+$ 233.1172; Found 233.1176 **Rf** = 0.4 (20% EtOAc in hexanes); Stain: Hanessian's Stain

Data for **41-P2**:

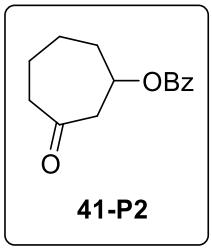

41-P2

^{1}H NMR (600 MHz, $CDCl_3$): δ 8.03 (d, *J* = 8.0 Hz, 2H), 7.59 (t, *J* = 7.4 Hz, 1H), 7.46 (t, *J* = 7.7 Hz, 2H), 5.44 (tt, *J* = 7.5, 2.7 Hz, 1H), 3.08 – 2.86 (m, 1H), 2.63 (m, 1H), 2.22 (m, 1H), 2.05 – 1.93 (m, 1H), 1.94 – 1.73 (m, 4H).

Ylide oxidation of compound 42

Following Condition A, **42** (73.0 mg, 0.3 mmol), HFIP (0.2 mL), Me_4NBF_4 (16.0 mg, 0.1 mmol), ylide **Y7** (99.7 mg, 0.3 mmol) and $NaHCO_3$ (63.2 mg, 0.75 mmol) were added to O_2 saturated MeCN (2.00 mL). Purification by flash chromatography on silica gel eluting with 10% EtOAc/hexane afforded **42-P1** (20.8mg, 27% yield) and **42-P2** (14.7 mg, 19% yield) as a colorless amorphous solid. Spectral data matched reported values.[43]

Data for **42-P1**:

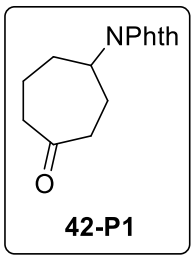

42-P1

^{1}H NMR (600 MHz, $CDCl_3$): δ δ 7.83 (dd, J = 5.4, 3.0 Hz, 2H), 7.71 (dd, J = 5.5, 3.0 Hz, 2H), 4.27 (ddt, J = 11.4, 9.3, 3.1 Hz, 1H), 2.73 – 2.50 (m, 5H), 2.47 – 2.30 (m, 1H), 2.04 (m, 2H), 1.94 – 1.87 (m, 1H), 1.82 – 1.61 (m, 1H).

Data for **42-P2**:

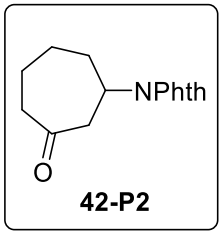

42-P2

^{1}H NMR (600 MHz, $CDCl_3$): δ 7.83 (dd, J = 5.4, 3.1 Hz, 2H), 7.72 (dd, J = 5.5, 3.0 Hz, 2H), 4.49 (tt, J = 11.9, 2.7 Hz, 1H), 3.65 (dd, J = 15.0, 12.1 Hz, 1H), 2.75 – 2.48 (m, 3H), 2.47 – 2.36 (m, 1H), 2.14 – 1.93 (m, 3H), 1.84 – 1.69 (m, 1H), 1.62 – 1.49 (m, 1H).

Ylide oxidation of compound 43

Following Condition B, **43** (19.8 mg, 0.10 mmol), H_2O (0.10 mL), Me_4NBF_4 (16.1 mg, 0.10 mmol), **Y7** (33.4 mg, 0.10 mmol), and $NaHCO_3$ (21.0 mg, 0.25 mmol) were added to O_2 saturated MeCN (2.00 mL). The reaction mixture was electrolyzed for 12 F/mol. Purification by flash chromatography (EtOAc/hexanes-25:75) afforded an inseparable mixture of **43-P1**, **43-P2**, and **43-P3** (6.8 mg, 32% yield, 2:1:0.2) as a colorless oil. Spectral data for compound **43-P3** matched reported values.[11]

Data for **43-P1**:

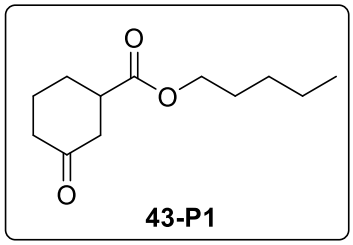

43-P1

^{1}H NMR (500 MHz, $CDCl_3$): δ 4.09 (2H), 2.79 (1H), 2.55 (2H), 2.38 (2H), 2.07 (2H), 1.86 (2H), 1.73 (2H), 1.36 – 1.28 (4H), 0.91 (3H).
^{13}C NMR (126 MHz, $CDCl_3$): δ 209.5, 173.9, 65.2, 43.5, 41.1, 28.4, 28.2, 27.9, 24.7, 14.1.

Data for **43-P2**:

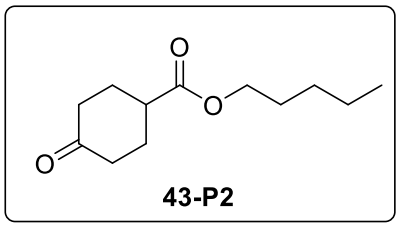

43-P2

^{1}H NMR (500 MHz, $CDCl_3$): δ 4.11 (2H), 2.75 (1H), 2.48 (2H), 2.35 (2H), 2.21 (2H), 2.03 (2H), 1.63 (2H), 1.34 (4H), 0.91 (3H).
^{13}C NMR (126 MHz, $CDCl_3$): δ 210.3, 174.4, 65.1, 40.9, 39.9, 28.7, 28.4, 28.2, 22.4, 14.1.

Data for **43-P3**:

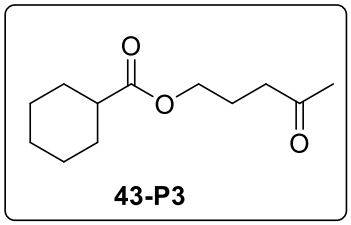

43-P3

^{1}H NMR (500 MHz, $CDCl_3$): δ 4.06 (2H), 2.51 (2H), 2.27 (1H), 2.16 (3H), 1.94 – 1.87 (4H), 1.76 – 1.72 (2H), 1.66-1.64 (1H), 1.47 – 1.38 (2H), 1.33-1.20 (3H).
^{13}C NMR (126 MHz, $CDCl_3$): δ 207.9, 176.3, 63.4, 43.4, 40.1, 30.1, 29.2, 25.9, 25.6, 23.0.

HRMS (ESI-TOF, m/z): HRMS (ESI) Calcd for $[M+H]^+$ 213.1485; Found 213.1485. $\mathbf{R_f}$ = 0.3 (20% EtOAc in hexanes); Stain: Hanessian's Stain.

Ylide oxidation of compound 44

Following Condition B, compound **44** (120.7 mg, 0.3 mmol), H_2O (0.1 mL), Me_4NBF_4 (48.0 mg, 0.3 mmol), ylide **Y7** (100.2 mg, 0.3 mmol), and $NaHCO_3$ (63.0 mg, 0.75 mmol) were added to MeCN (2.00 mL). The reaction mixture was electrolyzed for 5 F/mol. The reaction mixture was diluted with Et_2O (50 mL) and 1 M aq. HCl (30 mL), transferred into a separatory funnel, the organic phase was separated, and the aqueous phase was extracted with Et_2O (2 × 50 mL). Combined organic extracts were washed with 1 M aq. HCl (2 × 50 mL) and brine (80 mL), dried over $MgSO_4$, filtered, and concentrated under reduced pressure to afford crude product. Purification by flash chromatography (EtOAc/hexanes 1:2 → 1:1) afforded **44-P1** (58.9 mg, 47% yield) as a white solid.

Data for **44-P1**:

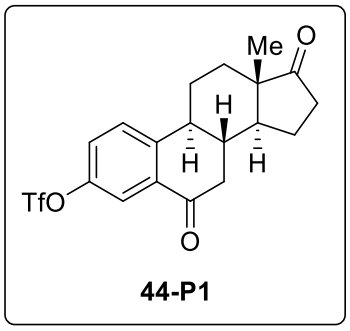

44-P1

^{1}H NMR (600 MHz, $CDCl_3$): δ 7.95 (d, *J* = 2.8 Hz, 1H), 7.54 (dd, *J* = 8.8, 1.1 Hz, 1H), 7.45 (dd, *J* = 8.7, 2.8 Hz, 1H), 2.93 (dd, *J* = 16.9, 3.4 Hz, 1H), 2.67 – 2.59 (m, 1H), 2.58 – 2.46 (m, 2H), 2.36 (dd, *J* = 17.0, 13.5 Hz, 1H), 2.24 – 2.10 (m, 2H), 2.06 (ddd, *J* = 13.4, 4.7, 2.8 Hz, 2H), 1.73 – 1.53 (m, 5H), 0.93 (s, 3H).
^{13}C NMR (151 MHz, $CDCl_3$): δ 219.2, 195.4, 148.6, 146.4, 134.4, 128.0, 126.5, 120.0, 118.8 (q, *J* = 320.9 Hz), 50.4, 47.7, 43.3, 43.1, 39.2, 35.7, 31.2, 25.2, 21.5, 13.7.
^{19}F NMR (376 MHz, $CDCl_3$): δ −75.4 ppm.
HRMS (ESI-TOF, m/z): HRMS (ESI) Calcd for $[M+H]^+$ 417.0978; Found 417.0980.
R_f = 0.4 (33% EtOAc in hexanes); Stain: Anisaldehyde.
$[\alpha]_D^{20}$ = 44.5 (*c*.0.60 in $CHCl_3$).

Ylide oxidation of compound 45

Following Condition B, **45** (85.2 mg, 0.3 mmol), H_2O (0.1 mL), Me_4NBF_4 (16.0 mg, 0.1 mmol), ylide (99.7 mg, 0.3 mmol) and $NaHCO_3$ (63.2 mg, 0.75 mmol) were added to O_2 saturated MeCN (2.00 mL). The reaction mixture was electrolyzed for 20 F/mol. Purification by flash chromatography on silica eluting with 10% Acetone/CH_2Cl_2 afforded **46a** (17.0 mg, 19% yield) and **46b** (6.3 mg, 7% yield) as a colorless amorphous solid.

Data for **46a**:

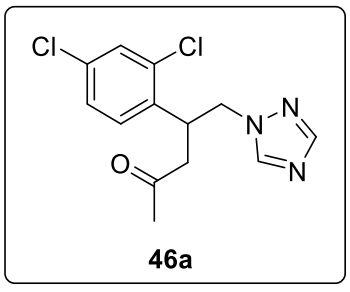

46a

^{1}H NMR (600 MHz, $CDCl_3$): δ 7.93 (s, 1H), 7.88 (s, 1H), 7.40 (s, 1H), 7.14 (d, *J* = 8.3 Hz, 1H), 6.86 (d, *J* = 8.4 Hz, 1H), 4.47 (ddt, *J* = 19.9, 14.0, 6.1 Hz, 2H), 4.24 (dt, *J* = 10.8, 5.4 Hz, 1H), 3.06 (dd, *J* = 17.9, 7.8 Hz, 1H), 2.84 (dd, *J* = 17.9, 6.0 Hz, 1H), 2.15 (s, 3H).
^{13}C NMR (151 MHz, $CDCl_3$): δ 205.5, 151.2, 143.5, 135.7, 134.5, 134.0, 130.0, 129.3, 127.6, 52.0, 44.6, 37.2, 30.3.
HRMS (ESI-TOF, m/z): HRMS (ESI) Calcd for $[M+H]^+$ 298.0508; Found 298.0517. **R_f** = 0.3 (30% acetone in CH_2Cl_2); Stain: Basic $KMnO_4$.

Data for **46b**:

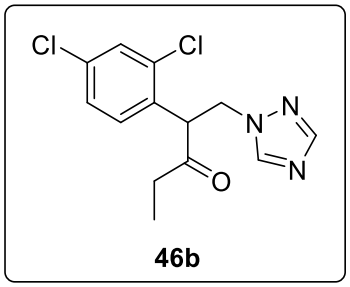

46b

^{1}H NMR (600 MHz, $CDCl_3$): δ 7.99 (s, 1H), 7.92 (s, 1H), 7.47 (d, *J* = 2.1 Hz, 1H), 7.26 – 7.21 (m, 1H), 7.06 (d, *J* = 8.3 Hz, 1H), 4.87 (m, 2H), 4.33 (q, *J* = 9.4 Hz, 1H), 2.35 (m, 2H), 0.97 (t, *J* = 7.2 Hz, 3H).
^{13}C NMR (151 MHz, $CDCl_3$): δ 207.0, 151.7, 143.7, 134.8, 134.7, 131.0, 129.9, 129.4, 127.7, 76.8, 76.6, 76.4, 53.0, 49.2, 35.0, 7.2.
HRMS (ESI-TOF, m/z): HRMS (ESI) Calcd for $[M+H]^+$ 298.0508; Found 298.0521. $\mathbf{R}_f$ = 0.3 (30% acetone in CH_2Cl_2); Stain: Basic $KMnO_4$

Ylide oxidation of 52

Following Condition B, **52** (90.6 mg, 0.3 mmol), H_2O (0.1 mL), Me_4NBF_4 (16.0 mg, 0.1 mmol), ylide **Y7** (99.7 mg, 0.3 mmol) and $NaHCO_3$ (63.2 mg, 0.75 mmol) were added to O_2 saturated MeCN (2.00 ml). The reaction mixture was electrolyzed for 20 F/mol. Purification by flash chromatography on silica gel eluting with 50% AcOEt /hexane afforded **53** (22.7 mg) and **52** (58.0 mg). To the recovered **52**, H_2O (0.1 mL), Me_4NBF_4 (16.0 mg, 0.1 mmol), ylide (66.8 mg, 0.20 mmol), $NaHCO_3$ (42.0 mg, 0.50 mmol) and O_2 saturated MeCN (2.00 mL) were added followed by the electrolysis again. The reaction mixture was electrolyzed for 20 F/mol. After the completion of the reaction, the crude mixture was purified by flash chromatography on silica gel to afford **53** (12.9 mg) and **52** (34.8 mg). Recovered **52** was subjected to another electrolysis following same protocol adding H_2O (0.1 mL), Me_4NBF_4 (16.0 mg, 0.1 mmol), ylide **Y7** (40.0 mg, 0.12 mmol), $NaHCO_3$ (25.2 mg, 0.3 mmol), and O_2 saturated MeCN (2.00 mL). The reaction mixture was electrolyzed for 20 F/mol. Purification by flash choromatography on silica afforded **53** (9.0 mg) and **52** (20.1 mg). Three runs of products were combined for a total of 47% yield.

Data for **53**:

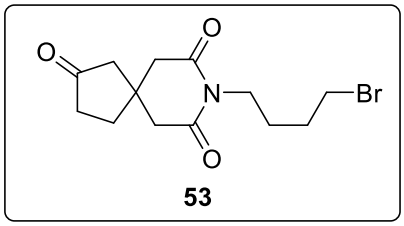

53

^{1}H NMR (600 MHz, $CDCl_3$) δ 3.87 – 3.79 (t, *J* = 6.4 Hz, 2H), 3.43 (t, *J* = 6.7 Hz, 2H), 2.73 (s, 4H), 2.42 (t, *J* = 8.0 Hz, 2H), 2.21 (s, 2H), 1.97 (t, *J* = 7.9 Hz, 2H), 1.87 (dq, *J* = 8.4, 6.7 Hz, 1H), 1.76 – 1.63 (m, 1H).
^{13}C NMR (151 MHz, $CDCl_3$) δ 214.2, 170.0, 48.9, 43.4, 38.4, 36.4, 35.8, 32.9, 32.5, 29.6, 26.3.
HRMS (ESI-TOF, m/z): HRMS (ESI) Calcd for $[M+H]^+$ 316.0543; Found 316.0548. $\mathbf{R}_f$ = 0.3 (50% EtOAc in hexanes); Stain: Basic $KMnO_4$.

Intramolecular ylide oxidation of compound 61

The reaction was performed by following General procedure A (HFIP). 0.2 mmol scale, 5 F/mol. After passing 5 F/mol, the reaction solution was transferred to a round-bottom flask, using CH_2Cl_2 for washing electrode and ElectraSyn vial. The solvents were removed by a rotary evaporator, followed by thorough removal of remaining HFIP in vacuo. The residue was re-dissolved to CH_2Cl_2 and insoluble solid (electrolyte) was filtered with Celite. The desired oxidation product was isolated by column chromatography of the residual organic compound (CH_2Cl_2/EtOAc/MeOH = 1:0.2:0.2), 28% yield containing small amount of impurity that could be either the rotamer or the regioisomer.

Data for compound **62**:

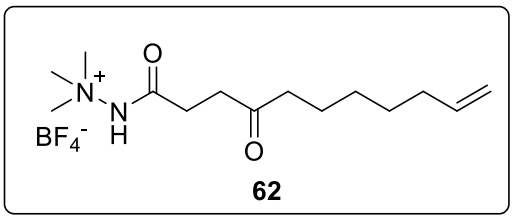

62

^{1}H NMR (600 MHz, $CDCl_3$): δ 5.77 (ddt, *J* = 17.0, 10.2, 6.7 Hz, 1H), 5.06 – 4.85 (m, 2H), 3.34 (s, 9H), 2.66 (t, *J* = 7.2 Hz, 2H), 2.46 – 2.37 (m, 2H), 2.30 (t, *J* = 7.3 Hz, 2H), 2.08 – 1.96 (m, 2H), 1.56 (dtt, *J* = 11.1, 7.6, 3.4 Hz, 2H), 1.43 – 1.32 (m, 2H), 1.32 – 1.20 (m, 2H).
^{13}C NMR (151 MHz, $CDCl_3$): δ 210.9, 175.2, 139.1, 114.4, 55.6, 42.7, 39.1, 35.7, 33.7, 30.3, 28.9, 23.8.
HRMS (ESI-TOF, m/z): HRMS (ESI) Calcd for $[M–BF_4]^+$ 255.2072; Found 255.2072.
R_f = 0.3 (CH_2Cl_2/EtOAc/MeOH = 1:0.2:0.2); Stain: Basic $KMnO_4$.

Comparison with other C-H Oxidation Conditions

FE(PDP) (INCLUDING CALIBRATION WITH KNOWN SUBSTRATES)

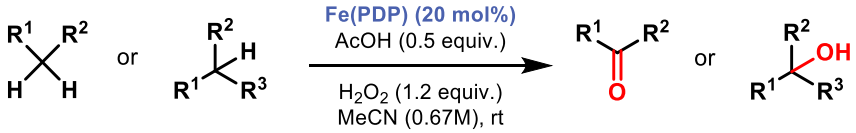

Scheme S2. Fe(*S*,*S*-PDP) oxidation of unactivated C(sp^3)-H bonds.

General Procedure

The C–H oxidation catalyzed by Fe(*S*,*S*-PDP) was carried out by following the literature procedure with minor modifications.[49] Substrate (0.2 mmol) and AcOH (5.7 μL, 0.1 mmol, 0.5 equiv.), MeCN (0.5 – 1.0 mL, depending on substrate solubility) and a magnetic stir bar were charged into a 20-mL vial. Solutions of H_2O_2 (54 μL, 50 wt. % in H_2O, 0.8 mmol, 4 equiv.) in MeCN (2.5 mL) and Fe(*S*,*S*-PDP) (37 mg, 0.04 mmol, 0.2 equiv,) in MeCN (0.25 mL) were charged into 10 and 1 mL plastic syringes, respectively, and syringe-pumped into the vigorously stirred solution of substate over 30 min. After the addition was complete, the reaction mixture was concentrated under reduced pressure. MeCN and Et_2O (50 mL) or Et_2O/EtOAc (50 mL, 10:1 – 10:2, depending on substrate and product polarity) was added to the reaction mixture, resulting in a brown precipitate. The mixture was filtered through a pad of Celite and concentrated under reduced pressure. The crude reaction mixture was analyzed by ^{1}H NMR analysis using CH_2Br_2 internal standard. Products were isolated by column chromatography or pTLC.

Experimental Setup

Figure S15. A) Used Fe(*S*,*S*-PDP) catalyst (commercially available from Strem Chemicals). **B)** Reactions were performed using the slow addition protocol with a syringe pump. **C)** Top-view of the reaction. MeCN solutions of H_2O_2 and Fe(*S*,*S*-PDP) catalyst (in separate syringes) were simultaneously added dropwise into a vigorously stirred solution of substrate and acetic acid.

Calibration

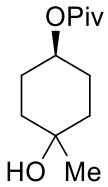

S1

Entry	Yield of S1
Original report	60% (GC yield)
Calibration	64% (NMR yield)

Table S1. Calibration of Fe(*S*,*S*-PDP) oxidation procedure using reported substrate **S1**.

Experimental Procedures

Fe(S,S-PDP) oxidation of compound 27

To a vial charged with compound **27** (72.1 mg, 0.2 mmol), AcOH (5.7 µL, 0.1 mmol, 0.5 equiv.), MeCN (1.0 mL), and a magnetic stir bar, syringe-pumped solutions of H_2O_2 (54 µL, 50 wt. % in H_2O, 0.8 mmol, 4 equiv.) in MeCN (2.5 mL) and Fe(*S*,*S*-PDP) (37 mg, 0.04 mmol, 0.2 equiv.) in MeCN (0.25 mL) were added over 30 min. The crude reaction mixture was concentrated under reduced pressure to a minimal amount of MeCN, 10% EtOAc in Et_2O (50 mL) was added, resulting in a brown precipitate and the mixture was filtered through a pad of Celite and concentrated under reduced pressure. The crude reaction mixture was then purified by column chromatography (hexanes/EtOAc 3:1 → 1:1) to afford **27** (12.0 mg, 17% RSM), ketone **27-P2** (9.4 mg, 13% yield) and a complex mixture of other unidentified oxidation products (31.0 mg).

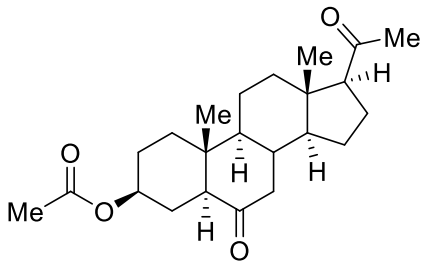

27-P2

Fe(S,S-PDP) oxidation of compound 28

This result has been previously reported.[20]

Fe(S,S-PDP) oxidation of compound 29

To a vial charged with compound **29** (50.5 mg, 0.2 mmol), AcOH (5.7 µL, 0.1 mmol, 0.5 equiv.), MeCN (1.0 mL), and a magnetic stir bar, syringe-pumped solutions of H_2O_2 (54 µL, 50 wt. % in H_2O, 0.8 mmol, 4 equiv.) in MeCN (2.5 mL) and Fe(*S*,*S*-PDP) (28 mg, 0.03 mmol, 0.15 equiv.) in MeCN (0.25 mL) were added over 30 min. The crude reaction mixture was concentrated under reduced pressure to a minimal amount of MeCN, 10% EtOAc in Et_2O (50 mL) was added, resulting in a brown precipitate. The reaction mixture was filtered through a pad of Celite and concentrated under reduced pressure. ^{1}H NMR spectroscopic analysis of the crude reaction mixture revealed starting material and trace amounts of product.

Fe(S,S-PDP) oxidation of compound 30

To a vial charged with compound **30** (33.6 mg, 0.2 mmol), AcOH (5.7 µL, 0.1 mmol, 0.5 equiv.), MeCN (0.5 mL), and a magnetic stir bar, syringe-pumped solutions of H_2O_2 (54 µL, 50 wt. % in H_2O, 0.8 mmol, 4 equiv.) in MeCN (2.5 mL) and Fe(*S*,*S*-PDP) (37 mg, 0.04 mmol, 0.20 equiv,) in MeCN (0.25 mL) were added over 30 min. The crude reaction mixture was concentrated under reduced pressure to a minimal amount of MeCN, then Et_2O (50 mL) was added, resulting in a brown precipitate. The reaction mixture was filtered through a pad of Celite and concentrated under reduced pressure. ^{1}H NMR spectroscopic analysis revealed **30-P5** was formed in 13% yield (dibromomethane was used as internal standard).

Data for compound 30-P5

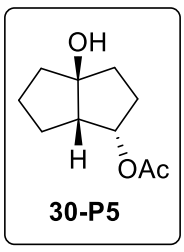

30-P5

^{1}H NMR (600 MHz, $CDCl_3$): δ 5.23 – 5.16 (m, 1H), 2.46 – 2.39 (m, 1H), 2.11 – 2.04 (m, 1H), 2.03 (s, 3H), 1.89 – 1.83 (m, 1H), 1.83 – 1.76 (m, 2H), 1.76 – 1.59 (m, 6H), 1.46 (ddt, *J* = 12.4, 10.3, 6.7 Hz, 1H).
^{13}C NMR (150 MHz, $CDCl_3$): δ 170.8, 90.3, 76.2, 54.9, 42.5, 37.7, 31.6, 26.8, 26.7, 21.2.
HRMS (ESI-TOF, m/z): HRMS (ESI) Calcd for $[M–OH]^+$ 167.1067; Found 167.1072. $\mathbf{R}_f$ = 0.45 (50% EtOAc in hexanes); Stain: Anisaldehyde.

Fe(S,S-PDP) oxidation of compound 31

To a vial charged with compound **31** (44.5 mg, 0.2 mmol), AcOH (5.7 µL, 0.1 mmol, 0.5 equiv.), MeCN (0.5 mL), and a magnetic stir bar, were syringe-pumped solutions of H_2O_2 (54 µL, 50 wt. % in H_2O, 0.8 mmol, 4.0 equiv.) in MeCN (2.5 mL) and Fe(*S*,*S*-PDP) (37 mg, 0.04 mmol, 0.20 equiv,) in MeCN (0.25 mL) were added over 30 min. The crude reaction mixture was concentrated under reduced pressure to a minimal amount of MeCN, then 10% EtOAc in Et_2O (50 mL) was added, resulting in a brown precipitate. The reaction mixture was filtered through a pad of Celite and concentrated under reduced pressure. The crude reaction mixture was separated by column chromatography (hexanes/EtOAc 2:1 → 1:1) to afford alcohol **31-P2** (7.6 mg, 16% yield).

Data for **31-P2**:

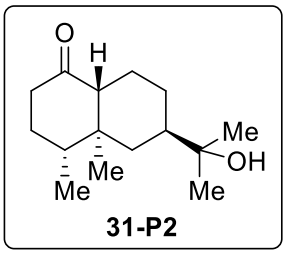

31-P2

^{1}H NMR (600 MHz, $CDCl_3$): δ 2.43 – 2.34 (m, 1H), 2.30 (ddd, *J* = 13.9, 5.4, 1.7 Hz, 1H), 2.11 (dd, *J* = 12.4, 3.3 Hz, 1H), 1.93 – 1.85 (m, 2H), 1.80 (dddt, *J* = 29.4, 13.2, 6.6, 3.0 Hz, 2H), 1.74 – 1.62 (m, 2H), 1.52 – 1.42 (m, 2H), 1.18 (d, *J* = 10.6 Hz, 6H), 0.96 (td, *J* = 12.8, 4.5 Hz, 2H), 0.91 (d, *J* = 6.7 Hz, 3H), 0.66 (s, 3H).
^{13}C NMR (150 MHz, $CDCl_3$): δ 213.1, 72.8, 58.0, 43.3, 43.0, 41.9, 41.4, 39.5, 31.6, 27.7, 27.1, 26.3, 20.7, 14.7, 12.2.
HRMS (ESI-TOF, m/z): HRMS (ESI) Calcd for $[M+H]^+$ 239.2006; Found 239.2014.
R_f = 0.25 (33% EtOAc in hexanes); Stain: Anisaldehyde.

Fe(S,S-PDP) oxidation of compound 32

To a vial charged with compound **32** (66.5 mg, 0.2 mmol), AcOH (5.7 µL, 0.1 mmol, 0.5 equiv.), MeCN (1.0 mL), and a magnetic stir bar, syringe-pumped solutions of H_2O_2 (54 µL, 50 wt. % in H_2O, 0.8 mmol, 4 equiv.) in MeCN (2.5 mL) and Fe(*S*,*S*-PDP) (37 mg, 0.04 mmol, 0.20 equiv.) in MeCN (0.25 mL) were added over 30 min. The crude reaction mixture was concentrated under reduced pressure to a minimal amount of MeCN, then Et_2O (50 mL) was added, resulting in a brown precipitate. The reaction mixture was filtered through a pad of Celite and concentrated under reduced pressure. The crude reaction mixture was separated by column chromatography (hexanes/EtOAc 2:1 → 1:1) to afford ketone **32-P1** (5.1 mg, 7% yield).

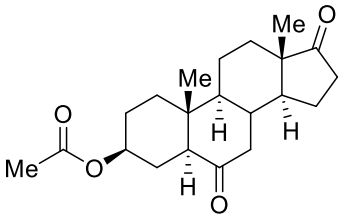

32-P1

Fe(S,S-PDP) oxidation of compound 33

To a vial charged with compound **33** (69.3 mg, 0.2 mmol), AcOH (5.7 µL, 0.1 mmol, 0.5 equiv.), MeCN (1.5 mL), and a magnetic stir bar, syringe-pumped solutions of H_2O_2 (54 µL, 50 wt. % in H_2O, 0.8 mmol, 4 equiv.) in MeCN (2.5 mL) and Fe(*S*,*S*-PDP) (37 mg, 0.04 mmol, 0.20 equiv,) in MeCN (0.25 mL) were added over 30 min. The crude reaction mixture was concentrated under reduced pressure to a minimal amount of MeCN, then 20% EtOAc in Et_2O (50 mL) was added, resulting in a brown precipitate. The mixture was filtered through a

pad of Celite and concentrated under reduced pressure. The crude reaction mixture was separated by pTLC (hexanes/EtOAc - 7:3) to afford ketone **33-P1** (4.0 mg, 6% yield).

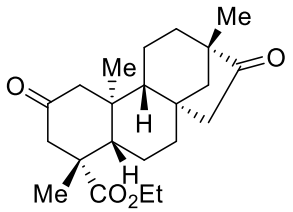

33-P1

Fe(S,S-PDP) oxidation of compound 34

To a vial charged with compound **34** (73.2 mg, 0.2 mmol), AcOH (5.7 µL, 0.1 mmol, 0.5 equiv.), MeCN (0.5 mL), and a magnetic stir bar, syringe-pumped solutions of H_2O_2 (54 µL, 50 wt. % in H_2O, 0.8 mmol, 4 equiv.) in MeCN (2.5 mL) and Fe(*S*,*S*-PDP) (37 mg, 0.04 mmol, 0.20 equiv,) in MeCN (0.25 mL) were added over 30 min. The crude reaction mixture was concentrated under reduced pressure to a minimal amount of MeCN, then 20% EtOAc in Et_2O (50 mL) was added, resulting in a brown precipitate. The reaction mixture was filtered through a pad of Celite and concentrated under reduced pressure. ^{1}H NMR spectroscopic analysis of the crude reaction mixture revealed starting material and trace amounts of product.

Fe(S,S-PDP) oxidation of compound 35

To a vial charged with compound **35** (40.7 mg, 0.2 mmol), AcOH (5.7 µL, 0.1 mmol, 0.5 equiv.), MeCN (0.5 mL), and a magnetic stir bar, syringe-pumped solutions of H_2O_2 (54 µL, 50 wt. % in H_2O, 0.8 mmol, 4 equiv.) in MeCN (2.5 mL) and Fe(*S*,*S*-PDP) (37 mg, 0.04 mmol, 0.20 equiv,) in MeCN (0.25 mL) were added over 30 min. The crude reaction mixture was concentrated under reduced pressure to a minimal amount of MeCN, then 10% EtOAc in Et_2O (50 mL) was added, resulting in a brown precipitate. The reaction mixture was filtered through a pad of Celite and concentrated under reduced pressure. ^{1}H NMR spectroscopic analysis of the crude reaction mixture revealed starting material and trace amounts of product.

Fe(S,S-PDP) oxidation of compound 36

To a vial charged with compound **36** (38.5 mg, 0.2 mmol), AcOH (5.7 µL, 0.1 mmol, 0.5 equiv.), MeCN (0.5 mL), and a magnetic stir bar, syringe-pumped solutions of H_2O_2 (54 µL, 50 wt. % in H_2O, 0.8 mmol, 4 equiv.) in MeCN (2.5 mL) and Fe(*S*,*S*-PDP) (37 mg, 0.04 mmol, 0.20 equiv,) in MeCN (0.25 mL) were added over 30 min. The crude reaction mixture was concentrated under reduced pressure to a minimal amount of MeCN, then Et_2O (50 mL) was added, resulting in a brown precipitate. The reaction mixture was filtered through a pad of Celite and concentrated under reduced pressure. ^{1}H NMR spectroscopic analysis of the crude reaction mixture revealed starting material and trace amounts of product.

Fe(S,S-PDP) oxidation of compound 37

To a vial charged with compound **37** (37.3 mg, 0.2 mmol), AcOH (5.7 μL, 0.1 mmol, 0.5 equiv.), MeCN (0.5 mL), and a magnetic stir bar, syringe-pumped solutions of H_2O_2 (54 μL, 50 wt. % in H_2O, 0.8 mmol, 4 equiv.) in MeCN (2.5 mL) and Fe(*S*,*S*-PDP) (37 mg, 0.04 mmol, 0.20 equiv,) in MeCN (0.25 mL) were added over 30 min. The crude reaction mixture was concentrated under reduced pressure to a minimal amount of MeCN, then Et_2O (50 mL) was added, resulting in a brown precipitate. The reaction mixture was filtered through a pad of Celite and concentrated under reduced pressure. ^{1}H NMR spectroscopic analysis of the crude reaction mixture using CH_2Br_2 as an internal standard revealed a mixture of ketone **37-P1**, ketone **37-P2**, and alcohol **37-P3** in a 2.5:1:1.3 ratio (35% combined yield).

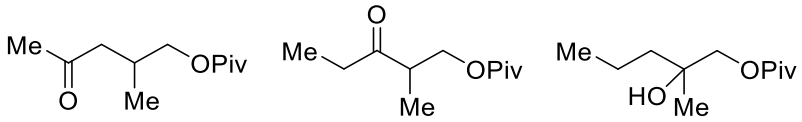

37-P1 **37-P2** **37-P3**

Data for compound **37-P3**
^{1}H NMR (600 MHz, $CDCl_3$): δ 3.98 (d, *J* = 11.3 Hz), 3.93 (d, *J* = 11.3 Hz), 1.48 (m, 2H), 1.38 (m, 2H), 1.19 (s, 3H), 0.93 (t, 3H).
^{13}C NMR (151 MHz, $CDCl_3$): δ 178.6, 72.1, 71.1, 41.7, 39.1, 27.4, 24.0, 17.1, 14.8.
HRMS (ESI-TOF, m/z): HRMS (ESI) Calcd for $[M–OH]^+$ 185.1536; Found 185.1544.

Fe(S,S-PDP) oxidation of compound 38

To a vial charged with compound **38** (41.3 mg, 0.2 mmol), AcOH (5.7 μL, 0.1 mmol, 0.5 equiv.), MeCN (0.5 mL), and a magnetic stir bar, syringe-pumped solutions of H_2O_2 (54 μL, 50 wt. % in H_2O, 0.8 mmol, 4 equiv.) in MeCN (2.5 mL) and Fe(*S*,*S*-PDP) (37 mg, 0.04 mmol, 0.20 equiv,) in MeCN (0.25 mL) were added over 30 min. The crude reaction mixture was concentrated under reduced pressure to a minimal amount of MeCN, then Et_2O (50 mL) was added, resulting in a brown precipitate. The reaction mixture was filtered through a pad of Celite and concentrated under reduced pressure. ^{1}H NMR spectroscopic analysis of the crude reaction mixture revealed starting material and trace amounts of product.

Fe(S,S-PDP) oxidation of compound 39

To a vial charged with compound **39** (31.2 mg, 0.2 mmol), AcOH (5.7 μL, 0.1 mmol, 0.5 equiv.), MeCN (0.5 mL), and a magnetic stir bar, syringe-pumped solutions of H_2O_2 (54 μL, 50 wt. % in H_2O, 0.8 mmol, 4 equiv.) in MeCN (2.5 mL) and Fe(*S*,*S*-PDP) (37 mg, 0.04 mmol, 0.20 equiv,) in MeCN (0.25 mL) were added over 30 min. The crude reaction mixture was concentrated under reduced pressure to a minimal amount of MeCN, then Et_2O (50 mL) was added, resulting in a brown precipitate. The reaction mixture was filtered through a pad of Celite and concentrated under reduced pressure. ^{1}H NMR spectroscopic analysis of the crude reaction mixture using CH_2Br_2 as an internal standard revealed a mixture of ketones **39-P1** and **39-P2** (70 %, **39-P1**/**39-P2** = 1.2:1).

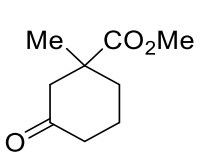

39-P1

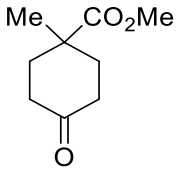

39-P2

Fe(S,S-PDP) oxidation of compound 40

To a vial charged with compound **40** (40.0 mg, 0.2 mmol), AcOH (5.7 µL, 0.1 mmol, 0.5 equiv.), MeCN (0.5 mL), and a magnetic stir bar, syringe-pumped solutions of H_2O_2 (54 µL, 50 wt. % in H_2O, 0.8 mmol, 4 equiv.) in MeCN (2.5 mL) and Fe(*S*,*S*-PDP) (37 mg, 0.04 mmol, 0.20 equiv,) in MeCN (0.25 mL) were added over 30 min. The crude reaction mixture was concentrated under reduced pressure to a minimal amount of MeCN, Et_2O (50 mL) was added, resulting in a brown precipitate. The reaction mixture was filtered through a pad of Celite and concentrated under reduced pressure. The crude reaction mixture was separated by preparative thin-layer chromatography (hexanes/EtOAc 2:3) to afford ketone **55** (19.5 mg, 46 %).

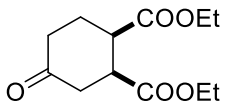

55

Fe(S,S-PDP) oxidation of compound 41

To a vial charged with compound **41** (43.7 mg, 0.2 mmol), AcOH (5.7 µL, 0.1 mmol, 0.5 equiv.), MeCN (0.5 mL), and a magnetic stir bar, syringe-pumped solutions of H_2O_2 (54 µL, 50 wt. % in H_2O, 0.8 mmol, 4 equiv.) in MeCN (2.5 mL) and Fe(*S*,*S*-PDP) (37 mg, 0.04 mmol, 0.20 equiv,) in MeCN (0.25 mL) were added over 30 min. The crude reaction mixture was concentrated under reduced pressure to a minimal amount of MeCN, then Et_2O (50 mL) was added, resulting in a brown precipitate. The reaction mixture was filtered through a pad of Celite and concentrated under reduced pressure. ^{1}H NMR spectroscopic analysis of the crude reaction mixture revealed starting material and trace amounts of product.

Fe(S,S-PDP) oxidation of compound 42

To a vial charged with compound **42** (48.7 mg, 0.2 mmol), AcOH (5.7 µL, 0.1 mmol, 0.5 equiv.), MeCN (0.5 mL), and a magnetic stir bar, syringe-pumped solutions of H_2O_2 (54 µL, 50 wt. % in H_2O, 0.8 mmol, 4 equiv.) in MeCN (2.5 mL) and Fe(*S*,*S*-PDP) (37 mg, 0.04 mmol, 0.20 equiv,) in MeCN (0.25 mL) were added over 30 min. The crude reaction mixture was concentrated under reduced pressure to a minimal amount of MeCN, then Et_2O (50 mL) was added, resulting in a brown precipitate. The reaction mixture was filtered through a pad of Celite and concentrated under reduced pressure. The crude reaction mixture was separated by pTLC (hexanes/EtOAc-7:3) to afford ketones **42-P1** and **42-P2** in 1.7:1 ratio (23.1 mg, 45% yield).

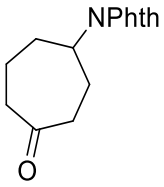

42-P1

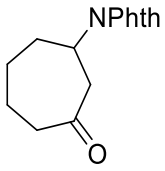

42-P2

Fe(S,S-PDP) oxidation of compound 43

To a vial charged with compound **43** (39.7 mg, 0.2 mmol), AcOH (5.7 µL, 0.1 mmol, 0.5 equiv.), MeCN (0.5 mL), and a magnetic stir bar, syringe-pumped solutions of H_2O_2 (54 µL, 50 wt. % in H_2O, 0.8 mmol, 4 equiv.) in MeCN (2.5 mL) and Fe(*S*,*S*-PDP) (37 mg, 0.04 mmol, 0.20 equiv,) in MeCN (0.25 mL) were added over 30 min. The crude reaction mixture was concentrated under reduced pressure to a minimal amount of MeCN, then Et_2O (50 mL) was added, resulting in a brown precipitate. The mixture was filtered through a pad of Celite and concentrated under reduced pressure. The crude reaction mixture was separated by column chromatography (CH_2Cl_2/Et_2O- 8:1) to afford ketones **43-P1**, **43-P2** and **43-P3** in 5:3:1 ratio (8.2 mg, 20% yield) and inseparable mixture of several other oxidation products (10.7 mg).

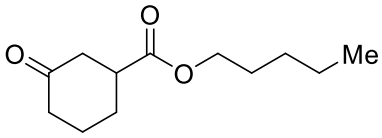

43-P1

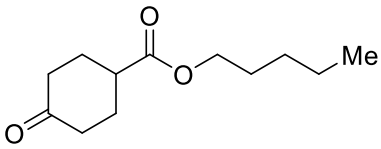

43-P2

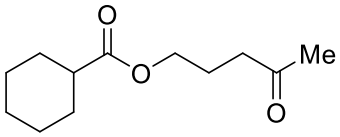

43-P3

Fe(S,S-PDP) oxidation of compound 44

To a vial charged with compound **44** (80.5 mg, 0.2 mmol), AcOH (5.7 µL, 0.1 mmol, 0.5 equiv.), MeCN (0.5 mL), and a magnetic stir bar, syringe-pumped solutions of H_2O_2 (54 µL, 50 wt. % in H_2O, 0.8 mmol, 4 equiv.) in MeCN (2.5 mL) and Fe(*S*,*S*-PDP) (37 mg, 0.04 mmol, 0.20 equiv,) in MeCN (0.25 mL) were added over 30 min. The crude reaction mixture was concentrated under reduced pressure to a minimal amount of MeCN, then Et_2O (50 mL) was added, resulting in a brown precipitate. The reaction mixture was filtered through a pad of Celite and concentrated under reduced pressure. The crude reaction mixture was separated by column chromatography (hexanes/EtOAc 2:1) to afford compound **44-P2** (25.8 mg, 30% yield).

Data for compound **44-P2**

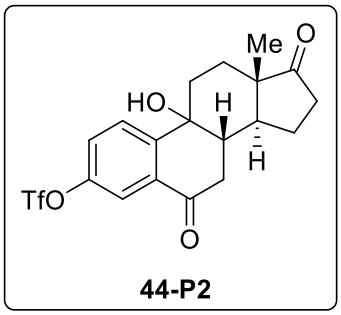

44-P2

^{1}H NMR (600 MHz, $CDCl_3$): δ 7.95 (d, *J* = 2.8 Hz, 1H), 7.71 (d, *J* = 8.7 Hz, 1H), 7.49 (dd, *J* = 8.6, 2.8 Hz, 1H), 2.92 (dd, *J* = 17.6, 13.1 Hz, 1H), 2.65 (dd, *J* = 17.6, 4.1 Hz, 1H), 2.56 – 2.45 (m, 2H), 2.37 (ddd, *J* = 13.1, 11.7, 4.2 Hz, 1H), 2.26 – 2.15 (m, 2H), 2.07 – 1.95 (m, 2H), 1.89 – 1.81 (m, 2H), 1.61 (dddd, *J* = 12.5, 9.0 Hz, 1H), 0.93 (s, 3H).
^{13}C NMR (126 MHz, $CDCl_3$): δ 219.4, 195.7, 149.6, 147.0, 134.0, 126.8, 126.7, 120.7, 118.8 (q, *J* = 320.8 Hz), 69.4, 47.6, 43.6, 40.9, 36.6, 35.8, 32.0, 27.4, 21.2, 12.9.
^{19}F NMR (376 MHz, $CDCl_3$): δ −75.4.
HRMS (ESI-TOF, m/z): HRMS (ESI) Calcd for $[M–OH]^+$ 415.0822; Found 415.0827.
$[\alpha]_D^{20}$ = 46.1 (*c*.0.76 in $CHCl_3$).

Fe(S,S-PDP) oxidation of compound 45

To a vial charged with compound **45** (56.8 mg, 0.2 mmol), AcOH (5.7 µL, 0.1 mmol, 0.5 equiv.), MeCN (0.5 mL), and a magnetic stir bar, syringe-pumped solutions of H_2O_2 (54 µL, 50 wt. % in H_2O, 0.8 mmol, 4 equiv.) in MeCN (2.5 mL) and Fe(*S*,*S*-PDP) (37 mg, 0.04 mmol, 0.20 equiv,) in MeCN (0.25 mL) were added over 30 min. The crude reaction mixture was concentrated under reduced pressure to a minimal amount of MeCN, then 10% EtOAc in Et_2O (50 mL) was added, resulting in a brown precipitate. The reaction mixture was filtered through a pad of Celite and concentrated under reduced pressure. ^{1}H NMR spectroscopic analysis of the crude reaction mixture revealed starting material and trace amounts of product.

Fe(S,S-PDP) oxidation of compound 52

To a vial charged with compound **52** (60.4 mg, 0.2 mmol), AcOH (5.7 µL, 0.1 mmol, 0.5 equiv.), MeCN (0.5 mL), and a magnetic stir bar, syringe-pumped solutions of H_2O_2 (54 µL, 50 wt. % in H_2O, 0.8 mmol, 4 equiv.) in MeCN (2.5 mL) and Fe(*S*,*S*-PDP) (37 mg, 0.04 mmol, 0.20 equiv,) in MeCN (0.25 mL) were added over 30 min. The crude reaction mixture was concentrated under reduced pressure to a minimal amount of MeCN, then Et_2O (50 mL) was added, resulting in a brown precipitate. The mixture was filtered through a pad of Celite and concentrated under reduced pressure. The crude reaction mixture was separated by column chromatography (hexanes/EtOAc 1:1) to afford compound **53** (18.0 mg, 28% yield).

Fe(S,S-PDP) oxidation of compound 63

To a vial charged with compound **63** (36.9 mg, 0.2 mmol), AcOH (5.7 µL, 0.1 mmol, 0.5 equiv.), MeCN (0.5 mL), and a magnetic stir bar, syringe-pumped solutions of H_2O_2 (54 µL, 50 wt. % in H_2O, 0.8 mmol, 4 equiv.) in MeCN (2.5 mL) and Fe(*S*,*S*-PDP) (37 mg, 0.04 mmol, 0.20 equiv,) in MeCN (0.25 mL) were added over 30 min. The crude reaction mixture was concentrated under reduced pressure to a minimal amount of MeCN, then Et_2O (50 mL) was added, resulting in a brown precipitate. The reaction mixture was filtered through a pad of Celite and concentrated under reduced pressure. ^{1}H NMR spectroscopic analysis of the crude reaction mixture using CH_2Br_2 as an internal standard revealed epoxide **64** (31% yield). The spectral data matched reported literature values.[21]

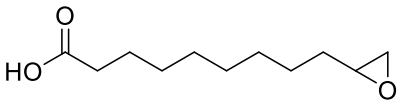

64

TFDO (INCLUDING CALIBRATION WITH KNOWN SUBSTRATES)

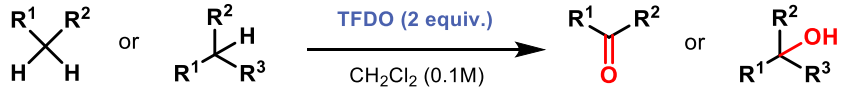

Scheme S3. TFDO oxidation of unactivated C(sp^3)–H bonds.

General Procedure

TFDO (ca. 0.4 M in trifluoroacetone) was prepared by following the procedure reported in the literature minor modifications.[22] (The details are described in the Baran Laboratory Blog: http://openflask.blogspot.com/2014/01/tfdo-synthesis-procedure.html). Following literature procedure,[52] the TFDO solution (0.2 mmol, 0.5 mL, 2.0 equiv.) was added to a stirred solution of a substrate (0.1 mmol, 1.0 equiv.) in CH_2Cl_2 (1.0 mL) at –78 °C. The reaction mixture was kept in a freezer at –20 °C for 48 h. The solvents were removed under reduced pressure, and the crude material was purified by either PTLC or flash column chromatography. The prepared TFDO solution (0.3 mL) was added to the CH_2Cl_2 solution of PPh_3 (0.1 mmol, 0.1 M), and the concentration of TFDO was determined by the NMR yield of PPh_3O.

Calibration

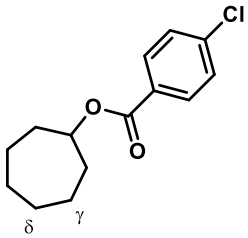

S2

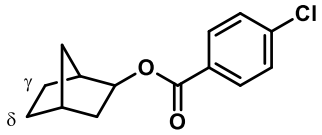

S3

Entry	NMR yield of S2	NMR yield of S2
Original report	100% (γ:δ = 15:85) (based on 2 equiv. of TFDO)	100% (γ:δ = 2:98) (based on 2 equiv. of TFDO)
Calibration	77% (γ:δ = 17:83) (based on 2 equiv. of TFDO)	72% (selectivity not determined) (based on 2 equiv. of TFDO)

Table S2. Calibration of TFDO procedure using reported substrates **S2** and **S3**.

Experimental Procedures

TFDO oxidation of compound 27

To a vial charged with compound **27** (36 mg, 0.1 mmol) in CH_2Cl_2 (1.0 mL) was added TFDO solution prepared following the described method (0.66 mL, 0.3 M, 0.2 mmol). The crude products were purified by flash column chromatography (EtOAc/hexanes-30:70) to afford 15.1 mg of inseparable mixture of **27-P1** and **27-P2** (11% based on ^{1}H NMR) and two unidentified oxidation products (combined 31% based on ^{1}H NMR).

TFDO oxidation of compound 28

This result has been previously reported.[28]

TFDO oxidation of compound 29

To a vial charged with compound **29** (25 mg, 0.1 mmol) in CH_2Cl_2 (1.0 mL) was added TFDO solution prepared following the described method (0.66 mL, 0.3 M, 0.2 mmol). The yield of oxidation products was determined by ^{1}H NMR using dibromomethane as the internal standard (92 %). Spectral data matched reported values.[43]

Data for compound **29-P3**

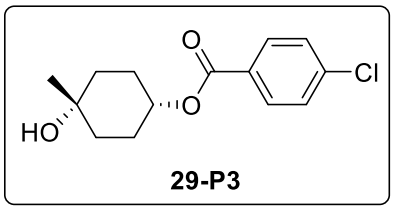

29-P3

^{1}H NMR (600 MHz, $CDCl_3$): δ 7.98 (d, *J* = 8.2 Hz, 2H), 7.41 (d, *J* = 8.2 Hz, 2H), 4.98 (dq, *J* = 9.5, 4.8 Hz, 1H), 1.87 (d, *J* = 4.5 Hz, 4H), 1.77 (d, *J* = 17.0 Hz, 2H), 1.57 (t, *J* = 10.3 Hz, 2H), 1.28 (s, 3H), 0.92 – 0.84 (m, 3H).
^{13}C NMR (151 MHz, $CDCl_3$): δ 165.2, 139.2, 131.0, 129.2, 128.7, 72.9, 68.7, 36.6, 29.7, 27.3.
HRMS (ESI-TOF, m/z): HRMS (ESI) Calcd for $[M–OH]^+$ 251.0833; Found 251.0844.

TFDO oxidation of compound 30

To a vial charged with compound **30** (17 mg, 0.1 mmol) in CH_2Cl_2 (1.0 mL) was added TFDO solution prepared following the described method (0.32 mL, 0.3 M, 0.1 mmol). The crude products were then purified by flash column chromatography (EtOAc/hexanes-20:80) to afford alcohol **30-P5** (5.6 mg, 61%). Yields were calculated based on 0.05 mmol scale to adjust the SM/TFDO ratio to the original conditions.

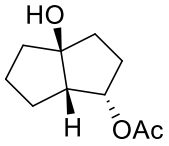

30-P5

TFDO oxidation of compound 31

To a vial charged with compound **31** (22 mg, 0.1 mmol) in CH_2Cl_2 (1.0 mL) was added TFDO solution prepared following the described method (0.66 mL, 0.3 M, 0.2 mmol). The crude products were then purified by flash column chromatography (EtOAc/hexanes-30:70) to afford alcohol **31-P2** (20.2 mg, 85%).

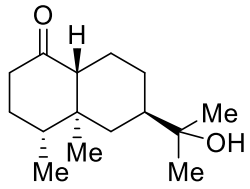

31-P2

TFDO oxidation of compound 32

To a vial charged with compound **32** (33 mg, 0.1 mmol) in CH_2Cl_2(1.0 mL) was added TFDO solution prepared following the described method (0.66 mL, 0.3 M, 0.2 mmol). The products obtained were purified by pTLC (EtOAc/hexanes-1:1) afforded **32-P1** (8.1 mg, 23% yield) as a white solid, and a complex mixture of oxidation products (15.3 mg, 44% yield), and recovered starting material (5.1 mg, 15% rsm).

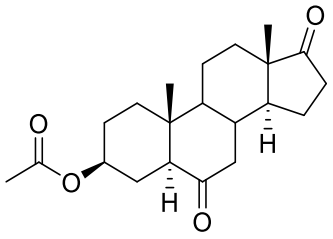

32-P1

TFDO oxidation of compound 33

To a vial charged with compound **33** (35mg, 0.1 mmol) in CH_2Cl_2(1.0 mL) was added TFDO solution prepared following the described method (0.66 mL, 0.3 M, 0.2 mmol). The products obtained were purified by pTLC (EtOAc/hexanes-3:7) afforded **33-P2** (6 mg, 17% yield) as a white solid, and a complex mixture of oxidation products (9.1 mg, 25% yield), and recovered starting material (15.8 mg, 46% rsm).

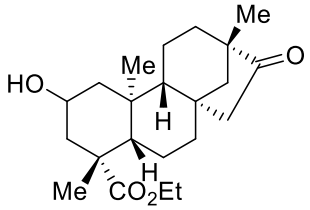

33-P2

TFDO oxidation of compound 34

To a vial charged with compound **34** (37 mg, 0.1 mmol) in CH_2Cl_2 (1.0 mL) was added TFDO solution prepared following the described method (0.32 mL, 0.3 M, 0.1 mmol). The crude reaction mixture was separated by pTLC (hexanes/EtOAc-1:1) to afford compound **34-P1** as a white solid (5.9 mg, 15 %).

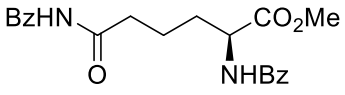

34-P1

TFDO oxidation of compound 35

To a vial charged with compound **35** (20 mg, 0.1 mmol) in CH_2Cl_2 (1.0 mL) was added TFDO solution prepared following the described method (0.32 mL, 0.3 M, 0.1 mmol). ^1H NMR spectroscopic analysis of the crude reaction mixture revealed starting material and trace amounts of product.

TFDO oxidation of compound 36

To a vial charged with compound **36** (19 mg, 0.1 mmol) in CH_2Cl_2 (1.0 mL) was added TFDO solution prepared following the described method (0.66 mL, 0.3 M, 0.2 mmol). The crude reaction mixture was purified by flash column chromatography (EtOAc/hexanes-25:75) to afford **36-P1** (10.3 mg, 50%) as a colorless oil.

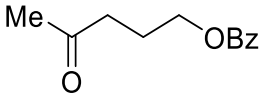

36-P1

TFDO oxidation of compound 37

To a vial charged with compound **37** (19 mg, 0.1 mmol) in CH_2Cl_2 (1.0 mL) was added TFDO solution prepared following the described method (0.66 mL, 0.3 M, 0.2 mmol). The crude reaction mixture was purified by flash column chromatography (EtOAc/hexanes-25:75) to afford a mixture of **37-P1, 37-P2,** and **37-P3** (9.6 mg, 48% yield, **37-P1**/**37-P2**/**37-P3** = 4:1:1.7)**.**

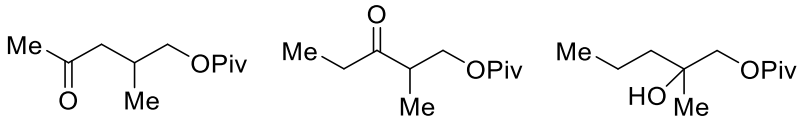

37-P1 **37-P2** **37-P3**

TFDO oxidation of compound 38

To a vial charged with compound **38** (21 mg, 0.1 mmol) in CH_2Cl_2 (1.0 mL) was added TFDO solution prepared following the described method (0.66 mL, 0.3 M, 0.2 mmol). The crude reaction mixture was purified by flash column chromatography (EtOAc/hexanes-25:75) to afford **38-P1** (18.2 mg, 83% yield)**.**

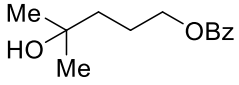

38-P1

TFDO oxidation of compound 39

To a vial charged with compound **39** (16 mg, 0.1 mmol) in CH_2Cl_2 (1.0 mL) was added TFDO solution prepared following the described method (0.32 mL, 0.3 M, 0.1 mmol). The crude

products were then purified by flash column chromatography (EtOAc/hexanes-25:75) to afford a mixture of **39-P1** and **39-P2** (7.1 mgs, **39-P1**:**39-P2** = 1:1.7).

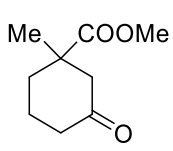

39-P1

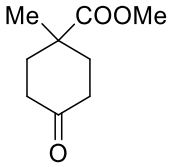

39-P2

TFDO oxidation of compound 40

To a vial charged with compound **40** (20 mg, 0.1 mmol) in CH_2Cl_2 (1.0 mL) was added TFDO solution prepared following the described method (0.32 mL, 0.3 M, 0.1 mmol). The yield of oxidation product **55** was determined to 32% by ^1H NMR using dibromomethane as the internal standard.

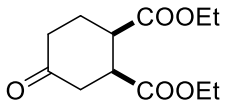

55

TFDO oxidation of compound 41

To a vial charged with compound **41** (22 mg, 0.1 mmol) in CH_2Cl_2 (1.0 mL) was added TFDO solution prepared following the described method (0.66 mL, 0.3 M, 0.2 mmol). The yield of oxidation products **41-P1** and **41-P2** were determined to be 40% (**41-P1**/**41-P2** = 5:1) by ^1H NMR using dibromomethane as the internal standard

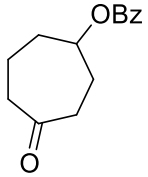

41-P1

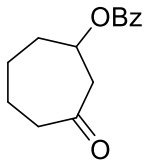

41-P2

TFDO oxidation of compound 42

To a vial charged with compound **42** (24 mg, 0.1 mmol) in CH_2Cl_2 (1.0 mL) was added TFDO solution prepared following the described method (0.32 mL, 0.3 M, 0.1 mmol). The crude products were then purified by flash column chromatography (EtOAc/hexanes-20:80) to afford **42-P1** (5.6 mg, 44%) and **42-P2** (1.9 mg, 14%).

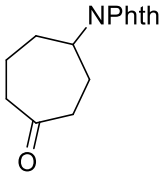

42-P1

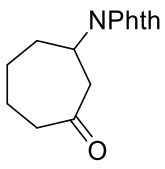

42-P2

TFDO oxidation of compound 43

To a vial charged with compound **43** (20 mg, 0.1 mmol) in CH_2Cl_2 (1.0 mL) was added TFDO solution prepared following the described method (0.66 mL, 0.3 M, 0.2 mmol). The crude reaction mixture was purified by flash column chromatography (EtOAc/hexanes-25:75) to afford an inseparable mixture of **43-P1, 43-P2,** and **43-P3** (5.9 mg, 28% yield, **43-P1**/**43-P2**/**43-P3** = 1:1:0.75).

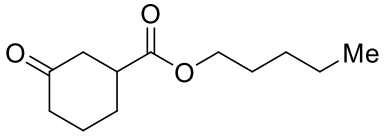

43-P1

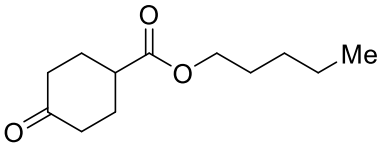

43-P2

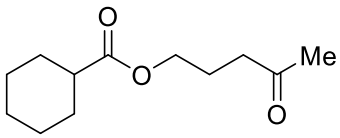

43-P3

TFDO oxidation of compound 44

To a vial charged with compound **44** (40 mg, 0.1 mmol) in CH_2Cl_2 (1.0 mL) was added TFDO solution prepared following the described method (0.66 mL, 0.3 M, 0.2 mmol). The crude reaction mixture was purified by pTLC (CH_2Cl_2/acetone - 100:1) to afford compound **44-P3** (4.5 mg, 11% yield) as a crystalline solid, and **44-P4** (6.1 mg, 15% yield).

Data for compound **44-P3**:

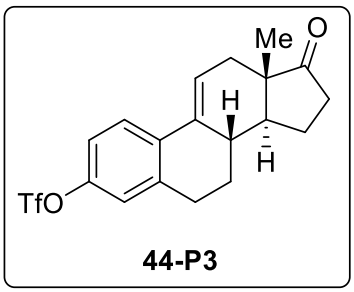

44-P3

^{1}H NMR (600 MHz, $CDCl_3$): δ 7.64 (d, *J* = 8.9 Hz, 1H), 7.04 (dd, *J* = 8.8, 2.8 Hz, 1H), 7.01 (d, *J* = 2.9 Hz, 1H), 6.31 – 6.30 (m, 1H), 2.96 – 2.93 (m, 2H), 2.57 – 2.51 (m, 1H), 2.38 – 2.18 (m, 6H), 1.71 – 1.64 (m, 2H), 1.51 – 1.44 (m, 1H), 0.94 (s, 3H).
^{13}C NMR (151 MHz, $CDCl_3$): δ 211.1, 148.3, 138.5, 134.71, 134.69, 126.1, 121.7, 121.4, 119.0, 118.9 (q, *J* = 321.0 Hz), 47.9, 46.2, 38.0, 36.3, 34.3, 29.8, 27.4, 22.6, 14.7.
^{19}F NMR (376 MHz, $CDCl_3$): δ -75.6 ppm.
HRMS (ESI-TOF, m/z): HRMS (ESI) Calcd for $[M+H]^+$ 401.1029; Found 401.1039.
R_f = 0.55 (5% Et_2O in CH_2Cl_2); Stain: Anisaldehyde.
$[\alpha]_D^{20}$ = 78.4 (*c*.0.50 in $CHCl_3$).

Data for compound **44-P4**:

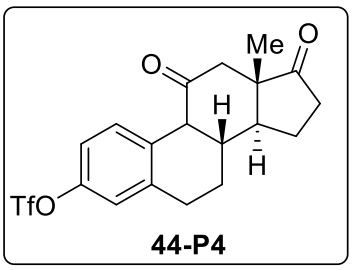

44-P4

^{1}H NMR (500 MHz, $CDCl_3$): δ 7.08 – 7.07 (m, 2H), 7.02 (dd, *J* = 9.0, 2.2 Hz, 1H), 3.75 (d, *J* = 5.4 Hz, 1H), 2.98 – 2.82 (m, 2H), 2.63 – 2.46 (m, 3H), 2.30 – 2.06 (m, 5H), 1.90 – 1.83 (m, 1H), 1.76 – 1.72 (m, 1H), 0.96 (s, 3H).
^{13}C NMR (151 MHz, $CDCl_3$): δ 216.8, 210.0, 148.4, 138.5, 131.4, 129.8, 122.6, 119.6, 118.2 (q, *J* = 321.0 Hz), 54.1, 50.5, 46,7, 41.9, 36.1, 32.7, 24.8, 22.8, 21.5, 15.0.
^{19}F NMR (376 MHz, $CDCl_3$): δ -75.6 ppm.
HRMS (ESI-TOF, m/z): HRMS (ESI) Calcd for $[M+H]^+$ 417.0978; Found 417.0982.
R_f = 0.45 (10% hexanes in CH_2Cl_2); Stain: Anisaldehyde. **$[\alpha]_D^{20}$** = 89.4 (*c*.0.50 in $CHCl_3$).

Structural assignment of these two compounds is based on literature precedents for dioxirane oxidation at C9 position,[23,24] on our NMR spectroscopic data and on comparison with NMR data previously reported for structurally related estrone derivatives. Dioxirane oxidation affords C9-hydroxy derivatives which have been reported to undergo facile dehydration to $\Delta^{9,11}$ unsaturated derivate (**44-P3** in our case). Subsequent epoxidation and 1,2-hydride shift would then afford C11-ketone, which has also been suggested for a related estrone derivative.[25] Moreover, the ^{1}H chemical shift and interaction constant of benzylic C–H in **44-P4** (3.75 ppm, d, 1H, J = 5.8 Hz) is similar to the same signal of related mesylate-protected estrone (3.70 ppm, d, 1H, J = 5.4 Hz).

TFDO oxidation of compound 45

To a vial charged with compound **45** (28 mg, 0.1 mmol) in CH_2Cl_2 (1.0 mL) was added TFDO solution prepared following the described method (0.32 mL, 0.3 M, 0.1 mmol). ^{1}H NMR spectroscopic analysis of the crude reaction mixture revealed no reaction.

TFDO oxidation of compound 52

To a vial charged with compound **52** (30 mg, 0.1 mmol) in CH_2Cl_2 (1.0 mL) was added TFDO solution prepared following the described method (0.32 mL, 0.3 M, 0.1 mmol). ^{1}H NMR spectroscopic analysis of the crude reaction mixture revealed low conversion.

TFDO oxidation of compound 63

To a vial charged with compound **63** (18 mg, 0.1 mmol) in CH_2Cl_2 (1.0 mL) was added TFDO solution prepared following the described method (0.32 mL, 0.3 M, 0.1 mmol). The yield was determined by ^{1}H NMR analysis of the crude mixture (quantitative).

TBADT (INCLUDING CALIBRATION WITH KNOWN SUBSTRATES)

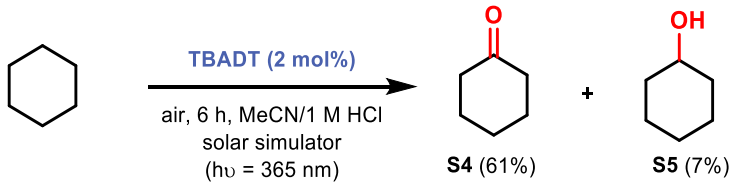

Scheme S4. TBADT oxidation of unactivated C(sp^3) –H bonds.

Preface

TBADT photocatalyzed C(sp^3)–H oxidation in flow has been reported.[51] Therein, a single example in batch (see Scheme S4) was shown to convert cyclohexane into cyclohexanone (**S4**) and cyclohexanol (**S5**). Our comparison was carried out utilizing this batch procedure with some modifications for ease and accessibility of setup. As depicted in Figure S17, we used 16 × 125 mm reaction tubes and 8 × 9W LED light bulbs (hν = 365 nm) instead of the solar window ledge glassware and solar simulator (hν = 365 nm) that were used respectively in this reported procedure. Notably, our set-up has been previously reported for use in decatungstate catalyzed C–H fluorination reactions.[26] Tetrabutylammonium decatungstate (TBADT) was purchased from Sigma Aldrich.

General Procedure

To a vial charged with substrate in a solvent mixture of MeCN/1 M aq. HCl (0.14 M, 2.5:1), was added TBADT catalyst (2 mol %). The resulting reaction mixture was placed under an O_2 atmosphere and irradiated with 365 nm light for 6 h. Subsequently, the reaction mixture was filtered over Celite and concentrated under reduced pressure. The crude products were then purified by flash column chromatography as indicated.

Experimental Setup

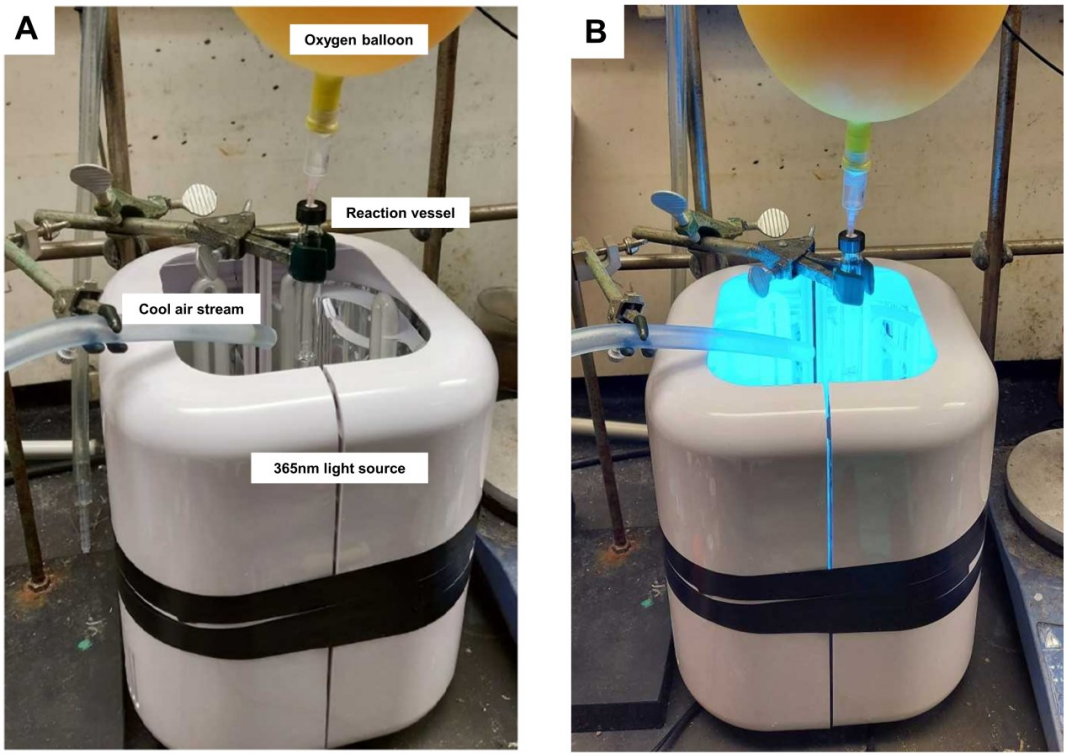

Figure S17. **A)** Experimental setup. **B)** Sample under irradiation.

Calibration

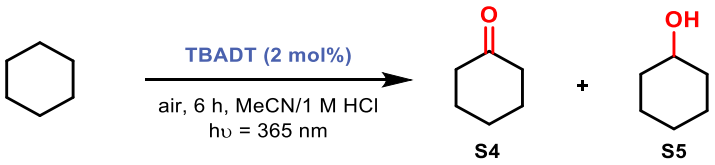

Entry	GC yield of S4	GC yield of S5
Original report	61%	7%
Calibration	26%	trace

Table S3. Calibration of TBADT oxidation using reported substrate cyclohexane.

A dilute solution in diethyl ether containing a 1:1 mixture of 2-methylcyclohexanone (internal standard) and S4 (product) were used to calibrate the instrument. The average of three separate runs of this solution determined S4 to be 94% sensitive relative to the internal standard.

Experimental Procedures

TBADT oxidation of compound 27

To a vial charged with compound **27** (12.5 mg, 0.035 mmol) in 0.25 mL of MeCN/CH_2Cl_2 (2.5:1), was added TBADT catalyst (2.3 mg). The crude products were then purified by flash column chromatography (EtOAc/hexanes-30:70). ^{1}H NMR spectroscopic analysis of the crude

reaction mixture and of several fractions obtained from purification revealed a complex mixture of possible oxidation products.

TBADT oxidation of compound 28

To a vial charged with compound **28** (19.8 mg, 0.100 mmol) in a 0.70 mL of MeCN/1 M aq. HCl (2.5:1), was added TBADT catalyst (6.6 mg). The crude products were then purified by flash column chromatography (EtOAc/hexanes-40:60) to afford a mixture of several oxidation products (6.1 mg, 20% yield) including **28-P1**, **28-P2**, and **28-P3** (**28-P1**/**28-P2**/**28-P3** = 0.6:1:2). Spectral data matched reported values for **28-P3**.[14]

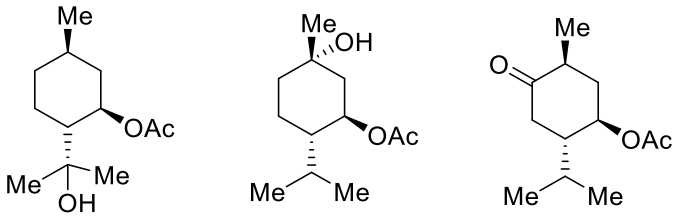

28-P1 **28-P2** **28-P3**

TBADT oxidation of compound 29

To a vial charged with compound **29** (75.9 mg, 0.300 mmol) in 2.14 mL of MeCN/CH_2Cl_2 (2.5:1), was added TBADT catalyst (49.8 mg, 5 mol%). ^{1}H NMR spectroscopic analysis of the crude reaction mixture revealed a trace amount product and recovered starting material.

TBADT oxidation of compound 30

To a vial charged with compound **30** (16.8 mg, 0.100 mmol) in a 0.70 mL of MeCN/CH_2Cl_2 (2.5:1), was added TBADT catalyst (6.6 mg). The crude products were then purified by flash column chromatography (EtOAc/hexanes-25:75) to afford a mixture of **30-P1** and **30-P2** (2.4 mg, 11% yield).

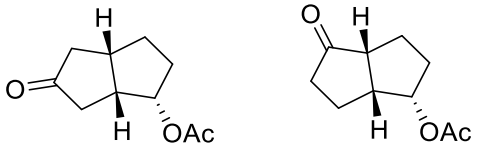

30-P1 **30-P2**

TBADT oxidation of compound 31

To a vial charged with compound **31** (22.2 mg, 0.100 mmol) in 0.70 mL of MeCN/1 M aq. HCl (2.5:1), was added TBADT catalyst (6.6 mg). ^{1}H NMR spectroscopic analysis of the crude reaction mixture revealed a complex mixture of possible oxidation products.

TBADT oxidation of compound 32

To a vial charged with compound **32** (33.3 mg, 0.100 mmol) in 0.70 mL of MeCN/CH_2Cl_2 (2.5:1), was added TBADT catalyst (6.6 mg). The crude reaction mixture was then purified by flash column chromatography (EtOAc/hexanes-25:75) to afford a mixture of several oxidation products (11.1 mg, 32% yield) including **32-P1** (3.3 mg, 10% yield).

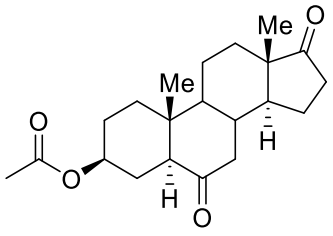

32-P1

TBADT oxidation of compound 33

To a vial charged with compound **33** (34.7 mg, 0.100 mmol) in 0.70 mL of MeCN/1 M aq. HCl (2.5:1), was added TBADT catalyst (6.6 mg). The crude products were then purified by flash column chromatography (EtOAc/hexanes-50:50). ^{1}H NMR spectroscopic analysis of the crude products and several fractions obtained from purification revealed a complex mixture of possible oxidation products.

TBADT oxidation of compound 34

To a vial charged with compound **34** (36.8 mg, 0.100 mmol) in a 0.70 mL of MeCN/CH_2Cl_2 (2.5:1), was added TBADT catalyst (6.6 mg). ^{1}H NMR spectroscopic analysis of the crude reaction mixture revealed starting material and trace amounts of product.

TBADT oxidation of compound 35

To a vial charged with compound **35** (20.3 mg, 0.100 mmol) in a solvent mixture of MeCN/CH_2Cl_2 (2.5:1), was added TBADT catalyst (6.6 mg). After 6 h, 3 M aq. HCl was added to the reaction mixture. The desired dealkylation product was not detectable by ^{1}H NMR spectroscopic analysis of the crude reaction mixture.

TBADT oxidation of compound 36

To a vial charged with compound **36** (57.7 mg, 0.300 mmol) in 2.14 mL of MeCN/1 M aq. HCl (0.14 M, 2.5:1), was added TBADT catalyst (6.6 mg). The crude products were then purified by flash column chromatography (EtOAc/hexanes-10:90) to afford **36-P1** (4.3 mg, 7% yield) and **36-P2** (2.1 mg, 3% yield).

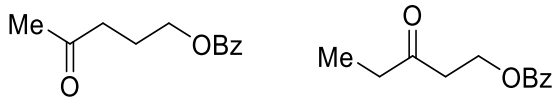

36-P1 **36-P2**

TBADT oxidation of compound 37

To a vial charged with compound **37** (55.9 mg, 0.300 mmol) in 2.14 mL of MeCN/1 M aq. HCl (2.5:1), was added TBADT catalyst (49.8 mg, 5 mol %). ^{1}H NMR spectroscopic analysis of the crude reaction mixture revealed trace amounts of product.

TBADT oxidation of compound 38

To a vial charged with compound **38** (61.9 mg, 0.300 mmol) in 2.14 mL of MeCN/1 M aq. HCl (0.14 M, 2.5:1), was added TBADT catalyst (19.9 mg). The crude products were then purified by flash column chromatography (EtOAc/hexanes-10:90) to afford **38-P1** (4.0 mg, 6% yield).

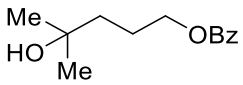

38-P1

TBADT oxidation of compound 39

To a vial charged with compound **39** (15.6 mg, 0.100 mmol) in 0.70 mL of MeCN/1 M aq. HCl (2.5:1), was added TBADT catalyst (6.6 mg). The crude products were then purified by flash column chromatography (EtOAc/hexanes-25:75) to afford a mixture of **39-P1** and **39-P2** (7.4 mg, 44% yield, **39-P1**/**39P2** = 1:4).

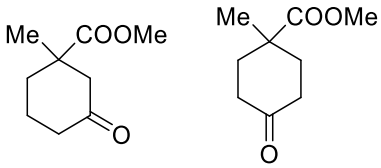

39-P1 **39-P2**

TBADT oxidation of compound 40

To a vial charged with compound **40** (60.1 mg, 0.300 mmol) in 2.14 mL of MeCN/1 M aq. HCl (2.5:1), was added TBADT catalyst (19.9 mg). The crude products were then purified by flash column chromatography (EtOAc/hexanes – 20:80) to afford **55** (20.4 mg, 32% yield).

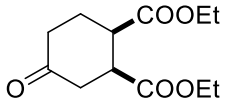

55

TBADT oxidation of compound 41

To a vial charged with compound **41** (21.8 mg, 0.100 mmol) in 0.70 mL of MeCN/CH_2Cl_2 (2.5:1), was added TBADT catalyst (6.6 mg). The crude products were then purified by flash column chromatography (EtOAc/hexanes-20:80) afforded a mixture of **41-P1** and **41-P2** (12.5 mg, 54% yield, **41-P1**/**41-P2** = 1.8:1).

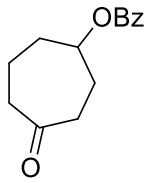

41-P1

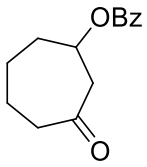

41-P2

TBADT oxidation of compound 42

To a vial charged with compound **42** (24.9 mg, 0.100 mmol) in 0.70 mL of MeCN/CH_2Cl_2 (2.5:1), was added TBADT catalyst (6.6 mg). The crude products were then purified by flash column chromatography (EtOAc/hexanes-40:60) to afford a mixture of **42-P1** and **42-P2** (14.0 mg, 53%, **42-P1**/**42-P2** = 2:1).

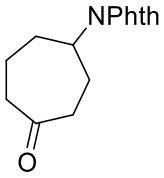

42-P1

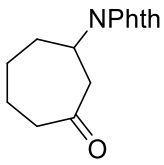

42-P2

TBADT oxidation of compound 43

To a vial charged with compound **43** (59.5 mg, 0.300 mmol) in 2.14 mL of MeCN/1 M aq. HCl (2.5:1), was added TBADT catalyst (24.9 mg). The crude products were then purified by flash column chromatography (EtOAc/hexanes-25:75) to afford a mixture of **43-P1** and **43-P2** (16.4 mg, 26% yield, **43-P1**/**43-P2** = 1.3:1).

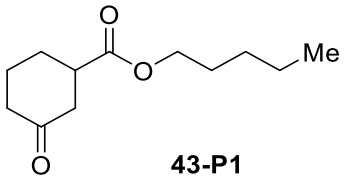

43-P1

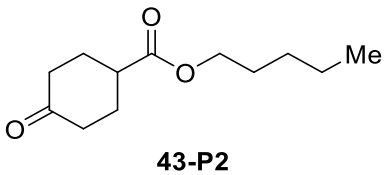

43-P2

TBADT oxidation of compound 44

To a vial charged with compound **44** (40 mg, 0.100 mmol) in 0.70 mL of MeCN:CH_2Cl_2 (2.5:1), was added TBADT catalyst (6.6 mg). The crude product was then purified by pTLC (CH_2Cl_2) to afford **44-P1** (6.0 mg, 14% yield).

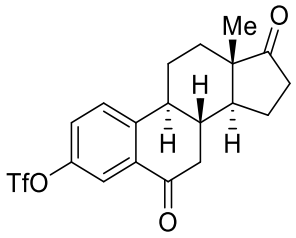

44-P1

TBADT oxidation of compound 45

To a vial charged with compound **45** (28.4 mg, 0.100 mmol) in a solvent mixture of MeCN/1 M aq. HCl (2.5:1), was added TBADT catalyst (2 mol %). ^{1}H NMR spectroscopic analysis of the crude reaction mixture revealed no detectable products.

TBADT oxidation of compound 52

To a vial charged with compound **52** (30.2 mg, 0.100 mmol) in 0.70 mL of MeCN/1 M aq. HCl (2.5:1), was added TBADT catalyst (6.6 mg). The crude products were then purified by flash column chromatography (EtOAc/hexanes-70:30) to afford **53** (13.1 mg, 42%).

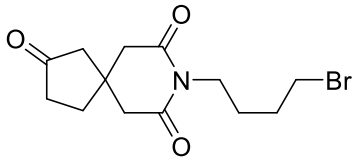

53

TBADT oxidation of compound 63

To a vial charged with compound **63** (30.2 mg, 0.100 mmol) in 0.70 mL of MeCN/1 M aq. HCl (2.5:1), was added TBADT catalyst (6.6 mg). ^{1}H NMR spectroscopic analysis of the crude reaction mixture revealed trace amounts of **64**.

RUTHENIUM (INCLUDING CALIBRATION WITH KNOWN SUBSTRATES)

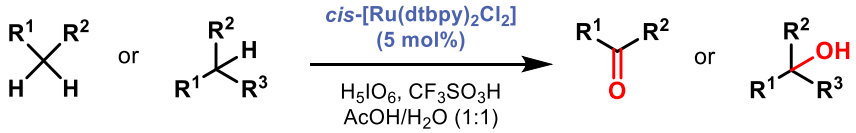

Scheme S5. *cis*-[Ru(dtbpy)$_2$Cl$_2$] oxidation of unactivated C(sp^3)–H bonds.

General Procedure

Catalyst *cis*-[Ru(dtbpy)$_2$Cl$_2$] was prepared following a literature procedure.[50] Physical and spectroscopic properties of *cis*-[Ru(dtbpy)$_2$Cl$_2$] match those reported in the literature.[27]

Methods A, B and C were adapted from a literature procedure.[50]

Method A. A 10-mL glass vial containing substrate (0.2 mmol) was charged with a solution of *cis*- [Ru(dtbpy)$_2$Cl$_2$] (7.1 mg, 0.01 mmol, 5 mol %) in 1.6 mL of AcOH. To this solution was added aqueous trifluoromethanesulfonic acid (1.6 mL, 0.75 M, 1.20 mmol, 6.0 equiv). The purple solution was stirred for 2 min before a single portion of solid H_5IO_6 (91.2 mg, 0.40 mmol, 2.0 equiv.) was added. After stirring for 8 h, the reaction mixture was transferred to a separatory funnel with 4 mL of H_2O and 4 mL of a 3:1 $CHCl_3$/*i*-PrOH solution. The pH of the aqueous mixture was then made basic (pH ~14) with ~30 mL of 2 M aq. NaOH. The aqueous layer was extracted with 3 × 10 mL of a 3:1 $CHCl_3$/*i*-PrOH solution. The combined organic extracts were dried over Na_2SO_4, filtered, and concentrated under reduced pressure to give a purple oil. Purification of the isolated material was performed by chromatography on silica gel or by pTLC.

Method B. A 10-mL glass vial containing substrate (0.2 mmol) was charged with a solution of *cis*- [Ru(dtbpy)$_2$Cl$_2$] (7.1 mg, 0.01 mmol, 5 mol%) in 1.6 mL of AcOH. To this solution was added 1.6 mL of H_2O. The purple solution stirred for 2 min before a single portion of solid H_5IO_6 (91.2 mg, 0.40 mmol, 2.0 equiv.) was added. After stirring for 8 h, the reaction mixture was transferred to a separatory funnel with 4 mL of CH_2Cl_2 and 30 mL of H_2O. Then, the aqueous layer was extracted with 3 × 10 mL of CH_2Cl_2. The combined organic extracts were dried over Na_2SO_4, filtered, and concentrated under reduced pressure. Residual AcOH was removed by dissolving this material in ~10 mL of heptanes and concentrating this solution under reduced pressure (this co-evaporation was performed twice). Purification of the isolated material was performed by pTLC.

Method C. A 10-mL glass vial containing substrate (0.2 mmol) was charged with a solution of *cis*-[Ru(dtbpy)$_2$Cl$_2$] (7.1 mg, 0.01 mmol, 5 mol %) in 1.6 mL of AcOH. To this solution was added 1.6 mL of H_2O. The purple solution stirred for 2 min before a single portion of solid H_5IO_6 (91.2 mg, 0.40 mmol, 2.0 equiv) was added. After stirring for 8 h, the reaction mixture was transferred to a separatory funnel with 4 mL of CH_2Cl_2 and 30 mL of sat. aq. $NaHCO_3$ solution. The aqueous layer was extracted with 3 × 10 mL of CH_2Cl_2. The combined organic extracts were dried over Na_2SO_4, filtered, and concentrated under reduced pressure to give a purple oil. Purification of the isolated material was performed by chromatography on silica gel or by pTLC.

Calibration

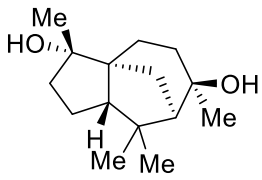

S6

Entry	yield of S6
Original report	55%
Calibration	47%

Table S4. Calibration of *cis*-[Ru(dtbpy)$_2$Cl$_2$] oxidation procedure using reported substrate cedrol.

cis-[Ru(dtbpy)$_2$Cl$_2$] oxidation of compound 9

Compound **9** (51.7 mg, 0.2 mmol) was reacted according to **Method C**. The resulting crude products were purified by pTLC (CH_2Cl_2/Et_2O –5:2) to afford **10a** (5.6 mg, 11% yield) as a white solid, **10d** (4.9 mg, 9% yield) as a white solid, a mixture of other unidentified oxidation products (7 mg, 13% yield), and recovered starting material (24 mg, 46% rsm). Spectral data for **10d** matched reported literature values.[12]

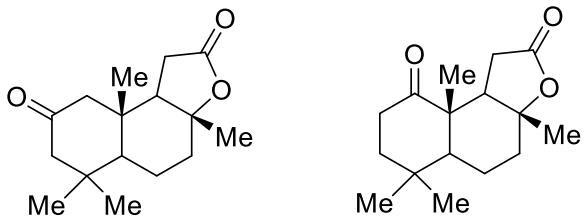

cis-[Ru(dtbpy)$_2$Cl$_2$] oxidation of compound 27

Compound **27** (72.1 mg, 0.2 mmol) was reacted according to **Method C**. The resulting crude products were purified by column chromatography (EtOAc/hexanes 1:3 → 1:1) to afford **27-P2** (3.9 mg, 5% yield) as a white solid, a mixture of other unidentified oxidation products (16.6 mg, 23%), and recovered starting material (11.5 mg, 16% rsm).

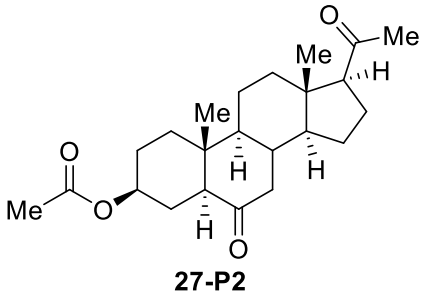

cis-[Ru(dtbpy)$_2$Cl$_2$] oxidation of compound 28

Compound **28** (39.7 mg, 0.2 mmol) was reacted according to **Method C**. The resulting crude products were purified by pTLC (EtOAc/hexanes-1:1) to afford **28-P2a/b** (23.3 mg, 54% yield, **28-P2a**/**28-P2b** = 4:1) as a colorless oil and **28-P4** (7.6 mg, 17% yield) as a colorless oil. Spectral data for **28-P2a** and **28-P2b** matched literature values (*62*, *70*).

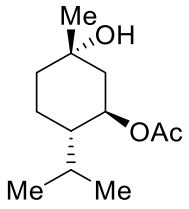

28-P2a

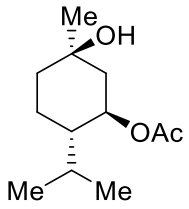

28-P2b

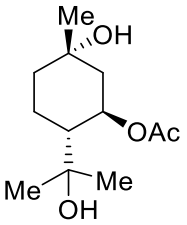

28-P4

Data for compound **28-P4:**

^{1}H NMR (600 MHz, $CDCl_3$): δ 5.17 (td, *J* = 11.0, 4.3 Hz, 1H), 2.09 (d, *J* = 12.8 Hz, 1H), 2.06 (s, 3H), 1.74 (s, 1H), 1.68 (d, *J* = 26.7 Hz, 2H), 1.52 – 1.46 (m, 1H), 1.43 – 1.39 (m, 1H), 1.39 – 1.34 (m, 1H), 1.25 (s, 3H), 1.18 (d, *J* = 6.0 Hz, 6H).

^{13}C NMR (151 MHz, $CDCl_3$): δ 169.8, 73.9, 73.2, 71.1, 51.7, 44.8, 38.1, 31.3, 28.7, 26.0, 23.1, 21.8.

HRMS (ESI-TOF, m/z): HRMS (ESI) Calcd for $[M+Na]^+$ 253.1410; Found 253.1422.

cis-[Ru(dtbpy)$_2$Cl$_2$] oxidation of compound 29

Compound **29** (50.5 mg, 0.2 mmol) was reacted according to **Method C**. The resulting crude products were purified by pTLC (EtOAc/hexanes-3:7) to afford **29-P3** (5.4 mg, 10% yield) as a white solid, and recovered starting material (11.5 mg, 23% rsm).

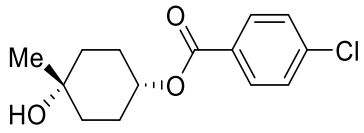

29-P3

cis-[Ru(dtbpy)$_2$Cl$_2$] oxidation of compound 30

Compound **30** (33.6 mg, 0.2 mmol) was reacted according to **Method C**. The resulting crude products were purified by column chromatography (EtOAc/hexanes 1:4 → 1:1) to afford **30-P5** (14.9 mg, 40% yield) as a colorless oil.

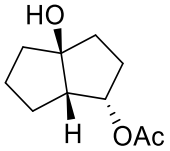

30-P5

cis-[Ru(dtbpy)$_2$Cl$_2$] oxidation of compound 31

Compound **31** (44.5 mg, 0.2 mmol) was reacted according to **Method C**. The resulting crude products were purified by column chromatography (EtOAc/hexanes-1:2) to afford **31-P2** (25.2 mg, 53% yield) as a colorless oil.

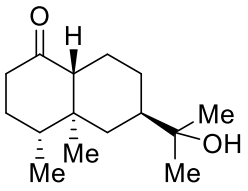

31-P2

cis-[Ru(dtbpy)$_2$Cl$_2$] oxidation of compound 32

Compound **32** (66.5 mg, 0.2 mmol) was reacted according to **Method C**. The resulting crude products were purified by pTLC (EtOAc/hexanes-1:1) to afford **32-P1** (5.5 mg, 8% yield) as a white solid, a mixture of several oxidation products (19.4 mg, 28% yield), and recovered starting material (17.6 mg, 26% rsm).

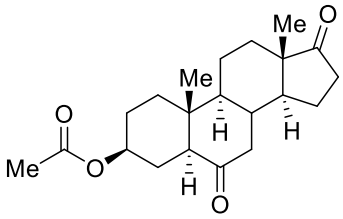

32-P1

cis-[Ru(dtbpy)$_2$Cl$_2$] oxidation of compound 33

Compound **33** (69.3 mg, 0.2 mmol) was reacted according to **Method C** and afforded trace amounts of product (<5%).

cis-[Ru(dtbpy)$_2$Cl$_2$] oxidation of compound 34

Compound **34** (73.3 mg, 0.2 mmol) was reacted according to **Method A**. The resulting crude products were purified by column chromatography (EtOAc/hexanes-1:2 → 1:1) to afford **34-P1** (10.4 mg, 14% yield) as a white solid.

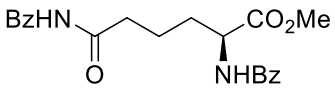

34-P1

cis-[Ru(dtbpy)$_2$Cl$_2$] oxidation of compound 35

Compound **35** (40.7 mg, 0.2 mmol) was reacted according to **Method A**. The resulting crude products were purified by pTLC (CH_2Cl_2/MeOH-9:1) to afford **35-P1** (8.3 mg, 34% yield) as a white solid.

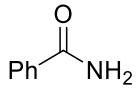

35-P1

cis-[Ru(dtbpy)$_2$Cl$_2$] oxidation of compound 36

Compound **36** (38.5 mg, 0.2 mmol) was reacted according to **Method C**. The resulting crude products were purified by pTLC (EtOAc/hexanes-3:7) to afford **36-P1** (5.9 mg, 14% yield), and recovered starting material (29 mg, 75% rsm).

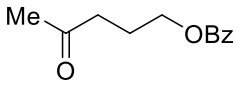

36-P1

cis-[Ru(dtbpy)$_2$Cl$_2$] oxidation of compound 37

Compound **37** (37.3 mg, 0.2 mmol) was reacted according to **Method C** and afforded trace amounts of product (<5%).

cis-[Ru(dtbpy)$_2$Cl$_2$] oxidation of compound 38

Compound **38** (41.3 mg, 0.2 mmol) was reacted according to **Method C**. The resulting crude products were purified by column chromatography (EtOAc/hexanes 1:10 → 2:3) to afford **38-P1** (27.1 mg, 61% yield) as a colorless oil.

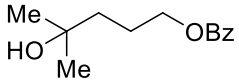

38-P1

cis-[Ru(dtbpy)$_2$Cl$_2$] oxidation of compound 39

Compound **39** (31.2 mg, 0.2 mmol) was reacted according to **Method C** and afforded trace amounts of product (<5%).

cis-[Ru(dtbpy)$_2$Cl$_2$] oxidation of compound 40

Compound **40** (40.0 mg, 0.2 mmol) was reacted according to **Method C** and afforded trace amounts of product (<5%).

cis-[Ru(dtbpy)$_2$Cl$_2$] oxidation of compound 41

Compound **41** (43.7 mg, 0.2 mmol) was reacted according to **Method C**. The resulting crude products were purified by pTLC (EtOAc: hexanes-2:8) afforded **41-P1** (14 mg, 30% yield) and recovered starting material (12.3 mg, 28% rsm).

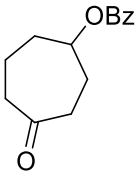

41-P1

cis-[Ru(dtbpy)$_2$Cl$_2$] oxidation of compound 42

Compound **42** (48.7 mg, 0.2 mmol) was reacted according to **Method A**. The resulting crude products were purified by column chromatography (EtOAc/hexanes-3:7) to afford **42-P1** and **42-P2** (8.5 mg, 17%, **42-P1**/**42-P2** = 1.3:1) as a white solid and recovered starting material (23.9 mg, 49% rsm).

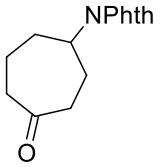

42-P1

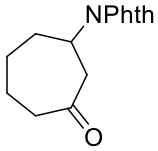

42-P2

cis-[Ru(dtbpy)$_2$Cl$_2$] oxidation of compound 43

Compound **43** (39.7 mg, 0.2 mmol) was reacted according to **Method C**. The resulting crude products were purified by column chromatography (CH_2Cl_2/Et_2O - 8:1) to afford a mixture of **43-P1** and **43-P3** (5.5 mg, 13%, **43-P1**/**43-P2** = 1:1).

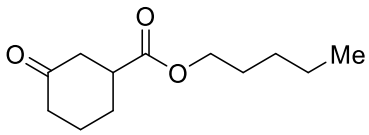

43-P1

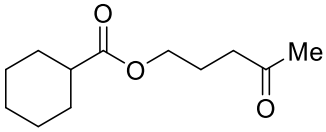

43-P3

cis-[Ru(dtbpy)$_2$Cl$_2$] oxidation of compound 44

Compound **44** (80.5 mg, 0.2 mmol) was reacted according to **Method C**. The resulting crude products were purified by pTLC (EtOAc/hexanes-1:2) to afforded **44-P1** (29.3 mg, 35% yield), **44-P2** (26.4 mg, 31% yield), as a white solid, and recovered starting material (7.8 mg, 10% rsm).

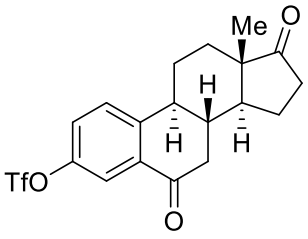

44-P1

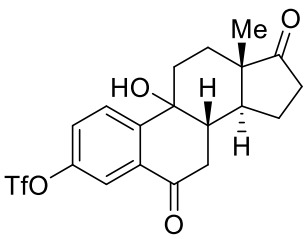

44-P2

cis-[Ru(dtbpy)$_2$Cl$_2$] oxidation of compound 45

Compound **45** (50 mg, 0.2 mmol) was reacted according to **Method A**. This afforded a complex mixture of oxidation products (10 mg, 17% yield) and recovered starting material (21.6 mg, 43% rsm).

cis-[Ru(dtbpy)$_2$Cl$_2$] oxidation of compound 50

Compound **50** (60.4 mg, 0.2 mmol) was reacted according to **Method A**. The resulting crude products were purified by preparative TLC (EtOAc/hexanes-1:1) to afford **53** (3.3 mg, 5% yield), and recovered starting material (25.7 mg, 43% rsm).

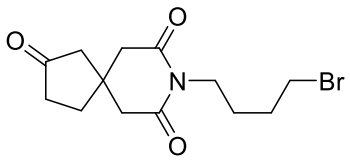

53

cis-[Ru(dtbpy)$_2$Cl$_2$] oxidation of compound 63

Compound **63** (36.9 mg, 0.2 mmol) was reacted according to **Method B** and afforded a complex mixture of oxidation products.

QUINUCLIDINE ELECTROCHEMICAL C–H OXIDATION

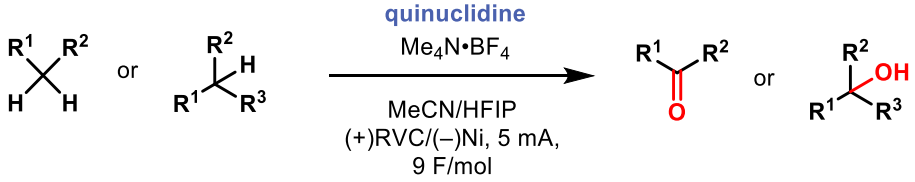

Scheme S6. Quinuclidine electrochemical C–H oxidation of unactivated C–H bonds.

General Procedure

Quinuclidine mediated electrochemical C–H oxidation was evaluated following procedures from our previous report.[43] To an ElectraSyn reaction vial charged with substrate (1 equiv) in 2.00 mL of MeCN was added HFIP (0.20 mL), tetramethylammonium tetrafluoroborate (Me_4NBF_4) (1.0 equiv.) and quinuclidine (1.0 equiv.). As depicted in the graphical guide (see page S11), using a RVC anode and a Ni-plate cathode the resulting reaction mixture was electrolyzed under a constant current of 5 mA for 9 F/mol. Subsequently, the resulting reaction mixture was concentrated under reduced pressure and the crude product was purified by either flash column chromatography or pTLC.

Experimental Procedures

Quinuclidine oxidation of compound 27

To an ElectraSyn vial charged with compound **27** (72.0 mg, 0.2 mmol) in 2.00 mL of MeCN was added 0.20 mL of HFIP, Me_4NBF_4 (32 mg, 0.2 mmol) and quinuclidine (22.2 mg, 0.2 mmol). ^{1}H NMR spectroscopic analysis of the crude reaction mixture revealed no reaction.

Quinuclidine oxidation of compound 28

To an ElectraSyn vial charged with compound **28** (39.7 mg, 0.2 mmol) in 2.00 mL of MeCN was added 0.20 mL of HFIP, Me_4NBF_4 (32 mg, 0.2 mmol) and quinuclidine (22.2 mg, 0.2 mmol). ^{1}H NMR spectroscopic analysis of the crude reaction mixture revealed no reaction.

Quinuclidine oxidation of compound 29

This result has been previously reported.[43]

Quinuclidine oxidation of compound 30

To an ElectraSyn vial charged with compound **30** (33.6 mg, 0.2 mmol) in 2.00 mL of MeCN was added 0.20 mL of HFIP, Me_4NBF_4 (32 mg, 0.2 mmol) and quinuclidine (22.2 mg, 0.2 mmol). The crude products were then purified by flash column chromatography (EtOAc/hexanes-30:70) to afford **30-P4** (11.9 mg, 30% yield) and the mixture of **30-P1** and **30-P2** (3.3 mg, 9% yield).

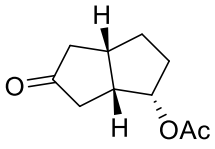

30-P1

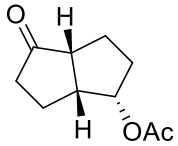

30-P2

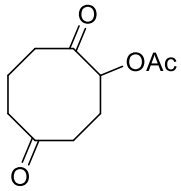

30-P4

Data for compound **30-P4**:

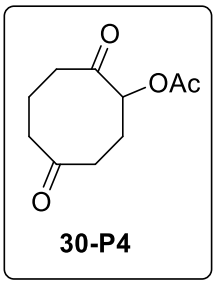

30-P4

^{1}H NMR (600 MHz, $CDCl_3$): δ 5.20 (dd, *J* = 7.4, 3.4 Hz, 1H), 2.79 – 2.60 (m, 3H), 2.60 – 2.49 (m, 3H), 2.46 (ddd, *J* = 13.3, 8.1, 3.8 Hz, 1H), 2.29 – 2.19 (m, 3H), 2.18 (s, 3H).
^{13}C NMR (151 MHz, $CDCl_3$): δ 212.4, 207.9, 170.4, 77.3, 42.3, 39.6, 37.3, 27.2, 22.6, 20.78.
HRMS (APCI-TOF, m/z): HRMS (APCI) Calcd for $[M+H]^+$ 199.0965; Found 199.1110. $\mathbf{R}_f$ = 0.3 (30% EtOAc in Hexane); Stain: Hanessian's Stain.

Quinuclidine oxidation of compound 31

To an ElectraSyn vial charged with compound **31** (40.6 mg, 0.2 mmol) in 2.00 mL of MeCN was added 0.20 mL of HFIP, Me_4NBF_4 (32 mg, 0.2 mmol) and quinuclidine (22.2 mg, 0.2 mmol). ^{1}H NMR spectroscopic analysis of the crude reaction mixture revealed no product.

Quinuclidine oxidation of compound 32

To an ElectraSyn vial charged with compound **32** (34.6 mg, 0.1 mmol) in 2.00 mL of MeCN was added 0.20 mL of HFIP, Me_4NBF_4 (16.1 mg, 0.1 mmol) and quinuclidine (11.1 mg, 0.1 mmol). ^{1}H NMR spectroscopic analysis of the crude reaction mixture revealed no product (<5%).

Quinuclidine oxidation of compound 33

This result has been previously reported.[43]

Quinuclidine oxidation of compound 34

To an ElectraSyn vial charged with compound **34** (34.6 mg, 0.1 mmol) in 2.00 mL of MeCN was added 0.20 mL of HFIP, Me_4NBF_4 (16.1 mg, 0.1 mmol), and quinuclidine (11.1 mg, 0.1 mmol). The crude products were then purified by flash column chromatography. ^{1}H NMR spectroscopic analysis of the crude reaction mixture revealed no product.

Quinuclidine oxidation of compound 35

To an ElectraSyn vial charged with compound **35** (40.6 mg, 0.2 mmol) in 2.00 mL of MeCN was added 0.20 mL of HFIP, Me_4NBF_4 (32 mg, 0.2 mmol) and quinuclidine (22.2 mg, 0.2 mmol). After the electrolysis, 12 M aq. HCl (1 mL) was added to reaction mixture followed by the stirring for another 2 h. LC-MS analysis of the crude mixture revealed a complex mixture of unidentified products.

Quinuclidine oxidation of compound 36

To an ElectraSyn vial charged with compound **36** (38.5 mg, 0.200 mmol) in 2.00 mL of MeCN was added 0.21 mL of HFIP, Me_4NBF_4 (32.2 mg, 0.200 mmol) and quinuclidine (22.2 mg, 0.200 mmol). The crude products were then purified by flash column chromatography (EtOAc/hexanes-20:80) to afford **36-P1** (13.9 mg, 34%) and **36-P2** (4.1 mg, 10%).

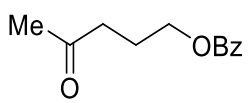

36-P1

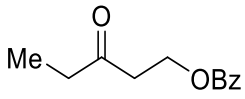

36-P2

Quinuclidine oxidation of compound 37

To an ElectraSyn vial charged with compound **37** (37.3 mg, 0.200 mmol) in 2.00 mL of MeCN was added 0.21 mL of HFIP, Me_4NBF_4 (32.2 mg, 0.200 mmol) and quinuclidine (22.2 mg, 0.200 mmol). The crude products were then purified by flash column chromatography (EtOAc/hexanes-15:85) to afford a mixture of **37-P1** and **37-P3** (12.4 mg, 31%, **37-P1**/**37-P3** = 2:1).

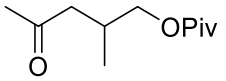

37-P1

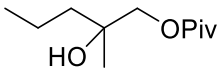

37-P3

Quinuclidine oxidation of compound 38

To an ElectraSyn vial charged with compound **38** (38.5 mg, 0.200 mmol) in 2.00 mL of MeCN was added 0.20 mL of HFIP, Me_4NBF_4 (32.2 mg, 0.200 mmol) and quinuclidine (22.2 mg, 0.200 mmol). The crude products were then purified by pTLC (EtOAc/hexanes-30:70) afforded **38-P2** (26.3 mg, 59% yield) as a colorless oil.

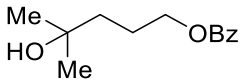

38-P2

Quinuclidine oxidation of compound 39

To an ElectraSyn vial charged with **39** (46.9 mg, 0.300 mmol) in 2.00 mL was added 0.20 mL of HFIP (0.20 mL), Me_4NBF_4 (48.3 mg, 0.300 mmol) and quinuclidine (33.3 mg, 0.300 mmol). Purification by flash chromatography (EtOAc/hexanes-25:75) afforded an inseparable mixture of **39-P1** (15.6 mg, 31% yield) and **39-P2** (10.4 mg, 20% yield) as a colorless oil.

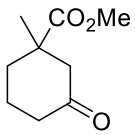

39-P1

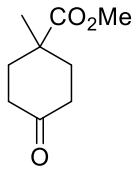

39-P2

Quinuclidine oxidation of compound 40

This result has been previously reported.[43]

Quinuclidine oxidation of compound 41

To an ElectraSyn vial charged with compound **41** (43.6 mg, 0.2 mmol) in 2.00 mL of MeCN was added 0.20 mL of HFIP, Me_4NBF_4 (32.2 mg, 0.2 mmol) and quinuclidine (22.2 mg, 0.2 mmol). ^1H NMR spectroscopic analysis of the crude reaction mixture revealed products **41-P1** (27% yield) and **41-P2** (13% yield) (dibromomethane was used as an internal standard).

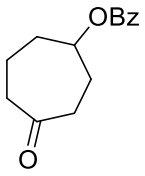

41-P1

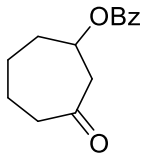

41-P2

Quinuclidine oxidation of compound 42

This result has been previously reported.[43]

Quinuclidine oxidation of compound 43

To an ElectraSyn vial charged with compound **43** (39.6 mg, 0.2 mmol) in 2.00 mL of MeCN was added 0.21 mL of HFIP, Me_4NBF_4 (32.2 mg, 0.2 mmol) and quinuclidine (22.2 mg, 0.2 mmol). The crude products were then purified by flash column chromatography (EtOAc/hexanes-25:75) to afford a mixture of **43-P1**, **43-P2**, and **43-P3** (10.5 mg, 25%, **43-P1/43-P2/43-P3** = 2:1:0.6) and several other oxidation products (15.5 mg, 37%).

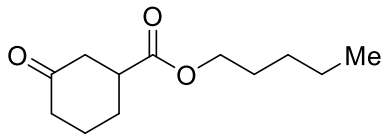

43-P1

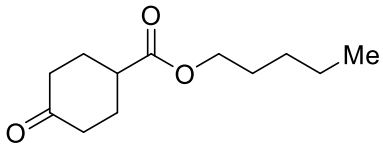

43-P2

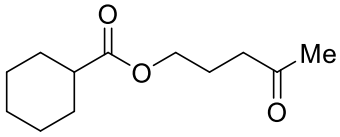

43-P3

Quinuclidine oxidation of compound 44

To an ElectraSyn vial charged with compound **44** (80.5 mg, 0.2 mmol) in 1.80 mL of MeCN was added 0.20 mL of HFIP, Me_4NBF_4 (32.0 mg, 0.2 mmol) and quinuclidine (22.2 mg, 0.2 mmol). The crude products were then purified by pTLC (CH_2Cl_2/acetone-100:1) to afford **44** (7.7 mg, 10 %), **44-P1** (35.7 mg, 43 %) and **44-P2** (9.2 mg, 11%).

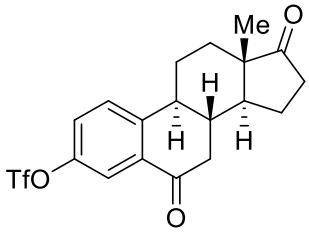

44-P1

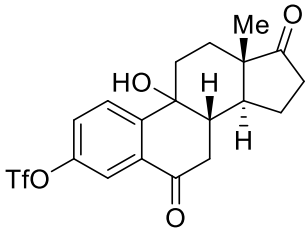

44-P2

Quinuclidine oxidation of penconazole (45)

To an ElectraSyn vial charged with penconazole (56.8 mg, 0.2 mmol) in 2.00 mL of MeCN was added 0.20 mL of HFIP, Me_4NBF_4 (32.0 mg, 0.2 mmol) and quinuclidine (22.2 mg, 0.2 mmol). The crude products were then purified by flash column chromatography

(EtOAc/hexanes-30:70). ^{1}H NMR spectroscopic analysis of the crude reaction mixture revealed no reaction.

Quinuclidine oxidation of 52

To an ElectraSyn vial charged with compound **52** (60.4 mg, 0.2 mmol) in 2.00 mL of MeCN was added 0.20 mL of HFIP, Me_4NBF_4 (32.0 mg, 0.2 mmol) and quinuclidine (22.2 mg, 0.2 mmol). ^{1}H NMR spectroscopic analysis of the crude reaction mixture revealed no reaction.

Scale-up

PROCEDURE FOR 10 G SCALE YLIDE OXIDATION OF 40

Dimethyl cyclohexane-1,2-dicarboxylate (10.0 g, 0.05 mol, 1.0 eq.), ylide **Y7** mediator (16.7 g, 0.05 mol, 1.0 eq.), sodium bicarbonate (10.5 g, 0.125 mol, 2.5 eq.) and tetramethylammonium tetrafluoroborate (8.0 g, 0.05 mol, 1.0 eq.) was dissolved with 500 mL MeCN (0.1 M) in a 1.0 L beaker under vigorous stirring, then HFIP (52.6 mL, 0.5 mol, 10.0 eq.) was added dropwise followed by stirring 15 min. RVC (15 cm × 5 cm × 0.8 cm) as anode and stainless steel (15 cm × 5 cm × 0.2 cm) as cathode was connected to a direct current power and placed parallel into reaction mixture. The reaction was electrolyzed at a constant current of 420 mA. After passing 11 F/mol, the reaction mixture was transferred to a 2.0 L round-bottom and the solvent was removed under reduced pressure. The residue was then dissolved in ethyl acetate and the organic phase was washed with water (2 × 500 mL) and brine (1 × 500 mL). The organic phase was then dried over $MgSO_4$, filtered, and concentrated under reduced pressure. The crude reaction mixture was then purified by column chromatography with 1:2 EtOAc/hexanes to furnish the desired product **55** (4.07 g, 38% yield).

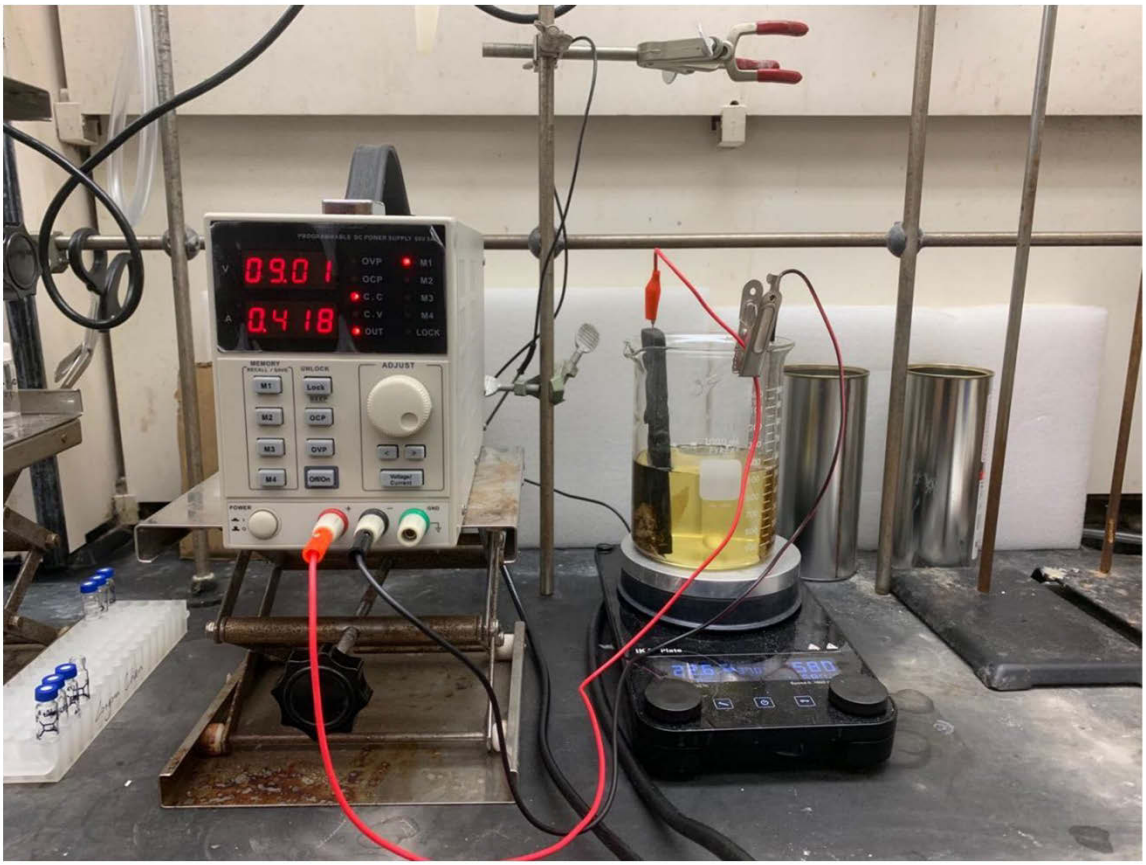

Figure S18. Setup for 10 g oxidation of compound **40**. Permission granted by IKA.

Figure S19. Setup for 10 g oxidation of compound **40**. Permission granted by IKA.

Figure S20. Setup for 10 g oxidation of compound **40**. Permission granted by IKA.

COST CALCULATION FOR 10 GRAM SCALE OXIDATIONS OF COMPOUND **40**

Prices of reagents were obtained from Sigma Aldrich (accessed on 01 Feb 2021) unless indicated. The scale of the reaction is 0.05 mol (10 g).

TFDO oxidation

Trifluoroacetone (T62804-100G, $231.00) calculation based on 3 equiv. of TFDO is required for the oxidation (this is consistent with literature [52]) and the yield of TFDO is taken as 2% from trifluoroacetone. See Baran Laboratory Blog for details: http://openflask.blogspot.com/2014/01/tfdo-synthesisprocedure.html

$2.31/g × 0.05 mol × 3 equiv. × 128 g/mol (TFDO) ÷ 2% = $2217.60

Cost of reaction: $2217.60 USD

Fe oxidation

Fe(*S*,*S*-PDP) (Stream Chemicals Inc., MFCD16038114, $702/g)

$702/g × 10 mmol × 931g/mol ÷ 1000 = $6536.60

Cost of reaction: $6536.60 USD

Ru oxidation

$RuCl_3 \cdot xH_2O$ (206229-25G, $24/g)
4,4'-Di-*tert*-butyl-2,2'-bipyridine (515477-25G, $12.44/g)

($24/g × 2.5 mmol × 207.4g/mol + $12.44/g × 5.0 mmol × 268g/mol) ÷ 1000 = $29.09

Cost of reaction: $29.09 USD

TBADT oxidation

Tetrabutylammonium decatungstate (900432-1G, $362)

$362/g × 1.0 mmol × 3320g/mol ÷ 1000 = $1201.80

Cost of reaction: $1201.8 USD
This work

Item	Name	Unit price	Quantity	Cost
Chemical	cis-1,2-Cyclohexanedicarboxylic anhydride	$35.43/100g	15 g	$5.30
	H_2SO_4	$24.8/1L	1.5 mL	$0.10
	Methyl Iodide	$57.9/100g	20 g	$11.60
	1,1-Dimethylhydrazine	$280/500g	20 g	$11.20

	Oxalyl Chloride	$62.7/100g	20 g	$12.50
	2-(Trifluoromethyl)benzoic acid	$45/100g	20 g	$9
	HFIP	$247/100g	52.6 mL	$207.90
	Me_4NBF_4	$262/100g	8.0 g	$21.00
	Acetonitrile	$245/2.5L	500 mL	$49.00
	$NaHCO_3$	$48.1/500g	10.5 g	$1.01
Total				$328.61

Mechanistic Discussion

The proposed mechanism involves five steps: A) anodic oxidation to generate *N*-ammonium amidyl radical, B) C–H abstraction by the reactive *N*-centered radical, C) reaction of the resulting carbon radical with atmospheric oxygen, D) formation of both ketone and alcohol products by decomposition of the peroxy radical. E) re-oxidation of the alcohol to the ketone. The oxidation of *N*-ammonium ylide was unambiguously confirmed by the observation of oxidation peak in cyclic voltammetry. The result of the intramolecular reaction strongly suggests the intermediacy of *N*-centered radical during this oxidation since intramolecular C–H abstraction by such radical species is well-described. Alternatively, elusive *N*-oxide or *N*-oxyl species that undergo oxygen-transfer to the C–H bond may also be hypothesized. However, the observation of no epoxidation of the double bond nor ylide *N*-oxide formation suggests that it is unlikely that these two species contribute significantly to this reaction. ^{18}O incorporation into both the ketone and the alcohol products suggests that the carbon radical reacts with oxygen, resulting in the formation of the ketone and the alcohol by a known mechanism.[45] The alcohol product could be further oxidized to the ketone. This step is likely mediated due to the dependency of ketone/alcohol ratio ON ylide structure (see Figure S21).

• *Proposed mechanism*

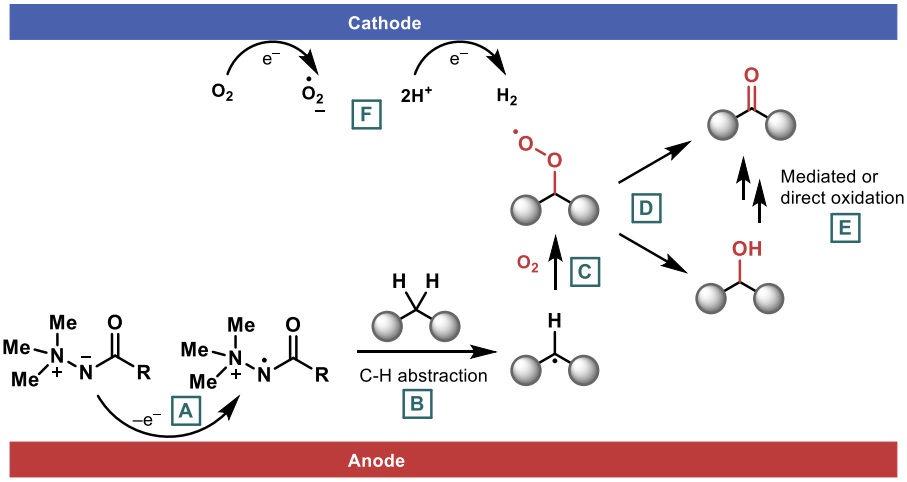

A Oxidation of N-ammonium ylide is observable around 1.8V in cyclic voltammetry.

B Proven by intramolecular C-H oxidation

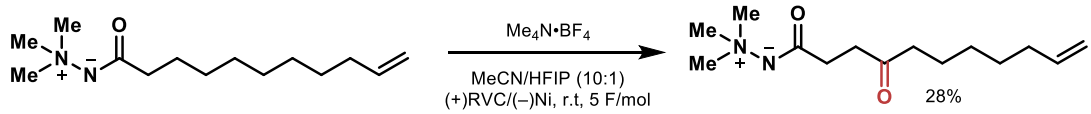

C

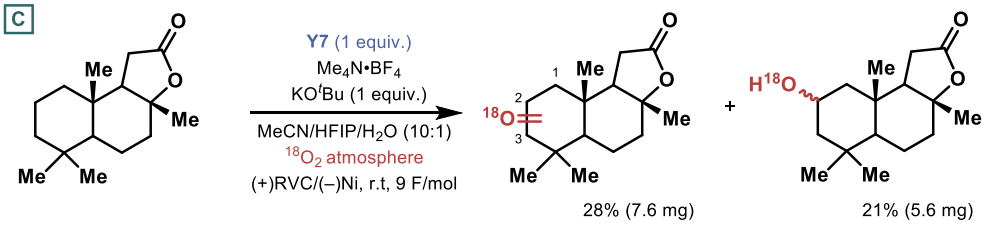

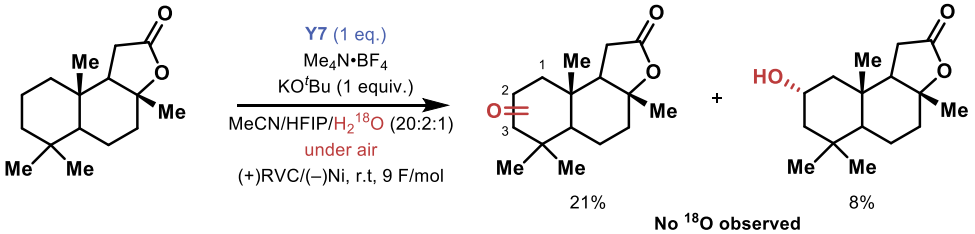

D Both alcohol and ketone are derived from peroxy radical based on Russell mechanism (*24*)

E

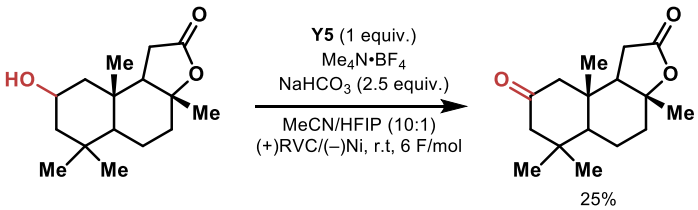

F Cathodic potential measured was 1.2 V. This potential is close to the reduction potential of O_2; however, reduction of H^+ could take place at the same time.

Figure S21. Mechanistic studies of ylide mediated oxidation.

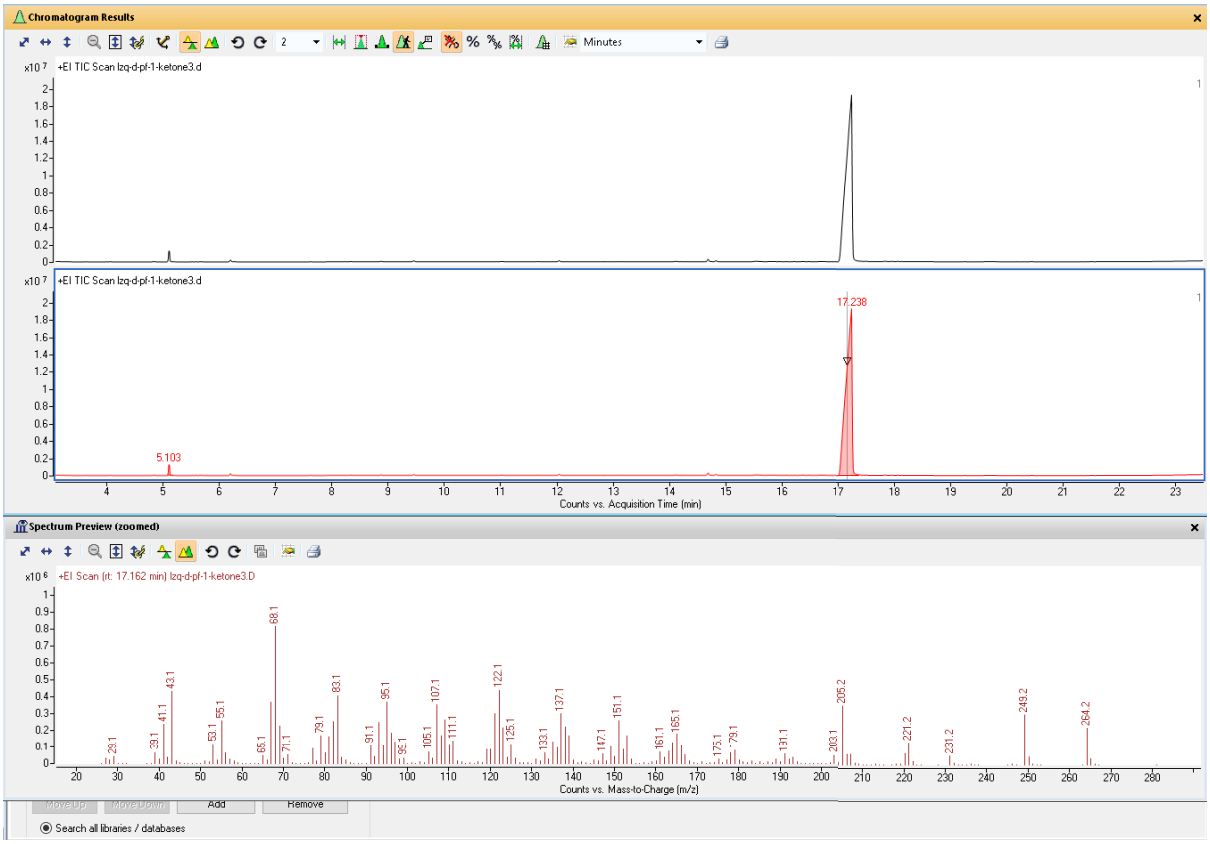

Figure S22. GC trace of product from sclareolide oxidation.

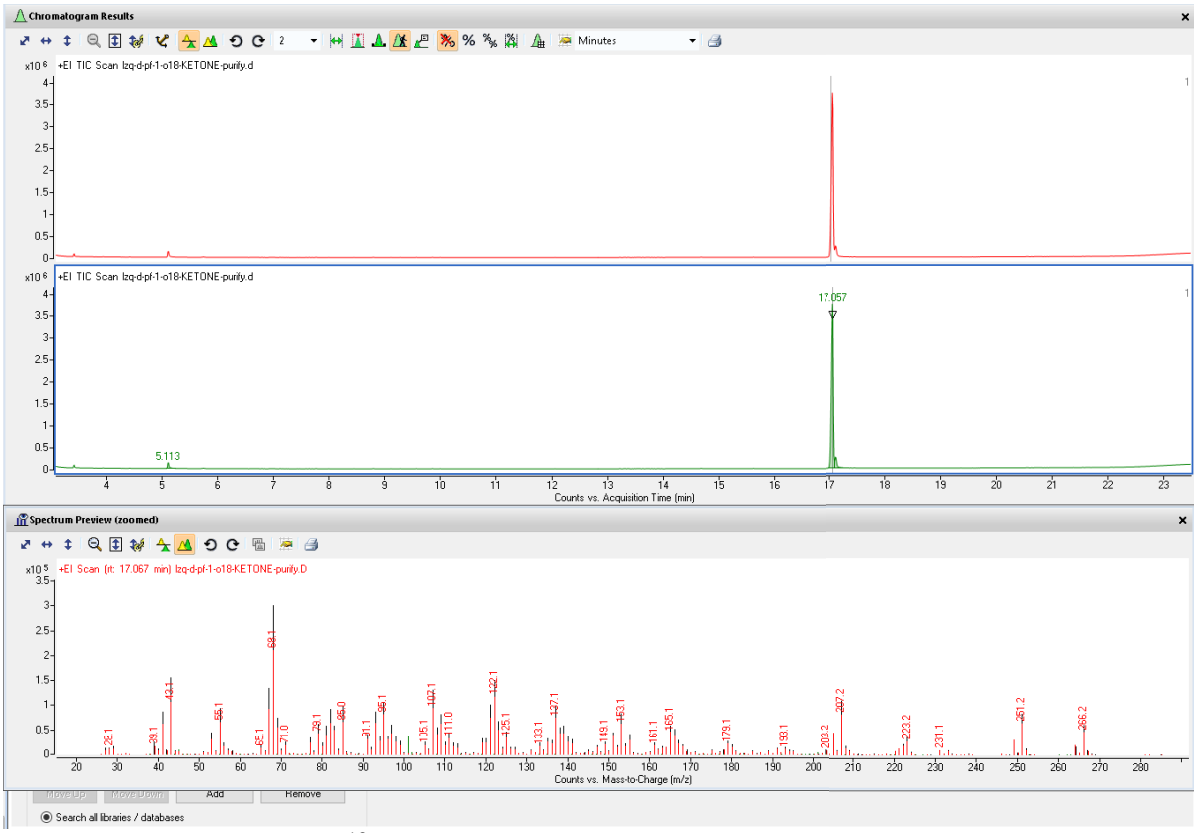

Figure S23. GC trace of the ^{18}O-labeled 2-oxo product from sclareolide oxidation. Note: The ^{18}O-labeled 2-hydroxy product was converted into the ^{18}O-labeled 2-oxo product via Dess-Martin Periodinane oxidation and then also detected in GC-MS.

Computational Detail

Gaussian parameters

The Gaussian 16 software program was used to carry out all of the density functional theory calculations reported herein.[29] The M06-2X functional was used to model nonlocal exchange and correlation effects.[30] The 6-311++G(d,p) basis set was used with an auto fitting set to describe all the main group elements except for Iodine,[31–33] and the Stuttgart/Dresden effective core potentials with the SDD basis set were used for Fe and I atoms.[34] The SMD solvation model was employed to capture the solvation effects of the acetonitrile solvent.[35] The self-consistent field (SCF) calculations were carried out using an ultrafine grid and a convergence criterion of 10^{-8} Ha. All reactant, intermediate, and product structures were optimized until the maximum force, root-mean-square force, maximum displacement, and root-mean-square displacement reached values of $4.5*10^{-4}$ Ha/a_0, $3.0*10^{-4}$ Ha/a_0, $1.8*10^{-3}$ a_0, and $1.2*10^{-3}$ a_0, respectively where a_0 is the Bohr radius. The transition state structures were determined using the Berny algorithm.[36] The optimization of the

respective structures was confirmed by examining their vibrational modes and ensuring that there were no negative vibrational frequencies for the reactant, product, and intermediate structures, and precisely one negative vibrational frequency corresponding to the reaction coordinate for the transition state structure. The frequencies computed were subsequently used to determine the zero-point energy (ZPE) as well as the entropic factors at 1 atm pressure and 298 K temperature for all the reactant, intermediate, transition state, and product structures.

Calculation methodology

The catalytic cycle for the mediator's activation and the substrate's subsequent oxidation was discussed in the main text and presented in Figure 2A. The mediator precursor **M-H** is initially deprotonated by a base to form $\mathbf{M}^-$. This species is subsequently oxidized at the electrode surface to form the active mediator $\mathbf{M}^\bullet$, which can then abstract hydrogen from the substrate, thus facilitating subsequent downstream C-H oxidation pathways. To model this system, we calculated the deprotonation of **M-H** (step B in Fig. 2A), the oxidation potential of $\mathbf{M}^-$ (step C in Fig. 2A) and the free energy of hydrogen binding to the mediator $\mathbf{M}^\bullet$ (step A in Fig. 2A) as descriptors of the elementary steps in the catalytic cycle.

The free energy for hydrogen binding to the mediator, $\Delta G_{H\text{-}bind}$, was calculated as:

$$\Delta G_{H-bind} = G(M-H) - G(M^\bullet) - \frac{G(H_2)}{2} \quad (1)$$

where, G(M-H) is the free energy of the mediator precursor, $G(M^\bullet)$ is the free energy of the active mediator, and $G(H_2)$ is the free energy of dihydrogen, as shown in equation (1).

While equation (1) was universally used for all the mediators to calculate their respective hydrogen binding free energies, a different calculation methodology had to be adopted to calculate the oxidation potentials depending on the mediator class and the nature of its deprotonated form. For mediators such as **11, 12, 22, 23** (Class 1), the mediator that forms upon deprotonation takes on an overall *neutral charge* over the molecule. For such mediators, the oxidation potentials were calculated as:

$$E_{ox} \text{ in V (vs. SHE)} = \frac{[G(M^\bullet) - G(M^-)]}{F} - 4.28 \quad (2)$$

where, E_{ox} is the oxidation potential in V vs. SHE required to generate the active mediator from its deprotonated form, $G(M^\bullet)$ is the free energy of the active mediator, $G(M^-)$ is the free

energy of the deprotonated mediator, and *F* is the Faraday's constant (96500 C/mol), as shown in equation (2).

As discussed in the main text, the oxidation potential values calculated via equation (2) for this mediator class were in good agreement with the experimental oxidation potential values, validating this methodology's reliability for redox potential calculations for such similar mediators.

However, for mediators such as **18-21, 24** (Class 2), wherein the mediator upon deprotonation results in an overall *negative charge* over the molecule, it is seen that oxidation potentials calculated using equation (2) lead to erroneous predictions. For example, in the NHPI mediator's case (**19**), the oxidation potential was computed to be 0.08 V vs. SHE as per equation (2), which is 0.91 V off from its reported experimental oxidation potential value of 0.99 V vs. SHE.[37]

Computation of the oxidation potentials using a base-NHPI complex with pyridine as the base gave a resultant oxidation potential of 1.13 V vs. SHE, which is in good agreement with the experimental value. In this case, the oxidation of the base-mediator complex results in deprotonation of the mediator followed by the subsequent loss of an electron from the system. This is consistent with a proton-coupled electron transfer (PCET) mechanism, as shown in Figure S24. Hence, we believe that oxidation reactions likely proceed via a PCET mechanism at the electrode surface for this class of mediators, as reported in a previous study.[38] The oxidation potentials for this class of mediators (**18-21, 24**) were therefore calculated as:

$$\mathrm{E_{ox}\ in\ V\ (vs.\ SHE)} = \frac{[\mathrm{G(M^{\bullet} \bullet\bullet\bullet H^{+} - B)} - \mathrm{G(M - H \bullet\bullet\bullet B)}]}{F} - 4.28 \quad (3)$$

where, E_{ox} is the oxidation potential in V vs. SHE required to generate the active mediator, G(M-H•••B) is the free energy of the mediator precursor-base complex, G($M^{\bullet}$•••H^{+}-B) is the free energy of the corresponding oxidized complex (active mediator-protonated base complex), and *F* is the Faraday's constant, as shown in equation (3).

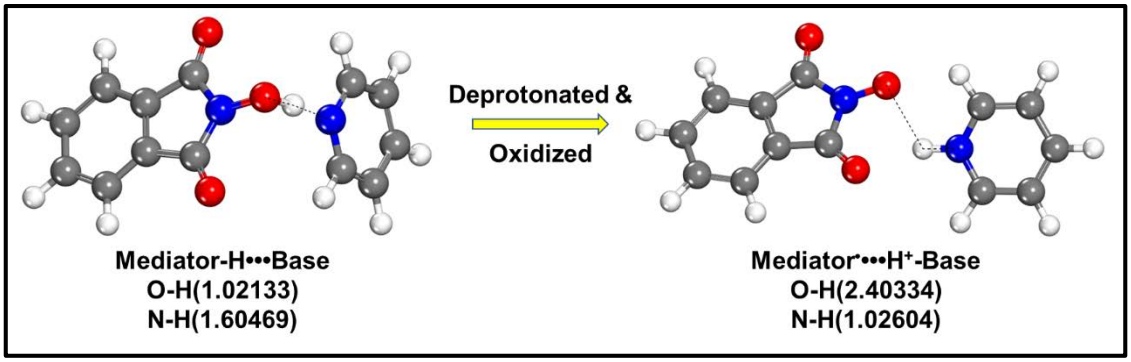

Figure S24. *Optimized structures for the mediator precursor-base complex (left) and the corresponding oxidized complex (active mediator-protonated base complex) (right) for the TCNHPI mediator. The parenthesis values are the corresponding bond distances in Å. Hydrogen (), Carbon (), Nitrogen (), and Oxygen ().*

The deprotonation free energies for the Class 1 type of mediators (**11, 12, 22, 23**), which proceed by separate proton transfer and electron transfer steps, were calculated as:

$$\mathrm{DPFE} = \mathrm{G(M^-)} + \mathrm{G(H^+)} - \mathrm{G(M-H)} \quad (4)$$

where, DPFE is the deprotonation free energy of the mediator, G(M^-) is the free energy of the deprotonated mediator precursor, G(H^+) is the free energy of the proton, and G(M-H) is the free energy of the mediator precursor, as shown in equation (4).

Transition state calculations

Transition state calculations were carried out to elucidate the mediator-specific factors that govern the selectivity to different oxidation products. Herein, we specifically examine the interactions between the substrate **29**, 1,4 substituted cyclohexane, and the quinuclidine and ylide mediators, both of which show unique selectivity towards the different oxidation products as discussed in the main text. While quinuclidine selectively abstracts hydrogen from C4, the ylide mediator (**Y4**) abstracts hydrogens from C2 and C3 sites. The bond dissociation energy (BDE) for any substrate R-H was calculated as:

$$\mathrm{BDE} = \mathrm{G(R^\bullet)} + \mathrm{G(H^\bullet)} - \mathrm{G(R-H)} \quad (5)$$

where, BDE is the bond dissociation energy of the substrate R-H, G($R^\bullet$) is the free energy of the corresponding radical, G($H^\bullet$) is the free energy of the hydrogen radical, and G(R-H) is the free energy of the substrate, as shown in equation (5).

The BDEs (Figure S25) of the different hydrogens present in the substrate indicate that the tertiary C4-H1 hydrogen's abstraction should be the easiest. The BDEs of the axial and equatorial hydrogens on the C2 and the C3 sites, on the other hand, are higher than that at the C4 site but comparable to one another, as is shown in Figure S25. Thus, based on simple BDE calculations, radical generation at the C4 site is thermodynamically the most favored. More detailed transition state calculations (Figure S26) for the ylide and quinuclidine mediated C-H abstractions, on the other hand, show that quinuclidine prefers to abstract the H1, whereas ylide **Y4** preferentially abstracts the hydrogens at the equatorial C3 (H2) and C2 (H4) positions. The abstraction of axial H3 and H5 hydrogens is less favorable for both the quinuclidine and ylide **Y4** mediators due to increased steric hindrance versus that at the equatorial positions.

While the H1 is the easiest to cleave, as seen in the BDE values in Figure S25, its activation depends upon its interaction with the mediator accepting site. The nitrogen on the ylide is a *neutral radical* which strongly interacts with and abstracts the substrate's hydrogen. On the other hand, the nitrogen on quinuclidine is a *radical cation* that more weakly interacts with the substrate's hydrogens. This is also evident in the more exergonic hydrogen binding free energy with ylide **Y4** ($\Delta G_{H\text{-}bind}$ = -229 kJ/mol) than quinuclidine ($\Delta G_{H\text{-}bind}$ = –183 kJ/mol). The stronger electronic interactions allow the ylide to begin to activate the hydrogen at a longer distance than that involved with quinuclidine. This allows ylide to activate the less sterically hindered H2 and H4 hydrogens over the axial H3 and H5 hydrogens. However, the steric effects are significantly higher for the ylide's approach to the tertiary C4-H1 bond, which outweighs any gain in activating the weaker C4-H1 bond, resulting in a higher activation free energy for H1.

Quinuclidine, on the other hand, much more weakly interacts with the hydrogens on the substrate. As such, the nitrogen on the quinuclidine must approach the hydrogen much more closely to enable activation. This leads to significantly higher activation free energy barriers for quinuclidine versus those for the ylide. The stabilization that results from the close contact with the hydrogen dominates over steric repulsion. As such, quinuclidine preferentially abstracts the weakest tertiary C4-H1 hydrogen. The higher steric repulsions at the C4 site are overridden by the gain in the stronger interaction with the weaker C-H bond. Thus, the interplay of steric-electronic interactions governs the overall selectivity trends in the two mediators.

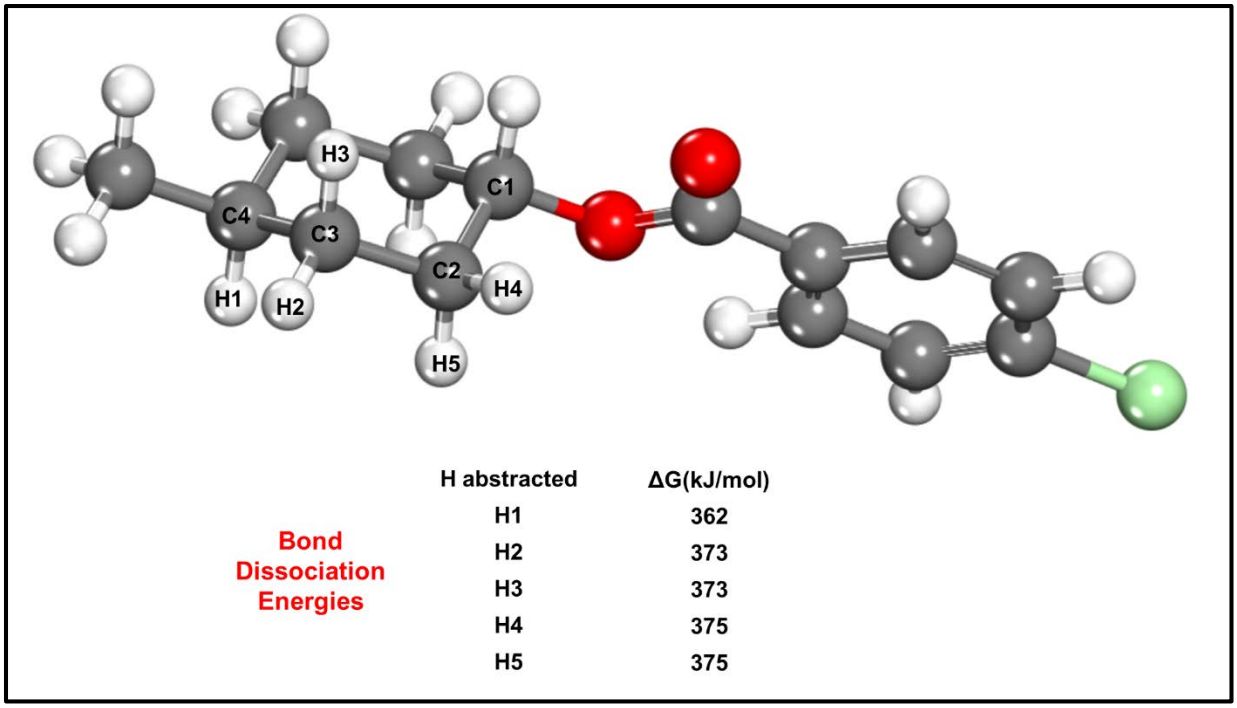

Figure S25. Optimized structure of the 1,4 substituted cyclohexane. The different hydrogens within the substrate targeted using quinuclidine and ylide mediators are labeled along with their corresponding bond dissociation energies reported in kJ/mol. Hydrogen (), Carbon (), Oxygen (), and Chlorine ().

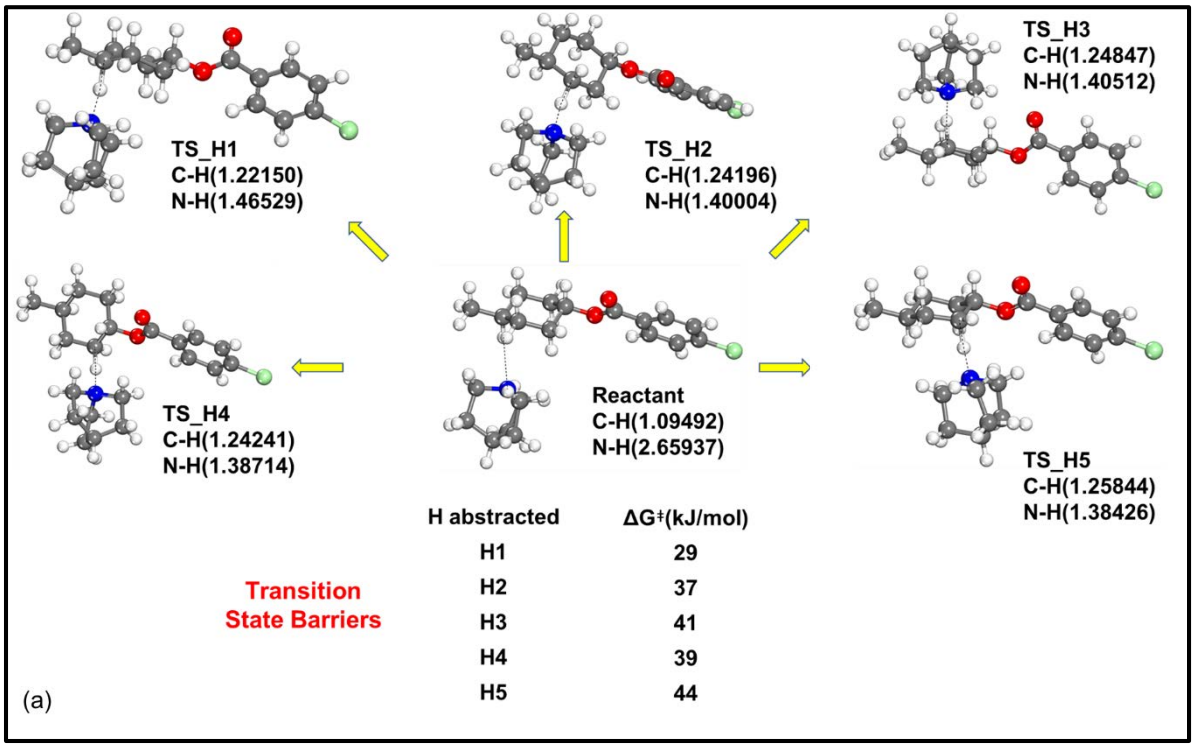

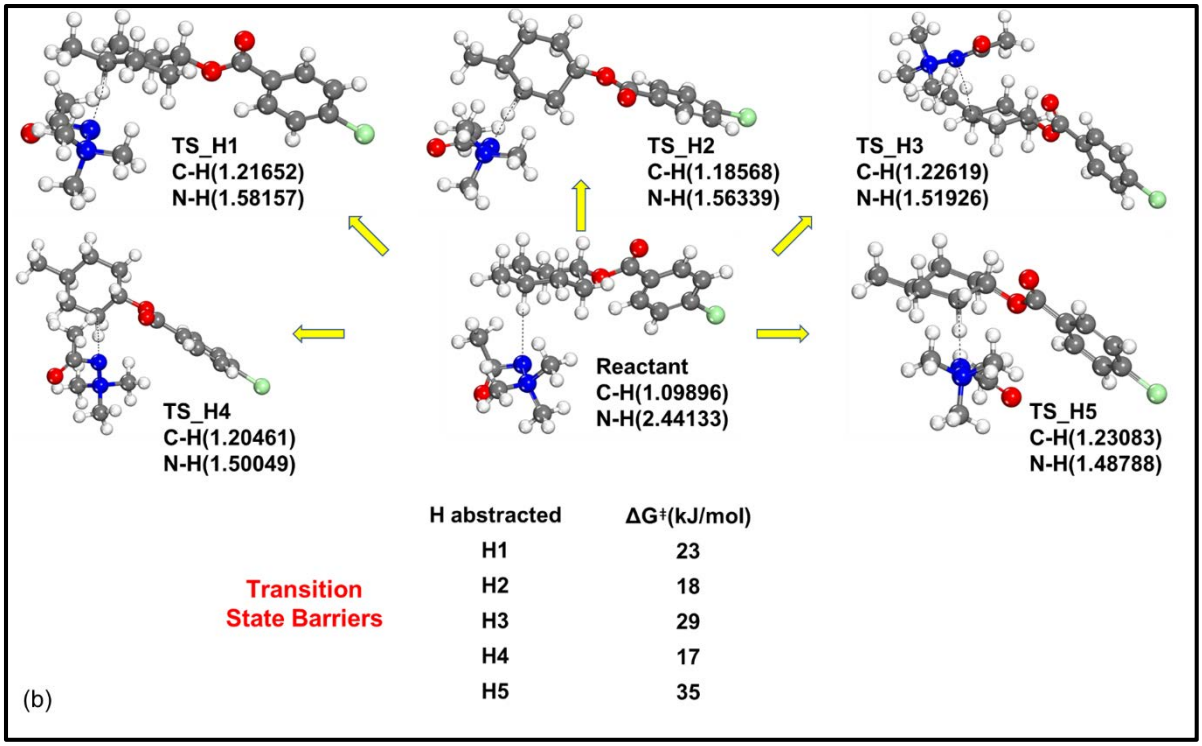

Figure S26(a, b). Transition state structures of hydrogen abstraction at different labeled C-H positions of the 1,4 substituted cyclohexane using mediators (a) quinuclidine and (b) ylide as the abstracting agent. The value in parenthesis corresponds to the bond distances in Å. All the energies are reported in kJ/mol. Hydrogen (), Carbon (), Nitrogen (), Oxygen (), and Chlorine ().

Chemical Space Analysis

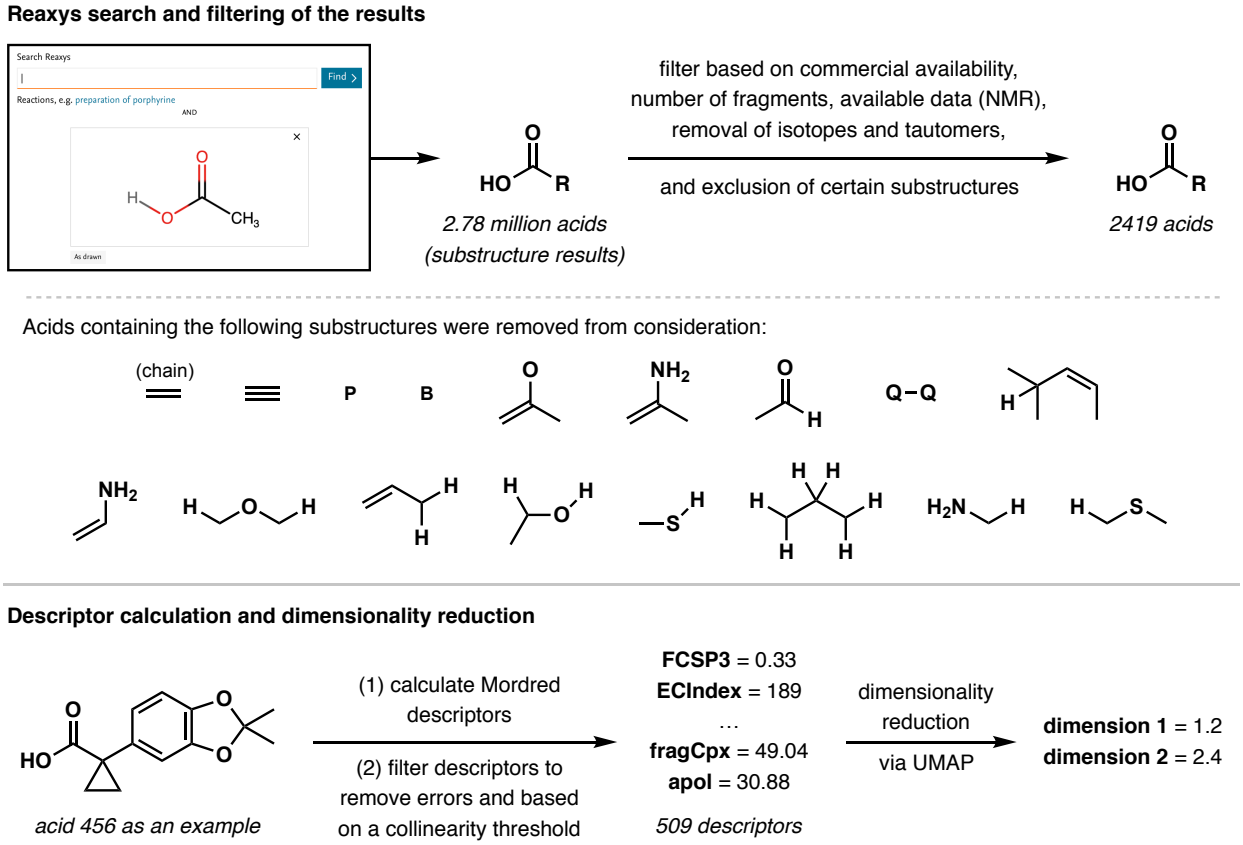

Figure S27. Overview of Reaxys search, descriptor calculation, and dimensionality reduction.

A Reaxys substructure search for carboxylic acids was performed using the input shown in Figure S27. The resulting 2.78 million acids were filtered based on a variety of criteria including availability, number of fragments, available data, and substructures. SMILES for the final 2419 acids were exported. >1800 two- and three-dimensional Mordred descriptors were calculated for the acids using the SMILES and a Python script.[39,40,46] The descriptors were filtered to remove any errors and based on a collinearity threshold of 0.95 R^2. An excel file containing the resulting 509 descriptors for each of the 2419 acids was exported. Dimensionality reduction was performed using the Uniform Manifold Approximation and Projection (UMAP) technique via a Python script.[40,47] UMAP was chosen for dimensionality reduction due to its ability to preserve the global structure of the data.[48] An interactive plot was used to evaluate the coverage of the chemical space by the acids chosen for initial screening.

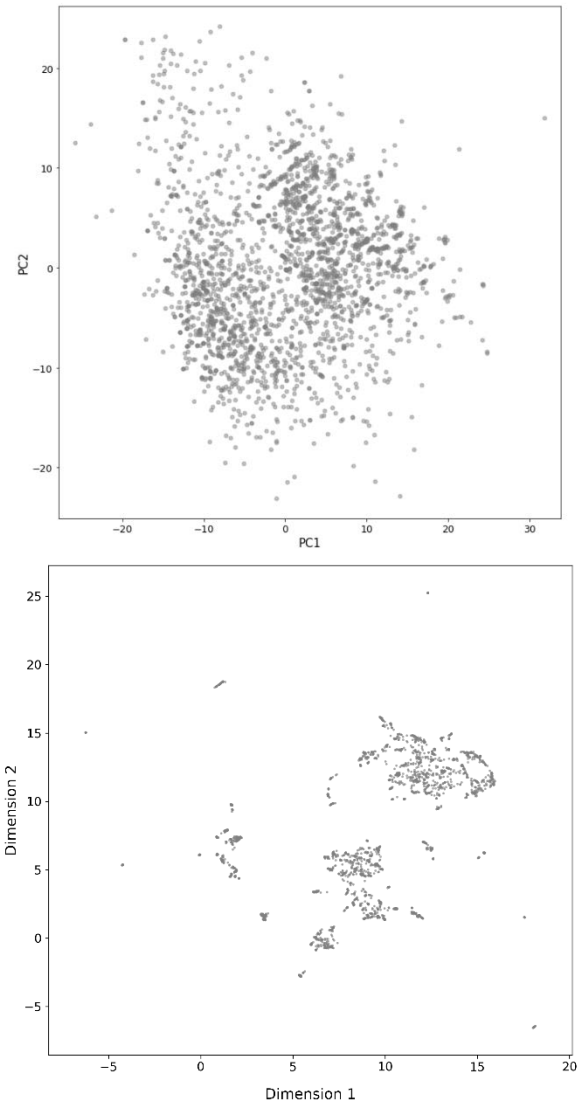

Figure S28. Visualization of the 2419 acids using principal component analysis (left, top two PCs explain 25% of the variance) and UMAP (right).

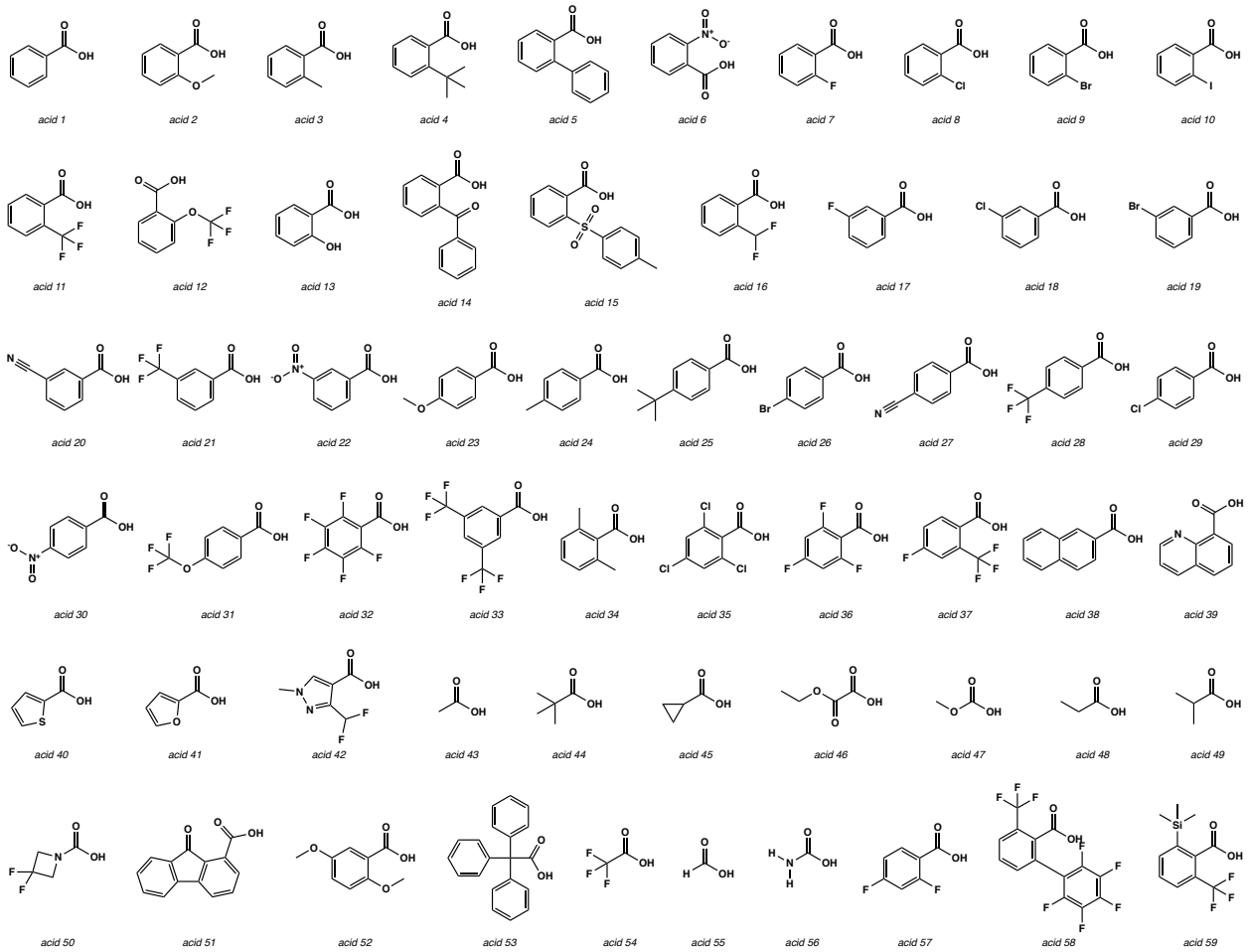

Figure S29. 59 acids that were screened (as the corresponding mediators).

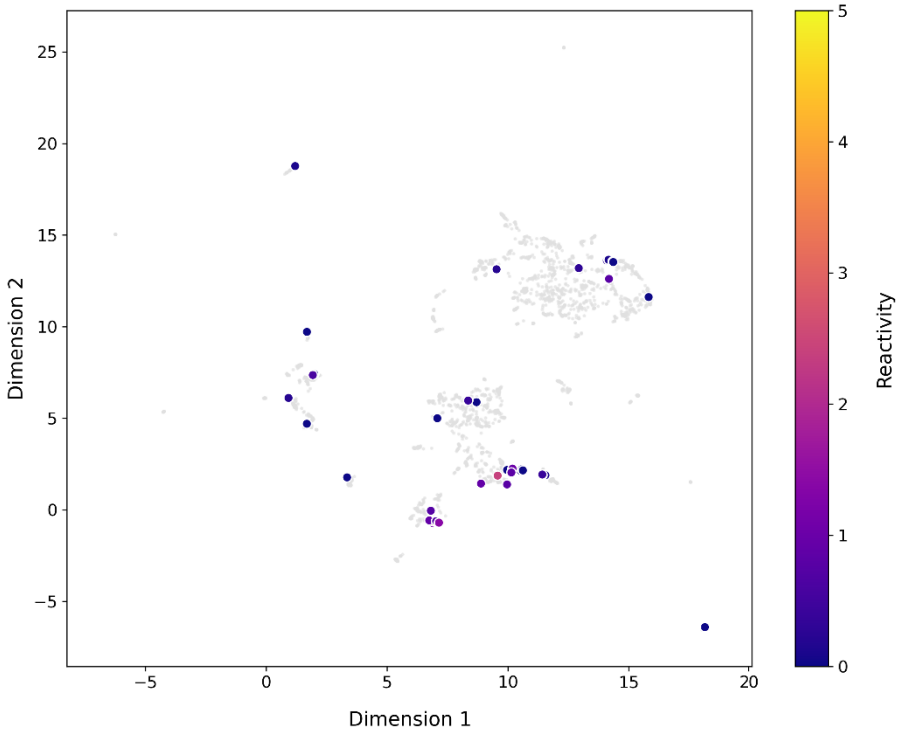

Figure S30. UMAP plot of the 2419 acids with reactivity results for the 59 screened acids colorized (see Figure S35-36 for relative reactivity).

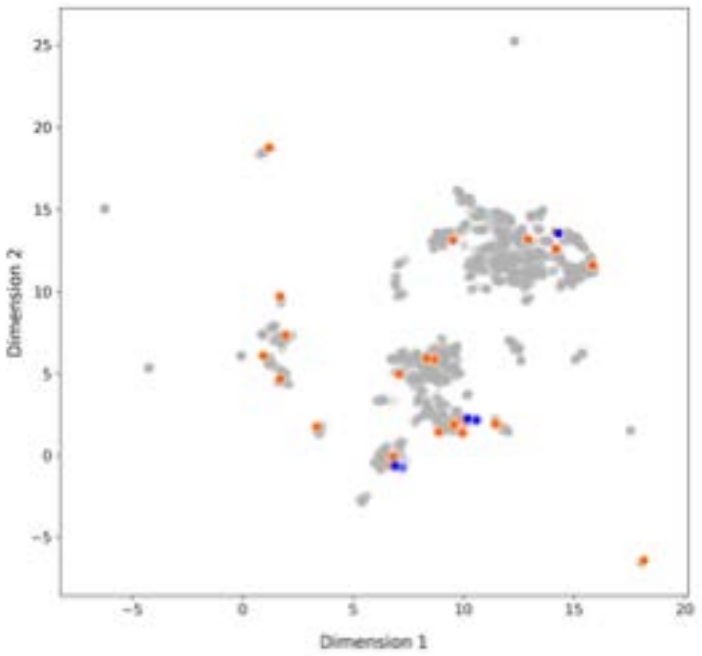

Figure S31. UMAP plot of the 2419 acids (grey) with screened acids (orange) and **Y2**-**Y7** (blue).

Hydrogen binding free energy ($\Delta G_{H\text{-}bind}$), deprotonation free energy (DPFE) and oxidation potential (E_{ox}) were calculated for the 59 screened acids. These values are available in "baran_acid_identifiers.xlsx" (column F) and "baran_acid_descriptors.xlsx" (columns SQ to SS).[40]

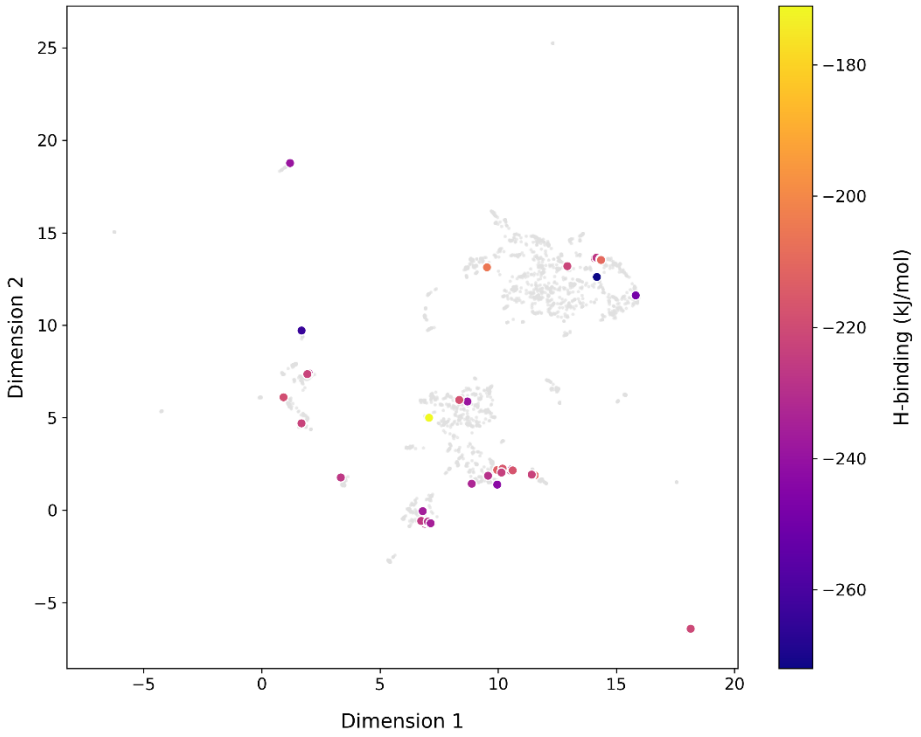

Figure S32. UMAP plot of the 2419 acids with $\Delta G_{H\text{-}bind}$ for the 59 screened acids colorized.

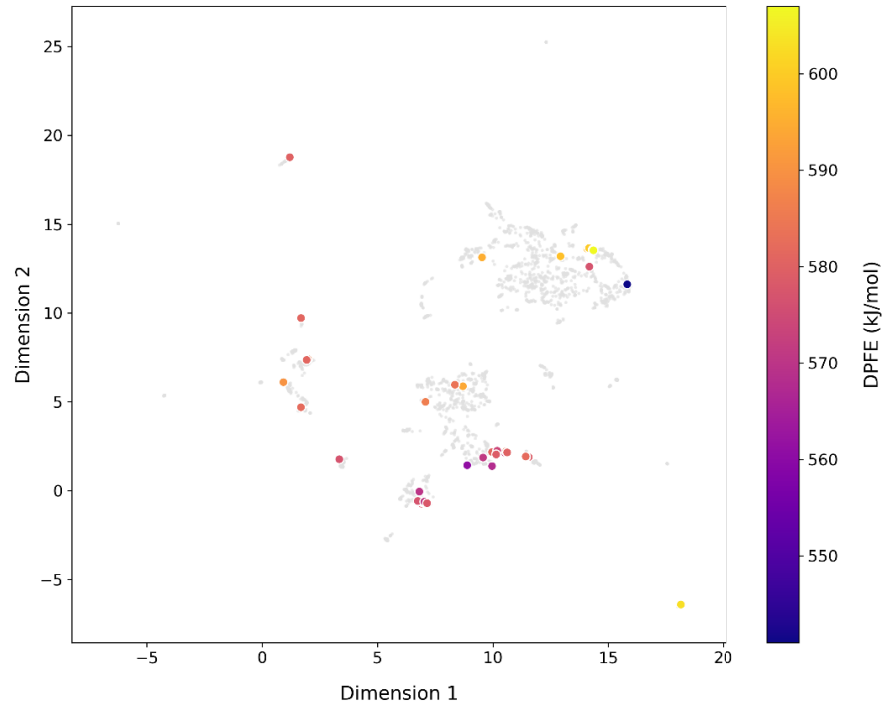

Figure S33. UMAP plot of the 2419 acids with DPFE for the 59 screened acids colorized.

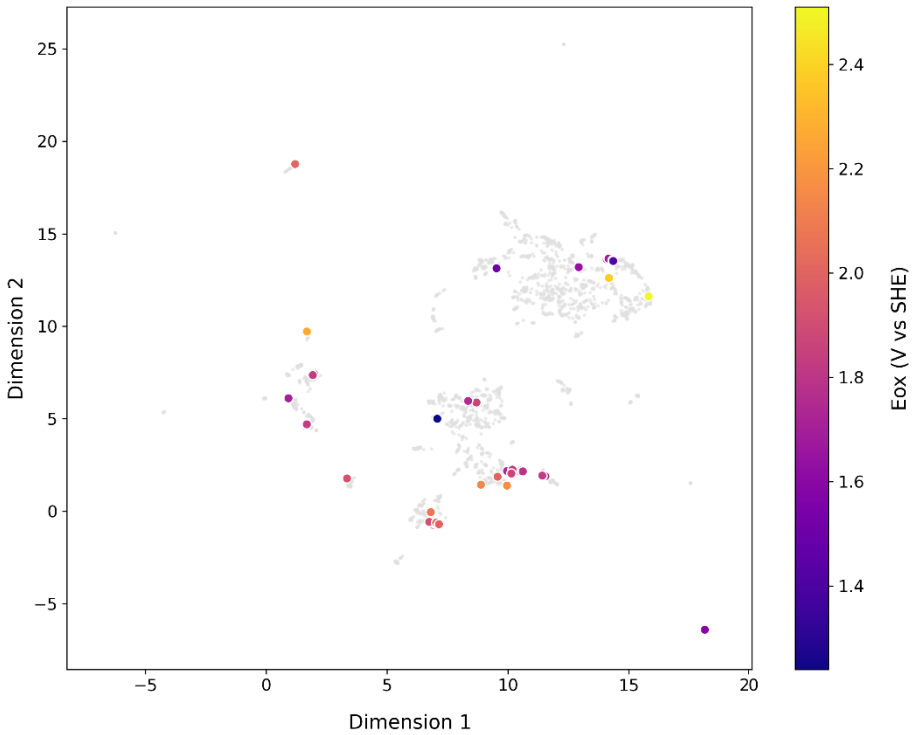

Figure S34. UMAP plot of the 2419 acids with E_{ox} for the 59 screened acids colorized.

Ylide Reactivity Study

The efficacy of each mediator was evaluated in C–H oxidation of tetrahydroionone. The amount of the oxidation products was quantified by gas chromatography. The relative reactivity of a given ylide was calculated based on the product GC area divided by that of product GC area from **Y5**. Comprehensive reactivity screening was carried out with Cs_2CO_3 as base. In selected cases, reactivity with $NaHCO_3$ was also evaluated.

SCREENING WITH TETRAHYDROIONONE

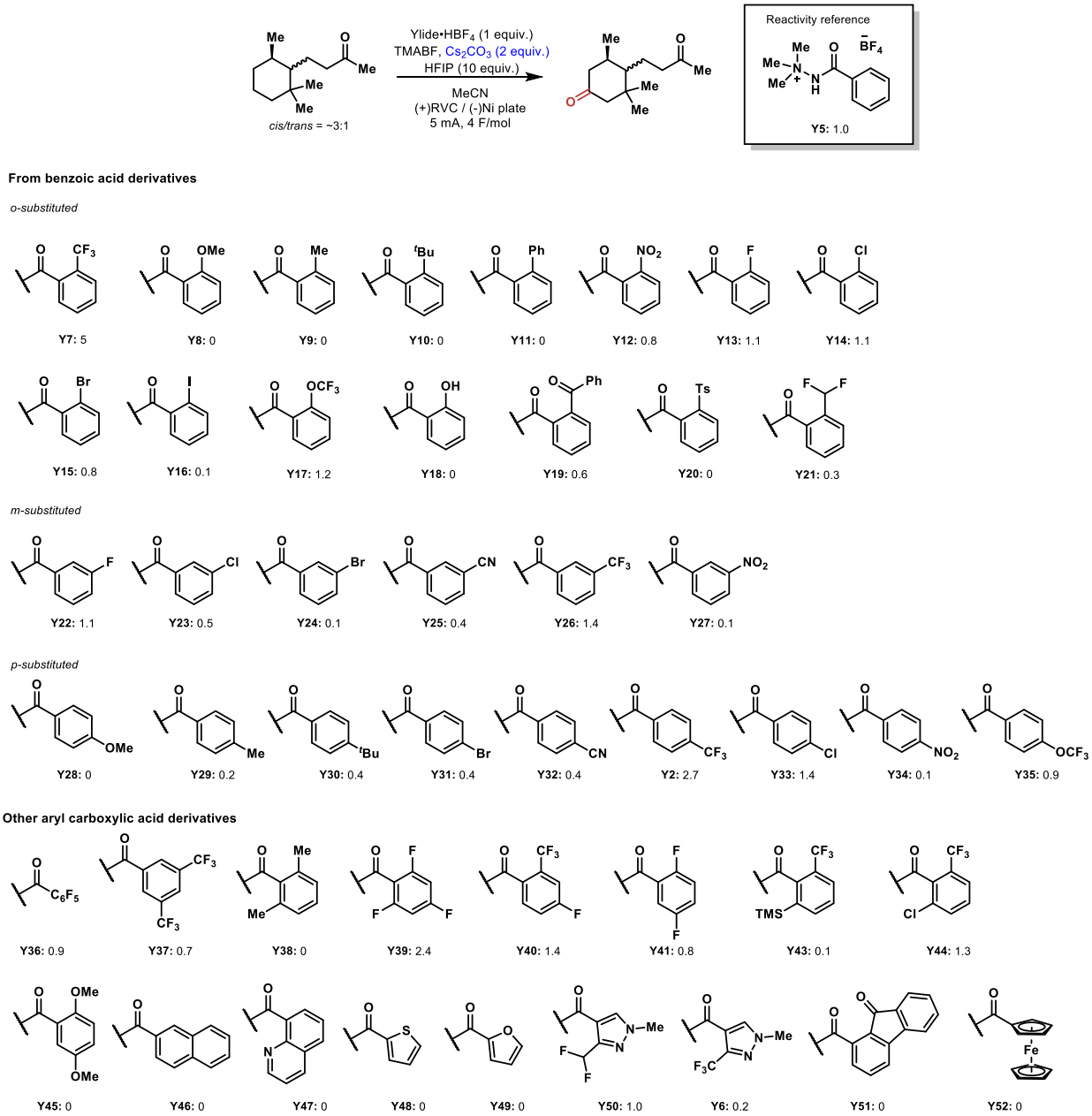

Figure S35. Ylide reactivity screening Part I.

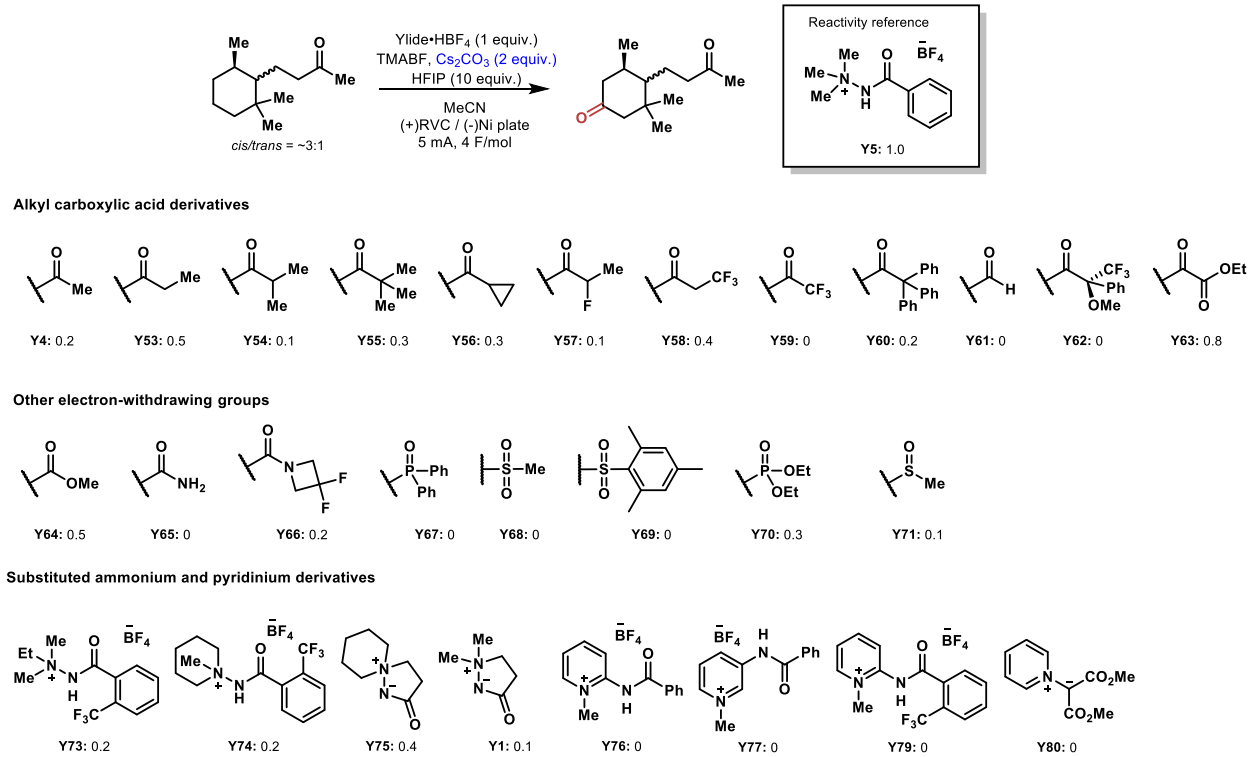

Figure S36. Ylide reactivity screening Part II.

SCREENING RESULTS USING $NAHCO_3$

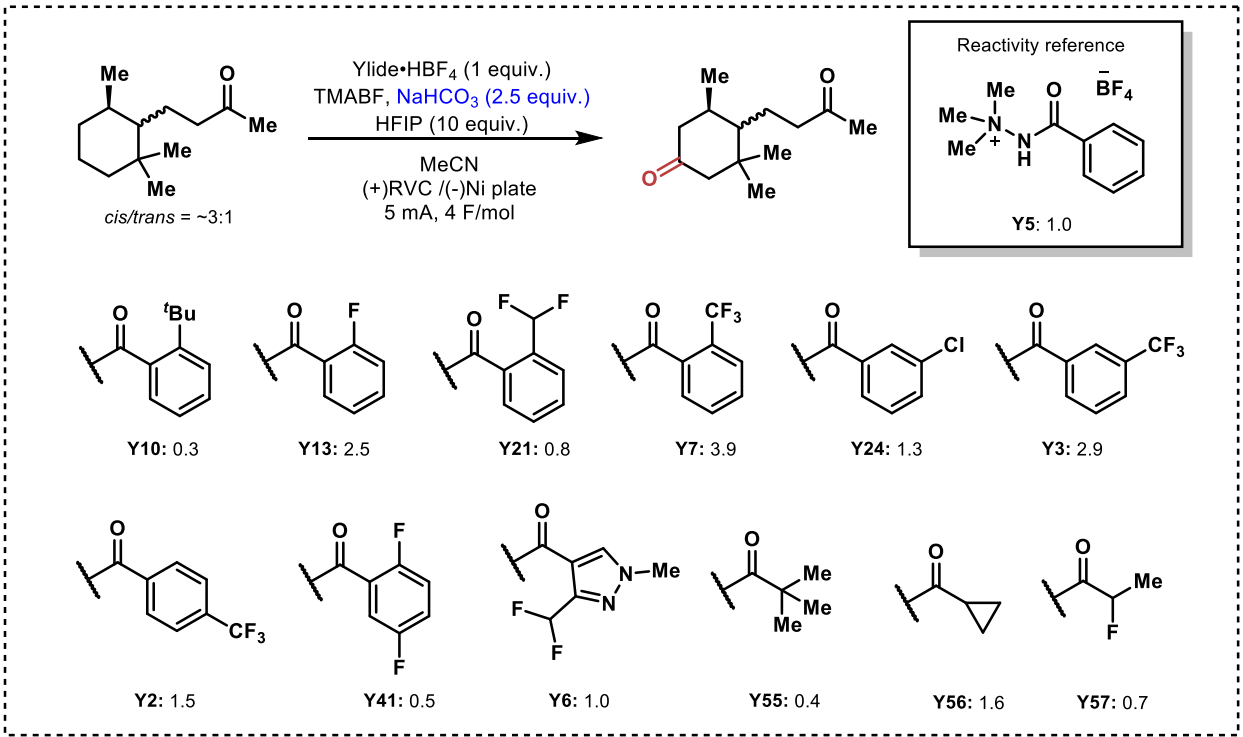

Figure S37. Ylide reactivity screening using $NaHCO_3$ as base

REGIOSELECTIVITY IN SCLAREOLIDE OXIDATION

The selectivity of ylides were evaluated by following General Procedures, Condition A. 2-oxo and 3-oxo products were obtained as an inseparable mixture when purified by preparative TLC with the eluent (CH_2Cl_2/Et_2O-5:2). 1-oxo product was found in some cases, but it was not quantified due to its small quantity. The alcohol product was obtained as single diastereomer, and the stereochemistry was determined by comparing the ^1H NMR with reported spectrum.[14]

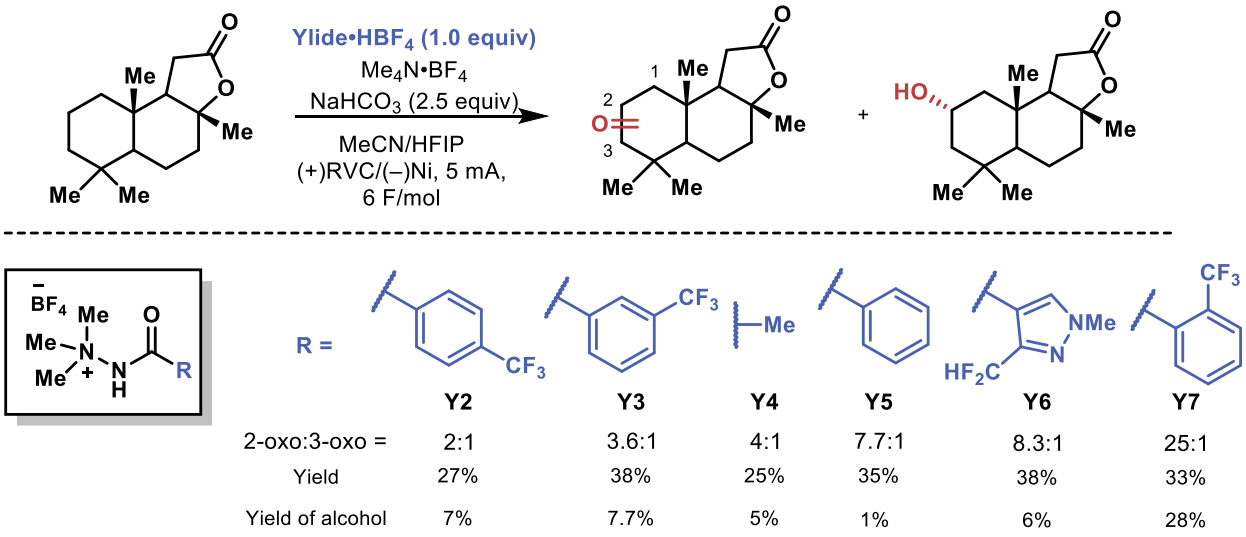

	Y2	Y3	Y4	Y5	Y6	Y7
2-oxo:3-oxo =	2:1	3.6:1	4:1	7.7:1	8.3:1	25:1
Yield	27%	38%	25%	35%	38%	33%
Yield of alcohol	7%	7.7%	5%	1%	6%	28%

Figure S38. Oxidation of sclareolide with ylides **Y2-Y7**.

Cyclic Voltammetry Data for Ylides

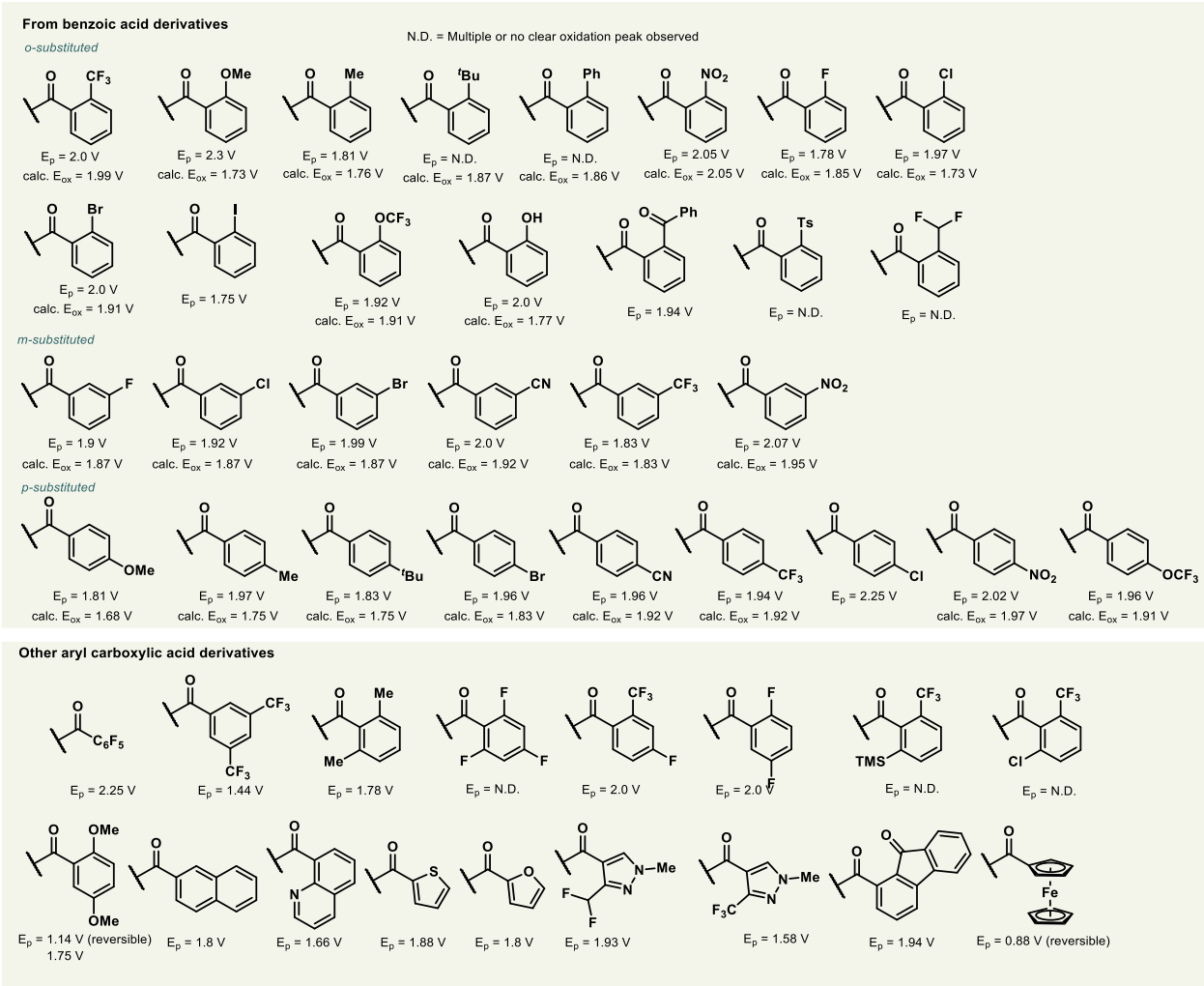

Figure S39. CV values for ylides Part I.

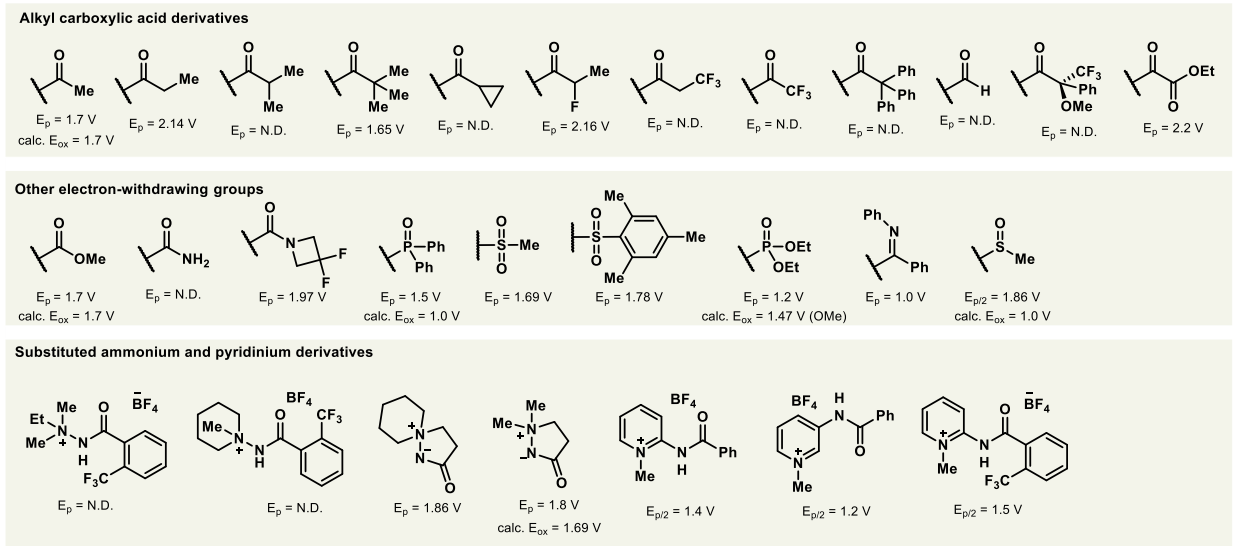

Figure S40. CV values for ylides Part II.

Cyclic voltammograms for ylides **Y1-Y7**

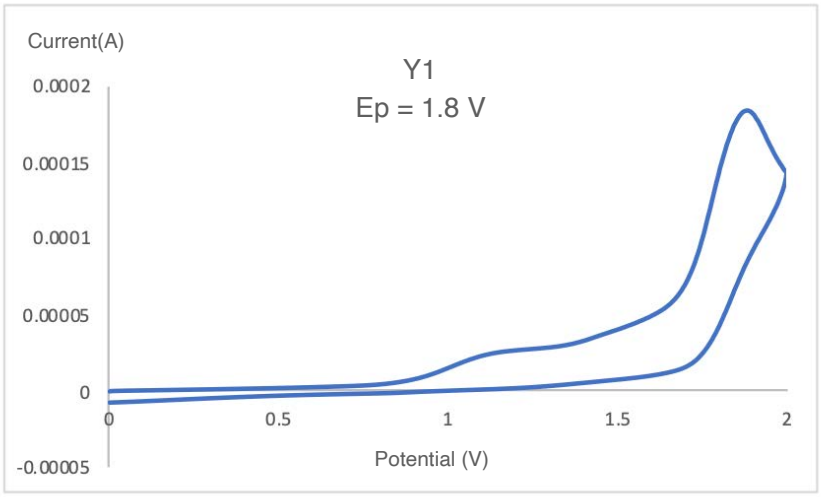

Figure S41. Optimized CV conditions: 5 mM ylide, 0.1 M $TBABF_4$ in MeCN, performed under Air. Ag/AgCl was used as reference and converted to SHE.

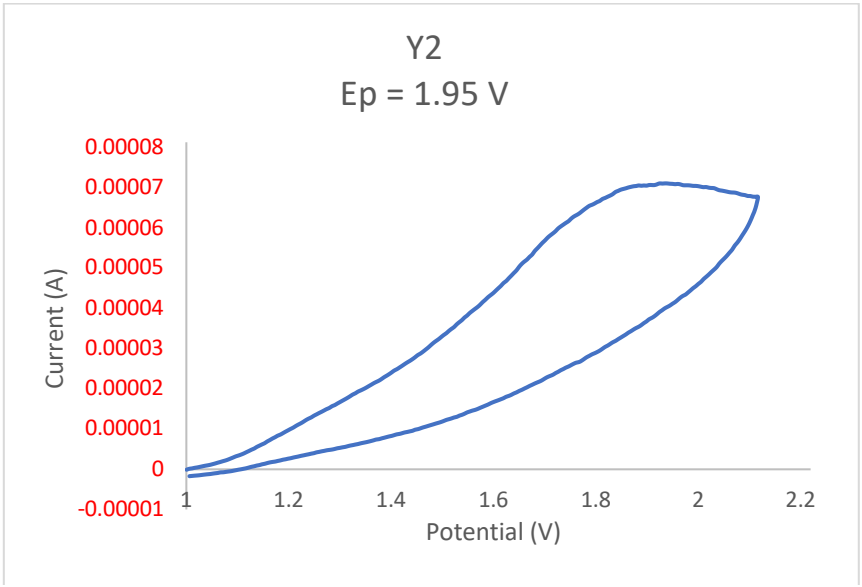

Figure S42. Optimized CV conditions: 1 mM ylide, 2 mM Cs_2CO_3 (saturated), 0.1 M $TBABF_4$ in MeCN, performed under Air. Ag/AgCl was used as reference and converted to SHE.

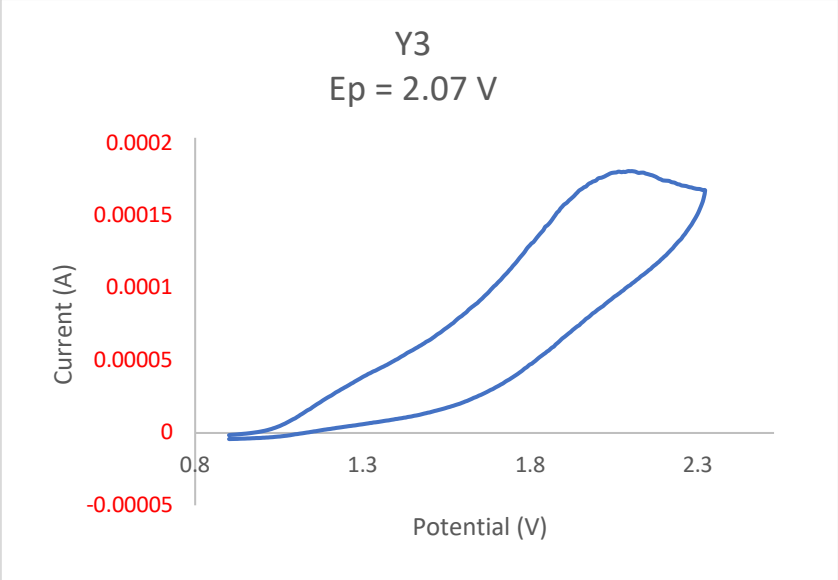

Figure S43. Optimized CV conditions: 1 mM ylide, 2 mM Cs_2CO_3 (saturated), 0.1 M $TBABF_4$ in MeCN, performed under Air. Ag/AgCl was used as reference and converted to SHE.

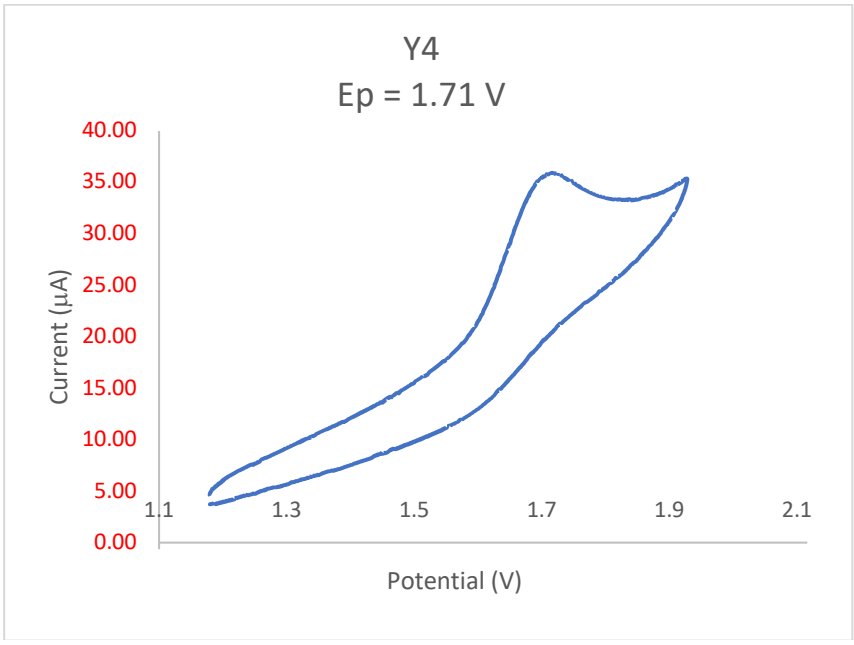

Figure S44. Optimized CV conditions: 1 mM ylide, 2 mM Cs_2CO_3 (saturated), 0.1 M $TBAPF_6$ in MeCN, all performed under Ar. Ag/AgCl was used as reference and converted to SHE.

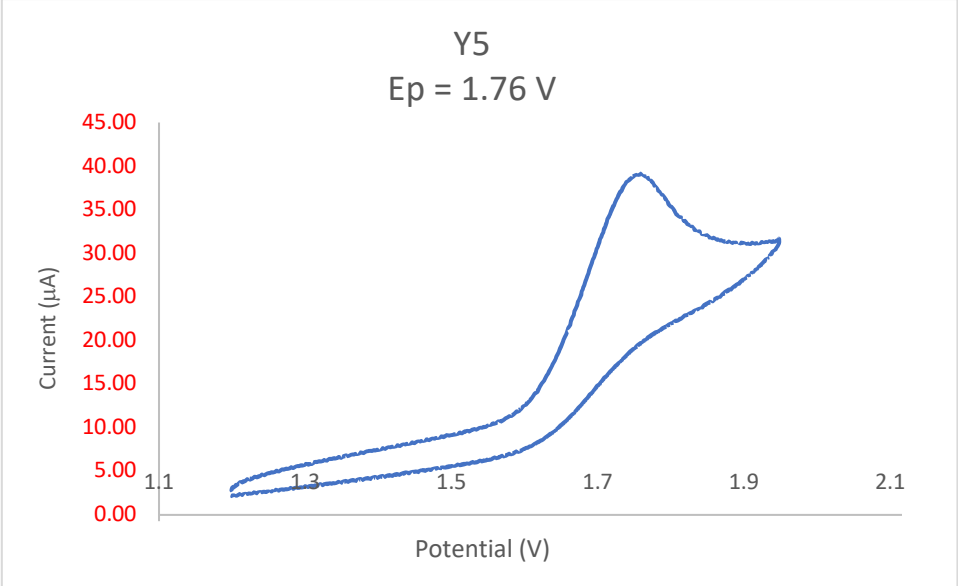

Figure S45. Optimized CV conditions: 1 mM ylide, 2 mM Cs_2CO_3 (saturated), 0.1 M $TBAPF_6$ in MeCN, all performed under Ar. Ag/AgCl was used as reference and converted to SHE.

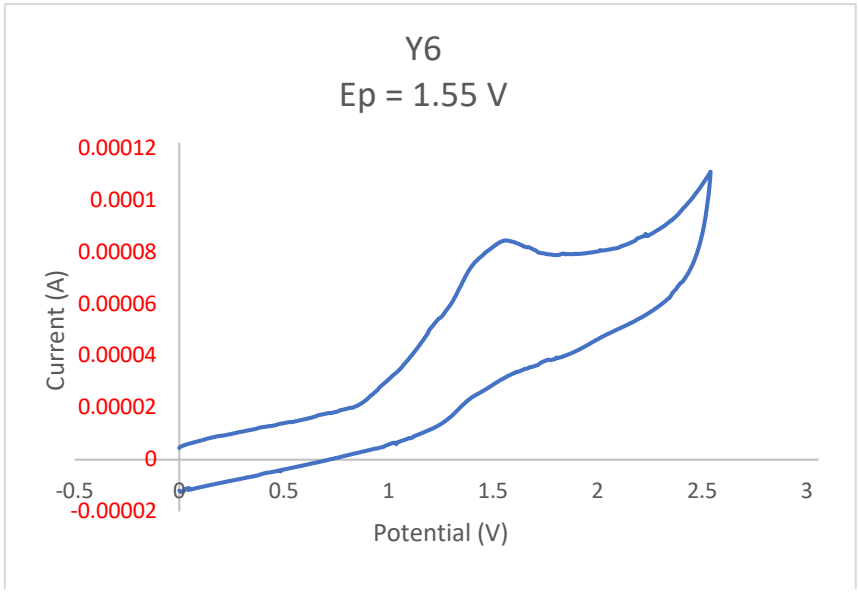

Figure S46. Optimized CV conditions: 1 mM ylide, 2 mM $NaHCO_3$ (saturated), 0.1 M $TBABF_4$ in MeCN, performed under Air. Ag/AgCl was used as reference and converted to SHE.

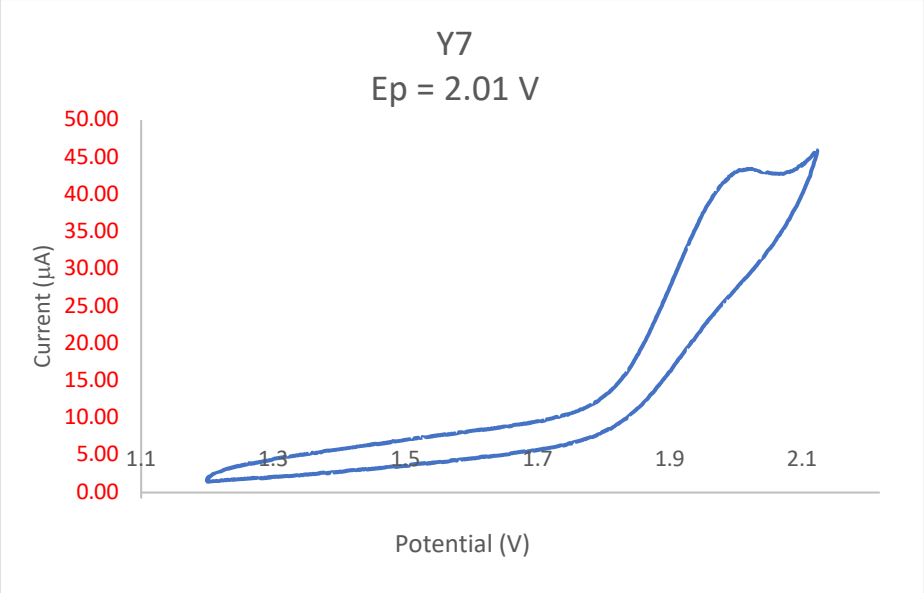

Figure S47. Optimized CV conditions: 1 mM ylide, 2 mM Cs_2CO_3 (saturated), 0.1 M $TBAPF_6$ in MeCN, all performed under Ar. Ag/AgCl was used as reference and converted to SHE.

Additional Studies and Information

SYNTHESIS AND CHARACTERIZATION OF CF_3-QUINUCLIDINE

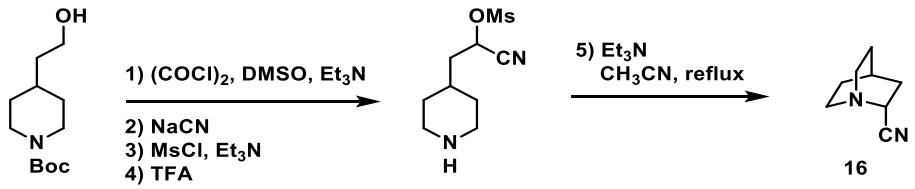

Figure S48. The CN-QNC (**16**) was prepared following the literature reported method in 5 steps from commercially available starting material.[44]

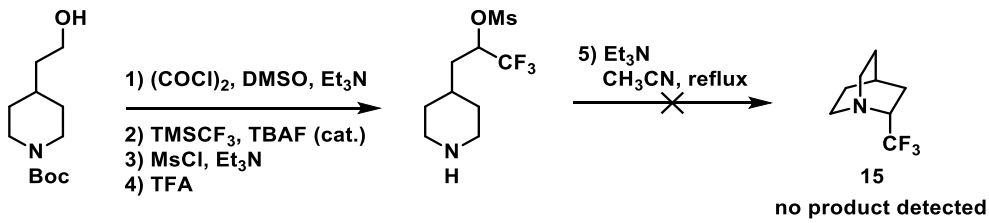

Figure S49. A similar route is not amenable for CF_3-QNC (**15**).

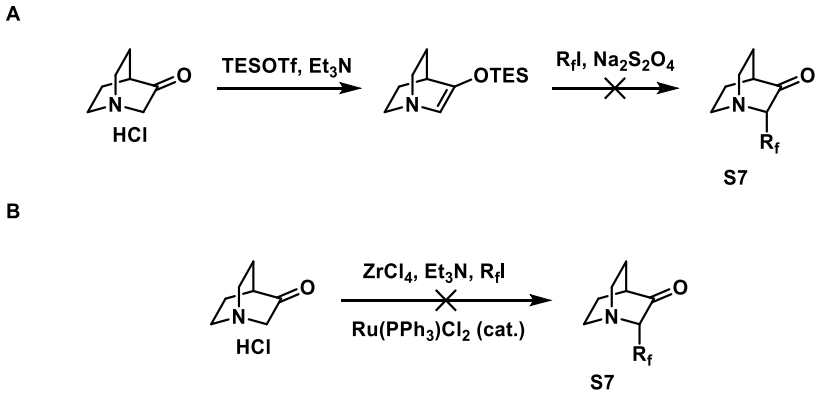

Figure S50. Additional unsuccessful routes A [41] and B [42] towards CF_3-QNC (**15**).

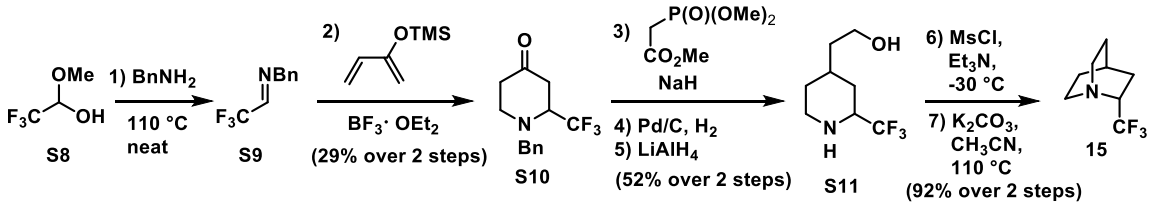

Figure S51. CF_3-QNC (**15**) was synthesized in 7 steps following the sequence.

To a 25 mL flask was added technical grade trifluoroacetaldehyde methyl hemiacetal **S8** (7.23 g, 50.0 mmol, 1 equiv) and benzyl amine (5.36 g, 50.0 mmol, 1 equiv). The flask was attached to a drying tube filled with anhydrous $CaCl_2$ and heated to 115 °C. After 10 h, it was cooled down to laboratory temperature and the imine product **S9** was directly used in the next step without purification. The imine **S9** was transferred to a flame-dried 500 mL flask and dissolved with anhydrous CH_2Cl_2 (250 mL), followed by the addition of 2-(trimethylsilyloxy)-1,3-butadiene (8.54 g, 60.0 mmol, 1.2 equiv). The flask was cooled to −78 °C under Ar and BF_3•OEt_2 (7.81 g, 6.8 mL, 55.0 mmol, 1.1 equiv) was added dropwise over 10 min. The reaction was stirred for 5 h before being quenched with 1N HCl (100 mL) and stirred for 1h. The mixture was transferred to a separatory funnel and the organic layers were separated. The aqueous phase was exacted with CH_2Cl_2 (3 × 100 mL) and the organic layers were combined, dried over $MgSO_4$, concentrated and further purified via column chromatography (SiO_2, hexanes/EtOAc 20:1 → 5:1) to give the desired product **S10** (3.78 g, 29% yield assumed) as a colorless oil, which contains impurities that cannot be removed via repeated column chromatography. This step has not been optimized.

To a flame-dried flask was added NaH (60% in mineral oil, 1.18 g, 29.4 mmol, 2.0 equiv), anhydrous THF (50 mL) and cooled to 0 °C. Trimethyl phosphonoacetate (6.59 g, 29.4 mmol, 2.0 equiv) was added dropwise over 10 min. The reaction was kept at 0 °C for 30 min followed by the addition of **S10** (3.78 g assumed, 14.7 mmol, 1.0 equiv) in THF (20 mL). The reaction was warmed to laboratory temperature and stirred for 2 h before being quenched with sat. NH_4Cl solution (50 mL). The resulting mixture was diluted with H_2O (100 mL),

transferred to a separatory funnel and extracted with EtOAc (3 × 50 mL). The combined organic phase was then washed with brine (100 mL), dried over $MgSO_4$, concentrated, and used in the next step without further purification. Next, the HWE reaction product was dissolved in absolute EtOH (50 mL), and Pd/C (5 wt%, 3.20 g, 1.5 mmol, 1.0 equiv.) was added. The reaction flask was equipped with a hydrogen balloon and stirred at laboratory temperature for 12 h before TLC indicated full consumption of starting material. The resulting mixture was filtered through Celite, concentrated, and directly used in the next step without purification. The hydrogenation product was dissolved in THF (100 mL) and $LiAlH_4$ (760 mg, 20 mmol, 1.36 equiv) solid was added at 0 °C. The reaction was stirred at 23 °C and then carefully quenched by adding H_2O (1 mL), 3 N NaOH (1 mL) and H_2O (3 mL). The mixture then solidified and suspended in EtOAc (100 mL). After filtration through Celite, the cake was washed with EtOAc (3 × 50 mL) and the combined filtrate was dried via $MgSO_4$, concentrated and purified via column chromatography (SiO_2, hexanes/EtOAc 5:1 → 1:1) to give product **S11** (1.51 g, 52% over 3 steps) as a colorless oil.

Data for **S11**:

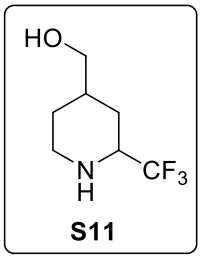

S11

^{1}H NMR (600 MHz, $CDCl_3$): δ 3.68 – 3.62 (m, 2H), 3.15 (ddd, *J* = 12.2, 4.4, 2.6 Hz, 1H), 3.12 – 3.04 (m, 1H), 2.63 (td, *J* = 12.3, 2.7 Hz, 1H), 2.08 – 2.00 (m, 2H), 1.87 (ddt, *J* = 12.7, 3.7, 2.3 Hz, 1H), 1.72 – 1.65 (m, 1H), 1.62 – 1.54 (m, 1H), 1.54 – 1.48 (m, 2H).
^{13}C NMR (126 MHz, $CDCl_3$): δ 125.8 (q), 60.1, 58.2 (q), 45.9, 39.7, 32.3, 31.8, 31.5.
^{19}F NMR (376 MHz, $CDCl_3$): δ −80.5
HRMS (ESI-TOF, m/z): Calcd for $C_{13}H_{15}F_3NO^+$ $[M+H]^+$: 198.1100; Found 198.1108. $\mathbf{R_f}$ = 0.33 (hexanes/EtOAc-1:4)

To **S11** (490 mg, 2.49 mmol, 1.0 equiv) and Et_3N (754.4 mg, 7.46 mmol, 3.0 equiv) in CH_2Cl_2 (25 mL) at -30 °C was added MsCl (0.300 g, 0.2 mL, 2.61 mmol, 1.05 equiv) slowly over 20 min. After 2 h, the reaction was quenched by the addition of sat. aq. NH_4Cl (10 mL) and diluted with H_2O (20 mL). The mixture was transferred to a separatory funnel and the organic phase was separated. The aqueous layer was exacted with CH_2Cl_2 (3 × 20 mL) and the combined organic phase was dried over $MgSO_4$, concentrated, and further purified via column chromatography to give the desired product **S12** (630 mg, 92%) as a colorless oil.
Note: The reaction temperature is crucial; reaction at 0 °C gave both *O*- and *N*- mesylation product.

Data for **S12**:

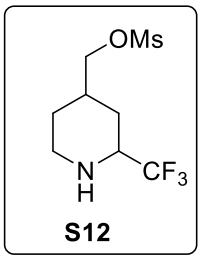

S12

^{1}H NMR (600 MHz, $CDCl_3$): δ 4.33 – 4.26 (m, 2H), 3.23 – 3.18 (m, 1H), 3.18 – 3.10 (m, 1H), 3.01 (s, 3H), 2.68 (td, *J* = 12.3, 2.7 Hz, 1H), 1.92 – 1.86 (m, 1H), 1.83 – 1.76 (m, 1H), 1.76 – 1.70 (m, 3H), 1.69 – 1.60 (m, 1H), 1.21 – 1.10 (m, 2H). 2.68 (td, *J* = 12.3, 2.7 Hz, 1H)
^{13}C NMR (126 MHz, $CDCl_3$): δ 125.6 (q), 67.2, 58.0 (q), 45.7, 37.6, 36.1, 31.7, 31.6, 31.2.
HRMS (ESI-TOF, m/z): Calcd for $C_{13}H_{17}F_3NO_3S^+$ $[M+H]^+$: 276.0876; Found 276.0887. $\mathbf{R_f}$ = 0.43 (hexanes/EtOAc-1:4).

To **S12** (200 mg, 0.726 mmol, 1.0 equiv) in anhydrous MeCN (1.5 mL) was added anhydrous K_2CO_3 (301.2 mg, 2.10 mmol, 2.9 equiv). The reaction was sealed and heated to 110 °C for 12 h. Then it was passed through a shot pad of SiO_2. The SiO_2 was washed with anhydrous MeCN (2 mL) and the stock solution of **15** (0.2 M, 3.5 mL, 96%) in MeCN was used in the

electrochemical C-H oxidation reaction without further purification. The same procedure was repeated on a 20-mg scale with CD_3CN as the solvent (0.5 mL) and eluent (0.5 mL) to obtain a sample for NMR experiments.

Note: **15** turned out to be non-basic and volatile. Treating **15** with HBF_4 failed to deliver the salt. A pure sample can be obtained by diluting the solution of **15** (0.2 M, 3 mL) with Et_2O (20 mL), followed by washing with H_2O (5 × 20 mL), dried over $MgSO_4$, and carefully concentrated on a rotary evaporator with the bath temperature at 0 °C. Significant material loss was observed during the concentration process. A ^1H NMR spectrum in $CDCl_3$ was obtained with this sample.

Data for **15**:

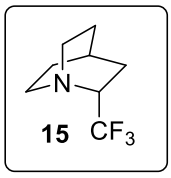

^{1}H NMR (600 MHz, $CDCl_3$): δ 3.36 – 3.23 (m, 1H), 3.20 – 3.10 (m, 1H), 3.02 – 2.85 (m, 2H), 2.81 – 2.71 (m, 1H), 1.95 – 1.89 (m, 1H), 1.78 (dddd, *J* = 12.7, 10.1, 4.4, 2.5 Hz, 1H), 1.67 – 1.59 (m, 2H), 1.59 – 1.45 (m, 4H).
^{1}H NMR (600 MHz, CD_3CN): δ 3.49 – 3.32 (m, 1H), 3.07 – 2.96 (m, 1H), 2.83 – 2.75 (m, 1H), 2.79 (dt, *J* = 13.4, 8.4 Hz, 1H), 2.67 (ddd, *J* = 14.6, 9.8, 5.2 Hz, 1H), 1.88 – 1.84 (m, 1H), 1.78 (dddd, *J* = 12.5, 10.0, 4.5, 2.3 Hz, 1H), 1.61 – 1.42 (m, 5H).
^{13}C NMR (126 MHz, CD_3CN): δ 57.7 (q), 50.8, 43.9, 26.5, 26.3, 25.5, 22.0.
^{19}F NMR (376 MHz, CD_3CN): δ −76.8
HRMS (ESI-TOF, m/z): Calcd for $C_8H_{13}F_3N^+$ $[M+H]^+$: 180.0995; Found 180.1004.
R_f = 0.53 (hexanes/EtOAc-1:4)

ACIDITY STUDY BY ^{1}H NMR

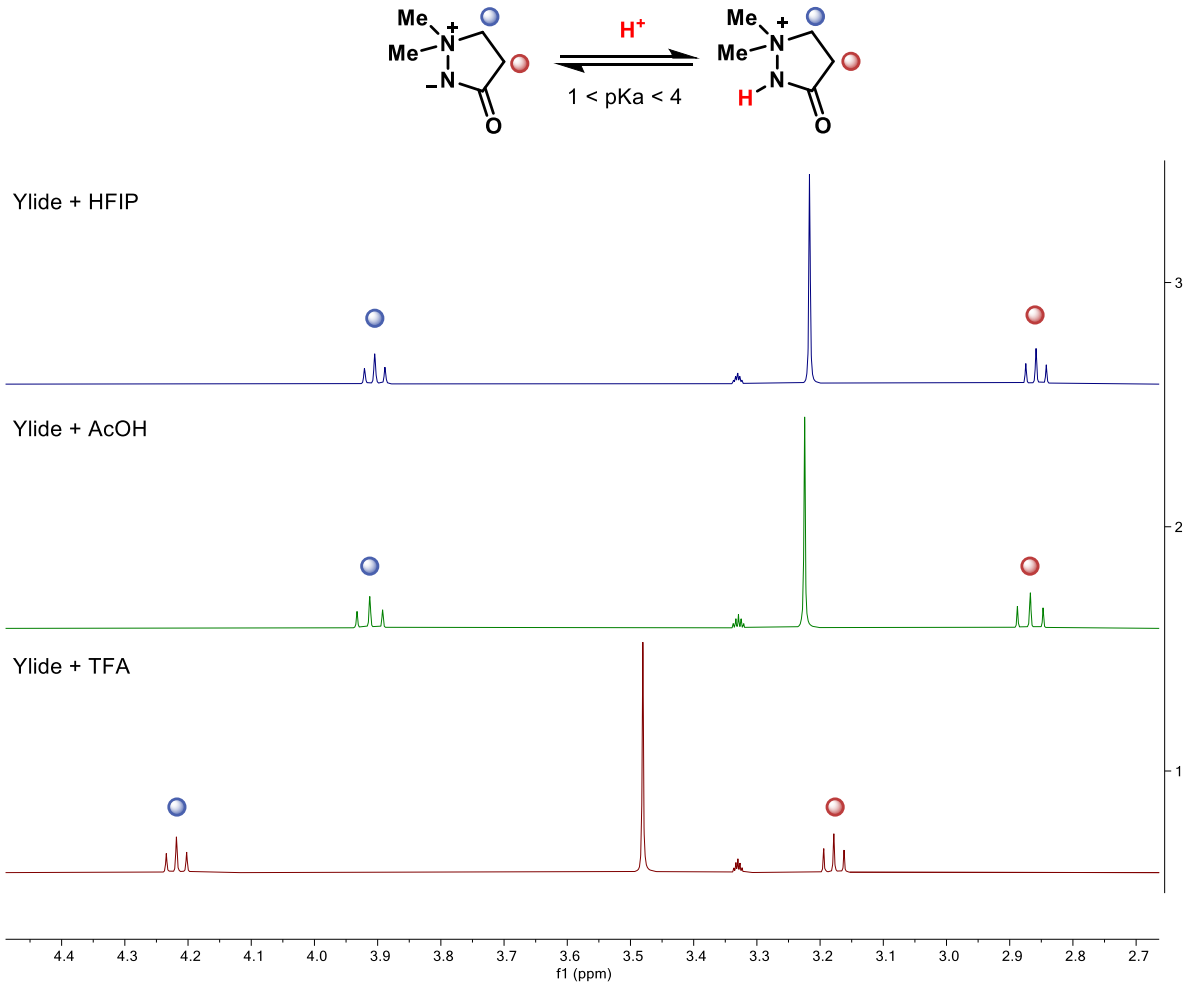

Figure S52. The above ^{1}H NMR spectra were taken in MeOH-d_4 solvent with 1 equiv. of HFIP, AcOH, and TFA respectively. A large shift was observed between AcOH and TFA, suggesting that pKa of the [ylide-H]$^{+}$ lies between the pKa of these acids.

LIST OF REFERENCES FOR COUNTING DERIVATIVES

TFDO

C. J. Pierce, M. K. Hilinski, Chemoselective hydroxylation of aliphatic sp^3 C–H bonds using a ketone catalyst and aqueous H_2O_2. *Org. Lett.* **16**, 6504–6507 (2014).
W. G. Shuler, S. L. Johnson, M. K. Hilinski, Organocatalytic, dioxirane-mediated C–H hydroxylation under mild conditions using oxone. *Org. Lett.* **19**, 4790–4793 (2017).
L. D'Accolti, C. Annese, C. Fusco, Continued progress towards efficient functionalization of natural and non-natural targets under mild conditions: Oxygenation by C−H bond activation with dioxirane. *Chem. Eur. J.* **25**, 12003–12017 (2019).

Oxaziridine

N. D. Litvinas, B. H. Brodsky, J. Du Bois, C–H hydroxylation using a heterocyclic catalyst and aqueous H_2O_2. *Angew. Chem. Int. Ed.* **48**, 4513–4516 (2009).
A. M. Adams, J. Du Bois, Organocatalytic C–H hydroxylation with Oxone® enabled by an aqueous fluoroalcohol solvent system. *Chem. Sci.* **5**, 656–659 (2014).

Quinuclidine

H.-B. Yang, A. Feceu, D. B. C. Martin, Catalyst-controlled C–H functionalization of adamantanes using selective H-atom transfer. *ACS Catal.* **9**, 5708–5715 (2019).
M. A. Ashley, C. Yamauchi, J. C. K. Chu, S. Otsuka, H. Yorimitsu, T. Rovis, Photoredox-catalyzed site-selective α-C(sp^3)−H alkylation of primary amine serivatives. *Angew. Chem. Int. Ed.* **58**, 4002–4006 (2019).
V. Dimakos, H. Y. Su, G. E. Garrett, M. S. Taylor, Site-selective and stereoselective C–H alkylations of carbohydrates via combined diarylborinic acid and photoredox catalysis. *J. Am. Chem. Soc.* **141**, 5149–5153 (2019).
J. Ye, I. Kalvet, F. Schoenebeck, T. Rovis, Direct α-alkylation of primary aliphatic amines enabled by CO_2 and electrostatics. *Nature Chem.* **10**, 1037–1041 (2018).
X. Zhang, D. W. C. MacMillan, Direct aldehyde C–H arylation and alkylation via the combination of nickel, hydrogen atom transfer, and photoredox catalysis. *J. Am. Chem. Soc.* **139**, 11353–11356 (2017).
C. Le, Y. Liang, R. W. Evans, X. Li, D. W. C. MacMillan, Selective sp^3 C–H alkylation via polarity-match-based cross-coupling. *Nature* **547**, 79–83 (2017).
J. L. Jeffrey, J. A. Terrett, D. W. C. MacMillan, O–H hydrogen bonding promotes H-atom transfer from α C–H bonds for C-alkylation of alcohols. *Science* **349**, 1532–1536 (2015).

Fe-oxo

L. Vicens, G. Olivo, M. Costas, Rational design of bioinspired catalysts for selective oxidations. *ACS Catal.* **10**, 8611–8631 (2020).
M. C. White, J. Zhao, Aliphatic C–H oxidations for late-stage functionalization. *J. Am. Chem. Soc.* **140**, 13988–14009 (2018).
J. M. Howell, K. Feng, J. R. Clark, L. J. Trzepkowski, M. C. White, Remote oxidation of aliphatic C–H bonds in nitrogen-containing molecules. *J. Am. Chem. Soc.* **137**, 14590–14593 (2015).
P. E. Gormisky, M. C. White, Catalyst-controlled aliphatic C–H oxidations with a predictive model for site-selectivity. *J. Am. Chem. Soc.* **135**, 14052–14055 (2013).
M. S. Chen, M. C. White, Combined effects on selectivity in Fe-catalyzed methylene oxidation. *Science*. **327**, 566–571 (2010).

PREVIOUS ROUTES FOR PENCONAZOLE METABOLITE SYNTHESES

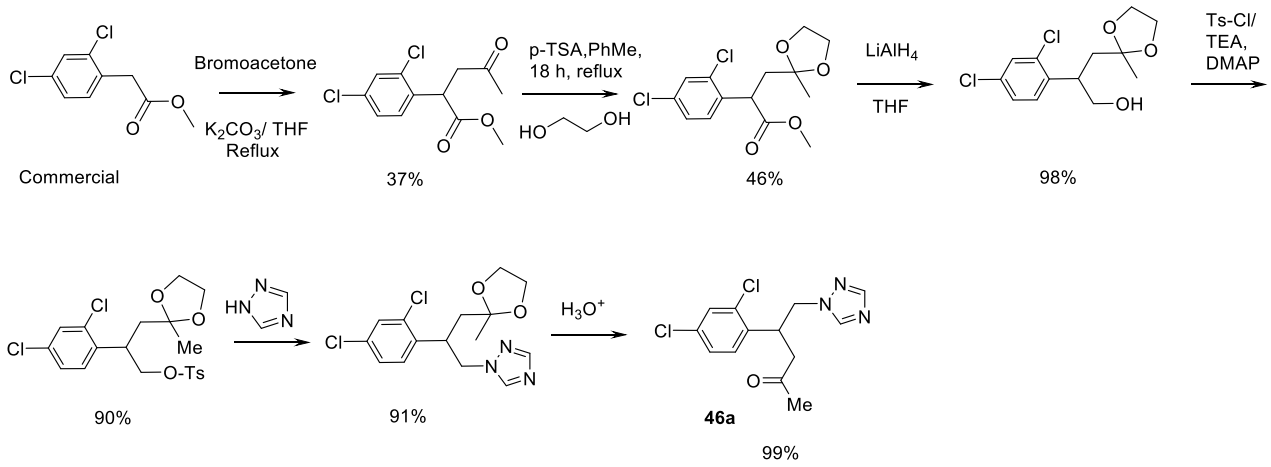

Scheme S7. Current route (6 steps) to penconazole metabolite **46a**.

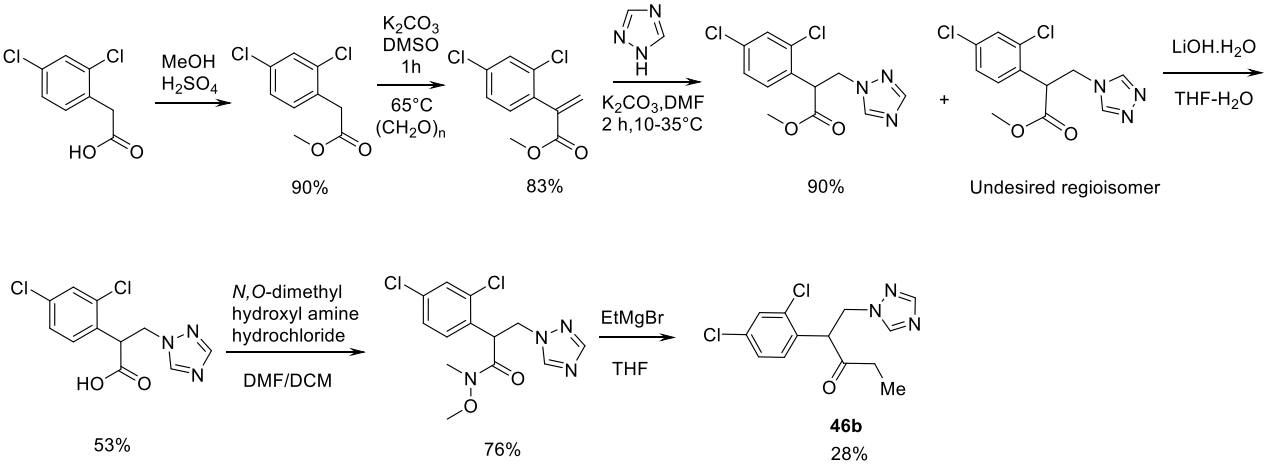

Scheme S8. Current route (6 steps) to penconazole metabolite **46b**.

Troubleshooting: Frequently Asked Questions

Question #1: The reaction is not reproducible. What should I do?

There are a few possible reasons, some of which are covered in more detail in the remaining questions. However, here is a brief overview of key factors. We found that contamination by redox active impurities (i.e., transition metals, iodides) can severely hinder the reaction. Furthermore, the oxygen content can at times vary so conducting the reaction under an O_2 atmosphere will help ensure a high degree of reproducibility. Maintaining both an appropriate voltage (see Question #2) and electrode charge density (see Question #5) is also important.

Question #2: What are suitable voltage values for these reactions?

For reactions run using Condition A, we observed successful reactions had voltage values ranging from 3.5V – 5.0V. Similarly, when using Condition B these values were reliably between 2.5V– 4.0V. In general, you can add additional electrolyte to reduce the

resistance/voltage. If you observe excessively large voltage values (>10V), check that the electrode cap (see graphical guide) is securely attached to the ElectraSyn.

Question #3: What can I do if the starting material is not completely consumed after electrolysis?

You can increase the reaction time. However, excessively long reaction times (i.e. >12 F/mol for Condition A, >18 F/mol for Condition B) often led to reduced yields due to decomposition of starting material and product.

Question #4: What can I do if my starting material and/or product readily decomposes during electrolysis?

In these cases, we found replacing HFIP with H_2O (Condition B) reduced decomposition. When this failed, we used shorter reaction times (3 – 4 F/mol) which may also allow for recycling of the remaining starting material.

Question #5: Does the size of the electrodes matter?

Yes. While the Nickel plate electrode comes in a specific size, the RVC electrode has to be cut from a larger block of RVC. It is important that the RVC electrode is similar in size to the Ni plate to ensure a desirable charge density (6 –10 A/m^2).

Question #6: How do you clean the electrodes?

Solids that build up on the Ni plate electrode during electrolysis can easily be removed by rinsing the electrode with 1 M aq. HCl, water, and acetone. RVC can also be cleaned with water and acetone and should be subsequently dried in the oven. See Figure S53 for a visual depiction.

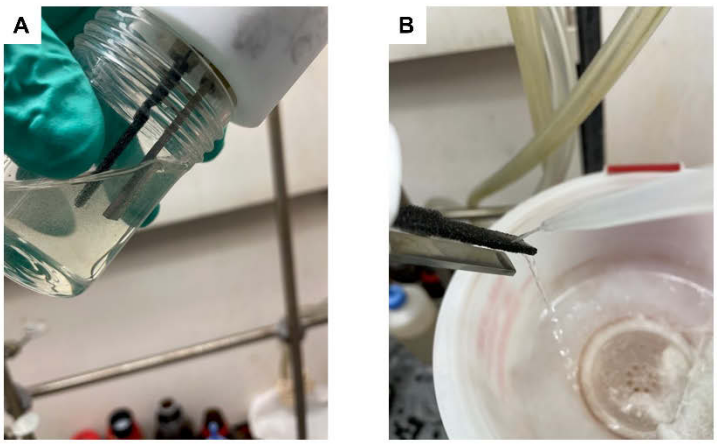

Figure S53. A) Electrodes are immersed into 1 M aq. HCl. **B)** Electrodes (particularly porous RVC) are washed with distilled water, MeOH, CH_2Cl_2 or EtOAc and acetone.

Question #7: Are electrodes reusable?

After reactions employing Condition A, both Ni plate and RVC electrodes, following proper cleaning, are reusable for several runs (up to 10 times). However, when using Condition B, we noticed partial degradation of the RVC electrode (see Figure S54) and thus it is recommended in these cases to not reuse the RVC electrode.

Figure S54. Photo of degraded RVC electrode from water conditions

Question #8: How to change reaction scale?

Up to 0.300 mmol of substrate can be reacted in these ElectraSyn vials without having to adjust solvent quantities. However, we found that when using Condition A that increasing the amount of HFIP (~19 equiv.) for larger scale reactions was required to obtain similar yields.

References

1) Ers., L. E. V. I.; Mccombie, S.W.; Lin, S.; Vice, S. E. *Tetrahedron Lett.* **1999**, *40*, 8767.
2) Xu, P.; Guo, S.; Wang, L.; Tang, P. *Angew. Chem. Int. Ed*. **2014**, 53, 5955.
3) Kato, H.; Hirano, K.; Kurauchi, D.; Toriumi, N. *Chem. Eur. J.* **2015**, *21*, 3895.
4) Zhu, C.; Yoshimura, A.; Ji, L.; Wei, Y.; Nemykin, V. N.; Zhdankin, V.V. *Org. Lett*. **2012**, *14*, 3170.
5) Bume, D. D.; Pitts, C. R.; Ghorbani, F.; Harry, S. A.; Capilato, J. N.; Siegler, M. A.; Lectka, T. *Chem Sci*. **2017**, *8*, 6918.
6) Ye, P.; Shao, Y.; Ye, X.; Zhang, F.; Li, R.; Sun, J.; Xu, B.; Chen, J. *Org. Lett*. **2020**, *22*, 1306.
7) He, H.; Zhang, H.; Ma, M.; Shi, Y.; Gao, Z.; Chen, S.; Wang, X. *Nanoscale* **2020**, *12*, 12146.
8) Subaramanian, M.; Ramar, P. M.; Rana, J.; Gupta, V. K.; Balaraman, E. *Chem. Commun.* **2020**, *56*, 8143.
9) Mukherjee, S.; Maji, B.; Tlahuext-Aca, A.; Glorius, F. *J. Am. Chem. Soc.* **2016**, *138*, 16200.

10) Zhang, C.; Zhang, G.; Luo, S.; Wang, C.; Li., H. *Org. Biomol. Chem*. **2018**, *16*, 8467.
11) Lu, L.; Cheng, D.; Zhan, Y.; Shi, R.; Chiang, C.-W.; Lei, A. *Chem. Commun*. **2017**, *53*, 6852.
12) Cooper, P.; Crisenza, G. E. M.; Feron, L. J.; Bower, J. F. *Angew. Chem. Int. Ed* **2018**, *57*, 14198.
13) Oba, G.; Coleman, B. E.; Hart, J. D.; Zakin, J.; Zhang, Y.; Kawaguchi, Y.; Talmon, Y. *Tetrahedron* **2006**, *62*, 10193.
14) Canta, M.; Font, D.; Gómez, L.; Ribas, X.; Costas, M. *Adv. Synth. Catal.* **2014**, *356*, 818.
15) Song, L.; Claessen, S.; Van der Eycken, E.V. *J. Org. Chem*. **2020**, *85*, 8045.
16) Fuse, H.; Mitsunuma, H.; Kanai, M. *J. Am. Chem. Soc.* **2020**, *142*, 4493.
17) Kiyokawa, K.; Ito, R.; Takemoto, K.; Minakata, S. *Chem. Commun*. **2018**, *54*, 7609.
18) Sohda, T.; Megaro, K.; Kawamatsu, Y. *Chem. Pharm. Bull.* **1984**, *32*, 2267.
19) Hao, B.; Gunaratna, M. J.; Zhang, M.; Weerasehera, S.; Seiwald, S. N.; Nguyen, V.T.; Meier, A.; Hua, D. H. *J. Am. Chem. Soc.* **2016**, *238*, 16839.
20) Chen., M. S.; White, C. *Science* **2007**, *318*, 783.
21) Sharma Shallu, M. L.; Singh, J. *Synth. Commun*. **2012**, *42*, 1306.
22) Adam, W.; van Barneveld, C.; Golsch, D. *Tetrahedron* **1996**, *52*, 2377.
23) Bovicelli, P.; Lupattelli, P.; Mincione, E.; Prencipe, T.; Curci, R. *J. Org. Chem.* **1992**, 57, 2182.
24) D'Accolti, L.; Fusco, C.; Lampignano, G.; Capitelli, F.; Curci, R. *Tetrahedron Lett.* **2008**, *49*, 5614.
25) Adams, M.; Du Bois, J. *Chem. Sci.* **2014**, *5*, 656–659.
26) Nodwell, M. B.; Yang, H.; Čolovic, M.; Yuan, Z.; Merkens, H.; Martin, R. E.; Bénard, F.; Schaffer, P.; Britton. R. *J. Am. Chem. Soc*. **2017**, *139*, 3595.
27) Viala, C.; Coudret, C. *Inorg. Chim. Acta* **2006**, *359*, 984.
28) Cipollina, J. A.; Ruediger, E. H.; New, J. S.; Wire, M. E.; Shepherd, T. A.; Smith, D. W.; Yevich, J. P. *J. Med. Chem.* **1991**, *34*, 3316.
29) Frisch, J.; Trucks, G. W.; Schlegel, H. B.; Scuseria, G. E.; Robb, M. A.; Cheeseman, J. R.; Scalmani, G.; Barone, V.; Petersson, G. A.; Nakatsuji, H.; Li, X.; Caricato, M.; Marenich, A.; Bloino, J.; Janesko, B. G.; Gomperts, R.; Mennucci, B.; Hratchian, H. P.; Ortiz, J. V.; Fox, D. J. "Gaussian, Inc." Wallingford CT, **2016**.
30) Zhao, Y.; Truhlar, D. G. *Theor. Chem. Acc.* **2008**, *120*, 215.
31) Hariharan, P. C.; Pople; J. A. *Mol. Phys.* **1974**, *27*, 209.
32) Krishnan, R.; Binkley, J. S.; Seeger, R.; Pople, J. A. *J. Chem. Phys.* **1980**, *72*, 650.
33) Ditchfield, R.; Hehre, W. J.; Pople, J. A. *J. Chem. Phys.* **1971**, *54*, 720.
34) Dolg, M.; Wedig, U.; Stoll, H.; Preuss, H. *J. Chem. Phys.* **1986**, *86*, 866.
35) Marenich, V.; Cramer, C. J.; Truhlar, D. G. *J. Phys. Chem. B* **2009**, *113*, 6378.
36) Peng, P. Y.; Ayala, H. B.; Schlegel, M. J. *J. Comput. Chem.* **1996**, *17*, 49.
37) Horn, E. J.; Rosen, B. R.; Chen, Y.; Tang, J.; Chen, K.; Eastgate, M. D.; Baran, P. S. *Nature* **2016**, *533*, 77.
38) Nutting, J. E.; Rafiee, M.; Stahl, S. S. *Chem. Rev.* **2018**, *118*, 4834.
39) Zuranski, A. **2020** https://github.com/PrincetonUniversity/auto-qchem/blob/master/notebooks/Fast%20featurize%20with%20Mordred.ipynb
40) Excel files containing the descriptors/identifiers and the UMAP Python script are available at https://github.com/SigmanGroup/umap_baran_mediators
41) Plenkiewicz, H.; Dmowski, W.; Lípinski, M. *J. Fluor. Chem.* **2001**, *111*, 227.
42) Herrmann, T.; Smith, L. L.; Zakarian, A. *J. Am. Chem. Soc*. **2012**, *134*, 6976.
43) Kawamata, Y.; Yan, M.; Liu, Z.; Bao, D.-H.; Chen, J.; Starr, J. T.; Baran, P. S. *J. Am. Chem. Soc.* **2017**, *139*, 7448.

44) Mi, Y.; Corey, E. J. *Tetrahedron Lett.* **2006**, *47*, 2515.
45) Recupero, F.; Punta, C. *Chem. Rev.* **2007**, *107*, 3800.
46) Moriwaki, H.; Tian, Y.-S.; Kawashita, N.; Takagi, T. *J Cheminform*. **2018**, *10*, 4.
47) McInnes, L.; Healy, J.; Melville, J. UMAP: Uniform Manifold Approximation and Projection for Dimension Reduction. arXiv, September 18, 2020, 1802.03426v3. https://arxiv.org/abs/1802.03426
48) Probst, D.; Reymond, J.-L. *J Cheminform.* **2020***, 12*, 1.
49) Vermeulen, N. A.; Chen, M. S.; White, M. C. *Tetrahedron* **2009**, *65*, 3078.
50) J Mack, J. B. C.; Gipson, J. D.; Du Bois, J.; Sigman, M. S. *J. Am. Chem. Soc.* **2017**, *139*, 9503.
51) Laudadio, G.; Govaerts, S.; Wang, Y.; Ravelli, D.; Koolman, H. F.; Fagnoni, M.; Djuric, S. W.; Noël, T. *Angew. Chem. Int. Ed.* **2018**, *57*, 4078.
52) Asensio, G.; Castellano, G.; Mello, R.; González Núñez, M. E. *J. Org. Chem.* **1996**, *61*, 5564.
53) Mercadante, R.; Polledri, E.; Scurati, S.; Moretto, A.; Fustinoni, S. *Chem. Res. Toxicol.* **2016***, 29*, 1179.

Addendum: Copyright permission/license for use of published figures and text

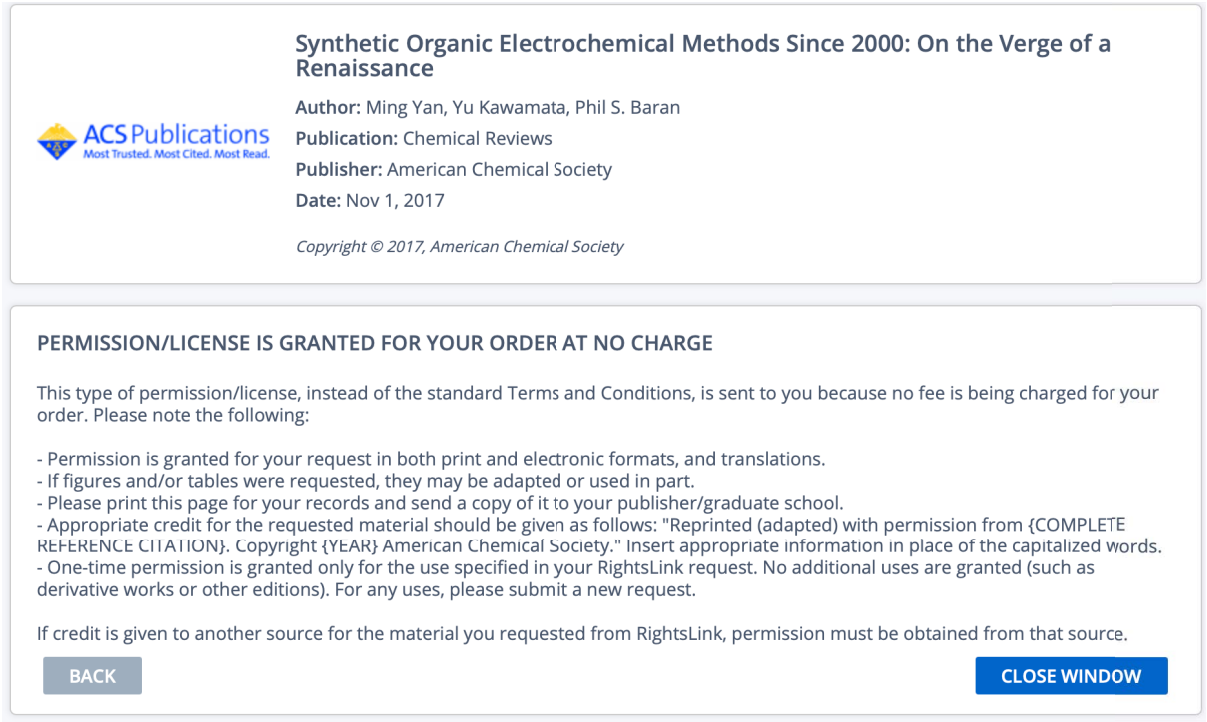

Synthetic Organic Electrochemical Methods Since 2000: On the Verge of a Renaissance

Author: Ming Yan, Yu Kawamata, Phil S. Baran

Publication: Chemical Reviews

Publisher: American Chemical Society

Date: Nov 1, 2017

Copyright © 2017, American Chemical Society

PERMISSION/LICENSE IS GRANTED FOR YOUR ORDER AT NO CHARGE

This type of permission/license, instead of the standard Terms and Conditions, is sent to you because no fee is being charged for your order. Please note the following:

- Permission is granted for your request in both print and electronic formats, and translations.
- If figures and/or tables were requested, they may be adapted or used in part.
- Please print this page for your records and send a copy of it to your publisher/graduate school.
- Appropriate credit for the requested material should be given as follows: "Reprinted (adapted) with permission from {COMPLETE REFERENCE CITATION}. Copyright {YEAR} American Chemical Society." Insert appropriate information in place of the capitalized words.
- One-time permission is granted only for the use specified in your RightsLink request. No additional uses are granted (such as derivative works or other editions). For any uses, please submit a new request.

If credit is given to another source for the material you requested from RightsLink, permission must be obtained from that source.

BACK CLOSE WINDOW

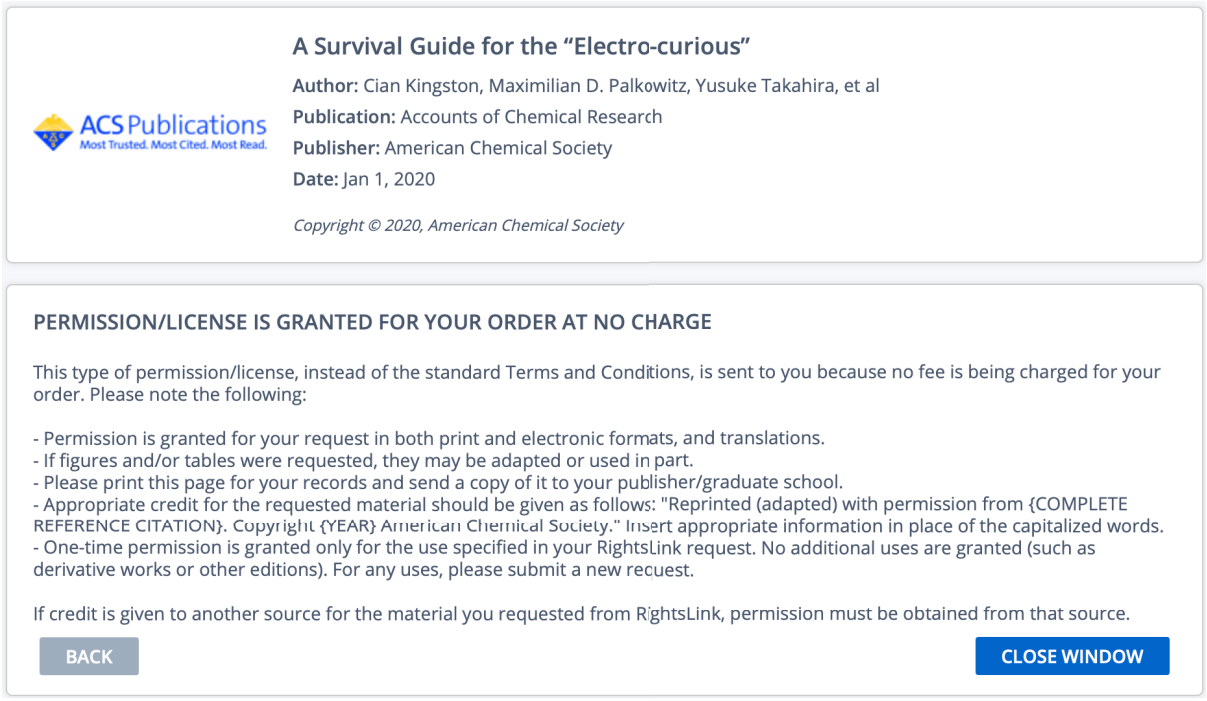

A Survival Guide for the "Electro-curious"

Author: Cian Kingston, Maximilian D. Palkowitz, Yusuke Takahira, et al

Publication: Accounts of Chemical Research

Publisher: American Chemical Society

Date: Jan 1, 2020

Copyright © 2020, American Chemical Society

PERMISSION/LICENSE IS GRANTED FOR YOUR ORDER AT NO CHARGE

This type of permission/license, instead of the standard Terms and Conditions, is sent to you because no fee is being charged for your order. Please note the following:

- Permission is granted for your request in both print and electronic formats, and translations.
- If figures and/or tables were requested, they may be adapted or used in part.
- Please print this page for your records and send a copy of it to your publisher/graduate school.
- Appropriate credit for the requested material should be given as follows: "Reprinted (adapted) with permission from {COMPLETE REFERENCE CITATION}. Copyright {YEAR} American Chemical Society." Insert appropriate information in place of the capitalized words.
- One-time permission is granted only for the use specified in your RightsLink request. No additional uses are granted (such as derivative works or other editions). For any uses, please submit a new request.

If credit is given to another source for the material you requested from RightsLink, permission must be obtained from that source.

BACK CLOSE WINDOW